Unravelling the complex inflammatory landscape of hidradenitis suppurativa

Conor M. Smith MSc

School of Biochemistry and Immunology

A thesis submitted to Trinity College Dublin as completion of the degree of Doctor of Philosophy

2024

Supervisor: Dr Jean Fletcher

Co-Supervisor: Dr Andreea Petrasca

Declaration of authorship

I declare that this thesis has not been submitted as an exercise for a degree at this or any other university and it is entirely my own work.

I agree to deposit this thesis in the University's open access institutional repository or allow the library to do so on my behalf, subject to Irish Copyright Legislation and Trinity College Library conditions of use and acknowledgement.

I consent to the examiner retaining a copy of the thesis beyond the examining period, should they so wish (EU GDPR May 2018).

Conor Smith

Student Number: 19331956

Abstract

Hidradenitis suppurativa (HS) is a chronic, relapsing, inflammatory skin disease characterised by painful lesions at hair follicles of the inframammary fold, genitals, groin, buttocks and perianal areas. Follicular occlusion is an initiating event in HS, resulting in cyst formation which subsequently rupture leading to a bloody, foul-smelling discharge. Severe HS may also lead to the development of dermal tunnels and hypertrophic scarring. A poor understanding of HS pathogenesis has limited the development of effective therapies, with the only approved biologics, adalimumab and secukinumab, proving moderately effective in a cohort of HS patients. Evidence suggests immune dysregulation plays an important role in driving HS inflammation; however detailed investigation into both immune and non-immune cells, and their interaction, has yet to be pursued. Identifying potential interactions between immune and non-immune cells would be invaluable to the field.

This project utilised state-of-the-art bulk and single cell RNA sequencing and high-parameter flow cytometry to study both immune and non-immune cells in HS skin.

The data presented in this thesis identified B cells and immunoglobulins as key features which distinguish HS from other inflammatory dermatoses, psoriasis and atopic dermatitis. For the first time, this study characterised the keratinocyte and fibroblast populations present in HS lesions. Of note, T cells were shown to promote the development of inflammatory phenotypes which are likely responsible for distinct clinical features including epidermal hyperplasia, dermal tunnel formation and hypertrophic scarring. This study identified a dendritic cell subset (cDC2) as the major source of IL-1β and the NLRP3 inflammasome and finally, provided proof of concept that targeting NLRP3 inflammasome activation effectively inhibits IL-1β, as well as other inflammatory mediators including IL-17A, IFN-γ and TNF, in HS lesions.

These data highlight the complex nature of HS pathogenesis, implicating B cells, T cells, keratinocytes, fibroblasts and dendritic cells in HS inflammation. Importantly, this study outlines the potential for therapeutic suppression of the NLRP3 inflammasome in HS patients, providing additional benefits to current therapies by reducing a broader range of inflammatory mediators in HS lesions.

Acknowledgements

Putting my thoughts into words is not my strong point and writing this section took longer than Chapter 4 of this thesis, but I want to thank everyone who was part of this journey.

Firstly, I would like to thank my supervisor Dr Jean Fletcher. An exceptional mentor who always had her door open and willing to help in any way she can. I really appreciate all the time you have invested in me and the encouragement you have given me throughout this project. From letting me try (and fail) new experiments to tirelessly reading through this thesis, I want to thank you for giving me the opportunity to be part of your lab and I look forward to working together post-PhD.

To my co-supervisor Dr Andreea Petrasca, thank you for your support throughout this project. Listening to my nonsense everyday can't have been easy, but you did it with a smile on your face. I really appreciate all of the scientific support and guidance you have given me and for keeping the Fletcher lab in order. Most importantly, I want to thank you for introducing me to Oreo truffles, they have changed my life. I hope that I am the first of many PhD students you get to supervise.

To the members of my thesis committee, Prof Kingston Mills and Dr Emma Creagh, thank you for your invaluable advice throughout the years.

To the past and present members of the Fletcher and Fearon labs, thank you for your scientific help and friendship. To Dr Barry Moran, the FACS guru, thank you for coming in to save the day whenever I broke your cytometers. Your exceptional eye for detail was always so helpful in our lab meetings and was a fantastic help for reviewing this thesis, I really appreciate the time and effort you have put in. To the newbie Orlaith, thank you for taking care of all of the lab duties while I was at home writing, it has been a massive help for me.

To everyone in the reading room, thank you for making these past 4 years so enjoyable. In particular I want to mention Brianne, who initiated a baking war which benefitted us all and Orla, who was always ready to go down a rabbit hole of philosophical thinking, you both are exceptional scientists. To Dr Megan Hanlon, you allowed me to be in the presence of a podcast sensation for which I am forever grateful. Thank you for allowing me to be part of your macrophage project, it has been a pleasure working with you over the years, and I hope our scientific paths cross again in the future.

To Dr Viviana Marzaioli, thank you for the chats and listening to me complain about the smallest of problems. You have also been a great mentor for me and helped me get me first ever grant, I will be eternally grateful. I have been lucky to be surrounded by fantastic scientists who have always offered advice whenever I asked for it. Dr Mary Canavan, thank you for trusting me with analysing some of your RNA-seq data and I hope we can work together again in the future. To Prof Ursula Fearon, thank you for allowing me to work so closely on some of your projects and for coming in and talking about rugby when nobody else in the reading room was interested.

None of the clinical work in this project would be possible without the patients and healthy controls who donated samples for these studies. I am particularly grateful to the clinical collaborators in St Vincent's University Hospital and St. Michael's Hospital. Roisin and Emily, you both have been so helpful collecting samples whenever needed and made this work possible. To Prof Brian Kirby, thank you for helping put the value of our work in a clinical context, your enthusiasm and support has been unwavering since I joined, and I look forward to continuing this collaboration.

To Dr Karsten Hokamp, thank you for sharing your RNA-seq expertise and for paving the path for me to start my bioinformatics journey. To Dr Achilleas Floudas, thank you for helping me troubleshoot the so many problems I encountered in R, it was a pleasure to work with you.

To the Provost PhD award which funded my PhD and to TBSI who awarded me the early career researchers grant, thank you for funding this project.

To my friends back home, Rory, Josh, Kevin, Chris, Ciza, Jake and Jack, thank you for making sure my feet were always kept on the ground. You guys have been there through thick in thin and I couldn't ask for a better group of friends.

Lastly, to my wife Kirsty. You have been amazing over these past 4 years. You have dragged me from a struggling undergraduate student to where I am today and more importantly, made me a better man. I can't put into words how much you have helped me throughout these years but this achievement is as much yours as it is mine. You have sacrificed many evenings and Saturdays to spend time with me in the lab, from labelling tubes to proofreading this thesis you have been an essential part of this journey. I am lucky to have you in my life. I love you.

Contents

List of Tables

List of Figures

Author publications

Moran, B.*, **Smith, C. M.***, Zabarowski, A., Ryan, M., Karman, J., Dunstan, R. W., Smith, K. M., Hambly, R., Musilova, J., Petrasca, A., Fabre, A., O'Donnell, M., Hokamp, K., Mills, K. H. G., Housley, W. J., Winter, D. C., Kirby, B. and Fletcher, J. M. (2023) 'Targeting the NLRP3 inflammasome reduces inflammation in hidradenitis suppurativa skin', Br J Dermatol.

* Equal contribution

Smith, C. M., Hambly, R., Gatault, S., Iglesias-Martinez, L. F., Kearns, S., Rea, H., Marasigan, V., Lynam-Loane, K., Kirthi, S., Hughes, R., Fletcher, J. M., Kolch, W. and Kirby, B. (2023) 'B-cell-derived transforming growth factor-β may drive the activation of inflammatory macrophages and contribute to scarring in hidradenitis suppurativa', Br J Dermatol, 188(2), pp. 290-310.

Hambly, R., Gatault, S., Smith, C. M., Iglesias-Martinez, L. F., Kearns, S., Rea, H., Marasigan, V., Lynam-Loane, K., Kirthi, S., Hughes, R., Fletcher, J. M., Kolch, W. and Kirby, B. (2023) 'B-cell and complement signature in severe hidradenitis suppurativa that does not respond to adalimumab', Br J Dermatol, 188(1), pp. 52-63.

Fletcher, J. M., Moran, B., Petrasca, A. and Smith, C. M. (2020) 'IL-17 in inflammatory skin diseases psoriasis and hidradenitis suppurativa', Clin Exp Immunol, 201(2), pp. 121-134.

Petrasca, A., Hambly, R., Kearney, N., Smith, C. M., Pender, E. K., Mac Mahon, J., O'Rourke, A. M., Ismaiel, M., Boland, P. A., Almeida, J. P., Kennedy, C., Zaborowski, A., Murphy, S., Winter, D., Kirby, B. and Fletcher, J. M. (2023a) 'Metformin has anti-inflammatory effects and induces immunometabolic reprogramming in hidradenitis suppurativa via multiple mechanisms', Br J Dermatol.

Petrasca, A., Hambly, R., Molloy, O., Kearns, S., Moran, B., Smith, C. M., Hughes, R., O'Donnell, M., Zaborowski, A., Winter, D., Fletcher, J. M., Kirby, B. and Malara, A. (2023b) 'Innate lymphoid cell (Montero-Vilchez *et al.*) subsets are enriched in the skin of patients with hidradenitis suppurativa', PLoS One, 18(2), pp. e0281688.

Floudas, A., Smith, C. M., Tynan, O., Neto, N., Krishna, V., Wade, S. M., Hanlon, M., Cunningham, C., Marzaioli, V., Canavan, M., Fletcher, J. M., Mullan, R. H., Cole, S., Hao, L. Y., Monaghan, M. G., Nagpal, S., Veale, D. J. and Fearon, U. (2022) 'Distinct stromal and immune cell interactions shape the pathogenesis of rheumatoid and psoriatic arthritis', Ann Rheum Dis.

Barker, B. E., Hanlon, M. M., Marzaioli, V., Smith, C. M., Cunningham, C. C., Fletcher, J. M., Veale, D. J., Fearon, U. and Canavan, M. (2023) 'The mammalian target of rapamycin contributes to synovial fibroblast pathogenicity in rheumatoid arthritis', Front Med (Lausanne), 10, pp. 1029021.

Pending Author Publications

Hanlon, M. M., Smith, C. M., Canavan, M., Neto, N. G. B., Song, Q., Lewis, M., Gallagher, P., Mullan, R., Hurson, C., Moran, M., Monaghon, M. M., Pitzalis, C., Fletcher, J. M., Nagpal, S., Veale, D. J., Fearon, U. (Manuscript under review at ScienceAdvances). Loss of synovial tissue macrophage homeostasis precedes Rheumatoid Arthritis clinical onset.

Abbreviations

µg	microgram
µl	microlitre
µm	micrometer
AD	atopic dermatitis
adj	adjusted
aDC	activated dendritic cells
AhR	Aryl hydrocarbon
AMPs	antimicrobial peptides
ANOVA	analysis of variance
APCs	antigen presenting cells
BAFF	B cell activating factor
BMI	body mass index
BSA	bovine serum albumin
CAPS	Cryopyrin-associated periodic syndrome
CCL	chemokine (C-C motif) ligand
CCR	chemokine receptor
CD	cluster of differentiation
CD	Crohn's disease
cDC	conventional dendritic cells
cDNA	Complimentary DNA
cIMDM	complete Iscove's Modified Dulbecco's Medium
CLEC	C-type lectin domain containing
Con	healthy control group samples
cRPMI	Complete Roswell Park Memorial Institute media
CTLA4	cytotoxic T-lymphocyte-associated protein 4
CX_3CL	chemokine (C-X_3-C motif) ligand
CXCL	chemokine (C-X-C motif) ligand
CyTOF	Cytometry by Time Of Flight
DAMP	damage associated molecular pathogen
DCs	dendritic cells
DGE	differential gene expression
DEGs	differentially expressed genes
dH_2O	distilled water
DMKN	dermokine
DNA	deoxyribonucleic acid
dNTPs	Deoxynucleotide triphosphate
EASI	Eczema Area and Severity Index
EDTA	Ethylenediaminetetraacetic acid
ELISA	Enzyme Linked Immunosorbent Assay
EMA	European medicines agency

EudraCT	European union drug regulating authorities clinical trials
E-S	ex-smoker
Ex-Th17	extinguished Th17 cells
F	female
FACS	Fluorescence-Activated Cell Sorting
FBS	Fetal bovine serum
FC	fold change
Fc block	Fc receptor binding inhibitor
FDA	food and drug administration (US)
FGFR2	fibroblast growth factor-receptor 2
FixVia eF506	Fixable Viability Dye eFluor™ 506
FoxP3	forkhead box P3
FSC	forward scatter channel
FSC-A	forward scatter channel area
FSC-H	forward scatter channel height
FSC-W	forward scatter channel width
g	gram
g	standard gravity
G-CSF	granulocyte-colony-stimulating factor
GEM	gel bead-in-emulsion
GEM-RT	Gel bead-in-emulsion reverse transcription
GM-CSF	granulocyte-macrophage colony-stimulating factor
GO	gene ontology
H_2SO_4	sulfuric acid
h	hours
hi	high expression
IHS4	international hidradenitis suppurativa severity score system
HiSCR	hidradenitis suppurativa clinical response score
HS	hidradenitis suppurativa
HS-hi	HS samples with a high inflammatory load
HS-lo	HS samples with a low inflammatory load
HS-TCM	HS sinus tract skin derived T cell conditioned media
I	ionomycin
IFN	interferon
Ig	immunoglobulin
IL	interleukin
ILCs	innate lymphoid cells
IMDM	Iscove's Modified Dulbecco's Media
JAK	Janus kinase
KRT	keratin
kg	kilogram

l	litre
lo	low expression
log	logarithm
LSD	least significant difference
LPS	lipopolysaccharide
M	male
MACS	Magnetic-activated cell sorting
MAIT cells	Mucosal associated invariant T cells
MAPK	mitogen-activated protein kinase
MERTK	MER proto-oncogene tyrosine kinase
MFI	mean fluorescence intensity
mg	milligram
MHC I/II	major histocompatibility complex class I / class II
m	meter
mins	minutes
ml	millilitre
mm	millimeter
MMP	matrix metalloproteinase
MPO	myeloperoxidase
mRNA	messenger ribonucleic acid
MSD	Meso Scale Discovery
n	number
n/a	Data not available
N-S	non-smoker
NETs	neutrophil extracellular traps
NF-κB	nuclear factor kappa-light-chain-enhancer of activated B cells
ng	nanogram
NK cells	natural killer cells
NLR	Neutrophil to lymphocyte ratio
NLR	Nod-like receptor
NLRP	Nucleotide-binding oligomerization domain, Leucine rich Repeat and Pyrin domain containing
nm	nanometer
Nrm	no relevant medications
nUMI	number of unique molecular identifiers
ORS	outer root sheath
p	probability
PAMP	pathogen associated molecular pathogen
PASI	Psoriasis Area and Severity Index
PBMC	peripheral blood mononuclear cells
PBS	phosphate buffered saline

PBS-T	phosphate buffered saline tween
PCA	principal component analysis
PCR	polymerase chain reaction
pDC	plasmacytoid dendritic cells
pg	picogram
pH	potential of hydrogen
PDPN	podoplanin
PMA	phorbol-12-myristate-13-acetate
PRR	pattern recognition receptors
PSG	L-Glutamine/Penicillin/Streptomycin
PsO	psoriasis
QC	quality control
RA	rheumatoid arthritis
RNA	ribonucleic acid
RNases	ribonucleases
RNA-seq	RNA sequencing
ROS	Reactive oxygen species
RPMI	Roswell Park Memorial Institute media
RT	Reverse transcription
RT	room temperature
RT-PCR	real time polymerase chain reaction
S	smoker
scRNA-seq	single cell RNA sequencing
SD	standard deviation
SELE	E-selectin
SEM	standard error of the mean
SSC	side scatter channel
STATs	signal transducers and activators of transcription
TCA	Citrate acid cycle
TCD	Trinity College Dublin
TCR	T cell receptor
Tfh	T follicular helper cell
TGF-β	transforming growth factor beta
Th	T helper
TLRs	toll-like receptors
3,3',5,5'-TMB	3,3',5,5'-Tetramethylbenzidine
TNF	tumour necrosis factor
Treg cells	regulatory T cells
TRM cells	resident memory T cells
WGCNA	weighted gene co-expression network analysis
UC-SFM	Ultra-CULTURE serum free medium

UCD	University College Dublin
UMAP	uniform manifold approximation and projection
UMI	Unique molecular identifier
XCR	X-C motif chemokine receptor
vs	versus
y	years

Chapter 1

Introduction

1 Introduction

1.1 Skin Immunity

The skin is the largest organ in the human body and acts a physical barrier to provide protection from injury, microbes and environmental pathogens, while also providing structural integrity, regulating body temperature and acting as the first line of immunological protection. The skin comprises of 3 layers: the epidermis, the dermis and subcutaneous fat. The outermost layer, the epidermis, is subdivided into the outermost stratum corneum, the stratum granulosum, the stratum spinosum and the stratum basale (**Figure 1.1**) (Pasparakis, Haase and Nestle, 2014).

The stratum corneum comprises of terminally differentiated keratinocytes, which provide a physical barrier to the internal environment. Rows of flat, anucleated, cornified keratinocytes make this layer impermeable to external toxins, while sweat ducts and hair follicles provide channels for the movement of small molecules and water (Murphrey, 2023). Filaggrin plays an important role in the formation of cornified keratinocytes, aggregating keratin filaments made by keratinocytes into tight bundles, inducing the collapse of the keratinocyte into a flattened structure, providing rigidity and strengthening the structure of the stratum corneum (Madison, 2003).

The stratum corneum prevents the entry of foreign pathogens into the body while also limiting the loss of water from the skin (Kubo *et al.*, 2013). Pathogens that enter the skin are greeted with an acidic environment with a pH of 5.4-5.9, which is inhospitable for budding pathogens (Schmid-Wendtner and Korting, 2006). The pH of blood in comparison is ~7.4, with this dramatic pH change serving as a secondary defensive mechanism preventing microbes that have breached the skin from entering the circulation (Nguyen and Soulika, 2019). Filaggrin aids in the maintenance of this low pH. Filaggrin is broken down into histidine and further processed by histidase expressed by corneocytes into trans-urocanic acid, lowering the pH of the skin microenvironment (Nguyen and Soulika, 2019).

The basal layer of the epidermis is responsible for the continuous generation of new keratinocytes which will ultimately replace the cornified keratinocytes following a full differentiation program. This basal layer is predominantly comprised of basal keratinocytes which express many structural proteins vital for the structural integrity of the skin

(Madison, 2003). Basal keratinocytes can be identified based on the expression of a KRT5 and KRT14 heterodimer which makes up the basal keratinocyte cytoskeleton.

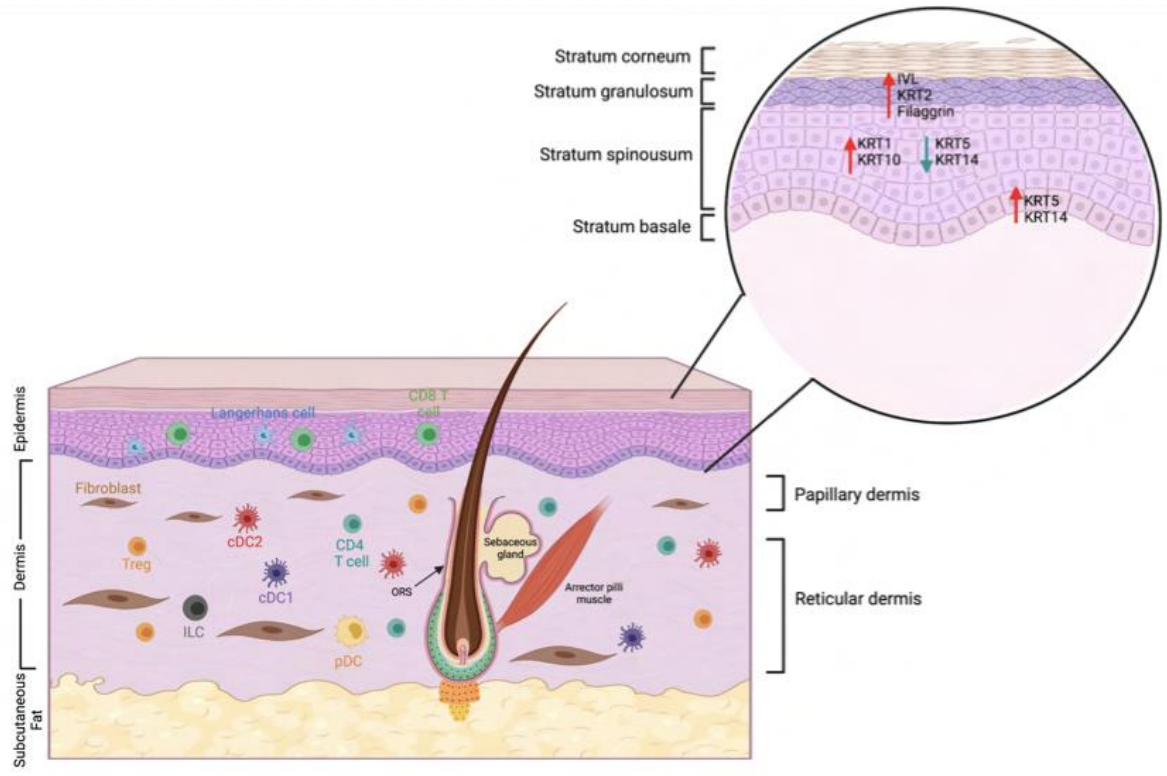

Figure 1.1 Structure and cell populations in healthy human skin. Human skin is comprised of 2 major layers, a thick dermis which lies below a thinner epidermis. Immuno-privileged hair follicles extend from the lower layer of the dermis, with the hair shaft protruding through the epidermis. Immune cells such as Langerhans cells, mast cells and tissue resident CD8 T cells reside in the epidermis alongside keratinocytes. The dermis mainly comprises of fibroblasts with tissue resident CD8 T cells, ILCs, DCs, pericytes and endothelial cells residing in the dermal compartments of the skin. The epidermis is separated into 4 major layers, the stratum basale, where stem cell-like keratinocytes reside, the stratum spinous and stratum granulosum where keratinocytes undergo differentiation and a superficial stratum corneum comprising of terminally differentiated corneocytes.

The stratum spinosum lies above the basal layer. Here, keratinocytes form intercellular attachments through desmosomes, which act as protein channels. As keratinocytes begin to migrate towards the granular layer of the skin, filaggrin expression increases, facilitating the aggregation of keratin filaments (Baroni *et al.*, 2012). Keratinocytes begin to lose their organelles and gradually become more compact until they have a flat structure when terminally differentiated. Once keratinocytes collapse into the flattened structure, keratinisation is completed and these cornified keratinocytes can bind to one another via desmosomes, forming a brick-like pattern surrounded by a lipid envelope which is responsible for moisture regulation in the skin (Madison, 2003). KRT1 and KRT10 are the

earliest known markers of keratinocyte differentiation in normal epidermis. As keratinocytes differentiate from a granular to a cornified keratinocyte, there is an increase in involucrin, filaggrin and loricrin expression (Zhang, Yin and Zhang, 2019). These structural proteins reinforce the cornified envelope which begins to form under the plasma membrane. In hyperproliferative skin conditions such as psoriasis, the differentiation markers KRT1 and KRT10 can be replaced by KRT6 and KRT16 which play a direct role in regulating cell proliferation (Mommers *et al.*, 2000).

Keratinocytes are not only crucial for the maintenance of the physical barrier of the skin, but they also play a role in the immune response. Keratinocytes secrete antimicrobial peptides (AMPs), cytokines and chemokines, playing an active role in immunity. They also produce biologically active IL-1α and IL-1β which allows a rapid response to epidermal injury (Kupper and Groves, 1995). Once keratinocytes sense danger signals, the production of proinflammatory mediators including TNF, IL-6 and IL-1β is increased (Albanesi *et al.*, 2005). Furthermore, keratinocytes express toll-like receptors (TLRs) which, when activated, induce the production of TNF, IL-8 and AMPs (Uchi *et al.*, 2000). The expression of key chemokines CCL17, CCL27, CXCL1 and CXCL8 by keratinocytes facilitates the migration of T cells, dendritic cells (DCs) and neutrophils to the site of inflammation (Giustizieri *et al.*, 2001; Li *et al.*, 2014). CCL20, also expressed by keratinocytes, is essential for the recruitment of T cells and DCs to the epidermis (Albanesi *et al.*, 2005). Similar to keratinocytes in the epidermis, fibroblasts are the structural cells of the dermis. The primary function of fibroblasts is to produce extracellular matrix components such as collagen. Like keratinocytes, fibroblasts also express a number of TLRs, however at a significantly higher level than keratinocytes, suggesting that fibroblasts may play a central role in the detection of foreign pathogens (Yao *et al.*, 2015).

Beneath the overlaying epidermis lies the dermis which is separated into papillary and reticular layers (**Figure 1.1**). The papillary dermis contains capillaries which transport nutrients to the epidermis (Shirshin *et al.*, 2017). The reticular dermis contains skin appendages such as hair follicles, sweat glands and sebaceous glands. The reticular dermis contains dense collagenous and reticular fibres making it significantly thicker than the papillary dermis (Woodley, 2017). Fibroblasts contribute to the structural integrity of the dermis by producing collagens, proteoglycans and elastic fibres (Tracy, Minasian and

Caterson, 2016). Fibroblasts and immune cells such as macrophages, DCs, T cells, B cells and mast cells reside in both layers of the dermis (Nguyen and Soulika, 2019). Fibroblasts also play an active role in the immune response, expressing a number of functionally active TLRs to detect invading pathogens (Jang *et al.*, 2012). In response to the detection of foreign pathogens, fibroblasts produce AMPs, defensins, growth factors and proinflammatory cytokines (IFN-γ, IL-6 , IL-8, TNF) and chemokines (CCL1, CCL2, CCL5, CXCL1, CXCL10 and CX_3CL1) (Bautista-Hernández *et al.*, 2017). This facilitates the coordination of an effective immune response in parallel with conventional immune cells once pathogens invade the skin.

Langerhans cells, predominantly residing in the epidermis, are professional antigen presenting cells (APCs) which form a dense network of dendrites through intercellular tight junctions to sense antigens that have not yet penetrated the epidermal barrier (Banchereau and Steinman, 1998; Ouchi *et al.*, 2011). Langerhans cells promote the expansion and activation of skin resident regulatory T cells (Treg cells) and are critical for CD8 T cell mediated immunity (Seneschal *et al.*, 2012; van der Aar *et al.*, 2011). While Langerhans cells possess similar features to DCs, developmental studies have that shown Langerhans cells are monocyte-derived tissue-resident macrophages which develop a DC-like phenotype in the skin (Ginhoux *et al.*, 2006). Langerhans cells differ from dermal macrophages as they are capable of migrating to draining lymph node to promote a further T cell response (Pasparakis, Haase and Nestle, 2014).

While Langerhans cells populate the epidermis, dermal macrophages and dermal DCs are the primary APCs found in the dermis. Dermal macrophages play a critical role in all phases of wound healing and tissue remodelling while also constantly monitoring the skin microenvironment for signs of cellular stress, injury or infection (Yanez *et al.*, 2017). Upon detection of antigen, dermal macrophages rapidly produce cytokines and chemokines which can recruit cells to the site of insult to induce an effective inflammatory response (Murphy and Weaver, 2017). Blood monocytes can also be recruited to the skin and differentiate into macrophages to help eradicate the pathogen (Murphy and Weaver, 2017). Macrophages can be distinguished from dermal DCs based on the expression of CD64 and MERTK (Singh *et al.*, 2016).

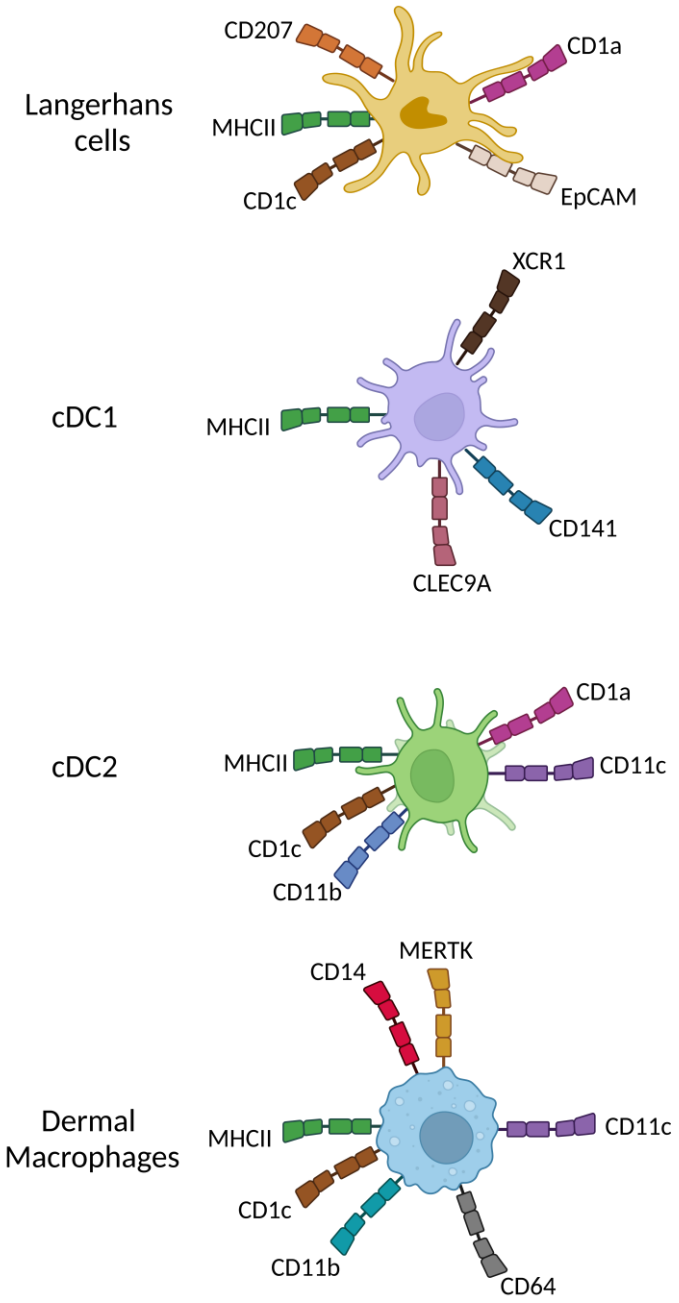

Figure 1.2 Distinguishing markers of APC subsets in human skin. 4 major APC subsets reside in human skin, including Langerhans cells, cDC1 cells, cDC2 cells and dermal macrophages. While it is often difficult to distinguish between subsets, surface expression of distinctive markers in combination can delineate APC subsets. Illustration was generated using BioRender software.

Conventional DCs (cDCs) are commonly found in both lymphoid and non-lymphoid tissues, including the dermis of the skin (Nestle *et al.*, 1993). Dermal DCs expressing MHC II and low levels of CD11c can be subdivided into $CD141^{+}$ cDC1 and $CD1c^{+}$ cDC2 DC (**Figure 1.2**) (Haniffa, Gunawan and Jardine, 2015). cDC1 are a relatively rare population in skin, characterised by the expression of XCR1, CLEC9A, TLR3 and CD141 (Dutertre *et al.*, 2019; Jongbloed *et al.*, 2010). cDC1s have a key role in cross presentation of keratinocyte antigens

(Bedoui *et al.*, 2009; Henri *et al.*, 2010) and can also rapidly migrate to the deep T cell zone of the lymph node (Liu *et al.*, 2021). Despite their low abundance in human skin, cDC1s can constitute 20-40% of lymph node-resident DCs (Henri *et al.*, 2010; Shortman and Heath, 2010; Vremec and Shortman, 1997). cDC2s on the other hand, are the most abundant DC population in the human dermis (Malissen, Tamoutounour and Henri, 2014). cDC2 cells are characterised by their expression of CD11b and CD1c and distinguished from Langerhans cells by increased CD11c expression and lower CD207 expression (**Figure 1.2**) (Kashem, Haniffa and Kaplan, 2017). In contrast to cDC1s, cDC2s secrete IL-23, IL-1β, TNF and IL-8 and are potent activators of Th17 and CD8 T cells (Leal Rojas *et al.*, 2017).

T cells are crucial for efficient adaptive immune response in skin with twice as many T cells found to infiltrate healthy skin as there are in peripheral blood (Clark *et al.*, 2006a). T cells develop from common lymphoid progenitor cells in the thymus and ultimately emerge in the periphery as naïve T cells (Murphy and Weaver, 2017). Naïve T cells recirculate between the blood and secondary lymphoid organs through the lymphatic system, eventually interacting with DCs presenting their cognate antigen (Murphy and Weaver, 2017). Following antigen recognition, naïve T cells undergo clonal expansion and differentiate into different effector T cells (Murphy and Weaver, 2017).

Following activation, CD4 T cells differentiate into T helper (Th) cell subsets, depending on differing cytokines in the local microenvironment (**Figure 1.3**). The different Th cell subsets are defined by the cytokines they secrete and the presence of particular transcription factors driving the expression of characteristic cell markers. Th1 cells are induced by IL-12 and IFN-γ cytokines and can be identified by their expression of T-bet (**Figure 1.3**) (Raphael *et al.*, 2015). Th1 cells signal through the signal transducers STAT1 and STAT4 and predominantly secrete IFN-γ (**Figure 1.3**) (Murphy and Weaver, 2017). IFN-γ directly activates macrophages, increases antigen presentation and phagocytosis and upregulates TLR expression (Hu, Chakravarty and Ivashkiv, 2008). The primary function of Th1 cells is to recognise and eradicate microbial infections presented by macrophages. Once antigen is recognised, IFN-γ increases microbicidal activity by recruitment of macrophages and B cells and also further promoting Th1 activation in an autocrine loop (Nathan *et al.*, 1983).

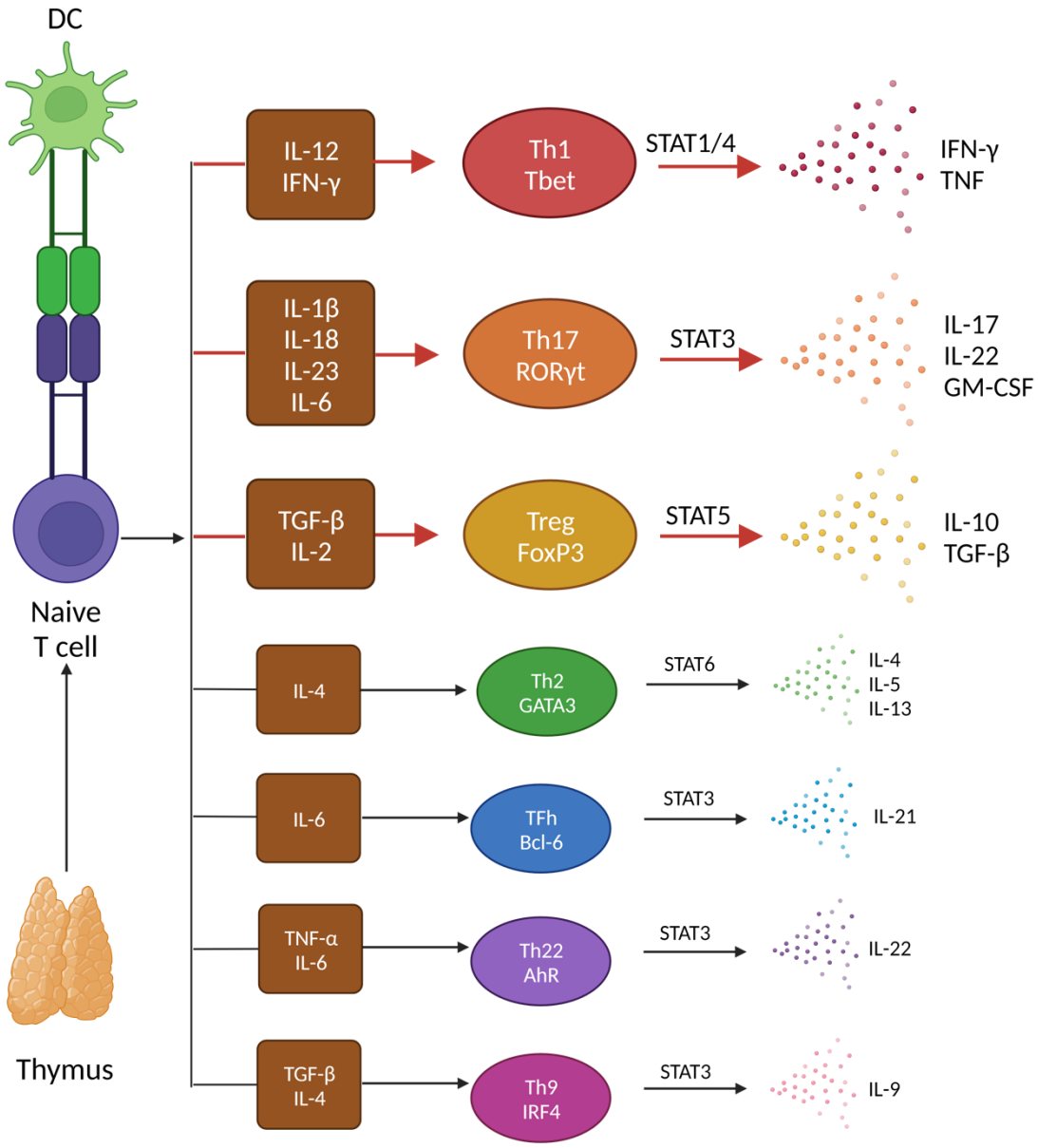

Figure 1.3 Differentiation of CD4 T cell subsets. Following recognition of pathogens via pattern recognition receptors, DCs phagocytose pathogen and present antigen via MHC II. Naïve T cells recognise antigen presented by MHCII and form a complex with MHC II and TCR. A second co-stimulatory signal involving CD28 on T cells and CD80/86 on APCs provides co-stimulation to the naïve T cell. Upon activation CD4 T cells undergo clonal expansion and differentiate into an effector subset depending on the polarising cytokines present. The function of each Th cell subset is regulated by transcription factors and specific STATs which mediate the expression of signature cytokines. Th cell subsets previously implicated in hidradenitis suppurativa are represented with red arrows. Illustration was generated using BioRender software.

Treg cells are important for constraining the immune response, suppressing inflammation and halting inappropriate immune responses. Defined by their expression of CD25 and the transcription factor FoxP3, Treg cells can develop directly in the thymus during T cell development (Murphy and Weaver, 2017) or CD4 T cells stimulated with TGF-β and IL-2 can differentiate into Treg cells (**Figure 1.3**) (Miyara and Sakaguchi, 2007). Treg cells in turn

secrete the suppressive cytokines IL-10 and TGF-β (Murphy and Weaver, 2017). Treg cells have an intrinsic link to Th17 cells, both requiring TGF-β for their differentiation. In the absence of IL-6, TGF-β induces the differentiation into Treg cells, while the combination of IL-6 and TGF-β promotes Th17 development (**Figure 1.3**) (Bettelli *et al.*, 2006; Mangan *et al.*, 2006). Other cytokines, including IL-23 and IL-1β have also been implicated in Th17 differentiation (Revu *et al.*, 2018; Acosta-Rodriguez *et al.*, 2007). Th17 cells secrete their signature cytokines IL-17A and IL-17F, while also secreting IL-22 and GM-CSF (**Figure 1.3**). Th17 cells can also be identified by CD161 and CCR6 expression in humans (Cosmi *et al.*, 2008). Th17 cells have been implicated in numerous inflammatory diseases, including psoriasis, rheumatoid arthritis (RA) and multiple sclerosis. Once triggered, Th17 cells induce the expression of chemokines by epithelial cells resulting in the recruitment of neutrophils to the site of inflammation. Th17 cells also appear to be highly plastic and can switch from expressing IL-17A to IFN-γ. *Ex vivo*, this occurs in the presence of IL-12 rather than IL-23, generating ex-Th17 cells (extinguished Th17 cells) (Annunziato *et al.*, 2007; Lexberg *et al.*, 2010). Similar to Th17 cells, ex-Th17 cells express CD161 and CCR6, while also expressing the Th1 cell-associated chemokine CXCR3 (Maeda *et al.*, 2019). These cells are more polyfunctional than Th17 cells and are resistant to Treg cell suppression (Basdeo *et al.*, 2017).

While Th17, Th1 and Treg cells have previously been implicated in HS, other Th cell subsets include Th2, follicular helper T cells (Tfh), Th22 and Th9 cells. Th2 cells, known for their role in driving atopic dermatitis (AD) inflammation, secrete the inflammatory cytokines IL-4, IL-5 and IL-13 (Raphael *et al.*, 2015). Th2 differentiation requires IL-4, and Th2 cells can be distinguished by expression of the transcription factor GATA3 (**Figure 1.3**) (Murphy and Weaver, 2017). Tfh cells are regulated by the transcription factor Bcl-6 which regulates the expression of IL-21 (**Figure 1.3**) (Murphy and Weaver, 2017). Tfh cells remain in the lymphoid tissue and have been found to support B cell development of class-switched antibodies in the germinal centre (Murphy and Weaver, 2017). The transcription factor AhR promotes the differentiation of naïve CD4 T cells into Th22 cells (**Figure 1.3**) (Trifari *et al.*, 2009). Th22 cells secrete IL-22 (Eyerich *et al.*, 2009) and under the appropriate conditions can differentiate into Th1 or Th2 cells (Plank *et al.*, 2017). TGF-β and IL-4 induce the differentiation of Th9 cells which characteristically secrete IL-9 (**Figure 1.3**) (Zhang *et al.*, 2019). Th9 cells have been shown to promote Treg cell survival and enhance Treg cell-

mediated suppression. Despite this anti-inflammatory function, Th9 cells appear to play a role in asthma and systemic lupus erythematosus.

Following activation, T cells are known to migrate into tissues and elicit their effector functions. Subsequently, the majority of effector T cells die by apoptosis, while a small cohort survive as memory T cells. Resident memory T (TRM) cells, identified at peripheral barrier sites including lungs, nose, gastrointestinal tract and skin, are a memory T cell subset which do not migrate out of the tissue and provide local immunosurveillance (Clark, 2015). Skin TRM cells can be identified by the expression of CD69 and/or CD103 and have been found to typically reside around hair follicles (Collins *et al.*, 2016). TRM cells are primed to rapidly respond to secondary infection or insult, demonstrated by never-lesional psoriasis skin having a skewed TRM profile, poised to drive inflammation following local activation (Gallais Serezal *et al.*, 2019).

1.2 HS

1.2.1 Symptoms

Hidradenitis suppurativa (HS), commonly referred to as acne inversa, is a chronic inflammatory follicular skin disease clinically defined by recurrent inflammatory nodules in areas of apocrine-bearing skin such as the axillary, inguinal and perianal areas (**Figure 1.4**). Painful, erythematous HS nodules often form in combination with severe acne (Jemec, 2012). HS is characterised by pus formation, irreversible tissue damage and subsequent scarring, discriminating this debilitating skin disease from other chronic inflammatory skin conditions (Jemec, 2012).

The rupture of HS lesions leads to the release of foul-smelling, bloody, suppurative discharge, with these areas healing with atrophic scarring. Typically, HS patients experience 4.6 abscesses per month with 62% of patients describing persistent painful inflammatory lesions (Hoffman, Ghias and Lowes, 2017). Inflammatory nodules may burst internally forming suppurative dermal tunnels (also called sinus tracts or dermal fistulae). Dermal tunnels, constant suppuration and hypertrophic scarring can also form following persistent HS inflammation, which leads to the formation of dermal contractures and a hardening of the affected skin (Martorell *et al.*, 2015). Fibrotic scarring in sensitive areas, such as the groin and axillae, can result in restricted and painful movement. Combined with the bloody,

odorous discharge released from ruptured lesions, HS patients experience a significantly lower quality of life compared with other inflammatory skin conditions, such as psoriasis (Schneider-Burrus *et al.*, 2021). HS patients often suffer from systemic complications, including cardiovascular and metabolic comorbidities associated with obesity, inflammatory bowel disease and depression (Miller, McAndrew and Hamzavi, 2016).

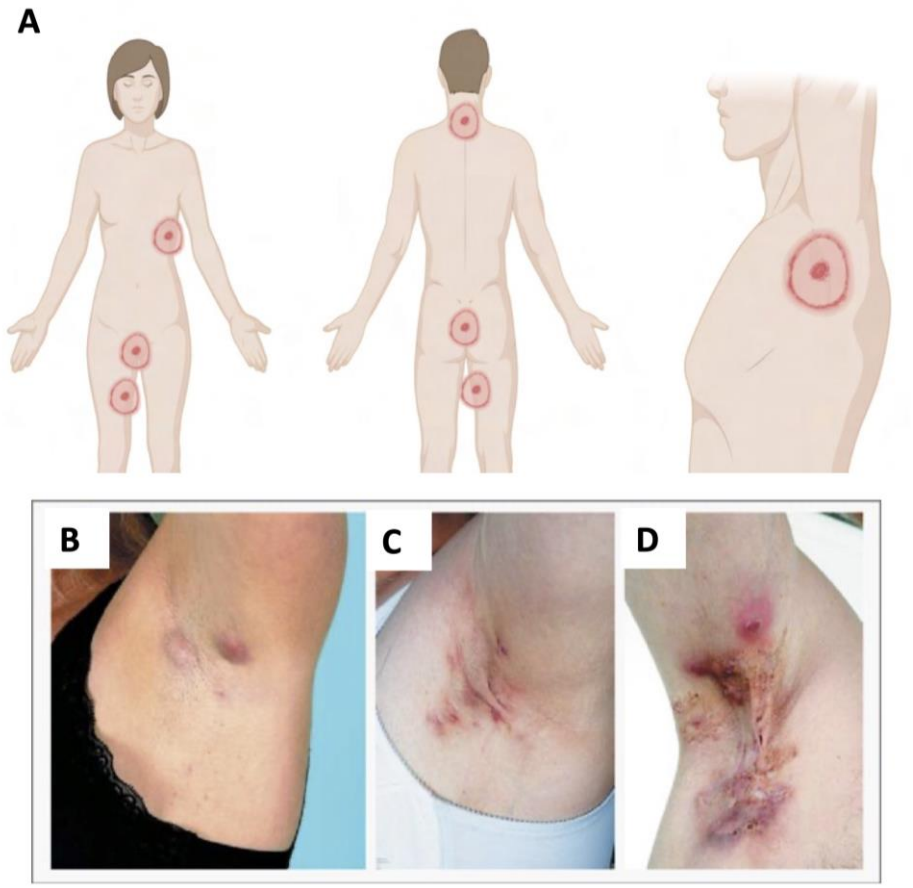

Figure 1.4 Schematic and real-life images of HS inflammatory sites. HS is a chronic inflammatory skin disease which affects apocrine-bearing skin. HS lesions commonly affect the groin, perianal, axilla and inframammary skin folds (A). Panel B displays Hurley stage 1 disease, with multiple inflammatory nodules formed, absence of sinus tracts or scarring. Hurley stage 2 of HS involves recurrent abscesses and sinus tract formation with potential scarring on widely spread lesions (C). Hurley stage 3 disease is characterised by multiple interconnected sinus tracts and inflammatory lesions across a larger area (D). Real life images were taken from Jemec, 2012 (Jemec, 2012). Illustration was generated using BioRender software.

1.2.2 Prevalence

HS commonly arises post-puberty and frequently persists until middle and old age. Although considered uncommon, HS is not defined as a rare disease with ~1% of the population suffering from this chronic inflammatory skin disease, however other studies

dispute this (Revuz *et al.*, 2008; Vazquez *et al.*, 2013). Due to long delays in disease diagnosis and the frequency of misdiagnosis, estimations of disease prevalence are inconsistent. General practitioners are often the first point of contact with undiagnosed HS patients; however, they may have no experience with this disease. Due to the location of HS lesions in sensitive areas, such as the perianal and groin areas, patients are often reluctant to present for examination, delaying diagnosis (Kokolakis *et al.*, 2020). The average time for diagnosis for HS patients is 7 years, which is in stark contrast to other inflammatory skin diseases such as psoriasis, which is typically diagnosed after 1.6 years (Saunte *et al.*, 2015).

1.2.3 Impact

HS patients suffer from a range of social and psychological consequences of the disease. An Australian study previously showed HS patients were more likely to have lower income or be unemployed compared with non-HS individuals (Calao *et al.*, 2018). This may be a consequence of additional sick days that HS patients take from work compared with the general public. Studies assessing privately insured patients with HS in the US demonstrated that HS patients lose ~12 days of work per year more than the general public (Tzellos *et al.*, 2019).

HS patients have heightened negative emotions due to the location and appearance of lesions, combined with their malodorous discharge. Delayed diagnosis and fear that prospective treatments will not be successful meaning patients may suffer for decades with severe symptoms, contributes to the anger and depression associated with HS (Esmann and Jemec, 2016). Social anxiety is a major problem associated with HS, with patients avoiding social interactions over fear of being perceived negatively by others (Keary, Hevey and Tobin, 2020). The depression and isolation associated with HS correlates with disease activity and tends to be much more severe than in other dermatological conditions (Onderdijk *et al.*, 2013).

1.2.4 Classification

Clinicians use a number of classification systems to characterise HS disease severity, although a universal gold standard has yet to be decided. The simplest and most widely

used classification system is the Hurley Classification System (Horváth *et al.*, 2017). This system is a static scale and is therefore limited. The HS Severity Index (Grant *et al.*, 2010), the modified Sartorius System (Sartorius *et al.*, 2009) and the HS Physician's Global Assessment classification system (Kimball *et al.*, 2012) have been developed to improve upon the Hurley classification system. More recently, the International Hidradenitis Suppurativa Severity Score System (IHS4) has been developed (Zouboulis *et al.*, 2017). This simple, dynamic, consensus-driven method has proven popular amongst dermatologists in characterising HS clinical severity.

To assess the treatment efficacy in HS patients the Hidradenitis Suppurativa Clinical Response (HiSCR) system is used (Kimball *et al.*, 2014). This scoring system considers clinical characteristics such as inflammatory lesions, abscesses and draining fistulae. A positive HiSCR result is defined as at least a 50% reduction in inflammatory lesions with no increase in abscesses or draining fistulae compared with baseline.

1.2.5 Risk factors

HS has been shown to be more prevalent in females than males, with a 3:1 female: male ratio reported (Garg *et al.*, 2017). HS often initiates at menarche and flares can coincide with menstrual cycle indicating a potential role for hormones in the pathogenesis of HS, however results remain inconclusive (Hoffman, Ghias and Lowes, 2017).

Smoking is widely regarded as a significant risk factor for developing HS, with up to 90% of patients having smoked tobacco (Sartorius *et al.*, 2009). Smokers are twice as likely to develop HS as non-smokers (Garg *et al.*, 2018). While smoking may not drive HS disease severity, it does seem to act as a triggering factor, with smoking increasing neutrophil chemotaxis, downregulating production of AMPs and inducing TNF production by keratinocytes (Canoui-Poitrine *et al.*, 2009; Hana *et al.*, 2007).

Obesity is commonly reported in HS patients, with an average body mass index (BMI) of 31 reported in HS patients (Kelly *et al.*, 2015; Reddy, Strunk and Garg, 2019). Obesity is thought to contribute to disease initiation, with large skin folds driving enhanced friction which leads to follicular occlusion (de Winter, van der Zee and Prens, 2012). During obesity, skin becomes thickened in a process known as acanthosis, which may also play a role in follicular

occlusion and enhance subsequent inflammation (Stone, 1976). Adipose tissue has its own immune system, which includes macrophages, B cells, T cells and innate lymphoid cells (ILCs) (Lynch *et al.*, 2012); these cells may contribute to HS. Moreover, signaling molecules found in the adipose tissue, known as adipokines, are dysregulated in HS, with anti-inflammatory adiponectin reduced and proinflammatory resistin and leptin elevated in HS (Malara *et al.*, 2018).

The assessment of genetic risk factors in HS is difficult due to large-scale under-reporting and the varying clinical phenotypes and severities of HS. Despite these challenges, mutations to genes involved in the γ-secretase complex have been identified, particularly in *NCSTN* (Pink *et al.*, 2013). Over 30 different mutations have been described in *NCSTN* in HS patients, 14 mutations in *PSENEN* and 4 mutation in *PSEN1*, most of which attenuate NOTCH signaling (Wang, Yan and Wang, 2021). The γ-secretase complex stimulates the intramembrane proteolysis of NOTCH receptors, with dysregulated NOTCH signaling implicated in HS skin (Nomura, 2020). *NOTCH1*$^{-}$/*NOTCH2*$^{-}$ and *PSEN1*$^{-}$/*PSEN2*$^{-}$ knockout mice develop epidermal cysts and hyperkeratosis with follicular occlusion, mirroring the histological features seen in HS lesions (Pan *et al.*, 2004; Li *et al.*, 2007). However, these mutations are seen in only a small cohort of HS patients.

Ultimately, the role of certain risk factors in HS development and progression remains unclear. It is likely that a complex interaction of genes contributes to the predisposition to HS or disease severity, however environmental factors and a dysregulated immune response appear to drive HS pathogenesis.

1.2.6 Pathogenesis

HS pathogenesis is not completely understood, however immune dysregulation plays an important role in disease aetiology. An initiating event in HS appears to be hair follicle occlusion induced by hyperkeratosis and follicular epithelium hyperplasia, which ultimately leads to cyst development (Yazdanyar and Jemec, 2011; Yu and Cook, 1990). The subsequent cyst rupture induces a potent immune response following the release of damage-associated molecular patterns (DAMPs). The influx of immune cells in HS lesions induces chronic inflammation (Lima *et al.*, 2016) and ultimately leads to abscess formation, sinus tract development and scarring (Sabat *et al.*, 2020).

Initial follicular occlusion in HS patients may be driven by genetic predisposition to infundibulum keratinisation or by exogenous factors such as microbiota, smoking, obesity or mechanical stress (Wang *et al.*, 2010; von Laffert *et al.*, 2010). Keratinocytes derived from the follicular outer root sheath (ORS) in HS patients have a proinflammatory phenotype with dysregulated production of CXCL10 and CCL5 (Hotz *et al.*, 2016). Upon pattern recognition receptor (PRR) stimulation, these keratinocytes have increased production of IL-1β which drives TNF, IL-6 and IL-8 expression. A dysregulated cell cycle in ORS stem cells, from which these keratinocytes originate, may contribute to this inflammatory phenotype. ORS stem cells from HS patients have a 2-3 fold increase in replication fork speed compared with healthy control ORS stem cells which may induce DNA replicative stress and genomic instability (Orvain *et al.*, 2020; Maya-Mendoza *et al.*, 2018). The subsequent accumulation of endogenous cytoplasmic single stranded DNA as a result of increased replication induces type I IFN production in HS lesional skin (Orvain *et al.*, 2020).

Rupture of the hair follicle likely disperses its contents throughout the dermis, including keratin fibres, dermal detritus and a variety of pathogen-associated molecular patterns (PAMPs) and DAMPs (van der Zee *et al.*, 2012b). This likely initiates downstream inflammatory pathways such as IL-17A/IL-23 signaling, the NLRP3 inflammasome and TLR activation, invoking immune cell infiltration and subsequent sinus tract and abscess formation (Fletcher *et al.*, 2020). Fibrotic factors and activated epithelial cells simultaneously drive an immune response which results in fibrotic scarring and dermal tunnel formation (Navrazhina *et al.*, 2021a).

HS research is complicated by the heterogenous nature of the disease. One clinical feature which epitomises this heterogeneity is the formation of dermal tunnels. Dermal tunnels are unique to HS and have not been identified in any other inflammatory skin disease, however not every HS patient develops dermal tunnels (Frew *et al.*, 2019). Tunnels are often associated with a more aggressive disease and traditionally develop in Hurley Stage III patients at the fibrotic, end stage of disease (Goldburg, Strober and Payette, 2019; Vanlaerhoven *et al.*, 2018; Vossen, van der Zee and Prens, 2018).

Recently, HS dermal tunnels have been identified as active players in HS inflammation (Navrazhina *et al.*, 2021a). During disease development, the epidermis of HS lesions

becomes thickened and is characterised by epidermal psoriasiform hyperplasia (Navrazhina, Frew and Krueger, 2020). HS tunnels primarily comprise of keratinocytes which adopt similar psoriasiform features to the overlying epidermis (Navrazhina *et al.*, 2021a). Biofilms thrive in these dermal tunnels and are responsible for the suppurative, malodorous discharge that is characteristic of HS (Ring *et al.*, 2017a). Dermal tunnels have increased lipocalin-2 expression, a marker of IL-17A-activated keratinocytes, and HS lesions containing tunnels have increased neutrophil, DC and T cell infiltration and a unique proinflammatory transcriptomic profile compared with HS lesions without dermal tunnels (Navrazhina *et al.*, 2021a).

1.2.7 Immune dysregulation in HS

It is widely accepted that a dysregulated immune response is important in HS pathogenesis (**Figure 1.5**). This idea is strengthened by the association of HS with other autoimmune conditions such as Crohn's disease (CD). Aberrant proinflammatory cytokine production in HS lesions has been confirmed in numerous studies and immune-modifying therapies have been an effective treatment for moderate to severe HS (Kimball *et al.*, 2023a; Kimball *et al.*, 2016). In particular, increased TNF, IL-1β and IL-17A levels are seen in HS lesions compared with healthy skin (Kelly *et al.*, 2015).

1.2.7.1 Innate immune cells

Increased infiltration of macrophages and DCs has been reported in HS lesions (Moran *et al.*, 2023) and studies utilising single cell RNA sequencing (scRNA-seq) and mass cytometry (CyTOF) have attempted to characterise myeloid cells in HS lesions, albeit in only a small cohort of HS patients (Lowe *et al.*, 2020). Major myeloid populations identified in HS lesions included cDC2 cells, $CD14^+$ macrophages, $CD163^+$ macrophages, cDC1 cells and Langerhans cells (Lowe *et al.*, 2020). Further scRNA-seq studies demonstrated that the macrophages in HS lesions may have an activated M1 phenotype with increased FcyR signaling which regulates phagocytosis, oxidative burst and cytokine secretion (Mariottoni *et al.*, 2021). The important role of innate immune cells in HS is epitomised by the central role of TNF in HS pathogenesis. Increased expression of TNF in HS lesions has been described in multiple studies (Kelly *et al.*, 2015; van der Zee *et al.*, 2012a). TNF was first identified as a potential therapeutic target in HS when improvements in HS disease were observed following

infliximab treatment in CD patients with concomitant HS (Martínez *et al.*, 2001). Further, myeloid cells have been found to be the predominant source of TNF and major producers of IL-1β in HS lesions (Lowe *et al.*, 2020), indicating a central role for dysregulated myeloid cells in HS immunopathogenesis. Coupled with the increased levels of IL-1β in HS lesions, increased expression of NLRP3 has also been detected in HS lesions (Witte-Handel *et al.*, 2019), implicating dysregulated NLRP3 inflammasome signaling in HS inflammation.

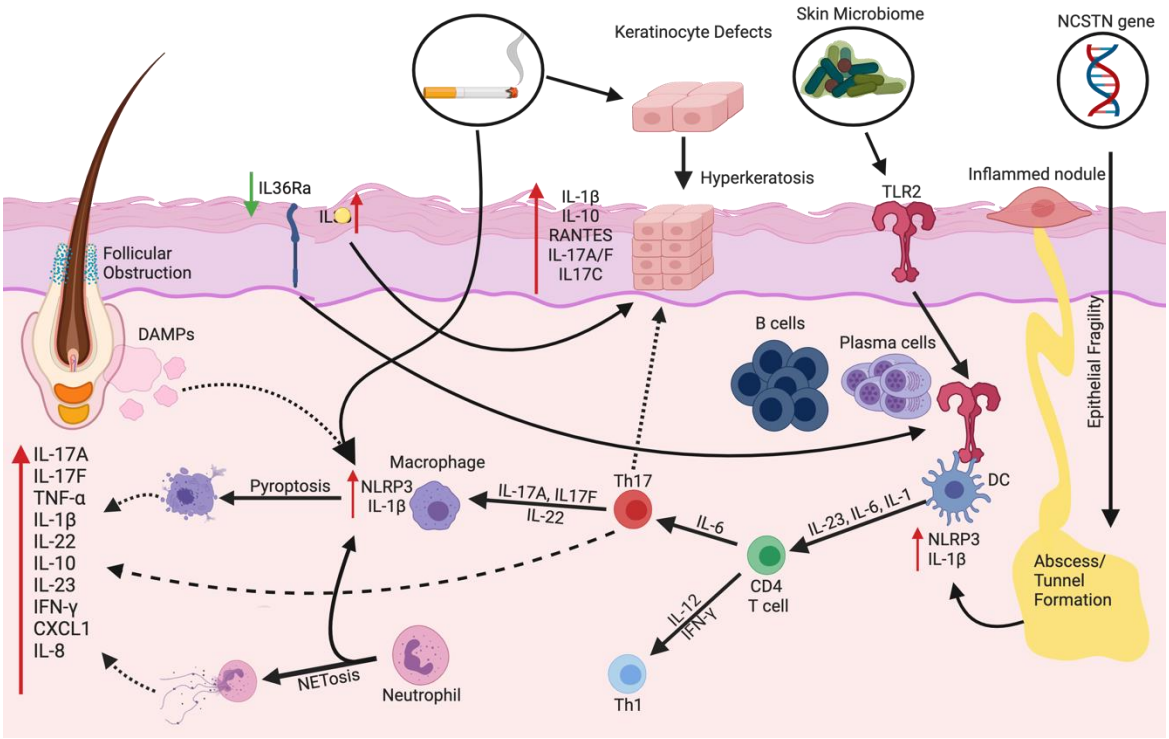

Figure 1.5 Schematic of HS pathogenesis. HS is likely triggered by endogenous factors, such as genetic predisposition or obesity, or exogenous factors such as smoking or bacterial infections. Follicular obstruction occurs early in disease, followed by cyst development and subsequent rupture which releases DAMPs into the dermis. IL-1β is a key feature of HS and could be driven by the activation of the NLRP3 inflammasome by DAMPs. Activated dendritic cells (DC) drive CD4 differentiation into T helper 1 (Th1) or Th17 subsets. Neutrophils recruited to the skin can undergo NETosis and release proinflammatory cytokines, activating the NLRP3 inflammasome. Th17 cells proliferate in response to DC-derived IL-23 and NLRP3-derived IL-1β, producing IL- 17A and IL-17F. IL-17 cytokines activate keratinocytes which release antimicrobial peptides and chemokines such as IL-8, that act on neutrophils. Keratinocytes also secrete IL-36γ and IL-17C that act in an autocrine manner to further potentiate keratinocyte activation and proliferation. Illustration was generated using BioRender software.

NLRP3 is a PRR, expressed by neutrophils, macrophages, lymphocytes, epithelial cells and DCs (Rada *et al.*, 2014; Zahid *et al.*, 2019), which sense PAMPs and DAMPs. PAMPs are conserved structural moieties commonly found in microorganisms such as LPS found on Gram-negative bacteria, viral nucleic acids, bacterial peptides such as flagellin and polysaccharides such as β-glucans (Chen and Nuñez, 2010). DAMPs on the other hand are

molecules released following cellular stress or damage and can include heat shock proteins and extracellular matrix fragments (Chen and Nuñez, 2010).

The NLRP3 inflammasome is a multiprotein complex consisting of a sensor protein (NLRP3), an adaptor protein (ASC) and an effector protein (caspase-1). The NLRP3 inflammasome facilitates the activation of caspase-1 and subsequent cleavage of pro-IL-1β and pro-IL-18 into their active conformations (**Figure 1.6**). NLRP3 inflammasome activation requires two signals, a priming signal through the TLR/NF-κB pathway which upregulates NLRP3 expression and a second signal of PAMPs or DAMPs which initiates the assembly and activation of the multi-protein complex of the NLRP3 inflammasome (Jo *et al.*, 2016). While the signals that may activate the inflammasome in HS lesions have yet to be defined, a variety of stimuli, including ATP, particulate aggregates, viral nucleic acids and bacterial pathogens can induce inflammasome activation (Latz, Xiao and Stutz, 2013; Jo *et al.*, 2016). The NLRP3 inflammasome has also been implicated in a number of inflammatory disorders, including Alzheimer's disease, atherosclerosis, osteoarthritis and Cryopyrin-associated periodic syndrome (CAPS). CAPS is an inflammatory disorder characterised by a gain-of-function mutation to NLRP3 (Hoffman *et al.*, 2001), making the NLRP3 inflammasome a prime target for these patients.

Since the discovery of the NLRP3 inflammasome, multiple inhibitors have been developed to directly inhibit this inflammatory pathway. MCC950 is a small molecule inhibitor which specifically inhibits the NLRP3 inflammasome by blocking the structural rearrangements which need to occur for inflammasome activation, blocking inflammasome activity. (Coll *et al.*, 2019). While the specific inhibition of the NLRP3 inflammasome makes MCC950 a suitable small molecule inhibitor for *in vivo* and *in vitro* experimental models, a number of alternative inhibitors are currently in development and phase 2 and 3 trials assessing the safety and efficacy of these inhibitors in CAPS, heart failure, melanoma and lung fibrosis are underway (Schwaid and Spencer, 2021).

While the NLRP3 inflammasome has been previously implicated in HS inflammation (Witte-Handel *et al.*, 2019) its cellular source has yet to be fully elucidated in HS lesions. scRNA-seq indicated cDC2 cells were the predominant source of *IL1B* expression in HS lesions (Lowe *et al.*, 2020), however immunohistochemistry demonstrated that keratinocytes rather than myeloid cells or neutrophils were the main source of NLRP3 and IL-1β in HS

lesions (Lima *et al.*, 2016). Further, IL-18, which is processed by the NLRP3 inflammasome in a similar fashion to IL-1β (**Figure 1.6**), was found to be predominantly expressed by keratinocytes (Gudjonsson *et al.*, 2020).

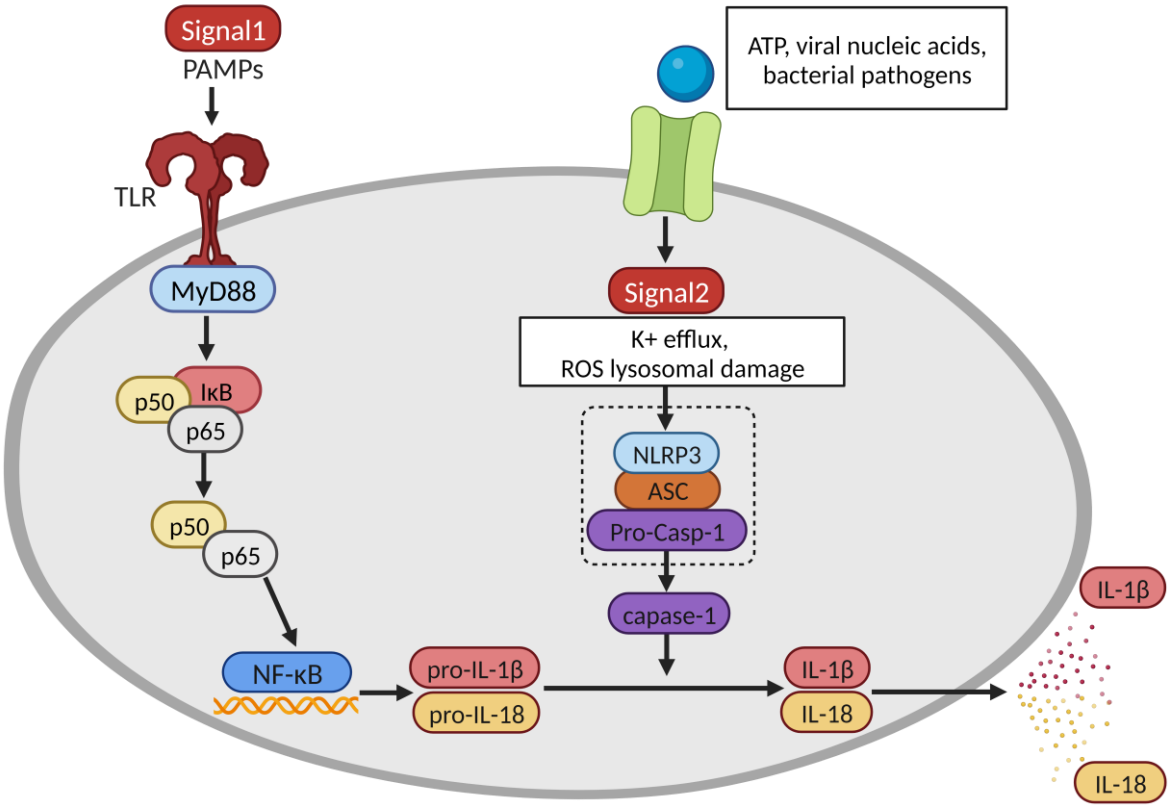

Figure 1.6 NLRP3 inflammasome activation. The NLRP3 inflammasome requires 2 signals for activation. The first, priming signal typically comes from TLRs which recognise PAMPs and activate NF-κB. This upregulated the expression of immature IL-1β and IL-18 and increases the expression of NLRP3. A second signal typically comes from ATP, nucleic acids or bacterial pathogens which induces, potassium efflux, ROS production or lysosomal damage which is recognised by NLRP3 and induces the assembly and activation of the NLRP3 inflammasome and subsequent maturation of caspase-1. Caspase-1 can then cleave immature IL-1β and IL-18 into their active conformations which can then be released into the extracellular environment. Illustration was generated using BioRender software.

1.2.7.2 T cells

An aberrant T cell landscape has been noted in HS lesions by numerous studies. From these studies, a number of T cell subsets have been postulated to play a role in HS inflammation, including Treg cells, Th17 and Th1 cells.

An influx of immune cells infiltrate HS lesions with a large proportion of these being CD4 T cells. Coinciding with the increased frequency of Th17 cells in HS lesions (Moran *et al.*, 2017), a 30-fold increase in IL-17A expression has been detected in HS lesions compared

with healthy control skin. Along with increased levels of IL-17A, elevated TNF and IFN-γ have been reported in HS lesions (Kelly *et al.*, 2015; Banerjee, McNish and Shanmugam, 2017). Further, HS lesional CD4 T cells were also found to produce elevated TNF, while both CD4 and CD8 T cells have elevated production of IFN-γ in HS lesions relative to healthy control skin (Moran *et al.*, 2017), indicating a potential role for cytotoxic CD8 T cells and Th1 cells in HS inflammation. Th1 cells and IFN-γ^+ CD8 T cells were found to be elevated in HS lesions indicating a dysregulated T cell landscape beyond this Th17-Treg cell axis (Lowe *et al.*, 2020). Surprisingly, Treg cells, known for their role in constraining T cell effector functions, were also found elevated in HS lesions (Moran *et al.*, 2017). Nonetheless, the Th17:Treg cell ratio was dramatically skewed in favour of Th17 cells in HS lesions, suggesting unconstrained Th17 cell activity promotes inflammation in HS lesions (Moran *et al.*, 2017).

While multiple studies have implicated IL-17A in HS pathogenesis, limited investigation into the role of IL-17F has been performed. IL-17A and IL-17F can form homo- or heterodimers, which then bind to different IL-17 receptors. IL-17A homodimer binds to the heterodimeric IL-17RA receptor (Gaffen, 2009), as does the IL-17A/F heterodimer. However, the IL-17F homodimer binds heterodimeric IL-17RA/RC or to the homodimeric IL-17RC receptor (Gaffen, 2009), indicating the possibility of IL-17RA-independent IL-17 signaling. IL-17A and IL-17F share 55% homology at the amino acid level (Akimzhanov, Yang and Dong, 2007), and a high proportion of CD4 T cells that make IL-17A have been found to also produce IL-17F. However, studies suggest IL-17A may be up to ten times more potent at inducing chemokine responses than IL-17F (Zrioual *et al.*, 2009). Recently, a study investigating IL-17F producing T cells in HS lesions has been performed using scRNA-seq (Kim *et al.*, 2023). HS lesional T cells expressing IL-17F, but not IL-17A were found to express lower levels of IL-17F than T cells expressing both IL-17A and IL-17F (Kim *et al.*, 2023). Further, these IL-17A$^+$ IL17F$^+$ T cells had higher expression of *IL1R1* and CD103 (*ITGAE*) relative to T cells only producing IL-17A. Interestingly, IL-17F$^+$ IL-17A$^-$ T cells in HS lesions expressed higher levels of *IL17F* and *IL1R1* compared to the same population found in psoriasis lesions, while psoriatic IL-17F$^+$ IL-17A$^-$ T cells notably had higher expression of *IL23R* (Kim *et al.*, 2023). This suggests IL-1β may drive the development of IL-17F$^+$ TRM cells in HS lesions, while psoriatic IL-17F$^+$ T cells are more dependent on IL-23 signaling and migrate to psoriatic lesions from the periphery (Kim *et al.*, 2023).

1.2.7.3 Neutrophils

HS peripheral blood has significantly higher levels of neutrophil counts relative to healthy controls. The ratio of neutrophils to lymphocytes (NLR) in peripheral blood has been shown to be elevated in HS patients relative to healthy controls, indicative of systemic inflammation in HS (Miller *et al.*, 2016). Further, the NLR was reduced in HS patients following 12 week treatment with adalimumab (Kearney, Hughes and Kirby, 2023) demonstrating the impact adalimumab has on systemic inflammation. Increased neutrophils were found in both HS blood and HS skin, with elevated frequencies of neutrophils found in the deep dermal infiltrate of HS lesions (Lima *et al.*, 2016), indicating a prominent role for neutrophils in later stages of HS inflammation. Increased frequencies of myeloperoxidase (MPO) and neutrophil elastase positive cells in HS lesions further implicating neutrophils in HS lesional inflammation (Gamell *et al.*, 2023). MPO catalyses the formation of potent antimicrobial reactive oxygen intermediates (Parker and Winterbourn, 2012) and neutrophil elastase promotes the release of IL-8 from epithelial cells (Lee *et al.*, 2015), promoting inflammation and attracting more neutrophils to the HS lesion. CXCR1, a key receptor for neutrophil migration is elevated in HS peripheral neutrophils and increased CXCR1 expression on the surface of neutrophils positively correlated with disease severity (Gamell *et al.*, 2023). Interestingly, HS patients who failed to respond to adalimumab treatment had elevated expression of CXCR1 in HS lesions, implicating neutrophils in HS lesions refractory to adalimumab treatment (Lowe *et al.*, 2020).

G-CSF is a major regulator of neutrophil survival and function, and importantly is elevated in HS lesional skin compared with healthy control skin and other inflammatory dermatoses (Wolk *et al.*, 2021). Interestingly, expression of G-CSF was downregulated in HS tunnels and scars relative to inflammatory nodules and abscesses (Wolk *et al.*, 2021), which suggests that neutrophils may not be evenly distributed in HS skin and localise in inflammatory nodules and abscesses. G-CSF, secreted by keratinocytes and fibroblasts, is induced by inflammatory mediators typically found to be upregulated in HS lesions, including IL-17A, TNF and IL-1β (Wolk *et al.*, 2021). Importantly, blocking the G-CSF receptor with CSL324 inhibited neutrophil migration (Gamell *et al.*, 2023), outlining a potential future therapeutic avenue which could dampen the effects of neutrophils in HS lesions.

Neutrophils are prominent in HS lesions with IL-17A and Th17 responses inducing neutrophil migration to the HS lesion and inducing tissue inflammation (Lima *et al.*, 2016; Griffin *et al.*, 2012). Immunohistology suggested that neutrophils were the main source of IL-17A in HS lesions, however *IL17A* and *IL17F* mRNA expression is absent from neutrophils indicating that rather than being a primary producer of IL-17A, neutrophils may sequester IL-17A from other cellular sources via IL-17 receptors (Lima *et al.*, 2016; Tamarozzi *et al.*, 2014).

Neutrophils form web-like structures called neutrophil extracellular traps (NETs) following activation (Brinkmann *et al.*, 2004). NETs subsequently promote innate and adaptive immune responses activating plasmacytoid DC (pDC) to produce IFN-α and the NLRP3 inflammasome to promote inflammatory cytokine release (Lande *et al.*, 2011; Karmakar *et al.*, 2016). Elevated NET formation was found in both HS blood and HS lesional neutrophils relative to healthy controls, and NET formation positively correlated with disease severity (Byrd *et al.*, 2019). The effective removal of NETs is required to prevent dysregulated autoantigen production. NETs have been shown to externalise autoantigens and alarmins which promote an aberrant inflammatory response (Carmona-Rivera *et al.*, 2017). Improper NET clearance has been implicated in systemic lupus erythematosus and more recently, dysregulated NET clearance has been shown in HS patients (Leffler *et al.*, 2012; Oliveira *et al.*, 2023). 94% of HS patients have impaired NET degradation which is not fully rectified with exogenous DNase, the natural version of which mediates NET clearance, indicating additional factors protect NETs from clearance in HS (Oliveira *et al.*, 2023). Interestingly, antibodies against Dnase1 and Dnase1L3 were found to be elevated in HS lesions and correlate with disease severity (Oliveira *et al.*, 2023). Importantly, immunoglobulins in HS serum were found to impair NET degradation by neutralising DNase activity (Oliveira *et al.*, 2023).

1.2.7.4 B and Plasma cells

B cells are largely absent in healthy skin and multiple studies have reported increased frequencies of infiltrating B cells and plasma cells in HS lesions (Byrd *et al.*, 2019; Gudjonsson *et al.*, 2020; Moran *et al.*, 2023; Musilova *et al.*, 2020). Further, antibody

producing B cells have been found to reside in high concentrations around hair follicles in chronic skin inflammation (Wilson *et al.*, 2019). B and plasma cells are key producers of immunoglobulins, which are elevated in HS serum (Byrd *et al.*, 2019). Immunoglobulins specifically against citrullinated proteins found in NETs were found elevated in the serum of HS patients (Byrd *et al.*, 2019). Further investigation identified autoantibodies to multiple components of NETs, including MPO, double stranded DNA, chromatin and citrullinated histones in HS lesions (Carmona-Rivera *et al.*, 2022). Interestingly, the increased neutrophils in HS lesions also appeared to correlate with elevated B and plasma cells (Sabat *et al.*, 2023). This link between neutrophils and B cells in HS is further enhanced with the finding that neutrophil-derived BAFF (B cell activating factor) supports the persistence and function of B and plasma cells in HS lesions (Sabat *et al.*, 2023). The importance of B cells in HS further emphasised by the recent discovery that HS patients who fail to respond to adalimumab treatment have an increased B cell signature (Hambly *et al.*, 2023).

1.2.7.5 Keratinocytes

Non-immune cells have also been shown to actively participate in skin inflammation. Keratinocytes are a primary target for IL-17A, expressing chemokines and cytokines and promoting epidermal hyperproliferation following IL-17A stimulation (Furue *et al.*, 2020). HS keratinocytes demonstrate an inflammatory profile, suggesting that they are primarily dysfunctional in HS and contribute to chronic inflammation rather than enhancing a tissue protective response (Jones *et al.*, 2018; Lima *et al.*, 2016; Hotz *et al.*, 2016). IL-17A signaling enhances the expression of key proinflammatory mediators such as S100A8, S100A9, defensins, CXCL1 and IL-8, all of which are upregulated in HS lesions (Hotz *et al.*, 2016).

A central role for IL-17 signaling in HS inflammation, is further strengthened by the implication of IL-17C in HS pathogenesis. IL-17C is produced by keratinocytes following stimulation with IL-17A, TNF, microbes or TLR agonists (Ramirez-Carrozzi *et al.*, 2011). HS skin has elevated *IL17C* mRNA expression which localised to the suprabasal epidermis (Navrazhina, Frew and Krueger, 2020). IL-17C induced the production of IL-8, CXCL1, and IL-36γ (Ramirez-Carrozzi *et al.*, 2011) as well as elevating IL-17A and IL-17F production by Th17 cells (Chang *et al.*, 2011), creating an inflammatory feed forward loop (Guttman-Yassky and Krueger, 2018).

1.2.7.6 Fibroblasts

Dermal tunnels and hypertrophic scarring are key features of HS, which appear to be driven by immune dysregulation (Navrazhina *et al.*, 2021a; Frew *et al.*, 2019). Dermal tunnels are associated with more severe disease (Vanlaerhoven *et al.*, 2018) and the presence of dermal tunnels reduces the likelihood of adalimumab response in HS patients (Frew *et al.*, 2021a). Fibroblasts drive the development of hypertrophic scars, with an imbalance of collagen production and extracellular matrix degradation a critical process in scar formation (Zhu *et al.*, 2013). $CD163^+$ macrophages have been implicated in scar formation in HS, with $CD163^+$ macrophages and fibroblasts found embedded within the collagen bundles in chronic HS lesions, but not perilesional or normal skin (Byrd *et al.*, 2018). TGF-β has been shown to promote the development of hypertrophic scars (Wang *et al.*, 2000). TGF-β, elevated in HS lesional skin (Dajnoki *et al.*, 2022), potentially activates dermal macrophages in HS lesions and regulates their expression of matrix metalloproteinase (MMP) 9 which is directly involved extracellular matrix degradation and regulating subsequent scar formation (Smith *et al.*, 2023).

1.2.7.7 Skin microbiome

Healthy human skin is home to an extensive array of microorganisms which are essential for maintaining homeostasis in the skin and protect against pathogens. In healthy sebaceous skin, members of the *Cutibacterium* and *Staphylococcus* genus dominate, while generally dry areas (limbs) primarily comprise of *Proteobacteria*, *Bacteroidetes* and *Actinobacteria* (Grice and Segre, 2011). The diverse commensal bacteria found in healthy human skin provide a protective role against pathogens. The role of the skin microbiome in HS development remains controversial with a range of bacterial strains associated with HS which may potentially trigger the onset of disease (Guet-Revillet *et al.*, 2014). Increased abundances of anaerobes, including *Prevotella*, *Actinomyces*, *Mobiluncus* and *Campylobacter ureolyticus* and lower abundances of *Staphylococcus epidermis* and *Staphylococcus hominis* were found on the surface of HS skin relative to healthy controls (Riverain-Gillet *et al.*, 2020; Ring *et al.*, 2017b). Other studies supported these findings, while also highlighting an increase in *Finegoldia magna* in HS lesions (McCarthy *et al.*, 2022). Importantly, *F. magna* has been shown to promote NET formation (Neumann, Björck and Frick, 2020). The luminal biofilm identified in HS dermal tunnels primarily consists of

anaerobic bacteria, including *Porphyromonas* and *Prevotella* species (Ring *et al.*, 2019). These microbes may also promote inflammation by TLR activation inducing the secretion of IL-1β and TNF (Chu and Mazmanian, 2013). *Prevotella* has previously been shown to trigger Th17 responses and activate TLR2, increasing IL-1 and IL-23 production in mouse models of RA and in germ free mice (Maeda *et al.*, 2016; Huang *et al.*, 2020).

1.2.8 Treatment

1.2.8.1 Current therapies

As HS is frequently under-reported and often misdiagnosed, it is unlikely that patients will present to a specialised dermatologist at the early stage of disease. This may partially account for the unsatisfactory treatment outcomes for HS (Alikhan, Lynch and Eisen, 2009). HS patients are typically initially encouraged to introduce lifestyle changes, including weight loss, smoking cessation, and wearing loose clothing (Kromann *et al.*, 2014; Sartorius *et al.*, 2009). Often topical agents are prescribed to patients, providing some relief, while antibiotics can prevent infection and further breakouts.

The use of antibiotics can be effective for early stage treatment of HS, however HS symptoms frequently return (Molinelli *et al.*, 2023). Rifampicin, clindamycin and tetracycline can act as immunomodulators in HS, with tetracycline proven to inhibit bacterial products which promotes inflammation (Perret and Tait, 2014). Tetracycline also limits MMP synthesis (Griffin, Ceballos and Villarreal, 2011). MMPs contribute to the degradation of the extracellular matrix and subsequent fibrosis that is characteristic of HS.

HS patients may be treated with metformin for concomitant metabolic syndrome. Metabolic syndrome has a close association with HS, with HS patients having an increased likelihood of being diagnosed with metabolic syndrome compared with the general population (Miller *et al.*, 2014). Fortunately, treatment with metformin for metabolic syndrome has also proved effective in reducing HS disease severity. Metformin has proven to be effective in HS, with preliminary trials indicating 68%-76% of HS patients have reduced disease activity following metformin treatment (Jennings *et al.*, 2020; Verdolini *et al.*, 2013). Patients on metformin have reduced expression of *IL17A*, *IFNG*, *TNF* and *IL6*, demonstrating anti-inflammatory effects, and metformin has been shown to normalise the dysregulated cellular metabolic profile of HS lesions (Petrasca *et al.*, 2023a). Metformin

elicited these anti-inflammatory effects at least in part via NLRP3 inflammasome inhibition (Petrasca *et al.*, 2023a).

Surgical interventions are an important treatment option in HS, with laser surgery, de-roofing (turning deep sinus tracts into scars), incision and drainage or excision and skin grafts used to treat HS lesions (Alharbi, Kauczok and Pallua, 2012). The placement of setons in HS lesions is a specialised technique whereby non-absorbable nylon structures are placed within the HS lesion and tied externally (Lajevardi and Abeysinghe, 2015). The compression caused by this procedure, along with the ensuing local inflammatory reaction initiates fibrosis and acts as an intervention for anal fistulae (Kelly *et al.*, 2014).

The TNF inhibitor, adalimumab, is the only FDA approved treatment for moderate/severe HS. This monoclonal antibody targets soluble and membrane-bound TNF and is shown to significantly reduce HS severity (Kimball *et al.*, 2016). Other TNF inhibitors such as infliximab have shown promise in treating HS. Currently licensed for the treatment of RA, ankylosing spondylitis, ulcerative colitis, psoriatic arthritis, psoriasis and CD, the efficacy of TNF inhibition in HS was first noted when CD patients treated with infliximab noticed improvements to their HS (Katsanos, Christodoulou and Tsianos, 2002; Martínez *et al.*, 2001). Despite this, relatively few HS patients reached the primary endpoint during randomised clinical trial with infliximab (Grant *et al.*, 2010).

Beyond directly blocking TNF, adalimumab has been shown to alter the immune cell landscape of HS lesions. Adalimumab reduced the infiltration of Th17 cells, cytotoxic CD8 T cells, B cells, plasma cells, monocytes, DCs and macrophages in HS lesions, while having no impact on Treg cell frequencies (van der Zee *et al.*, 2012a). Ultimately, TNF inhibition, normalised the skewed Th17:Treg ratio and reduced the polyfunctionality of CD4 T cells in HS lesions (Moran *et al.*, 2017). Taken together, this suggests an important role for TNF in promoting Th17 cell proliferation and IL-17 signaling in HS lesions.

Targeting the IL-17 signaling pathway is a promising strategy in HS, with secukinumab recently approved by the European Medicines Agency (EMA) for treatment of HS (**Figure 1.7**). Two phase 3 trials assessing the efficacy of secukinumab in HS patients, SUNSHINE and SUNRISE trials, concluded that 45% and 42% of HS patients, respectively, achieved HiSCR following secukinumab treatment every 2 weeks (Kimball *et al.*, 2023a). While the

most common adverse effect in these trials was a headache, adverse reactions have been reported in trials of secukinumab in ankylosing spondylitis where five new cases of CD were reported (Schreiber *et al.*, 2019). While this may be problematic for HS patients given the association between HS and CD, similar adverse effects have not been seen in these phase 3 trials for HS (Parkes, Whelan and Lindsay, 2014; Kimball *et al.*, 2023a).

1.2.8.2 Clinical trials

Bimekizumab, a dual IL-17A and IL-17F inhibitor has completed Phase III trials for HS (NCT04242446, NCT04242498), yielding promising results (UCB, 2023). This is supported by the phase 2 trial in which 46% of patients had at least a 75% reduction in disease activity and 32% had at least a 90% reduction in disease activity (Glatt *et al.*, 2021). In this trial bimekizumab outperformed adalimumab, with only 35% of adalimumab patients having at least a 75% reduction in disease activity, and 15% having at least a 90% reduction in disease activity (Glatt *et al.*, 2021). Given the elevated expression of IL-17A, IL-17F and IL-17C in HS, targeting their shared receptor, IL-17RA, with brodalumab is an attractive therapeutic avenue. Promising results have emerged in two small open label trials, with 100% and 87.5% of patients reporting reduced disease activity, respectively (Frew *et al.*, 2020; Kearney, Hughes and Kirby, 2023). Brodalumab treatment reduced the expression of neutrophil associated *CSF3* and *CXCL1*, Th17-associated *IL21R* and the B cell chemoattractant *CXCL13* (Navrazhina *et al.*, 2022a). Brodalumab also reduced the infiltration of T cells, DCs and naïve B cells in HS lesions (Navrazhina *et al.*, 2022a). Upon treatment with brodalumab, HS patients had reduced epidermal thickness compared with baseline, indicating an important role for IL-17 cytokines in promoting epidermal thickening and keratinocyte proliferation in HS lesions (Navrazhina *et al.*, 2022a).

A nanobody targeting IL-17A and IL-17F, sonelokimab, has been developed and is currently under investigation in a phase 2 trial in HS (NCT05322473). Proven to be effective in phase 2 trials for psoriasis, sonelokimab treatment was effective in >75% of psoriasis patients, even at low doses (Papp *et al.*, 2021). The phase 2 trial currently underway in HS also has an adalimumab arm to the trial, facilitating a direct comparison between adalimumab and sonelokimab (NCT05322473). Izokibep is another novel small molecule inhibitor targeting IL-17A which has recently been developed and has outperformed secukinumab in pre-clinical models (Klint *et al.*, 2023). This IL-17 anti-mimetic small molecular inhibitor is

currently being evaluated in a phase 2 trial for HS (NCT05355805). Izokibep proved to be moderately effective in psoriasis patients in a phase 2 trial with 71% of patients having a 90% reduction in psoriasis disease severity (Gerdes *et al.*, 2023).

Inhibiting upstream of Th17 cells is another therapeutic strategy available for HS treatment. Ustekinumab inhibits both IL-12 and IL-23 binding to the p40 subunit of these cytokines, perturbing both Th1 and Th17 responses. Although appearing to elicit a clinical meaningful improvement in HS (Blok *et al.*, 2016; Montero-Vilchez *et al.*, 2022), similar to secukinumab, there have been case reports of psoriasis patients developing HS following treatment with ustekinumab (Gkini and Bewley, 2018). Larger trials are required to evaluate the safety and efficacy of ustekinumab in HS.

Guselkumab, which targets IL-23p19 has recently been evaluated in a phase 2 trial of 20 HS patients (Dudink *et al.*, 2023). 65% of HS patients with moderate-to-severe HS achieved HiSCR, while 35% of patients had at least a 75% reduction in disease activity, reaching the trials clinical endpoint and highlighting the importance of the Th17:IL-23 axis in HS (Dudink *et al.*, 2023). After 16 weeks of guselkumab treatment, HS lesional skin had reduced expression of *KRT6A*, *KRT16*, *S100A8* and *S100A9* relative to untreated lesional skin (Dudink *et al.*, 2023), suggesting that Th17 cells may promote inflammatory keratinocyte development which in turn releases AMPs known to be elevated in HS lesions. Similar to guselkumab, risankizumab is a monoclonal antibody which specifically inhibits IL-23 by binding to the p19 subunit. In a phase 2 trial in HS, 46.8% of HS patients achieved HiSCR in response to risankizumab, however a high placebo response (41.5%) indicates that risankizumab may not be an effective treatment for moderate-to-severe HS (Kimball *et al.*, 2023b).

JAK-STAT inhibitors have also been predicted to be potential future effective strategies in HS considering their proven efficacy in other chronic inflammatory diseases including RA and inflammatory bowel disease (Cohen and Frahm, 2017; Kim and Kim, 2021). Provorcitinib, a specific JAK1 inhibitor, was assessed in two phase 2 trials for HS, demonstrating mixed results. In the first phase 2 trial, 43% of HS patients achieved HiSCR, however 70% of patients experienced treatment-associated adverse events (Alavi *et al.*, 2022). In the second study, 88% of HS patients achieved HiSCR, but 81% of patients experienced adverse effects of provorcitinib (Alavi *et al.*, 2022). Despite these adverse

effects, two phase 3 trials are currently underway to assess the efficacy of provorcitinib in HS (NCT05620836; NCT05620823).

Tofacitinib, a small molecule inhibitor of JAK1 and JAK3, initially demonstrated efficacy in individual case reports (Sadeghzadeh Bazargan, Pashaei and Goodarzi, 2023; Savage *et al.*, 2020). In one case report, one HS patient with Hurley stage 3 disease achieved remission following tofacitinib treatment (Savage *et al.*, 2020). A report of tofacitinib-induced HS in a RA patient receiving tofacitinib highlights potential adverse effects associated tofacitinib treatment which may limit its use in HS (Shaharir *et al.*, 2020). Ruxolitinib, a JAK1 and JAK2 inhibitor is also currently under investigation in two phase 2 trials in HS (NCT04414514; NCT05635838). Ruxolitinib has benefits over other JAK inhibitors as it can be taken orally, and has proved to be effective in phase 2 trials for vitiligo (Rosmarin *et al.*, 2020). A small retrospective cohort study of HS patients on updacitinib, a small molecule inhibitor of JAK1, demonstrated high efficacy, with 100% of patients achieving HiSCR after 24 weeks of treatment (Kozera, Flora and Frew, 2022). Unfortunately, phase 2 trials, proved upadacitinib was less effective, with only 38% of HS patients achieving HiSCR (NCT04430855).

Other therapeutic strategies such as blocking IL-1 cytokines or IL-1 receptors have proven to be moderately successful in clinical trials for moderate to severe HS (NCT02643654 and NCT01516749). In a small cohort of patients, 78% of patients treated with anakinra achieved HiSCR (Tzanetakou *et al.*, 2016), however painful reactions at the site of injection have also been reported following anakinra treatment (André *et al.*, 2019; Leslie *et al.*, 2014). Case reports of HS patients failing to respond to anakinra have also put into question the efficacy of anakinra in HS patients (Russo and Alikhan, 2016; Menis *et al.*, 2015). A larger randomised, placebo-controlled trial is required to evaluate the true efficacy of anakinra in HS. Bermekimab, an anti-IL-1α monoclonal antibody was evaluated in two phase II clinical trial for the treatment of HS (Gottlieb *et al.*, 2020). One open label trial involved 42 patients split into a TNF inhibitor naïve group and a group of HS patients previously treated with a TNF inhibitor. 61% of HS patients in the TNF inhibitor naïve cohort achieved HiSCR, while 63% of HS patients previously treated with TNF inhibitors achieved HiSCR following bermekimab treatment (Gottlieb *et al.*, 2020). However, this trial was limited by the absence of a placebo control. Once measured in a placebo-controlled phase 2 trial,

bermekimab failed to outperform placebo (NCT04019041). Targeting IL-1β directly with canakinumab has demonstrated mixed results in single case reports (Sun *et al.*, 2017; Houriet *et al.*, 2017).

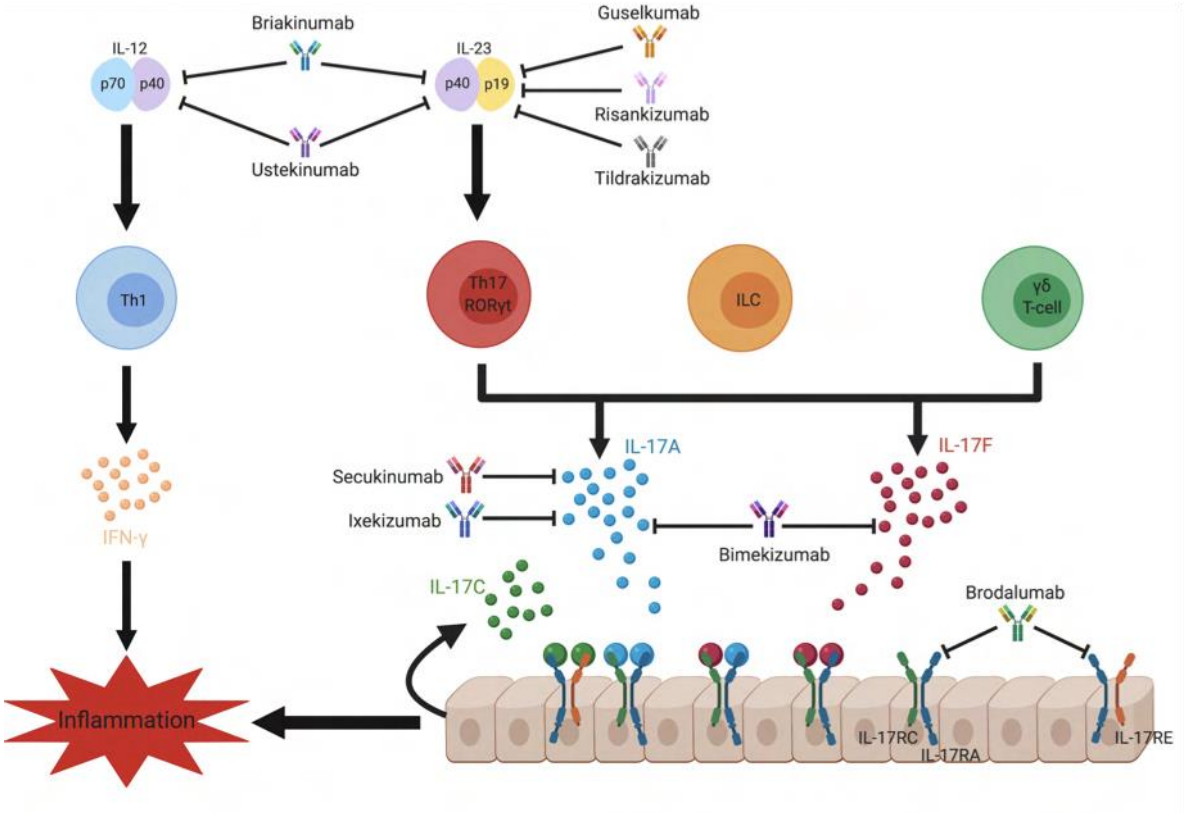

Figure 1.7 Current therapeutic strategies targeting the IL-17 pathway. IL-17A and IL-17F are signature cytokines of Th17 cells. IL-17 cytokines can also come from ILCs and γδ T cells. Dimers of IL-17A, IL-17F or IL-17A/F bind to their cognate receptor, IL-17RA or IL-17RC expressed on epithelial cells. In turn, epithelial cells produce IL-17C in response to IL-17 cytokine stimulation. In response to IL-17 stimulation, epithelial cells secrete AMPs, proinflammatory cytokines and recruit neutrophils to the site of inflammation. Blocking IL-17A directly with secukinumab, IL-17A/F directly with bimekizumab or IL-17RA with brodalumab are potential therapeutic strategies in HS. Alternatively, blocking IL-23 alone, upstream of Th17 cells with guselkumab or both IL-23 and IL-12 with ustekinumab could be useful for the treatment of HS. Illustration was generated using BioRender software (Fletcher *et al.*, 2020).

1.3 Working Hypothesis

HS is a poorly understood chronic inflammatory skin disease, characterised by aberrant immune responses. Identifying key cellular players and their transcriptional profile will contribute to the understanding of HS pathology and may propose novel therapeutic targets for HS.

Chapter 2

Materials and Methods

2 Materials and Methods

2.1 Materials

2.1.1 T cell crawl out media preparation

Product	Company
Roswell Park Memorial Institute Medium (RPMI)	Labtech
Fetal Bovine Serum (FBS)	Sigma
L-Glutamine/ Penicillin/ Streptomycin (PSG)	Sigma
Hepes Buffer	Gibco
IL-2	Miltenyi Biotec

2.1.2 T cell stimulation

Product	Company
Phorbol 12-myristate 13-acetate (PMA)	Sigma
Ionomycin	Sigma
Brefeldin A	Sigma
Anti-CD3	Invitrogen
Anti-CD28	Invitrogen

2.1.3 Keratinocyte isolation

Product	Company
Miltenyi Epidermis Dissociation Kit	Miltenyi Biotec
gentleMacs C tubes	Miltenyi Biotec
Pre-Separation Filter (70 µM)	Fisher scientific

2.1.4 Complete EpiLife preparation

Product	Company
EpiLife serum free media	Gibco
EpiLife Defined Growth Supplement (1X)	Gibco
ROCK inhibitor	Becton Dickinson

2.1.5 Peripheral blood mononuclear cells (PBMC) preparation

Product	Company
Phosphate buffered saline (PBS)	Sigma
Lithium heparin phlebotomy tubes	Cruinn
Lymphoprep	Stemcell Technologies

2.1.6 Monocyte Isolation

Product	Company
CD14 microbeads	Miltenyi Biotec
MACS buffer	Miltenyi Biotec
LS columns	Miltenyi Biotec

2.1.7 Cytokine secretion assay

Product	Company
S100A8 ELISA kit	R&D biotechne
MMP3 ELISA kit	R&D biotechne
IL-36γ ELISA kit	R&D biotechne
IL-17A ELISA kit	BioLegend
TNF ELISA kit	Invitrogen
IL-1β ELISA kit	Invitrogen
IFN-γ ELISA kit	BioLegend
IL-17F ELISA kit	Invitrogen
Bovine Serum Albumin (BSA)	Sigma
Tween	Sigma
Stop Solution (1M H_2SO_4)	ThermoFischer
MesoScale Discovery (MSD) U-plex kit	MesoScale Discovery

2.1.8 Other Materials

Product	Company
UltraCulture media	Lonza
Iscoves Modified Dulbecco Media (IMDM)	Sigma
MCC950	Inflazome
Adalimumab	AbbVie
Secukinumab	Novartis
Human serum	Sigma
ATP	Sigma
Whole Skin Dissociation Kit	Miltenyi Biotec
CyroStor cryopreservation media	StemCell Technologies
Qiagen RNA isolation kit	Qiagen
cDNA reverse transcription kit	Applied Biosystems
Lipopolysaccharide (LPS)	Enzo Sciences
Zymosan	Invivogen
Ethylenediaminetetraacetic acid (EDTA)	Sigma

2.1.9 Flow cytometry panel for analysis of digested epidermis.

Antibody	Fluorochrome	/50 µl	Supplier	Clone
KRT14	AF488	1.5	Novus Biotechne	KRT14/2375
CD90	PE-CF594	1.5	Becton Dickinson	5E10
KRT10	AF647	1.5	Santa Cruz Biotechnology	RKSE60
KRT6	DyLight405	1	Novus Biotechne	LHK6
CD45	BV711	1.5	Becton Dickinson	HI30

2.1.10 Flow cytometry panel for analysis of PMA and ionomycin stimulated T cells in emigrating cells from human skin

Antibody	Fluorochrome	/50 µl	Supplier	Clone
CD45RO	BV421	2.5	Becton Dickinson	UCHL1
IL-17F	eFluor450	1.25	Invitrogen	SHLR17
IFN-γ	BV605	0.65	Becton Dickinson	B27
CD3	BV711	1.5	Becton Dickinson	UCHT1
CD69	BV786	1.5	Becton Dickinson	FN50
IL-17A	AF488	1.25	BioLegend	BL168
CD103	PerCP-eFluor710	1.2	Invitrogen	Ber-ACT8
CD4	PECF594	1.5	Becton Dickinson	L200
CD161	PE-Cy7	1.5	Invitrogen	HP-3G10
CD45	AF700	1.5	Invitrogen	2D1
CD8	APC-eFluor700	1.5	Invitrogen	SK1
CCR7	APC	1.5	BioLegend	G043H7

2.1.11 Flow cytometry panel for analysis of LPS and zymosan stimulated monocytes in PBMC.

Antibody	Fluorochrome	/50 µl	Supplier	Clone
CD64	BV421	1.25	Becton Dickinson	10.1
CD40	eFluor450	1.5	Invitrogen	5C3
CD16	BV785	2	BioLegend	3G8
CD86	FITC	3	Becton Dickinson	FUN-1
TNF	PerCP	1.5	BioLegend	Mab11
CD80	PerCP-eFluor710	1.5	Invitrogen	B7-1
IL-12 (p40/p70)	PE	0.5	Miltenyi Biotec	C8.6
CD14	PE-Dazzle594	1.5	Miltenyi Biotec	M5E2
HLA-DR	PE-Cy7	1.5	Becton Dickinson	G46-6
Lineage	APC	6	BioLegend	UCHT1 (CD3); HIB19 (CD19); 2H7 (CD20); 5.1H11 (CD56)
IL-1β	AF647	1.5	Invitrogen	CRM56
IL-6	AF700	1.5	Invitrogen	MQ2-13A5
CD45	APC-Fire810	1.5	BioLegend	HI30

2.2 Methods

2.2.1 Patient recruitment

Studies were reviewed and approved by the St. Vincent's Healthcare Group Ethics and Medical Research Committee, Dublin. Patients were recruited during dermatology and surgical consultations at St Vincent's Hospital Dermatology Department, and St Michael's Hospital Surgical Theatres, respectively. Healthy controls were recruited through mammoplasty surgeries at St Vincent's Private Hospital Plastic and Reconstructive Surgery Clinic. Patients were fully consulted, and presented with an information leaflet, full project details and consent form. It was clearly outlined that participation would not affect their medical care in any way. All participants provided full informed consent. Clinical information is detailed in the relevant sections.

For samples in **Chapter 3**, regulatory approval for the clinical trial (DERMMARK) was granted by the Health Product Regulatory Authority in Ireland and the trial was registered with the European Clinical Trials Register (EudraCT number 2016-001566028). For this study, HS patients were recruited as part of an investigator-led, open-label, single arm clinical trial of adalimumab treatment in HS patients with moderate-to-severe disease. Patient recruitment was performed by members of the dermatology research team led by Prof. Brian Kirby in St Vincent's University Hospital, particularly Drs Roisin Hambly, Helen Rea, Vivien Marasigan and Shivashini Kirthi. Human skin (a 3 or 6 mm biopsy, excised surgical tissue from a HS tract, or excess tissue from abdominoplasty and mammoplasty surgeries) was transferred in a dry sterile tube from surgery for processing in Trinity College Dublin (TCD).

2.2.2 Isolation and stimulation of emigrating T cells from human skin

Skin samples were weighed and approximately cut into 1 mm sections and cultured in 1.5 ml of media supplemented with 10 ng/ml IL-2 (**Section 2.1.1**) for 10 days (Clark *et al.*, 2006b). IL-2 enhanced the survival and expansion of T cells which emigrated from the tissue. Half of the media was removed and replaced with fresh IL-2 supplemented media every 3 days.

For intracellular cytokine analysis (**Section 2.1.10**), emigrating T cells from HS and healthy control skin were stimulated with 50 ng/ml PMA and 500 ng/ml ionomycin and treated with

5 µg/ml Brefeldin A to inhibit protein trafficking to the Golgi apparatus. Samples were then placed in an incubator at 37°C for 4 hours (h). Unstimulated controls were treated with 5 µg/ml Brefeldin A alone.

T cell conditioned media was generated using T cells which emigrated from HS tracts/fistulae (HS-TCM). For this, 1 x 10^6 emigrating T cells/ml from HS tracts or healthy control skin were stimulated with 1 µg/ml anti-CD3 and 0.5 µg/ml anti-CD28 for 5 days.

2.2.3 Keratinocyte isolation and culture

Skin sample was weighed and then processed using the Epidermis Dissociation Kit (Miltenyi Biotec). Biopsies were washed with PBS and subcutaneous fat removed using scissors and a scalpel. Biopsies were placed in a 1.5 ml tube (Eppendorf tube) containing 1 ml RPMI and 25 µl of Enzyme G. Samples were incubated at 4°C for 18 h on a tube rotator. Skin samples were then removed and placed in a petri dish for 30 minutes (mins) at 37°C to facilitate easier removal of the epidermal layer. Using curved tweezers, the epidermis was removed from the dermis and placed in a new Eppendorf tube containing 1 ml RPMI, 25 µl Enzyme P and 5 µl Enzyme A from the Epidermis Dissociation Kit (Miltenyi Biotec). Unfortunately, due to company proprietary information, the enzymes used could not be disclosed. The skin samples were then incubated for 1 h at 37°C. Following incubation, the epidermis was layered on the rotator of the gentleMACS C tube (Miltenyi Biotec) and the contents of the Eppendorf tube added to the C tube. 1 ml cold 1% BSA in PBS was then added to stop the enzymatic reaction. The gentleMACS C tube was then inserted into the mechanical gentleMACS Dissociator (Miltenyi Biotec) and the h_skin_01 program was run, which mechanically dissociates the epidermal tissue. C tubes were centrifuged at 400 standard gravity (g) for 30 seconds (s) to collect sample material at the bottom of the C tube. Sample was resuspended by pipetting and then passed through a 70 µM strainer into a 15 ml tube. The 70 µM strainer was then washed through with cold 1% BSA in PBS. The sample was then centrifuged at 300 g for 10 mins at room temperature (RT). Keratinocytes were resuspended with cEpiLife media (EpiLife media, EpiLife Defined Growth Supplement, 10 µM ROCK inhibitor, 1% PSG) for long term culture, or keratinocytes were used for same day cytometric analysis (**Section 2.1.9**). Keratinocytes isolated from healthy control skin using the gentleMACS Epidermis dissociation kit were grown to 80% confluence in cEpiLife media and used between passages 1 and 3. 1 x 10^4 keratinocytes were plated in 96 well plates for

stimulation with recombinant cytokines or HS-TCM and treated with adalimumab (10 µg/ml) or secukinumab (10 µg/ml) for 24 h.

2.2.4 Fibroblast isolation and culture

During isolation of emigrating T cells from human skin (**Section 2.2.2**), fibroblasts also crawl out (Clark *et al.*, 2006b). To maximise fibroblast isolation from the human skin, healthy biopsies were cultured for an additional 4 days in cRPMI (RPMI, 10% FBS, 1% PSG) following the removal of the emigrating T cells. Dermal fibroblasts were cultured in cRPMI to 90% confluence and used between passages 2 and 6. 1 x 10^4 fibroblasts were plated in 96 well plates for stimulation with recombinant cytokines or HS-TCM and treated with adalimumab (10 µg/ml) or secukinumab (10 µg/ml) for 24 h.

2.2.5 Isolation of PBMC from HS patient and healthy control blood

Healthy donor and HS patient blood samples were collected in heparin tubes by a trained, authorised phlebotomist. Blood was kept at RT and processed within 3 h of collection. Blood was mixed 1:1 with PBS and 30 ml layered over 20 ml Ficoll-Hypaque (Lymphoprep) per tube. PBMC were isolated by density-gradient centrifugation at 800 g for 20 mins at RT, with the brake off for this step. The subsequent PBMC layer was removed with a Pasteur pipette, resuspended in 50 ml sterile PBS and centrifuged at 600 g for 10 mins. The supernatant was discarded and the PBMC pellet was resuspended in 20 ml sterile PBS and centrifuged at 400 g for 10 mins. Supernatants were discarded and the PBMC pellet was resuspended in cold, heat-inactivated FBS before cells were counted (**Section 2.2.7**).

2.2.6 Purification of monocytes

PBMC were isolated from HS patients and healthy donors as described in **Section 2.2.5** and total $CD14^+$ monocytes were isolated from PBMC using Miltenyi CD14 microbeads according to the manufacturer's instruction. After determining the cell number in the isolated PBMC (**Section 2.2.7**), cell suspension was centrifuged at 300 g for 10 mins. Cell pellet was resuspended in 80 µl MACS buffer per 1 x 10^7 PBMC and 20 µl CD14 microbeads were added per 1 x 10^7 PBMC. Cell suspension was mixed well with CD14 microbeads by vortex and incubated for 15 mins at 4°C. PBMC were washed by adding 2 ml MACS buffer

per 1 x 10^7 cells and centrifuged at 400 g for 10 mins. Supernatants were discarded and cells were resuspended in 500 µl MACS buffer.

LS columns were placed on the MACS magnetic separator. LS columns were prepared by first passing 3 ml MACS buffer through the column. The cell suspension was then passed through, which was washed a further 3 times with 3 ml MACS buffer. Unlabelled cells that passed through the columns were discarded. The column was then removed from the magnetic separator and 3 ml of MACS buffer added. CD14 labelled cells were flushed out of the column by firmly pushing the plunger into the column and collected in a fresh 15 ml tube. The purity of the $CD14^+$ cell sort was routinely > 95%.

2.2.7 Cell counting

Cells in suspension were diluted in trypan blue and viable mononuclear cells were counted on a light microscope using a haemocytometer. Dead cells stain dark blue in trypan blue, while the number of clear, viable cells were counted in 3 squares (each containing 9 sections) and the total number of cells was calculated using the following formula:

Total cells = average cells counted per square x dilution factor x 10^4 cells per ml

For cytometric analysis, the cell counts were calculated as follows:

$$\text{Absolute count (cells/µl)} = \frac{\text{No. of events}}{\text{Total volume analysed}} \times \text{Original resuspended volume}$$

2.2.8 Surface staining for flow cytometry

Following appropriate treatment (e.g., rested, stimulated), cells were washed with 2 ml of PBS and centrifuged at 400 g for 5 mins, and the supernatant discarded. 50 µl of the viability dye FixVia eFluor506 (1:250 in PBS) was added to cells and incubated at RT for 15 mins in the dark. 2 ml FACS buffer (PBS, 4% FBS, 0.5 mM EDTA) was added to cells and centrifuged at 400 g for 5 mins, and the supernatant discarded. Cells were treated with 1.5 µl Fc block to minimise non-specific Fc receptor-antibody binding. Cells were then incubated with 50 µl containing BD Brilliant Stain Buffer and antibodies targeting surface membrane proteins.

Samples were incubated in the dark for 15 mins at RT before being washed with 2 ml FACS buffer, centrifuged at 400 g for 5 mins, and the supernatant discarded. Cell pellets were resuspended in 200 µl FACS buffer. Where intracellular staining was required, see **Section 2.2.9** below.

2.2.9 Intracellular staining for flow cytometry

When staining with antibodies for intracellular proteins, Invitrogen's Cell Permeabilization Kit was used. Following surface staining (**Section 2.2.8**), cells were washed with 2 ml FACS buffer, centrifuged at 400 g for 5 mins and the supernatant was discarded. Cells were treated with 50 µl of Part A from the kit, for 15 mins at RT in the dark, to fix cells. Cells were washed with 2 ml FACS buffer and centrifuged at 400 g for 5 mins. Samples were then treated with 50 µl of Part B from the kit containing antibodies targeting intracellular proteins for 15 mins at RT, in the dark to permeabilise the cells. Cells were then washed with 2 ml FACS buffer, centrifuged for 5 mins at 400 g and the supernatant discarded. Cell pellets were resuspended in 200 µl FACS buffer and kept at 4°C until acquired on the cytometer.

2.2.10 *In vitro* inflammasome assay and TLR stimulations

5 x 10^5 PBMC/well were plated in a 24-well plate in cRPMI. To induce inflammasome activation, PBMC were stimulated with 100 ng/ml LPS for 3 hours and 5 mM ATP for an additional hour. 30 mins prior to ATP stimulation, PBMC were treated with 100 nM MCC950 to block inflammasome activation. Cell supernatants were harvested and the concentrations of IL-1β and TNF were evaluated by ELISA.

To evaluate different TLR stimulations in HS and healthy control monocytes, 5 x 10^5 PBMC in cRPMI were stimulated with zymosan (1 µg/ml) or LPS (100 ng/ml) for 3 hours. Cells were harvested and stained for monocyte markers (**Section 2.1.11**). Additionally, 5 x 10^5 purified $CD14^+$ monocytes (**Section 2.2.6**) were stimulated with zymosan (1 µg/ml) or LPS (100 ng/ml) for 24 hours. Supernatants were harvested and concentration of IL-1β, TNF and IL-6 were evaluated by ELISA.

2.2.11 Complete media selection and preparation

UltraCULTURE serum free medium (UC-SFM) supplemented with 1% PSG and 0.5% human serum was previously determined in our lab to be the optimal media for the explant culture. Other media, such as RPMI, Dulbecco's Modified Eagle Medium, IMDM and HL-1 were compared to UC-SFM, with higher cytokine levels found in the supernatants of skin biopsies cultured in UC-SFM compared to other media. Due to the discontinuation of UC-SFM medium during the course of this study, IMDM supplemented with 1% PSG and 0.5% human serum (cIMDM) was used as an alternative culture medium for HS113-HS115.

2.2.12 *Ex vivo* preparation of human skin biopsy

Skin sample was initially washed in PBS, removing any excess blood. The sample was cut into 4 approximately equal sections using a surgical blade and each piece weighed. Each section, which contained all skin layers, was placed into an appropriate-sized well containing complete UC-SFM, or cIMDM, at a concentration of 10 mg/ml (i.e., a 5 mg biopsy placed in a 24-well plate with 500 µl medium). One section was left untreated, with various inhibitors added to the other 3 sections. The NLRP3 inflammasome inhibitor MCC950 (a gift from Inflazome), was added to one section at a concentration of 100 nM. Supernatants were collected following 24 h incubation at 37°C and 5% CO_2, then centrifuged at 500 g for 5 mins to remove any cells. Supernatants were aliquoted and stored at -20°C for subsequent ELISA and MSD analyses. The remaining skin biopsies were flash frozen in liquid nitrogen and stored at -80°C for downstream RT-PCR analysis.

2.2.13 Measurement of cytokine secretion by MSD assay

The MSD sandwich immunoassay system is a multiplex assay which allows for a customised combination of analytes. In brief, a biotinylated capture antibody couples with a linker which binds to specific spots on the MSD plate, with a unique linker for each antibody. The biotinylated antibody and linker were combined and incubated at RT for 30 mins. A stop solution was added and incubated for 30 mins. The solution was incubated at RT for 1 h on a plate shaker. The plate was washed 3 times (x 3) with PBS-Tween wash buffer (PBS-T). Samples and standard calibrators (see **Table 2.1** for dynamic range of assay) were added to each well for 1 h at RT. The plate was washed x 3 with PBS-T. Detection antibody was added

to each well, the plate sealed and incubated at RT for 1 h on a plate shaker. After 1 h, the wells were washed x 3 with PBS-T. MSD Read Buffer was added to each well immediately prior to reading the plate on an MSD sector imager. Data were analysed using the MSD Discovery Workbench software. The Discovery Workbench calculates the electochemiluminescent signal from each analyte in every well. From this signal a standard curve was created, and the analyte concentration calculated. Data were displayed, and statistical analysis performed, using Prism software (Graphpad Prism v10).

Table 2.1 Dynamic ranges of cytokines used in the MSD assay.

Analyte	Dynamic Range (pg/ml)
IL-1α	1.4 – 5680
IL-1β	1 – 4260
IL-18	9 – 37,400
CCL20	6 – 25,000
IL-17A	6 – 24,500
TNF	0.9 – 3,680
IL-8	0.5 – 2,230
IFN-γ	6 – 24,800
IL-17C	4.76 – 19,500
CXCL1	0.6 – 2,570

2.2.14 Measurement of cytokine secretion by ELISA

The concentrations of S100A8, IL-36γ, MMP3, IL-17A, IL-17F, TNF and IFN-γ were quantified by ELISA. 50 µl of capture antibody diluted in PBS was added to high affinity 96-well plates. Plates were incubated overnight at RT, then the capture antibody removed and 150 µl reagent diluent (1% BSA in PBS) added. After 1 h, plates were washed in wash buffer (PBS-T) x 3, blotted dry and 50 µl of supernatant samples were added to single wells. A standard curve of serial diluted recombinant cytokine standard was loaded onto the plate in duplicate. Blank wells containing only reagent diluent were included to subtract background from each sample. Samples were incubated at RT for 2 h. Supernatants were removed, and wash buffer added, then blotted dry. 50 µl biotinylated detection antibody, diluted with reagent diluent, was then added and incubated at RT for 2 h. Plates were washed and 50 µl horseradish-peroxidase conjugated to streptavidin was added for 30 mins at RT in the dark. Wells were washed and 50 µl 3,3',5,5'-Tetramethylbenzidine (TMB) substrate was added. Plates were left at RT in the dark while the enzyme-mediated colour

reaction developed. The reaction was stopped by the addition of 25 µl 1M H_2SO_4 when a sufficient colour change had occurred. The absorbance at 450 nm wavelength was measured using a microtiter plate reader (BioTek, Epoch). Cytokine concentrations were calculated from the standard curve.

2.2.15 Measurement of relative gene expression by Polymerase chain reaction

RNA was extracted from fresh skin biopsies flash frozen with liquid nitrogen. First, skin biopsies were pulverised using a BioPulveriser pre-chilled in liquid nitrogen and transferred to 700 µl Qiazol to lyse the cells. 140 µl chloroform was then added and the sample vigorously shaken for 15 secs and centrifuged at 8,000 g for 15 mins at 4°C. RNA was then isolated from DNA and protein by transferring 350 µl of the aqueous phase into a new Eppendorf tube. Following addition of 525 µl 100% ethanol, 700ul of the RNA solution was transferred to an RNeasy RNA isolation column (Qiagen). RNA was isolated following the manufacturer's instructions, which included a series of wash steps before the RNA was finally isolated in RNA-free water.

The yield and quality of the isolated RNA was measured by NanoDrop spectrophotometer and samples of sufficient quality were reverse-transcribed into cDNA. To do this, the Applied Biosystems High Capacity cDNA Reverse Transcriptase kit and RNase Inhibitor were used as per the manufacturer's instructions and reverse transcription was performed using the G-Storm GS-1 PCR/Thermal Cycler. 10 µl of 100 ng RNA was added to the reverse transcription master mix (**Table 2.2**) and placed in the thermal cycler. This reaction involved 10 mins at 25°C, 120 mins at 37°C, 5 mins at 85°C and 4°C to finish.

Real time Polymerase Chain Reaction (RT-PCR) was carried out using the PowerSYBR green PCR master mix and oligonucleotide primers. Reactions were made up as detailed in **Table 2.3** in a 96-well PCR microplate. RT-PCR was performed using the QuantStudio RT-PCR system. For each sample, mRNA concentration was normalised to the housekeeping gene *HPRT1*. Expression of *KRT14*, *KRT6A* and *KRT17* (Section **Table 2.4**) were measured in HS and healthy control skin.

Table 2.2 Components for cDNA synthesis master mix.

Reverse transcription master mix	Per tube (µl)
dH_2O	3.2
10X RT buffer	2
10X random primers	2
dNTPs	0.8
Multiscribe	1
RNase Inhibitor	1

Table 2.3 Components of RT-PCR master mix.

RT-PCR master mix	Per tube (µl)
dH_2O	3.75
10 µM forward primer	1
10 µM reverse primer	1
2X Sybr green master mix	6.25

Table 2.4 Primer sequences. Table containing the forward and reverse primer sequences for keratin markers.

Gene	Forward Primer	Reverse Primer
HPRT1	ATGGACAGGACTGAACGTCTTG	GGCTACAATGTGATGGCCTC
KRT14	GCGGCCTGTCTGTCTCAT	CCACCAGAAGCCCATCAC
KRT6A	GGGTTTCAGTGCCAACTCAG	CCAGGCCATACAGACTGCGG
KRT17	CCAGGCCATACAGACTGCGG	CCAGGCCATACAGACTGCGG

2.2.16 RNA isolation, cDNA synthesis and bulk RNA sequencing of HS, psoriasis, atopic dermatitis and healthy skin biopsies

A 6 mm punch biopsy was collected from lesional skin of HS, psoriasis and AD patients. Samples were snap frozen in liquid nitrogen and stored at -80^{o}C. RNA was extracted from the skin biopsies using the RNeasy Fibrous Tissue Mini Kit (Qiagen) by Dr Solene Gatault and Dr Roisin Hambly (Hambly *et al.,* 2023). Samples of sufficient quality were shipped to AbbVie, IL, USA for RNA sequencing using the HiSeq 4000 Illumina sequencer. Raw sequencing reads were aligned by Dr Luis Fernando Iglesias Martinez, using default parameters of Rsubread (Liao, Smyth and Shi, 2019).

2.2.17 Bulk RNA-sequencing analysis

Raw data were normalised using default parameters in DESeq2 in R (Love, Huber and Anders, 2014). The Wald test was used to identify differentially expressed genes between two conditions in this bulk RNA-sequencing (RNA-seq) dataset (Love, Huber and Anders, 2014). Differentially expressed genes were defined as an adjusted (adj) p value ≤0.05. Pathway enrichment was performed using PathfindR (Ulgen, Ozisik and Sezerman, 2019) and both gene ontology and Kegg databases were utilised.

Transcription factor usage analysis was performed using DoRothEA (Garcia-Alonso *et al.,* 2019) which uses the statistical framework of VIPER (Alvarez *et al.*, 2016) to determine significant relationships between transcription factors and inflammatory dermatoses. Rather than evaluating the expression of a particular transcription factor, DoRothEA computes the expression of genes known to be regulated by that transcription factor, providing a better indication of its activity.

Weighted gene co-expression network analysis (WGCNA) is a systems biology technique to identify groups of highly correlated genes (clusters/modules) in big data (Langfelder and Horvath, 2008). Hierarchal clustering of the correlated gene modules identified genes with elevated co-expression in each inflammatory dermatosis. Gene ontology pathways enriched in these gene modules were displayed identifying unique inflammatory pathways which differentiate, HS, psoriasis and AD lesional skin.

The xCell enrichment tool was used to predict cell populations present in the skin biopsies, based on the transcriptional signature identified by bulk RNA-seq (Aran, Hu and Butte, 2017). Using previously curated gene signatures of different cell types, this tool calculates enrichment scores within the bulk RNA-seq data for each individual sample.

2.2.18 Patient details for single cell RNA sequencing

Clinical details for the HS patient group are shown in **Table 2.5**, the healthy control group in **Table 2.6**. HS patients were recruited from St Michael's Hospital, Dublin during surgical consultations and from HS clinics in St Vincent's Hospital, Dublin. All samples were 6 mm punch biopsies or surgical excisions of lesional skin. Healthy control skin was donated from

breast reduction surgeries (mammoplasty) at St Vincent's Private Hospital Plastic and Reconstructive Surgery Clinic, Dublin. All samples were processed within 2 h of sampling. The mean age of the HS patient cohort was 38.7 y ± (standard deviation) SD of 14.7 compared with 41 y ± SD of 13.88 in the healthy control group. All of the healthy controls were female, whereas 83% of the HS patients were female. 83% of HS patients had Hurley stage 3 disease and 17% had Hurley stage 2 disease. HS patients had a higher BMI (44.9 kg/m^2 ± SD of 5.6) than healthy controls (25 kg/m^2 ± SD of 0.6). No healthy controls were smokers, whereas 33.3% of HS patients were current smokers and 33.3% were ex-smokers.

Table 2.5 Clinical details for HS patient group. Clinical details of HS patients at the time of sampling, including age, sex, Hurley stage, body mass index (BMI), smoking status and medication HS patients were on at the time of sampling. E-S: ex-smoker, F: female, M: male, N-S: non-smoker, S: smoker.

Patient ID	Age (y)	Sex	Hurley	BMI	Smoker	Treatments
HS1	22	F	3	45.2	N-S	Liraglutide, flamazine, infliximab, seton sutures
HS2	43	F	3	38.7	S	Adalimumab, seton sutures
HS3	62	F	3	43.4	E-S	Metformin, seton sutures
HS4	31	M	2	43.6	S	Metformin, seton sutures
HS5	51	F	3	56.6	N-S	Seton sutures
HS6	23	F	3	42.1	E-S	Liraglutide, seton sutures
	Mean 38.7 SD 14.7	F 83% M 17%	1 – 0% 2 – 17% 3 – 83%	Mean 44.9 SD 5.6	S – 33.3% E-S – 33.3% N-S – 33.3%	

Table 2.6 Clinical details for healthy control group. Clinical details of healthy controls at the time of sampling, including age, sex, Hurley stage, body mass index (BMI), smoking status and medication HS patients were on at the time of sampling. F: female, N-S: non-smoker.

Patient ID	Age (y)	Sex	BMI	Smoker
Con1	58	F	24.2	N-S
Con2	41	F	25.2	N-S
Con3	24	F	25.7	N-S
	Mean 41 SD 13.88	F 100%	Mean 25 SD 0.6	N-S – 100%

2.2.19 Sample preparation for scRNA-seq

Skin sample was cut in half (approximately) using a scalpel, with one half preserved in 10% formalin for histopathology analysis. The remaining half was weighed and processed into a single cell suspension using the Whole Skin Dissociation Kit (Miltenyi Biotec). The samples were washed in PBS, diced into ~1 mm pieces, and transferred into a gentleMACS C tube containing 435 µl of Buffer L, 12.5 µl Enzyme P, 50 µl Enzyme D and 2.5 µl Enzyme A. The tube was incubated in a water bath at 37°C for 3 h. 500 µl of cold IMDM containing 5% FBS, 1% PSG was added to the tube prior to mechanical dissociation using the h_skin_01 program of the gentleMACS Dissociator. The sample was briefly centrifuged to collect the sample at the bottom of the tube, then passed through a 70 µM filter into a 50 ml falcon tube. The filter was washed with 4 ml cold IMDM before centrifugation for 10 mins at 300 g at 4°C. The cell pellet was resuspended in CryoStor cryopreservation media (StemCell Technologies), added in cryovials and frozen immediately in CoolCell freezing containers at -80°C.

Cryovials were transferred to liquid nitrogen following 24 h at -80°C and subsequently shipped to collaborators at AbbVie Bioresearch Centre, Mass., USA. There, the frozen cells were thawed with warm RPMI media and maintained at 4°C. Samples were centrifuged twice at 514 g and the cell pellet was resuspended with 100 µl PBS/0.5% BSA. 2 µl of CD45 antibody was added to samples for 30 mins, followed by addition of 2 ml PBS/0.5% BSA and subsequent centrifugation at 300 g. Supernatants were aspirated and cell pellet resuspended in 200 µl PBS/0.5% BSA before filtration through a 35 µM filter. 1 µl of SYTOX Blue dead stain was added to identify dead cells. Live, single $CD45^+$ and $CD45^-$ cells were sorted using the FACSAria II cytometric cell sorter into 50 µl of PBS/0.5% BSA. Sorted cells were centrifuged, supernatants aspirated, and cells resuspended at 1 x 10^3 cells/µl in PBS/0.5% BSA.

The 10X Single Cell 3' Reagent Kits v2 Rev C User Guide was followed to generate Gel Bead-in-Emulsion (GEM) and barcoding, post GEM-RT clean up and cDNA amplification (10X Genomics, Pleasanton, USA). To generate the cDNA library the Chromium Single Cell 3' Library & Gel Bead Kit v2, Chromium Single Cell A Chip Kit and Chromium & Multiplex Kit (10X Genomics) were used, producing a $CD45^+$ and $CD45^-$ library for each donor. The

quantity and quality of cDNA libraries were assessed using D1000 Screen Tapes (Agilent Technologies, San Francisco, USA). In one batch, 22 µl of each of the 9 libraries from each donor were sequenced on the Illumina HiSeq RNA sequencing system at AbbVie Genomics Research Center (Mass., USA). Cell recoveries ranged between 860- 4,800 cells per sample (**Table 8.59**).

2.2.20 scRNA-seq data analysis

scRNA-seq data were processed using Cell Ranger v.3.0.2 with the 10X human transcriptome GRCh38-3.0.0 acting as a reference. $CD45^+$ and $CD45^-$ data were analysed separately using the same protocol. Further analysis was performed in R v.3.6.3. Firstly, cell-containing droplets were identified in each individual sample using the programme EmptyDrops (Lun *et al.,* 2019), at a false discovery rate of 1%. Droplets identified as lacking a cell were removed from subsequent analysis. Only genes found in a minimum of 3 cells were included in downstream analysis in Seurat v.3 (Stuart *et al.,* 2019). Data were processed and clustered using the SCT workflow and Harmony to correct for batch effects (Korsunsky *et al.,* 2019). A number of quality control measures were used to remove low quality and decaying cells (**Figure 2.1A-D**). Apoptotic or decaying cells were identified and removed using a mitochondrial gene expression cut-off of 10% (**Figure 2.1C**). Doublets, i.e. single droplets containing more than one cell, were identified and excluded using the DoubletFinder package (McGinnis, Murrow and Gartner, 2019).

SCTransform, a recent method for data normalisation and variance stabilisation in scRNA-seq data, accounts for variation caused by sequencing depth using a regularised negative bimodal model, while also adjusting the variance based on pooling information across genes which have similar quantities (Hafemeister and Satija, 2019). SCTransform regresses out sequencing depth or number of unique molecular identifiers (nUMI), although other sources of variation, such as cell cycle phase, batch effects or non-biological differences were also accounted for before downstream analysis. The SCTransform workflow replaces data normalisation, data scaling and finding variable genes in a single command. SCTransform also allows the removal of confounding sources of variation, aside from nUMI, such as mitochondrial mapping percentage.

Following the SCTransform workflow, principal component analysis (PCA) was performed which maps cells onto a 2-dimensional space to overcome the technical noise which can be associated with any single gene in the scRNA-seq data. The closest cells to each individual cell were found using the FindNeighbors function in Seurat which constructs a shared nearest neighbour graph. 23 unique cell clusters were identified in the $CD45^-$ dataset using the FindClusters function in Seurat which uses this shared nearest neighbour graph. Uniform Manifold Approximation and Projection (UMAP) plots were used for dimensionality reduction and for visualisation of this scRNA-seq data. In the $CD45^+$ scRNA-seq dataset (GSE212721), T cell and myeloid cell clusters were isolated and reprocessed to generate cell type specific datasets.

To mitigate this clustering bias based on technical differences, Harmony, a single cell integration tool was used (Korsunsky *et al.,* 2019). Harmony uses PCA embedding, which is created following the SCT workflow, and in this PCA space Harmony iteratively removes any batch effects present. With each iteration, similar cells are clustered together from different donors while also maximising the diversity of donors within each cell population calculating a correction score which is applied to each cell.

To validate cell cluster annotation an automated cell annotation tool, SingleR, was used (data not shown)(Aran *et al.,* 2019). SingleR employs the Human Primary Cell Atlas, Blueprint, ENCODE and Database of Immune Cell Expression databases and data from sorted immune cell RNA-seq experiments and microarray experiments. However, these databases are not skin-specific, meaning all cell clusters need to be annotated manually based on systematic visualisation of specific cell markers based on literature.

Differential gene expression (DGE) was performed using Wilcoxon Rank Sum test. DGE was displayed using heatmaps or by volcano plots. Enriched pathways were identified using pathfindR (Ulgen, Ozisik and Sezerman, 2019) and pathway activity scores were created using the AddModuleScore function in Seurat based on gene lists of interest or gene lists curated by the Kegg database. This function was used to generate *IFNG*, *TNF*, *IL17A*, *IL1B* signaling scores, proliferation and inflammation scores, collagen pathway scores and a CD40 and NLRP3 signature scores (**Table 2.7**).

Ligand:receptor interactions were identified using the nichenetr R package which combines single cell data along with established ligand:target signaling pathways to predict what ligand:receptor interactions may drive gene expression changes (Browaeys, Saelens and Saeys, 2020). Monocle3 was used to perform pseudotime trajectory analysis, which facilitates the identification of cell transitions from one cell state to another (Cao *et al.,* 2019). Nebulosa was used to display gene expression density on the UMAP (Alquicira-Hernandez and Powell, 2021).

Table 2.7 Genes involved in specific pathway activity analysis.

AddModuleScore()	**Genes**
IFNG signaling	*AKT1, CAMK2A, CAMK2B, CAMK2D, CAMK2G, CASP1, CBL, CEBPB, CREBBP, CRKL, DAPK1, EP300, IFNG, IFNGR1, IL1B, IRF1, IRF9, JAK1, JAK2, MAP2K1, MAP3K1, MAP3K11, MAPK1, MAPK3, MTOR, PIAS1, PIAS4, PIK3CA, PIK3R1, PRKCD, PTGES2, PTPN11, RAP1A, RAP1B, RAPGEF1, SMAD7, SOCS1, STAT1, STAT3*
TNF signaling	*AKT3, DNM1L, TAB1, CREB3, CEBPB, RIPK3, CHUK, MAP3K8, CREB1, ATF2, ATF6B, MAPK14, CSF1, CSF2, CREB3L4, DAB2IP, CYLD, JAG1, EDN1, PGAM5, MLKL, AKT1, AKT2, VEGFD, TAB2, FOS, TAB3, CXCL1, CXCL2, CXCL3, BIRC2, BIRC3, XIAP, ICAM1, IFNB1, FAS, IKBKB, IL1B, IL6, IL15, CXCL10, IRF1, JUN, JUNB, LIF, LTA, MAP3K5, MMP3, MMP9, MMP14, ATF4, NFKB1, NFKBIA, PIK3CA, PIK3CB, PIK3CD, PIK3R1, PIK3R2, MAPK1, MAPK3, MAPK8, MAPK11, MAPK9, MAPK10, MAPK13, MAP2K1, MAP2K3, MAP2K6, MAP2K7, PTGS2, RELA, BCL3, MAPK12, CCL2, CCL5, CCL20, CXCL6, CXCL5, CX3CL1, SELE, NOD2, MAP2K4, CREB3L2, MAP3K7, TNF, TNFAIP3, TNFRSF1A, TNFRSF1B, TRAF1, TRAF2, TRAF3, TRAF5, VCAM1, VEGFC, CASP3, ITCH, CASP7, CASP8, CASP10, CREB3L3, PIK3R3, IKBKG, TRADD, RIPK1, FADD, IL18R1, CFLAR, RPS6KA4, MAP3K14, SOCS3, CREB3L1, RPS6KA5, BAG4, CREB5*
IL17A signaling	*DEFB4B, CEBPB, TRAF3IP2, IL17F, CHUK, IL17RE, MAPK14, CSF2, CSF3, DEFB4A, ELAVL1, MAPK15, TAB2, FOS, FOSB, IL17RA, TAB3, IL17C, IL17B, TBK1, CXCL1, CXCL2, CXCL3, GSK3B, USP25, HSP90AA1, HSP90AB1, S100A7A, IFNG, IKBKB, IL1B, IL4, IL5, IL6, CXCL8, IL13, IL17A, CXCL10, JUN, JUND, LCN2, MMP1, MMP3, MMP9, MMP13, MUC5AC, NFKB1, NFKBIA, ANAPC5, IL17D, IL17RB, MAPK1, MAPK3, MAPK4, MAPK6, MAPK7, MAPK8, MAPK11, MAPK9, MAPK10, MAPK13, PTGS2, RELA, S100A7, S100A8, S100A9, MAPK12, CCL2, CCL7, CCL11, CCL17, CCL20, CXCL6, CXCL5, SRSF1, IL25, MAP3K7, TNF, TNFAIP3, HSP90B1, TRAF2, TRAF3, TRAF5, TRAF6, MUC5B, FOSL1, CASP3, CASP8, IL17RC, IKBKG, TRADD, FADD, TRAF4, IKBKE*
IL1B signaling	*AKT1, ATF2, C11orf52, CCL2, CHUK, ECSIT, HSPB2, IKBKB, IKBKG, IL1A, IL1B, IL1R1, IL1RAP, IRAK1, IRAK2, IRAK3, IRAK4, JUN, LOC100996792, MAP2K1, MAP2K2, MAP2K3, MAP2K4, MAP2K6, MAP2K7, MAP3K1, MAP3K2, MAP3K3, MAP3K7, MAPK1, MAPK14, MAPK3, MAPK8, MAPK9, MAPKAPK2, MYD88, NFKB1, NFKBIA, NFKBIB, PELI1, PELI2, PIK3R1, PIK3R2, PLCG1, PRKCZ, PTPN11, REL, RELA, SQSTM1, TAB1, TAB2, TAB3, TMEM189, TOLLIP, TRAF6, UBE2N, UBE2V1*
Proliferation and Differentiation	*KRT6A, KRT6B, KRTC, KRT16, KRT17, WWOX, TP63, TRPS1, SPRR2A, KRT2, CDH13, MEF2A, CUX1, STIM1, JARID2, IGF1R, MACROH2A1, EGFR, JUND,*

	IFI27, CLASP2, KAZN, SLC39A1, PTPRK, SH3PXD2A, GRHL2, PDE4D, BNC2, BCL11B, KMT2C, CALML5, TEAD1, CDH1, NU98, EVPL, FTO, EPHA4, SOX6, FGFR2, SERPINB2, JUN, FABP5, TACSTD2, KRT15, PNRC1, CALM2, CTSB, HEXIM1, AMD1, PPP2CA, CD99, KLF4, YBX1, SOX4, DCN, DUSP1, MCL1
Inflammation	*S100A7, S100A9, SERPINB4, S100A8, DOCK5, PATJ, SREBF2, PHLPP1, DYRKIA, PUM2, NLRC5, SERPINB3, C10orf99, FTO, CCL27, NFKBIA, CXCL14, AREG, EIF4A1, ARF6, PFN1, HBEGF, JUNB, CXCL8, CXCL2,TNFAIP3*
Collagen pathway	*COL21A1, COL8A2, COL4A3BP, COL8A1, COL24A1, COL10A1, COL6A6, COL27A1, COL4A2, COL4A1, COL14A1, COL15A1, COL6A5, COL5A3, COL6A2, COL16A1, COL7A1, COL12A1, COL1A2, COL6A1, COL18A1, COL1A1, COL5A1, COL6A3, COL3A1, COL5A2*
CD40 signature	*HLA-DRB1, CD80, CD86, TNF, IL6, IL1B, IL1A, IL10, IL12, CD40, IL23A, NOS2, TRAF1, TRAF2, TRAF4, TRAF6, ICAM1, NFKB1, FOS, REL, STAT3, MMP3, VEGFA*
NLRP3 signature	*IL1B, NLRP3, NEK7, IL18, CXCL8, CXCL1, CXCL2, CCL5, MAP3K7, MAPK3, MAPK11, MAPK12, MAPK14, ATG5, ATG12, GABARAP, GABARAPL2, SUGT1, SHARPIN, RBCK1, XIAP, CARD6, IKBKE, TANK, IRF7, ANTXR1, PYCARD, CASP1, CTSB, TRPM2, PLCB4, ITPR1, VDAC1, MCU, OAS1, OAS2, OAS3, DHX33, MFN1, NAMPT, CYBA, TXN2, CARD8, FADD, CARD16, NAIP, GBP2, GBP5, AIM2, IFI16, RHOA, PKN1, YWHAE, GBP1, GBP3, CASP4, GSDMD, IFNAR1, IFNAR2, STAT1, STAT2, IRF9*

2.2.21 Statistical analysis

Statistical analyses were generated using Prism 10 software (Graphpad, San Diego, USA). Throughout the studies, non-gaussian distribution was assumed and so non-parametric tests were performed. Differences between two groups were analysed by Mann Whitney U-test; using 2-way ANOVA with uncorrected Fisher's LSD test for differences between multiple groups.

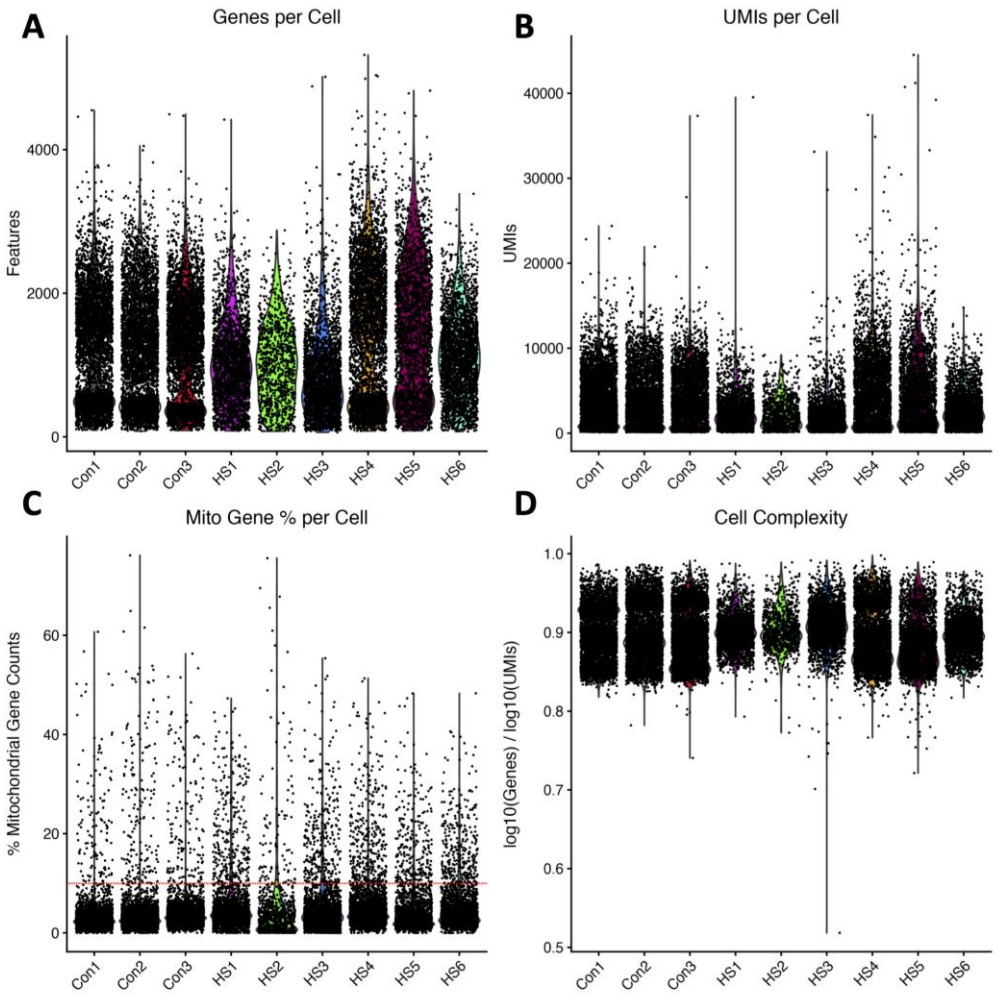

Figure 2.1 Quality control metrics of CD45$^-$ scRNA-seq data. Single cells isolated from healthy controls (Con; n=3) or HS lesional skin (HS; n=6) were purified based on absence of CD45 expression, barcoded and sequenced by 10X Genomics scRNA-seq. Quality control (QC) metrics display single cell data following the removal of doublets using DoubletFinder package. Violin plots display the number of genes per cell (A), the number of UMIs per cell (B), the percentage of mitochondrial genes per cell (C), and the cell complexity of each cell (D); all used to filter out low quality cells in each sample. The red line in (C) displays the cut-off used to remove decaying cells.

Chapter 3

Unique B/plasma cell signature differentiates HS from psoriasis and atopic dermatitis

3 Unique B/plasma cell signature differentiates HS from psoriasis and atopic dermatitis

3.1 Introduction

HS pathogenesis remains unclear, which has hindered the development of effective therapeutic strategies. The initiating event of HS is widely agreed to be hair follicle occlusion which leads to cyst formation (von Laffert *et al.*, 2010). The cyst ultimately ruptures, releasing PAMPs and DAMPs which subsequently drives an innate and adaptive immune response. Immune cells including T cells, B cells, neutrophils and mast cells have all been reported to promote HS inflammation (Moran *et al.*, 2023; List *et al.*, 2019). A strong Th17 response is evident in HS lesional skin, likely driven by innate immune cells and keratinocytes which in turn further activates keratinocytes and recruits neutrophils to the site of inflammation, creating a feed-forward inflammatory loop (Fletcher *et al.*, 2020). Inflammatory skin diseases such as psoriasis and atopic dermatitis (AD) have a relatively well defined immunopathogenesis relative to HS. Psoriasis is typically referred to as an IL-17-mediated disease due to the increased production of IL-17 cytokines, the expansion of Th17 cells in psoriasis lesions and the high success rate of anti-IL-17 therapies in treating psoriasis. On the other hand, AD is classically referred to as a Th2-mediated disease due to the prominent role of Th2 cells in driving AD pathogenesis. However, despite this, incidence of AD is twice as likely in HS patients compared with healthy individuals, indicating a clear association between HS and AD (Sherman *et al.*, 2021).

Understanding the complexities behind HS inflammation remains difficult due to the heterogenous nature of the disease (Kirby, 2021). However, bulk RNA-seq facilitates in-depth transcriptomic analysis of rare samples like HS lesional skin and allows for a greater number of samples to be analysed relative to scRNA-seq which is beneficial for a highly heterogenous disease like HS. Recently, some studies have attempted to reveal the key players responsible for HS inflammation using bulk RNA-seq analysis. Lowe *et al.,* demonstrated that HS lesional skin was distinguishable from healthy control skin and non lesional HS skin, while also indicating that HS lesions had increased activation of several inflammatory pathways including TNF, complement and B cell signaling (Lowe *et al.*, 2020). This study also used bulk RNA-seq to compare HS with psoriasis lesions, albeit from a previously published dataset, which may introduce variation when it comes to sample

preparation and sequencing (Lowe *et al.*, 2020). This analysis suggested that expression of IL-17 cytokines was comparable in HS and psoriasis lesional skin while also demonstrating that TNF signaling was elevated in HS lesions compared with psoriatic lesions.

Current treatment strategies for HS patients are limited, with the anti-TNF antibody adalimumab and the recently approved IL-17 inhibitor secukinumab the only biologics licensed for HS treatment. Approximately 60% of HS patients responded to adalimumab treatment in the PIONEER trials, with a response classified as a 50% reduction in abscess and inflammatory nodule count (Kimball *et al.*, 2016). In contrast, 80% of psoriasis patients responded to adalimumab in phase 3 clinical trials, which is characterised by a 75% improvement in disease (Gordon *et al.*, 2006).

Despite the upregulation of Th17 cell signaling in both HS and psoriasis inflammation, contrasting results are seen with IL-17 inhibition in both HS and psoriasis. IL-17A cytokine inhibition with secukinumab has proven to be a highly effective treatment in psoriasis, however secukinumab has been shown to be only moderately effective in treating HS, with only ~45% of patients responding to treatment (Langley *et al.*, 2014; Kimball *et al.*, 2023a). Simultaneous inhibition of IL-17A and IL-17F cytokines with bimekizumab has proven to be even more effective in psoriasis patients than IL-17A inhibition alone using secukinumab in a phase 3b head-to-head trial (Reich *et al.*, 2021). In HS, bimekizumab outperformed adalimumab in a phase 2 double-blind, placebo controlled randomized trial, however efficacy levels were much lower than those seen in psoriasis patients (Glatt *et al.*, 2021). Additionally, IL-17 receptor blockade with brodalumab has been shown to be a highly effective therapy in psoriasis and in a limited number of HS patients in open-labelled trials. 100% of HS patients treated weekly with brodalumab and 80% of HS patients treated fortnightly achieved a 75% clinical response (Reich *et al.*, 2022; Frew *et al.*, 2020; Frew *et al.*, 2021b). Targeting upstream of Th17 cells with IL-23 inhibitors has yielded remarkably contrasting results in HS and psoriasis patients. In psoriasis, guselkumab outperformed IL-17A inhibition with secukinumab, and recently guselkumab proved to be moderately effective in HS patients with 65% of a small cohort of patients achieving a clinical response (Reich *et al.*, 2019; Dudink *et al.*, 2023). Identifying the transcriptomic differences between HS and psoriasis lesions may explain why IL-17 inhibition is not as effective in HS as it is in psoriasis.

3.2 Aims

The aim of the experiments in this chapter was to characterise the inflammatory mediators present in HS lesional skin. First, to identify the inflammatory mediators upregulated in HS lesional skin compared with healthy control skin, and next to identify the immunological differences between HS, psoriasis and AD lesional skin.

Specifically, this chapter sought to:

- Characterise the transcriptomic profile of HS lesional skin.
    - Identify the key transcriptomic differences between HS lesional skin compared with healthy control skin using bulk RNA-seq.

- Compare the transcriptomic profile of HS, psoriasis and AD lesional skin.
    - Using bulk RNA-seq to characterise unique inflammatory mediators regulating HS inflammation compared with other inflammatory skin diseases.

3.3 Results

3.3.1 Clinical Details

Clinical details for the healthy individuals and HS, psoriasis and AD patients included in the RNA-seq analysis are shown in **Table 3.1**. HS patients were recruited as part of an investigator-led, open-label, single arm clinical trial of adalimumab in moderate-severe HS, including only HS patients with Hurley 2 or 3. HS lesional biopsies were taken within 2 cm of an inflammatory nodule or abscess (**Table 3.2**). Healthy individuals, psoriasis and AD patients were recruited as part of a non-interventional, case control study involving longitudinal biological sampling. Skin biopsies were collected from areas of active disease and from the arm, leg or trunk of the healthy controls (**Table 3.2**). Due to the typical anatomical locations of psoriasis, atopic dermatitis and HS, punch biopsies were taken from different anatomical locations in each disease group (**Table 3.2**).

The mean age of healthy individuals was 32.8 years (y) ± a SD of 9.7 (n=19), 37.4 y ± SD of 9.7 for HS patients (n=15), 47.9 y ± SD of 15.1 for psoriasis patients and 49.4 y ± SD of 17.1 for AD patients. 57.9% of healthy individuals, 92.85% of HS patients, 23.8% of psoriasis patients and 26.32% of AD patients were female. 62.5% of HS patients were Hurley stage 2 and 37.5% of HS patients were Hurley stage 3. No Hurley stage 1 patients were included in the HS cohort in this study. The mean PASI score for psoriasis patients was 11.8 ± SD of 4.8. The mean EASI score for AD patients was 15.6 ± SD of 8.2. Healthy individuals had a mean BMI of 25.3 kg/m^2 ± SD of 4.2, HS patients had a BMI of 35.1 kg/m^2 ± SD of 9, psoriasis patients had a BMI of 27.8 kg/m^2 ± SD of 5.2 and AD patients had a BMI of 26.5 kg/m^2 ± SD of 4.7. 57.2% of HS patients were smokers, 28.5% were ex-smokers and 14.3% were non-smokers, compared with healthy individuals who were predominantly non-smokers (63.2%), with 21.2% being current smokers and 15.8% being ex-smokers. 19% of psoriasis patients were smokers, 42.9% were ex-smokers and 38.1% were non-smokers. 7.1% of AD patients were smokers, 57.1% were ex-smokers and 35.7% were non-smokers.

Table 3.1 Clinical details of healthy individuals (HC; n=19), HS (n=15), psoriasis (PsO; n=21) and atopic dermatitis (AD; n=15) patients included in RNA-seq analysis. Statistical significance was calculated using Pearson's Chi-square test for categorical data and one-way ANOVA for numerical data.

		HC (n=19)	HS (n=14)	PsO (n=21)	AD (n=15)	p-value
Female (n, %)		11 (57.9%)	13 (92.85%)	5 (23.8%)	5 (33.33%)	**<0.001**
Age (years) (mean ± SD)		32.8 ± 9.7	37.4 ± 9.7	47.9 ± 15.1	49.4 ± 17.1	**0.0007**
Smoking Status (n,%)	Current Ex Non	4 (21.2%) 3 (15.8%) 12 (63.2%)	8 (57.2%) 4 (28.5%) 2 (14.3%)	4 (19%) 9 (42.9%) 8 (38.1%)	1 (6.67%) 8 (53.33%) 5 (33.33%)	**0.004**
Hurley Stage (n,%)	2 3	-	10 (62.5%) 6 (37.5%)	-	-	**-**
PASI (mean ± SD)		-	-	11.8 ± 4.8	-	**-**
EASI (mean ± SD)		-	-	-	15.6 ± 8.2	**-**
BMI (kg/m^2) (mean ± SD)		25.3 ± 4.2	35.1 ± 9.0	27.8 ± 5.2	26.5 ± 4.7	**<0.0001**
Waist circumference (cm) (mean ± SD)		85 ± 12.1	104.4 ± 26.8	98.4 ± 13.5	94.7 ±14.7	**0.015**

Table 3.2 Anatomical location of skin biopsy take from healthy individuals (HC; n=19) and HS (n=15), psoriasis (PsO; n=21) and atopic dermatitis (AD; n=15) patients for bulk RNA-seq analysis.

Biopsy Location	HC (n=19)	HS (n=14)	PsO (n=21)	AD (n=15)
Abdomen	0	1 (7.1%)	0	0
Arm	15 (78.9%)	0	3 (14.3%)	5 (33.3%)
Axilla	0	5 (35.7%)	0	0
Groin	0	3 (21.4%)	0	0
Intermammary	0	2 (14.3%)	0	0
Leg	3 (15.8%)	0	12 (57.1%)	8 (53.3%)
Thigh	0	3 (21.4%)	0	0
Trunk	1 (5.3%)	0	6 (28.6%)	1 (6.67%)

3.3.2 Transcriptomic differences between healthy control skin and HS lesional skin

The key inflammatory mediators which contribute to HS inflammation are not well defined, and this has limited the development of novel treatments for HS. In order to gain a better understanding of HS pathogenesis, the transcriptomic profile of HS lesions and healthy control skin were analysed by bulk RNA-seq. HS patients were recruited as part of an investigator-led, open-label, single arm clinical trial of adalimumab in moderate-to-severe HS (Hurley 2 and 3) (EudraCT number 2016-001566028). Biopsies from HS lesional skin (n=15) were taken from within 2 cm of an inflammatory nodule or abscess. Lesional skin from psoriasis (n=21) and AD patients (n=15) and healthy control skin (n=19) were recruited as part of a non-interventional case-control study with longitudinal biological sampling.

Patients (**Table 3.1**) were recruited from the dermatology department in St Vincent's University Hospital by members of the dermatology research team which included Dr Roisin Hambly, Dr Helen Rea, Dr Vivien Marasigan and Dr Shivashini Kirthi. 6 mm punch biopsies were collected (**Table 3.2**) and RNA isolation from skin biopsies and cDNA synthesis was performed by Dr Solene Gatault and Dr Roisin Hambly. Sample biopsies were snap frozen in liquid nitrogen and stored at -80°C until RNA isolation was completed as previously described (Kelly *et al.*, 2015). High quality samples were sent for bulk RNA-seq to AbbVie in Chicago, IL, USA. RNA-seq data were analysed as per **Section 2.2.17**. Bulk RNA-seq was performed by AbbVie and read alignment and quantification was performed by Dr Luis Fernando Iglesias Martinez in UCD. From here I performed normalisation, differential gene expression and subsequent pathway analysis of bulk RNA-seq data.

To estimate the broad transcriptomic landscape of HS lesions compared with healthy control skin, hierarchal clustering of individual samples was performed. To aid in differentiating HS lesional and healthy control samples, the distances created from the hierarchal clustering were displayed by heatmap (**Figure 3.1A**). This heatmap estimates sample similarities, clustering healthy control samples in two hierarchal branches which lie away from HS lesional skin. Despite some overlap between HS lesional and healthy control samples, PCA broadly clustered healthy control skin samples away from HS lesional skin, signifying a largely distinct transcriptome exists in HS lesions compared with healthy control skin (**Figure 3.1B**).

Differentially expressed genes (DEGs) between HS lesional and healthy control skin were identified using the Wald test in DESeq2 (adj p value≤ 0.05). 5,384 genes were identified as significantly differentially expressed, 3,004 of those were upregulated in HS lesions and 2,380 genes were significantly upregulated in healthy control skin (**Table 8.1**-**Table 8.2**). Volcano plot was used to visualise the DEGs between HS lesional and healthy control skin (**Figure 3.2A**). The X-axis of the volcano plot represents Log_2 fold change (FC); genes with a negative fold change had increased expression in HS lesional skin and genes with a positive fold change had increased expression in healthy control skin. The Y-axis of the volcano plot represents the significance of the differential expression. Genes in red are those which have a high log fold change (FC ≥ 1 or FC ≤ -1). Genes highly differentially expressed in HS lesions included immunoglobulin genes (*IGHG2*, *IGHG1*, *IGHG4*), B cell associated genes (*MZB1*, *JCHAIN*), antimicrobial genes (*S100A7*, *S100A8*, *S100A9*) and a number of proinflammatory mediators (*IL23R*, *CXCL1*, *CCL20*, *IFNG*, *IL6).* Of the genes significantly differentially expressed in healthy control skin, *IL12A,* which promotes Th1 differentiation (**Figure 1.3**), the antimicrobial dermicidin (*DCD*) and *VSTM2A,* which is involved in Wnt signaling, were of particular interest.

Relative expression of proinflammatory mediators further delineated the inflammatory profile that existed in HS lesions (**Figure 3.2B**). *TNF*, a target of currently approved biologics for HS treatment, and the AMPs *S100A8* and *S100A9* were significantly upregulated in HS lesions compared with healthy control skin, consistent with other studies (Wolk *et al.*, 2011; Moran *et al.*, 2023). Additionally, expression of Th17-associated genes including *CCL20*, *CXCL1* and *IL23R* were elevated in HS lesions, as were *IL6*, *CXCL13*, *TGFB1* and *IL1R1* demonstrating a broad range of inflammatory mediators elevated in HS lesions. Interestingly, the Th1 associated *IL12A* was significantly downregulated in HS lesional skin relative to healthy control skin.

To understand the biological processes altered in HS lesions compared with healthy control skin, pathway analysis was performed using the DEGs between HS lesions and healthy control skin. Looking at gene ontology terms enriched from the DEGs, 58 biological processes were significantly enriched (adj p value≤ 0.05) (**Figure 3.3A**). A number of T cell processes were enriched, including cellular response to IFN-γ (GO:0071346, p=0.0012), regulation of T cell activation (GO:0050863, p=0.0024), Th17 cell differentiation

(GO:0072539, p=0.016), and cellular response to IL-6 (GO:0071354, p=0.024199844). Innate immune processes including positive regulation of IL-1β production (GO:0032731, p=0.004462814), neutrophil chemotaxis (GO:0030593, p=0.045409118) and DC migration (GO:0036336, p=0.045409118) were also significantly enriched in HS lesions.

To confirm the upregulation in proinflammatory processes, pathway analysis was performed using the Kegg database as a reference. 180 Kegg pathways were significantly enriched from the DEGs between healthy control skin and HS lesions. To establish inflammatory pathway activity an enrichment score was calculated for each enriched Kegg pathway in each biological sample. The enrichment scores for inflammatory pathways of interest were visualised by heatmap (**Figure 3.3B**). Inflammatory pathways including T cell receptor, TNF, NLR, B cell receptor and IL-17 signaling were more active in the HS lesions demonstrating the broad range of inflammatory pathways which contribute to HS inflammation. Interestingly, oxidative phosphorylation was more active in healthy control skin suggesting a dysregulated metabolic profile may exist in HS lesions.

To understand what regulated the proinflammatory profile in HS, transcription factor activity was calculated. DoRothEA calculates an enrichment score based on the expression of genes which are regulated by transcription factors rather than the expression of the transcription factor itself (Garcia-Alonso *et al.*, 2019). Transcription factors which regulate inflammatory mediators including *STAT1*, *STAT2*, *STAT3* and *NFKB1* were highly enriched in HS lesions (**Figure 3.4A**). The most highly enriched transcription factor, *STAT1*, regulated the expression of multiple genes which were significantly differentially expressed in HS lesions (**Figure 3.4B**). Genes including *CCR5*, *CCR1*, *CCL3* and *IRF1* had elevated expressed in HS lesions and are known to be downstream of *STAT1*. The enrichment of *STAT3* in HS lesions is expected considering the increasingly prominent role of Th17 cells reported in HS inflammation. *STAT3* plays an important role in the generation of Th17 cells and regulates Th17 cell differentiation and cytokine production, reinforcing the previously reported importance of Th17 cells in HS inflammation (Yang *et al.*, 2007; Moran *et al.*, 2017). Given the increased expression of *TNF* in HS lesions, it is unsurprising that *NFKB*, which becomes activated by TNF, is enriched in HS lesions. NF-κB regulates the expression of IL-1β IL-6 and IL-8, all of which have been previously reported to be elevated in HS lesions (Hotz *et al.*, 2016; Witte-Handel *et al.*, 2019)

In conclusion, transcriptomic analysis of HS lesions revealed a unique proinflammatory profile existed in HS lesions compared with healthy control skin. HS lesions had increased expression of proinflammatory mediators and more active inflammatory pathways, contributing to inflammation in HS lesions.

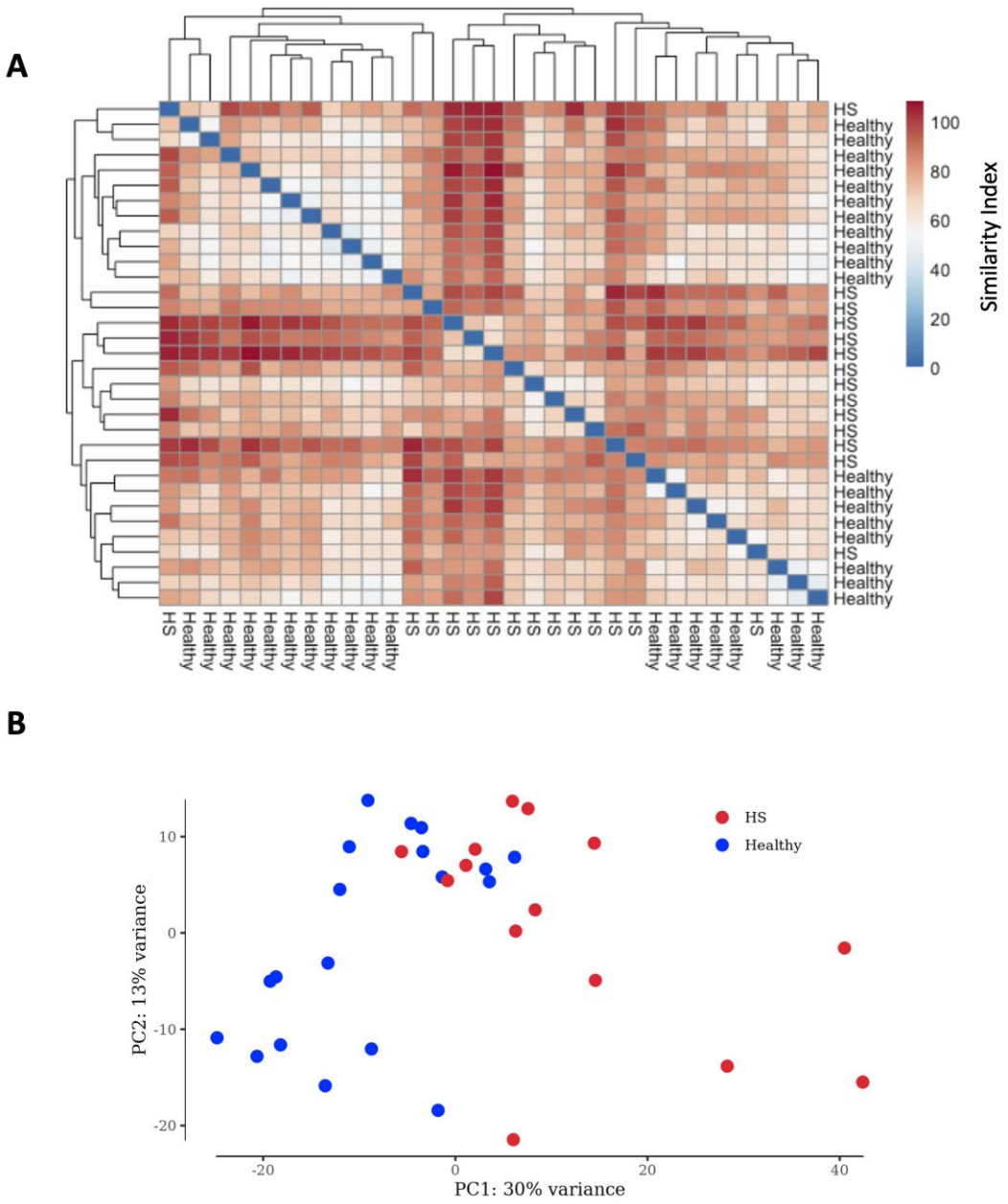

Figure 3.1 HS lesions exhibited a distinct transcriptome compared with healthy control skin. Bulk RNA-seq was performed on HS lesional biopsies (n=14) and healthy control skin (n=19). Heatmap of the transcriptomic similarities between HS lesions and healthy control skin based on hierarchal clustering distances (A). Principal component analysis demonstrates the transcriptomic differences between HS lesions (n=14) and healthy control skin (n=19) (B).

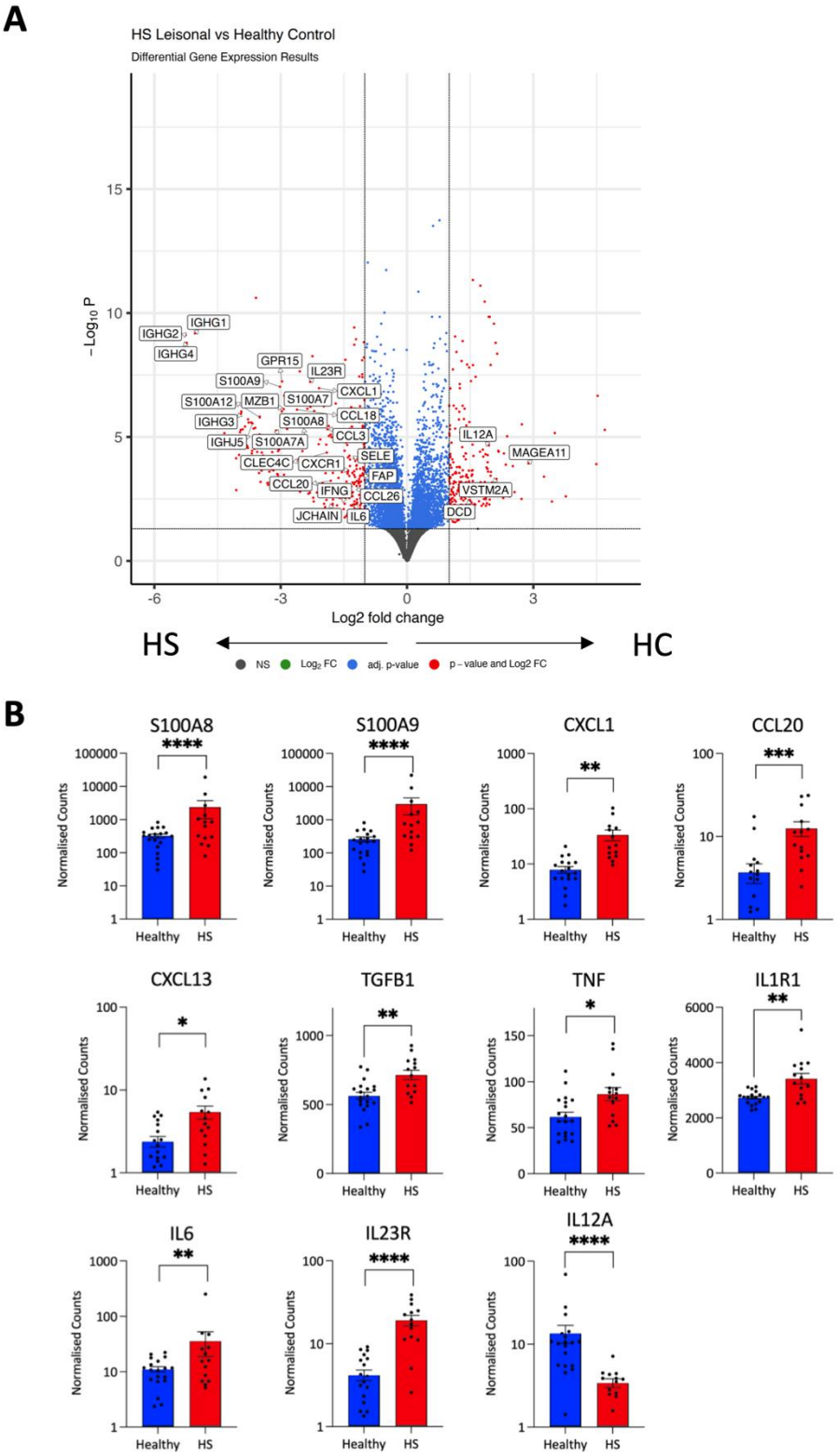

Figure 3.2 HS lesions had increased expression of proinflammatory mediators compared with healthy control skin. Bulk RNA-seq was performed on HS lesions (n=14) and healthy control skin (n=19). Differentially expressed genes between HS lesional and healthy control skin were displayed by volcano plot. Genes with elevated expression in HS lesions have a negative Log_2 fold change, genes with higher expression in healthy control skin have a positive fold change. The $-Log_{10}$ P Y axis is a measure of significance (A). Normalised expression of inflammatory genes of interest in HS lesions and healthy control skin (B). Graphs represent individual samples with mean ± SEM for each group. Statistical significance was calculated using Mann-Whitney t-test; * p≤ 0.05, ** p≤ 0.01, *** p≤ 0.001, **** p≤ 0.0001.

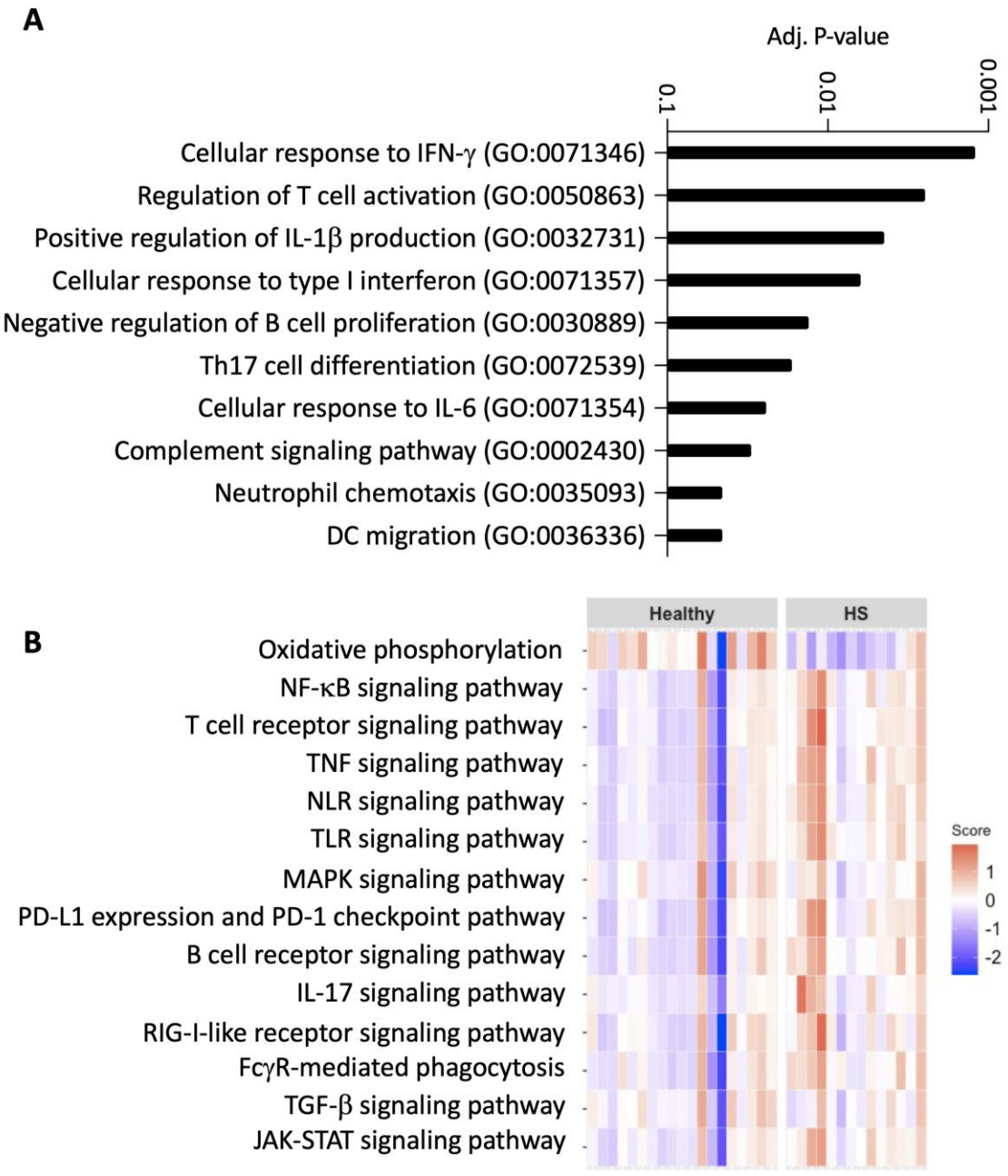

Figure 3.3 Enrichment of inflammatory pathways in HS lesions. Bulk RNA-seq was performed on HS lesions (n=14) and healthy control skin (n=19). Gene ontology terms of interest significantly enriched from the differentially expressed genes between HS lesions and healthy control skin (A). Enrichment scores of Kegg pathways of interest in individual samples. Significantly dysregulated pathways were enriched from the differentially expressed genes between HS lesions and healthy control skin (B).

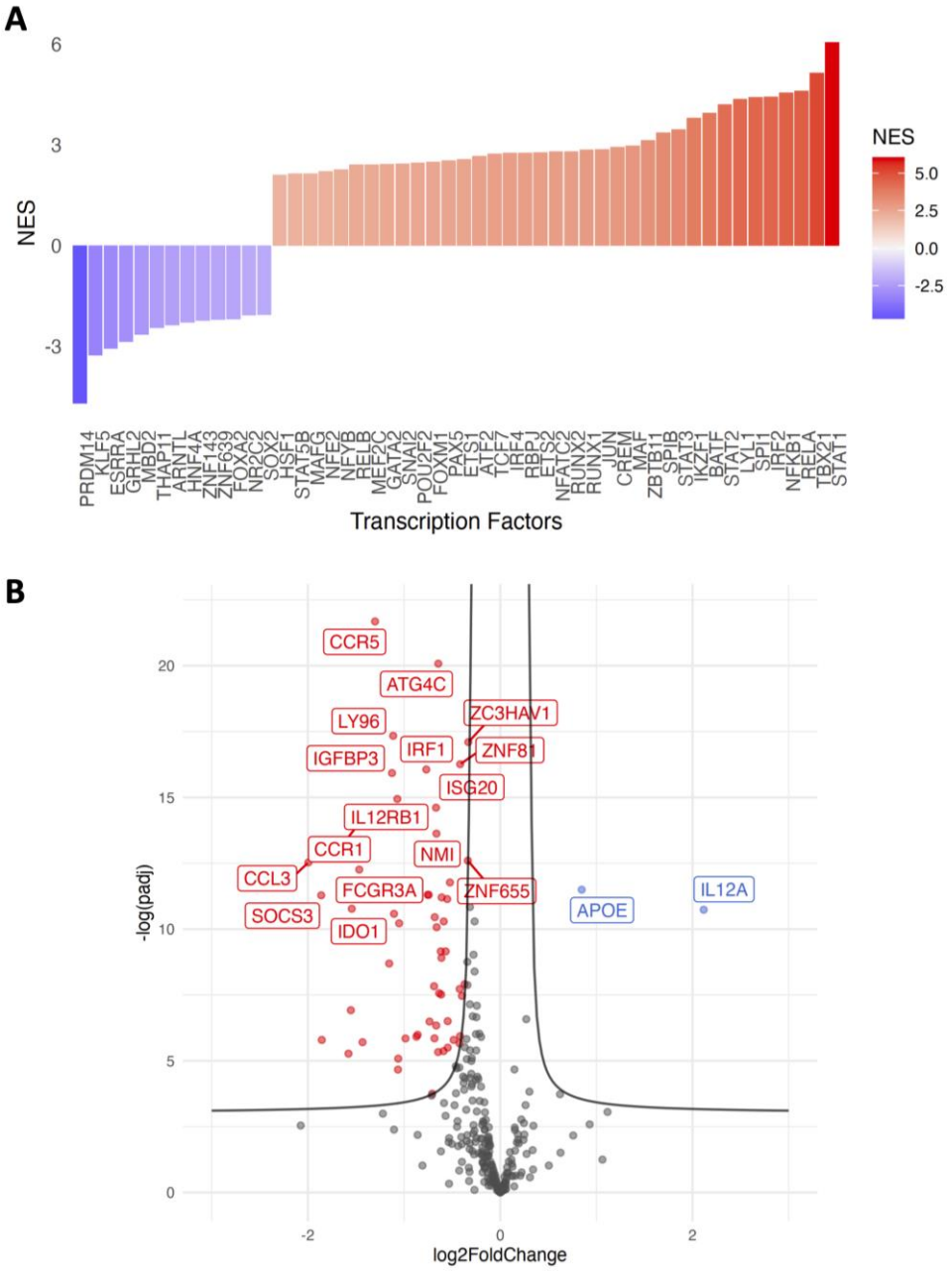

Figure 3.4 HS lesions have dysregulated transcription factor usage relative to healthy control skin. Bulk RNA-seq was performed on HS lesions (n=14) and healthy control skin (n=19). Transcription factor usage analysis highlights an enrichment of transcription factors in HS lesions which mediate proinflammatory responses (A). Volcano plot of genes regulated by the transcription factor STAT1. Genes significantly increased in HS lesions have a negative $\log_2$ fold change. Genes with higher expression in healthy control skin have a positive $\log_2$ fold change. The –log(padj) Y axis is a measure of significance (B).

3.3.3 HS and psoriasis lesions have distinct inflammatory mediators regulating inflammation

In the previous section, the data established clear differences in inflammatory gene expression between healthy control skin and HS lesional skin. Many of these inflammatory mediators also promote inflammation in other skin diseases including psoriasis, and so this section will further delineate the genes regulating HS inflammation from those mediating inflammation in psoriasis.

Hierarchal clustering of bulk RNA-seq data generated almost complete separation between HS and psoriasis lesions, suggesting that a unique transcriptomic profile existed in each of these inflammatory skin conditions (**Figure 3.5A**). Hierarchal clustering distances demonstrated a greater homogeneity among psoriasis lesions than among HS lesions. This is supported by PCA which clustered psoriasis lesional samples away from HS lesional samples (**Figure 3.5B**). Psoriasis samples also clustered more closely together than HS lesions which exhibited increased heterogeneity between samples.

Similar inflammatory mediators have previously been reported to be dysregulated in both HS and psoriasis lesions. To establish the transcriptomic differences between HS and psoriasis lesions, differential gene expression analysis was performed. Volcano plot visualised the 11,999 genes found to be differentially expressed between HS and psoriasis lesions (**Figure 3.6A**). 5,649 genes were upregulated in psoriasis lesions (**Table 8.3**), and 6,350 genes were upregulated in HS lesions (**Table 8.4**). The X-axis of the volcano plot represents Log_2 fold change (FC); genes with a negative fold change had increased expression in HS lesional skin and genes with a positive fold change had increased expression in psoriasis lesional skin. The Y-axis of the volcano plot represents the significance of the differential expression. Genes in red are those which have a high fold change ($FC \geq 1$ or $FC \leq -1$). The genes found to be most differentially expressed in psoriasis lesions included AMPs (*S100A7*, *S100A8*, *S100A9*), inflammatory keratins (*KRT6A*, *KRT16*, *KRT17*), IL-17 associated genes (*CXCL8*, *IL17A*, *IL17F*, *CCL20*), as well as the proinflammatory cytokines *IL1B* and *IFNG* (**Figure 3.6A**). Conversely, genes most differentially expressed in HS lesions included B cell and plasma cell associated genes (*MZB1*, *JCHAIN*, *IGHA1*, *IGHA2*, *IGLL5*) (**Figure 3.6A**).

Looking at the relative expression of genes can provide additional biological insight into the DEGs found above. IL-17 associated genes including *IL17A*, *CCL20*, *CXCL8*, *S100A8* and *KRT6A* were highly expressed in psoriasis lesions in comparison with HS lesions (**Figure 3.6B**). Similarly, *IL23A* found upstream of Th17 cells was elevated in psoriasis lesions, however *RORC*, which encodes a transcription factor selectively found in Th17 cells, and *IL17RC*, which encodes an IL-17A receptor, had increased expression in HS lesions (**Figure 3.6B**). Interestingly, HS IL-17^{+} have recently been found to have elevated expression of *RORC* relative to psoriasis IL-17^{+} cells, replicating these findings (Kim *et al.*, 2023). Psoriasis lesions also had increased expression of the inflammatory cytokine *IL1B* which is important for Th17 development (Revu *et al.*, 2018). Relative to psoriasis lesions, HS lesions had increased expression of the inflammasome component *NLRP1*, the B cell associated gene *CD79A* and *CCL27* which recruits T cells to the skin (Fenini *et al.*, 2020; Huse *et al.*, 2022; Homey *et al.*, 2002).

Differential gene expression highlighted B cell associated genes and immunoglobulin genes as highly upregulated in HS lesions. To elaborate on this, the relative expression of key B cell and immunoglobulin genes was visualised by heatmap (**Figure 3.7**). A cohort of HS lesions had high expression of this B cell signature, indicating the potential to stratify HS patients based on the presence of a B cell signature.

To understand the immunological pathways that differed between HS and psoriasis lesions pathway analysis was performed on DEGs upregulated in the respective diseases. Using the Kegg database as a reference, HS lesions had an enrichment of key inflammatory pathways, including Th17 cell differentiation and B cell receptor signaling (**Figure 3.8**). Psoriasis lesions had a strong enrichment of IL-17 signaling, oxidative phosphorylation and NLR signaling (**Figure 3.8**).

To gain a better understanding of how the pathogenesis of HS and psoriasis differ, each disease was compared to healthy control skin. This overcomes limitations associated with directly comparing HS and psoriasis lesions – for example high expression of a particular gene in psoriasis does not mean that the gene is not also dysregulated in HS, just to a lesser extent. 14,245 DEGs between psoriasis lesions and healthy control skin were identified and as previously determined, 5,313 DEGs were identified between HS lesions and healthy

control skin (**Figure 3.2**). Next, the DEGs were categorised based on whether they were uniquely differentially expressed in the psoriasis lesional and healthy control skin comparison (10,648 genes), uniquely differentially expressed in the HS lesional and healthy control skin comparison (1,716 genes) or if the genes were differentially expressed in both comparisons (3,597 genes) (**Figure 3.9A**). Unique to psoriasis pathogenesis were many IL-17 signaling genes including *IL17A*, *IL17F*, *IL17C*, *KRT16*, *KRT17*, *KRT6A*, *CXCL8*, as well as *IL1B* and *IL23A* (**Figure 3.9A**), giving a clear indication of the importance of IL-17 signaling in psoriasis pathogenesis. HS lesions had the unique upregulation of a broad variety of inflammatory mediators including IL-1 signaling gene *IL1R1*, B cell associated *CD79A* and *JCHAIN*, immunoglobulin genes, *EOMES,* which regulates T cell function, and the Th2 signature cytokine *IL5*.

3,597 genes were differentially expressed in both HS and psoriasis lesions when compared with healthy control skin (**Figure 3.9A**). Amongst these included a number of Th17 associated genes including *RORC*, *IL23R* and *KLRB1* and genes found downstream of IL-17 cytokines including *KRT6B*, *CXCL1* and *S100A8* (**Figure 3.9A**). Other genes of interest included the inflammatory cytokines *IFNG* and *IL36G* and the inflammasome associated *NLRP3* and *CASP1* (**Figure 3.9A**). Interestingly, both HS and psoriasis lesions had increased expression of *FAP*, indicative of fibroblast activation and increased expression of complement genes (**Figure 3.9A**).

Pathway analysis was performed to understand, beyond individual genes, what inflammatory pathways may be driving HS and psoriasis inflammation, and what pathways were similarly dysregulated in both diseases (**Figure 3.9B**). The most significant gene ontology terms enriched from the DEGs uniquely found in psoriasis lesions indicated that IL-1 signaling plays a key role in psoriasis pathogenesis (**Figure 3.9B**). Interestingly, from the genes which were shared between psoriasis and HS, cellular response to interferon-gamma and cytokine-mediated signaling pathway were significantly enriched (**Figure 3.9B**), highlighting the importance of cytokine signaling in both HS and psoriasis.

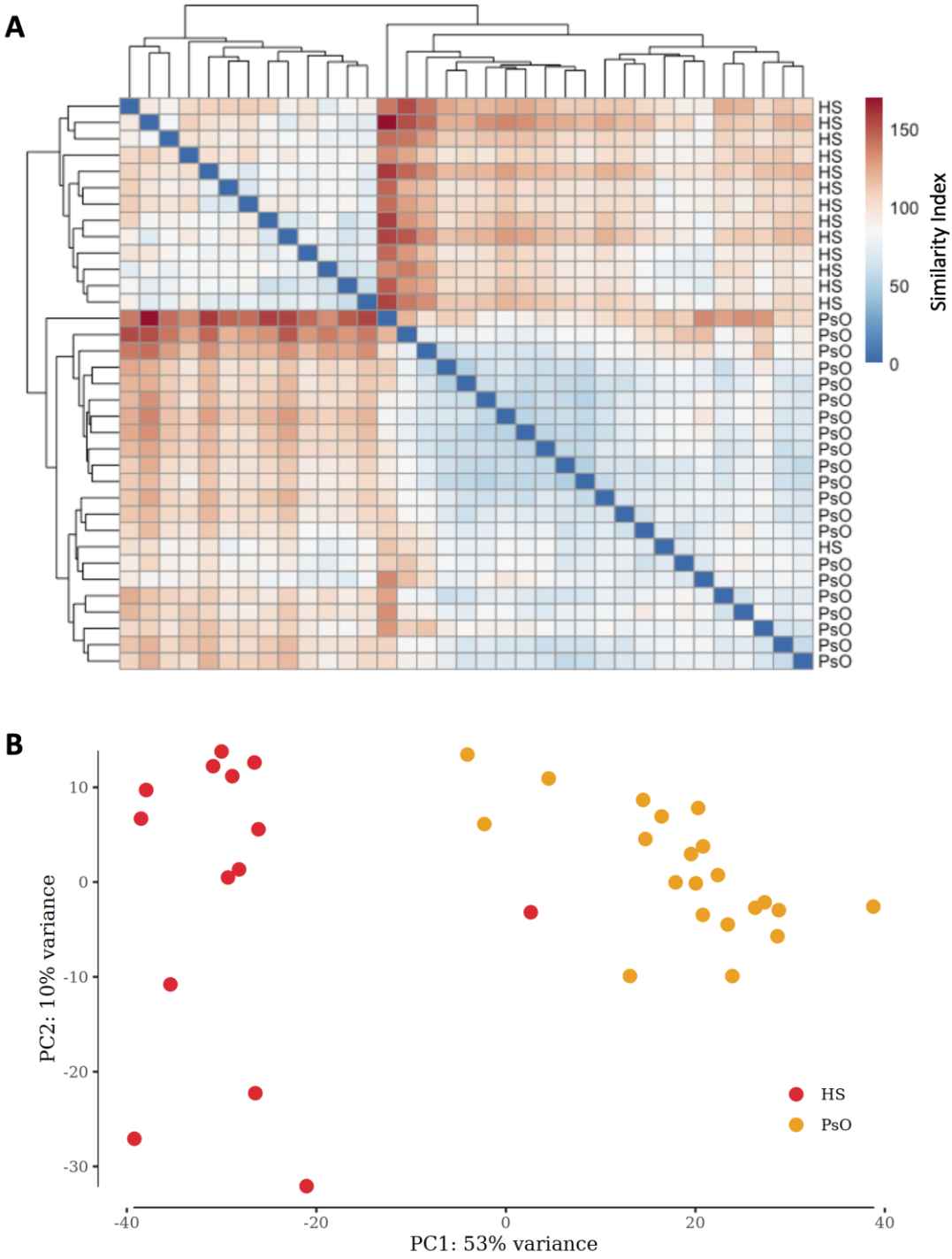

Figure 3.5 Evaluating transcriptomic differences in HS and psoriasis lesions by hierarchal clustering and principal component analysis. Bulk RNA-seq was performed on HS (n=14) and psoriasis lesions (n=21; PsO). Heatmap of transcriptomic similarities between HS and psoriasis lesions based on hierarchal clustering distances (A). Principal component analysis demonstrates distinct transcriptomic profiles between HS and psoriasis lesions (B).

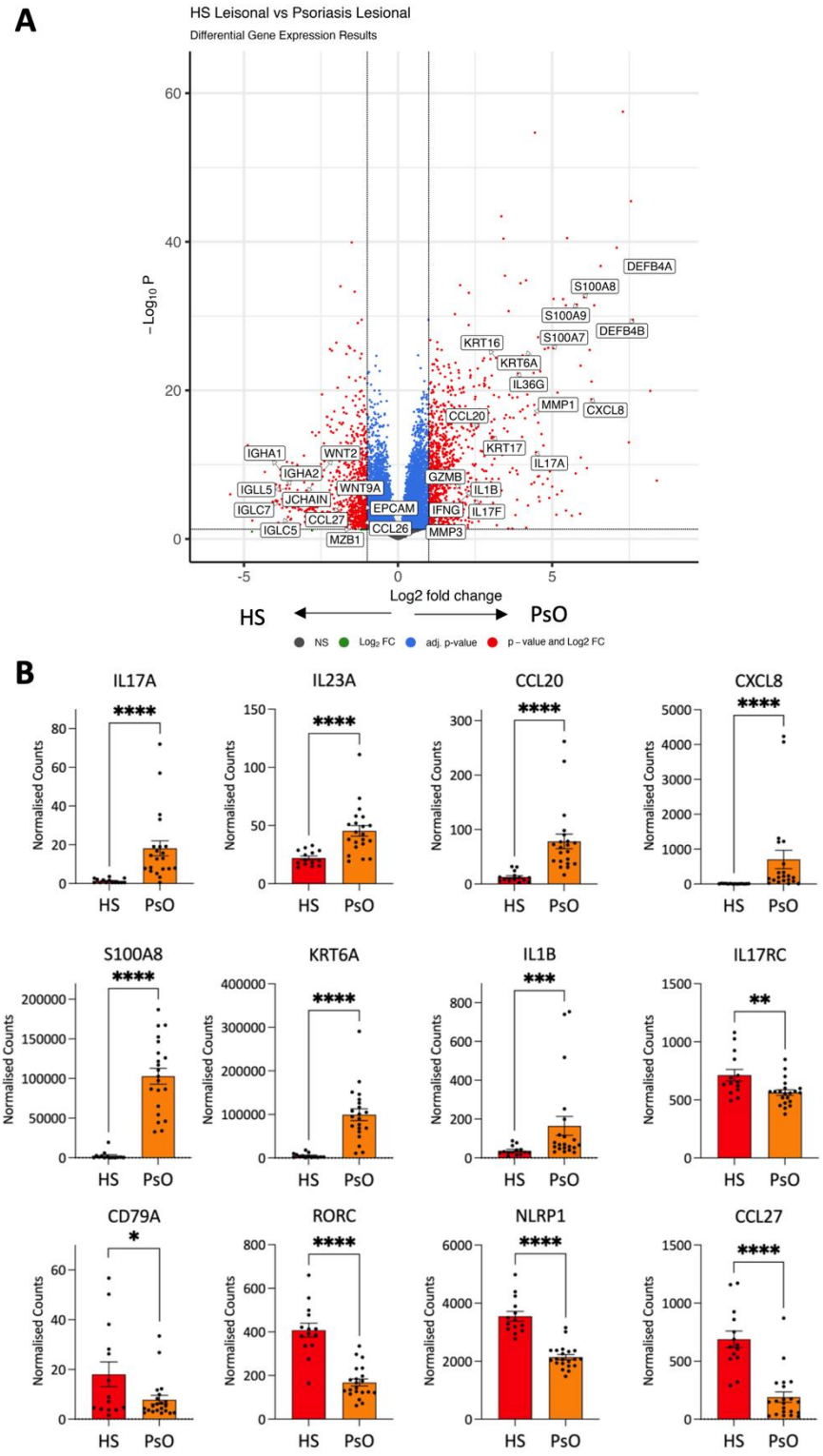

Figure 3.6 Differential gene expression analysis of HS and psoriasis lesions. Bulk RNA-seq was performed on HS (n=14) and psoriasis lesions (n=21; PsO). Differentially expressed genes between HS and psoriasis lesions are visualized by volcano plot. Genes with elevated expression in HS lesions have a negative Log_2 fold change, genes with higher expression in psoriasis lesions have a positive fold change. The $-Log_{10}$ P Y axis is a measure of significance (A). Normalised expression of inflammatory genes of interest in HS and psoriasis lesions (B). Graphs represent individual samples with mean ± SEM for each group. Statistical significance was calculated using Mann-Whitney t-test; * p≤ 0.05, ** p≤ 0.01, *** p≤ 0.001, **** p≤ 0.0001.

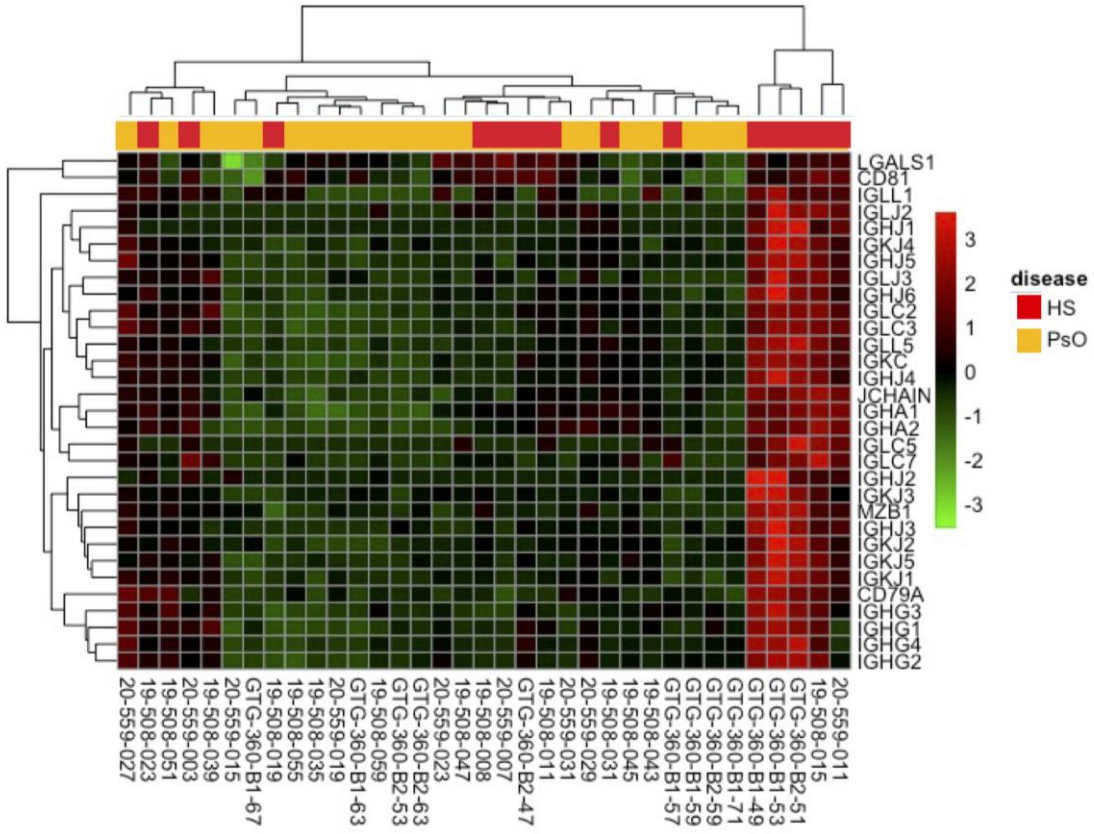

Figure 3.7 Increased expression of immunoglobulin and B cell associated genes in a subset of HS lesions. Bulk RNA-seq was performed on HS (n=14) and psoriasis lesions (n=21; PsO). Heatmap of relative gene expression of selected immunoglobulin and B cell associated genes in HS and psoriasis lesions.

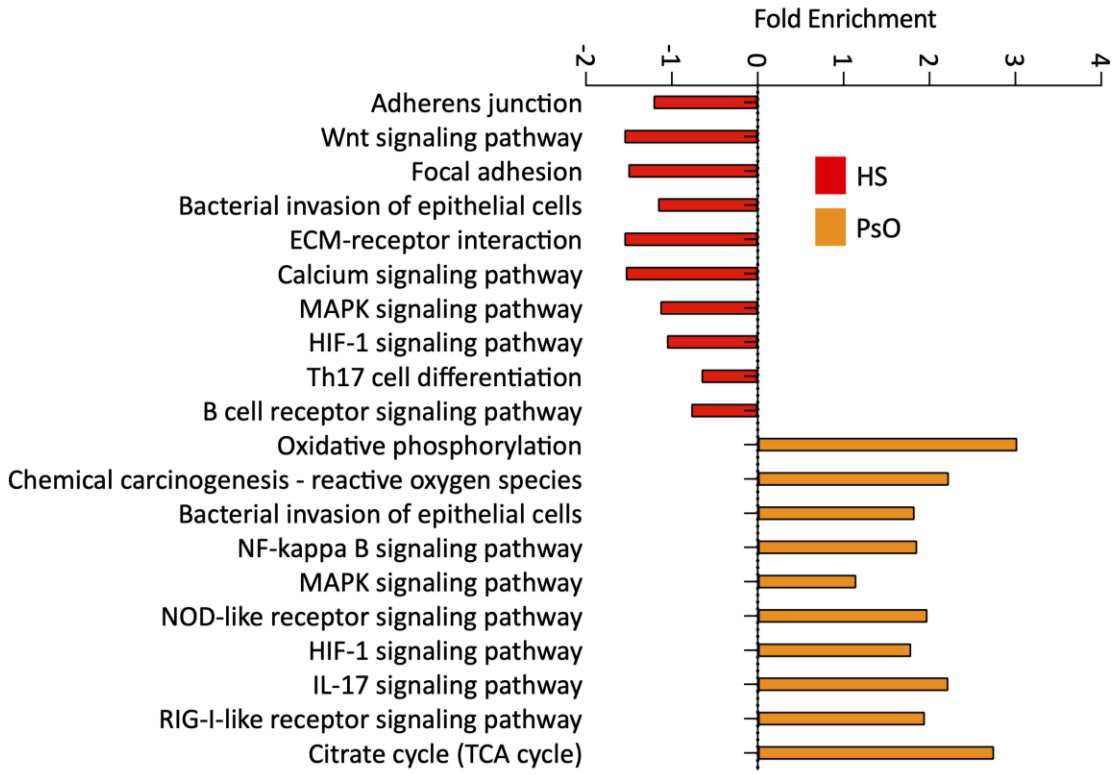

Figure 3.8 Pathway analysis displaying immune pathways enriched in HS and psoriasis lesions. Bulk RNA-seq was performed on HS (n=14) and psoriasis lesions (n=21). Bar chart displaying the fold enrichment of significantly enriched pathways from differentially expressed genes elevated in HS lesions (red) and psoriasis lesions (orange).

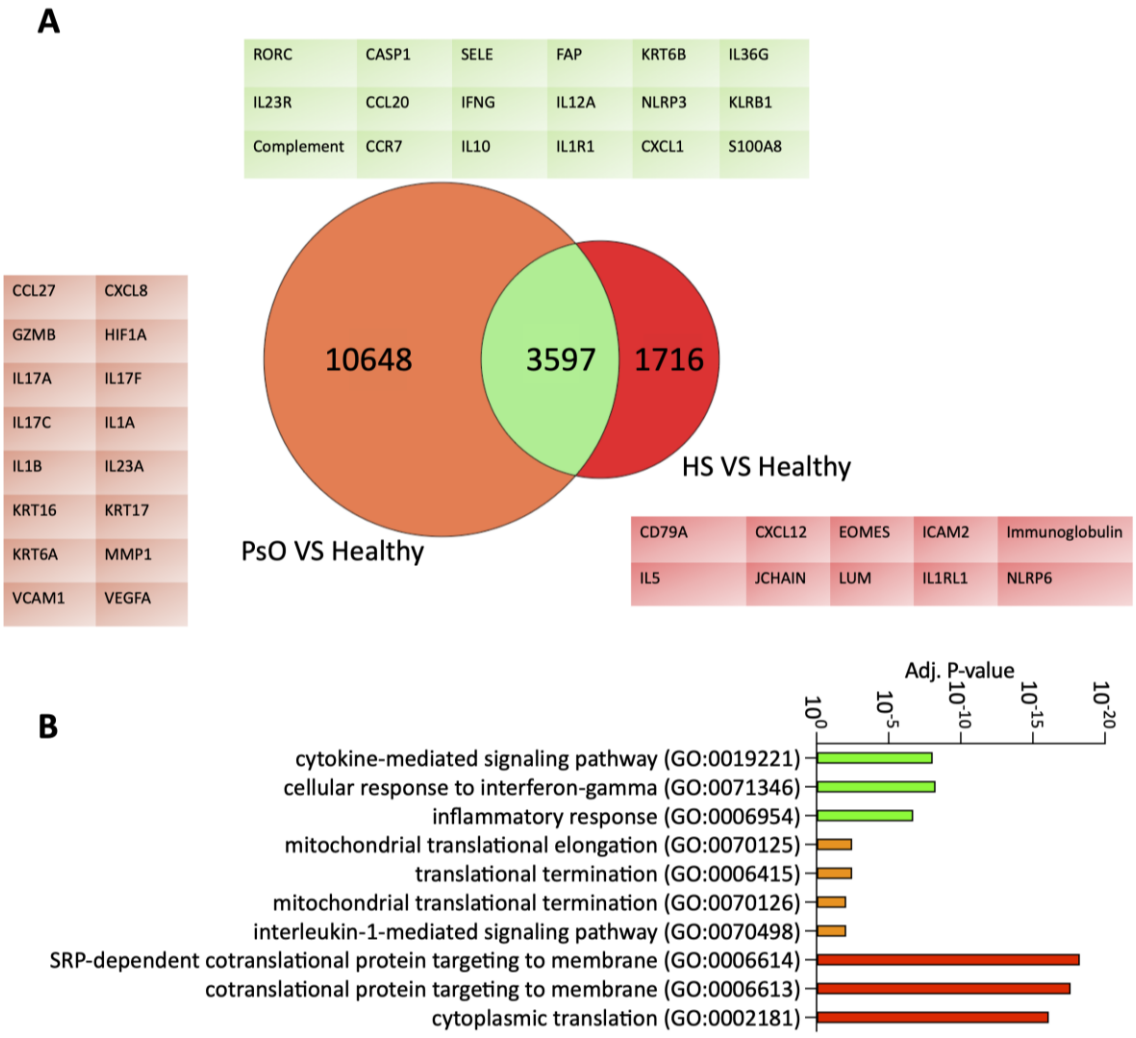

Figure 3.9 HS and psoriasis lesions have distinct drivers of inflammation. Bulk RNA-seq was performed on HS (n=14) and psoriasis lesions (n=21). Venn diagram illustrating the shared differentially expressed genes between HS and psoriasis lesions when compared to healthy control skin (A). Top 3 gene ontology terms enriched from the differentially expressed genes unique to HS (red) and psoriasis (orange) or shared (green) between them when compared with healthy control skin (B).

3.3.4 B cell and TNF signature differentiates HS and AD lesional skin

Having demonstrated the transcriptomic and pathogenic differences between HS and psoriasis lesions, next the transcriptomic differences between HS and AD were evaluated. AD has an interesting association with HS, as HS patients are twice as likely to develop AD (Sherman *et al.*, 2021). To further examine this association, bulk RNA-seq data of 14 HS lesions and 15 AD lesions were analysed.

Hierarchal clustering of HS and AD lesions broadly grouped a cohort of AD lesions together, distinct from HS lesions, while a minority of AD lesions more closely resembled some HS lesions (**Figure 3.10A**). To further investigate the broad transcriptomic differences between HS and AD lesions PCA was performed (**Figure 3.10B**). PCA grouped HS lesions away from AD lesions indicating a unique transcriptome exists in both dermatoses.

DEGs were identified between HS and AD lesional skin to understand what genes may be responsible for the differences seen in the PCA. Volcano plot visualised the 5,959 genes found to be differentially expressed between HS and AD lesions (**Figure 3.11A**). AD lesions had an upregulation of 3,052 genes (**Table 8.6**), while HS lesions had an upregulation of 2,907 genes (**Table 8.5**, **Figure 3.11A**). The X-axis of the volcano plot represents Log_2 fold change (FC), genes with a positive fold change had increased expression in HS lesional skin and genes with a negative fold change had increased expression in AD lesional skin. The Y-axis of the volcano plot represents the significance of the differential expression. Genes in red are those which have a high fold change (FC ≥ 1 or FC ≤ -1). Genes found to be upregulated in HS skin included B cell associated genes *CD79B*, *JCHAIN*, *MZB1* and immunoglobulin genes (**Figure 3.11A**). The IL23A receptor, *IL23R,* was significantly elevated in HS lesions as was *CXCL6* which acts as a neutrophil chemoattractant (**Figure 3.11A**). Conversely, AD lesions had increased expression of the AMP *S100A9*, Th2 signature cytokine *IL13*, inflammatory cytokines *IL36A* and *CXCL8* and inflammatory keratins *KRT6A* and *KRT16* (**Figure 3.11A**).

The relative expression of selected differentially expressed genes provides additional insight into the pathogenic mechanisms that drive each disease. HS lesions had significantly elevated expression of inflammasome components *NLR1* and *GSDMD*, indicating a potential novel driver of inflammation in HS lesions (**Figure 3.11B**). HS lesions also had

increased expression of *IL23R*, *MZB1* and *IL33* suggesting HS lesions have a broad inflammatory profile driven by multiple mechanisms (**Figure 3.11B**). On the other hand, AD lesions had significant upregulation of Th2 associated gene expression including *IL13*, *IL4R* and *IL13RA1* (**Figure 3.11B**). AD lesions also had increased expression of *MMP3*, *CXCL8*, *KRT6A* and *S100A8* pointing towards an important role for keratinocytes and fibroblasts in AD pathogenesis (**Figure 3.11B**).

To understand the impact the 5,959 DEGs have on HS and AD pathogenesis, pathway analysis was performed on genes upregulated in HS and AD, respectively (**Figure 3.12**). Consistent with previous findings, NLR, B cell and Notch signaling were significantly enriched in HS lesions (**Figure 3.12**) (Witte-Handel *et al.*, 2019; Gudjonsson *et al.*, 2020; Melnik and Plewig, 2013). Interestingly, mTOR signaling was significantly enriched in HS lesions, potentially implicating metabolic dysregulation in HS pathogenesis (**Figure 3.12**). This coincides with an enrichment of oxidative phosphorylation in AD lesions (**Figure 3.12**), which is consistent with the comparisons of HS with psoriasis and healthy control skin above, which suggests HS lesions have a downregulation of oxidative phosphorylation. AD lesions also had an increase in NF-κB signaling which regulates the expression of *GATA3* the master transcription factor for Th2 cells, highlighting their importance in AD pathogenesis (**Figure 3.12**).

Due to the clear association between HS and AD, both HS and AD lesions were directly compared with healthy control skin to identify genes uniquely upregulated in respective diseases and identify genes dysregulated in both HS and AD. 7,294 genes were uniquely differentially expressed in AD when compared with healthy control skin (**Figure 3.13**). This included the Th2 signature cytokine *IL13* and its corresponding receptors *IL13RA1* and *IL13RA2*, *GATA3* the master transcription factor of Th2 cells, *IL1B*, *CXCL8* and *MMP3* (**Figure 3.13**). *HK2* which is a key component of glycolysis and *HIF1A* which regulates glycolytic metabolism were also elevated in AD lesions. Conversely, 2,284 genes were uniquely differentially expressed in HS lesions when compared with healthy control skin (**Figure 3.13**). This included immunoglobulin genes, *CD79B* a marker of B cells and *TNF,* which is a target of a currently approved biologic for the treatment of HS (**Figure 3.13**).

Shared DEGs between HS and AD when compared with healthy control skin include genes involved in immune cell migration (*CCR7*) and specifically, Th17 and DC recruitment to the skin (*CCL20*) and the T cell activation marker *CD69* (**Figure 3.13**) (Yan *et al.*, 2019; Schutyser, Struyf and Van Damme, 2003; Cibrian and Sanchez-Madrid, 2017). Other inflammatory cytokines *IFNG*, *IL6* and *IL33* were also upregulated in both HS and AD as were the AMP *S100A8* and the inflammasome component *NLRP3*, suggesting that AD may have a more complex immunopathology beyond Th2 cells (**Figure 3.13**).

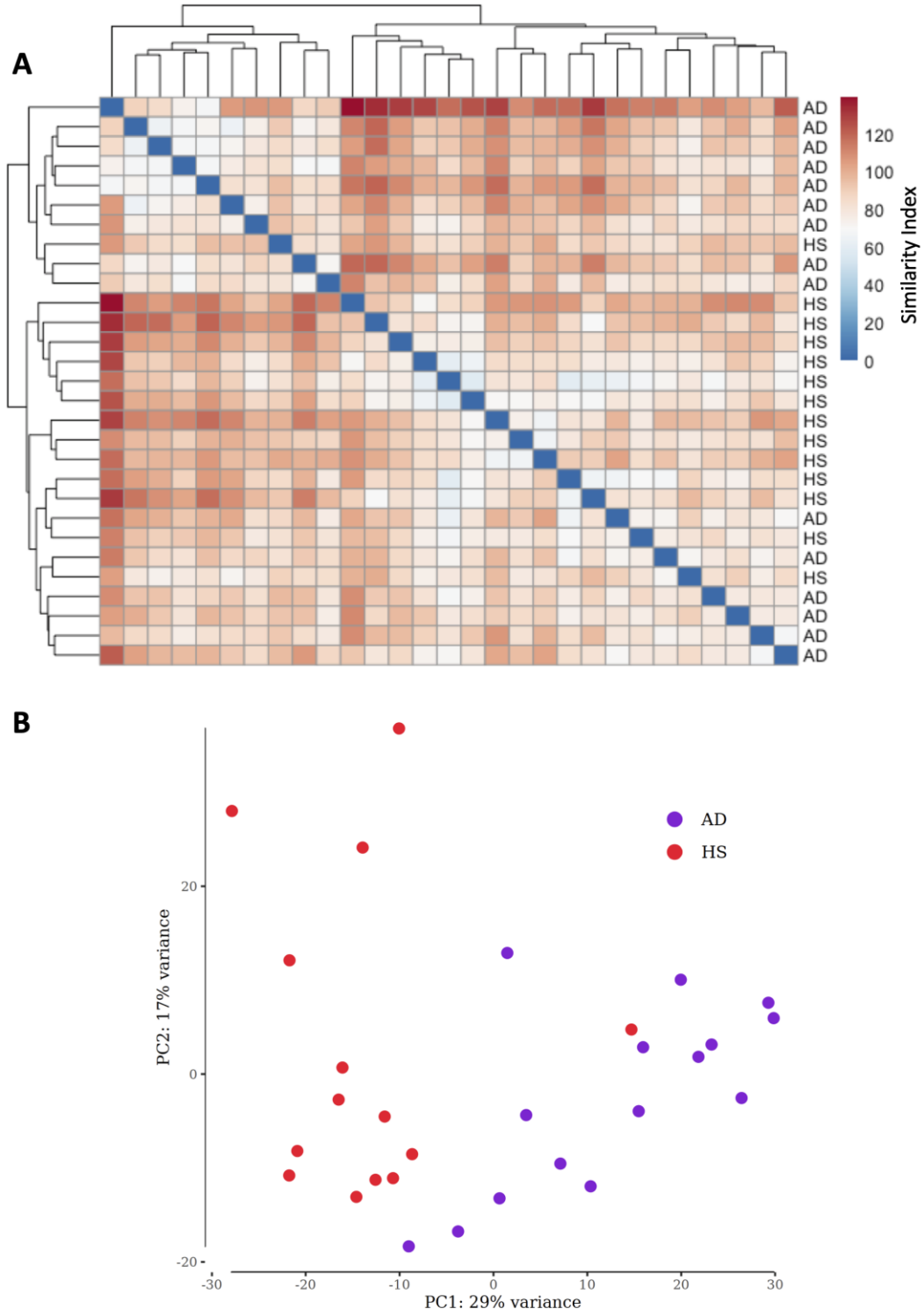

Figure 3.10 Evaluating transcriptomic differences in HS and AD lesions by hierarchal clustering and principal component analysis. Bulk RNA-seq was performed on HS (n=14) and AD lesions (n=15). Heatmap of the transcriptomic similarities between HS and AD lesion based on hierarchal clustering distances (A). Principal component analysis demonstrates distinct transcriptomic profiles between HS and AD lesions (B).

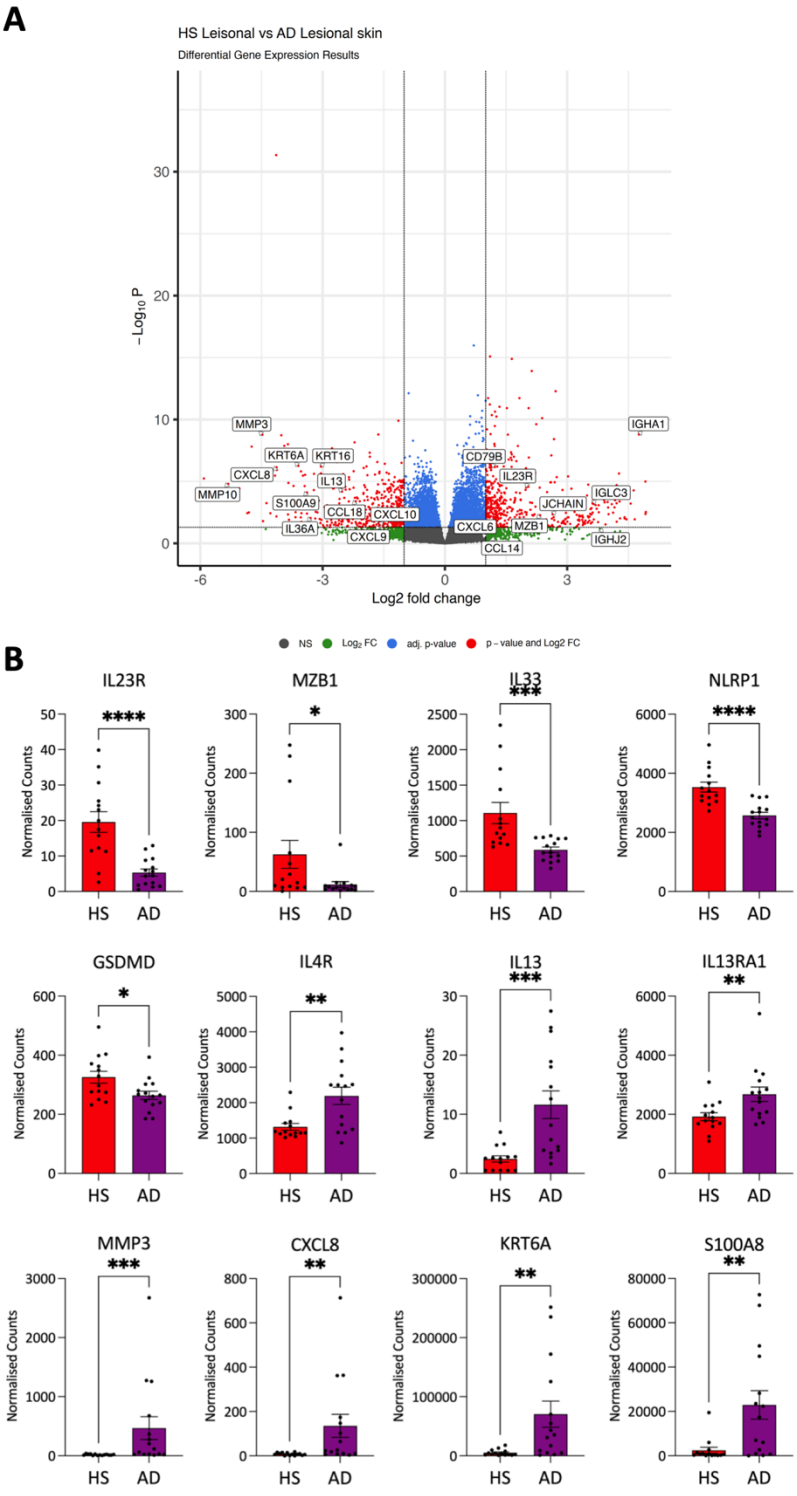

Figure 3.11 Differential gene expression analysis of HS and AD lesions. Bulk RNA-seq was performed on HS (n=14) and AD lesions (n=15). Differentially expressed genes between HS and AD lesions are visualized by volcano plot. Genes with elevated expression in HS lesions have a negative Log_2 fold change, genes with higher expression in AD lesions have a positive fold change. The $–Log_{10}$ P Y axis is a measure of significance (A). Normalised expression of inflammatory genes of interest in HS and AD lesions (B). Graphs represent individual samples with mean ± SEM for each group. Statistical significance was calculated using Mann-Whitney t-test; * p≤ 0.05, ** p≤ 0.01, *** p≤ 0.001, **** p≤ 0.0001.

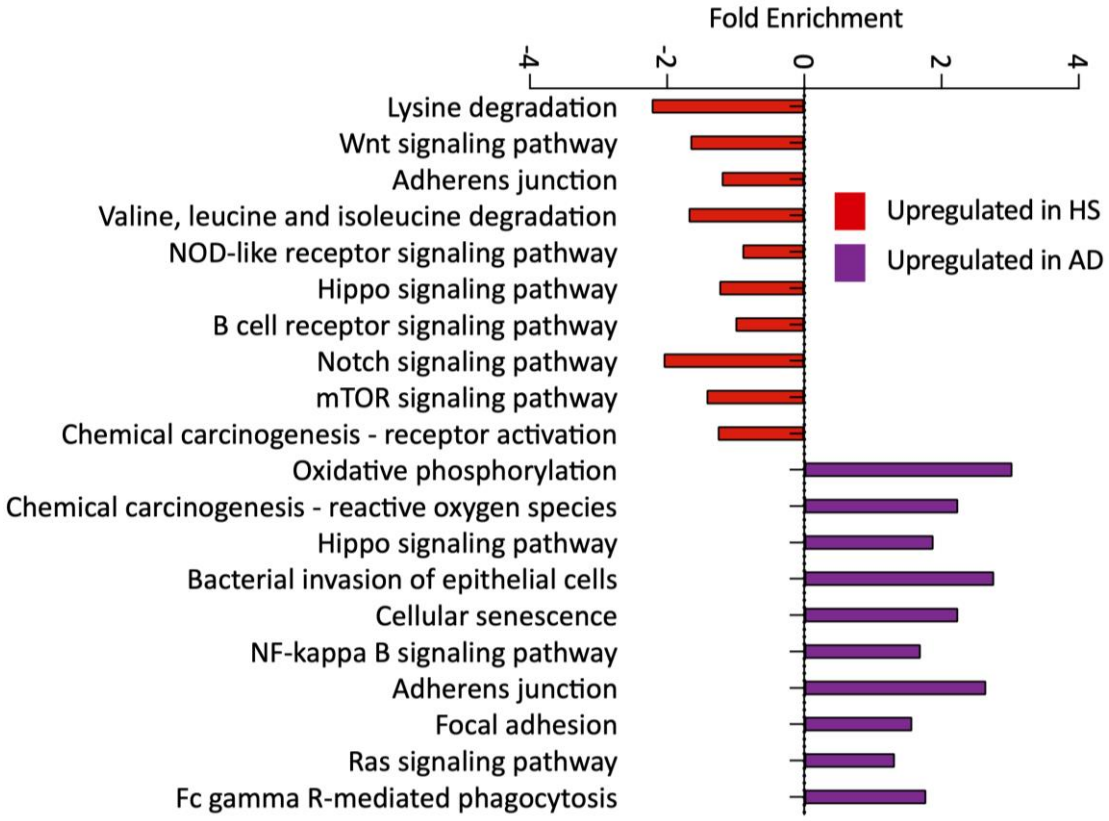

Figure 3.12 Pathway analysis displaying immune pathways significantly enriched in HS and AD lesions. Bulk RNA-seq was performed on HS (n=14) and AD lesions (n=15). Bar chart displaying the fold enrichment of significantly enriched pathways from differentially expressed genes elevated in HS lesions (red) and AD lesions (purple).

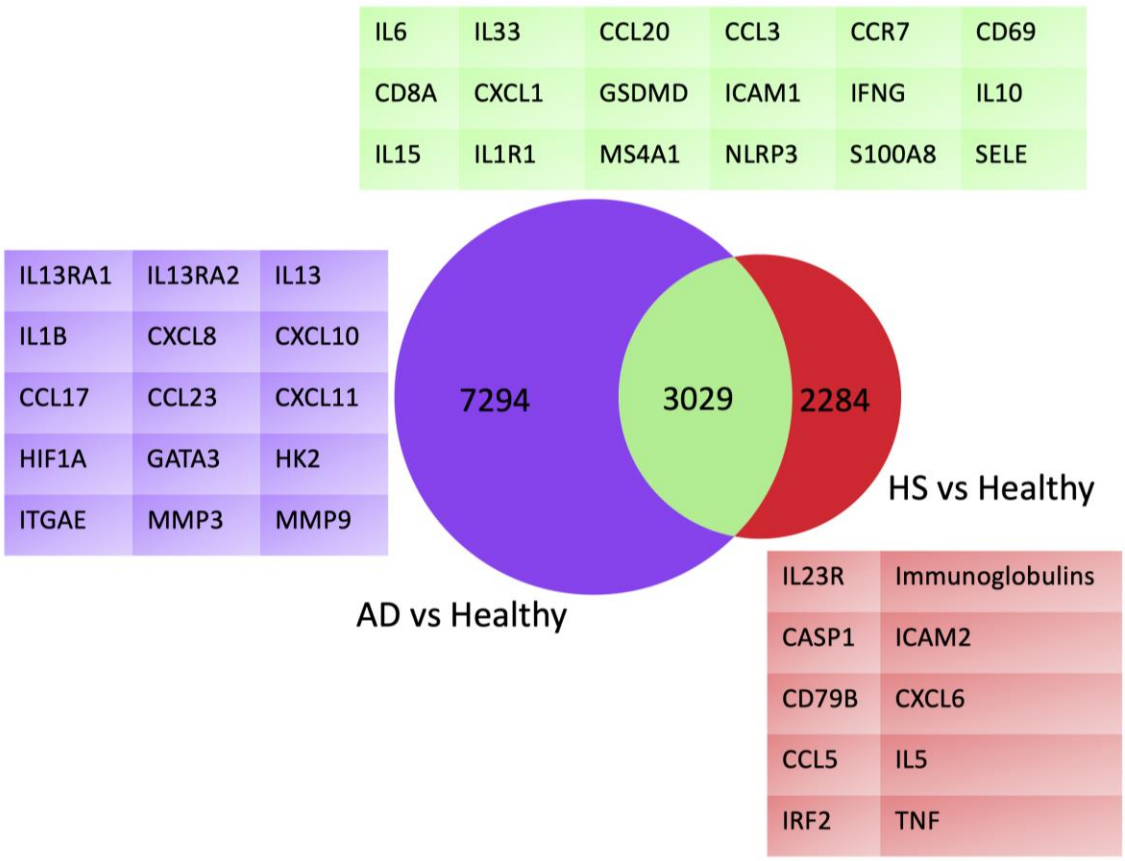

Figure 3.13 HS and AD lesions have distinct drivers of inflammation. Bulk RNA-seq was performed on HS (red; n=14) and AD lesions (purple; n=15). Venn diagram illustrating the shared differentially expressed genes (green) between HS and AD lesions when compared to healthy control skin.

3.3.5 B/plasma cell and complement signature differentiates HS from psoriasis and AD lesional skin

To gain a better understanding of the differences between HS and other inflammatory dermatoses, next a comparison between all disease groups was performed. Weighted gene co-expression network analysis (WGCNA) generates gene modules containing genes of similar functional relevance based on their expression patterns, thereby facilitating the identification of candidate biomarkers (Langfelder and Horvath, 2008). Gene modules were visualised by heatmap to identify clusters of gene modules enriched in each disease (**Figure 3.14A**). As the gene modules generated can contain hundreds of individual genes, pathway analysis provides a better indication of the functional relevance of the gene modules. The gene modules enriched in AD lesions related to cell migration and protein translation (**Figure 3.14B**). Psoriasis lesions had an enrichment of genes related to T cell and epidermal development (**Figure 3.14B**), highlighting the importance of both T cells and keratinocytes in psoriasis inflammation. Gene modules distinctly enriched in HS lesions included genes involved in a broad range of immune functions including complement activation, extracellular matrix organisation and the gene module ME11 contained a number of immunoglobulin genes (**Figure 3.14B**).

To estimate the cell populations in HS, psoriasis, and AD lesional skin and healthy control skin, cell type deconvolution was performed using the bulk RNA-seq data. The bioinformatic tool xCell was used to estimate enrichments of cell populations in bulk RNA-seq data using previously curated gene expression profiles from microarray and RNA-seq data (Aran, Hu and Butte, 2017). HS lesions had significant enrichment of B cells, class-switched memory B cells and mast cells compared with healthy control skin (**Figure 3.15**), consistent with findings from previous studies (Gudjonsson *et al.*, 2020). HS lesions also had a significant increase in plasma cells compared with AD lesions (**Figure 3.15**). Psoriasis lesions had significant enrichments of effector memory T cells, Th2 cells and Treg cells compared with healthy control skin (**Figure 3.15**). Expectedly, Th2 cells were significantly enriched in AD lesions compared with healthy control skin (**Figure 3.15**). Activated DC (aDC) were significantly elevated in HS, psoriasis, and AD lesional skin compared with healthy control skin (**Figure 3.15**). pDC and M1 macrophages were significantly elevated in psoriasis lesions compared with healthy control skin (**Figure 3.15**). Finally, keratinocytes were

significantly enriched in psoriasis lesions compared with healthy control skin which corresponds to the epidermal thickening characteristic of psoriasis lesions (**Figure 3.15**).

Considering the enrichment of B cell and plasma cells in HS lesions, next, expression of a B/plasma cell signature was evaluated in HS lesions compared with psoriasis and AD lesions and healthy control skin. Relative expression of B cell, plasma cell and immunoglobulin genes was visualised by heatmap (**Figure 3.16**). Hierarchal clustering identified a subset of genes uniquely upregulated in HS lesions compared with psoriasis and AD lesions and healthy control skin (**Figure 3.16**). This unique gene signature contained immunoglobulin genes, *JCHAIN*, *CD19* and *CD79A*, indicating that $CD19^{+}$ B cells are of potential therapeutic interest in HS.

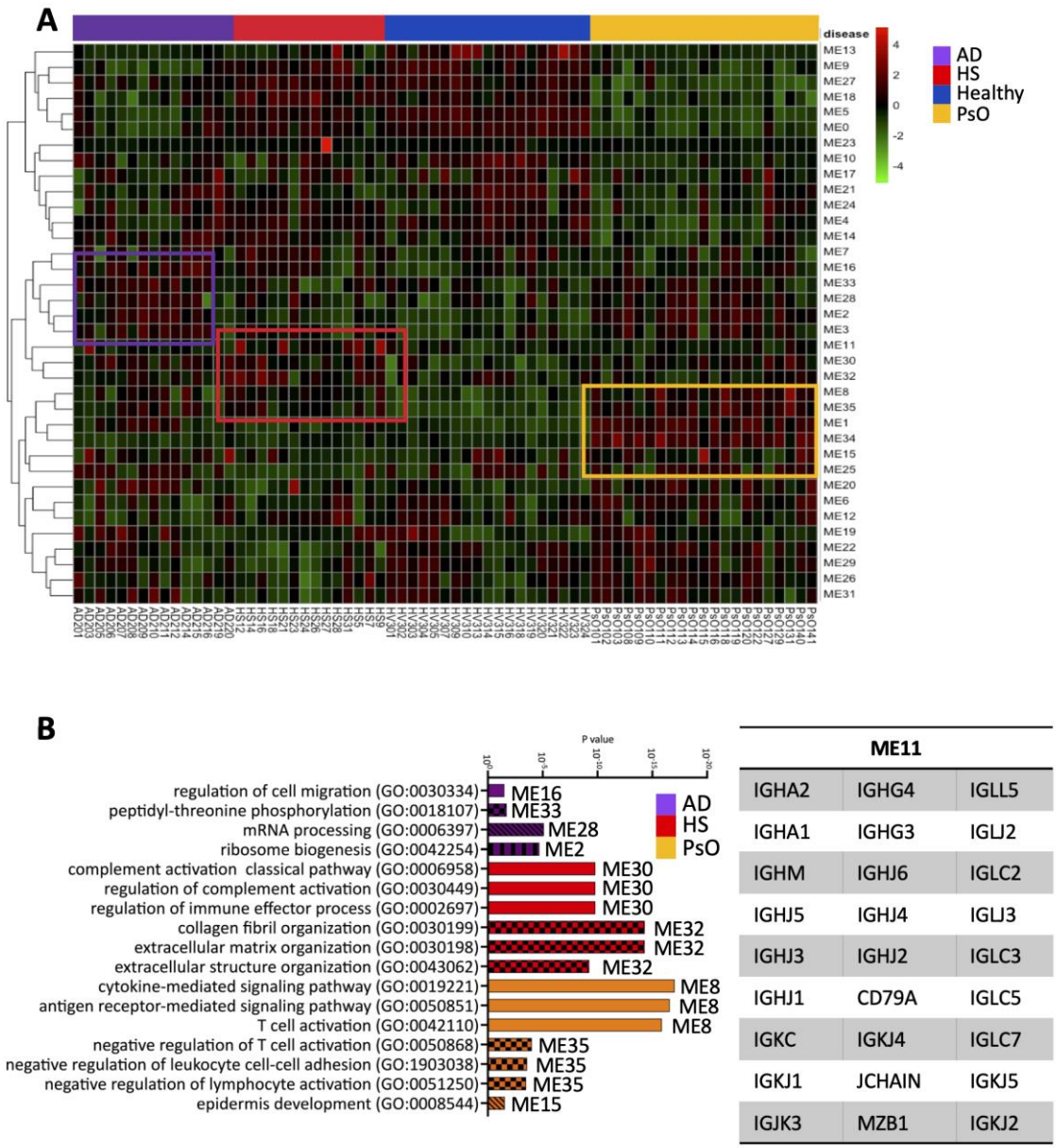

ME11		
IGHA2	IGHG4	IGLL5
IGHA1	IGHG3	IGLJ2
IGHM	IGHJ6	IGLC2
IGHJ5	IGHJ4	IGLJ3
IGHJ3	IGHJ2	IGLC3
IGHJ1	CD79A	IGLC5
IGKC	IGKJ4	IGLC7
IGKJ1	JCHAIN	IGKJ5
IGJK3	MZB1	IGKJ2

Figure 3.14 Psoriasis lesions defined by T cell signature; HS lesions have a complex immunopathology. Weighted gene co-expression analysis (WGCNA) of bulk RNA-seq data from healthy control skin (n=19), HS (n=14), psoriasis (n=21; PsO) and AD lesions (n=15) (A). Significantly enriched gene ontology terms from gene modules generated from the WGCNA (B).

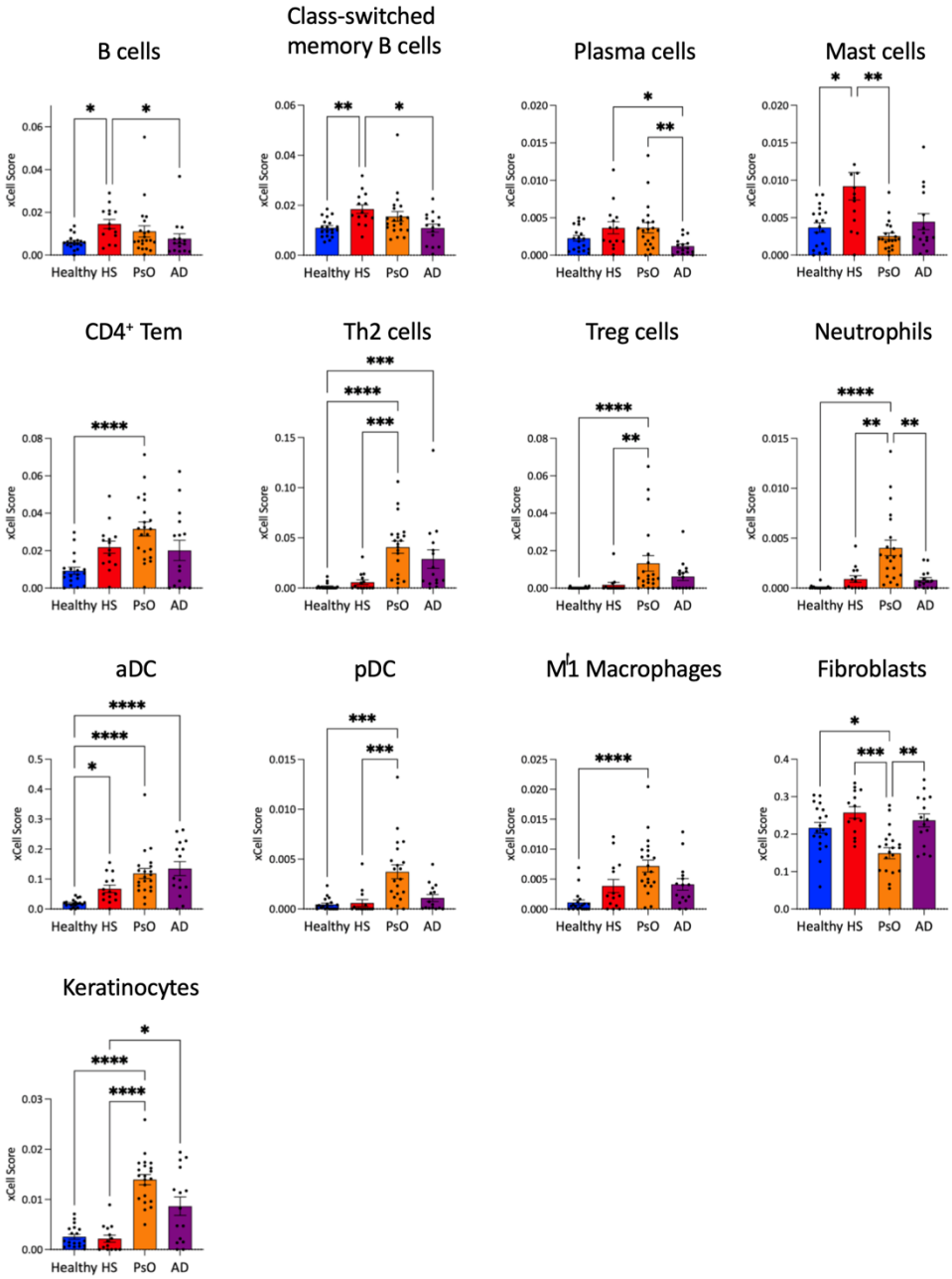

Figure 3.15 Cell type deconvolution predicts an enrichment of B and plasma cells in HS lesions. Bulk RNA-seq was performed on healthy control skin (n=19), HS (n=14), psoriasis (n=21; PsO) and AD lesions (n=15). Cell type deconvolution using xCell predicts the enrichment of cell populations from bulk RNA-seq data. Graphs represent individual samples with mean ± SEM for each group. Statistical significance was calculated using Kruskal-Wallis one-way ANOVA with Dunn's multiple comparisons test; * p≤ 0.05, ** p≤ 0.01, *** p≤ 0.001, **** p≤ 0.0001.

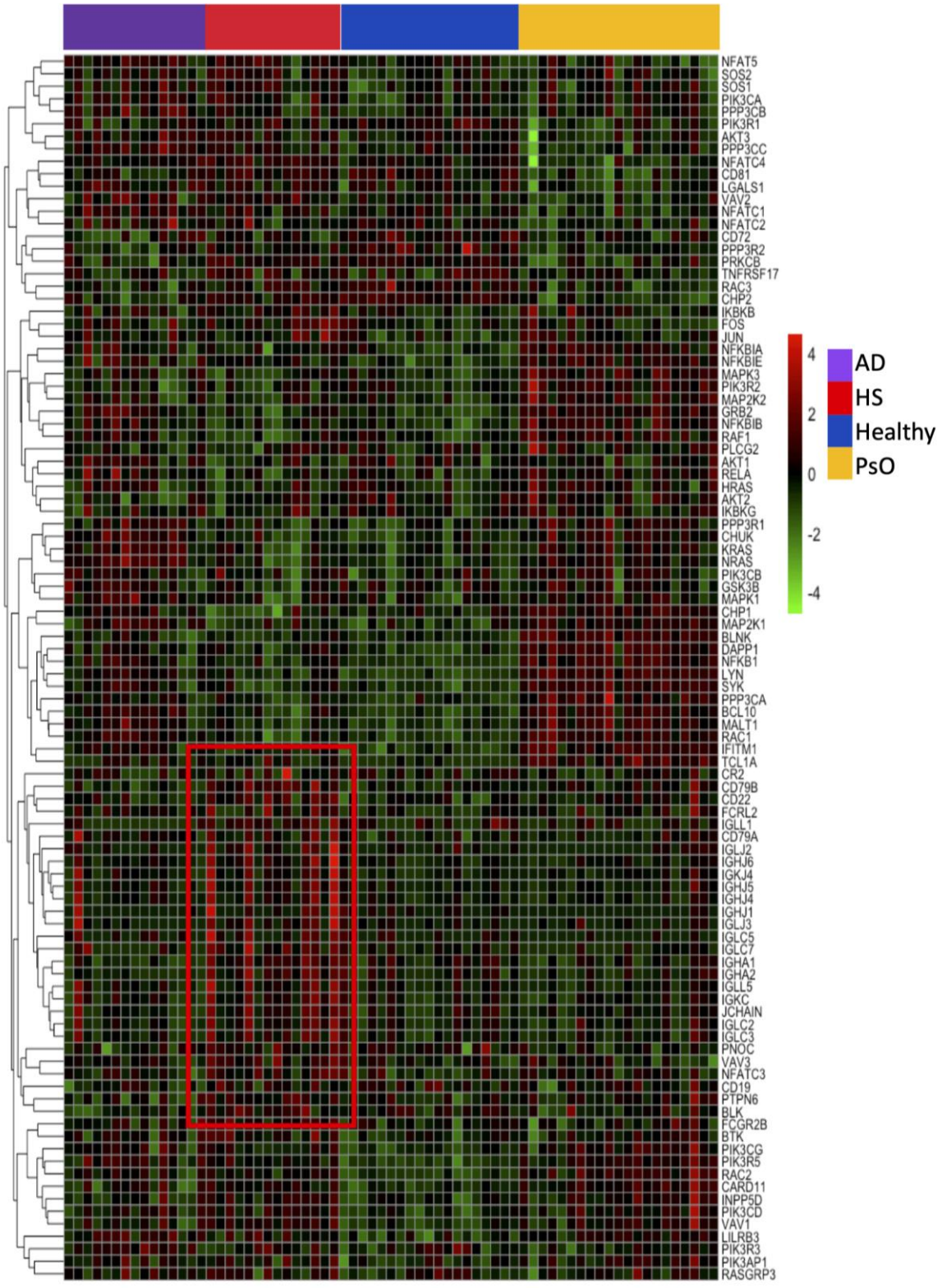

Figure 3.16 HS lesions are defined by a unique B/plasma cell signature absent in other chronic inflammatory skin diseases. Bulk RNA-seq was performed on healthy control skin (n=19), HS (n=14), psoriasis (n=21; PsO) and AD lesions (n=15). Heatmap of relative expression of immunoglobulin and B cell associated genes in healthy control skin, HS, psoriasis and AD lesions.

3.4 Discussion

This study characterised the transcriptome of HS lesional skin and directly compared it with lesional skin of psoriasis and AD and healthy control skin using bulk RNA-seq. These data convincingly show the distinctly complex immunological landscape that exists in HS lesions compared with other inflammatory skin diseases, while also highlighting the importance of complement and B cells in HS pathogenesis.

Elevated levels of Th17 cells, increased production of IL-17 cytokines and increased gene expression of IL-17-associated genes are key immunological features of both HS and psoriasis lesions (Fletcher *et al.*, 2020). Despite these similarities blocking the IL-17 pathway has differing results in HS and psoriasis patients. Blocking IL-17 cytokines directly with secukinumab or bimekizumab, the receptor with brodalumab or blocking upstream of Th17 cells with IL-23A inhibition (guselkumab) have proven to be highly effective in psoriasis (Langley *et al.*, 2014; Reich *et al.*, 2021; Papp *et al.*, 2016; Reich *et al.*, 2019). In contrast, blocking IL-17 signaling with secukinumab and brodalumab has had more limited success in HS patients (Kimball *et al.*, 2023a; Frew *et al.*, 2020). Similarly, IL-23 inhibition proved moderately effective in HS patients, further emphasising the role of Th17 cells in HS pathogenesis (Dudink *et al.*, 2023). The present study aimed to gain a better understanding of HS pathogenesis with the hope of gaining insight into why some targeted treatments are less effective in HS than in psoriasis.

Hierarchal clustering and PCA demonstrated that greater heterogeneity exists within HS lesions relative to other inflammatory dermatoses. Despite being characterised by painful inflammatory lesions, suppuration, development of sinus tracts and scar formation, there is a broad spectrum of clinical presentation and disease severity in HS (Jemec, 2012). The variable clinical presentation of HS and the evidential variable transcriptome between HS lesional skin has hindered our understanding of HS and subsequently limited the development of novel therapeutic strategies. The heterogeneity of HS may contribute to the limited efficacy of biologics including adalimumab and secukinumab, which are the only approved biologics for HS treatment. *TNF* gene expression was significantly higher in HS lesions compared with healthy control skin. Variability in TNF signaling was evident in HS lesions, with TNF signaling in some HS lesions comparable with healthy control skin, perhaps indicative of less severe disease (Hambly *et al.*, 2023; Navrazhina *et al.*, 2022b). In

psoriasis lesions *TNF* expression was significantly upregulated compared with healthy control skin, however there was no significant difference in *TNF* expression between HS and psoriasis lesions. These data complement the recent finding that TNF was significantly elevated in HS and psoriasis lesions compared with healthy control skin (Navrazhina *et al.*, 2022b).

The recent trials of IL-17 signaling inhibitors in HS emphasised the importance of IL-17 in HS inflammation. Despite this, there was no significant difference in *IL17A* or *IL17F* expression in HS lesions compared with healthy control skin. However, HS lesions had significantly increased expression of Th17 associated *CXCL1*, *CCL20* and *IL23R*, and an enrichment of IL-17 signaling pathways, indicating a potential role for IL-17 in HS inflammation. Psoriasis lesions had significantly increased expression of *IL17A* and *IL17F* compared with HS lesional skin, while HS lesions had significantly increased expression of *RORC* and *IL17RC* compared with psoriasis lesional skin demonstrating the importance of IL-17 signaling in both HS and psoriasis inflammation. While the increased expression of *RORC* in HS lesions is surprising considering psoriasis lesions had elevated expression of both *IL17A* and *IL17F* this may be explained by a recent scRNA-seq study which similarly demonstrated increased *RORC* expression by IL-17-producing T cells in HS relative to psoriasis (Kim *et al.*, 2023). Further, *IL17A*$^{+}$ *IL17F*$^{-}$ T cells expressed higher levels of *RORC* and lower levels of *IL17A* relative to *IL17A*$^{+}$ *IL17F*$^{+}$ T cells in HS lesions (Kim *et al.*, 2023). Taken together, this suggests that HS lesions may have an influx of IL-17A^{+} IL-17F^{-} T cells, whereas IL-17A^{+} IL-17F^{+} T cells may predominate psoriasis lesions.

Unfortunately, the cell type deconvolution technique used did not have a gene set representing Th17 cells and it was not possible to estimate Th17 enrichment. There was a significant increase in effector memory CD4 T cells in psoriasis lesions relative to healthy control skin, which encompasses Th17 cells (Kryczek *et al.*, 2011), and a non-significant increase in HS lesions. However, IL-17 signaling was significantly enriched in HS and psoriasis lesions relative to healthy control skin, implicating Th17 cells in both dermatoses.

AD inflammation is driven by an alternative T cell pathway, and this is reflected by the significant increase in Th2 cells in AD lesions. The significant enrichment of Th2 cells in psoriasis lesions was unexpected, however this may be a technical artifact of the analysis

which uses the expression of a gene set to estimate the enrichment of a cell population. It is possible that overlap may exist between genes expressed by T cell populations and those in the Th2 cell gene set, giving an artificial enrichment of Th2 cells in psoriasis lesions. Treg cells were significantly elevated in psoriasis lesions compared with healthy skin. This may be surprising due to their suppressive function, however, there have been reports of increased infiltration of Treg cells into psoriatic lesions relative to healthy control skin (Zhang *et al.*, 2010). Despite this increase of Treg cells in psoriasis lesions, these cells may be dysregulated or outnumbered by effector cells and hence fail to suppress effector T cell function and proliferation (Sugiyama *et al.*, 2005).

aDC were significantly elevated in HS, psoriasis and AD lesional skin compared with healthy control skin. DC have previously been identified as important regulators of inflammation in HS lesions. cDC2 cells are the main producers of *IL1B* (Lowe *et al.*, 2020) and, along with Langerhans cells, have been reported as the primary source of the NLRP3 inflammasome which regulates much of the IL-1β and IL-17 cytokines found in HS lesional skin (Moran *et al.*, 2023).

The expression of alarmins have been extensively investigated in inflammatory skin diseases. The AMPs *S100A7*, *S100A8* and *S100A9* are constitutively expressed by human epithelia, albeit at low levels which become upregulated upon infection or stimulation with specific mediators (Wolk *et al.*, 2011). These AMPs are crucial for preventing infection following epidermal barrier disruption. S100s were strongly upregulated in psoriasis lesional skin, while the increase of AMPs was much lower in AD patients, which may explain why cutaneous infections are so rare in psoriasis patients and why AD patients are more predisposed to gram negative bacterial infection (Wolk *et al.*, 2011). *S100A8* and *S100A9* expression was significantly elevated in HS lesions compared with healthy control skin, however both psoriasis and AD lesions had elevated expression of these AMPs compared with HS lesional skin. A similar trend has previously been shown by RT-PCR (Wolk *et al.*, 2011). *S100A8* and *S100A9* are DAMPs primarily expressed by neutrophils, however due to the likely absence of neutrophils in these data as a result of cryopreservation of biopsies prior to RNA extraction, their expression is most likely from keratinocytes and myeloid cells.

Given the increased activity of the transcription factor *STAT1* in HS lesional skin compared with healthy control skin, it is suggestive that *STAT1* regulates the expression of immune mediators responsible for HS inflammation. *STAT1* regulates the expression of *CD40*, *CD86*, *CX3CL1*, *CXCL8*, *ICAM1*, *IFNG*, *IL6* and *IRF1* all of which had significantly elevated expression in HS lesional skin compared with healthy control skin. Increased expression of *CD40*, *CD86*, and *CX3CL1* in HS lesions is indicative of increased myeloid activation in HS lesions. CD40 is typically expressed by APCs including DC, macrophages and B cells, and binds with CD40L on T cells resulting in costimulatory activity from the APC and subsequent T cell activation (Grewal *et al.*, 1996). Targeting CD40 has been suggested as a potential therapeutic strategy in hyperthyroidism and Sjogren's syndrome, potentially opening a novel therapeutic avenue in HS (Kahaly *et al.*, 2020; Fisher, 2020). *STAT1* also regulates important inflammatory cytokines *CXCL8*, *IFNG* and *IL6* which are elevated in HS lesional skin compared with healthy control skin (Vossen *et al.*, 2019b; Hotz *et al.*, 2016; Witte-Handel *et al.*, 2019). A *STAT1* signature has been identified in the epidermis of HS lesional skin, implicating keratinocytes in HS inflammation (Frings *et al.*, 2022).

Epidermal thickening is a key feature of psoriasis aetiology which is mediated by aberrant keratinocyte proliferation (Ortiz-Lopez, Choudhary and Bollag, 2022). This epidermal thickening is evident with the enrichment of keratinocytes in psoriasis lesions relative to healthy control skin. Additionally, psoriasis lesions had increased expression of proliferative and inflammatory keratins (*KRT6A*, *KRT16*, *KRT17*) compared with healthy control skin. Increased expression of inflammatory keratins and keratinocyte enrichment in AD lesions supports previous claims of keratinocyte dysregulation in AD (Chieosilapatham *et al.*, 2021). Interestingly, despite increased expression of the inflammatory keratin, *KRT6B,* in HS lesional skin, relatively similar levels of keratinocytes were found in HS lesional and healthy control skin. Keratinocytes were identified as a major producers of inflammatory cytokines in HS lesional epidermis, despite an influx of CD8 T cells, NK cells and neutrophils (Schell *et al.*, 2023). Although HS keratinocytes expressed similar inflammatory keratins and proinflammatory mediators as psoriatic keratinocytes, HS keratinocytes appear to lack the same proliferative capacity of psoriatic keratinocytes which culminate in the epidermal thickening characteristic of psoriasis.

A unique B/plasma cell signature was identified in HS lesional skin which distinguished HS from other inflammatory conditions. HS lesional skin had an enrichment of B cells, class switched memory B cells and plasma cells and increased expression of *MZB1*, *JCHAIN*, *CD79A* and several immunoglobulin genes. Despite distinguishing HS from other inflammatory dermatoses, this B/plasma cell signature was more strongly expressed in a subset of HS patients. A similar strategy to stratify patients has been previously reported, with patients with severe HS having increased B cell activation (Hambly *et al.*, 2023). These patients also failed to respond to adalimumab treatment, highlighting this B cell signature as a potential future biomarker to predict treatment response to adalimumab in HS patients.

Immunoglobulin production is a key function of B and plasma cells in HS lesions. Immunoglobulin genes were increased in HS lesions compared with lesional skin of psoriasis and AD and healthy control skin. This distinct expression of immunoglobulin genes in HS lesions may have a pathogenic role in HS. Autoantibodies produced by B or plasma cells against citrullinated proteins are increased in HS lesions, and this increased expression of immunoglobulin genes may promote inflammation via macrophage activation in HS lesions (Carmona-Rivera *et al.*, 2022). Furthermore, B cells are predicted to activate macrophages through TGF-β signaling which may also drive scarring in HS lesional skin (Smith *et al.*, 2023).

Complement activation was another defining feature of HS lesional skin which was relatively lower in other inflammatory dermatoses. Expression of individual complement genes was significantly higher in HS lesions (data not shown), including *C5* expression which has been linked to Th17 cell differentiation (Weaver *et al.*, 2010). C5 is capable of orchestrating neutrophil recruitment and activation, which may be an important mechanism in HS lesional inflammation (Hornum *et al.*, 2017).

In conclusion, this study has contributed to our overall understanding of HS pathogenesis, identifying the similarities and differences between HS and other inflammatory dermatoses. This study identified a unique B/plasma cell signature distinctly found in HS lesions. As this B/plasma cell signature was stronger in a cohort of HS patient, this study indicates potential to stratify patients, with previous data suggesting that patients with

elevated B cell signaling fail to respond to adalimumab treatment (Hambly *et al.*, 2023). This chapter has improved our understanding of HS pathogenesis, highlighting its complexity relative to other inflammatory dermatoses, suggesting that a larger arsenal of therapeutics or therapies with broader targets are required for HS compared with psoriasis or AD.

Chapter 4

HS is characterised by keratinocyte and fibroblast dysregulation

4 HS is characterised by keratinocyte and fibroblast dysregulation

4.1 Introduction

Significant strides have been made recently in uncovering HS aetiology, however, there has been a sparsity of research focusing on the interplay between immune and epithelial cells in the disease. The key initiating events which trigger HS have yet to be fully defined, although hair follicle occlusion is widely recognised as an important initiating event (von Laffert *et al.*, 2010). Hair follicle occlusion may arise from progenitor cells in the ORS which have enhanced proliferative capacity (Orvain *et al.*, 2020; Maya-Mendoza *et al.*, 2018). Cysts develop following hair follicle occlusion which subsequently rupture, releasing PAMPs, DAMPs and keratin fibres and inducing innate and adaptive immune responses (van der Zee *et al.*, 2012a). Abscesses and sinus tracts ultimately develop following hair follicle rupture. The moderate success of anti-TNF and anti-IL-17 therapies indicates that an aberrant immune response drives HS pathogenesis.

The immune cell populations in HS lesions involved in this aberrant immune response have been well characterised in recent years, with single cell transcriptomic analysis performed by multiple groups, implicating B cells (Gudjonsson *et al.*, 2020), macrophages, DCs (Lowe *et al.*, 2020; Mariottoni *et al.*, 2021) and Th17 cells (Moran *et al.*, 2023) in HS pathogenesis. Despite frequently being referred to as a fibrotic disease involving hyperkeratosis, an in-depth characterisation of fibroblasts and keratinocytes in HS lesions has thus far been lacking. Characterisation of non-immune cells present in HS lesions will provide a better insight into HS aetiology and improve our understanding of this chronic inflammatory disease.

Keratinocyte dysfunction has previously been implicated in HS (Hotz *et al.*, 2016). A thickened epithelium induced by ductal hyperkeratosis is characteristic of HS lesions (Frew, Hawkes and Krueger, 2018). HS keratinocytes have defective tissue protective responses and facilitate a chronic inflammatory response in HS lesions (Hotz *et al.*, 2016). HS keratinocytes have also been shown to express inflammatory cytokine responsive genes, with IL-17A, IL-36γ and TNF response genes having particularly high expression (Gudjonsson *et al.*, 2020). Coinciding with the increased expression of IL-17A responsive genes in keratinocytes, an increase in Th17 cells in HS lesions has also been described

(Moran *et al.*, 2017). IL17C, produced by keratinocytes in response to stimulation with IL-17A, TNF, TLR agonists or bacterial stimulation, has recently been implicated in HS pathogenesis, with HS patients having comparable levels of *IL17C* mRNA to psoriasis patients, which is significantly higher than that in healthy controls (Navrazhina, Frew and Krueger, 2020). IL-17C induced IL-1β, IL-8, CXCL1 and IL-36γ production in keratinocytes, as well as elevating expression of IL-17A and IL-17F in Th17 cells, creating a feed forward inflammatory loop (Guttman-Yassky and Krueger, 2018; Ramirez-Carrozzi *et al.*, 2011).

Uniquely, HS patients often develop hypertrophic scarring and dermal tunnels, suggesting an important role for fibroblasts in HS disease progression. Elevated MMPs and extensive matrix remodelling occurs during HS disease, likely driven by dermal fibroblasts in HS lesions (Frew, Hawkes and Krueger, 2018). Fibroblasts may also regulate dermal tunnel formation via matrix remodelling and epithelialisation of dermal tunnels via an aberrant form of wound healing (Frew *et al.*, 2019). These dermal tunnels may induce Th17-mediated inflammation and stimulate fibroblasts to produce IL-6 and IL-8 in a feed forward inflammatory loop (Navrazhina *et al.*, 2021a). Inflammasomes have previously been reported in fibroblasts, activation of which promotes inflammation and tissue fibrosis, highlighting a potential role of the NLRP3 inflammasome in HS inflammation (Ershaid *et al.*, 2019).

Studies characterising non-immune cells in HS thus far have combined immuno-histochemistry and mRNA analysis. However, the limited number of cell markers used in immunohistochemistry hinders the identification of different cell populations in HS lesions. A coherent study identifying the principal non-immune cells in HS lesional skin relative to healthy control skin via scRNA-seq would add value to the field. Comparing HS lesions and healthy control skin via scRNA-seq may provide a rationale for therapeutically targeting specific biological pathways for the treatment of HS.

4.2 Aims

The aim of the experiments in this chapter was to identify proinflammatory subsets of non-immune cells in HS lesions, currently an unexplored avenue in HS research.

Specifically, this chapter sought to:

- Define the cellular populations in HS lesions through single cell technologies.
    - Identify key $CD45^-$ cell populations in HS lesional and healthy control skin.

- Characterise the transcriptional profile of HS keratinocytes.
    - Identify keratinocyte subsets found in HS lesional and healthy control skin.
    - Evaluate DEGs and novel pathways enriched in HS keratinocytes relative to healthy control keratinocytes.
    - Examine potential changes in differentiation between HS and healthy control keratinocytes.

- Characterise the transcriptional profile of HS fibroblasts.
    - Identify fibroblast subsets in HS lesional and healthy control skin.
    - Evaluate DEGs and novel pathways enriched in HS fibroblasts relative to healthy control fibroblasts.

4.3 Results

4.3.1 Identifying non-immune cell populations in HS skin

The role of non-immune cells in HS skin has yet to be fully elucidated, thus limiting our understanding of HS pathogenesis. In order to characterise non-immune cells in HS patients and healthy controls, scRNA-seq was performed on HS lesional biopsies and healthy control skin from mammoplasty surgeries. Skin biopsies were processed, sequenced and data processed as per **Section 2.2.19**. While many studies, including from our own lab, have detailed the presence and frequency of immune cells in HS lesions, the complete characterisation of non-immune cells is lacking. This study aimed to define the cellular populations present in the $CD45^-$ cohort within HS lesions.

To characterise the scRNA-seq data from the $CD45^-$ cohort of cells isolated from HS lesional and healthy control skin, raw sequencing data was processed and analysed using Cell Ranger and Seurat (Zheng *et al.*, 2017; Stuart *et al.*, 2019). **Figure 4.1** displays a UMAP of 23 unique cell clusters from processed scRNA-seq data from 6 HS lesional and 3 healthy control skin samples. Each of the 23 clusters had a defining set of transcriptomic markers determined by Wilcoxon Rank Sum test (**Figure 8.2**). Clinical details for the 6 HS patients and 3 healthy controls used in this study can be found in **Section 2.2.18**.

To classify each cell cluster into common cell annotations, extensive visualisation of specific cell markers was performed. To determine the identity and function of each cell population, gene markers were visualised on the UMAP, expression ranged from relatively low in yellow to relatively high expression in purple (**Figure 4.2**). Cell clusters were annotated based on the expression of typically 10-15 transcriptomic markers in a similar fashion to phenotyping using flow cytometry. Briefly, cell clusters could be broadly grouped into keratinocytes, fibroblasts, endothelial cells, melanocytes, smooth muscle cells and pericytes based on prior knowledge of non-immune cell populations in skin and top ranked cluster-specific genes calculated by Wilcoxon Rank Sum test (**Figure 8.2**). Keratinocytes were identified based on the expression of keratins (*KRT1*, **Figure 4.2A**; *KRT5*, **Figure 4.2B**). Fibroblasts were identified based on the expression of *CD34* (**Figure 4.2C**), *COL1A1* (**Figure 4.2D**) and lumican (*LUM*, **Figure 4.2E**). Melanocytes had unique expression of *PMEL* (**Figure 4.2F**) and *MLANA* (**Figure 4.2G**), while endothelial cells expressed von Willebrand Factor

(*VWF*, **Figure 4.2H**), *CLDN5* (**Figure 4.2I**) and a subset of endothelial cells had high expression of *LYVE1* (**Figure 4.2J**), indicative of lymphatic endothelial cells. Despite having high transcriptomic similarity, pericytes and smooth muscle cells could be distinguished by the expression of *RGS5* (**Figure 4.2K**) and alpha actin (*ACTA2*, **Figure 4.2L**).

To ensure the robustness of data integration and in order to identify potential cell populations enriched in HS and hence of particular interest, an overlapping UMAP grouping cells derived from HS lesions (red) and healthy control skin (blue) was visualised (**Figure 4.3**). To illustrate potential cell clusters unique to HS lesions, separate UMAPs displaying healthy control-only cells (top) and HS-only cells (bottom) was generated (**Figure 4.4**). Taken together, these UMAPs demonstrate the efficacy of the data integration protocol used considering the high degree of overlap between healthy control and HS-derived cells, while also highlighting HS-specific clusters, including inflammatory keratinocytes and the inflammatory fibroblasts (2) cluster. Two cell clusters, located above keratinocytes on the UMAP, were classified as uncharacterised/debris due to the absence of specific cell markers while also having low UMI and low number of genes relative to other cell clusters.

Following extensive quality control measures (**Section 2.2.20, Figure 2.1**), the number of cells analysed per sample ranged from 861-3935 cells in HS lesional samples with a mean of 2365 cells ± 902 (n=6) and from 4069-4803 cells in healthy control samples with a mean of 4493 cells ± 310 (n=3). **Figure 4.5A** displays the proportion of each cell cluster in both HS lesional and healthy control skin. Fibroblasts make up a high proportion of cells in the $CD45^-$ cohort in both HS lesional and healthy control skin and while there is a general increase in all fibroblast clusters in HS lesions relative to healthy control skin, these failed to reach significance (**Figure 4.5B**). There were increases in the two spinous keratinocyte clusters in healthy controls relative to HS lesional skin while Inflammatory keratinocytes were enriched in HS lesional skin. The frequency of both clusters of endothelial cells were also elevated in HS lesional skin compared with healthy control skin.

Considering the variation in $CD45^-$ cell cluster frequency in HS lesional and healthy control skin, PCA was performed to calculate variations in transcriptomes between HS lesional and healthy control skin. PCA is a dimensionality reduction tool which calculates the variance between samples based on 3000 highly variable genes. **Figure 4.6** shows a homogenous

group of 3 healthy control samples (blue) close together, demonstrating little transcriptomic variation between the healthy control samples. The 6 HS lesional samples on this PCA plot displayed higher degrees of heterogeneity, with two HS lesional samples more closely resembling healthy control samples, and so these samples were termed HS-lo due to a potential lower inflammatory load. The remaining 4 HS samples were termed HS-hi due to their greater variance relative to healthy control samples and their potential higher inflammatory load. Importantly, similar stratification could be seen in $CD45^+$ cells (Moran *et al.*, 2023), with the same samples identified as HS-hi and HS-lo in both the $CD45^+$ and $CD45^-$ datasets.

To summarise this section, transcriptomic analysis revealed 23 distinct non-immune cell clusters within HS and healthy control skin samples. These clusters broadly grouped into fibroblasts, keratinocytes, endothelial cells, melanocytes, smooth muscle cells and pericytes. While healthy control samples were relative homogenous with regard to cellular frequencies and transcriptomic profiles, a higher degree of variance was found in HS lesional samples. Clear differences were seen in the cellular frequencies and the overall transcriptomic profile of HS lesional and healthy control skin, indicating potential dysregulation of $CD45^-$ cells in HS disease.

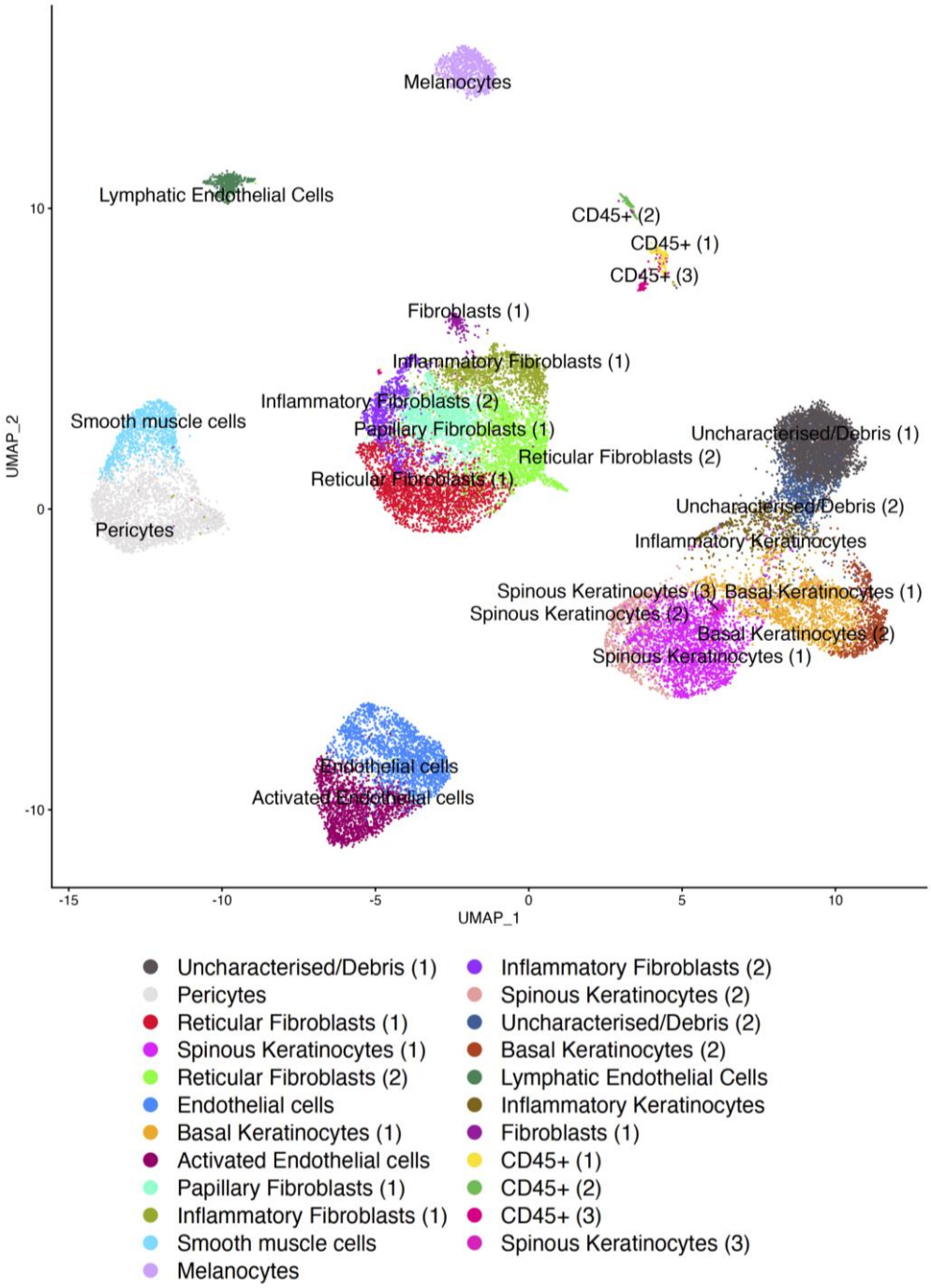

Figure 4.1 UMAP displaying 23 unique cell clusters from HS lesional and healthy control skin. Single cells isolated from healthy controls (Con; n=3) or HS lesional skin (HS; n=6) were purified based on absence of CD45 expression, barcoded and sequenced by 10X Genomics scRNA-seq. UMAP displays the individual cells isolated from HS lesional skin and healthy control skin integrated together following unsupervised classification of $CD45^-$ cells.

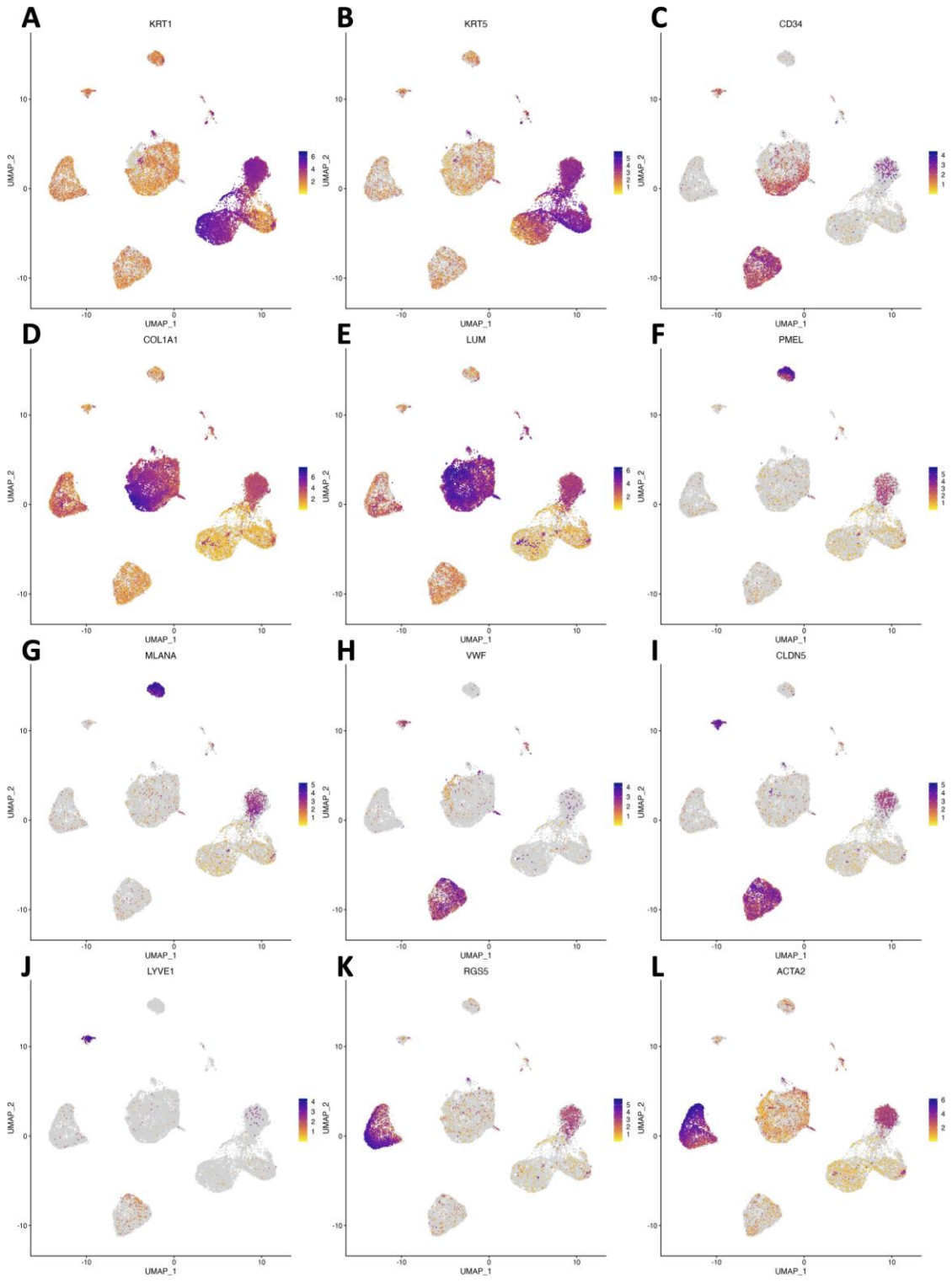

Figure 4.2 Expression of marker genes associated with keratinocytes, fibroblasts, melanocytes, pericytes and smooth muscle cells within HS patient lesions and healthy control skin. Single cells isolated from healthy controls (Con; n=3) or HS lesional skin (HS; n=6) were purified based on absence of CD45 expression, barcoded and sequenced by 10X Genomics scRNA-seq. UMAPs display gene expression for *KRT1* (A), *KRT5* (B), *CD34* (C), *COL1A1* (D), *LUM* I, *PMEL* (F), *MLANA* (G), *VWF* (H), *CLDN5* (I), *LYCE1* (J), *RGS5* (K), *ACTA2* (L) in CD45^{-} cells of HS lesional and healthy control skin.

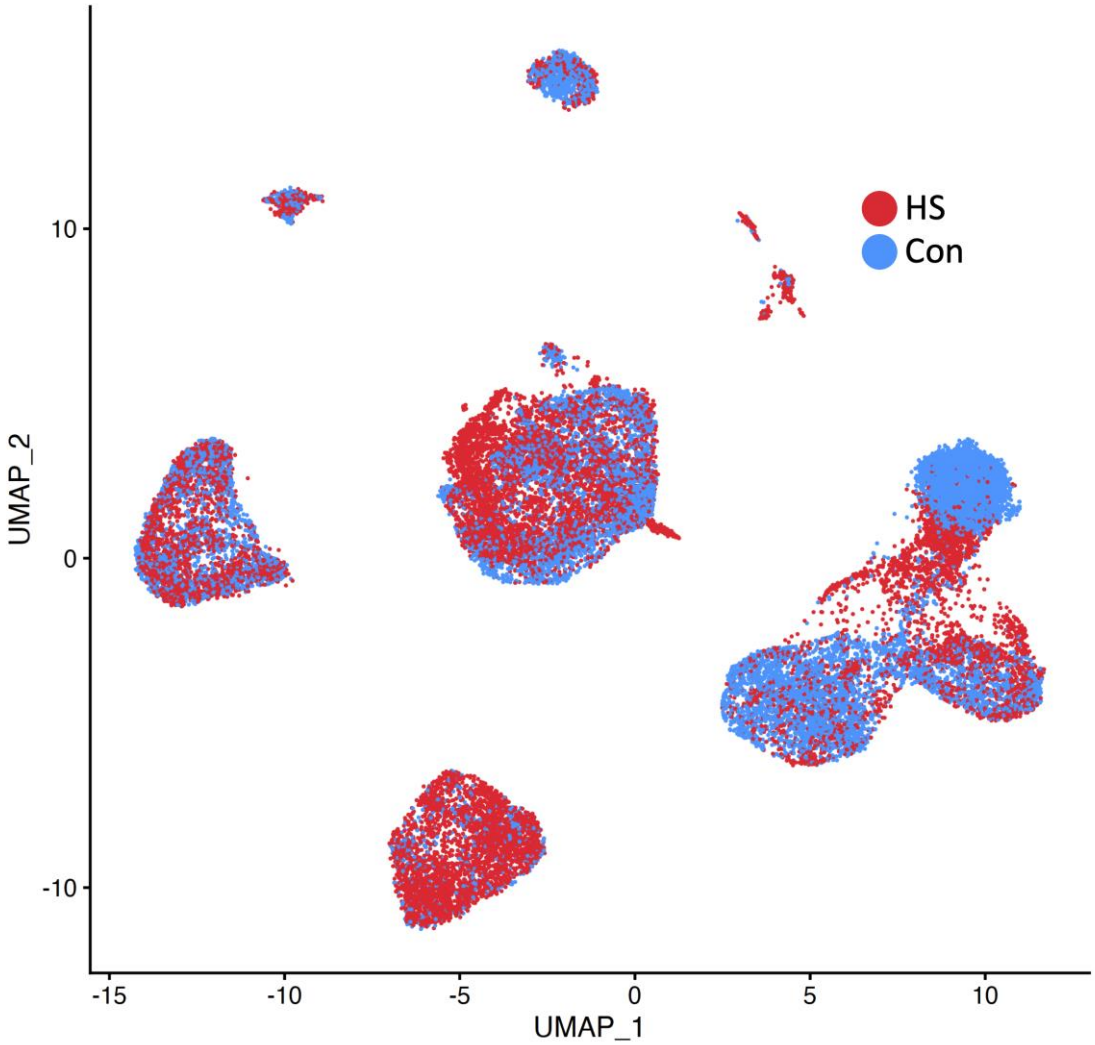

Figure 4.3 UMAP displaying cell populations specific to HS lesional and healthy control skin. Single cells isolated from healthy controls (Con; n=3) or HS lesional skin (HS; n=6) were purified based on absence of CD45 expression, barcoded and sequenced by 10X Genomics scRNA-seq. UMAP displays the individual cells isolated from HS lesional skin (red) and healthy control skin (blue) integrated together after unsupervised classification of $CD45^-$ cells.

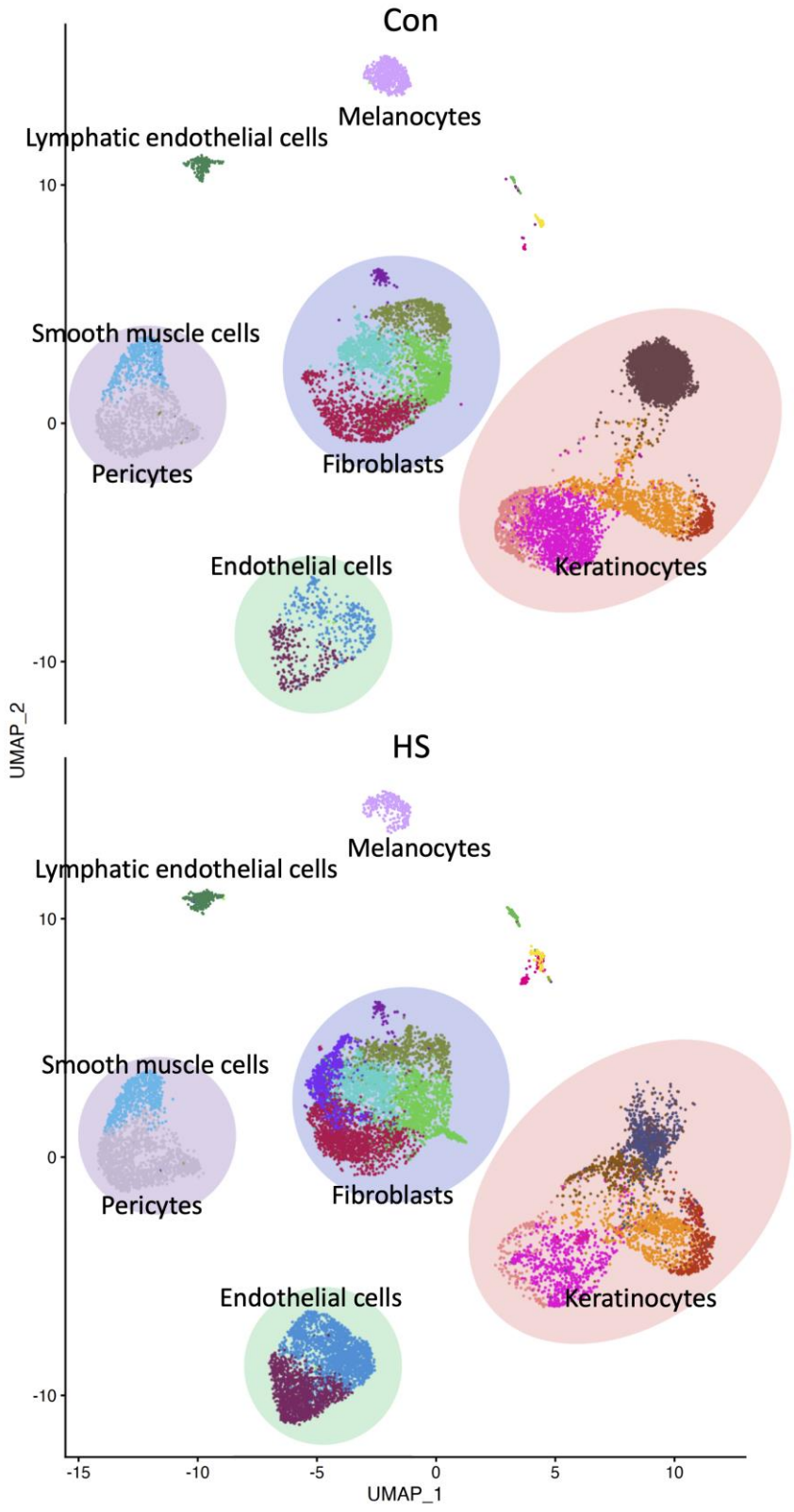

Figure 4.4 UMAP displaying cell populations in healthy control and HS lesional skin. Single cells isolated from healthy controls (Con; n=3) or HS lesional skin (HS; n=6) were purified based on absence of CD45 expression, barcoded and sequenced by 10X Genomics scRNA-seq. UMAP displays the individual cells isolated from healthy control skin (Con, top) and HS lesional skin (HS, bottom) after unsupervised classification of $CD45^-$ cells.

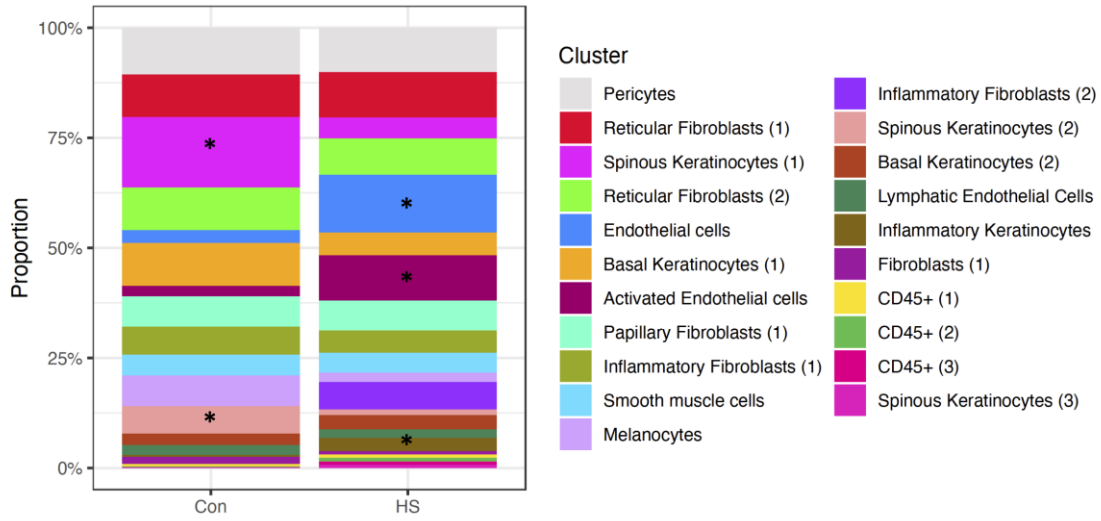

Figure 4.5 Keratinocytes and endothelial cell clusters are significantly enriched in HS lesional skin compared with healthy control skin. Single cells isolated from healthy controls (Con; n=3) or HS lesional skin (HS; n=6) were purified based on absence of CD45 expression, barcoded and sequenced by 10X Genomics scRNA-seq. Bar chart showing the proportion of each cell cluster relative to all cells in the $CD45^-$ dataset. Statistical significance was calculated using Mann Whitney U test; * $p \leq 0.05$.

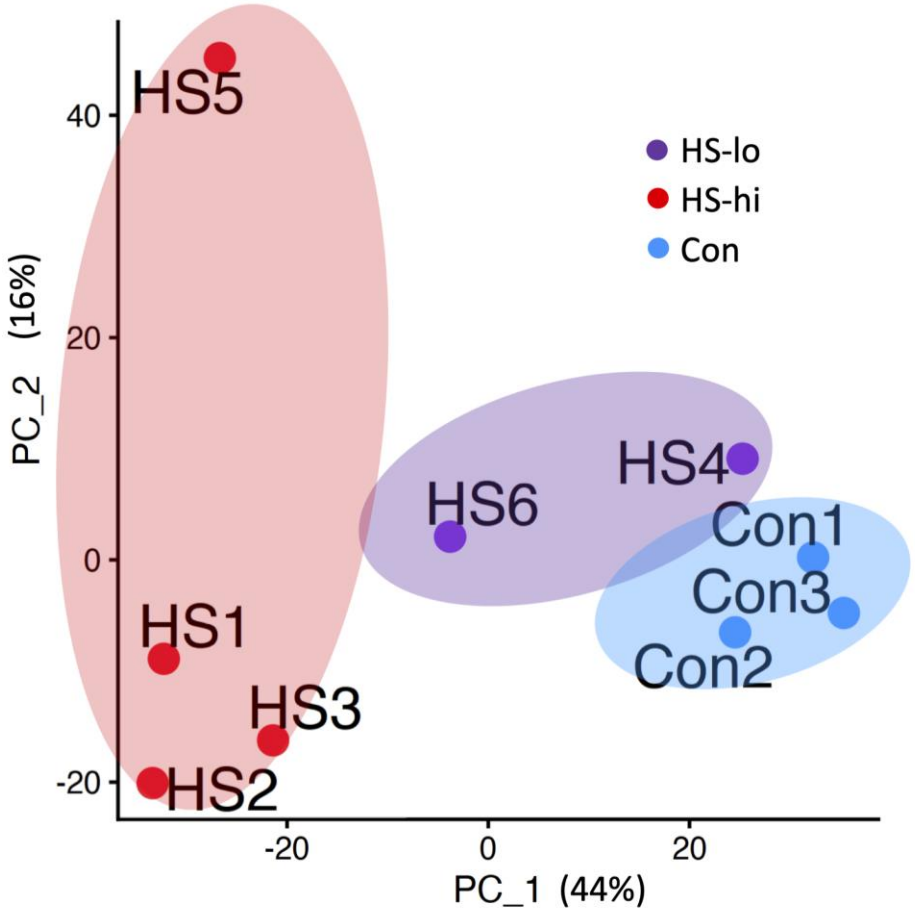

Figure 4.6 Principal component analysis (PCA) illustrates the heterogeneity within HS lesional skin (red) relative to healthy control skin (blue). Single cells isolated from healthy controls (Con; n=3) or HS lesional skin (HS; n=6) were purified based on absence of CD45 expression, barcoded and sequenced by 10X Genomics scRNA-seq. PCA demonstrates the homogeneity of healthy control samples relative to the heterogeneity of HS lesional skin where two HS samples (HS-lo, purple) group close to the healthy control samples, while the other HS samples are more distinct (HS-hi, red).

4.3.2 Transcriptomic differences between HS and healthy skin in CD45$^-$ cells

PCA illustrated clear differences between HS lesional and healthy control skin samples. This section further investigated these differences at a single cell level, identifying potential genes and inflammatory pathways which drive the transcriptomic differences between HS lesional and healthy control skin.

To examine the overall differences between CD45$^-$ cells in HS lesions and healthy controls, differential expression testing was performed using the Wilcoxon Rank Sum test. A volcano plot displays the DEGs between HS lesions and healthy controls (**Figure 4.7**). Genes with a log_2 fold change >0 were elevated in HS lesional skin, genes with a log_2 fold change <0 were downregulated in HS. Genes significantly differentially expressed are coloured in blue and those in red also have a high fold change and should be investigated in more detail. 6,571 genes were significantly differentially expressed between HS lesional and healthy control skin, 1,802 were upregulated in HS lesions (**Table 8.7**) and 4,759 and upregulated in healthy control skin (**Table 8.8**). Of particular interest, genes involved in IL-17 signaling including *S100A8*, *S100A9*, *CXCL8* and *CXCL1* were highly differentially expressed in HS lesions. Fibroblast associated genes were also elevated in HS lesions highlighting the importance of fibroblasts in HS disease. *MMP1, MMP3*, the collagen *COL1A1*, and fibroblast markers *LUM*, *PDPN* (podoplanin) and *THY1* (CD90) were among the most significantly elevated genes in HS lesional skin. Genes typically associated with endothelial cells, *VWF* and E-selectin (*SELE*), were also significantly elevated in HS lesional skin. Keratinocyte associated genes dermokine (*DMKN*), *KRT10* and *KRT1* were significantly downregulated in HS lesional skin, which coincides with reduced frequency of keratinocytes in HS lesions relative to healthy control skin. This reduced expression of keratins, along with the reduced frequency of certain keratinocyte populations in HS lesions, may be associated with the disrupted epithelial layers observed in severe HS lesions.

To establish an overall picture of the pathways dysregulated in HS lesions, pathway analysis was performed on the DEGs (adj p value <0.05 and log_2FC >0.1). Of the 168 pathways significantly enriched from the DEGs, the top 10 immune related pathways were visualised (**Figure 4.8A**). Pathways previously described to drive inflammation in HS including IL-17 and TNF signaling were significantly enriched in HS lesions from the CD45$^-$ cohort of cells.

Extracellular matrix interactions implicate fibroblasts in HS pathogenesis, while other inflammatory pathways including HIF-1, JAK-STAT and MAPK signaling demonstrate the broad inflammatory processes which contribute to inflammation in HS lesions. To understand the role of specific genes involved in each of these dysregulated pathways, a gene-pathway network was developed (**Figure 4.8B**). Genes represented by a blue circle were upregulated in healthy controls, while genes represented by a red circle, were upregulated in HS lesions.

The PCA (**Figure 4.9**) highlighted the potential to stratify HS samples into those with a high and low inflammatory load. To visualise the sources of transcriptomic variance between HS-hi and HS-lo samples, UMAPs display cells derived from healthy controls (top), HS-hi (middle) and HS-lo (bottom) samples (**Figure 4.9**). Despite the limited number of samples, the HS-hi UMAP had a visibly reduced frequency of keratinocytes and an increase in inflammatory fibroblasts relative to the HS-lo UMAP. The transcriptomic variance seen between HS-hi and HS-lo samples is replicated with cell frequencies in HS-hi and HS-lo samples (**Figure 4.10**). *KRT1*, *KRT5*, *KRT14*, *KRT10* and *KRT16* were significantly elevated in HS-lo samples reflecting the reduced frequency of keratinocytes in HS-hi samples (**Figure 4.11**). *MMP1*, *MMP3*, *MMP9*, *FAP* and collagen genes were upregulated in HS-hi samples indicating a potentially important role of fibroblasts in promoting severe HS inflammation. 6,303 genes were significantly differentially expressed between HS-hi and HS-lo samples, 1,189 genes were elevated in HS-hi lesions (**Table 8.9**) and 5,114 genes are elevated in HS-lo lesions (**Table 8.10**). 197 pathways were significantly enriched from the DEGs between HS-hi and HS-lo lesions. Among these enriched pathways, IL-17 and TNF signaling were among the top 10 immune related pathways enriched from the DEGs (**Figure 4.12A**). The gene-pathway network demonstrates the increased expression of oxidative phosphorylation and focal adhesion genes in HS-hi samples, suggesting fibroblast interactions and metabolic dysregulation are key features of severe HS inflammation (**Figure 4.12B**).

Interestingly, HS patients previously treated with TNF inhibitors had reduced expression of metabolic markers (*SLC2A1;* GLUT1), IL-17 regulated genes (*CXCL8*, *CXCL1*), AMPs (*S100A8*, *S100A9*), MMPs (*MPP1*, *MMP3*) (**Figure 8.11**) and an altered cellular profile compared with HS patients who weren't treated with any biologic prior to transcriptomic analysis (**Figure**

8.10). In addition, enriched pathways from the DEGs between HS lesions treated with or without TNF inhibitors highlighted IL-17 signaling as the most enriched pathway following anti-TNF treatment (**Figure 8.12**). IL-17 signaling genes were elevated in HS lesions not treated with TNF inhibitors, suggesting TNF signaling promotes IL-17 mediated inflammation in HS lesions (**Figure 8.12A-B**). To summarise this section, $CD45^-$ cells likely contribute to the chronic inflammatory processes in HS lesions. IL-17 signaling appears to play a prominent role in HS inflammation with a number of genes, downstream of IL-17, upregulated in the $CD45^-$ cells of HS lesions, while anti-TNF treatment significantly reduced the expression of IL-17 signaling genes.

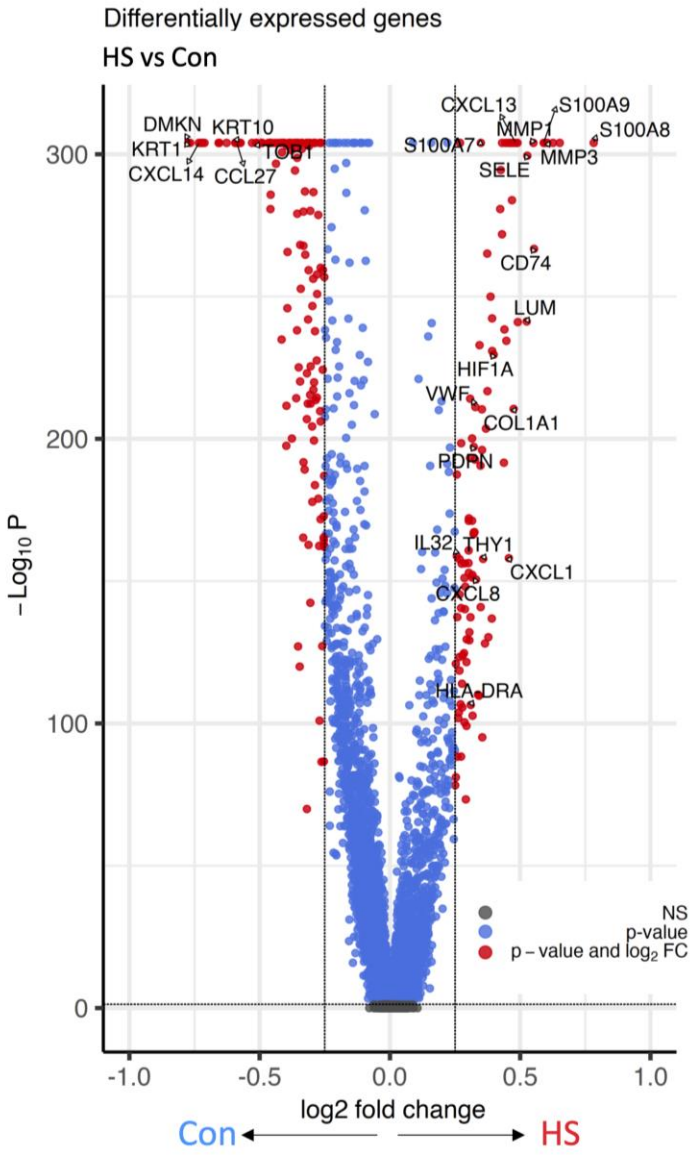

Figure 4.7 Differentially expressed genes between CD45$^-$ cells in healthy control and HS skin. Single cells isolated from healthy controls (Con; n=3) or HS lesional skin (HS; n=6) were purified based on absence of CD45 expression, barcoded and sequenced by 10X Genomics scRNA-seq. Volcano plot displays DEGs in HS lesional skin compared with healthy control skin. Genes with a $log_2FC > 0$ are upregulated in HS and a $log_2FC < 0$ are downregulated in HS. The $-Log_{10}$ P Y-axis is a measure of significance.

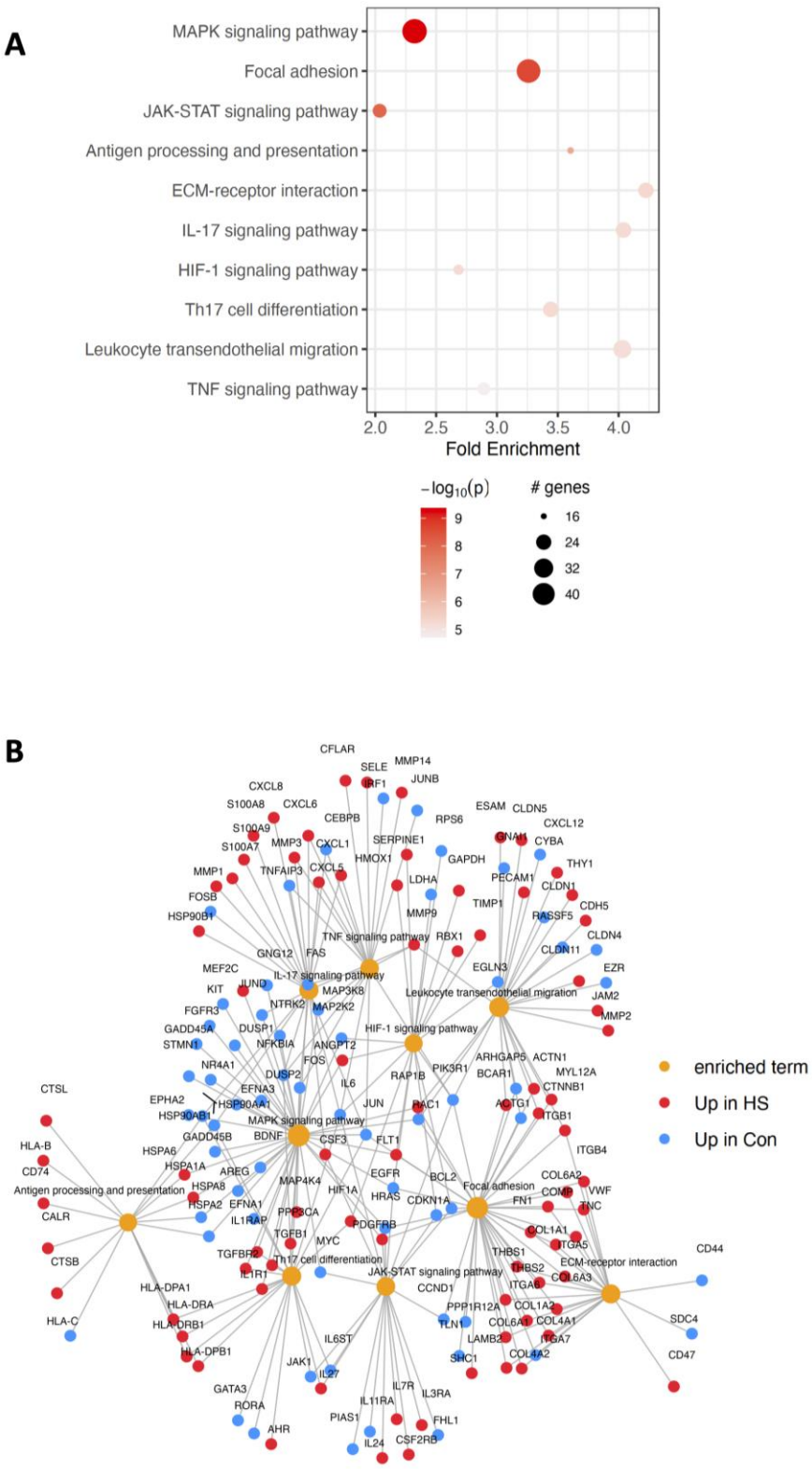

Figure 4.8 Differentially expressed genes drive diverse inflammatory pathways in HS lesional skin. Kegg pathways enriched by the DEGs were visualised by dotplot. The number of DEGs represented in each pathway is illustrated by the size of dot and increased significance of pathway enrichment is represented by increased coloration of dot (A). DEGs involved in enriched pathways were visualised by pathway network, genes upregulated in HS were coloured in red, genes downregulated in HS were coloured in blue (B).

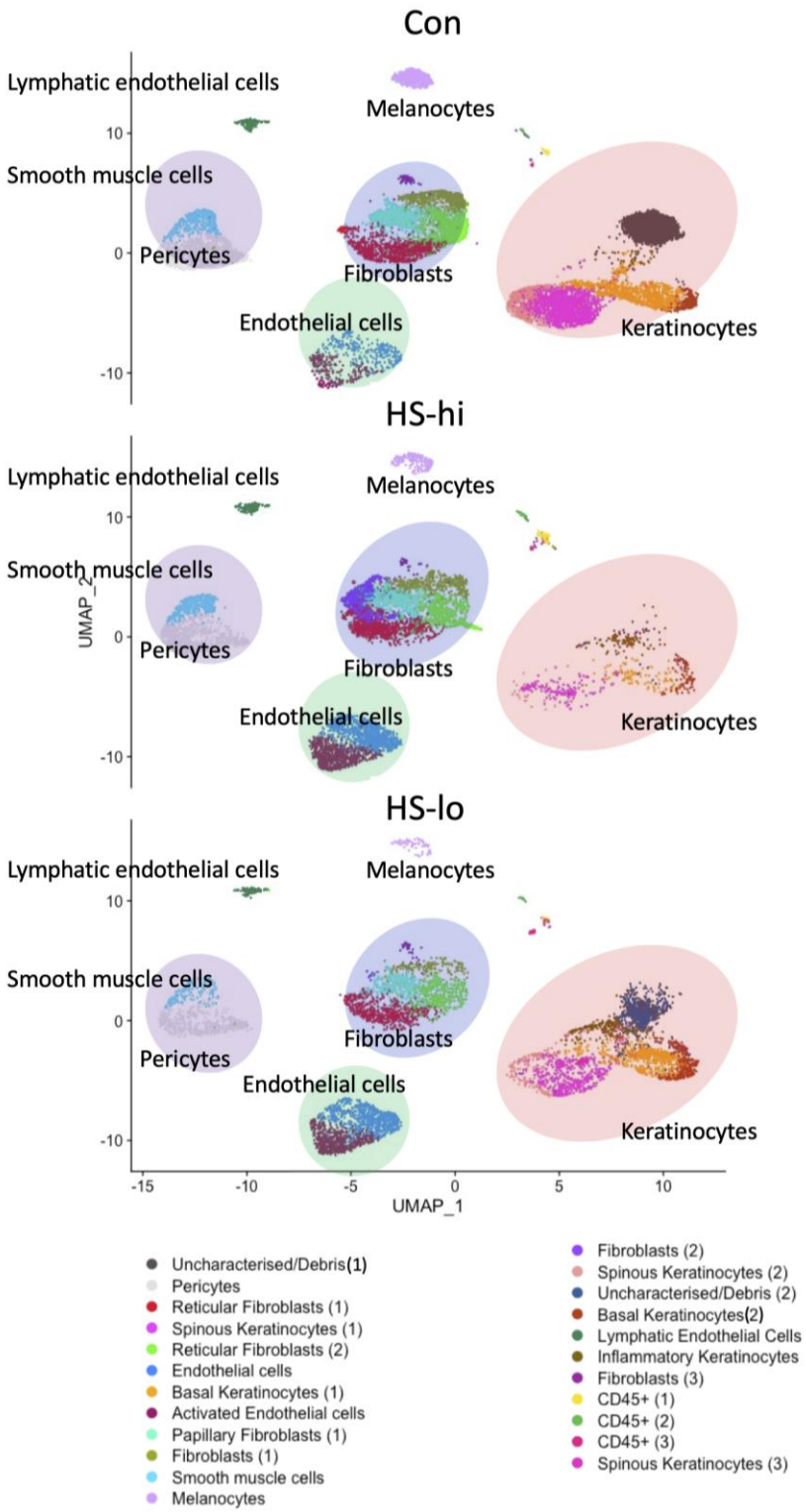

Figure 4.9 UMAP illustrating the cell populations identified in healthy control, HS-hi and HS-lo lesional skin. Single cells isolated from healthy controls (Con; n=3) or HS lesional skin (HS; n=6) were purified based on absence of CD45 expression, barcoded and sequenced by 10X Genomics scRNA-seq. UMAP displays the individual cells in 23 cell clusters isolated from healthy control skin (top), HS-hi (middle) and HS-lo (bottom) lesional skin after unsupervised classification of $CD45^-$ cells. HS-hi and HS-lo groups were identified based on relative variance to healthy control skin calculated by PCA.

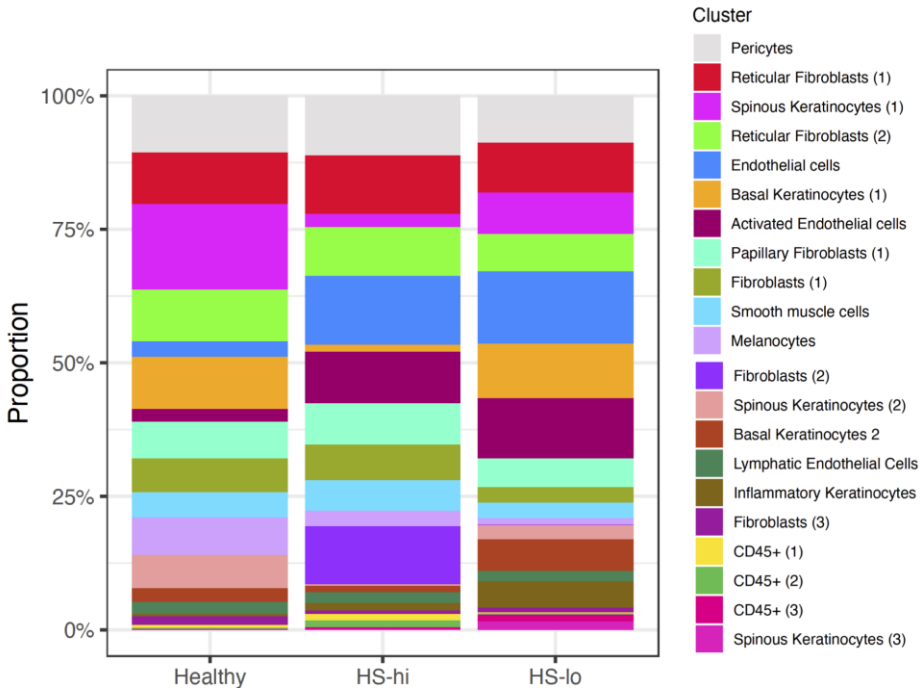

Figure 4.10 HS lesions with a higher inflammatory load had an altered cellular profile relative to HS lesions with a lower inflammatory load. Single cells isolated from healthy controls (Con; n=3) or HS lesional skin (HS; n=6) were purified based on absence of CD45 expression, barcoded and sequenced by 10X Genomics scRNA-seq. Bar chart showing the proportion of each cell cluster in healthy controls (n=3), HS-hi (n=4) and HS-lo (n=2) groups relative to all cells in the $CD45^-$ dataset.

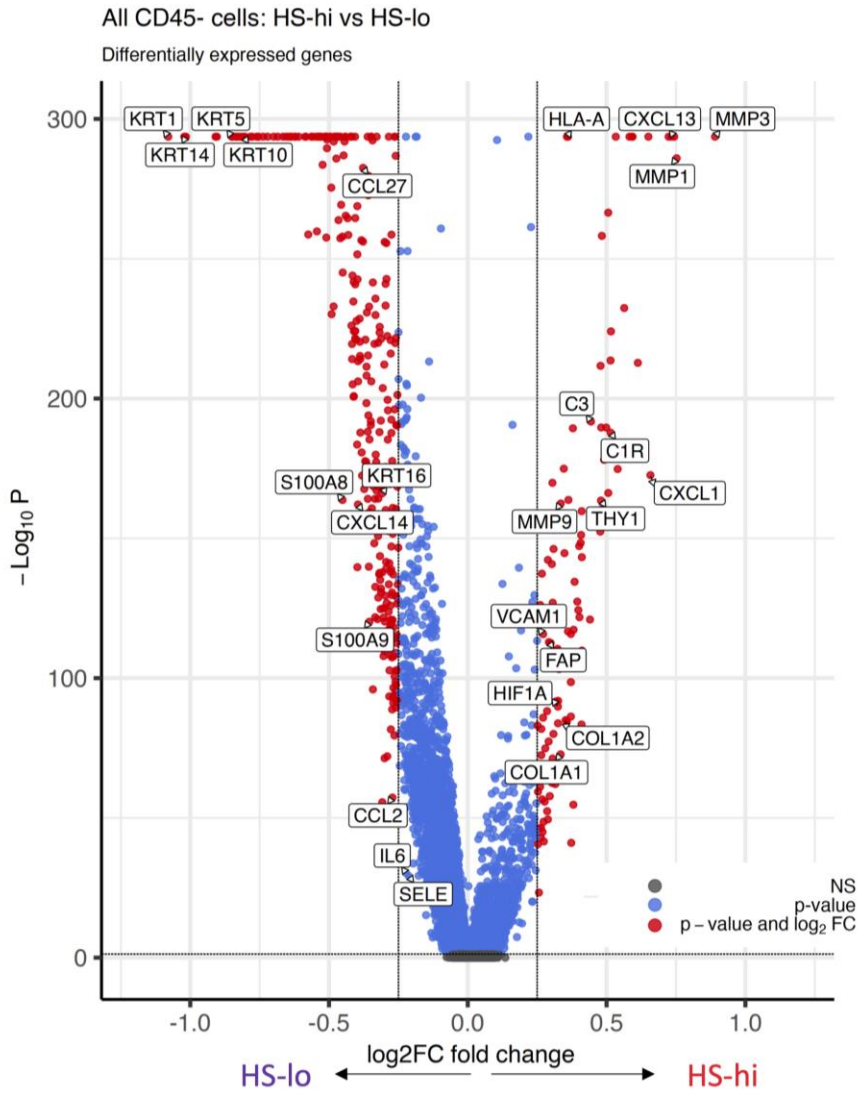

Figure 4.11 Volcano plot visualising DEGs between HS-hi and HS-lo lesions. Single cells isolated from healthy controls (Con; n=3) or HS lesional skin (HS; n=6) were purified based on absence of CD45 expression, barcoded and sequenced by 10X Genomics scRNA-seq. Volcano plot visualises DEGs in HS-hi (n=4) compared with HS-lo (n=2) lesions. Genes with a $log_2FC > 0$ are upregulated in HS-hi and a $log_2FC < 0$ are downregulated in HS-hi. The $-Log_{10}$ P Y-axis is a measure of significance.

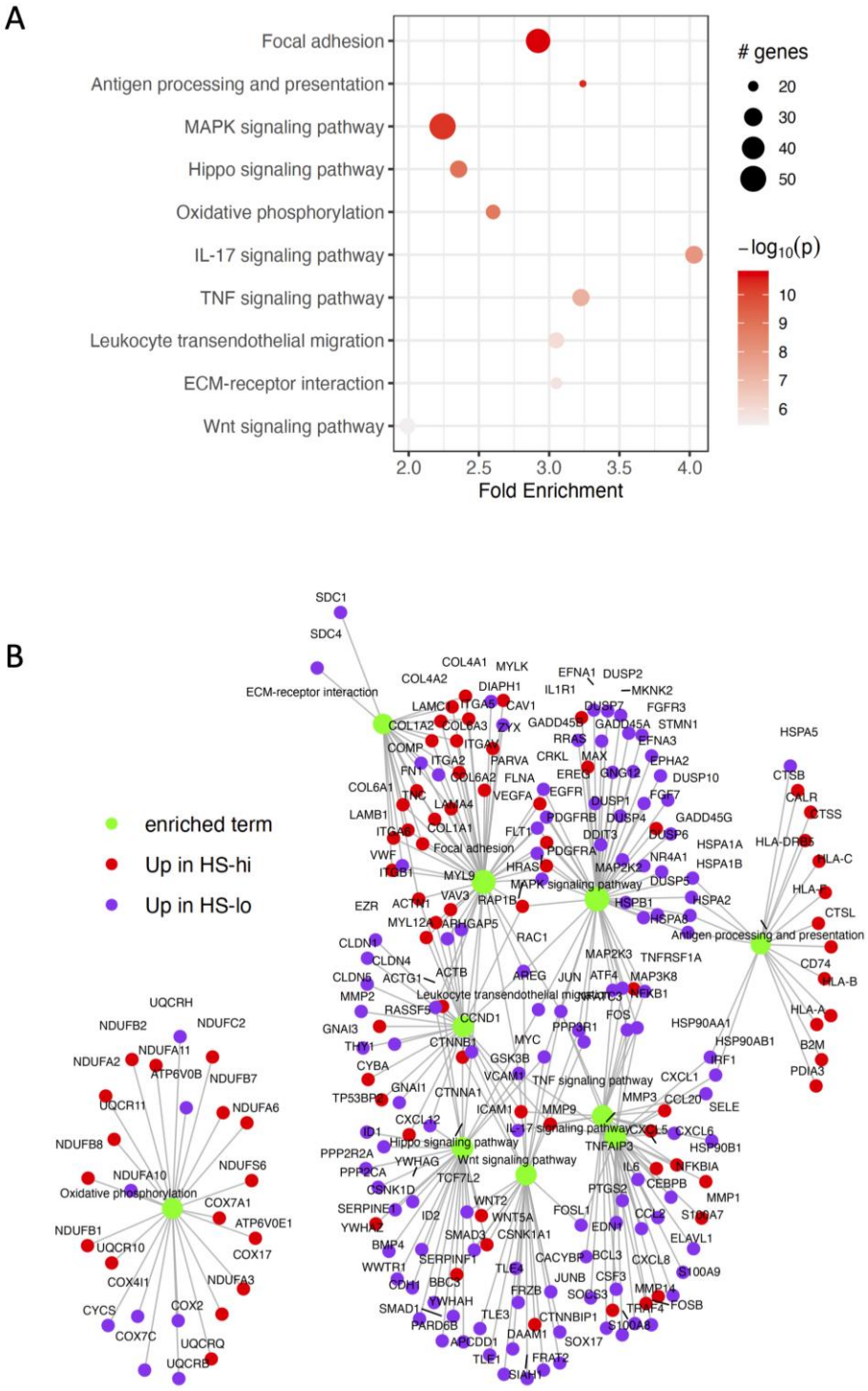

Figure 4.12 IL-17 and TNF signaling were key inflammatory pathways differentiating HS-lo from HS-hi lesions. Top 10 immune pathways enriched from the genes significantly differentially expressed between HS-lo and HS-hi lesions ($p < 0.05$ and $\log_2FC > 0.1$) (A). Gene-pathway network visualising the genes upregulated in HS-lo lesions (purple) or HS-hi lesions (red) in the top 10 immune pathways enriched from the DEGs between HS-lo and HS-hi lesions (B).

4.3.3 Characterisation of keratinocytes in HS lesions

As hyperkeratosis is an important element of HS pathogenesis (Frew, Hawkes and Krueger, 2018) an in-depth comparison of keratinocytes from HS lesions and healthy control skin was performed. HS lesional and healthy control skin comprised of 6 keratinocyte clusters identified following unsupervised clustering. This section characterises these 6 keratinocyte populations in HS lesional and healthy control skin.

Keratinocytes were categorised into 3 major populations, basal, spinous and inflammatory keratinocytes (**Figure 4.13A**). An overlapping UMAP displaying HS and healthy control keratinocytes highlighted inflammatory keratinocytes as a cell cluster of interest considering that they were predominantly found in HS lesions (**Figure 4.13B**).

To annotate the keratinocyte populations, characteristic cell markers were visualised on the keratinocyte UMAP (**Figure 4.14**). Basal keratinocytes were identified based on their elevated expression of the basal keratins *KRT5* (**Figure 4.14A**), *KRT14* (**Figure 4.14B**) and *KRT15* (**Figure 4.14C**), identifying two keratinocyte clusters as basal keratinocytes. Basal keratinocytes then differentiate into spinous keratinocytes downregulating the expression of the basal keratins and increasing the expression of *KRT1* (**Figure 4.14D**), *KRT10* (**Figure 4.14E**) and *KRTDAP* (**Figure 4.14F**), identifying three keratinocyte clusters as spinous keratinocytes. The final keratinocyte cluster had elevated expression of the inflammatory keratins *KRT6A* (**Figure 4.14G**), *KRT16* (**Figure 4.14H**) and *KRT17* (**Figure 4.14I**) and so was annotated as inflammatory keratinocytes. To confirm the annotation of basal, spinous and inflammatory keratinocytes, density plots display the co-expression of basal (**Figure 4.15A**), spinous (**Figure 4.15B**) and inflammatory keratins (**Figure 4.15C**) on the keratinocyte UMAP.

Visualising the frequency of keratinocyte clusters by bar chart confirmed the increase of inflammatory keratinocytes in HS lesional skin compared with healthy control skin (**Figure 4.16**). To validate these transcriptomic findings, keratinocytes were isolated into a single cell preparation from the epidermis of healthy control and HS lesional skin as per **Section 2.1.3**. Samples were then stained for surface expression of CD45 and intracellular expression of KRT10, KRT14 and KRT6 (**Section 2.1.9**) as per **Section 2.2.9**, fixed and analysed by flow cytometry. A gating strategy on how keratinocytes were identified is

shown in (**Figure 4.17**). All acquired events were initially gated as Forward Scatter Channel (FSC) vs the live/dead fixable viability dye eFluor506 (FixVia eF506). Live cells were identified within this plot (**Figure 4.17A**). Single cells were identified based on FSC-Area (FSC-A) vs FSC-Height (FSC-H) (**Figure 4.17B**). Immune cells and fibroblasts were removed based on the absence of the immune cell marker CD45 and the fibroblast marker CD90 ($CD45^-$ $CD90^-$; **Figure 4.17D**). Keratinocytes could be identified by expression of KRT14 and/or KRT10 (**Figure 4.17C**).

Keratinocytes were identified as $KRT10^-$ $KRT14^+$ basal keratinocytes or $KRT10^+$ $KRT14^+$ spinous keratinocytes (**Figure 4.17E**). Similar to the scRNA-seq data, there was a trend towards a decrease in the frequency of both basal and spinous keratinocytes in HS skin, however this failed to reach significance (**Figure 4.17F-G**). To estimate the frequency of inflammatory keratinocytes in basal and spinous keratinocytes the frequency of $KRT6^+$ keratinocytes in each population was calculated (**Figure 4.18**). There were significant increases in both basal ($p=0.037$) and spinous inflammatory keratinocytes ($p=0.0013$) in HS lesional skin compared with healthy control skin (**Figure 4.19A-B**). The median fluorescence intensity (MFI) for KRT6 expression was significantly increased in both basal ($p=0.0021$) and spinous keratinocytes ($p<0.0001$) from HS lesional skin relative to healthy control skin (**Figure 4.19C-D**), confirming the enrichment of inflammatory keratinocytes in HS skin.

In summary, there was a marked increase in the frequency of inflammatory keratinocytes in HS lesional skin relative to healthy control skin in our scRNA-seq data. These inflammatory keratinocytes express the inflammatory keratins *KRT6A*, *KRT16* and *KRT17* and this enrichment of inflammatory keratinocytes in HS skin was validated by flow cytometric analysis.

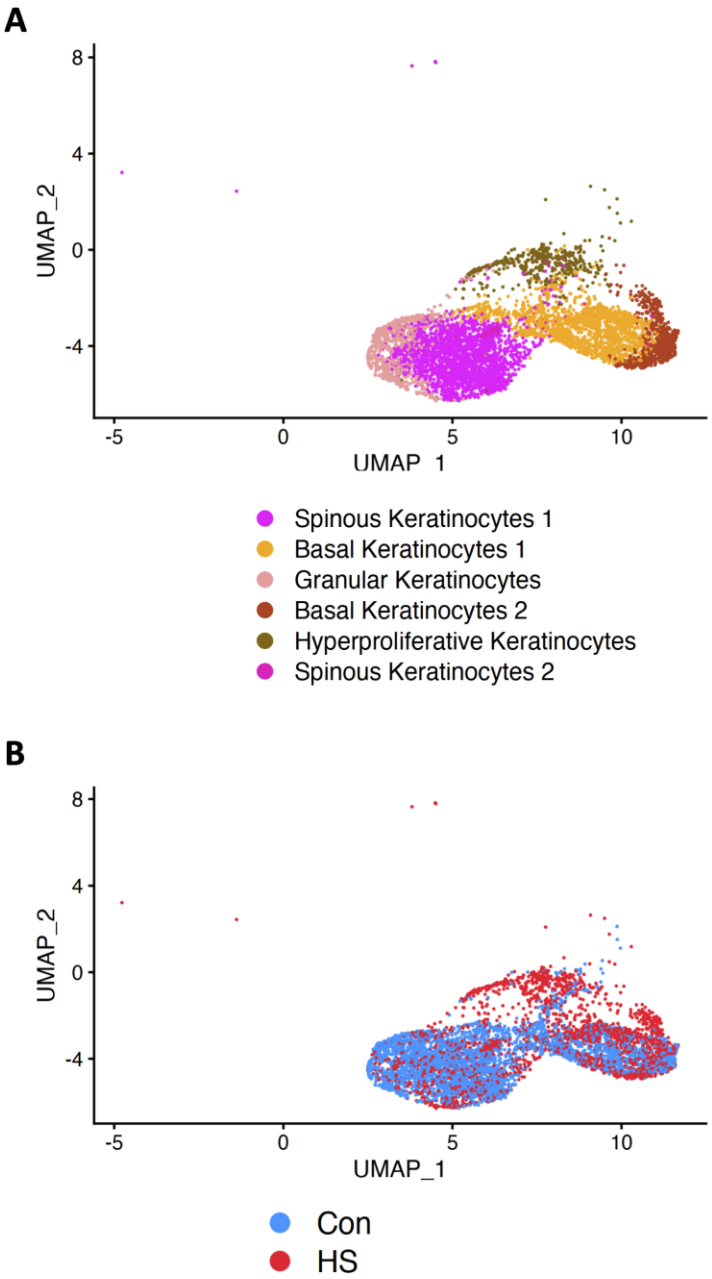

Figure 4.13 Inflammatory keratinocytes are enriched in HS lesional skin. Single cells isolated from healthy controls (Con; n=3) or HS lesional skin (HS; n=6) were purified based on absence of CD45 expression, barcoded and sequenced by 10X Genomics scRNA-seq. UMAP of 6 keratinocyte clusters identified by unsupervised classification in the $CD45^-$ dataset (A). UMAP plot overlaying keratinocytes from HS lesional skin (red) and healthy control skin (blue) (B).

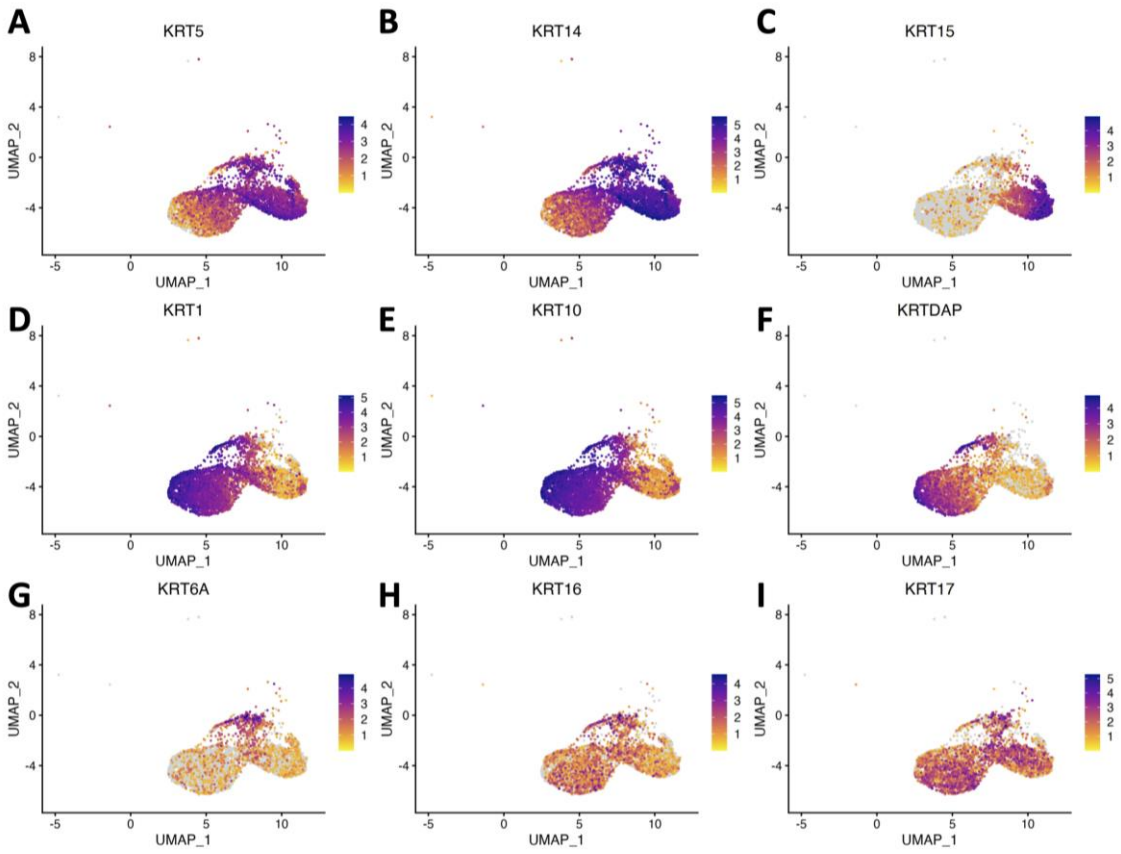

Figure 4.14 Characterisation of keratinocyte clusters. Single cells isolated from healthy controls (Con; n=3) or HS lesional skin (HS; n=6) were purified based on absence of CD45 expression, barcoded and sequenced by 10X Genomics scRNA-seq. UMAPs display gene expression for *KRT5* (A), *KRT14* (B), *KRT15* (C), *KRT1* (D), *KRT10* (E), *KRTDAP* (F), *KRT6A* (G), *KRT16* (H), *KRT17* (I) in keratinocytes from the $CD45^-$ cohort of HS lesional and healthy control skin.

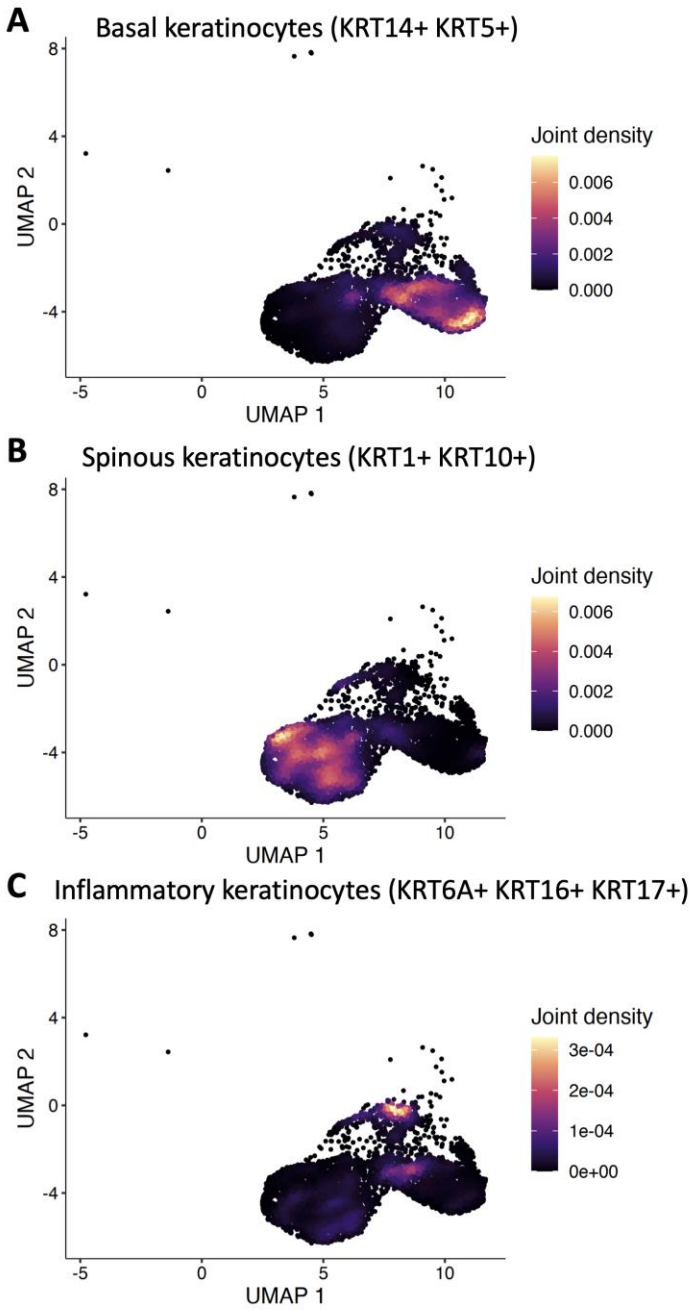

Figure 4.15 Density plot displaying basal, spinous and inflammatory keratinocytes. Single cells isolated from healthy controls (Con; n=3) or HS lesional skin (HS; n=6) were purified based on absence of CD45 expression, barcoded and sequenced by 10X Genomics scRNA-seq. Co-expression of basal (*KRT14*, *KRT5*; A), spinous (*KRT1*, *KRT10*; B) and inflammatory (*KRT6A*, *KRT16*, *KRT17*; C) keratinocyte markers in healthy control and HS lesional skin visualised on keratinocyte UMAP.

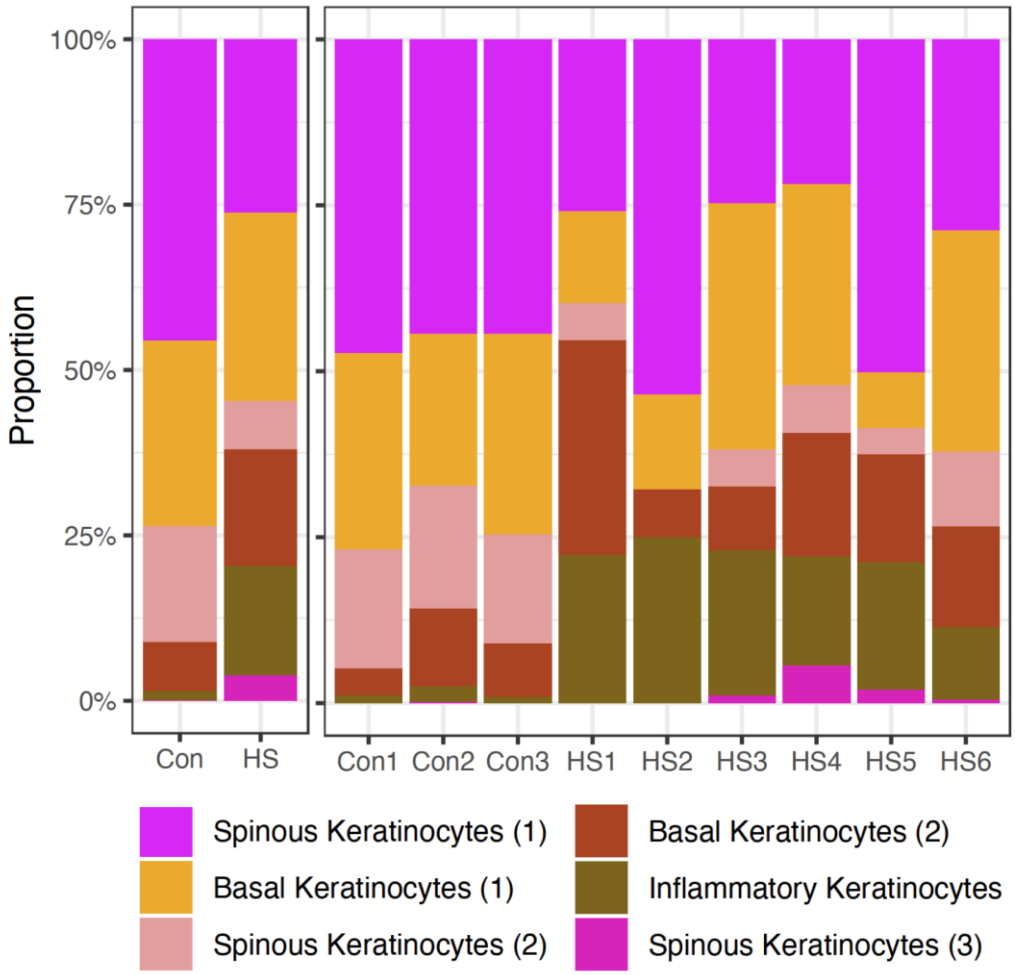

Figure 4.16 Inflammatory keratinocytes were elevated in HS lesional skin. Single cells isolated from healthy controls (Con; n=3) or HS lesional skin (HS; n=6) were purified based on absence of CD45 expression, barcoded and sequenced by 10X Genomics scRNA-seq. Bar chart showing the proportion of each cell cluster relative to all cells in the $CD45^-$ dataset.

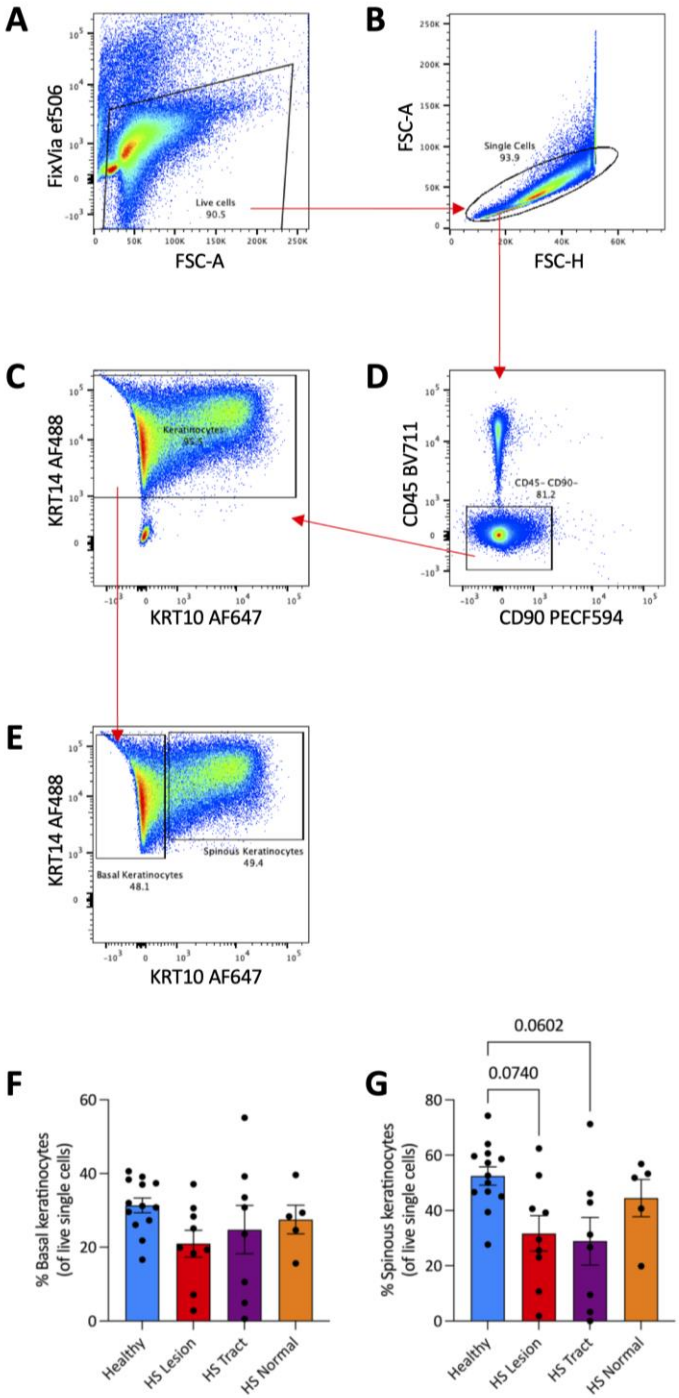

Figure 4.17 Keratinocyte frequencies in HS and healthy control epidermis. Cells isolated from the epidermis of healthy control (Healthy; n=13) or HS patients (HS Lesion, n=9; HS Tract, n=8; HS Normal, n=5) were stained for surface and intracellular markers in the presence of Fc block and analysed by flow cytometry. To identify single, viable $CD45^-$ $CD90^-$ keratinocytes, sequential gating was performed: Forward Scatter (FSC) vs Fixable-Viability-Dye^- to identify viable cells (A); FSC-Area vs FSC-Height to exclude doublets (B); CD45 vs CD90 to exclude immune cells and fibroblasts (C); KRT14 vs KRT10 to identify basal and spinous keratinocytes. Graphs show the frequency of basal (F) and spinous (G) keratinocytes calculated as a percentage of viable single cells. Graphs represent individual samples with mean ± standard error of mean (SEM) for each group. Statistical significance was calculated using Kruskal-Wallis one-way ANOVA with Dunn's multiple comparisons test.

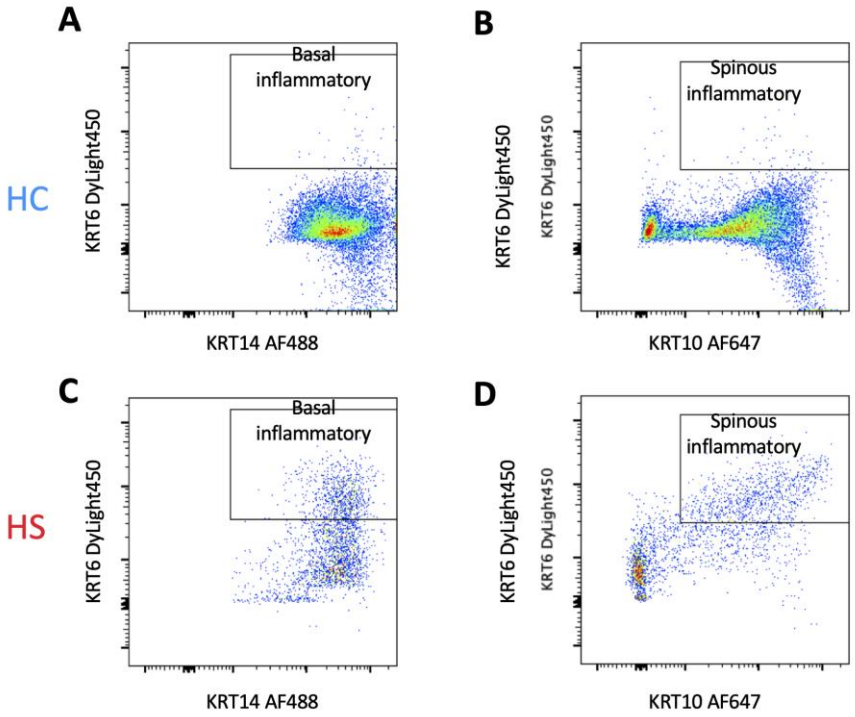

Figure 4.18 Representative plots displaying basal and spinous inflammatory keratinocytes in HS and healthy control skin. Cells isolated from the epidermis of healthy control (Healthy; n=13) or HS patients (HS Lesion, n=9; HS Tract, n=8; HS Normal, n=5) were stained for surface and intracellular markers in the presence of Fc block and analysed by flow cytometry. Basal and spinous inflammatory keratinocytes were identified as $KRT6^{+}KRT10^{+}$ (A, C) and $KRT6^{+}KRT14^{+}$ (B, D) keratinocytes in healthy control skin (A, B) and HS lesions (C, D).

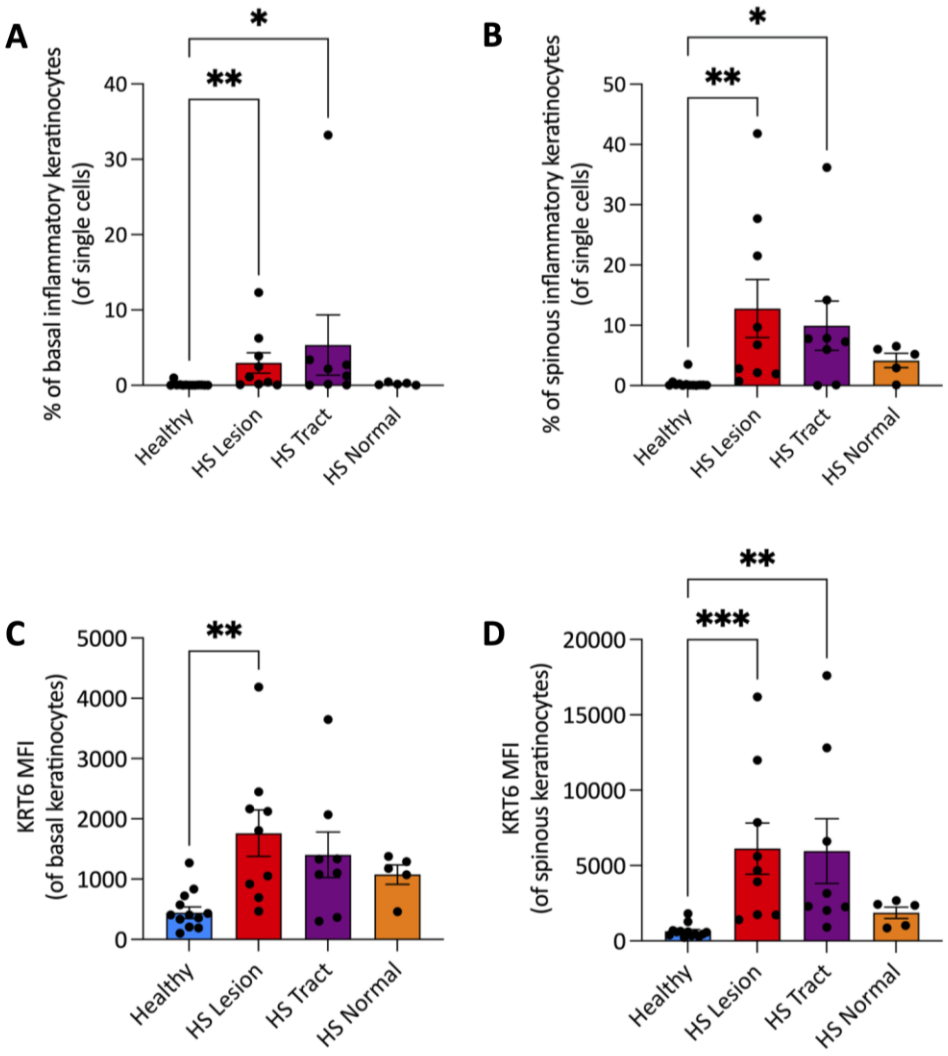

Figure 4.19 Inflammatory keratinocytes were enriched in HS skin compared with healthy control skin. Cells isolated from the epidermis of healthy control (Healthy; n=13) or HS patients (HS Lesion, n=9; HS Tract, n=8; HS Normal, n=5) were stained for surface and intracellular markers in the presence of Fc block and analysed by flow cytometry. Graphs show the frequency of inflammatory basal ($KRT6^+KRT14^+$)(A) and spinous ($KRT6^+KRT10^+$) (B) keratinocytes calculated as a percentage of viable single cells and the mean Fluorescence Intensity (MFI) of KRT6 in basal (C) and spinous (D) keratinocytes. Graphs represent individual samples with mean ± SEM for each group. Statistical significance was calculated using Kruskal-Wallis one-way ANOVA with Dunn's multiple comparisons test; * $p < 0.05$, ** $p < 0.01$, *** $p < 0.001$.

4.3.4 Transcriptomic differences between HS and healthy keratinocytes

An increased frequency of inflammatory keratinocytes was evident in HS lesions, however their role in HS inflammation has yet to be elucidated. This section details the transcriptomic differences between HS lesional and healthy control keratinocytes to evaluate their potential role in promoting HS inflammation.

PCA of keratinocytes confirmed that healthy control keratinocytes had homogenous transcriptomes. In contrast, keratinocytes from HS patients had a high degree of variation between samples (**Figure 4.20A**). Keratinocytes from 3 HS patients resembled those from healthy controls, while keratinocytes from the remaining 3 HS patients were highly heterogenous and had a much greater variance to the healthy control keratinocytes. Importantly, this variation did not match variation seen in all $CD45^-$ cells or in the $CD45^+$ cell cohort (Moran *et al.*, 2023).

Considering the broad transcriptomic differences between HS and healthy control keratinocytes, differential gene expression testing was performed on all keratinocytes to evaluate the transcriptomic differences at a single cell level. A volcano plot displayed the 2,908 DEGs between healthy control and HS lesional keratinocytes (**Figure 4.20B**). Genes with a $\log_2$ fold change >0 were elevated in HS lesional skin, genes with a $\log_2$ fold change <0 were downregulated in HS. Genes significantly differentially expressed were coloured in blue and those in red had a high fold change and warrant further investigation. 1,488 are upregulated in HS keratinocytes (**Table 8.11**) and 1,420 were upregulated in healthy control keratinocytes (**Table 8.12**). Of note, a number of genes found downstream of IL-17 cytokines were significantly upregulated in HS keratinocytes, including *S100A8* (**Figure 4.21A**), *S100A9* (**Figure 4.21B**), *S100A7* (**Figure 4.21C**), *KRT6A* (**Figure 4.21D**), *FABP5* **Figure 4.21E**), *CXCL8* (**Figure 4.21F**), *CXCL1* (**Figure 4.21G**), *CCL20* (**Figure 4.21H**) and *CXCL2* (**Figure 4.21I**) all of which were expressed by inflammatory keratinocytes. Genes downregulated in HS keratinocytes included *CCL27* (**Figure 4.21J**) and *DMKN* (**Figure 4.21K**), both of which have been linked to maintaining tissue homeostasis (Davila *et al.*, 2022; Utsunomiya *et al.*, 2020), and *TOB1* (**Figure 4.21L**) which may regulate keratinocyte differentiation (Park *et al.*, 2006). *CCL27*, *TOB1* and *DMKN* were predominantly expressed in basal and spinous keratinocytes.

Differential expression analysis of HS and healthy control keratinocytes confirmed an upregulation of proinflammatory mediators in HS keratinocytes. To further investigate the role of keratinocytes in HS inflammation, the expression of proinflammatory mediators was evaluated in each keratinocyte cluster (**Figure 4.22**). Spinous keratinocytes (1), basal keratinocytes (1) and inflammatory keratinocyte clusters had elevated expression of *CXCL8*, *CXCL1* and *CXCL2* in HS lesions relative to healthy controls. Interestingly, *CXCL2*, involved in neutrophil recruitment, had increased expression in HS keratinocytes across all keratinocyte clusters.

A diverse inflammatory milieu has been shown to promote HS inflammation (Del Duca *et al.*, 2020). To evaluate the cytokine signaling program which influences each keratinocyte cluster in HS and healthy controls, IFN-γ, TNF, IL-17 and IL-1β signaling pathway scores were calculated in each keratinocyte (**Table 2.7**). IFN-γ, TNF and IL-1β signaling scores were relatively similar across all keratinocyte clusters and between healthy control and HS keratinocytes (**Figure 4.23**). Of note, all keratinocyte clusters had elevated IL-17 signaling scores in HS relative to healthy controls, suggesting that all keratinocytes are impacted by IL-17 cytokines in HS lesions. Further, the inflammatory keratinocyte cluster had the highest IL-17 signaling score, suggesting that IL-17 cytokines may promote the development of inflammatory keratinocytes in HS.

Interestingly, HS lesions from HS-hi patients had a reduced frequency of keratinocytes relative to HS-lo or healthy control skin (**Figure 8.3**). The reason for this reduced frequency of keratinocytes is difficult to determine without histological examination of the HS lesional biopsies. Despite this, the relative frequency of inflammatory keratinocytes progressively increased in a stepwise fashion from healthy control skin to HS-lo to HS-hi lesions (**Figure 8.4A**). Coinciding with this, HS-hi keratinocytes had increased expression of the inflammatory keratin *KRT6A* and the IL-17 mediated *CXCL1* (**Figure 8.4B, Table 8.23Table 8.24**). Additionally, IL-17 signaling was enriched from the DEGs between HS-hi and HS-lo keratinocytes (**Figure 8.5C**). HS-hi keratinocytes had elevated expression of inflammatory keratins, AMPs, *CXCL1* and *CXCL8* relative to both HS-lo lesions and healthy control skin (**Figure 8.5B**).

To gain a better understanding of the transcriptomic differences between HS and healthy control keratinocytes, differential expression analysis was performed in each keratinocyte cluster. Identifying genes and inflammatory pathways that were distinctly elevated in each keratinocyte cluster provides unique insight into how different keratinocyte populations function in healthy control skin and HS lesions. A volcano plot illustrates the 1,753 DEGs between HS and healthy control keratinocytes in the spinous keratinocyte (1) cluster (**Figure 4.24**). HS spinous keratinocytes (1) had elevated expression of a number of genes found downstream of IL-17 cytokines, including *S100A8*, *S100A9*, *S100A7*, *KRT6A*, *CXCL1*, *CXCL8* and *CCL20* relative to healthy controls. 261 genes were elevated in HS spinous keratinocytes (1) (**Table 8.13**) and 1,492 genes were elevated in healthy control spinous keratinocytes (1) (**Table 8.14**). The top 5 immune related pathways enriched from the DEGs included oxidative phosphorylation, focal adhesion, MAPK signaling, TNF signaling and antigen presentation (**Figure 4.25A**). The focal adhesion pathway was particularly elevated in HS lesions relative to healthy controls, suggesting elevated epidermal renewal in HS lesions (**Figure 4.25A**). A gene-pathway network displays the DEGs from each enriched pathway. Of particular note, oxidative phosphorylation appeared to be markedly dysregulated in HS spinous keratinocytes (1) with a number of DEGs elevated in healthy controls (**Figure 4.25B**). Interestingly, **Figure 4.25B** displays the genes found differentially expressed between HS and healthy controls and indicates that DEGs which relate to oxidative phosphorylation are downregulated in HS. Contrastingly, **Figure 4.25A** displays the expression of all genes involved in that particular pathway, including genes not significantly differentially expressed between HS and healthy controls, and does not display a difference between HS and healthy controls.

Similar DEGs were among the most differentially expressed in the basal keratinocytes (1) as were seen in the spinous keratinocyte (1) cluster (**Table 8.15Table 8.16**). *S100A8*, *S100A9*, *S100A7*, *KRT6A*, *CCL20*, *CXCL1* and *CXCL8* were all elevated in HS keratinocytes in the basal keratinocyte (1) cluster (**Figure 4.26**). Interestingly, extracellular matrix interactions, FC-γ receptor mediated phagocytosis, focal adhesion, NLR and MAPK signaling were among the top 5 immune related pathways enriched from the DEGs (**Figure 4.27A**). Of particular interest, MAPK and NLR signaling are elevated in HS keratinocytes in the basal keratinocyte (1) cluster, suggesting HS basal keratinocytes had increased activation (**Figure 4.27B**). Further, the increased levels of ECM interactions- and focal adhesion-related genes

in HS keratinocytes suggests the HS basal keratinocytes (1) cluster has elevated epidermal renewal (**Figure 4.27B**), contributing to the epidermal thickening characteristic of HS.

The second cluster of spinous keratinocyte cluster, spinous keratinocytes (2), had 386 DEGs between HS lesions and healthy controls (**Figure 4.28**). 157 genes were significantly upregulated in HS keratinocytes (**Table 8.17**) and 229 were significantly upregulated in healthy control keratinocytes in this cluster (**Table 8.18**). Of note, *SERPINB4* and *AKR1B10* which play a role in keratinocyte proliferation were significantly elevated in HS lesions (Zhang *et al.*, 2023; Gao, Yi and Ding, 2017). Among the top 5 immune related pathways enriched from these DEGs were glycolysis, antigen presentation, TLR, MAPK, and JAK-STAT signaling (**Figure 4.29A**). A marked increase in glycolysis pathway scores were seen in HS keratinocytes in this spinous keratinocyte (2) cluster. Interestingly, the increased expression of *ENO1*, *TPI1*, *PKM* and *GAPDH* in HS keratinocytes and the reduced expression of *LDHB* suggests increased glycolytic activity which may subsequently drive the TCA cycle due to reduced conversion of pyruvate to lactate (**Figure 4.29B**).

Figure 4.30 displays the volcano plot of DEGs between healthy control samples and HS lesional keratinocytes in the basal keratinocyte (2) cluster. 1,117 genes were upregulated in HS lesions (**Table 8.19**) and 85 were upregulated in healthy controls from the basal keratinocyte (2) cluster (**Table 8.20**), demonstrating a clear dysregulation of HS keratinocytes in this cluster. Interestingly, a broader range of genes were differentially expressed in HS keratinocytes beyond genes found downstream of IL-17. *IFITM3*, an interferon inducible gene, *PYCARD* which is essential for NLRP3 inflammasome assembly (Ting, Kastner and Hoffman, 2006) and *SLC2A1* (GLUT1) were all significantly elevated in HS keratinocytes. Taken together, 158 pathways were significantly enriched from the DEGs. The top 5 immune pathways enriched included oxidative phosphorylation, FCγ receptor mediated phagocytosis, mTOR signaling, Hippo signaling and antigen presentation (**Figure 4.31A**). Oxidative phosphorylation was strikingly elevated in HS keratinocytes compared with healthy control keratinocytes from the basal keratinocyte (2) cluster. Increased expression of both mTOR and oxidative phosphorylation genes suggests that these HS keratinocytes have a high energy demand possibly due to their role in promoting inflammation (**Figure 4.31B**).

HS inflammatory keratinocytes had elevated expression of the AMPs *S100A7*, *S100A8* and *S100A9*, proliferation associated genes *AKR1B10* and *SERPINB4* and the NLRP3 inflammasome-associated *PYCARD,* compared with healthy keratinocytes (**Figure 4.32**, **Table 8.21Table 8.22**). The limited number of inflammatory keratinocytes found in healthy controls hindered this analysis, however oxidative phosphorylation, antigen presentation, IL-17, glucagon and MAPK signaling were significantly enriched from the DEGs between HS and healthy control keratinocytes in the inflammatory keratinocyte cluster (**Figure 4.33A**). Interestingly, oxidative phosphorylation and IL-17 signaling were distinctly upregulated in HS lesional keratinocytes relative to those from healthy controls (**Figure 4.33B**).

The final keratinocyte cluster, the spinous keratinocyte (3) cluster, had no healthy control keratinocytes in this cluster and so differential expression testing could not be performed.

In summary, this section demonstrates a clear dysregulation of HS keratinocytes which may be driven by IL-17 signaling. HS inflammatory keratinocytes had increased expression of *CXCL8* and *CXCL1*, as well as elevated IL-17 signaling relative to other keratinocyte clusters. HS keratinocytes also appeared to be metabolically dysregulated compared with healthy control keratinocytes, with both oxidative phosphorylation and glycolytic pathways enriched in HS keratinocytes.

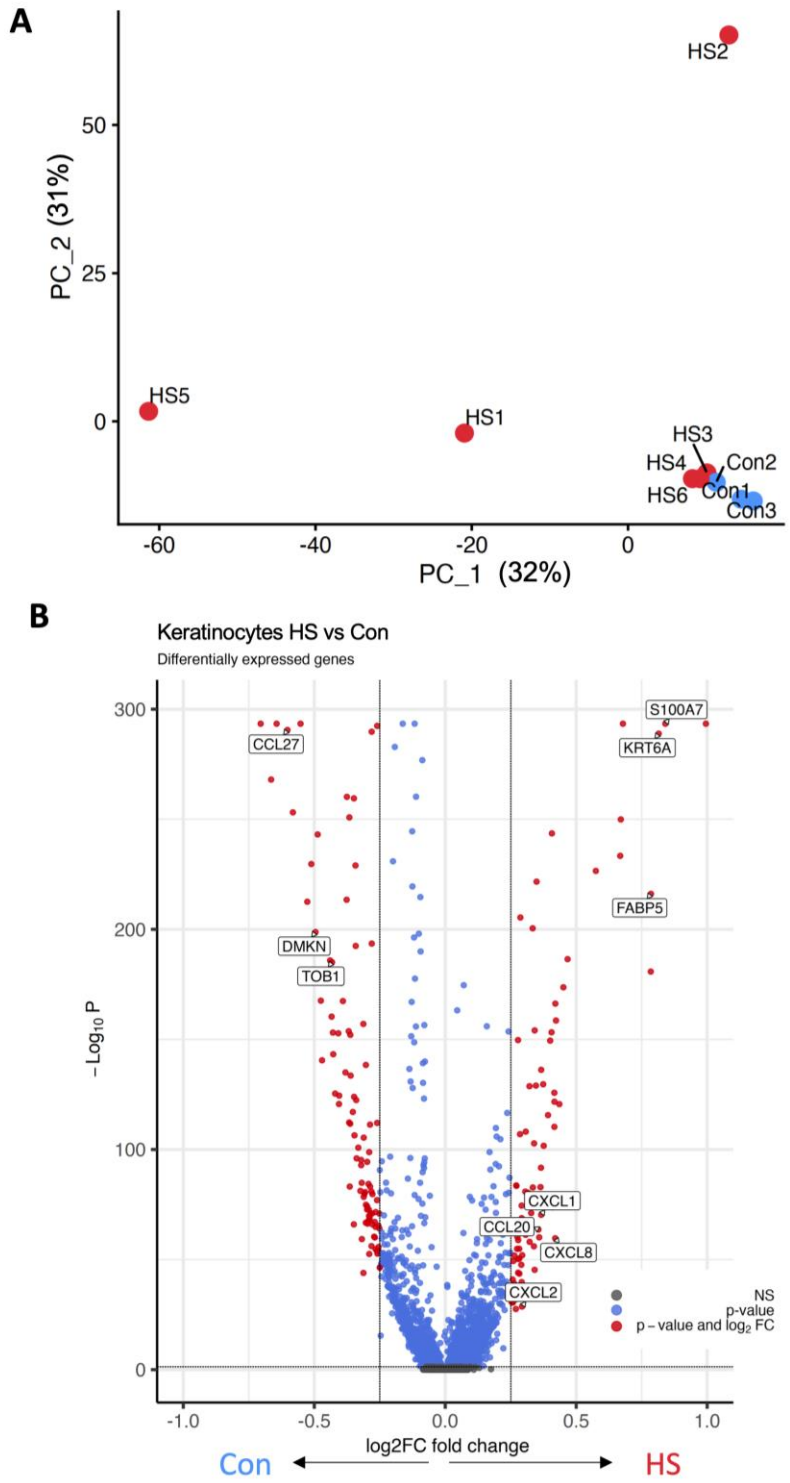

Figure 4.20 Volcano plot illustrating differentially expressed genes in healthy control and HS lesional keratinocytes. Single cells isolated from healthy controls (Con; n=3) or HS lesional skin (HS; n=6) were purified based on absence of CD45 expression, barcoded and sequenced by 10X Genomics scRNA-seq. Volcano plot visualises DEGs in HS keratinocytes compared with healthy control keratinocytes. Genes with a $log_2FC > 0$ are upregulated in HS and a $log_2FC < 0$ are downregulated in healthy controls. The $-Log_{10}P$ Y-axis is a measure of significance.

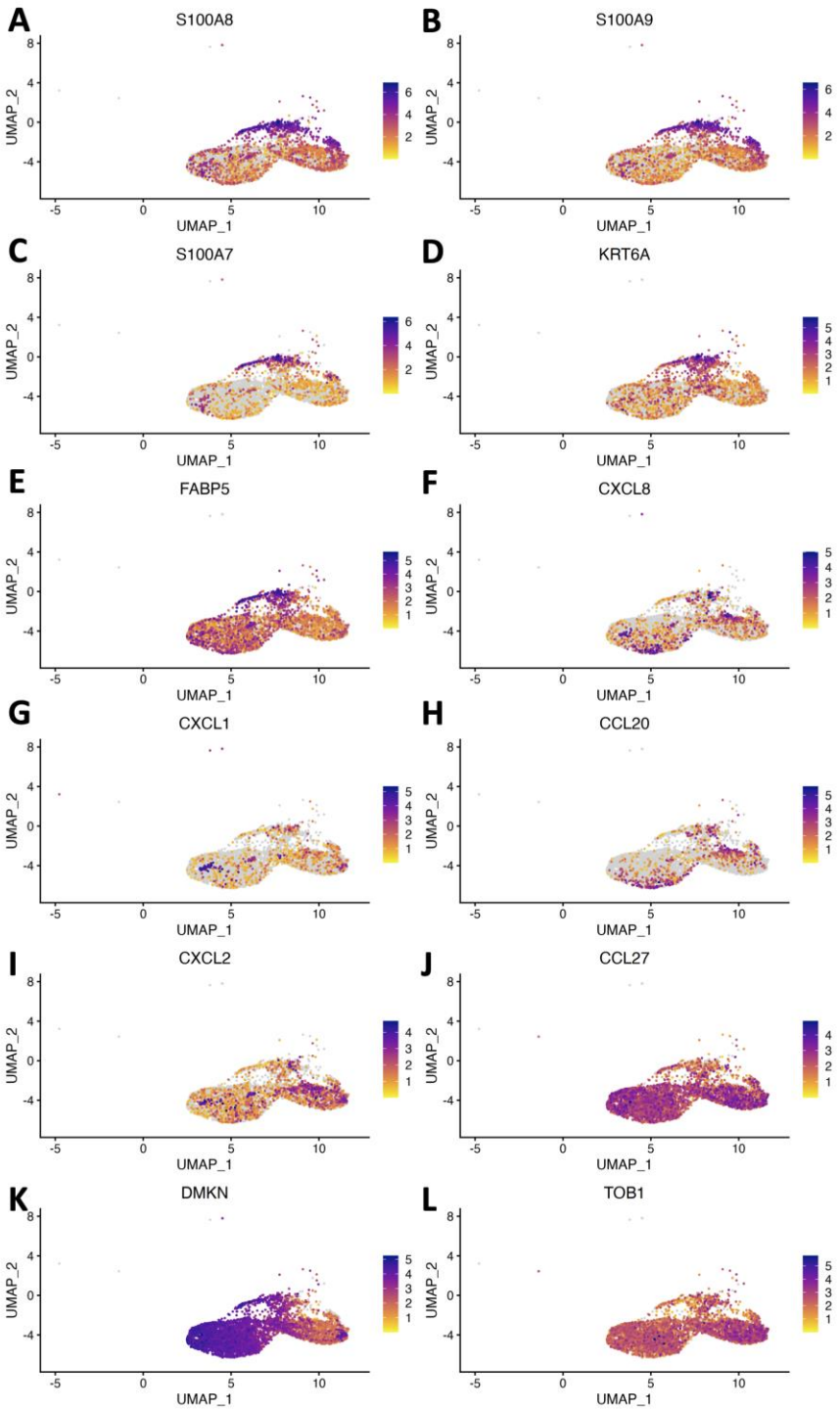

Figure 4.21 Inflammatory keratinocytes express key proinflammatory DEGs. Single cells isolated from healthy controls (Con; n=3) or HS lesional skin (HS; n=6) were purified based on absence of CD45 expression, barcoded and sequenced by 10X Genomics scRNA-seq. UMAP displays proinflammatory DEGs including *S100A8* (A), *S100A9* (B), *S100A7* (C), *KRT6A* (D), *FABP5* (E), *CXCL8* (F), *CXCL1* (G), *CCL20* (H), *CXCL2* (I), *CCL27* (J), *DMKN* (K), *TOB1* (L) in HS and healthy keratinocytes following unsupervised classification.

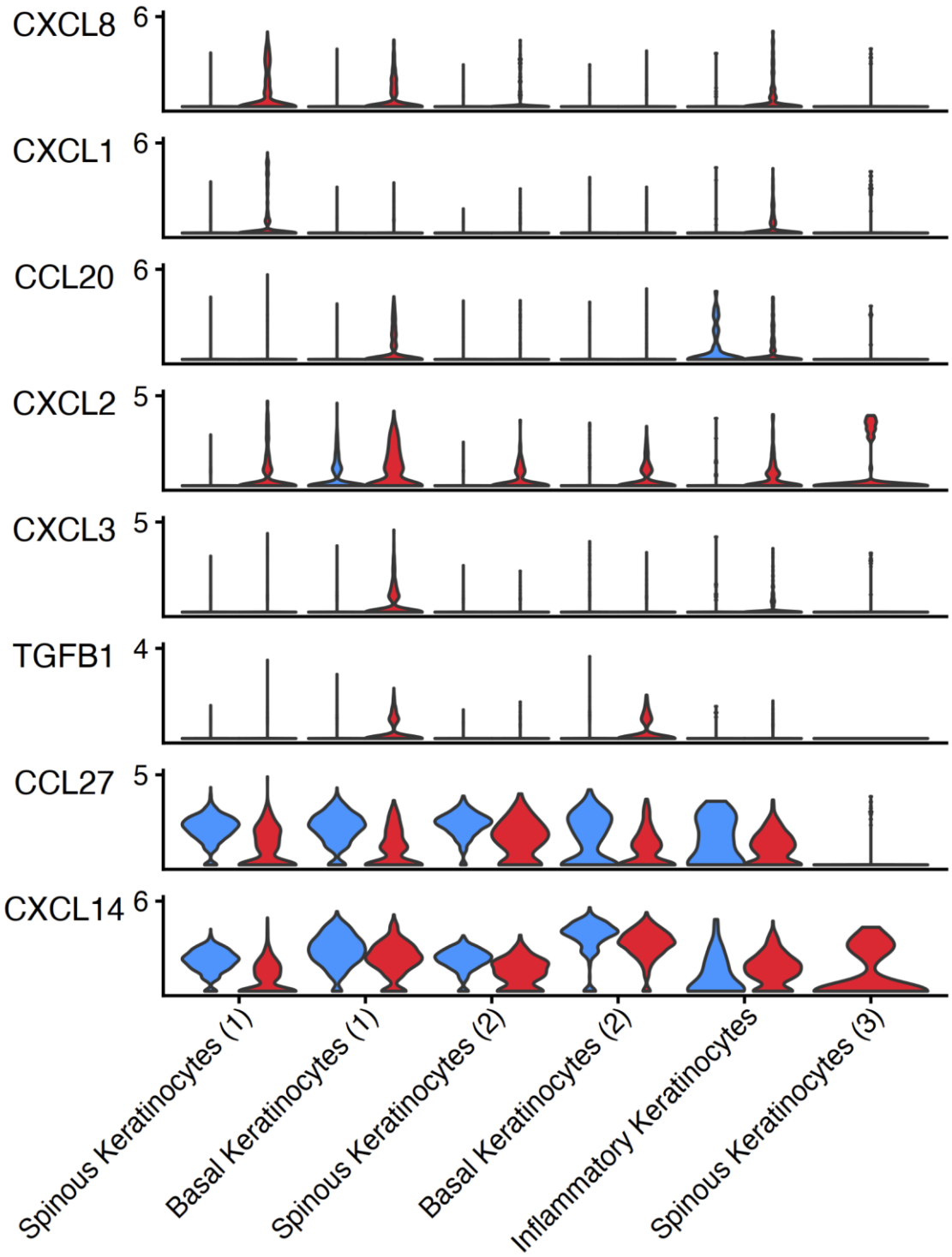

Figure 4.22 Inflammatory keratinocytes display increased expression of IL-17 signaling genes. Single cells isolated from healthy controls (Con; n=3) or HS lesional skin (HS; n=6) were purified based on absence of CD45 expression, barcoded and sequenced by 10X Genomics scRNA-seq. Violin plots visualising the expression of key inflammatory genes (*CXCL8*, *CXCL1*, *CCL20*, *CXCL2*, *CXCL3*, *TGFB1*, *CCL27*, *CXCL14*) in each keratinocyte cluster in both healthy (blue) and HS (red) keratinocytes.

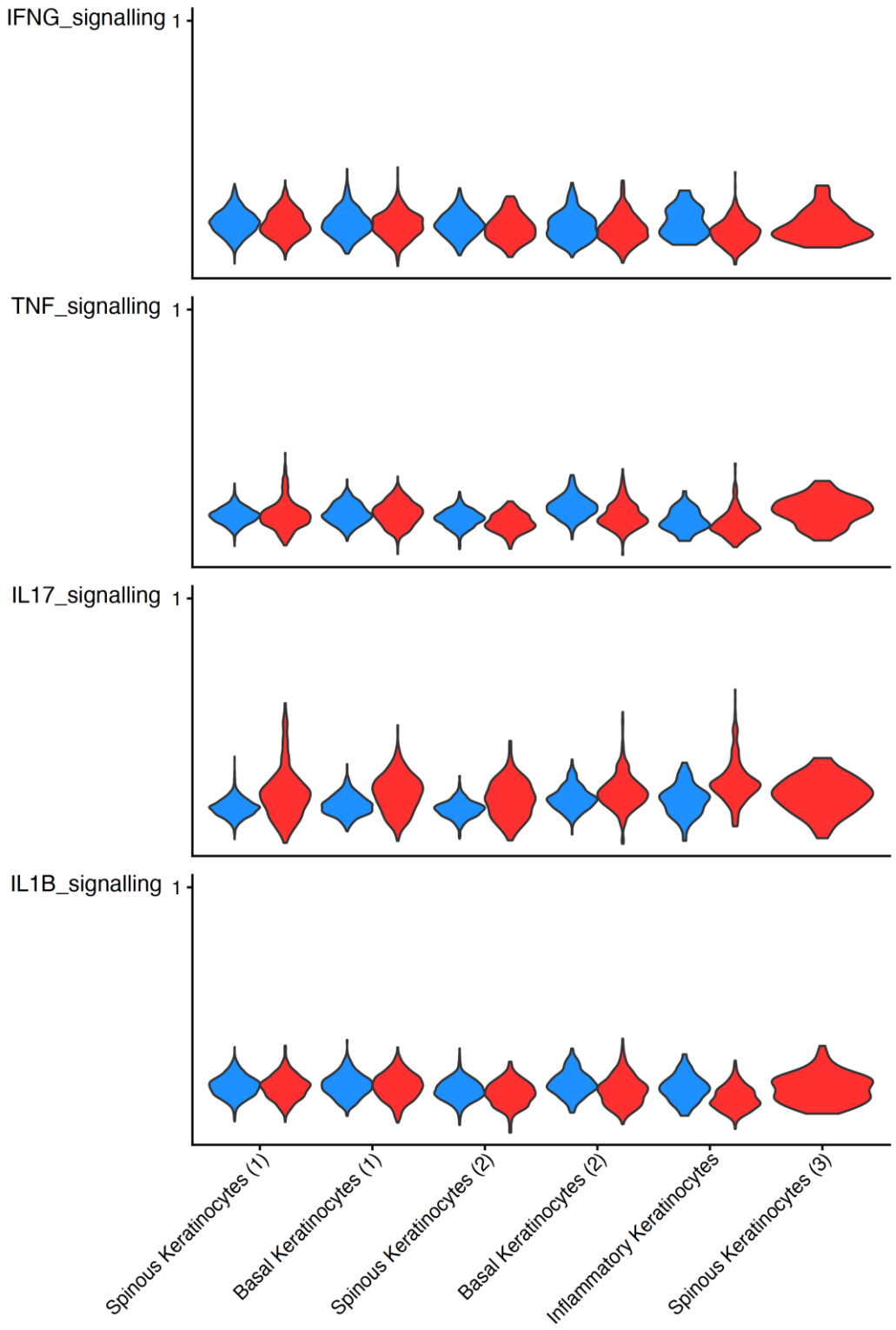

Figure 4.23 HS keratinocytes are highly regulated by IL-17 signaling. Single cells isolated from healthy controls (Con; n=3) or HS lesional skin (HS; n=6) were purified based on absence of CD45 expression, barcoded and sequenced by 10X Genomics scRNA-seq. Violin plots display the expression of IFN-γ, TNF, IL-17 and IL-1β signaling genes in individual keratinocyte clusters within HS lesional and healthy control skin.

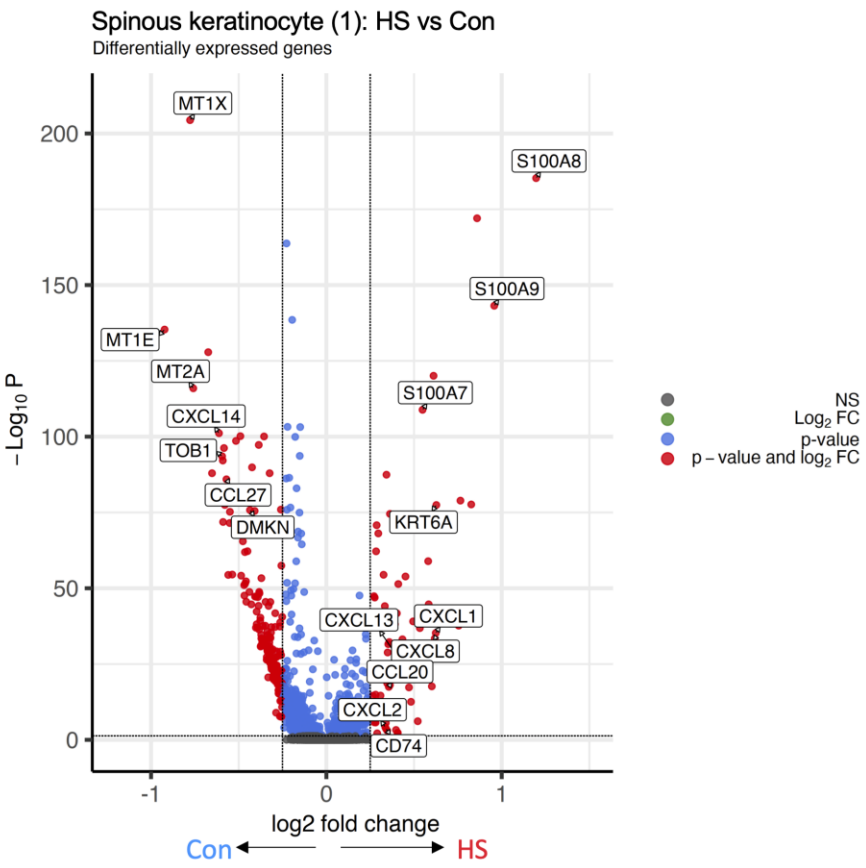

Figure 4.24 Volcano plot displaying DEGS between HS and healthy controls in the spinous keratinocyte (1) cluster. Single cells isolated from healthy controls (Con; n=3) or HS lesional skin (HS; n=6) were purified based on absence of CD45 expression, barcoded and sequenced by 10X Genomics scRNA-seq. Volcano plot visualises DEGs in HS compared with healthy control keratinocytes in the spinous keratinocyte (1) cluster. Genes with a $log_2FC > 0$ are upregulated in HS and a $log_2FC < 0$ are downregulated in HS. The $-Log_{10}P$ Y-axis is a measure of significance.

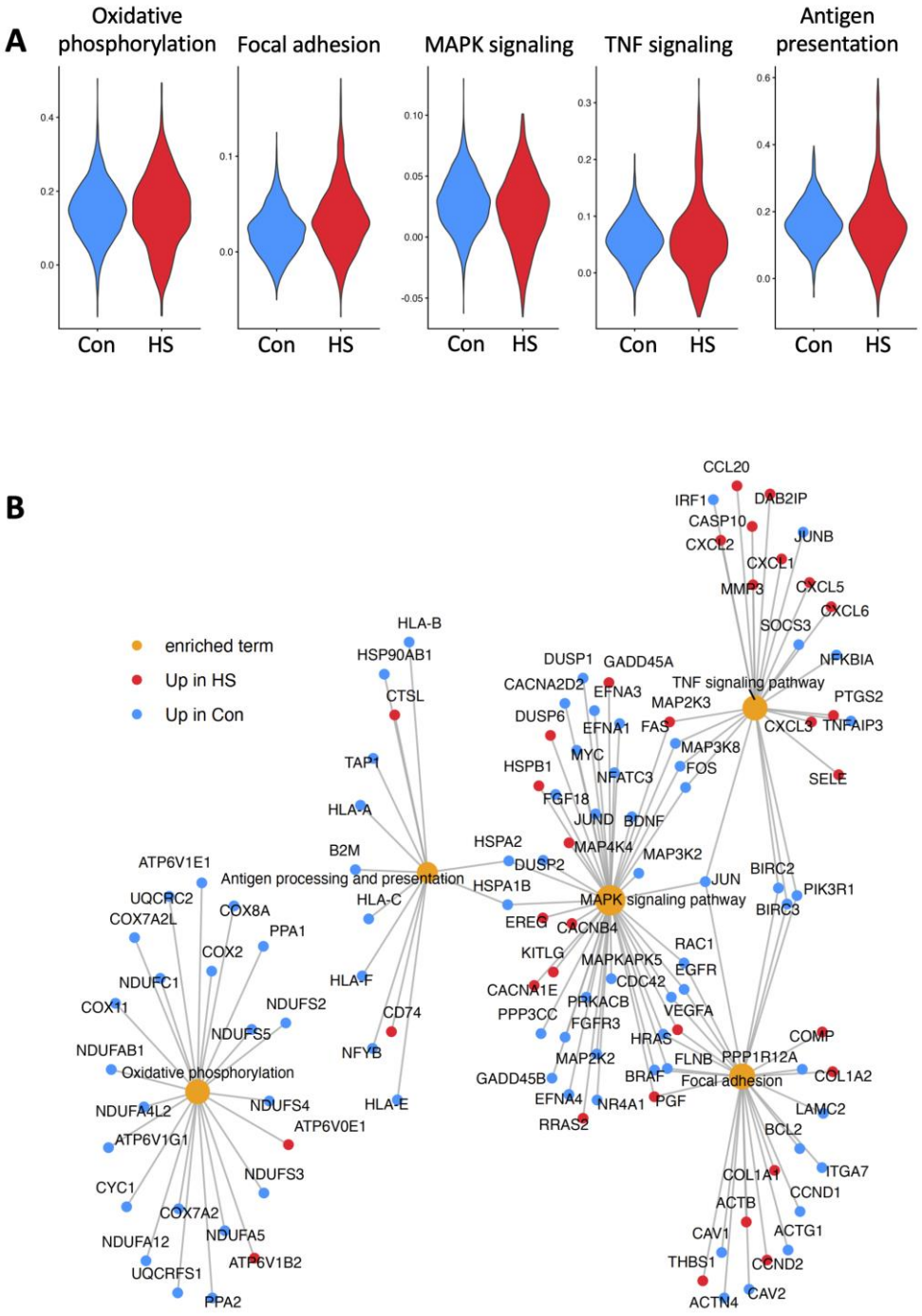

Figure 4.25 Pathways enriched from DEGs between HS and healthy controls in the spinous keratinocyte (1) cluster. Single cells isolated from healthy controls (Con; n=3) or HS lesional skin (HS; n=6) were purified based on absence of CD45 expression, barcoded and sequenced by 10X Genomics scRNA-seq. Violin plot of pathway activity score of top 5 immune pathways enriched from the DEGs between healthy control and HS lesional cells in the spinous keratinocytes (1) cluster (A). Gene-pathway network visualising the genes upregulated in Con (blue) or HS lesions (red) in the top 5 immune pathways enriched from the DEGs between healthy control and HS lesional cells in the spinous keratinocyte (1) cluster (B).

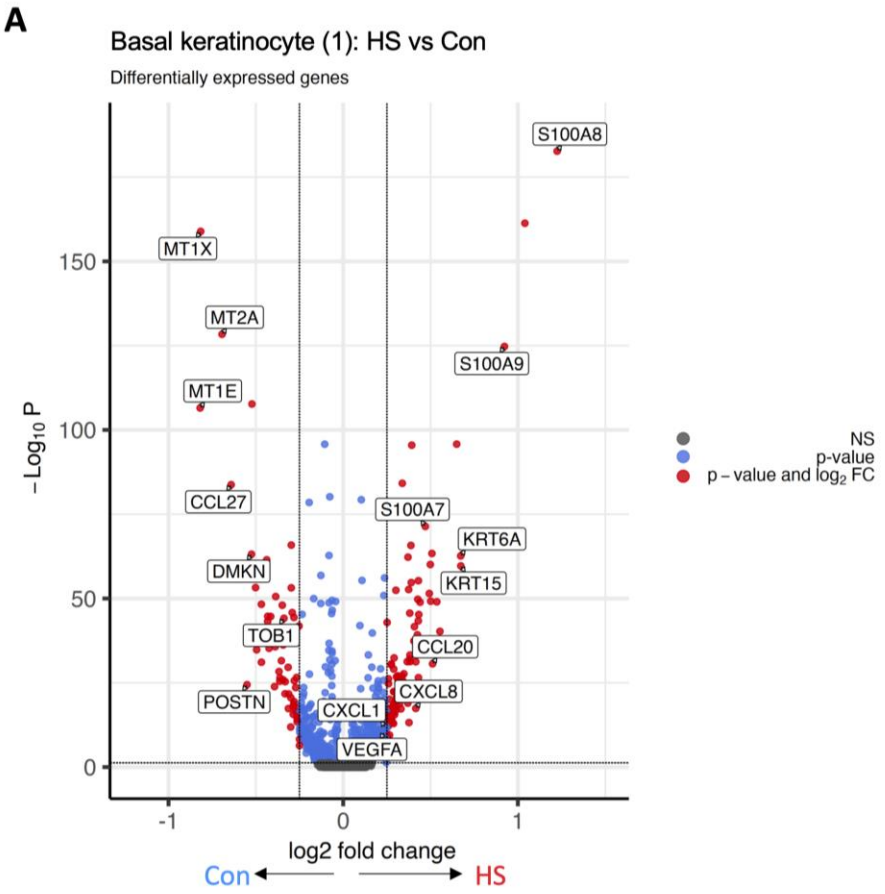

Figure 4.26 Volcano plot displaying DEGS between HS and healthy controls in the basal keratinocyte (1) cluster. Single cells isolated from healthy controls (Con; n=3) or HS lesional skin (HS; n=6) were purified based on absence of CD45 expression, barcoded and sequenced by 10X Genomics scRNA-seq. Volcano plot displays DEGs between HS lesional and healthy controls in the basal keratinocyte (1) cluster. Genes with a $log_2FC > 0$ are upregulated in HS and a $log_2FC < 0$ are downregulated in HS. The $-Log_{10}P$ Y-axis is a measure of significance.

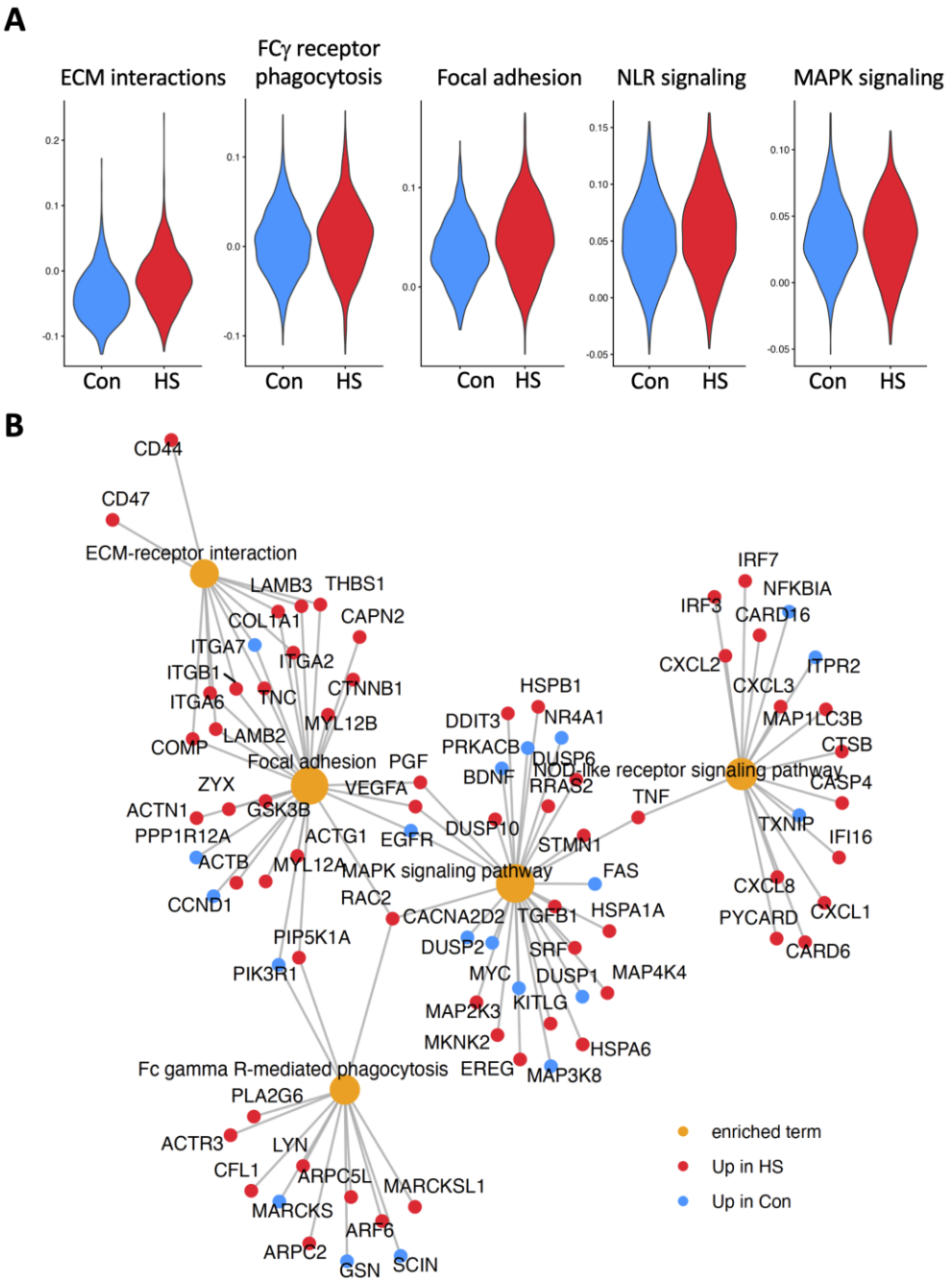

Figure 4.27 Extracellular matrix interactions, focal adhesion, NLR signaling and MAPK signaling differentiate healthy control and HS keratinocytes in the basal keratinocyte (1) cluster. Single cells isolated from healthy controls (Con; n=3) or HS lesional skin (HS; n=6) were purified based on absence of CD45 expression, barcoded and sequenced by 10X Genomics scRNA-seq. Violin plot of pathway activity scores of the top 5 immune pathways enriched from the DEGs between healthy control and HS lesional keratinocytes in the basal keratinocytes (1) cluster (A). Gene-pathway network visualising the genes upregulated in Con (blue) or HS lesions (red) in the top 5 immune pathways enriched from the DEGs between healthy control and HS lesional keratinocytes in the basal keratinocyte (1) cluster (B).

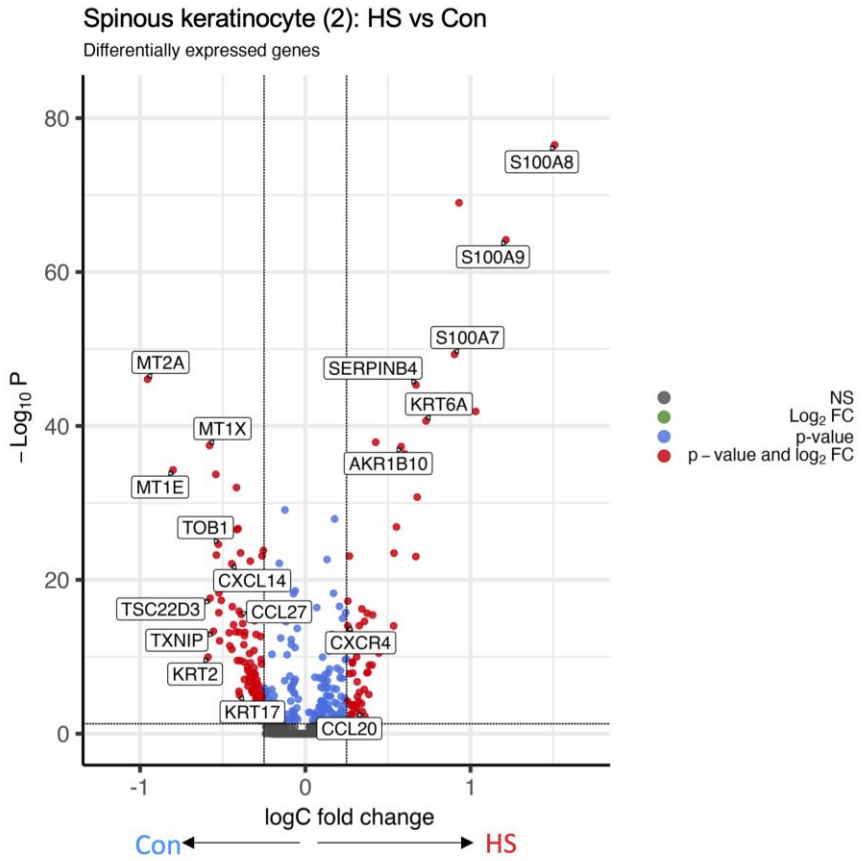

Figure 4.28 Volcano plot displaying DEGS between HS and healthy controls in the spinous keratinocyte (2) cluster. Single cells isolated from healthy controls (Con; n=3) or HS lesional skin (HS; n=6) were purified based on absence of CD45 expression, barcoded and sequenced by 10X Genomics scRNA-seq. Volcano plot displays DEGs between HS and healthy controls in the spinous keratinocytes (2) cluster. Genes with a $log_2FC > 0$ are upregulated in HS and a $log_2FC < 0$ are downregulated in HS. The $-Log_{10}P$ Y-axis is a measure of significance.

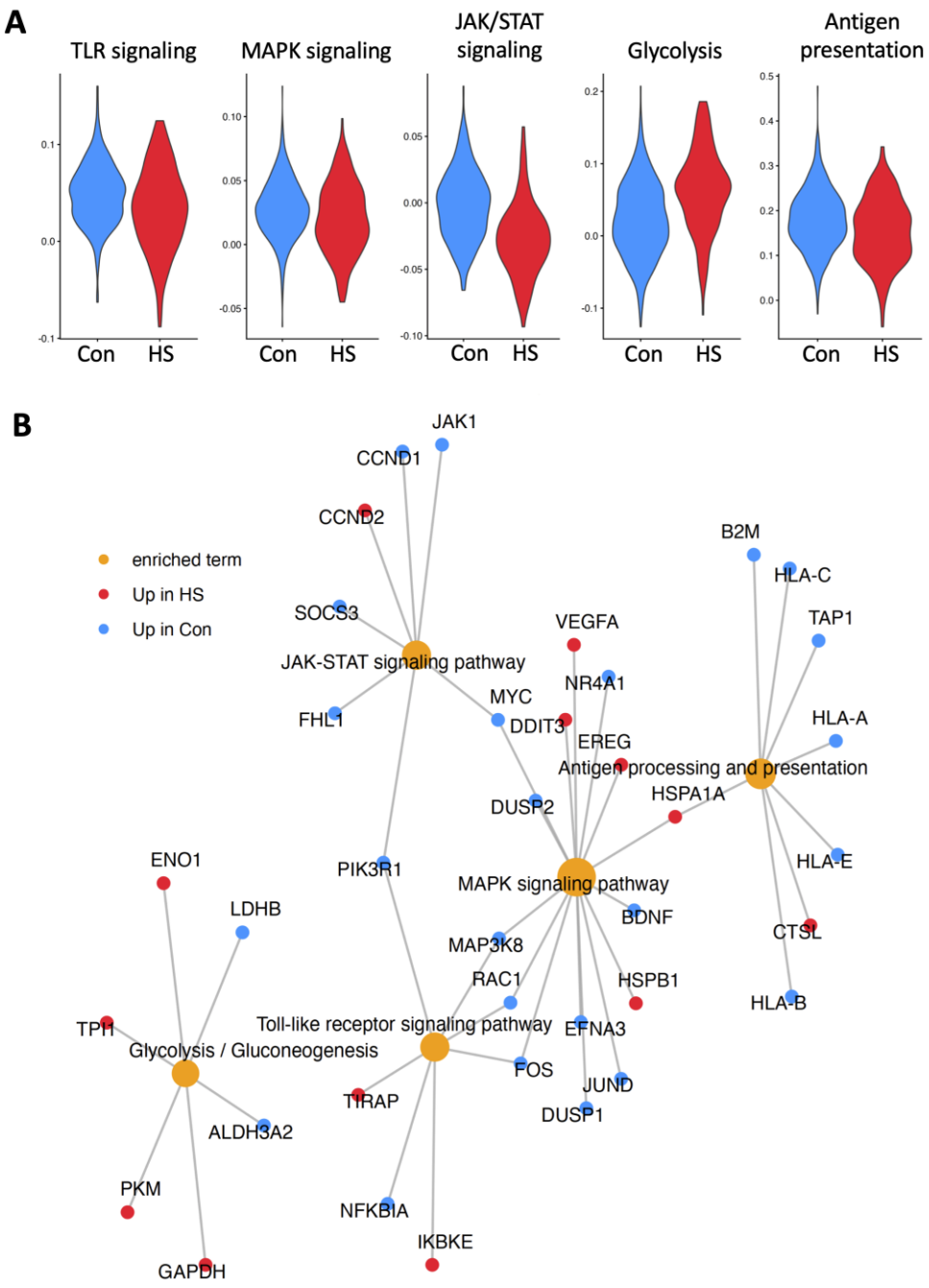

Figure 4.29 Glycolysis and JAK-STAT signaling differentiate healthy control and HS keratinocytes in the spinous keratinocyte (2) cluster. Single cells isolated from healthy controls (Con; n=3) or HS lesional skin (HS; n=6) were purified based on absence of CD45 expression, barcoded and sequenced by 10X Genomics scRNA-seq. Violin plot of pathway activity score of top 5 immune pathways enriched from the DEGs between healthy control and HS lesional keratinocytes in the spinous keratinocytes (2) cluster (A). Gene-pathway network visualising the genes upregulated in Con (blue) or HS lesions (red) in the top 5 immune pathways enriched from the DEGs between healthy control and HS lesional keratinocytes in the spinous keratinocyte (2) cluster (B).

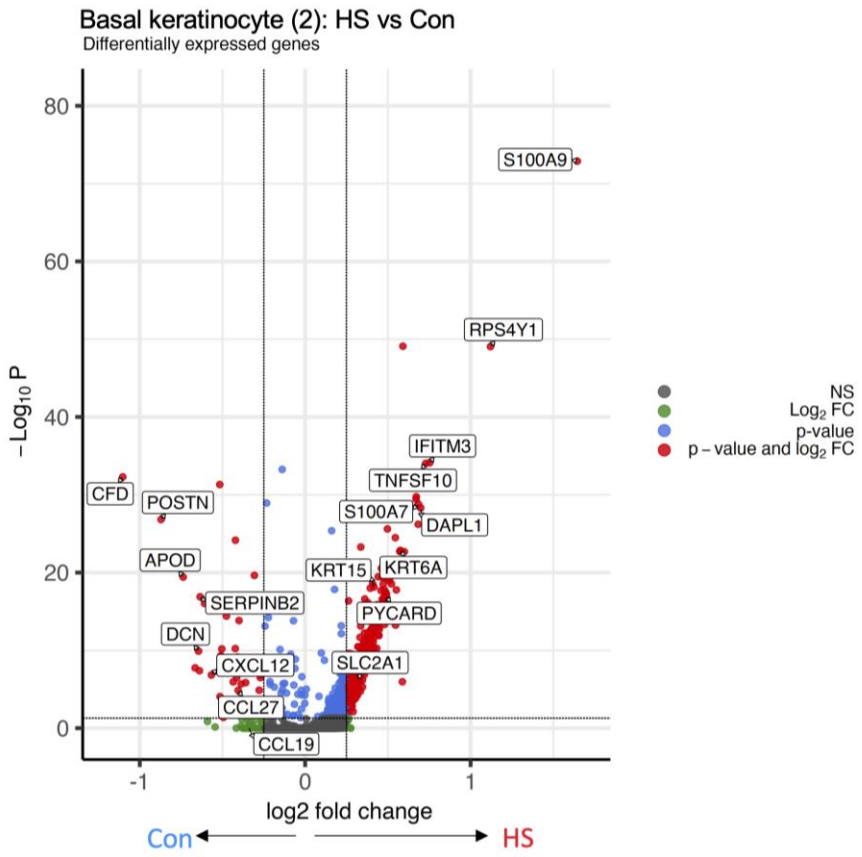

Figure 4.30 Volcano plot displaying DEGS between HS and healthy controls in the basal keratinocyte (2) cluster. Single cells isolated from healthy controls (Con; n=3) or HS lesional skin (HS; n=6) were purified based on absence of CD45 expression, barcoded and sequenced by 10X Genomics scRNA-seq. Volcano plot visualises DEGs between HS and healthy controls in the basal keratinocyte (2) cluster. Genes with a $log_2FC > 0$ are upregulated in HS and a $log_2FC < 0$ are downregulated in HS. The $-Log_{10}P$ Y-axis is a measure of significance.

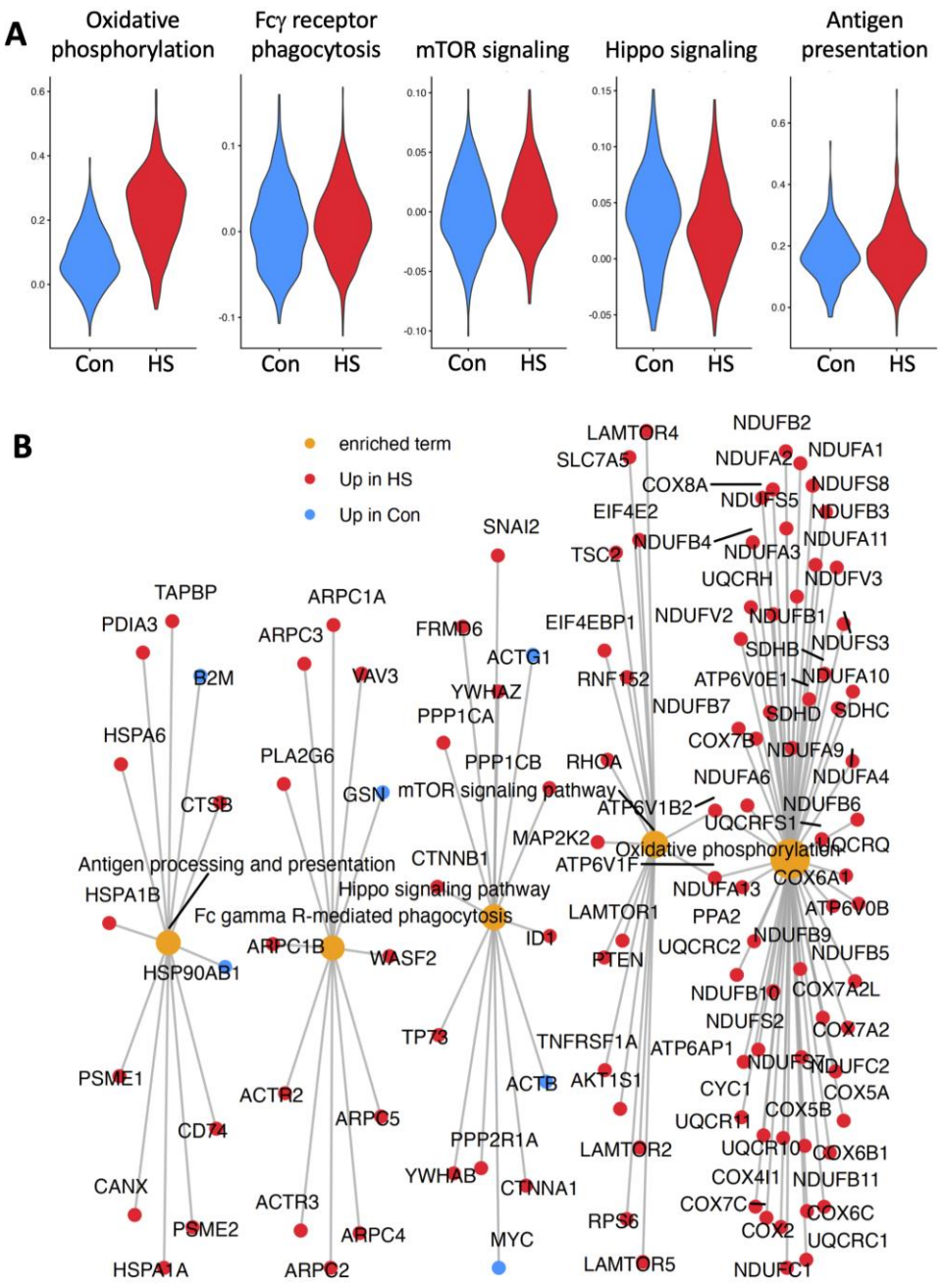

Figure 4.31 Oxidative phosphorylation and mTOR signaling differentiate healthy control and HS keratinocytes in the basal keratinocyte (2) cluster. Single cells isolated from healthy controls (Con; n=3) or HS lesional skin (HS; n=6) were purified based on absence of CD45 expression, barcoded and sequenced by 10X Genomics scRNA-seq. Violin plot of pathway activity score of top 5 immune pathways enriched from the differentially expressed genes between healthy control and HS lesional keratinocytes in the basal keratinocytes (2) cluster (A). Gene-pathway network visualising the genes upregulated in Con (blue) or HS lesions (red) in the top 5 immune pathways enriched from the differentially expressed genes between healthy control and HS lesional keratinocytes in the basal keratinocyte (2) cluster (B).

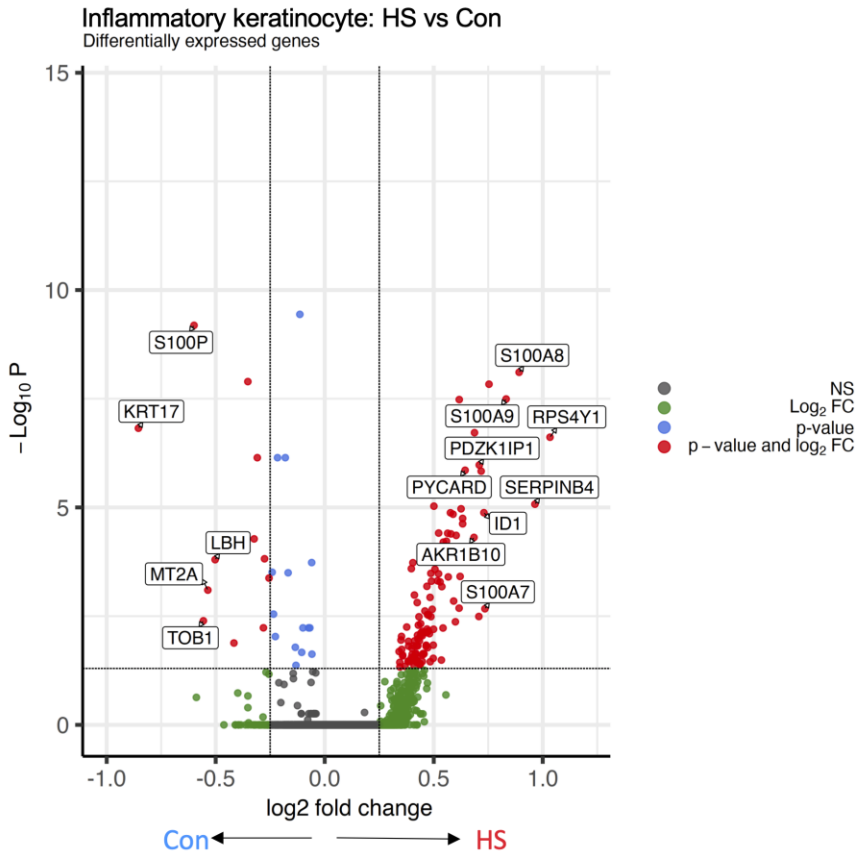

Figure 4.32 Volcano plot displaying DEGS between HS and healthy controls in the inflammatory keratinocyte cluster. Single cells isolated from healthy controls (Con; n=3) or HS lesional skin (HS; n=6) were purified based on absence of CD45 expression, barcoded and sequenced by 10X Genomics scRNA-seq. Volcano plot visualises DEGs between HS and healthy controls in the inflammatory keratinocyte cluster. Genes with a $log_2FC > 0$ are upregulated in HS and a $log_2FC < 0$ are downregulated in HS. The $-Log_{10}P$ Y-axis is a measure of significance.

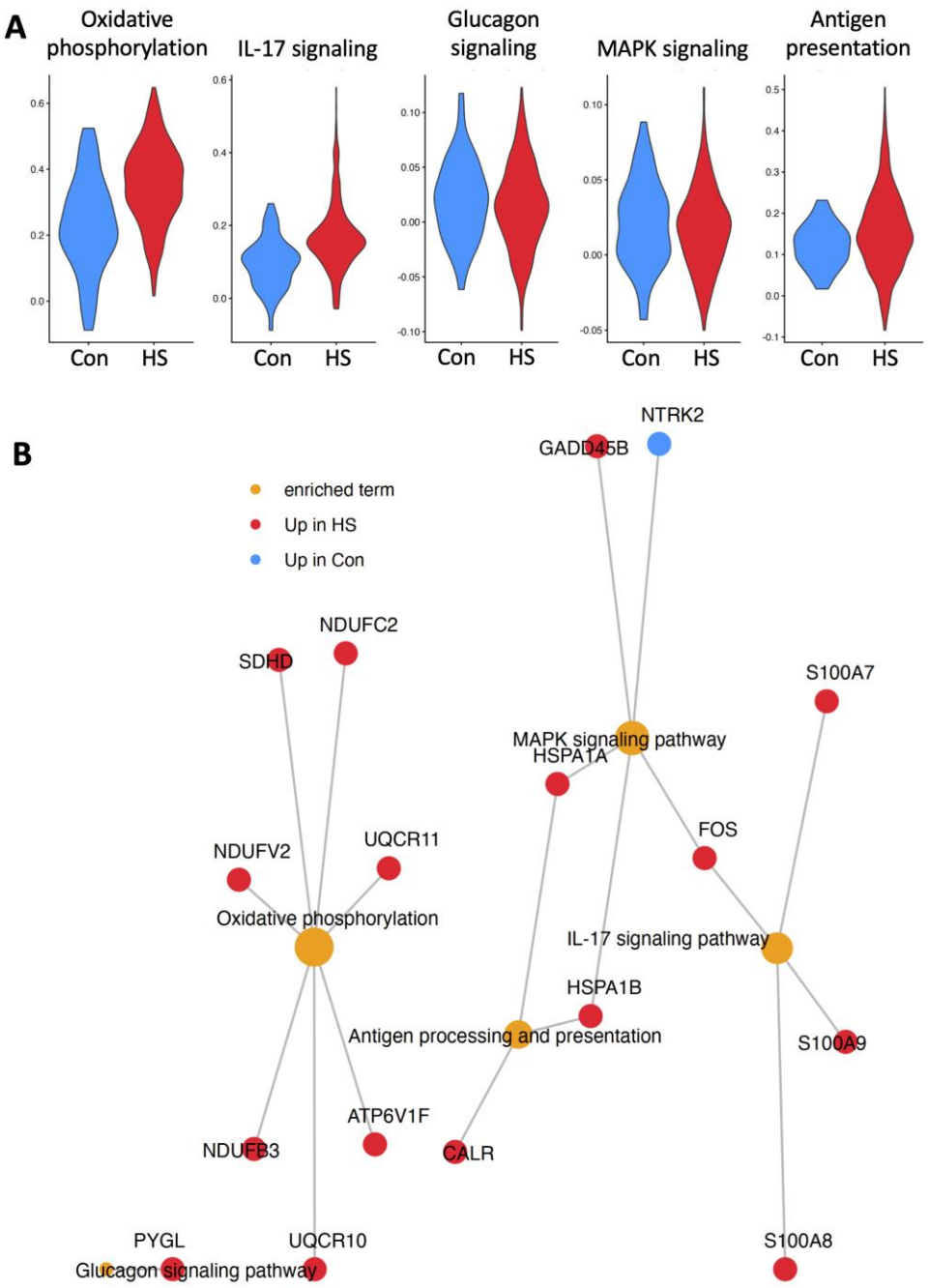

Figure 4.33 Oxidative phosphorylation and IL-17 signaling differentiate healthy control and HS keratinocytes in the inflammatory keratinocytes cluster. Single cells isolated from healthy controls (Con; n=3) or HS lesional skin (HS; n=6) were purified based on absence of CD45 expression, barcoded and sequenced by 10X Genomics scRNA-seq. Violin plot of pathway activity score of top 5 immune pathways enriched from the DEGs between healthy control and HS lesional keratinocytes in the inflammatory keratinocytes cluster (A). Gene-pathway network visualising the genes upregulated in Con (blue) or HS lesions (red) in the top 5 immune pathways enriched from the DEGs between healthy control and HS lesional keratinocytes in the inflammatory keratinocytes cluster (B).

4.3.5 HS keratinocytes have altered differentiation to healthy control keratinocytes

The previous section discussed the elevated expression of inflammatory genes in HS keratinocytes. This section will further examine the role of inflammatory mediators in keratinocyte differentiation in HS lesional skin.

Keratinocytes typically differentiate from a basal state to spinous keratinocytes, onto granular and then terminally differentiated keratinocytes. To evaluate keratinocyte differentiation in our scRNA-seq data, pseudotime trajectory analysis was performed (Cao *et al.*, 2017). This analysis tracks transcriptomic changes in neighbouring cells on the keratinocyte UMAP with the aim of developing a projected differentiation program. Beginning the pseudotime at basal keratinocytes (purple), keratinocytes appear to follow the typical differentiation program in healthy control samples, from a basal state to more differentiated spinous keratinocytes (yellow) (**Figure 4.34A**; left). HS keratinocytes had an altered differentiation program with multiple branching points allowing differentiation into inflammatory keratinocytes (**Figure 4.34A;** right). HS keratinocytes could differentiate into inflammatory keratinocytes immediately, or prior to differentiation into normal spinous keratinocytes. To confirm the altered differentiation program, expression of the inflammatory keratin *KRT6A* was mapped across the pseudotime trajectory (**Figure 4.34B**). HS keratinocytes had a marked increase in *KRT6A* expression during a specific point of the keratinocyte differentiation, indicating the point at which keratinocytes developed into inflammatory keratinocytes. This was in stark contrast to *KRT10* and *KRT5* which had similar expression profiles across healthy control and HS keratinocytes (**Figure 8.6**).

To identify genes that varied over the differentiation trajectory, graph-autocorrelation analysis was performed (**Figure 4.35**). Differentiation into inflammatory keratinocytes was characterised by elevated expression of *KRT6A*, *KRT6B* and *KRT6C*. The AMPs *S100A8*, *S100A9* and *S100A7A* and the inflammatory mediators *CXCL8* and *CCL20* were also elevated during this stage of differentiation. Beyond this, *SERPINB3* and *SERPINB4,* which promote keratinocyte inflammation (Sivaprasad *et al.*, 2015), and *FABP5*, involved in keratinocyte proliferation (Ogawa *et al.*, 2011), were significantly associated with differentiation into inflammatory keratinocytes.

To summarise, this section proposed an alternative differentiation program for HS keratinocytes relative to healthy keratinocytes, which directs HS keratinocytes to an inflammatory phenotype.

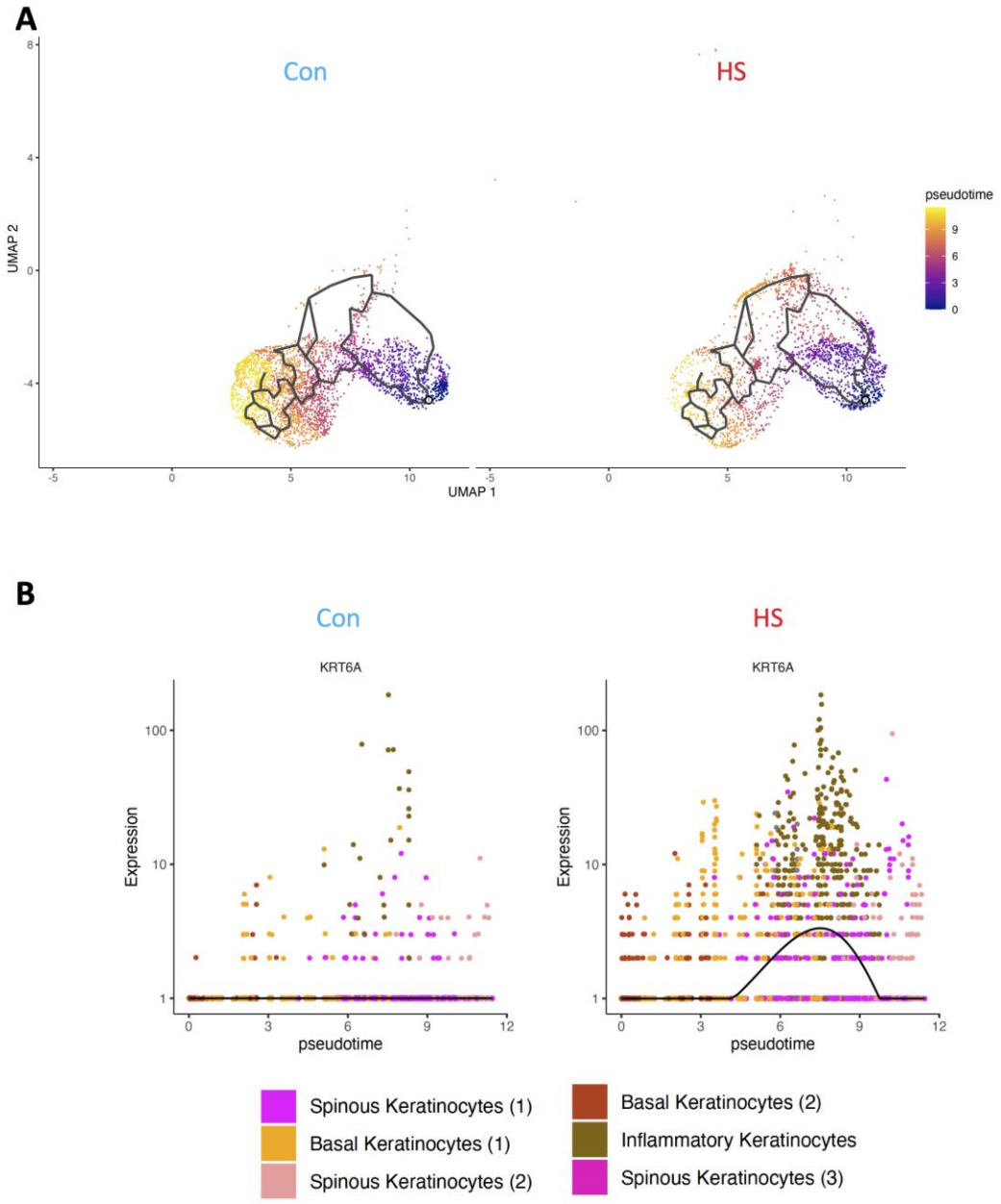

Figure 4.34 Basal keratinocytes modeled to differentiate into spinous keratinocytes or HS-specific inflammatory keratinocytes. UMAP displaying the pseudotime trajectory of keratinocytes beginning with basal keratinocytes (purple) and ending with differentiated spinous keratinocytes (yellow). Single cells isolated from healthy controls (Con; n=3) or HS lesional skin (HS; n=6) were purified based on absence of CD45 expression, barcoded and sequenced by 10X Genomics scRNA-seq. Pseudotime trajectory analysis performed using Monocle3 on the keratinocyte clusters (A). Scatter plot tracking the expression of *KRT6A* across pseudotime in healthy control and HS keratinocytes (B).

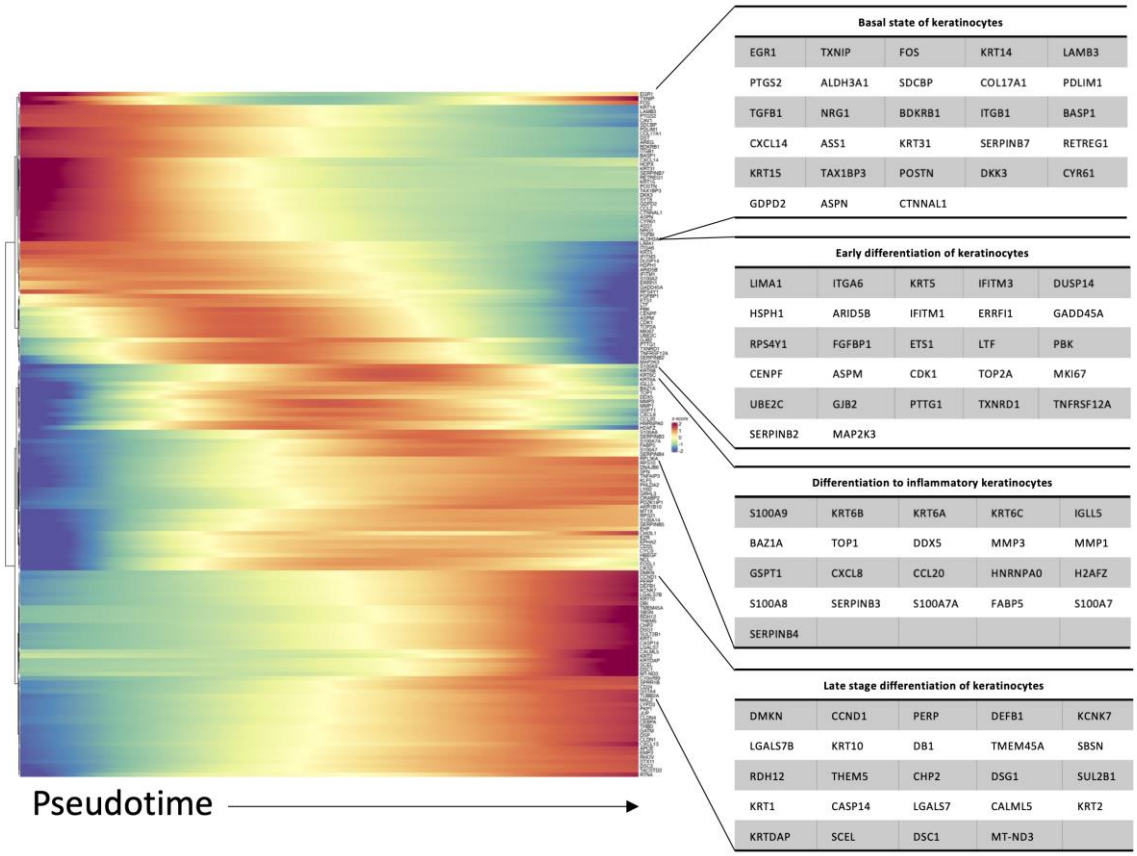

Basal state of keratinocytes

EGR1	TXNIP	FOS	KRT14	LAMB3
PTGS2	ALDH3A1	SDCBP	COL17A1	PDLIM1
TGFB1	NRG1	BDKRB1	ITGB1	BASP1
CXCL14	ASS1	KRT31	SERPINB7	RETREG1
KRT15	TAX1BP3	POSTN	DKK3	CYR61
GDPD2	ASPN	CTNNAL1		

Early differentiation of keratinocytes

LIMA1	ITGA6	KRT5	IFITM3	DUSP14
HSPH1	ARID5B	IFITM1	ERRFI1	GADD45A
RPS4Y1	FGFBP1	ETS1	LTF	PBK
CENPF	ASPM	CDK1	TOP2A	MKI67
UBE2C	GJB2	PTTG1	TXNRD1	TNFRSF12A
SERPINB2	MAP2K3			

Differentiation to inflammatory keratinocytes

S100A9	KRT6B	KRT6A	KRT6C	IGLL5
BAZ1A	TOP1	DDX5	MMP3	MMP1
GSPT1	CXCL8	CCL20	HNRNPA0	H2AFZ
S100A8	SERPINB3	S100A7A	FABP5	S100A7
SERPINB4				

Late stage differentiation of keratinocytes

DMKN	CCND1	PERP	DEFB1	KCNK7
LGALS7B	KRT10	DB1	TMEM45A	SBSN
RDH12	THEM5	CHP2	DSG1	SUL2B1
KRT1	CASP14	LGALS7	CALML5	KRT2
KRTDAP	SCEL	DSC1	MT-ND3	

Figure 4.35 Heatmap displaying keratinocyte gene expression changes throughout differentiation. Single cells isolated from healthy controls (Con; n=3) or HS lesional skin (HS; n=6) were purified based on absence of CD45 expression, barcoded and sequenced by 10X Genomics scRNA-seq. Pseudotime trajectory analysis performed using Monocle3 on the keratinocyte clusters. Pseudotime-dependent genes identified by graph autocorrelation analysis were tabulated.

4.3.6 Differentiating HS keratinocytes from psoriasis keratinocytes

The previous section outlined the importance of IL-17 for the development of inflammatory keratinocytes in HS lesions. These inflammatory keratinocytes were characterised by the expression of inflammatory keratins, similar to psoriatic keratinocytes which also express inflammatory keratins. Importantly, there are major physiological differences between keratinocytes found in psoriasis lesions and those in HS lesions. Psoriasis lesions are characterised by a build-up of scaly patches caused by a dramatic increase in keratinocyte proliferation which is not replicated in HS lesions. This section aimed to delineate potential transcriptomic changes which could explain these differences between HS and psoriatic keratinocytes.

In order to determine transcriptomic differences between HS and psoriatic keratinocytes, scRNA-seq data of psoriasis lesional skin was integrated with this HS scRNA-seq dataset (Gao *et al.*, 2021). **Figure 4.36A** displays a volcano plot of the 13,002 DEGs between HS and psoriatic keratinocytes. 10,781 were upregulated in psoriatic keratinocytes (**Table 8.26**) and 2,221 upregulated in HS keratinocytes (**Table 8.25**). Psoriatic keratinocytes had relatively increased expression of the inflammatory keratins *KRT6* and *KRT16*, the AMPs *S100A7*, *S100A8* and *S100A9,* and *WWOX,* which regulates keratinocyte proliferation, the most differentially expressed gene in psoriatic keratinocytes. HS keratinocytes had elevated expression of the proliferation and activation markers *FABP5*, *JUN* and *NFKBIA* suggesting an alternative pathway of activation for HS keratinocytes. In addition, HS keratinocytes had elevated expression of the inflammatory mediators *CXCL8, CXCL2* and *AREG* which are regulated by IL-17 signaling.

To determine if there are differences in the proliferative or inflammatory capacity of keratinocytes from HS and psoriasis lesions, the expression of proliferation and differentiation-associated genes and inflammation-associated were measured (**Table 2.7**). While HS keratinocytes had higher expression of proliferation and differentiation genes compared with healthy control keratinocytes, psoriatic keratinocytes had a striking increase relative to HS keratinocytes (**Figure 4.36B**; left). Despite the dramatic differences in the proliferative capacity of HS and psoriatic keratinocytes, there were similar levels of inflammatory genes in HS and psoriatic keratinocytes (**Figure 4.36B**; right).

Psoriatic keratinocytes had increased expression of the AMPs *S100A7*, *S100A8* and *S100A9*, the inflammatory keratins *KRT6A*, *KRT16* and *KRT17* and increased expression of proliferation regulators (*WWOX*, *TRPS1*, *CLASP2*, *CDH13*, *PTPRK*, *CALML5*) (**Figure 4.37**) (Chou *et al.*, 2020; Rybski, Zengin and Smoller, 2023; Shahbazi *et al.*, 2017; Wang *et al.*, 2018; Méhul, Bernard and Schmidt, 2001). HS keratinocyte proliferation appeared to be regulated by alternative mechanisms with increased expression of *CALM2*, *FABP5* and *PNRC1* (Kahl and Means, 2003; Ogawa *et al.*, 2011; Yao *et al.*, 2021). HS keratinocytes also had increased expression of *CCL27* which regulates T cell homing to the skin (Davila *et al.* 2022) and *CXCL8* and *AREG* which are regulated by IL-17 signaling (Gupta *et al.*, 2021).

In summary, this section detailed the transcriptomic differences between HS and psoriatic keratinocytes using two scRNA-seq datasets. Despite having an inflammatory profile, HS keratinocytes were distinct from psoriatic keratinocytes, with reduced proliferative capacity. Data suggests, HS keratinocytes may have heightened normal proliferation relative to psoriatic keratinocytes which have unique expression of diverse proliferation genes.

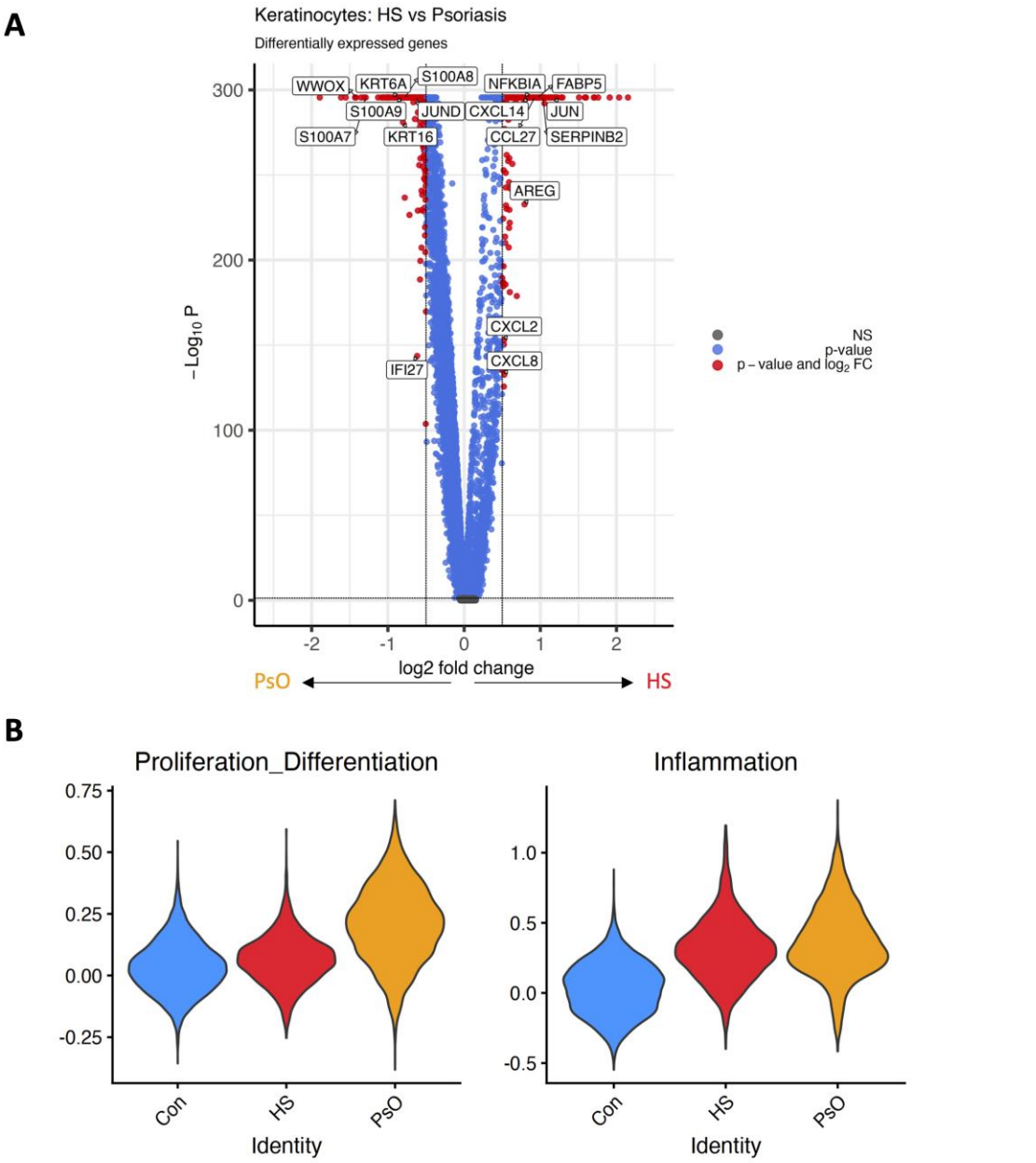

Figure 4.36 HS keratinocytes have elevated inflammatory, and reduced proliferative capacity, compared with psoriasis keratinocytes. Single cells isolated from healthy controls (Con; n=3), HS lesional skin (HS; n=6) were purified based on absence of CD45 expression, barcoded and sequenced by 10X Genomics scRNA-seq. Keratinocytes were identified and integrated with keratinocytes from the GSE162183 psoriasis (PsO; n=3) dataset. Volcano plot visualises DEGs in HS compared with PsO lesions. Genes with a log_2FC >0 are upregulated in HS and a log_2FC <0 are upregulated in PsO. The $-Log_{10}$ P Y-axis is a measure of significance (A). Violin plot displaying the activity scores for differentially expressed genes (adj p value<0.05 and log_2FC>0.5) involved in proliferation and differentiation or inflammation (B). Activity scores were calculated using the AddModuleScore function in Seurat.

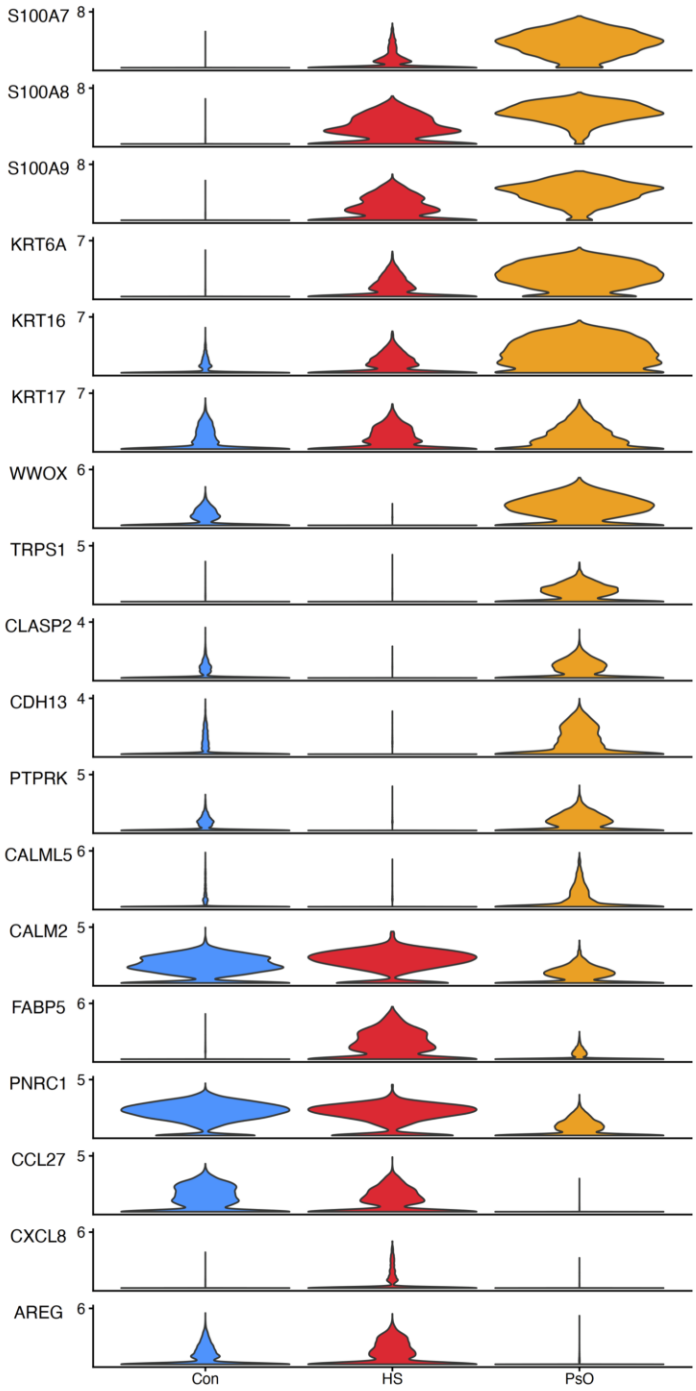

Figure 4.37 Psoriasis and HS keratinocytes have distinct proliferative and inflammatory gene expression. Single cells isolated from healthy controls (Con; n=3), HS lesional skin (HS; n=6) were purified based on absence of CD45 expression, barcoded and sequenced by 10X Genomics scRNA-seq. Keratinocytes were identified and integrated with keratinocytes from the GSE162183 psoriasis (PsO; n=3) dataset. Violin plot displaying the expression of inflammatory (*S100A7*, *S100A8*, *S100A9*, *KRT6A*, *KRT16*, *KRT17*, *CCL27*, *CXCL8*, *AREG*) and proliferative (*WWOX*, *TRPS1*, *CLASP2*, *CDH13*, *PTPRK*, *CALML5*, *CALM2*, *FABP5*, *PNRC1*) genes.

4.3.7 Characterisation of fibroblasts in HS skin

Fibroblasts make up a major proportion of the non-immune cells in HS lesional and healthy control skin. Unsupervised clustering identified 6 fibroblast clusters in HS lesional and healthy control skin (**Figure 4.38A**). This section will characterise these fibroblast populations, highlighting their specific functions and their potential role in promoting HS pathogenesis.

To identify potential fibroblast populations enriched in HS from the 6 fibroblast clusters, an overlapping UMAP was created (**Figure 4.38B**), grouping fibroblasts derived from HS lesions (red) and healthy control skin (blue). To visualise potential fibroblast clusters unique in HS lesions, separate UMAPs displaying healthy control-only fibroblasts (top) and HS-only fibroblasts (bottom) were generated (**Figure 4.39**). Taken together, these UMAPs highlight certain HS-specific clusters, including the inflammatory fibroblasts (2) cluster as potential clusters of interest.

To annotate fibroblast populations, characteristic cell markers were visualised on the fibroblast UMAP (**Figure 4.40**). Papillary fibroblasts were identified based on their elevated expression of *COL18A1* (**Figure 4.40A**), *APCDD1* (**Figure 4.40B**) and *COL23A1* (**Figure 4.40C**), identifying one fibroblast cluster as papillary fibroblasts. Reticular fibroblasts, found in a layer of the dermis above papillary fibroblasts had high expression of *MGP* (**Figure 4.40D**) and *MFAP5* (**Figure 4.40E**), identifying 2 reticular fibroblast clusters. Reticular fibroblasts also had high expression of *MMP2* (**Figure 4.40F**) and *CXCL14* (**Figure 4.40G**). One fibroblast population expressed high levels of *CCL19* (**Figure 4.40H**), which regulates T cell activation and T cell homing to tissue (Yan *et al.*, 2019), and another had high expression of *PDPN* (**Figure 4.40I**), indicating that these fibroblasts may be more motile (Suchanski *et al.*, 2017). These clusters were annotated as inflammatory fibroblast (1) and inflammatory fibroblast (2), respectively. To confirm the annotation of fibroblast populations, density plots were generated to display the co-expression of reticular markers (*COL13A1*, *APCDD1*, *COL23A1*) (**Figure 4.41A**), papillary markers (*MGP*, *MFAP5*) (**Figure 4.41B**), and inflammatory fibroblast markers (*CCL19*, *CCL2*; *PDPN*,*THY1*) (**Figure 4.41C-D**) on the fibroblast UMAP.

The six fibroblast clusters had unique transcriptomic profiles as visualised by heatmap (**Figure 4.42A**). To determine the functional profile of each fibroblast cluster, gene ontology

terms were identified for the unique cluster markers of each fibroblast population. The reticular fibroblast (1) cluster had an enrichment of gene ontology terms relating to extracellular matrix organisation. Papillary fibroblasts had an enrichment of Wnt signaling genes, while the 2 inflammatory fibroblast clusters had an enrichment of cytokine signaling and extracellular matrix organisation indicating potential regulation of inflammation and scar formation in HS lesions (**Figure 4.42B**).

In summary, this section characterised the 6 fibroblast clusters found in HS and healthy control skin. Papillary, reticular and the inflammatory fibroblast (1) clusters were found in both HS lesional and healthy skin, while the inflammatory fibroblast (2) cluster was uniquely found in HS lesional skin. Each fibroblast cluster had different biological functions, of particular interest, the inflammatory fibroblast (1) cluster was involved in cytokine signaling, while the inflammatory fibroblast (2) cluster may regulate scar formation in HS lesions.

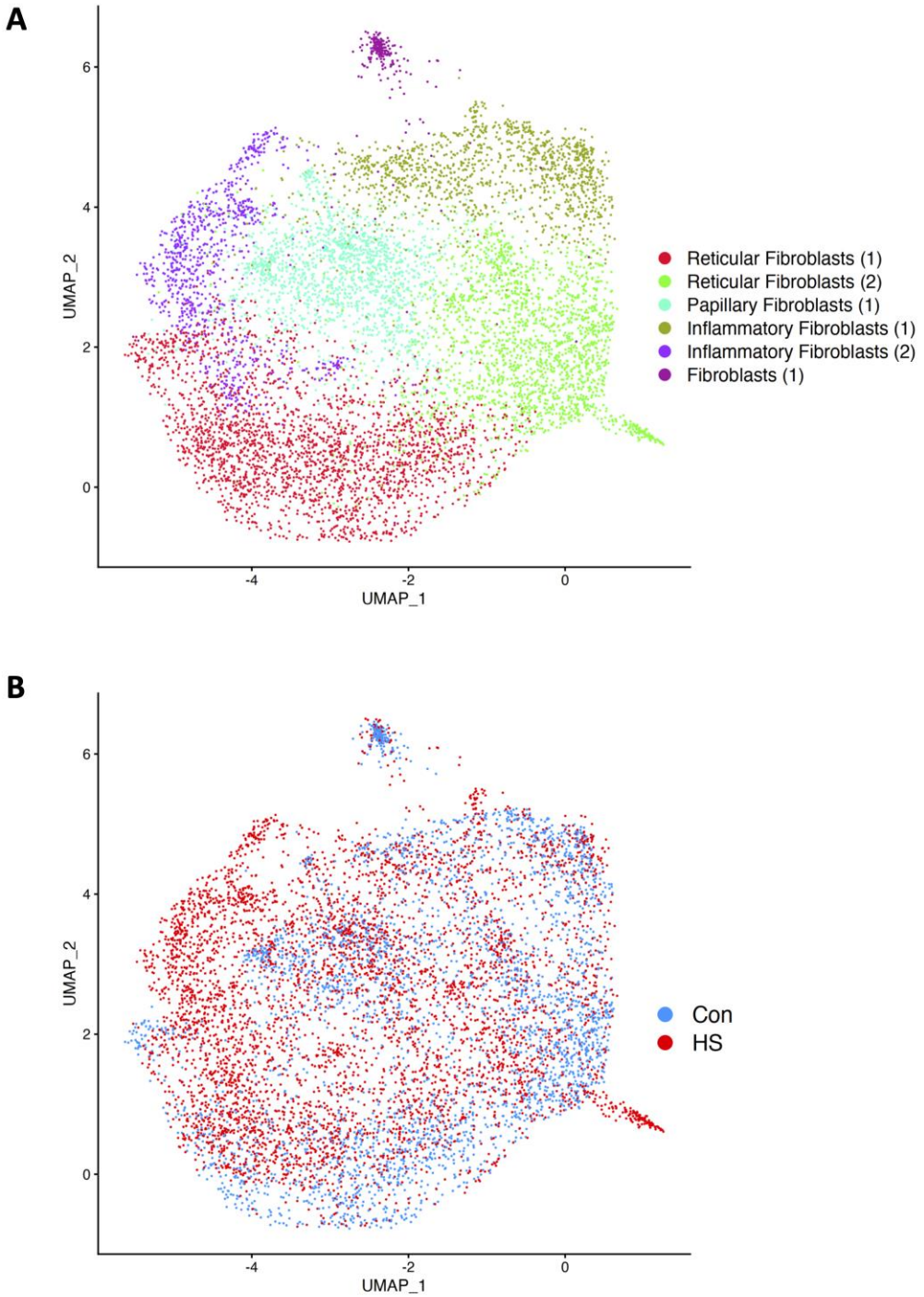

Figure 4.38 Inflammatory keratinocytes are enriched in HS lesional skin. Single cells isolated from healthy controls (Con; n=3) or HS lesional skin (HS; n=6) were purified based on absence of CD45 expression, barcoded and sequenced by 10X Genomics scRNA-seq. UMAP of 6 fibroblast clusters identified by unsupervised classification in the $CD45^-$ dataset (A). UMAP plot overlaying fibroblasts from HS lesional skin (red) and healthy control skin (blue) (B).

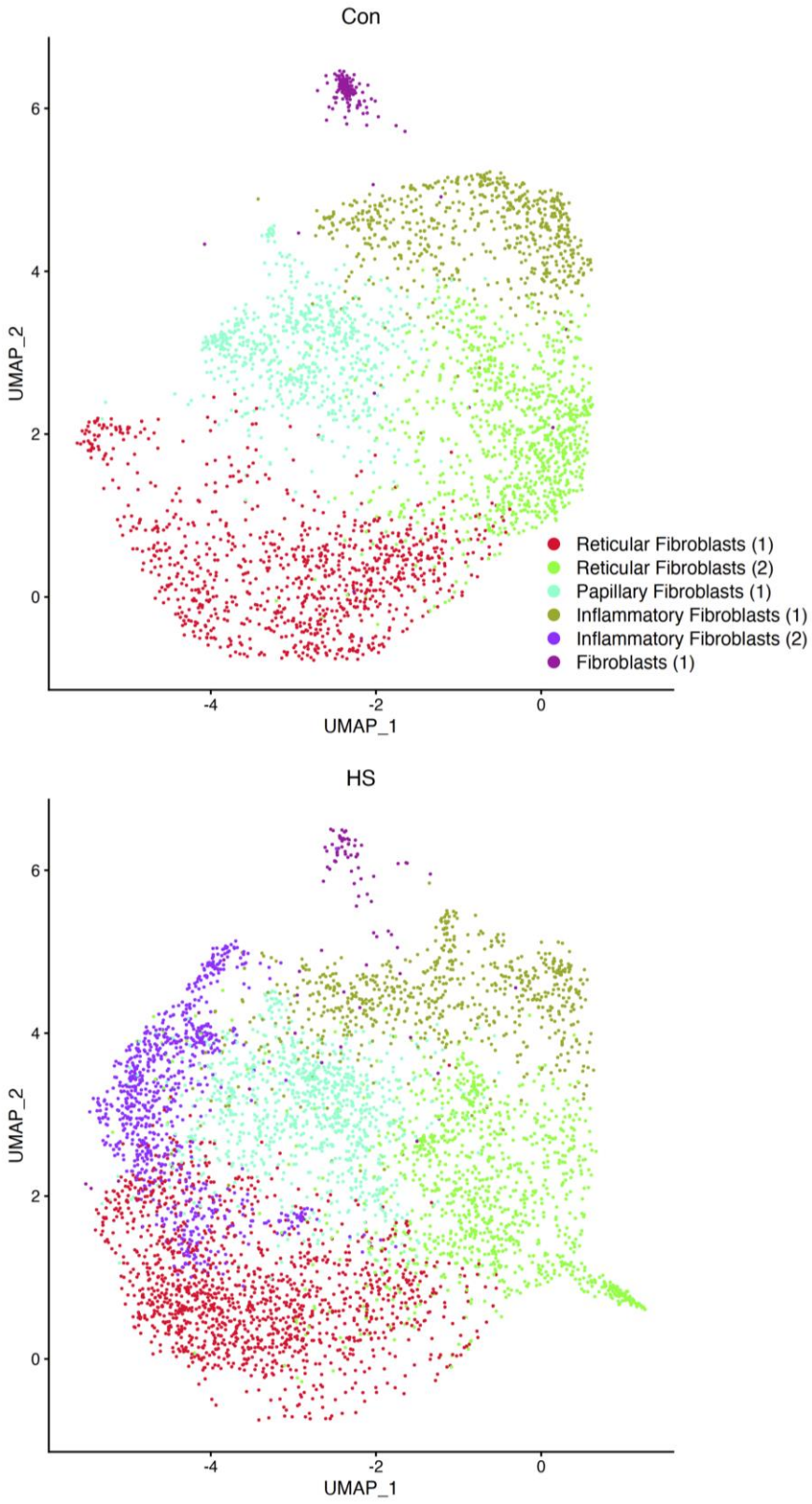

Figure 4.39 Inflammatory fibroblasts are enriched in HS lesions. Single cells isolated from healthy controls (Con; n=3) or HS lesional skin (HS; n=6) were purified based on absence of CD45 expression, barcoded and sequenced by 10X Genomics scRNA-seq. UMAP displays fibroblasts isolated from only healthy control skin (top) and only HS lesional skin (bottom), respectively.

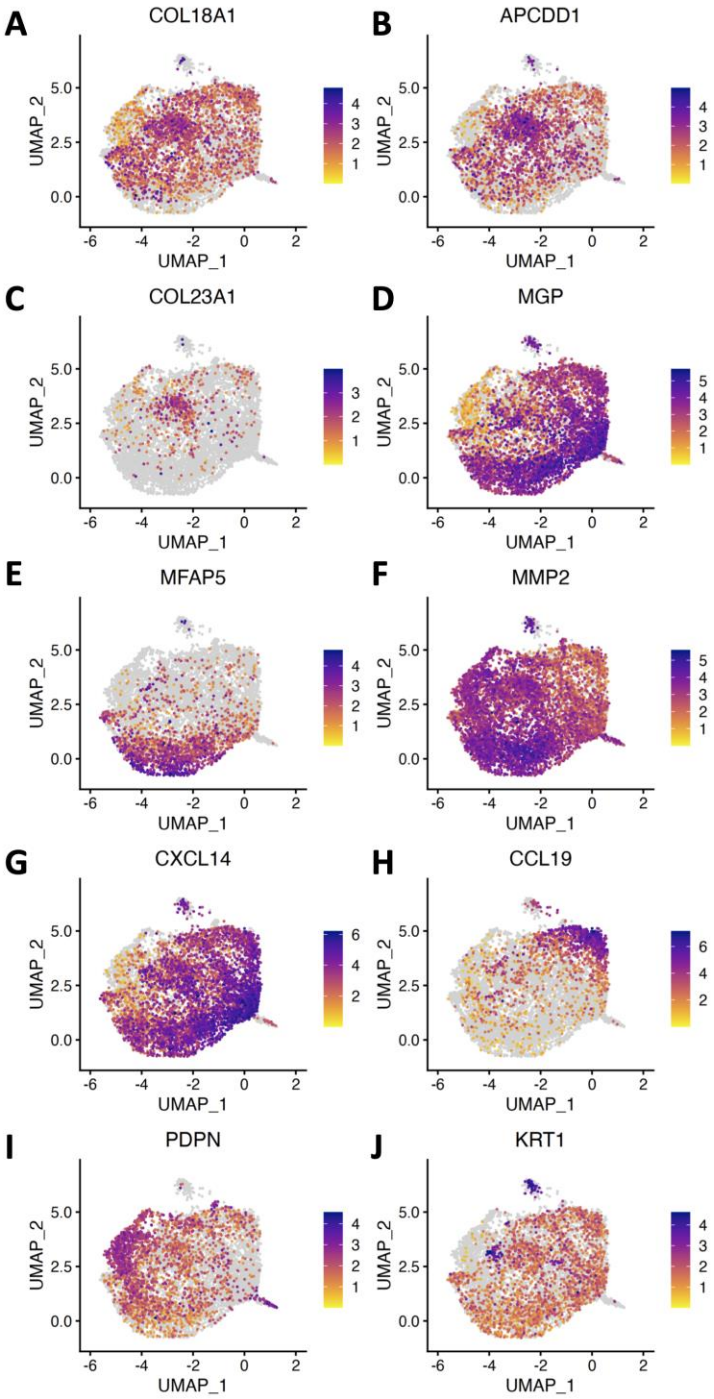

Figure 4.40 Characterisation of fibroblast clusters. Single cells isolated from healthy controls (Con; n=3) or HS lesional skin (HS; n=6) were purified based on absence of CD45 expression, barcoded and sequenced by 10X Genomics scRNA-seq. UMAPs display gene expression for *COL18A1* (A), *APCDD1* (B), *COL23A1* (C), *MGP* (D), *MFAP5* (E), *MMP2* (F), *CXCL14* (G), *CCL19* (H), *PDPN* (I), KRT1 (J) in fibroblasts from the $CD45^-$ cohort of HS lesional and healthy control skin.

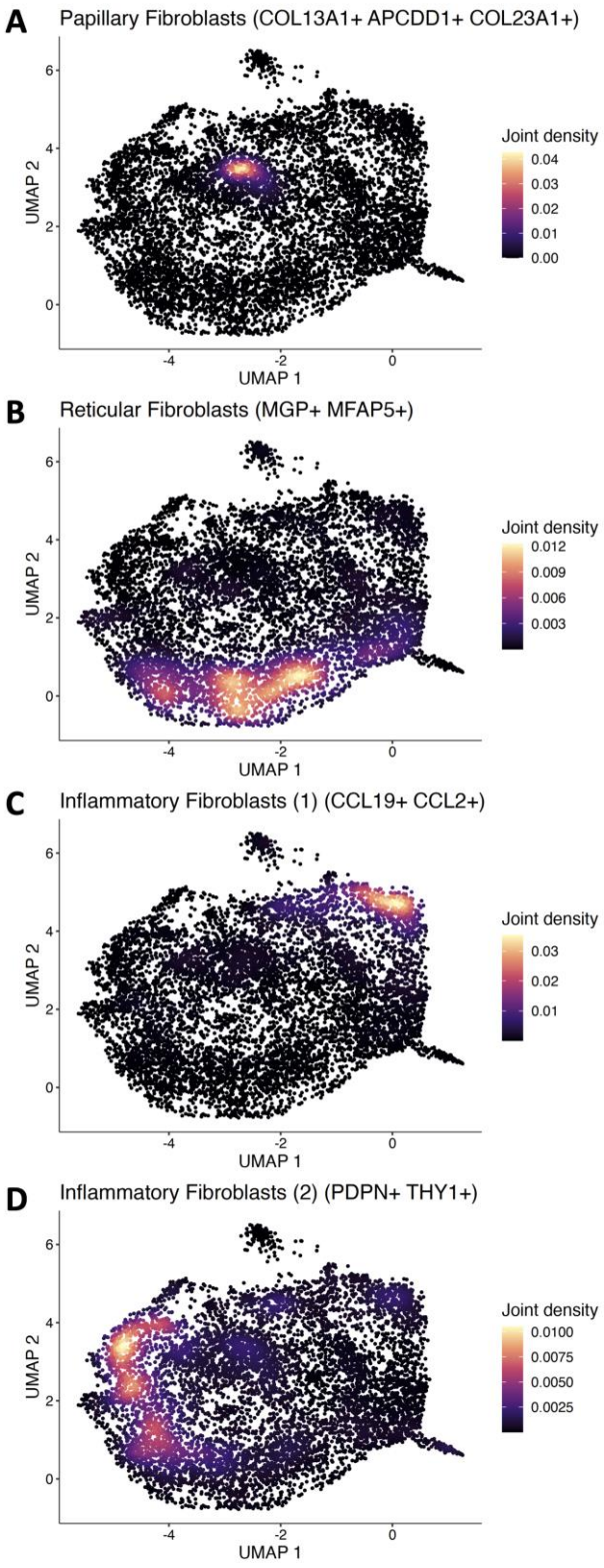

Figure 4.41 Density plot displaying reticular, papillary and inflammatory fibroblasts. Single cells isolated from healthy controls (Con; n=3) or HS lesional skin (HS; n=6) were purified based on absence of CD45 expression, barcoded and sequenced by 10X Genomics scRNA-seq. Co-expression of papillary (C*OL13A1, APCDD1, COL23A1*; A), reticular (*MGP, MFAP5*; B) and inflammatory (*CCL19*, *CCL2*; C)(*PDPN*, *THY1*; D) fibroblast markers in healthy control and HS lesional skin displayed on a fibroblast UMAP.

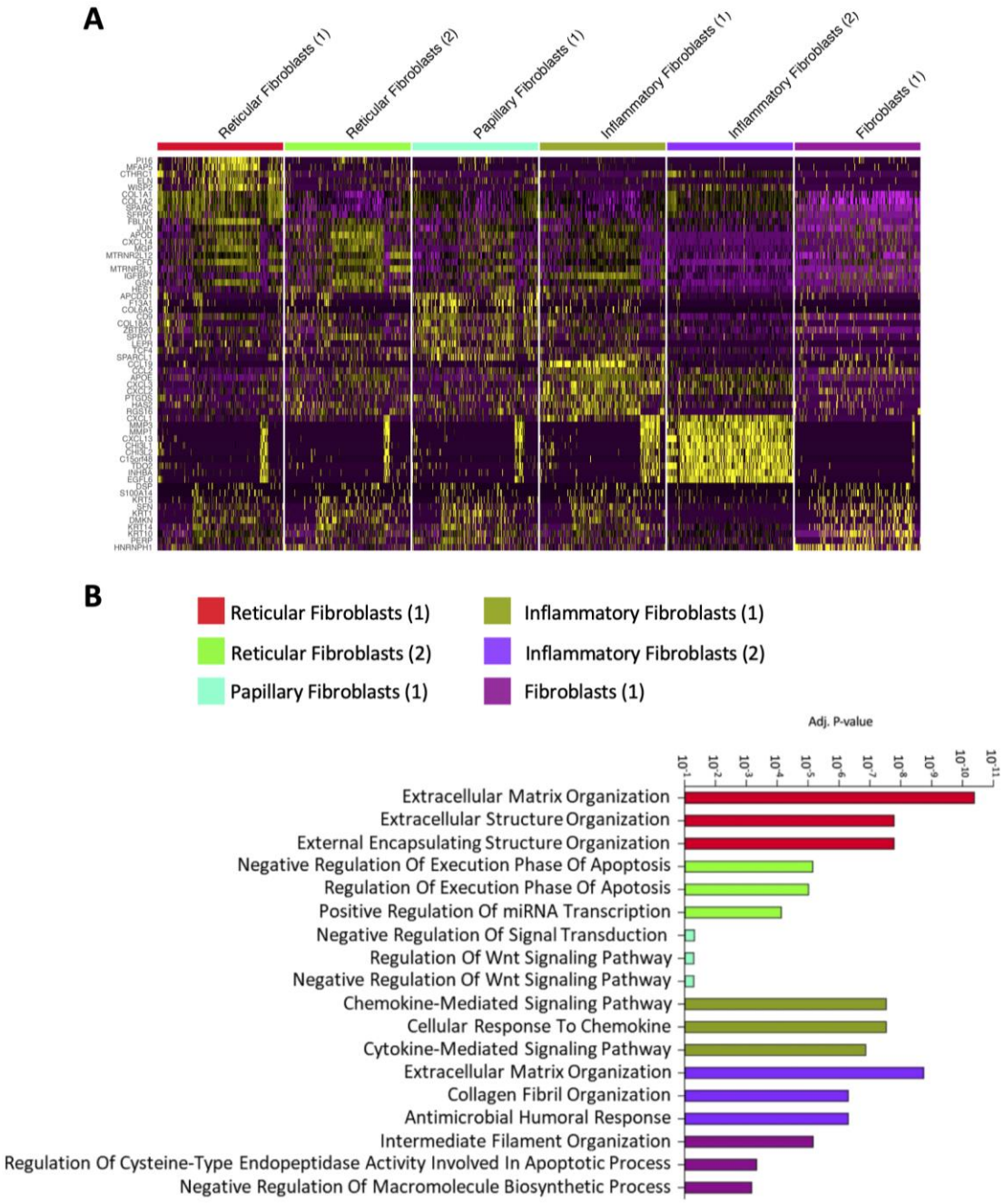

Figure 4.42 Fibroblast clusters display distinct transcriptomic and functional profiles. Single cells isolated from healthy controls (Con; n=3) or HS lesional skin (HS; n=6) were purified based on absence of CD45 expression, barcoded and sequenced by 10X Genomics scRNA-seq. Heatmap displayed cluster-specific genes identified by Wilcoxon Rank Sum test (A). Gene ontology terms enriched from the cluster-specific genes for each fibroblast cluster (B).

4.3.8 Transcriptomic differences in HS and healthy fibroblasts

The previous section identified fibroblast clusters in HS lesional and healthy control skin. In healthy skin, fibroblasts play an important role in regulating the balance between tissue homeostasis and scarring (Kirk, Ahmed and Rognoni, 2021; Jiang and Rinkevich, 2020). This section will examine the transcriptomic changes which occur in HS fibroblasts that help promote an inflammatory environment which may lead to hypertrophic scarring in HS lesional skin.

Similar frequencies of each fibroblast cluster were found in HS lesions and healthy control skin, aside from the inflammatory fibroblast (2) cluster which was predominantly found in 2 HS patients (**Figure 4.43A**). Despite these similarities, 3,610 genes were significantly differentially expressed between healthy control and HS fibroblasts (**Figure 4.43B**). 1,554 genes were significantly elevated in HS fibroblasts (**Table 8.27**), and 2,056 genes were elevated in healthy control fibroblasts (**Table 8.28**).

A broad range of cytokines have been reported to promote HS inflammation. To estimate the role of IFN-γ, TNF, IL-17 and IL-1β in HS fibroblasts, the expression of genes involved in each of these cytokine signaling pathways was calculated in HS and healthy control fibroblasts in each fibroblast cluster (**Figure 4.44**, **Table 2.7**). Interestingly, the inflammatory fibroblast (1) cluster had elevated TNF, IL-17 and IL-1β signaling relative to other fibroblast clusters. Contrastingly, the inflammatory fibroblast (2) cluster had elevated expression of TNF and IL-17 signaling only, highlighting how different cytokines may differentially regulate specific fibroblast clusters.

To gain a better understanding of how each fibroblast cluster becomes altered during disease, DEGs and enriched pathways between HS and healthy control fibroblasts were identified in each fibroblast cluster. **Figure 4.45** displays a volcano plot of 1,740 DEGs between HS and healthy control fibroblasts in the reticular fibroblast (1) cluster. 429 genes were significantly elevated in HS fibroblasts (**Table 8.29**) and 1,311 genes were significantly elevated in healthy control fibroblasts in the reticular fibroblast (1) cluster (**Table 8.30**). Of particular interest, *THY1*, *PDPN*, *MMP1*, *CXCL1* and *HIF1A* were significantly elevated in HS lesions. The top 5 immune related pathways enriched from these DEGs included MAPK signaling, JAK-STAT signaling, focal adhesion, Th17 differentiation and mTOR signaling

(**Figure 4.46A**). A marked increase in the focal adhesion pathway score suggests that HS reticular fibroblasts had elevated proliferation and motility (**Figure 4.46B**).

Figure 4.47 displays a volcano plot of the 2,375 DEGs between HS and healthy control fibroblasts in the reticular fibroblast (2) cluster. In this cluster, HS fibroblasts had elevated expression of *MMP1, MMP3* and the proinflammatory mediators *CXCL1*, *CXCL8*, *CXCL13*, *IL32* and *CSF3*. Interestingly, 154 genes were elevated in HS lesions (**Table 8.31**) and 2,221 genes were upregulated in healthy control fibroblasts (**Table 8.32**). The top 5 immune related pathways enriched from these DEGs included TCA cycle, JAK-STAT signaling, oxidative phosphorylation, MAPK signaling and focal adhesion (**Figure 4.48A**). Gene-pathway network analysis displays the genes involved in each of the enriched pathways (**Figure 4.48B**). This data suggests that HS fibroblasts are metabolically dysregulated relative to healthy control fibroblasts with increased expression of the oxidative phosphorylation pathway and the glycolytic regulator *HIF1A* (**Figure 4.48B**).

834 genes were differentially expressed between HS and healthy control fibroblasts in the papillary fibroblast (1) cluster (**Figure 4.49**, **Table 8.33Table 8.34**). HS papillary fibroblasts had elevated expression of MMPs, collagens and *HIF1A*, indicating a general increase in fibroblast activation in HS papillary fibroblasts. The top 5 immune pathways enriched in papillary fibroblasts included oxidative phosphorylation, HIF-1 signaling, focal adhesion, MAPK signaling and JAK-STAT signaling (**Figure 4.50A**). The elevated expression of oxidative phosphorylation and HIF-1 signaling in HS papillary fibroblasts suggests that papillary fibroblasts were metabolically dysregulated in HS lesions (**Figure 4.50B**).

Figure 4.51 displays 996 genes differentially expressed between HS and healthy control fibroblasts in the inflammatory fibroblast (1) cluster. 348 genes were significantly elevated in HS lesions (**Table 8.35**) and 638 genes were elevated in healthy controls (**Table 8.36**). HS inflammatory fibroblasts (1) had elevated expression of a number of proinflammatory mediators including *FAP*, *CXCL1*, *CXCL8*, *MMP1*, *MMP3*, *MMP9*, *S100A8* and *CCL3*. Oxidative phosphorylation, JAK-STAT signaling, antigen presentation, HIF-1 signaling, and TNF signaling were significantly enriched from the DEGs (**Figure 4.52A**). Of note, oxidative phosphorylation was elevated in HS inflammatory fibroblasts while JAK-STAT signaling was

markedly downregulated in HS fibroblasts in the inflammatory fibroblasts (1) cluster (**Figure 4.52B**).

This analysis could not be performed on the inflammatory fibroblast (2) cluster due to the absence of this cluster in healthy control samples. The final fibroblast cluster, fibroblast (1) only had 8 DEGs between HS and healthy control fibroblasts and so no pathways were enriched (**Figure 8.7**).

Considering collagen genes were often significantly elevated in HS fibroblasts and the suspected role of dysregulated collagen deposition in chronic HS scarring (Byrd *et al.*, 2018), the expression of collagen genes was estimated in HS lesional and healthy control fibroblasts. HS fibroblasts had increased expression of the collagen pathway in each fibroblast cluster relative to healthy control fibroblasts (**Figure 4.53A**). Interestingly, each fibroblast cluster had a unique collagen expression profile (**Figure 4.53B**).

As HS lesional fibroblasts had elevated expression of a range of inflammatory mediators, the expression of chemokines and cytokines expressed by fibroblasts in each fibroblast cluster was visualised by heatmap (**Figure 4.54A**). HS inflammatory clusters had elevated expression of *CXCL8*, *CXCL1*, *IL6* and *CCL20* and interestingly the inflammatory fibroblast (2) cluster had relatively high expression of the Th17 promoting cytokines *IL1B* and *IL23A*. Similarly, MMPs were frequently among the most differentially expressed genes in HS fibroblast. Interestingly, the inflammatory fibroblast (2) cluster had elevated expression of *MMP2*, *MMP9*, *MMP14*, *MMP1* and *MMP3*, suggesting that this fibroblast cluster may play a role in promoting scar formation and tissue destruction in HS skin (**Figure 4.54B**).

Fibroblasts derived from HS-hi lesions had elevated expression of inflammatory mediators relative to HS-lo fibroblasts. *CXCL1*, *CXCL8*, *MMP1*, *MMP9*, *HIF1A* and GLUT3 (*SLC2A3*) were more highly expressed in HS-hi fibroblasts compared with HS-lo fibroblasts, highlighting elevated IL-17 signaling and metabolic dysregulation as key drivers in HS-hi fibroblasts (**Figure 8.8**,
Table 8.37Table 8.38). In addition, oxidative phosphorylation, HIF-1 signaling, TNF and IL-17 signaling were enriched from the DEGs between HS-hi and HS-lo fibroblasts, suggesting

that HS-hi fibroblasts had a higher inflammatory load and were metabolically dysregulated compared with HS-lo fibroblasts (**Figure 8.9A-B**).

In summary, this section details the transcriptomic differences between HS and healthy control fibroblasts. HS fibroblasts appeared to be metabolically dysregulated compared with healthy control fibroblasts, while HS fibroblasts also had increased production of collagen and increased expression of key cytokines and chemokines which play an important role in HS inflammation. Additionally, the inflammatory fibroblast (2) cluster may regulate scar formation in HS skin with elevated expression of collagens and MMPs, an imbalance of which can lead to hypertrophic scarring.

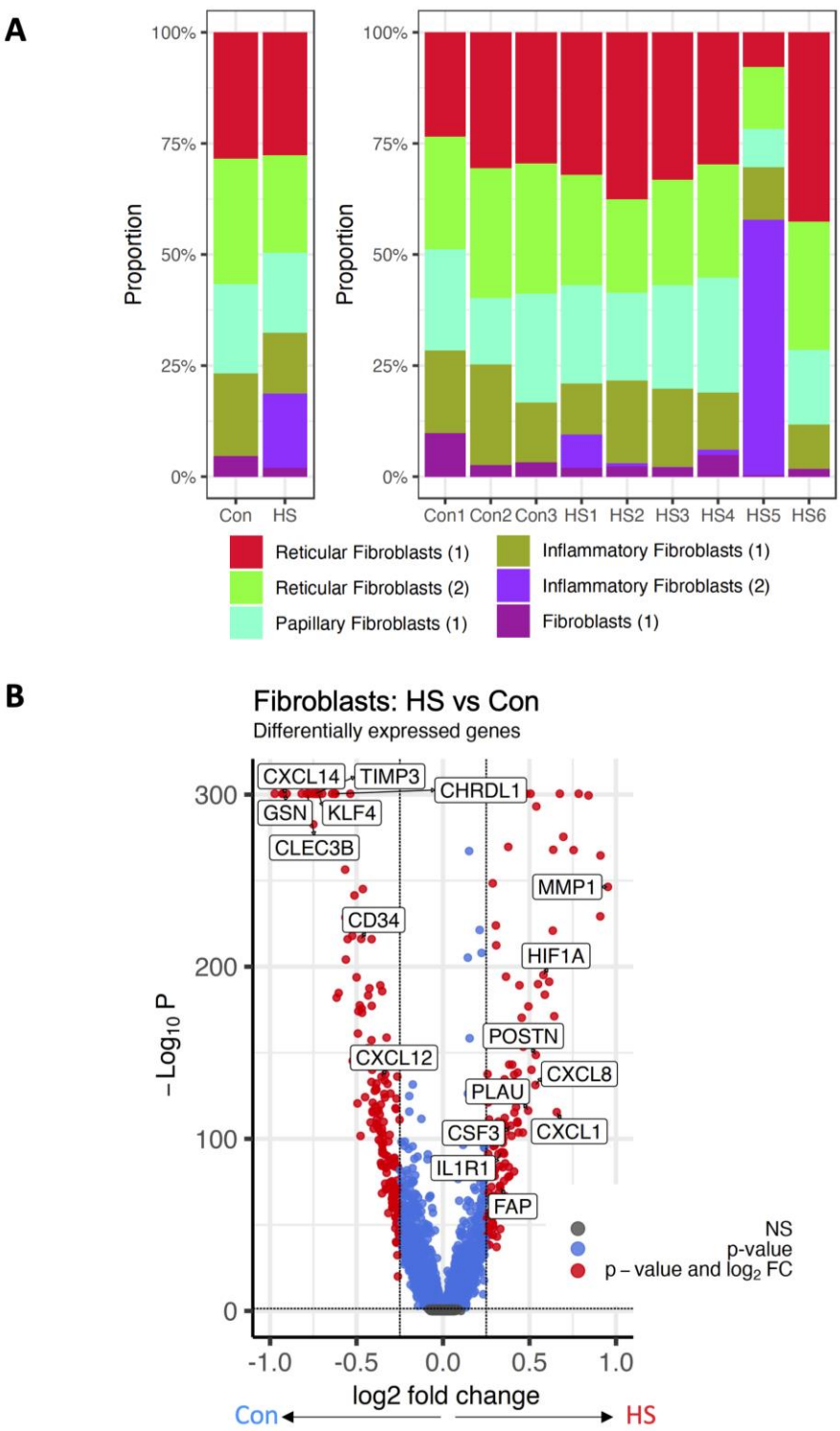

Figure 4.43 Inflammatory fibroblast cluster and proinflammatory gene expression are elevated in HS fibroblasts. Single cells isolated from healthy controls (Con; n=3) or HS lesional skin (HS; n=6) were purified based on absence of CD45 expression, barcoded and sequenced by 10X Genomics scRNA-seq. Bar chart visualises the relative frequency of fibroblast clusters in healthy control and HS lesional skin (A). Volcano plot visualises DEGs between HS and healthy control fibroblasts. Genes with a $log_2FC > 0$ are upregulated in HS and a $log_2FC < 0$ are downregulated in HS. The $-Log_{10}P$ Y-axis is a measure of significance (B).

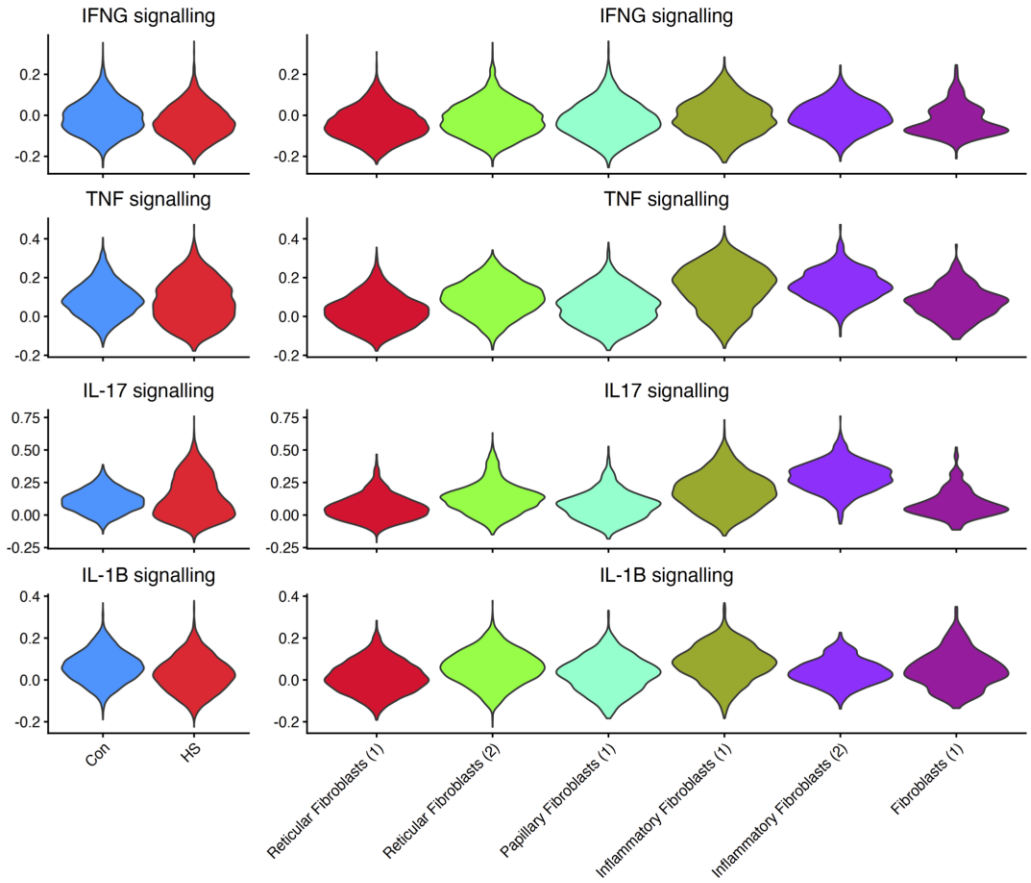

Figure 4.44 Inflammatory fibroblasts exhibited elevated TNF and IL-17 signaling relative to other fibroblast clusters. Single cells isolated from healthy controls (Con; n=3) or HS lesional skin (HS; n=6) were purified based on absence of CD45 expression, barcoded and sequenced by 10X Genomics scRNA-seq. Violin plot visualises the pathway activity scores of IFN-γ, TNF, IL-17 and IL-1β signaling in healthy control and HS fibroblasts and individual fibroblast clusters. Pathway activity scores were estimated for IFN-γ, TNF, IL-17 and IL-1β signaling using the AddModuleScore() function in Seurat.

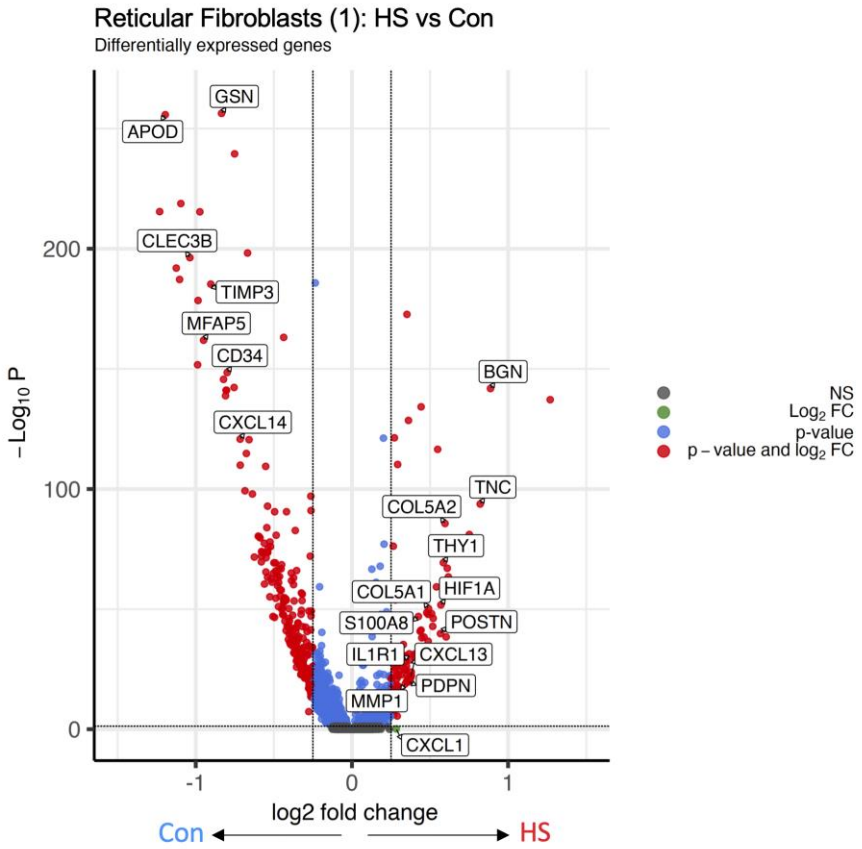

Figure 4.45 Volcano plot displaying DEGs between reticular fibroblasts in HS lesions and healthy control skin. Single cells isolated from healthy controls (Con; n=3) or HS lesional skin (HS; n=6) were purified based on absence of CD45 expression, barcoded and sequenced by 10X Genomics scRNA-seq. Volcano plot displays DEGs in reticular fibroblasts (1) from HS lesions compared with those in healthy control skin. Genes with a $log_2FC > 0$ are upregulated in HS and a $log_2FC < 0$ are downregulated in HS. The $-Log_{10}P$ Y-axis is a measure of significance.

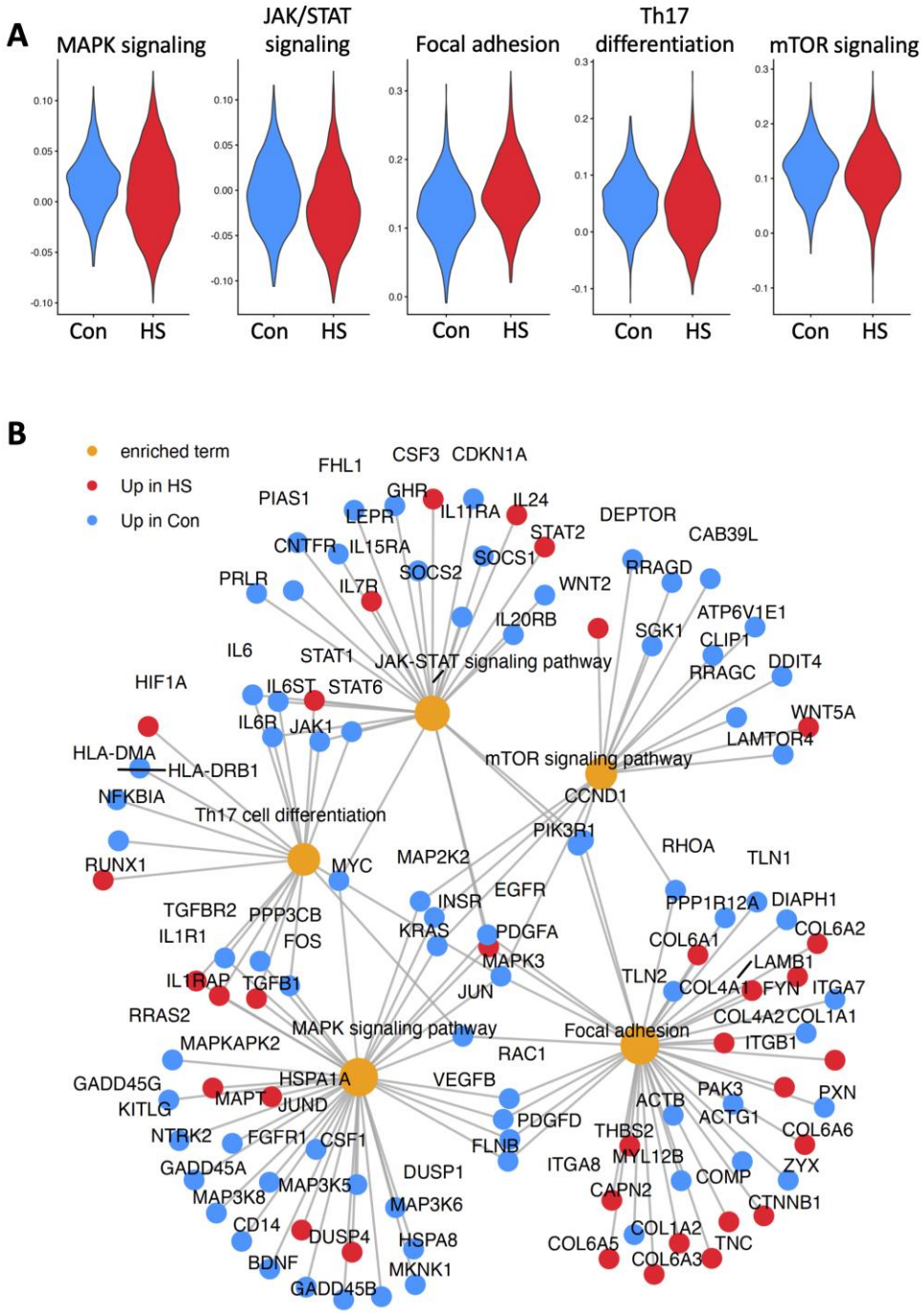

Figure 4.46 Reticular fibroblasts (1) have a distinct transcriptomic and functional profile in HS lesional skin. Single cells isolated from healthy controls (Con; n=3) or HS lesional skin (HS; n=6) were purified based on absence of CD45 expression, barcoded and sequenced by 10X Genomics scRNA-seq. Violin plot of pathway activity score of top 5 immune pathways enriched from the DEGs between healthy control and HS lesional fibroblasts in the reticular fibroblast (1) cluster (A). Gene-pathway network visualising the genes upregulated in Con (blue) or HS lesions (red) in the top 5 immune pathways enriched from the DEGs between healthy control and HS lesional fibroblasts in the reticular fibroblast (1) cluster (B).

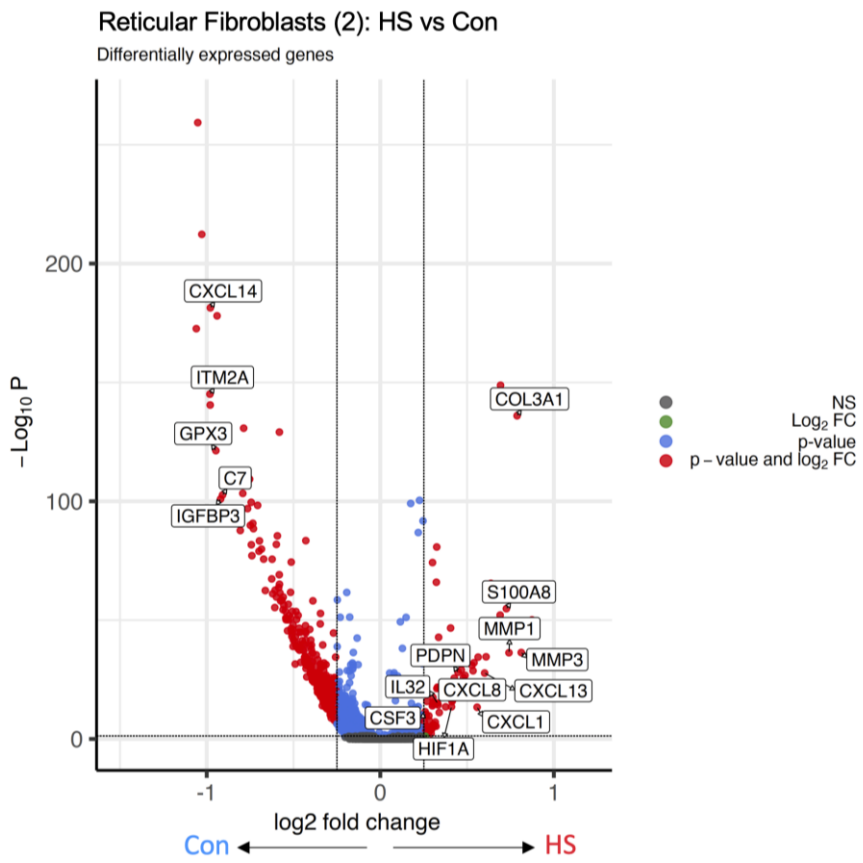

Figure 4.47 Volcano plot displaying DEGs between reticular fibroblasts (2) in HS lesions and healthy control skin. Single cells isolated from healthy controls (Con; n=3) or HS lesional skin (HS; n=6) were purified based on absence of CD45 expression, barcoded and sequenced by 10X Genomics scRNA-seq. Volcano plot visualises DEGs in reticular fibroblasts (2) from HS lesions compared with those in healthy control skin. Genes with a $log_2FC > 0$ are upregulated in HS and a $log_2FC < 0$ are downregulated in HS. The $-Log_{10}$ P Y-axis is a measure of significance.

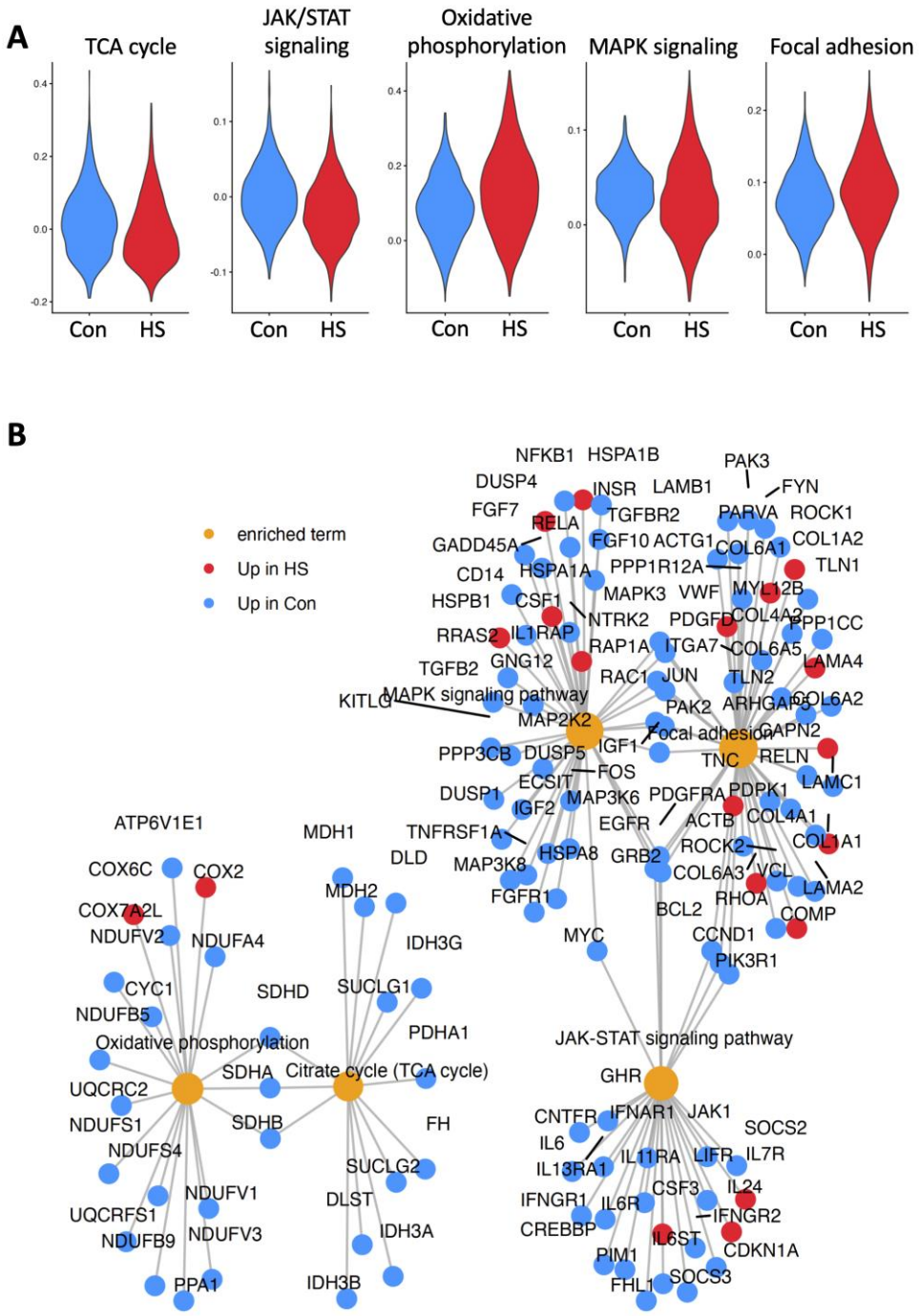

Figure 4.48 Reticular fibroblast (2) have a dysregulated metabolic profile in HS lesions compared with healthy control skin. Single cells isolated from healthy controls (Con; n=3) or HS lesional skin (HS; n=6) were purified based on absence of CD45 expression, barcoded and sequenced by 10X Genomics scRNA-seq. Violin plot of pathway activity score of top 5 immune pathways enriched from the DEGs between healthy control and HS lesional fibroblasts in the reticular fibroblast (2) cluster (A). Gene-pathway network displaying the genes upregulated in Con (blue) or HS lesions (red) in the top 5 immune pathways enriched from the DEGs between healthy control and HS lesional fibroblasts in the reticular fibroblast (2) cluster (B).

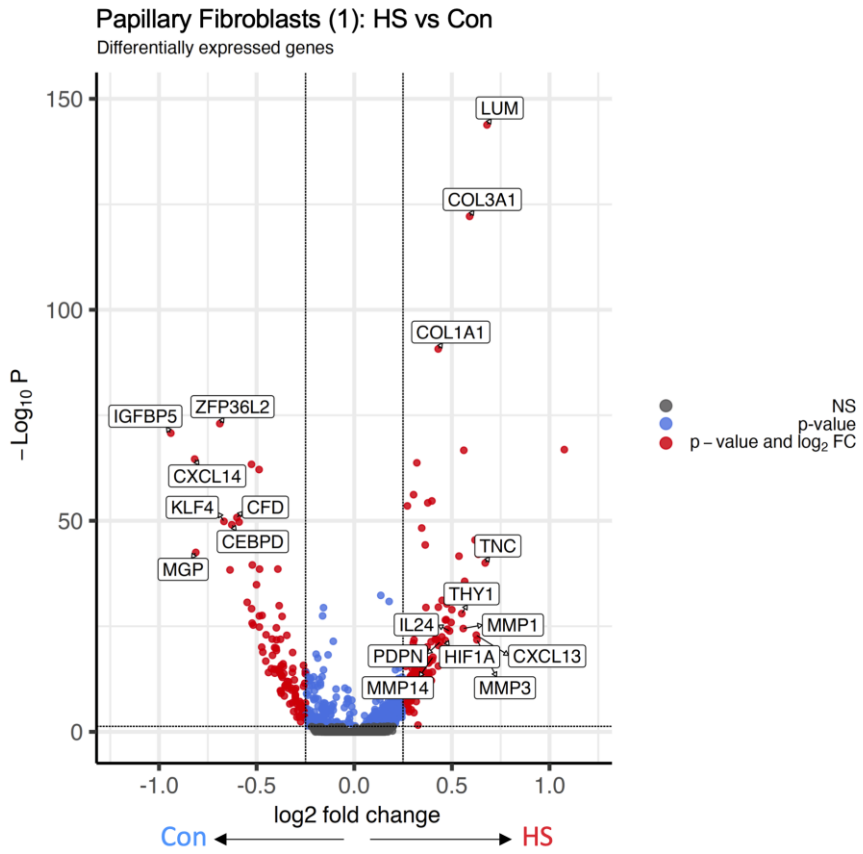

Figure 4.49 Volcano plot displaying DEGs in papillary fibroblasts (1) in HS lesions and healthy control skin. Single cells isolated from healthy controls (Con; n=3) or HS lesional skin (HS; n=6) were purified based on absence of CD45 expression, barcoded and sequenced by 10X Genomics scRNA-seq. Volcano plot visualises DEGs in papillary fibroblasts (1) from HS lesions compared with those in healthy control skin. Genes with a $log_2FC > 0$ are upregulated in HS and a $log_2FC < 0$ are downregulated in HS. The $-Log_{10}P$ Y-axis is a measure of significance.

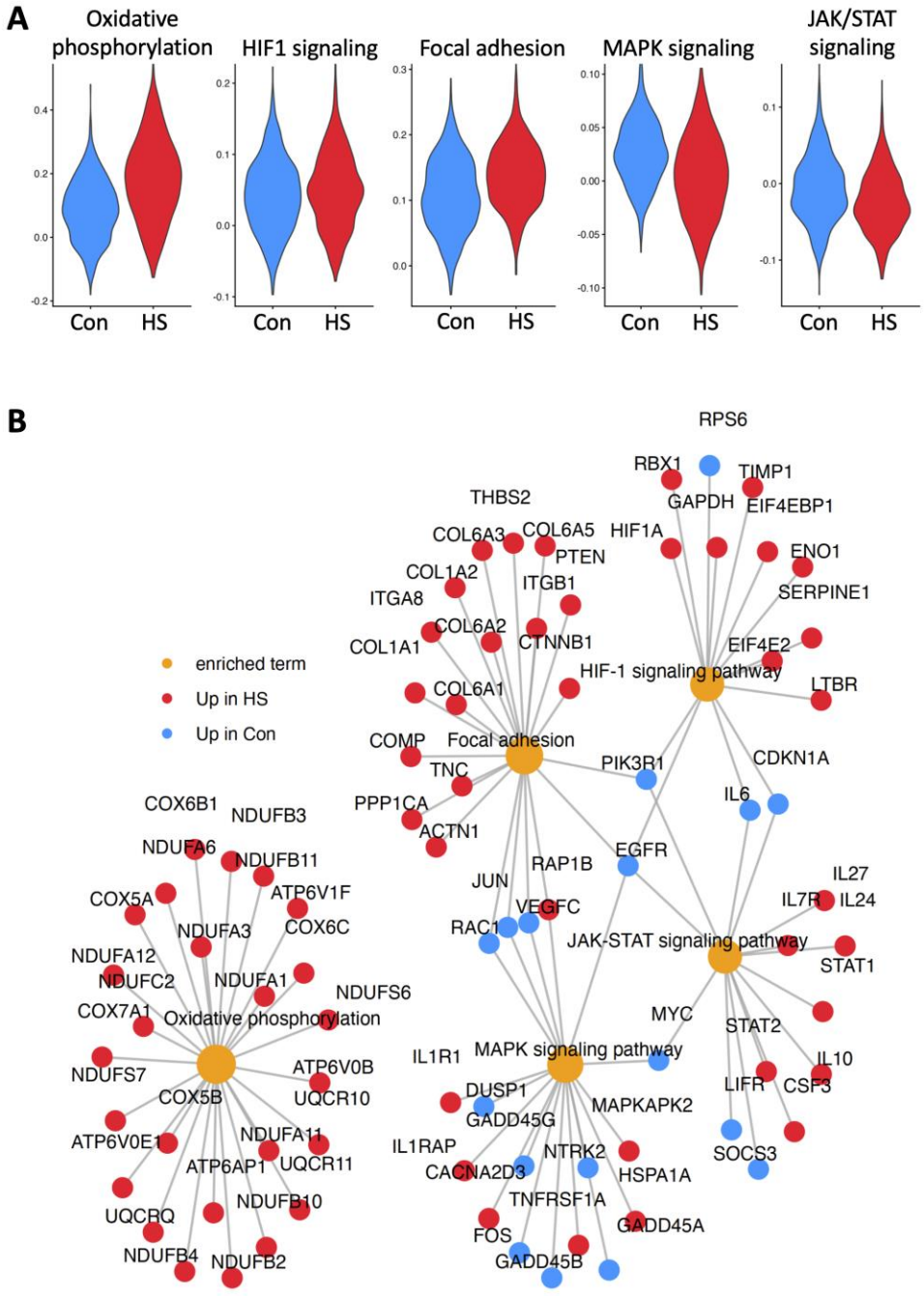

Figure 4.50 Papillary fibroblast (1) have elevated oxidative phosphorylation in HS lesions compared with healthy control skin. Single cells isolated from healthy controls (Con; n=3) or HS lesional skin (HS; n=6) were purified based on absence of CD45 expression, barcoded and sequenced by 10X Genomics scRNA-seq. Violin plot of pathway activity score of top 5 immune pathways enriched from the DEGs between healthy control and HS lesional fibroblasts in the papillary fibroblast (1) cluster (A). Gene-pathway network visualising the genes upregulated in Con (blue) or HS lesions (red) in the top 5 immune pathways enriched from the DEGs between healthy control and HS lesional fibroblasts in the papillary fibroblast (1) cluster (B).

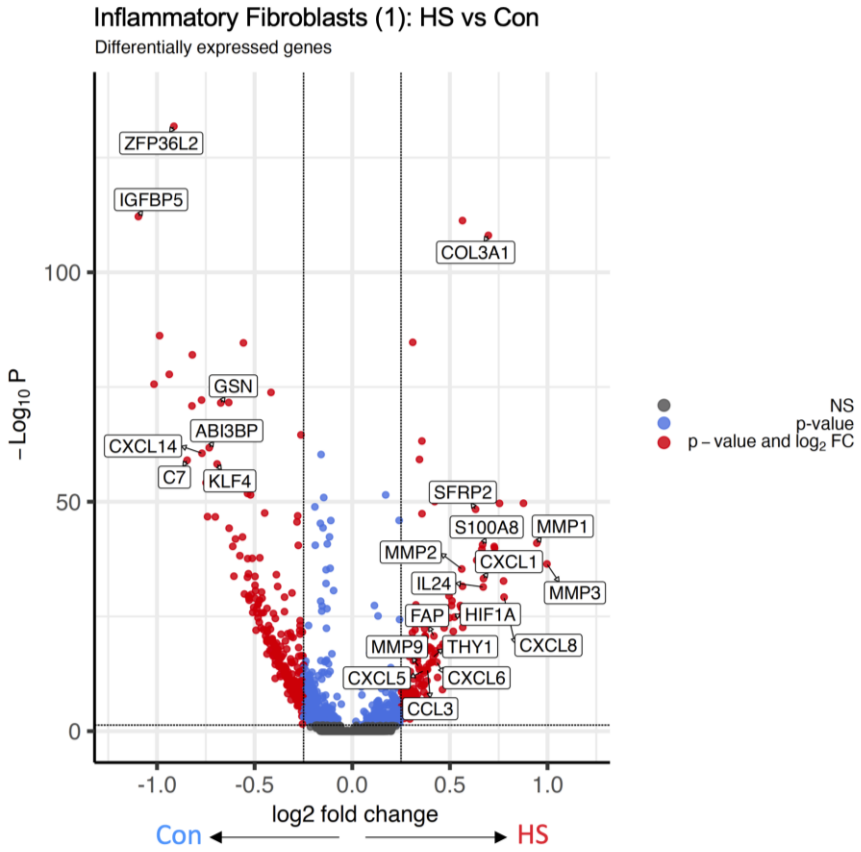

Figure 4.51 Volcano plot displaying DEGs between inflammatory fibroblasts (1) in HS lesions and healthy controls. Single cells isolated from healthy controls (Con; n=3) or HS lesional skin (HS; n=6) were purified based on absence of CD45 expression, barcoded and sequenced by 10X Genomics scRNA-seq. Volcano plot visualises DEGs in inflammatory fibroblasts (1) from HS lesions compared with those in healthy control skin. Genes with a $log_2FC > 0$ are upregulated in HS and a $log_2FC < 0$ are downregulated in HS. The $-Log_{10}P$ Y-axis is a measure of significance.

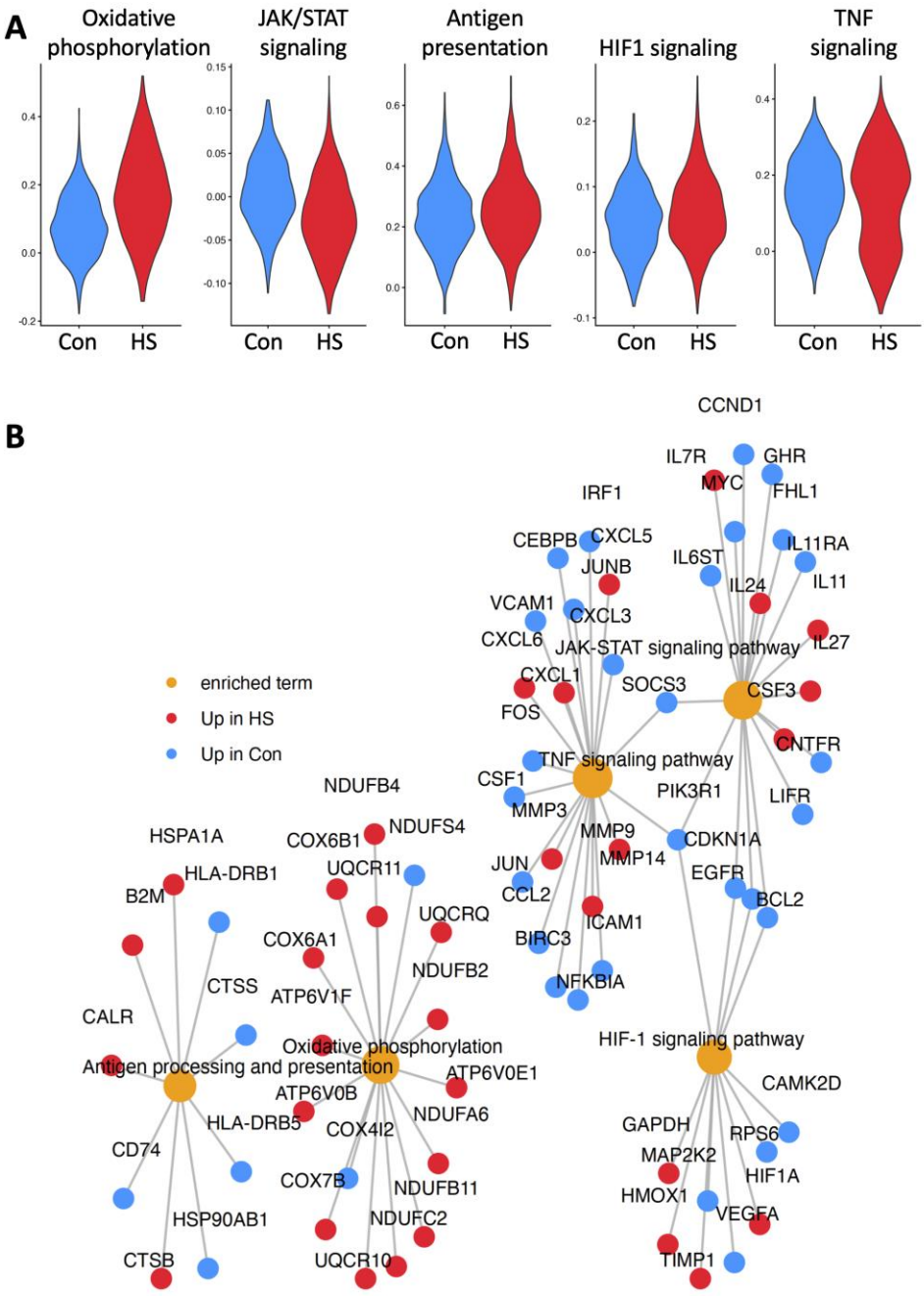

Figure 4.52 Increased oxidative phosphorylation and TNF signaling distinguished inflammatory fibroblasts (1) in HS lesions from healthy controls. Single cells isolated from healthy controls (Con; n=3) or HS lesional skin (HS; n=6) were purified based on absence of CD45 expression, barcoded and sequenced by 10X Genomics scRNA-seq. Violin plot of pathway activity score of top 5 immune pathways enriched from the DEGs between healthy control and HS lesional fibroblasts in the inflammatory fibroblast (1) cluster (A). Gene-pathway network visualising the genes upregulated in Con (blue) or HS lesions (red) in the top 5 immune pathways enriched from the DEGs between healthy control and HS lesional fibroblasts in the inflammatory fibroblast (1) cluster (B).

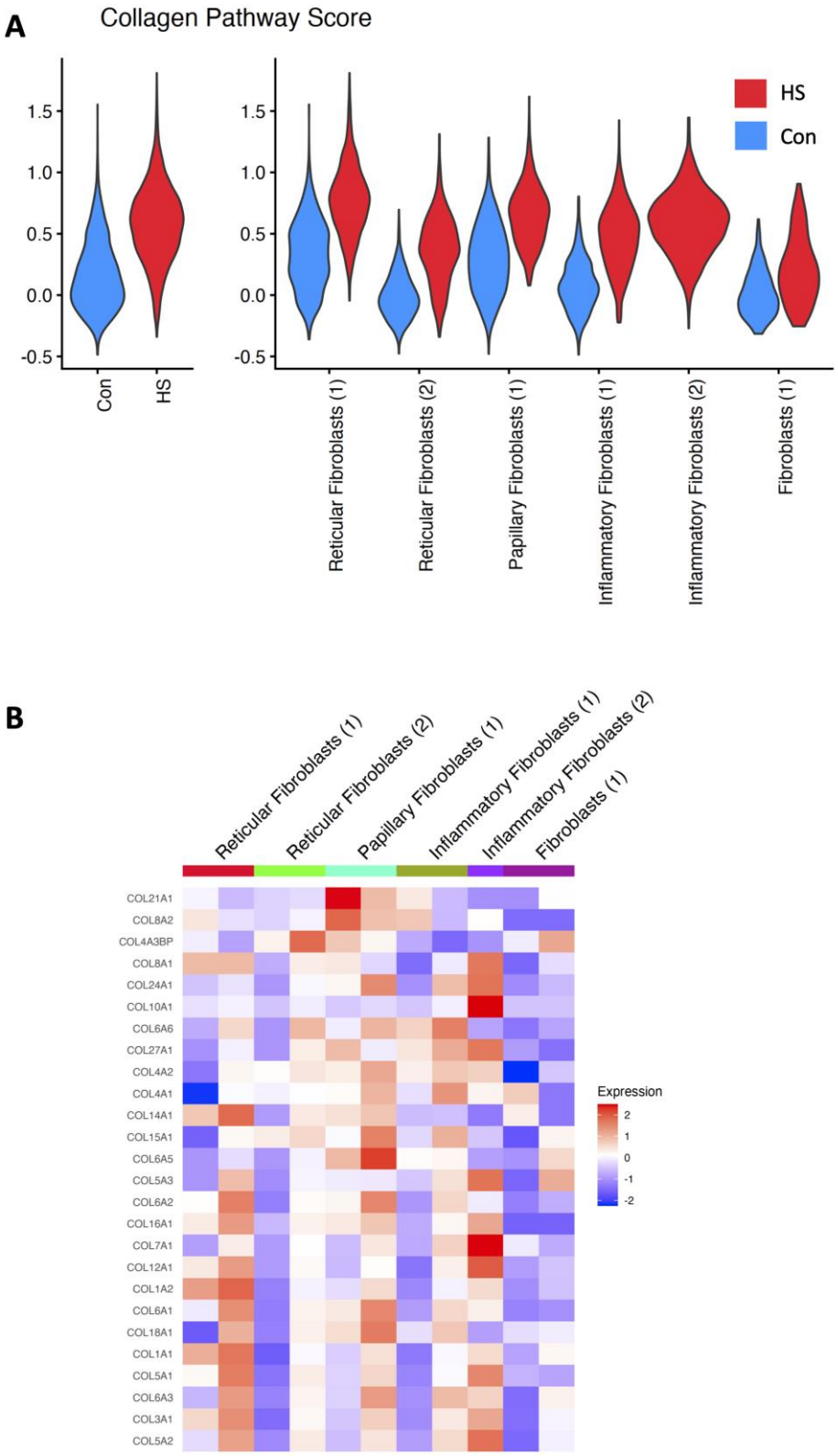

Figure 4.53 HS fibroblasts had increased collagen production. Single cells isolated from healthy controls (Con; n=3) or HS lesional skin (HS; n=6) were purified based on absence of CD45 expression, barcoded and sequenced by 10X Genomics scRNA-seq. Violin plot displays collagen pathway scores in HS and healthy control fibroblasts in each fibroblast cluster (A). Collagen pathway scores are calculated using the AddModuleScore function. Heatmap of relative expression of collagen genes in each fibroblast cluster in both healthy control and HS lesional fibroblasts (B).

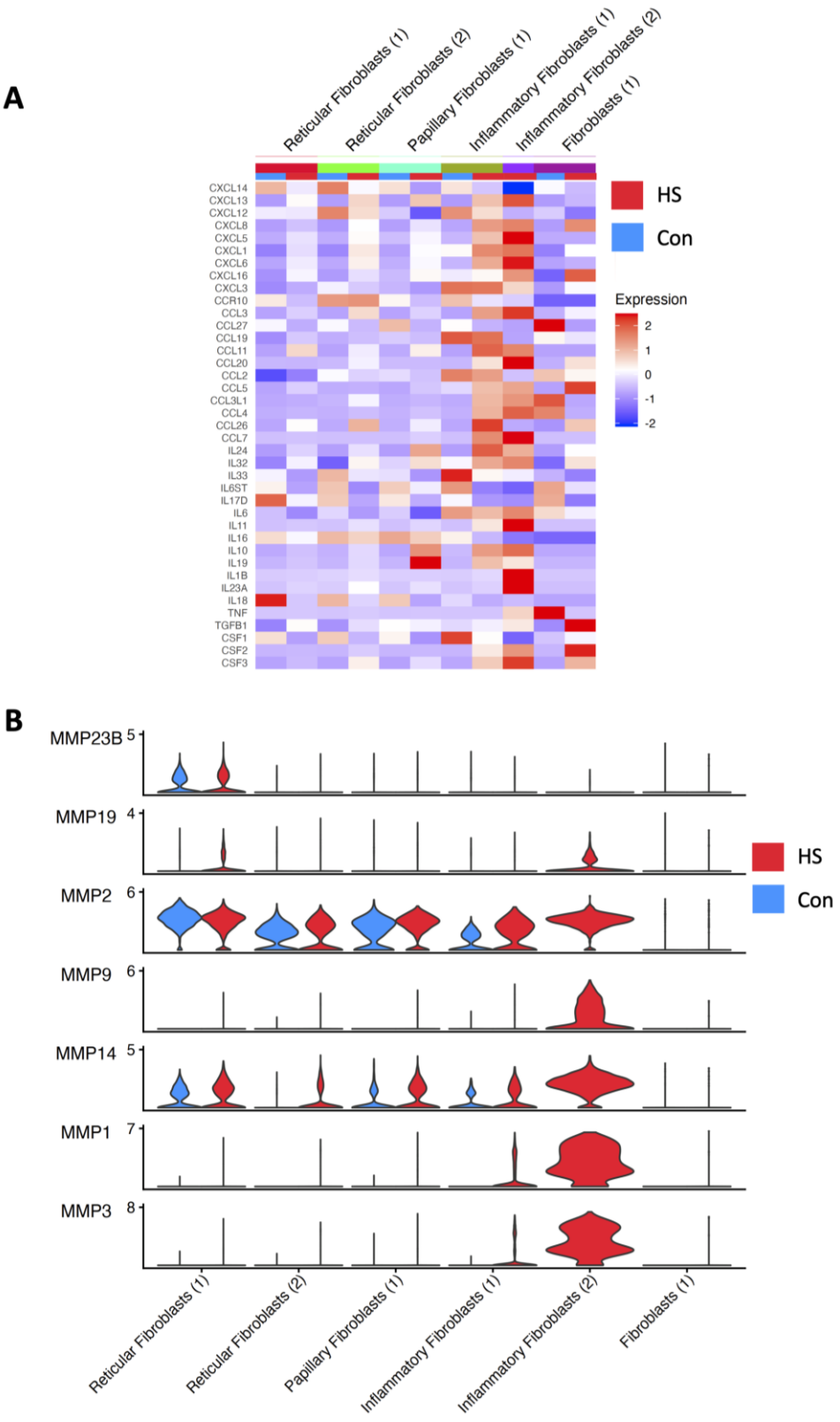

Figure 4.54 Inflammatory fibroblasts had elevated cytokine, chemokine and MMP expression in HS lesions. Single cells isolated from healthy controls (Con; n=3) or HS lesional skin (HS; n=6) were purified based on absence of CD45 expression, barcoded and sequenced by 10X Genomics scRNA-seq. Heatmap of the relative expression of chemokines and cytokines expressed by HS and healthy control fibroblasts in each fibroblast cluster (A). Violin plot displays the expression of MMPs in HS and healthy control fibroblasts in each fibroblast cluster (B).

4.4 Discussion

This chapter provided novel insights into the non-immune cells which reside in HS lesions. To my knowledge, this is the first comparative characterisation of $CD45^-$ cells from HS lesional and healthy control skin using state of the art single cell techniques. The identification and characterisation of inflammatory keratinocytes and fibroblasts in HS lesions has added much value to the field. These data convincingly highlight the important role of $CD45^-$ cells in promoting HS inflammation, detailing how different cytokines regulate the expression of proinflammatory mediators in HS fibroblast populations.

HS is a highly heterogenous disease, with many believing that HS could comprise of multiple different clinical phenotypes (Martorell *et al.*, 2020). In line with this, this study has outlined 2 transcriptomic profiles in HS which may replicate what is seen in the clinic. Samples HS4 and HS6 had similar transcriptomic profiles to healthy control skin, while HS1, HS2, HS3 and HS5 had a heterogenous transcriptomes with higher inflammatory loads. Unfortunately, histology could not be performed on all of these HS lesions due to the small biopsy sizes, which may have elucidated more details about their clinical phenotype.

Currently there is a paucity of research describing non-immune cells present in HS lesions and their role in HS pathogenesis. This study provides a detailed classification of the $CD45^-$ cells present in HS lesional and healthy control skin.

4.4.1 Keratinocytes in HS lesions

Despite being defined as a hyperkeratotic disease (Yazdanyar and Jemec, 2011), detailed characterisation of HS keratinocytes has yet to be performed. Previous studies have suggested keratinocyte dysfunction may play a prominent role in promoting HS inflammation (Hotz *et al.*, 2016; Gudjonsson *et al.*, 2020; Schell *et al.*, 2023). As keratinocytes differentiate from basal into spinous keratinocytes or if they become hyperproliferative, their expression of keratins changes. Immunohistochemistry previously demonstrated that HS lesions have normal expression of both KRT1 and KRT14, representing basal and spinous keratinocytes respectively, relative to healthy skin (Kurokawa *et al.*, 2002). Hyperproliferative keratinocytes are defined by increased expression of KRT16 and KRT17, with increased expression of both KRT16 and KRT17 found in the suprabasal layer of HS lesional epidermis (Kurokawa *et al.*, 2002), supporting findings

found here demonstrating the differentiation of HS basal keratinocytes into inflammatory keratinocytes. Inflammatory keratinocytes were characterised by elevated expression of *KRT6A* and *KRT16* which previously was believed to replace the expression of the spinous keratins *KRT1* and *KRT10* (Freedberg *et al.*, 2001). The increased expression of the inflammatory keratin *KRT6A* in HS lesions relative to healthy skin described here is supported by others (Coates *et al.*, 2019), while KRT6A has also been shown to be elevated in HS lesional skin relative to perilesional skin (Lima *et al.*, 2016), indicating that these inflammatory keratinocytes may uniquely develop in response to the HS lesional inflammatory microenvironment.

The identification of *KRT6A*, *KRT16* co-expressing keratinocytes has previously been described in HS lesions by scRNA-seq (Gudjonsson *et al.*, 2020). These keratinocytes had increased expression of inflammatory cytokine responsive genes, specifically genes related to IL-17, TNF, IFN-γ, IL-4, IL-13 and IL-36γ responses were elevated in these inflammatory keratinocytes (Gudjonsson *et al.*, 2020). The dramatic influx of immune cells which infiltrate the HS lesion contributes to the elevated cytokine signaling which HS keratinocytes experience (Lima *et al.*, 2016). An influx of B cells, CD4 and CD8 T cells, mast cells, macrophages and neutrophils have all been described in HS lesions (Lima *et al.*, 2016) and may contribute to dysregulated cytokine signaling in HS lesions. Importantly, an influx of immune cells into the HS lesional epidermis correlates with more severe disease (Schell *et al.*, 2023), indicating keratinocytes may be key promoters of severe HS inflammation. CD8 T cells and macrophages, in particular, infiltrate the HS epidermis (Schell *et al.*, 2023).

Keratinocytes themselves have been shown to play an active role in HS inflammation, expressing multiple chemokines which recruit immune cells to the HS lesion and cytokines which promote inflammation. This study found increased expression of *CXCL8*, *CXCL2* and *CXCL3* by HS keratinocytes relative to healthy control keratinocytes, supporting findings from a recent study (Schell *et al.*, 2023). Elaborating on the increased expression of *CXCL1* and *CCL20* described in HS lesions (Hotz *et al.*, 2016), the cellular sources of these neutrophil and T cell chemoattractants were defined in this chapter. Keratinocytes were also found to be a prominent source of *IL18* (Gudjonsson *et al.*, 2020), similarly high expression by keratinocytes was found in this dataset (data not shown), however there was no significant difference in expression between HS and healthy control keratinocytes.

Release of IL-18 can be regulated by the NLRP3 inflammasome, which has been reported to be expressed in epidermal keratinocytes (Dai *et al.*, 2017), however no expression of *NLRP3* or *IL1B* was found in keratinocytes in this dataset (data not shown). Interestingly, in the basal keratinocyte (1) cluster, NLR signaling was elevated in HS relative to healthy controls. This increase in NLR signaling may derive from the NLRP1 inflammasome, expression of which was detected in keratinocytes in this dataset (data not shown). While *NLRP1* expression was only slightly higher in HS keratinocytes compared with healthy, this may account for *IL18* expression by HS keratinocytes (Murphy *et al.*, 2016).

Multiple studies have described elevated expression of the S100 family of AMPs in HS lesional skin (Lima *et al.*, 2016; Hambly *et al.*, 2023; Coates *et al.*, 2019). Keratinocytes are a primary source of AMPs in this data, elaborating on previous studies (Hotz *et al.*, 2016; Lima *et al.*, 2016). These AMPs may act as DAMPs which can be recognised by the NLRP3 inflammasome, inducing the production of IL-1β (Simard *et al.*, 2013). IL-1β promotes the development of IL-17A-producing Th17 cells (Acosta-Rodriguez *et al.*, 2007) which subsequently stimulate keratinocytes to produced AMPs, creating an inflammatory feed forward loop. IL-17 signaling was particularly prominent in the inflammatory keratinocyte cluster in HS lesions, replicating previous findings which described an increase in IL-17 responsive genes by inflammatory keratinocytes (Gudjonsson *et al.*, 2020). Interestingly, IL-17 responsive genes, including *S100A8*, *S100A9*, *CXCL8*, *CCL20* and *KRT6A* were found to be key markers of keratinocyte differentiation into this inflammatory phenotype, indicating a potentially important role of IL-17A in dysregulating keratinocyte function in HS.

Keratinocytes have a well-known role in psoriasis inflammation, with epidermal thickening a key feature of psoriasis plaques. While HS lesions have a significantly thicker epidermal layer compared with healthy controls (Nisar *et al.*, 2019), the number of keratinocytes in the granular and corneous layers of the epidermis are dramatically reduced in HS relative to psoriasis (Kim *et al.*, 2023). Here, psoriatic keratinocytes had elevated expression of *KRT6A* and *KRT16*, indicative of increased inflammatory keratinocytes, and increased production of AMPs, supporting previous findings (Kim *et al.*, 2023; Wolk *et al.*, 2011). HS keratinocytes, on the other hand had elevated expression of *CXCL8*, *CXCL2*, *CCL27*, *JUN*, *NFKBIA*, *AREG* and *SERPINB2*. CXCL8 and CXCL2 are important neutrophil chemoattractants, emphasising the importance of neutrophils in HS relative to psoriasis

(Metzemaekers, Gouwy and Proost, 2020). *AREG*, which encodes amphiregulin, an epidermal growth factor has been found to be elevated in psoriasis lesions relative to healthy skin (Yu *et al.*, 2022). Furthermore, inhibition with secukinumab reduced the expression of *AREG* in psoriatic lesions (Yu *et al.*, 2022). Increased expression of *AREG* in HS keratinocytes, further emphases the importance of IL-17A in activating HS keratinocytes. *CCL27*, which can be induced by TNF or IL-1β, mediates the recruitment of skin-homing T cells via CCR10 interaction (Homey *et al.*, 2002). The elevated expression of *JUN* and *NFKBIA* indicate the complex inflammatory microenvironment of HS lesions may activate keratinocytes through different pathways relative to psoriatic keratinocytes which are primarily driven by IL-17 cytokines. Coinciding with this, there was increased expression of *SERPINB2* in HS keratinocytes relative to psoriatic keratinocytes. TNF has also been shown to induce the expression of *SERPINB2* in cultured keratinocytes, however greater expression was induced by IFN-γ (Vaher *et al.*, 2020), which is also elevated in HS lesions (Banerjee, McNish and Shanmugam, 2017). While *SERPINB2* has previously been shown to be elevated in psoriatic skin relative to healthy controls (Vaher *et al.*, 2020), its relative increase in HS keratinocytes may also be due to the more complex inflammatory microenvironment in HS lesions.

Importantly, this study demonstrated similar elevated expression of inflammatory genes in HS and psoriatic keratinocytes, but reduced expression of proliferation and differentiation genes by HS keratinocytes relative to psoriatic keratinocytes. These data replicate the physiological differences seen in HS and psoriasis lesions, with a dramatically thickened epithelium seen in psoriatic lesions compared with HS lesions. Despite this, keratinocytes play important roles in both HS and psoriasis inflammation. Psoriasis lesions had elevated expression of *WWOX*, *TRPS1*, *CLASP2*, *CDH13* and *CALML5*, which has been shown to regulate keratinocyte proliferation and differentiation (Chou *et al.*, 2020; Rybski, Zengin and Smoller, 2023; Shahbazi *et al.*, 2017; Wang *et al.*, 2018; Méhul, Bernard and Schmidt, 2001), and *PTPRK* which regulates the activation of keratinocytes (Xu *et al.*, 2015), relative to HS keratinocytes. HS keratinocytes had increased expression of *CALM2*, *FABP5* and *PNRC1,* demonstrating unique pathways regulating differentiation and proliferation compared with psoriasis keratinocytes (Kahl and Means, 2003; Ogawa *et al.*, 2011; Yao *et al.*, 2021).

Interestingly, the overall transcriptomic variation determined by PCA in keratinocytes was dramatically different to the PCA of all $CD45^-$ cells indicating that keratinocyte dysfunction may not reflect overall disease and the contribution of keratinocytes may vary between HS patients. This may have been due to reduced keratinocyte frequency in certain HS lesions. Without histological analysis of these samples, it is difficult to understand why some HS lesions may have a reduced frequency of keratinocytes, but this may be in part due to a disrupted epidermal layer caused as a result of the HS lesion or as a result of less severe disease which also correlated with reduced epidermal thickening (Schell *et al.*, 2023).

Dermal tunnels, a unique feature of HS, have been shown to be lined with keratinocytes (Kurokawa *et al.*, 2002; Navrazhina *et al.*, 2021a). Interestingly, these keratinocytes were shown to have a unique transcriptome to epidermal keratinocytes in HS lesions. Keratinocytes in HS dermal tunnels were found to have increased *IL6*, *IL1A* and *IL1B* expression, while epidermal keratinocytes had increased expression of *IL36G* and *IL1RL1* (Kim *et al.*, 2023) which may contribute to the highly inflammatory environment of HS dermal tunnels (Navrazhina *et al.*, 2021a).

The increased expression of genes related to oxidative phosphorylation, glycolysis and mTOR signaling demonstrated a dysregulated metabolic profile in HS keratinocytes. Interestingly, metformin, typically used to treat associated metabolic syndrome in HS patients, has been shown to normalise the cellular metabolic profile of HS lesions, and subsequently reduce the production of inflammatory cytokines (Petrasca *et al.*, 2023a). JAK-STAT, on the other hand, has long been touted as a potential therapeutic target in HS. INCB054707, a JAK1 inhibitor is currently in a phase 2 trial for treatment of HS. Phase 1 results involved a total of 45 patients, with 20 patients having at least a 50% reduction in disease severity at week 8 (Alavi *et al.*, 2022).

Importantly, these data have, for the first time, detailed the differentiation of keratinocytes into an inflammatory phenotype in HS lesions.

4.4.2 Fibroblasts in HS lesions

Hypertrophic scarring and dermal tunnels are unique features which distinguish HS from other inflammatory dermatoses. Fibroblasts have been previously linked with the development and progression of HS (Sanchez *et al.*, 2019). Despite the potential role of fibroblasts in the hypertrophic scarring seen in HS (Frew *et al.*, 2019), there was no significant difference between the frequency of fibroblast subsets in HS lesions compared with healthy control skin. This is an important finding as it suggests that rather than the development of HS-specific fibroblast populations, as with inflammatory keratinocytes, there is likely a global dysregulation of fibroblasts in HS.

6 fibroblast clusters were identified in this data, some of which have similarly been described in other scRNA-seq projects of healthy control and psoriatic skin. Dermal and papillary signatures have previously been defined in healthy skin, which aided in the annotation of fibroblasts in this dataset (Solé-Boldo *et al.*, 2020). While there was no significant difference in the frequency of any fibroblast cluster, the inflammatory fibroblast (2) cluster was unique to HS lesions, although this data was skewed by a dramatic increase of this fibroblast cluster in one HS patient. The elevated expression of MMPs, collagen genes and the prominent role of extracellular matrix remodelling in this inflammatory fibroblast (2) cluster suggested that these fibroblasts may be involved in scarring in HS lesions. This fibroblast cluster, which also expressed elevated levels of *FMO1* has previously been identified in healthy control skin (Tabib *et al.*, 2018), however more recent studies in ultra-violet B exposed skin and in AD skin have failed to identify this subset of fibroblasts (Solé-Boldo *et al.*, 2020; He *et al.*, 2020). Tabib *et al.,* described $FMO1^{+}$ fibroblasts similar to bone marrow stromal cells, which retain immune cells in the dermis and do not play an active role in matrix production (Tabib *et al.*, 2018). Contrastingly, the data from this study suggests that the inflammatory fibroblast (2) cluster plays a key role in matrix degradation and mediates immune cell migration into HS lesions, indicating that inflammatory fibroblasts may be pathogenic in the context of HS.

Sanchez *et al.,* previously detailed variations in collagen production between fibroblasts in the papillary and reticular dermis. This data elaborates on these findings, detailing collagen production in different fibroblast populations in both the papillary and reticular dermis (Sanchez *et al.*, 2019). Hypertrophic scarring develops following excessive deposition and

dysregulated degradation of the extracellular matrix. Collagen synthesis can be up to 20 times higher in hypertrophic scars than in normal skin (Xue and Jackson, 2015). This elevated production of collagen has been attributed to stronger proliferative capacity of fibroblasts (Abergel *et al.*, 1987). Elevated expression of TGF-β1 is a key feature of hypertrophic scars, with fibroblasts responsible for scarring having higher expression of TGF-β receptors and ultimately have a more potent response to TGF-β1 (Honardoust *et al.*, 2012; Abdou *et al.*, 2011). Interestingly, Decorin (*DCN*) which was significantly downregulated in HS fibroblasts here (data not shown), has been shown inhibit fibroblast proliferation, TGF-β production and collagen synthesis (Zhang *et al.*, 2007). The downregulation of this gene may account for the unregulated expression of collagen genes seen in this study. In normal skin, MMPs play an important role in degrading excess collagen, however in hypertrophic scarring collagen crosslinking makes collagens less susceptible to cleavage by MMPs (Romanic *et al.*, 1992). MMP1 has also been shown to mediate re-epithelisation, which may be crucial in the development of dermal tunnels in HS (Stevens and Page-McCaw, 2012). Similarly, reduced expression of *CXCL12* in inflammatory keratinocytes may contribute to the epithelialisation of dermal tunnels (Avniel *et al.*, 2006).

Neutrophils were found to infiltrate HS dermal tunnels, with CXCL1 and CXCL8 expression increasing towards the lumen of dermal tunnels (Navrazhina *et al.*, 2021a). In this data, HS inflammatory fibroblasts had elevated expression of both *CXCL1* and *CXCL8*, indicating a potential role in recruiting neutrophils to the dermal tunnel. In this data, inflammatory fibroblasts appeared to play a role in an antimicrobial response, which may be in response to the luminal biofilm of HS dermal tunnels. Unfortunately, clinical data detailing the presence or absence of dermal tunnels or hypertrophic scarring was not available for this study, limiting inferences which can be made about the role of fibroblasts in the development of dermal tunnels and scarring.

Supporting previous findings of elevated expression of *CSF3* in HS lesional skin (Wolk *et al.*, 2021), this study detailed fibroblasts as the primary cellular source of this increased expression of *CSF3*. The secretion of G-CSF, the protein encoded by *CSF3*, was elevated in dermal fibroblasts stimulated with a combination of IL-1β and TNF (Wolk *et al.*, 2021). The complex inflammatory microenvironment of HS lesions may explain why HS fibroblasts

have elevated expression of *CSF3* shown in this chapter. Interestingly, increased *CSF3* expression was found to correlate with the expression of neutrophil markers (Navrazhina *et al.*, 2021b), indicating that *CSF3* may drive neutrophil activity in HS lesions. Therapeutically targeting G-CSF by blocking its receptor with CSL324 is currently being assessed in a phase 1 trial in HS (NCT03972280).

Interestingly, the inflammatory fibroblast (2) cluster had relatively high expression of *IL1B* and *IL23A*. The NLRP3 inflammasome has previously been reported to be found in fibroblasts (Ershaid *et al.*, 2019) and could potentially regulate the production of IL-1β in HS fibroblasts, however no *NLRP3* expression was identified in these fibroblasts (data not shown). Human fibroblast-like synoviocytes were shown to produce IL-23A following IL-1β stimulation (Liu *et al.*, 2007). However, the expression of both *IL1B* and *IL23A* comes from the same small subset of fibroblasts in the inflammatory fibroblast (2) cluster and may simply represent a technical artifact.

In conclusion, this study has contributed to our understanding of both keratinocyte and fibroblast populations which contribute to the inflammatory microenvironment in HS lesions. Dysregulated inflammatory fibroblasts in HS lesions have increased expression of *CXCL8*, *CXCL1* and *CXCL5* which promote the infiltration of neutrophils and also potentially regulate the formation of hypertrophic scars through the dysregulated expression of collagen genes and MMPs.

Chapter 5

T cells drive keratinocyte and fibroblast inflammatory phenotypes in HS

5 T cells drive keratinocyte and fibroblast inflammatory phenotypes in HS

5.1 Introduction

Immune dysregulation and in particular, T cell dysregulation has emerged as a characteristic feature of HS. Studies have sought to characterise the T cell populations which can be found dramatically increased in HS lesions (Moran *et al.*, 2023; Kelly *et al.*, 2015). An increase of IL-17$^+$ CD4 T cells in HS skin has been reported by multiple groups (Kelly *et al.*, 2015; Schlapbach *et al.*, 2011; Moran *et al.*, 2017; Hotz *et al.*, 2016), with elevated frequencies of Th17 cells found in both lesional and perilesional HS skin (Moran *et al.*, 2017; Hotz *et al.*, 2016). Interestingly, considering the prominent role of IL-17 cytokines in psoriasis, IL-17A$^+$ T cells in HS lesional skin were found to have higher expression of IL-17F relative to those from psoriatic skin (Kim *et al.,* 2023). Similarly, increased expression of *IL1R1* was observed on IL-17-A$^+$ T cells in HS relative to psoriasis, emphasising the importance of the IL-1β-Th17 cell axis in HS (Kim *et al.,* 2023). Th17 cells appear to be a major source of IL-17A in HS skin (Moran *et al.,* 2017), which has previously been shown to be elevated in HS skin (Kelly *et al.,* 2015) and is the primary target of secukinumab which has recently been licenced by the EMA for use in HS (Kimball *et al.*, 2023a).

While TNF blockade has been effective in a number of chronic inflammatory diseases including psoriasis, RA and CD, it has only been moderately effective in HS, reducing inflammatory nodules by at least 50% in ~60% of HS patients (Kimball *et al.,* 2016). Multiple studies have described an increase of TNF in HS lesions without describing its cellular source (Kelly *et al.*, 2015; van der Zee *et al.*, 2011), while previous work in our lab has described an increase in the frequency of TNF$^+$ CD4 T cells in HS skin (Moran *et al.,* 2017).

Perhaps counterintuitively, an increase in Treg cells has previously been described in HS skin (Moran *et al.,* 2017). Treg cells are well known for their regulatory role in autoimmunity where they suppress and constrain effector T cells, preventing T cell mediated inflammation (Sojka, Huang and Fowell, 2008). Considering this, the increase of Treg cells in HS skin is surprising. Importantly however, the ratio of Th17:Treg cells was dramatically skewed in favour of Th17 cells in HS skin, suggesting that Treg cells were unable to constrain

inflammation (Moran *et al.,* 2017). A similar imbalance of Th17 and Treg cells has also been described in pyoderma gangrenosum and Crohn's disease (Caproni *et al.*, 2015; Brand, 2009). Transcriptomic analysis of Treg cells in HS and psoriasis lesions suggested that HS Treg cells had elevated expression of IL-17 cytokines and *IL1R1*, whereas Treg cells in psoriasis lesions had increased expression of *TGFB1* and *IL10* relative to HS, suggesting that HS Treg cells may be dysfunctional and contribute to HS inflammation rather than effectively constraining effector T cell function (Kim *et al.,* 2023). An enrichment of CD8 T cells described in HS lesions, coupled with elevated frequencies of IFN-γ^+ CD8 T cells seen in HS lesions relative to healthy controls and psoriatic lesions, suggests that CD8 T cells may also be dysregulated in HS and contribute to the complex inflammatory milieu in HS lesions (Lowe *et al.*, 2020). Furthermore, IFN-γ expression has been shown to be elevated in HS lesions relative to healthy control skin (Hotz *et al.,* 2016).

Much of these studies have utilised low-parameter flow cytometry, immunohistochemistry and mRNA analysis. A detailed investigation into the transcriptomic landscape of HS T cells isolated directly from HS lesions has thus far been lacking. In-depth scRNA-seq analysis of HS T cells would provide novel insight into T cell mediated inflammation in HS lesions. The previous chapter outlined the dysregulated transcriptomic landscape of keratinocytes and fibroblasts in HS lesions. This, coupled with other studies highlighting keratinocyte and fibroblast dysfunction in response to inflammatory cytokines suggests that interactions with immune cells may drive dysregulation and dysfunction in HS fibroblasts and keratinocytes (Witte-Handel *et al.*, 2019; Hotz *et al.*, 2016).

Characterisation of immune and non-immune cell interactions by scRNA-seq has previously been reported in HS (Gudjonsson *et al.,* 2020). Gudjonsson *et al.,* detailed the top ranked receptor:ligand interactions between immune and stromal cells in HS lesions and focused particularly on specific interactions between keratinocytes and inflammatory cytokines (Gudjonsson *et al.,* 2020). This chapter elaborates on these findings with the inclusion of healthy controls, allowing the identification of particular cellular interactions which drive HS keratinocytes and fibroblasts into an inflammatory state. Detailing the interactions between T cells, keratinocytes and fibroblasts in HS lesions should add value to the field and direct potential new therapeutic avenues.

5.2 Aims

The aim of the experiments in this chapter was to examine the interactions between T cells, keratinocytes and fibroblasts and how these interactions contribute to HS inflammation.

Specifically, this chapter sought to:

- Examine the transcriptional profile of HS lesional T cells.
    - Using scRNA-seq, identify T cell populations in HS lesions and determine inflammatory pathways driving T cell mediated inflammation in HS.

- Characterise the T cell interactions which drive keratinocytes and fibroblasts into inflammatory states.
    - Using *in silico* and *in vitro* techniques, identify T cell inflammatory mediators which regulate gene expression in HS keratinocytes and fibroblasts.

5.3 Results

5.3.1 Clinical details

Clinical details for HS patients and healthy controls used for the scRNA-seq analysis in this study can be found in **Section 2.2.18**. Clinical details for the healthy control group are shown in **Table 5.1**, the HS patient group in **Table 5.2** for the *in vitro* analysis in this study. HS patients were recruited during surgical consultations at St Michael's Hospital, Dublin. All HS samples were small surgical excisions. All HS patients included for the *in vitro* analysis donated skin from dermal tracts. Healthy control samples were skin tissue donated from patients undergoing abdominoplasty surgery at the Plastic and Reconstructive Surgery clinic at St Vincent's Private Hospital, Dublin.

The mean age of healthy controls was 45.3 y ± SD of 10 (n=19) and 38 y ± SD of 9 (n=7) for HS patients. There were 100% females in the healthy control group and 86% females in the HS patient group. 40% of HS patients were classified with Hurley stage 3 disease, 20% had Hurley stage 2 disease and 40% had Hurley stage 1 disease. HS patients had a mean BMI of 37.6 kg/m^2 ± SD of 10 in the HS patient group, unfortunately the BMI could not be calculated for the healthy control group who underwent abdominoplasty surgery. Smoking status could not be obtained from the healthy control group, however 60% of the HS group were smokers. One HS patient was receiving guselkumab, the IL-23 inhibitor, one HS patient was on the antibiotic doxycycline and one HS patient was receiving infliximab (TNF inhibitor) and the antibiotics clindamycin and rifampicin.

Table 5.1 Clinical details for healthy control group. Clinical details of HS patients at the time of sampling, including age and sex, F: female, n/a: data not available

Patient ID	Age (y)	Sex	Analysis
UCD05	n/a	n/a	Fibroblast, T cell
UCD06	43	F	Fibroblast, T cell
UCD10	46	F	Fibroblast
UCD13	63	F	T cell
UCD14	47	F	T cell
UCD15	48	F	T cell
UCD16	47	F	T cell
UCD17	n/a	F	T cell
UCD18	41	F	Fibroblast, T cell
UCD19	n/a	F	T cell
UCD20	n/a	F	Fibroblast, T cell
UCD21	44	F	T cell
UCD22	n/a	F	T cell
UCD23	46	F	T cell
UCD24	43	F	T cell
UCD25	38	F	T cell
UCD26	58	F	Keratinocyte, Fibroblast, T cell
UCD27	45	F	T cell
UCD28	52	F	Keratinocyte, Fibroblast, T cell
UCD30	17	F	Fibroblast
	Mean 45.3 SD 10	100% F	

Table 5.2 Clinical details for HS patient group. Clinical details of HS patients at the time of sampling, including age, sex, Hurley stage, body mass index (BMI), smoking status and medication HS patients were on at the time of sampling. E-S: ex-smoker, F: female, M: male, Nrm: no relevant medications, N-S: non-smoker, S: smoker, n/a: data not available.

Patient ID	Age (y)	Sex	Hurley	BMI	Smoker	Medication	Analysis
HS MI29	33	F	2	41.5	N-S	Infliximab, Clindamycin, Rifampicin	T cell
HS MI30	38	F	1	36.6	n/a	Nrm	T cell
HS MI31	27	F	3	56.5	N-S	Nrm	T cell
HS MI32	30	F	n/a	27	S	Nrm	T cell
HS MI33	51	M	3	27	S	Doxycycline	T cell
HSMI34	49	F	1	37.2	S	Nrm	T cell
HS MI37	46	F	n/a	n/a	n/a	Guselkumab	T cell
	Mean 38 SD 9.12	86% F, 14% M	40% 1 20% 2 40% 3	Mean 37.6 SD 10	60% S 40% N-S		

5.3.2 Th17 cells are enriched in HS lesions

The previous chapter outlined inflammatory dysregulation as a key feature of HS keratinocytes and fibroblasts. A number of immune cell-mediated signaling pathways, and T cell mediated pathways in particular, were found to be dysregulated in both keratinocytes and fibroblasts in HS lesions. Many studies, including from our lab, have detailed the presence and frequency of immune cells in HS lesions (Moran *et al.*, 2017; Hotz *et al.*, 2016), however further characterisation of the communication between immune and non-immune cells is warranted. To understand how T cells may drive keratinocytes and fibroblasts into inflammatory phenotypes, first detailed scRNA-seq characterisation of T cells in HS skin was performed. For this analysis, skin biopsies were processed by Dr Barry Moran in TCD using enzymatic and mechanical digestion as described (**Section 2.2.19**). Cryopreserved tissue samples were subsequently shipped to AbbVie, Massachusetts, where single, viable $CD45^+$ and $CD45^-$ cells were purified, barcoded and sequenced (**Section 2.2.19**).

To characterise T cells from HS lesional and healthy control skin, raw sequencing data was processed and analysed using Cell Ranger and Seurat (Zheng *et al.,* 2017; Stuart *et al.,* 2019). Following the removal of B cells, plasma cells, mast cells and myeloid cells in the scRNA-seq data (**Figure 8.1**), 14 T cell clusters were identified in 6 HS lesional and 3 healthy control skin samples (**Figure 5.1**). To identify specific T cell clusters enriched in HS lesions relative to healthy controls, UMAPs displaying only HS and only healthy control T cells were generated (**Figure 5.2**). Clusters of Th17 cells and Treg cells, in particular, appeared to be enriched in HS lesions. To confirm this, the frequency of T cell clusters relative to all lymphocytes analysed was calculated (**Figure 5.3**). A small cluster of B cell contaminants were identified despite the removal of B cell and plasma cells from this analysis.

To aid in the identification and annotation of the T cell clusters, specific cluster markers were identified by Wilcoxon Rank Sum test. The top 5 cluster markers for each cluster were displayed by dot plot (**Figure 5.4**). Th17 clusters had distinct expression of *KLRB1* (CD161), *IL17A*, *IL17F* and *CCL20*. Interestingly, Th17 cells were identified in two cell clusters, with the Th17 (2) cluster having increased expression of *IL17A* and *IL17F*, while the Th17 (1) cluster had elevated *KLRB1* expression (**Figure 5.5A-D**). Further, the Th17 (2) cluster had high expression of *TNF*, emphasising the potential importance of these cells in HS

pathogenesis (**Figure 5.5E**). *TNF* was most highly expressed by the CD4 T cells (1) cluster which also had *CD69*, *JUN* and *FOS* within the top 5 cluster markers suggesting that this cluster may contain activated CD4 T cells (**Figure 5.4**). As *CD69* is a marker of TRM cells, the expression of TRM and central memory markers were displayed on the T cell UMAP (**Figure 5.6**). While *CD69* was elevated in the CD4 T cells (1) cluster, expression was detected in every T cell cluster (**Figure 5.6A**). CD103 is also typically used to identify resident memory T cells, however expression was not concentrated in any particular cell cluster (**Figure 5.6B**). Many of the cell clusters also lacked the expression of CCR7, absence of which can be used to identify effector memory T cells (Sallusto *et al.,* 1999). The $CCR7^{+}$ CD4 T cell cluster had distinctly elevated expression of *CCR7* and *SELL*, suggesting this cluster may contain central memory T cells (Watanabe *et al.,* 2015) (**Figure 5.6C**).

While the classical Treg cell markers, including *FOXP3*, *CD25*, *ICOS* and *CTLA4* weren't identified within the top 5 cluster-specific markers, Treg cells distinctly expressed these markers when displayed by UMAP (**Figure 5.7A-D**). A cluster, termed $CD52^{+}$ CD4 T cells due to elevated expression of *CD52* (**Figure 5.7E**) had high expression of *IL32*, similar to levels found in Treg cells which had the highest expression of *IL32* indicating potential functional similarities between these clusters (**Figure 5.4**).

CD8 T cells had high expression of *CD8A* and could be identified within two cell clusters (**Figure 5.8A**). The cytotoxic CD8 T cell cluster had increased expression of granzymes (*GZMA*, *GZMK*) and elevated expression of *IFNG* in comparison to the CD8 T cells cluster (**Figure 5.8B-C**). This second CD8 T cell cluster had elevated expression of the chemokine *XCL1* relative to cytotoxic CD8 T cells (**Figure 5.8D**) but lower expression relative to NK cells, which also had distinct expression of *CTSW* (Cathepsin W), *GNLY* (Granulysin) and *XCL2* (**Figure 5.4**).

In summary, this section revealed 14 distinct T cell clusters with HS lesional and healthy control skin. Clusters of CD4 T cells, Th17, Treg cells, CD8 T cells, cytotoxic CD8 T cells and NK cells were identified, each of which had a unique transcriptomic profile.

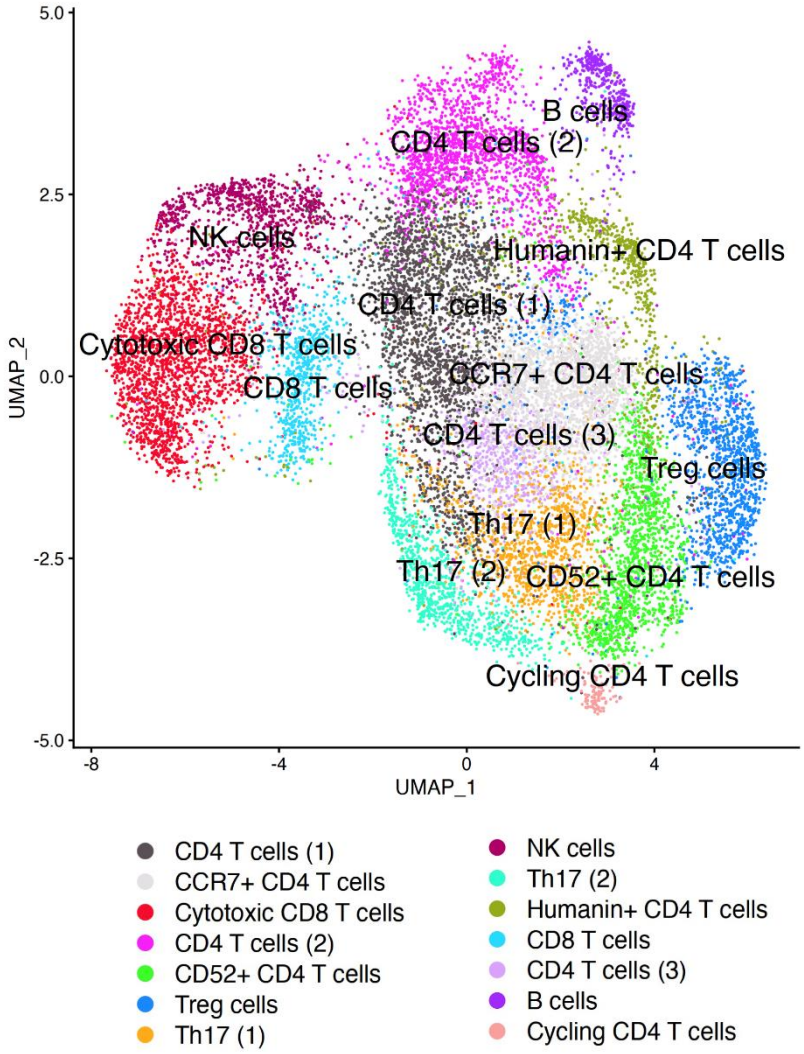

Figure 5.1 14 distinct T cell clusters identified within HS patient lesions and healthy control skin. Cells isolated from healthy control skin (Con, n=3) or HS lesional skin (HS, n=6) were purified based on CD45 expression, barcoded and their gene expression determined by 10X Genomics scRNA-seq. Myeloid cells, NK cells, B cells, plasma cells and mast cells were identified and removed from further analysis. T cells were identified and subclustered into 14 unique clusters generated by unsupervised classification.

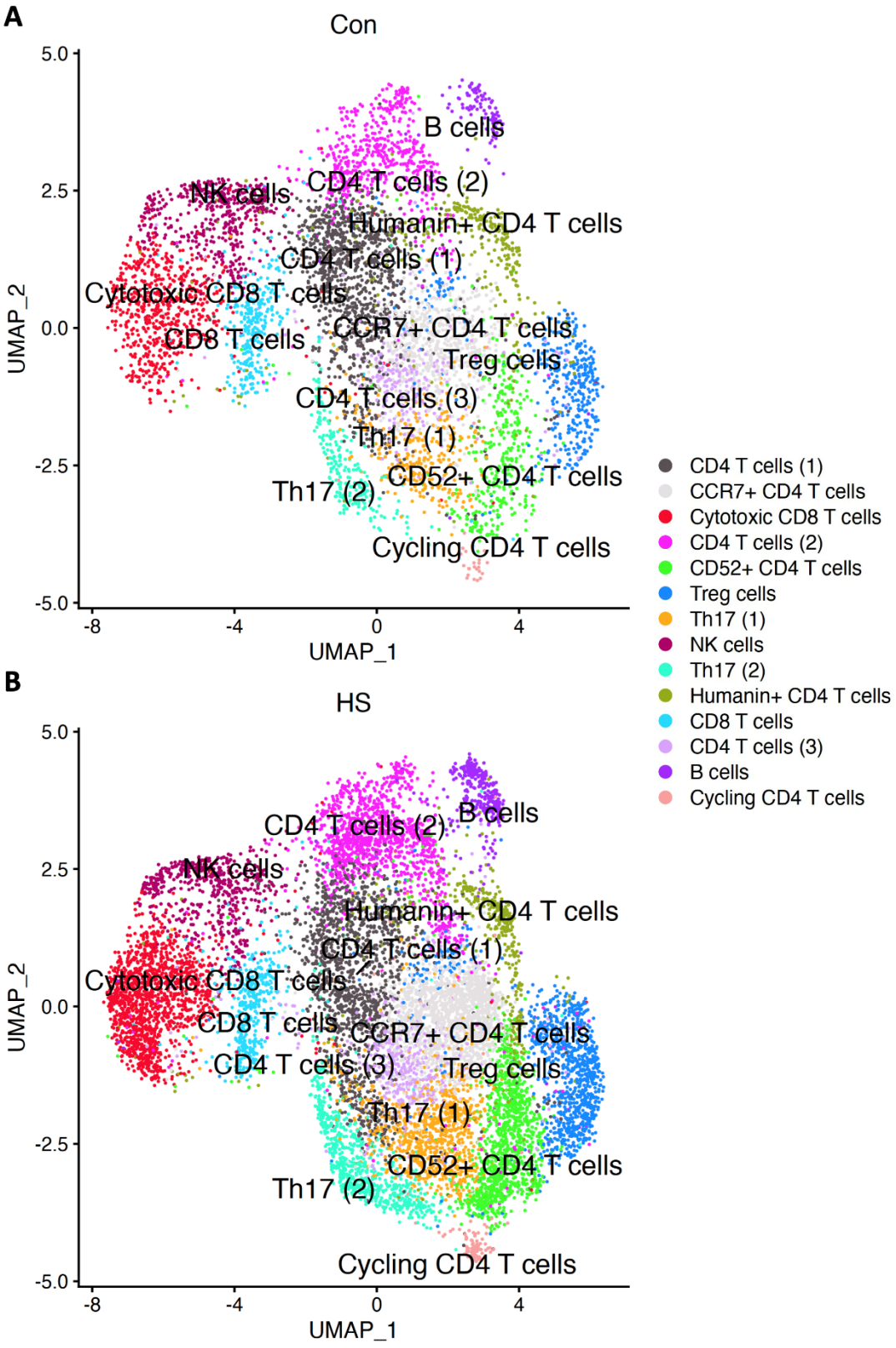

Figure 5.2 UMAP visualising T cell populations identified in healthy control and HS lesional skin. Cells isolated from healthy control skin (Con, n=3) or HS lesional skin (HS, n=6) were purified based on CD45 expression, barcoded and their gene expression determined by 10X Genomics scRNA-seq. UMAP displays T cells isolated from healthy control skin (Con; A) and HS lesional skin (HS; B) following unsupervised classification of T cells.

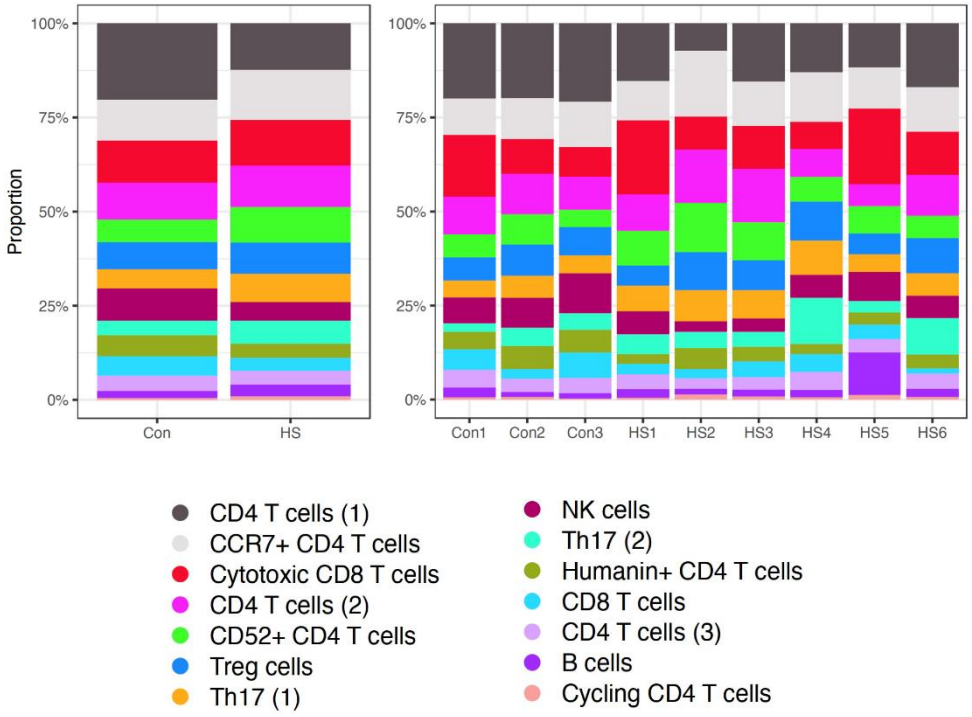

Figure 5.3 Frequency of T cell clusters in HS lesional skin compared with healthy control skin. Cells isolated from healthy control skin (Con, n=3) or HS lesional skin (HS, n=6) were purified based on CD45 expression, barcoded and their gene expression determined by 10X Genomics scRNA-seq. Bar chart showing the proportion of each cell cluster relative to total T cells in the $CD45^{+}$ dataset.

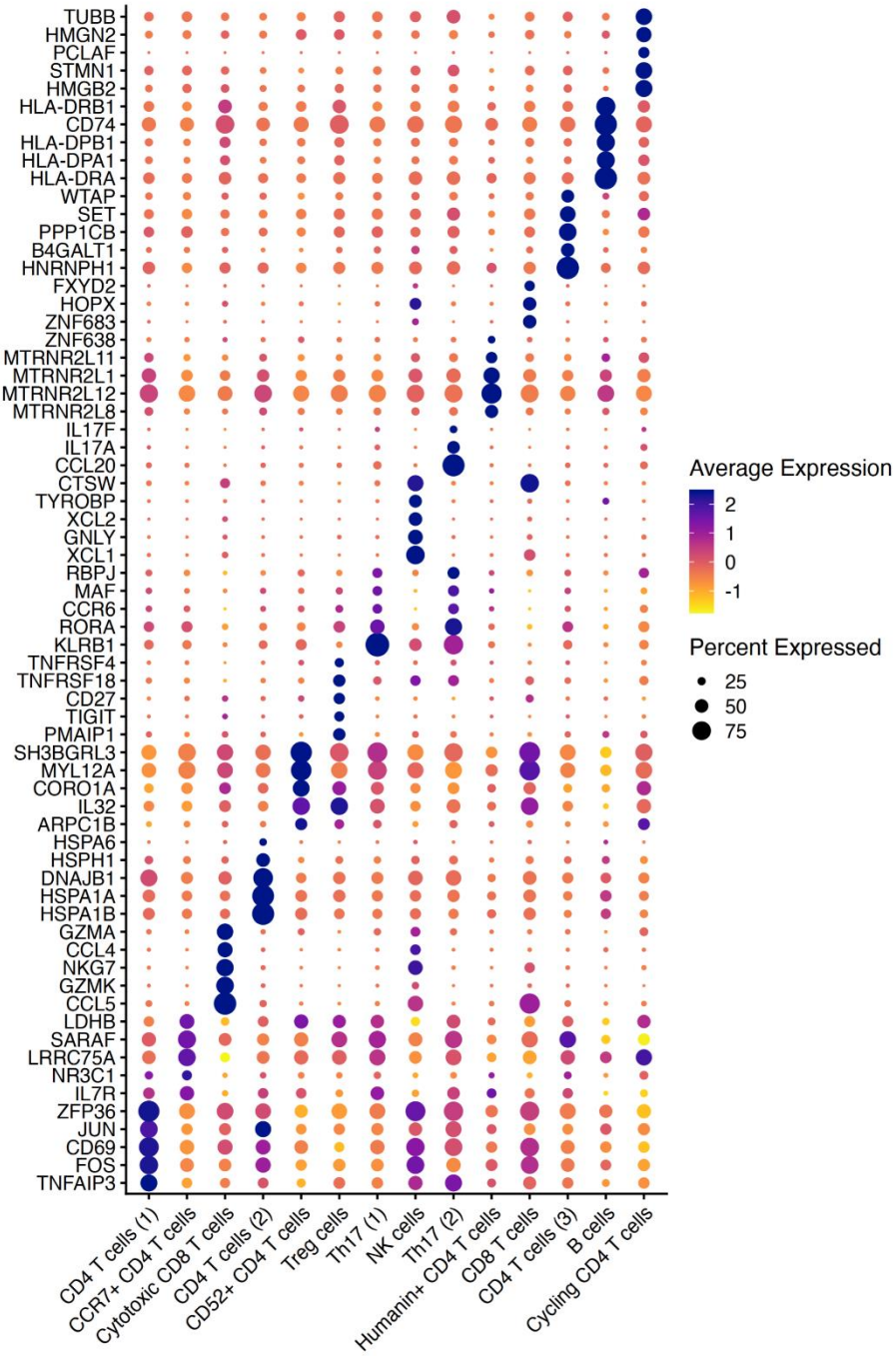

Figure 5.4 Dotplot displaying cluster-specific markers. Cells isolated from healthy control skin (Con, n=3) or HS lesional skin (HS, n=6) were purified based on CD45 expression, barcoded and their gene expression determined by 10X Genomics scRNA-seq. Dot plot displays cluster-specific genes identified by Wilcoxon Rank Sum test.

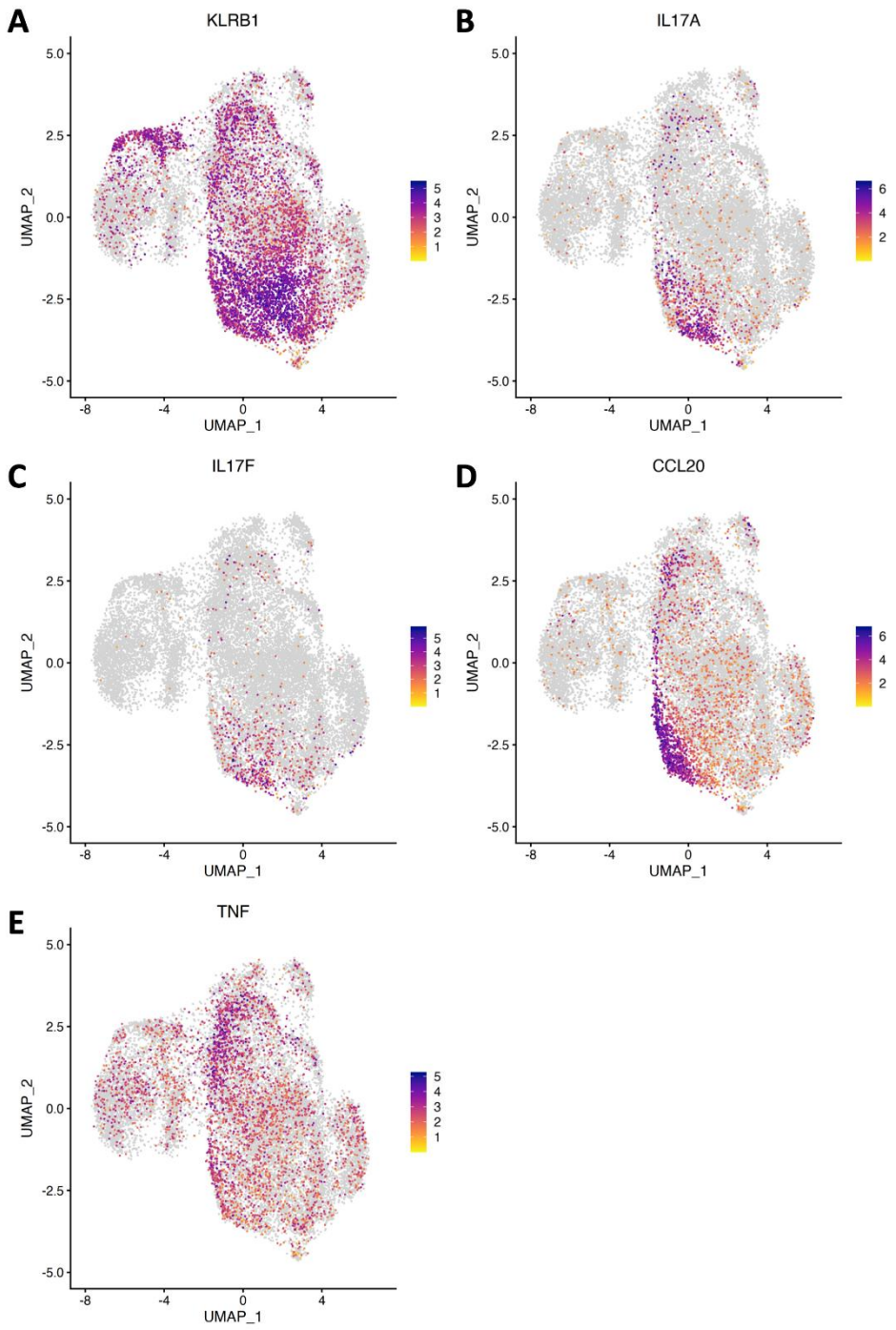

Figure 5.5 Expression of Th17 markers in HS and healthy control T cells. Cells isolated from healthy control skin (Con, n=3) or HS lesional skin (HS, n=6) were purified based on CD45 expression, barcoded and their gene expression determined by 10X Genomics scRNA-seq. UMAP displays Th17 cell markers including *KLRB1* (CD161; A), *IL17A* (B), *IL17F* (C), *CCL20* (D) and TNF (E) in HS and healthy T cells following unsupervised classification.

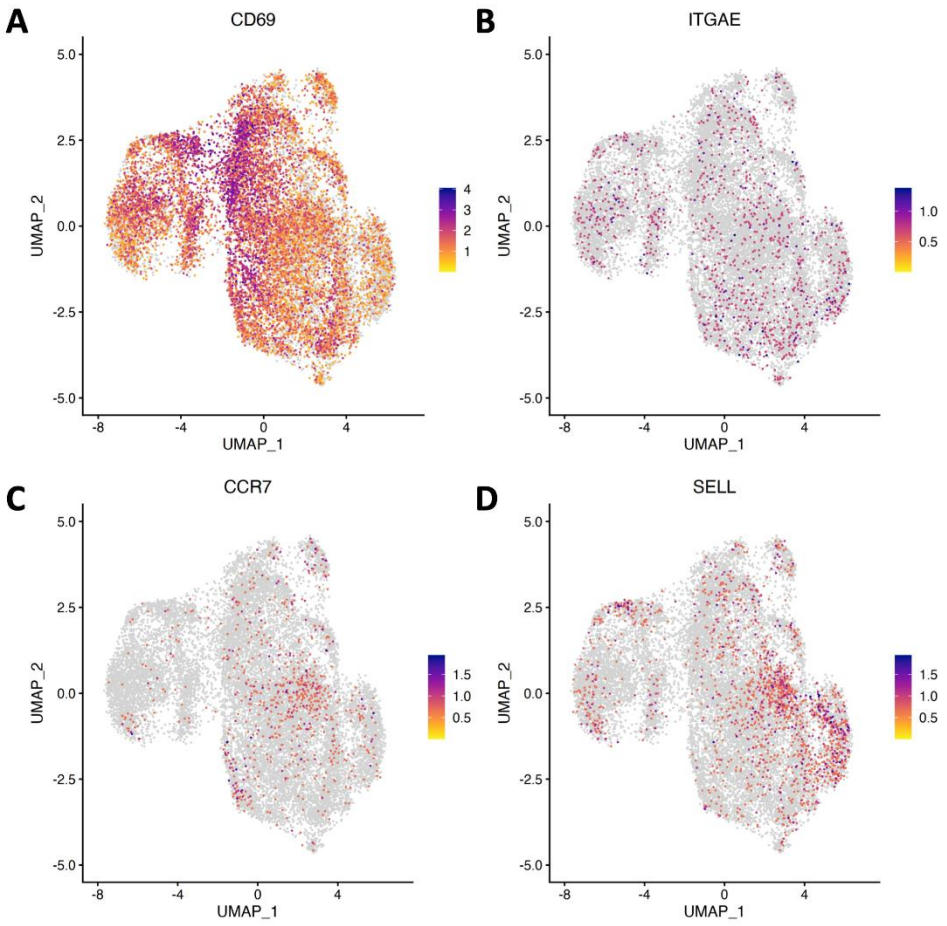

Figure 5.6 Expression of resident and central memory markers in HS and healthy control T cells. Cells isolated from healthy control skin (Con, n=3) or HS lesional skin (HS, n=6) were purified based on CD45 expression, barcoded and their gene expression determined by 10X Genomics scRNA-seq. UMAP displays resident and central memory T cell markers including *CD69* (A), *ITGAE* (CD103; B) *CCR7* (C) and *SELL* (D) in HS and healthy T cells following unsupervised classification.

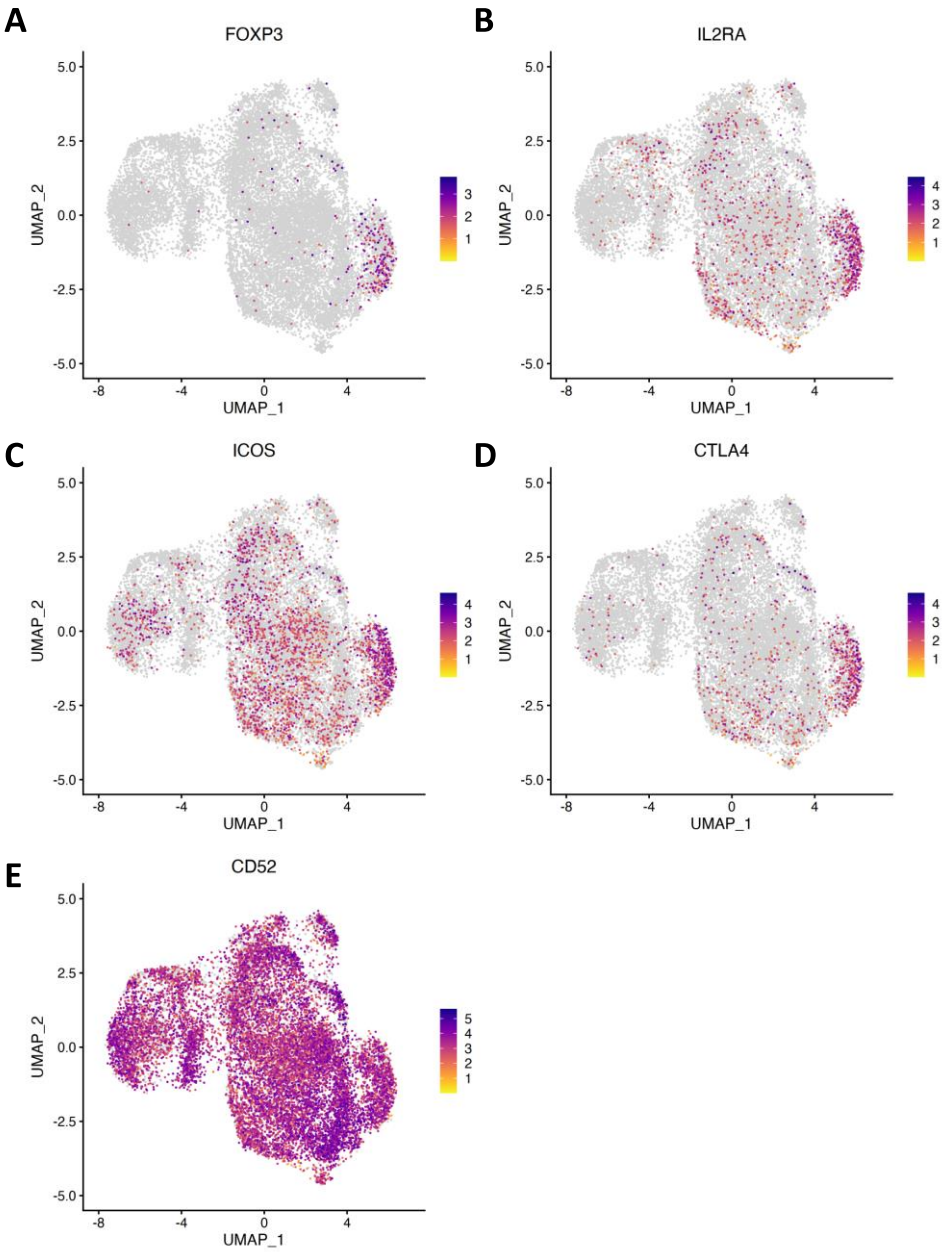

Figure 5.7 Expression of Treg cell markers in HS and healthy control T cells. Cells isolated from healthy control skin (Con, n=3) or HS lesional skin (HS, n=6) were purified based on CD45 expression, barcoded and their gene expression determined by 10X Genomics scRNA-seq. UMAP displays Treg cell markers including *FOXP3* (A), *IL2RA* (CD25; B), and *ICOS* (C), *CTLA4* (D), *CD52* (E) in HS and healthy T cells following unsupervised classification.

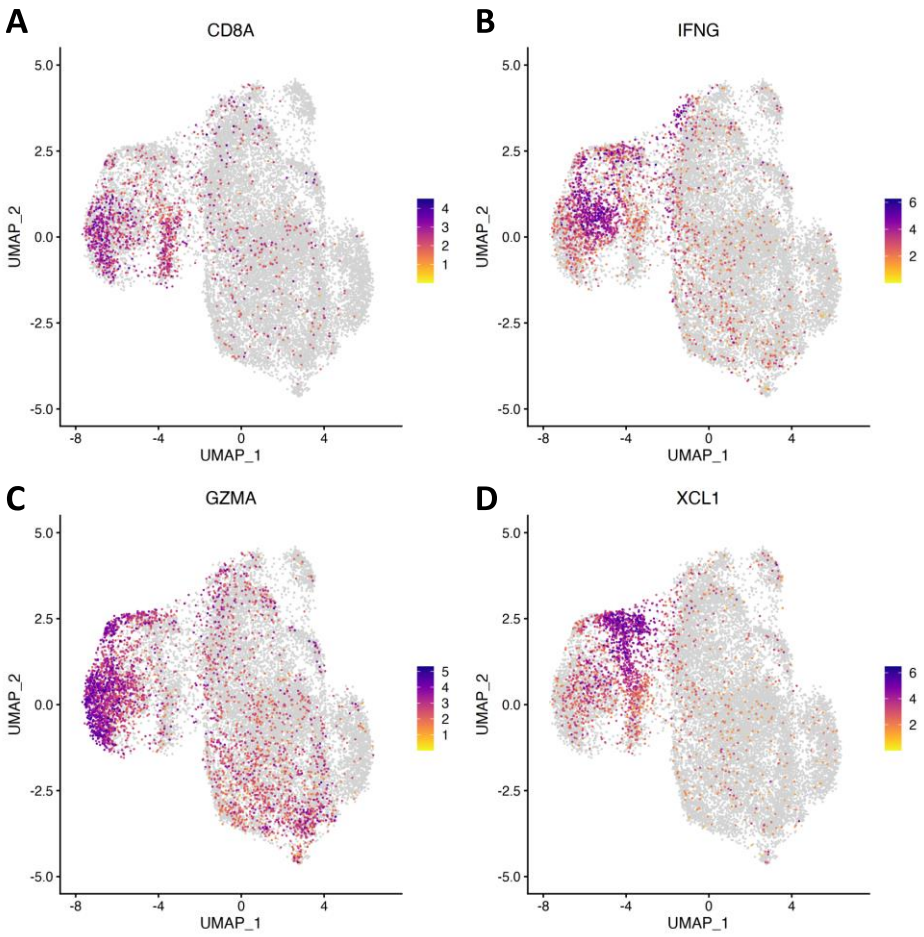

Figure 5.8 Expression of CD8 T cell markers in HS and healthy control T cells. Cells isolated from healthy control skin (Con, n=3) or HS lesional skin (HS, n=6) were purified based on CD45 expression, barcoded and their gene expression determined by 10X Genomics scRNA-seq. UMAP displays CD8 T cell markers including *CD8A* (A), *IFNG* (B), and *GZMA* (C) and *XCL1* (D) in HS and healthy T cells following unsupervised classification.

5.3.3 Dysregulated cytokine signaling in HS T cells

The previous section outlined the presence of T cell subsets in HS lesional and healthy control skin. This section further investigates the role of T cells in promoting HS inflammation by evaluating the transcriptomic differences between T cells found in HS lesions from those in healthy control skin.

A volcano plot illustrates the 3,044 DEGs identified between T cells from HS patients and those from healthy controls following Wilcoxon Rank Sum test (**Figure 5.9A, Table 8.39Table 8.40**). Of the genes significantly elevated in HS lesions, a number of Th17 cell-associated genes were among the most differentially expressed, including *KLRB1*, *CCL20* and the inflammatory cytokines, *IL17A* and *IL17F* (**Figure 5.9B**). HS T cells had elevated expression of *GZMK*, indicating an important role of cytotoxic CD8 T cells in HS inflammation, while *ICOS*, an activation marker and expressed predominantly by Treg cells was also significantly elevated in HS T cells (**Figure 5.9A**). Genes significantly downregulated in HS T cells included *DUSP1*, *DUSP2, PRDM1*, and *TOB1*, all of which have previously been shown to suppress T cell activation and function (Zhang *et al.*, 2009; Dan Lu *et al.*, 2020; Guo *et al.*, 2022; Baranzini, 2014) (**Figure 5.9A**). To understand the overall impact the DEGs have in driving HS inflammation, pathway analysis was performed on the 3,044 DEGs between T cells in HS lesions and healthy control skin. The top 10 immune related pathways enriched from the DEGs were displayed by dotplot (**Figure 5.9B**). TNF and TGF-β signaling pathways were among the top 10 immune pathways enriched, as was Th17 differentiation, implicating Th17 cells as an important contributor to T cell-mediated inflammation in HS lesions (**Figure 5.9B**).

Considering that TNF, TGF-β and Th17 cell pathways were significantly enriched among the DEGs between HS and healthy control T cells, and due to the previously reported role of IFN-γ in HS inflammation, the expression of each of these cytokines was evaluated in each T cell cluster (**Figure 5.10**). Interestingly, *TGFB1* was expressed by all T cell clusters, in contrast to *IL17A* and *IL17F* which was predominantly expressed by the Th17 (2) cluster but also expressed, albeit less so, by the Th17 (1) and the CD4 T cells (1) clusters (**Figure 5.10A-F**). Although *TNF* expression could be seen in each T cell cluster; it was most highly expressed by the CD4 T cells (1) cluster (**Figure 5.10G-H**). Cytotoxic CD8 T cells and NK cells were the main source of *IFNG* in HS lesions and healthy control skin (**Figure 5.10I-J**).

IL17A and *IL17F* were identified among the top ranked DEGs between HS and healthy control T cells (**Figure 5.9A**). Interestingly, when the expression of both *IL17A* and *IL17F* was displayed across healthy control, HS-lo and HS-hi patients, a dramatic increase in expression was found in HS-hi patients (**Figure 5.11A-B**). Similarly, HS-hi patients had elevated expression of *TNF*, *IFNG* and *TGFB1* relative to healthy controls and HS-lo patients (**Figure 5.11C-E**).

IL-23A, IL-1β, IL-6 and TGF-β play an important role in the differentiation and development of Th17 cells (Lalor *et al.*, 2011; Wilson *et al.*, 2007; Acosta-Rodriguez *et al.*, 2007; Yang *et al.*, 2008). Considering this, as well as the important role of Th17 cells in HS, the expression of cytokine receptors was evaluated in HS T cells (**Figure 5.12A-D**). Expression of *IL1R1*, *IL23R*, *TGFBR1* and *IL6R* was relatively low in this T cell dataset (data not shown), however, the limited expression of *IL1R1* and *IL23R* was most highly concentrated in Th17 cells, suggesting an important role of IL-1β and IL-23 in the development of Th17 cells in HS lesions (**Figure 5.12A-B**). Contrastingly, the expression of *TGFBR1* and *IL6R* could not be localised to a single T cell cluster, with scattered expression seen across all T cell clusters (**Figure 5.12C-D**).

Taken together, these data suggest that dysregulated cytokine signaling is a key feature of HS lesional T cells. IL-1β and IL-23A may play a pivotal role in the development of Th17 cells in HS lesions which subsequently promote IL-17 and TNF signaling, driving HS inflammation.

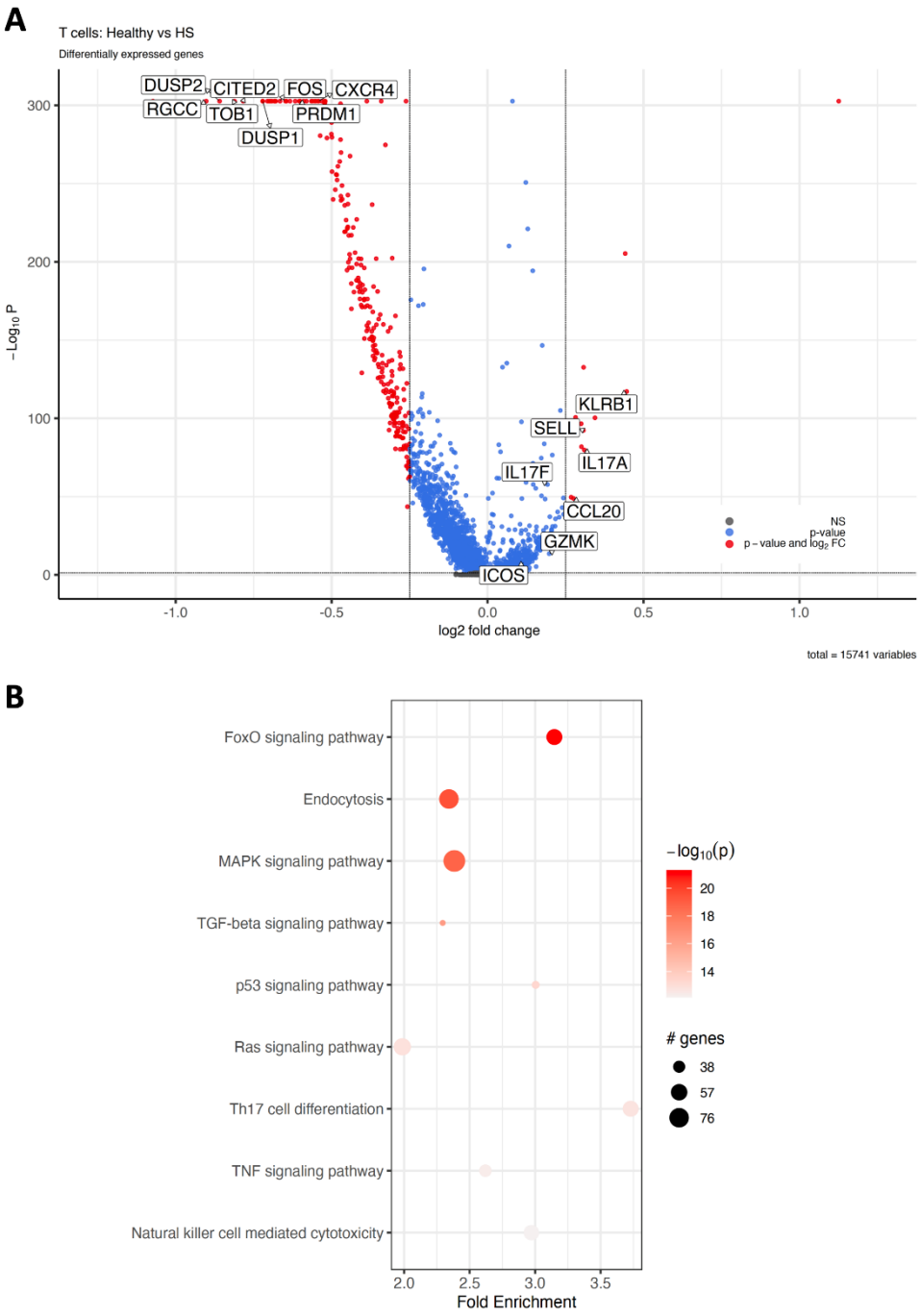

Figure 5.9 HS lesional T cells have dysregulated inflammatory cytokine signaling. Cells isolated from healthy control skin (Con, n=3) or HS lesional skin (HS, n=6) were purified based on CD45 expression, barcoded and their gene expression determined by 10X Genomics scRNA-seq. The volcano plot displays DEGs in HS compared with healthy control T cells. Genes with a $log_2FC > 0$ are upregulated in HS T cells and a $log_2FC < 0$ are downregulated in HS T cells. The $-Log_{10}$ P Y-axis is a measure of significance (A). Top 10 immune pathways enriched from the genes significantly differentially expressed between HS and healthy control T cells (B).

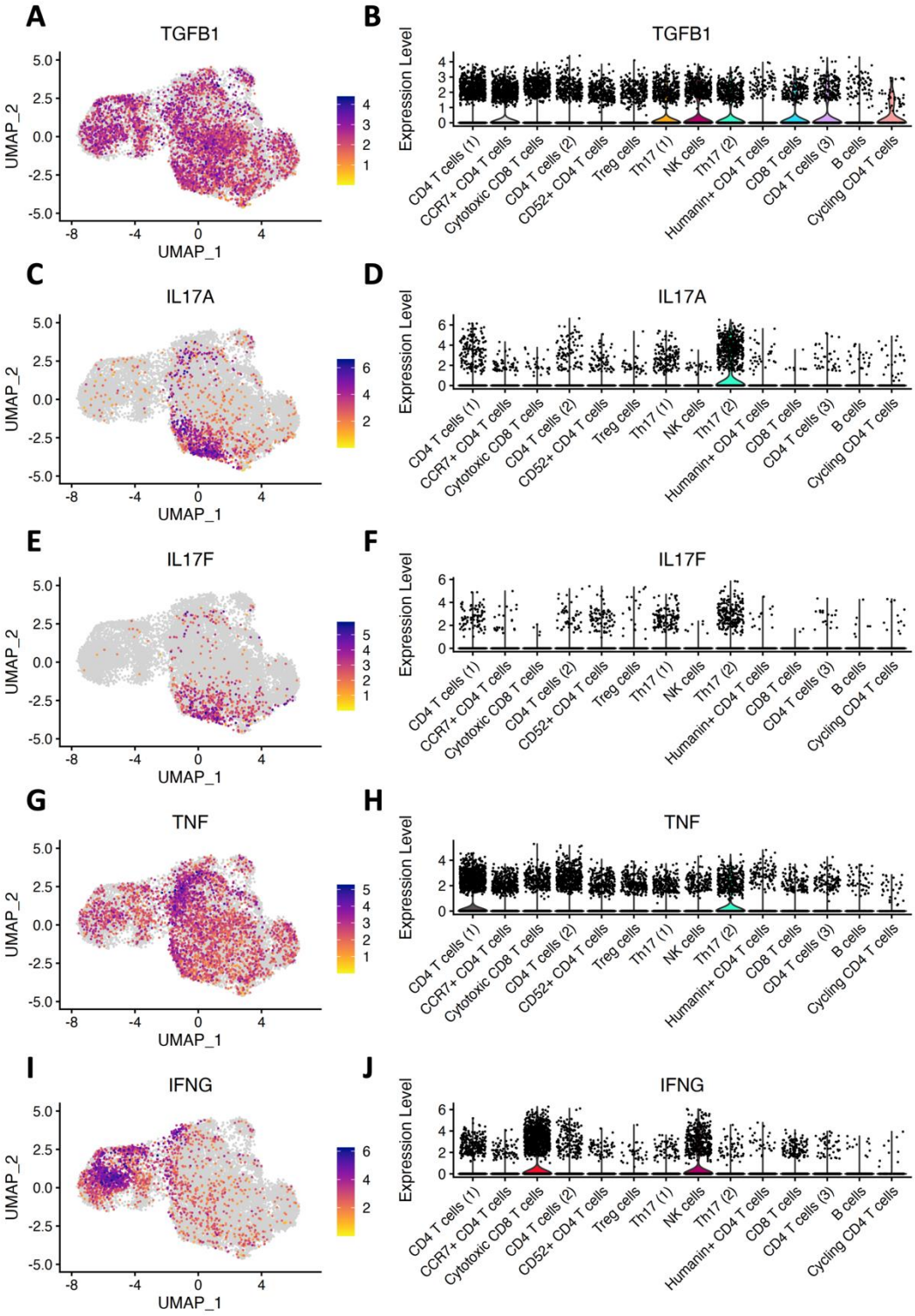

Figure 5.10 Expression of inflammatory cytokines in HS and healthy control T cells. Cells isolated from healthy control skin (Con, n=3) or HS lesional skin (HS, n=6) were purified based on CD45 expression, barcoded and their gene expression determined by 10X Genomics scRNA-seq. Expression of *TGFB1* (A, B), *IL17A* (C, D), *IL17F* (E, F) and *TNF* (G, H), *IFNG* (I, J) was displayed on the T cell UMAP and by violin plot displaying expression in each cell cluster.

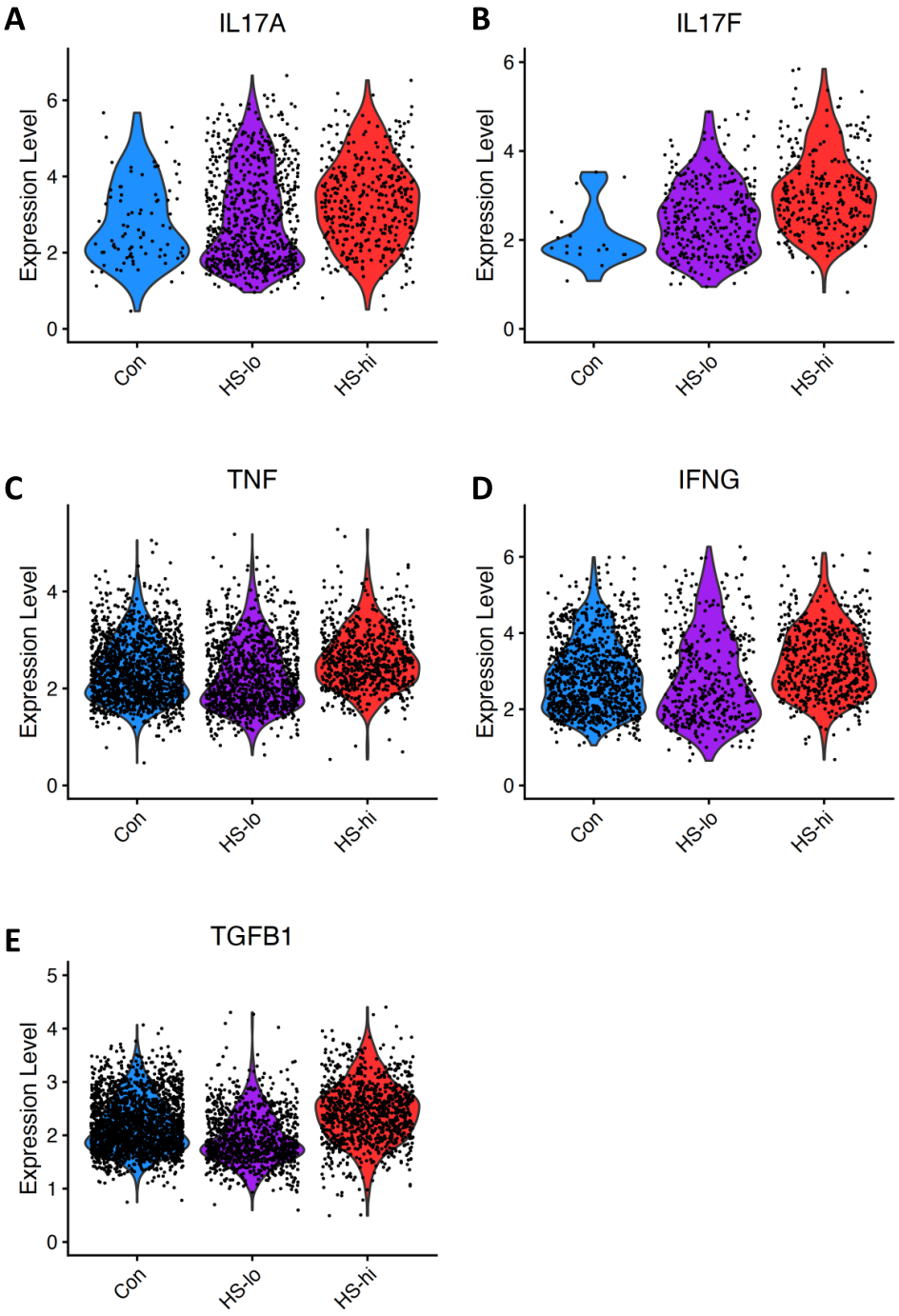

Figure 5.11 Inflammatory cytokines were elevated in in HS-hi T cells. Cells isolated from healthy control skin (Con, n=3) or HS lesional skin (HS, n=6) were purified based on CD45 expression, barcoded and their gene expression determined by 10X Genomics scRNA-seq. Violin plot displays the expression of *IL17A* (A), *IL17F* (B), *TNF* (C), *IFNG* (D), *TGFB1* (E), where present, in healthy controls, HS-lo and HS-hi T cells.

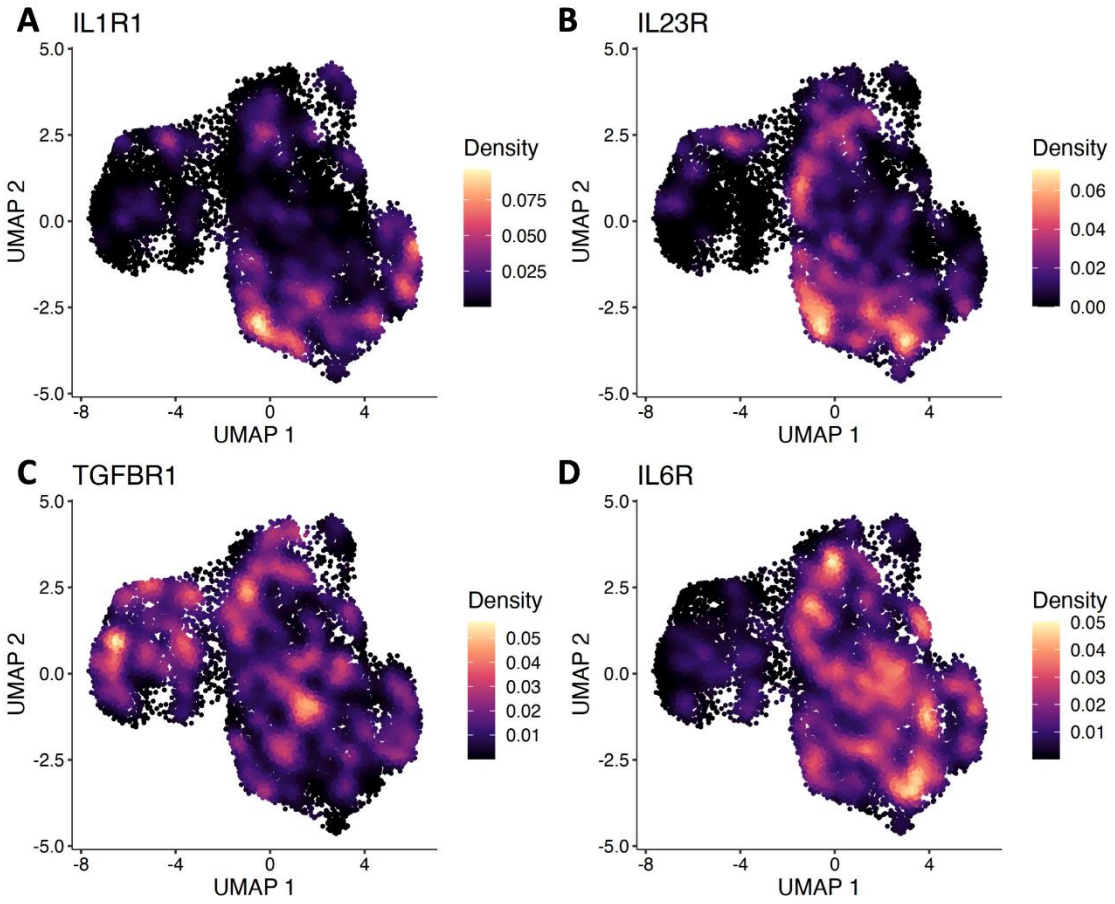

Figure 5.12 Expression of IL-1 and IL-23 receptors were concentrated on Th17 cells. Cells isolated from healthy control skin (Con, n=3) or HS lesional skin (HS, n=6) were purified based on CD45 expression, barcoded and their gene expression determined by 10X Genomics scRNA-seq. Density plots display where expression of *IL1R1* (A), *IL23R* (B), *TGFBR1* (C) and *IL6R* (D) was concentrated on the T cell UMAP.

5.3.4 TNF inhibition dampened T cell cytokine signaling in HS skin

Dysregulated TNF signaling is a key feature of HS inflammation, and this was supported in the previous section which detailed elevated *TNF* expression in HS patients with a higher inflammatory load. Dysregulated TNF and IL-17 signaling was prominent in HS T cells and in considering this, the effect of TNF inhibition on HS T cells was evaluated.

HS patients treated with TNF inhibitors had reduced frequency of both the Th17 (2) and CD4 T cells (1) clusters compared with untreated HS patients (**Figure 5.13**). HS patients treated with anti-TNF therapies also had an increased frequency of the $CD52^+$ CD4 T cells and $CCR7^+$ CD4 T cells clusters, suggesting TNF inhibition changes the T cell landscape of HS lesions (**Figure 5.13**).

HS patients treated with TNF blockade had dramatically reduced expression of a number of inflammatory mediators in HS T cells including, *TNF*, *IL17A*, *IFNG* and *CXCL8*, indicating a significant reduction in inflammatory cytokine output from T cells following TNF inhibition (**Figure 5.14**, **Table 8.42**). HS T cells also appear to have reduced activation following TNF inhibition with reduced expression of *CD69*, *FOS* and *JUNB* (**Figure 5.14**). TNF inhibition reduced the expression of *ICOS* which was distinctly expressed by Treg cells, supporting **Figure 5.13** which detailed a reduced frequency of Treg cells following TNF inhibition (**Figure 5.14**, **Figure 5.7C**). Blocking TNF may also impact the metabolic profiles of HS T cells with a significant increase in GLUT3 (*SLC2A3*) expression in untreated HS patients (**Figure 5.14**). On the other hand, HS T cells treated with anti-TNF therapies had elevated expression of the naïve/central memory T cell markers *CD27* and *SELL*, as well as an increase in *CD52* expression (**Figure 5.14**, **Table 8.41**), corresponding to the enrichment of $CD52^+$ CD4 T cells and $CCR7^+$ CD4 T cells in anti-TNF treated HS patients (**Figure 5.13**).

2,808 genes were differentially expressed between T cells from HS patients treated with anti-TNF therapies compared with HS patients not currently on biologic therapies (**Figure 5.14**). As many of the top ranked DEGs related to inflammatory cytokine signaling and T cell activation, pathway analysis was performed to identify specific inflammatory pathways impacted by TNF inhibition in HS T cells (**Figure 5.15A**). The top 10 immune pathways enriched from the DEGs included TNF, IL-17, TGF-β and chemokine and T cell receptor signaling pathways. This suggested that TNF inhibition had a greater effect than just

blocking TNF signaling, with a broad range of inflammatory processes downregulated. Reduced chemokine signaling suggested that TNF inhibition may reduce the recruitment of immune cells to the HS lesion, potentially reducing the overall inflammatory environment of HS lesions (**Figure 5.15**). TNF inhibition reduced the level of expression and the frequency of T cells expressing *TNF*, *IL17A*, *IL17F* and *TGFB1* in HS T cells, while there was no major change in the expression of *IFNG* (**Figure 5.16**).

Taken together, these data suggest that TNF inhibition can dampen the dysregulated cytokine profile of HS T cells. TNF inhibition also reduced the frequency of Th17 cells while increasing the frequency of $CCR7^+$ and $CD52^+$ CD4 T cells. Unfortunately, the small number of patients in this study prevents statistical analysis and limits the conclusions which can be made.

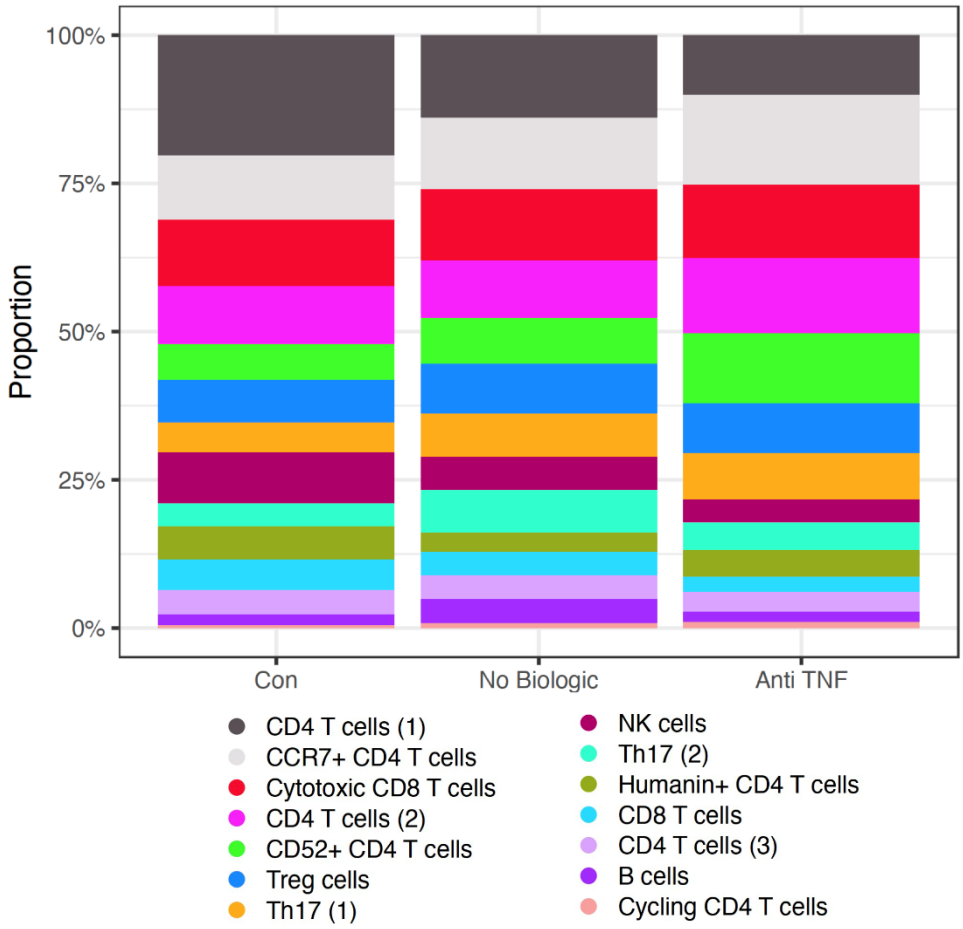

Figure 5.13 Effect of TNF inhibition on T cell frequencies in HS lesional skin Cells isolated from healthy control skin (Con, n=3) or HS lesional skin (HS, n=6) were purified based on CD45 expression, barcoded and their gene expression determined by 10X Genomics scRNA-seq. Bar chart illustrates the relative frequency of T cell clusters in healthy controls and HS lesional skin treated (n=2) with or without (n=4) TNF inhibitors.

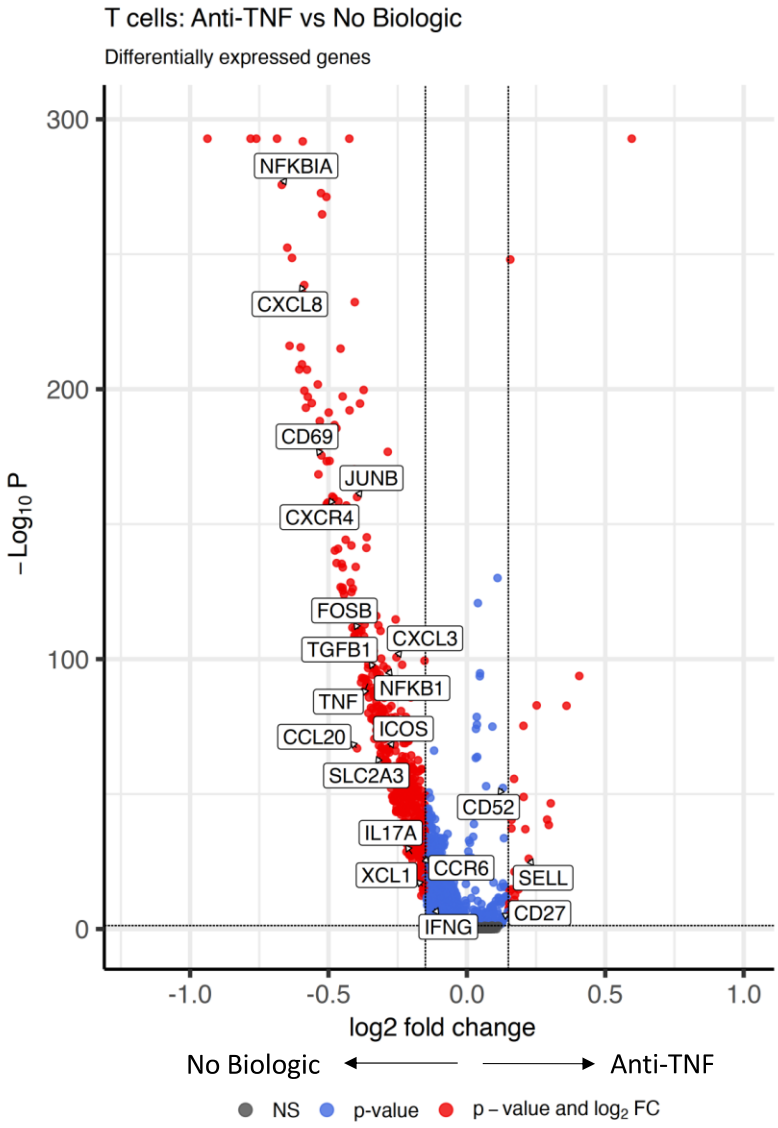

Figure 5.14 TNF inhibition reduced the expression of inflammatory mediators in HS T cells. Cells isolated from healthy control skin (Con, n=3) or HS lesional skin (HS, n=6) were purified based on CD45 expression, barcoded and their gene expression determined by 10X Genomics scRNA-seq. Volcano plot visualises DEGs in T cells from HS patients treated with (n=2) anti-TNF therapy compared with those not currently on biologic treatments (n=4). Genes with a $log_2FC > 0$ are upregulated in T cells from HS patients treated with TNF inhibitors and those with a $log_2FC < 0$ are downregulated in T cells from HS patients treated with biologic therapies. The $-Log_{10}$ P Y-axis is a measure of significance.

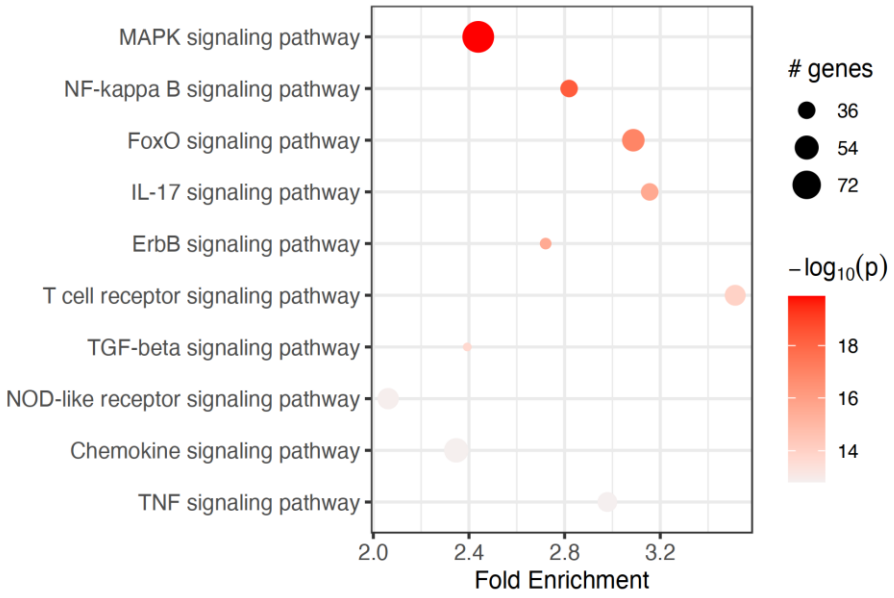

Figure 5.15 TNF inhibition reduced inflammatory cytokine signaling. Cells isolated from healthy control skin (Con, n=3) or HS lesional skin (HS, n=6) were purified based on CD45 expression, barcoded and their gene expression determined by 10X Genomics scRNA-seq. Plot displays the top 10 immune pathways enriched from the genes significantly differentially expressed in T cells derived from HS patients treated with anti-TNF therapy (n=2) compared with those not currently on biologic treatments (n=4).

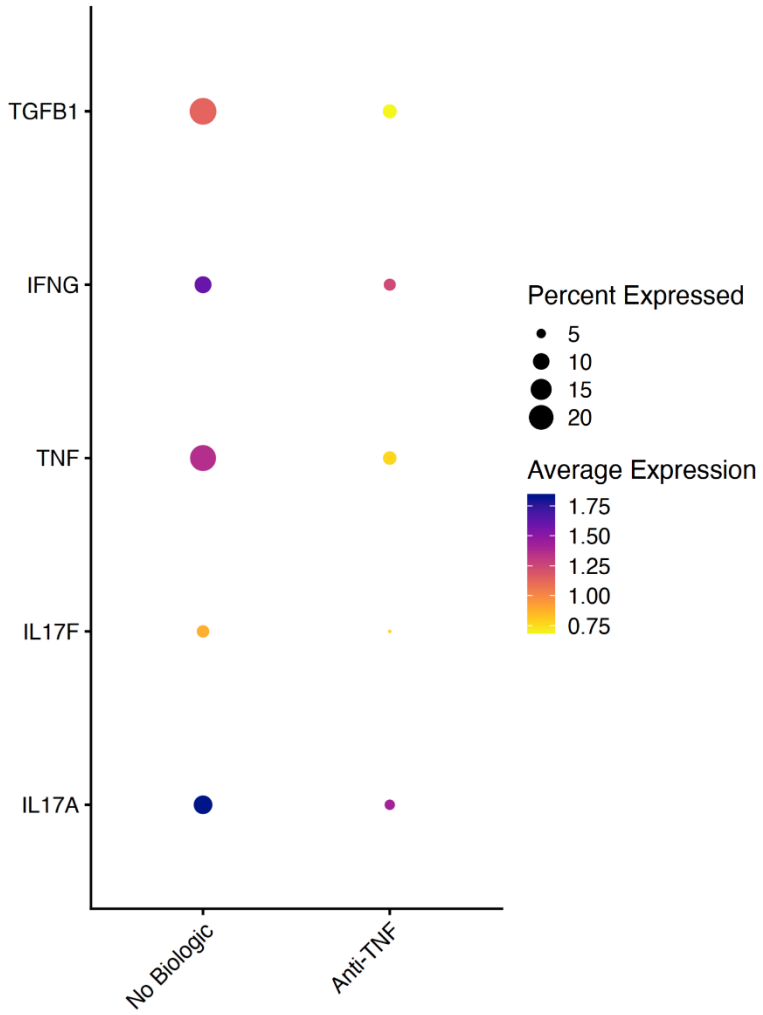

Figure 5.16 TNF inhibition reduced TNF, IL-17 and TGF-β cytokine expression in HS T cells. Cells isolated from healthy control skin (Con, n=3) or HS lesional skin (HS, n=6) were purified based on CD45 expression, barcoded and their gene expression determined by 10X Genomics scRNA-seq. Dotplot visualises the expression of *TNF*, *IL17A*, *IL17F*, *IFNG* and *TGFB1* in T cells from HS patients treated with (n=2) or without (n=4) TNF inhibitors.

5.3.5 Th17 cells predicted to drive HS keratinocytes into an inflammatory phenotype

As HS keratinocytes appeared to have dysregulated differentiation (**Figure 4.34**), it was important to determine what drives this aberrant differentiation and the development of inflammatory keratinocytes. Considering the enrichment of IL-17 signaling in HS keratinocytes, the interactions between T cells and keratinocytes were evaluated using Nichenetr (Browaeys, Saelens and Saeys, 2020). This ligand:receptor interaction analysis identified the ligands expressed by T cells most likely to interact with keratinocytes based on the expression of their corresponding receptor and the expression of genes found downstream of these receptors. *IL17A, IL17F, TNF, TGFB1* and *IFNG* were among the top ranked ligands expressed by T cells predicted to interact with HS keratinocytes (**Figure 5.17A**). *IL17A* had a relatively high Pearson correlation coefficient which indicates the ability of a ligand to predict the DEGs seen in HS keratinocytes (**Figure 5.17A**). **Figure 5.17B** displays the expression of the top ranked ligands in T cells which potentially interact with keratinocytes in HS lesions. Outlining the importance of IL-17 cytokines in HS inflammation, *IL17A* and *IL17F* were markedly increased in HS Th17 cells relative to healthy controls (**Figure 5.17C**). **Figure 5.18** displays the regulatory potential of the top ranked ligands on their downstream target genes, demonstrating the broad range of genes regulated by inflammatory cytokines in HS keratinocytes.

To visualise how T cell ligands regulate gene expression in keratinocyte clusters, a circos plot was generated (**Figure 5.19**). Using the nichenetR R package, ligands expressed by HS T cells which had corresponding receptors expressed by keratinocytes were identified. Downstream target genes from these identified ligands expressed by keratinocytes were ranked based on the regulatory potential of the upstream T cell-derived ligand. The highest ranked T cell:target gene interactions were displayed on the circos plot. Interactions with a higher regulatory potential are represented by more intense coloration. *IL17A* and *IL17F* regulate the expression of key inflammatory mediators in inflammatory keratinocytes including *S100A8*, *S100A9*, *KRT17*, *CXCL8* and *CCL20,* indicating Th17 cells may drive the differentiation of keratinocytes via IL-17 cytokines into an inflammatory phenotype (**Figure 5.19**). Many of these genes were also identified as key elements for keratinocyte differentiation into an inflammatory phenotype, including *S100A8*, *S100A9*, *CCL20* and *CXCL8* (**Figure 4.35**). *KRT17*, regulated by *IL17A*, *TNF* and *IFNG*, was also a defining marker of inflammatory keratinocytes (**Figure 4.14**) *TGFB1, IFNG* and *TNF* also regulate a number

of downstream target genes expressed by HS keratinocytes, suggesting multiple inflammatory cytokines may drive HS keratinocytes into an inflammatory phenotype.

Taken together, these data suggested that CD4 T cells and Th17 cells in particular, drive the expression of a number of proinflammatory mediators in HS keratinocytes via IL-17 signaling.

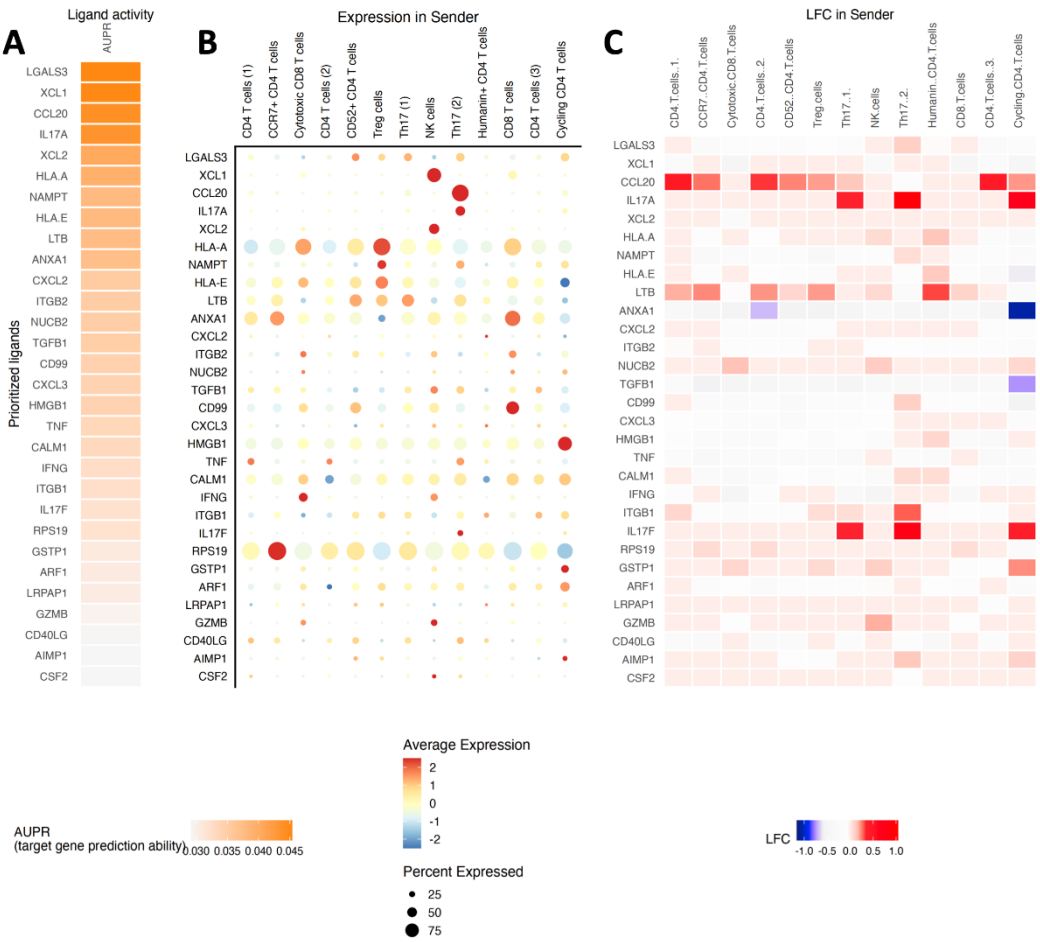

Figure 5.17 Th17 cells interact with keratinocytes via IL-17A to induce differential gene expression. Pearson correlation scores were generated using ligands expressed in T cells and DEGs in keratinocytes. A Pearson correlation score above 0.1 represents good capacity for inducing the DEGs seen in HS keratinocytes (A). Dotplot illustrating the expression of potential ligands in T cells (B). Heatmap displaying the relative change in expression of potential ligands in HS T cells compared with healthy control T cells (C).

Figure 5.18 Heatmap displaying the regulatory potential of T cell ligands on HS keratinocyte genes. Heatmap of the regulatory potential of potential ligands expressed by HS T cells on the downstream target genes expressed by HS keratinocytes.

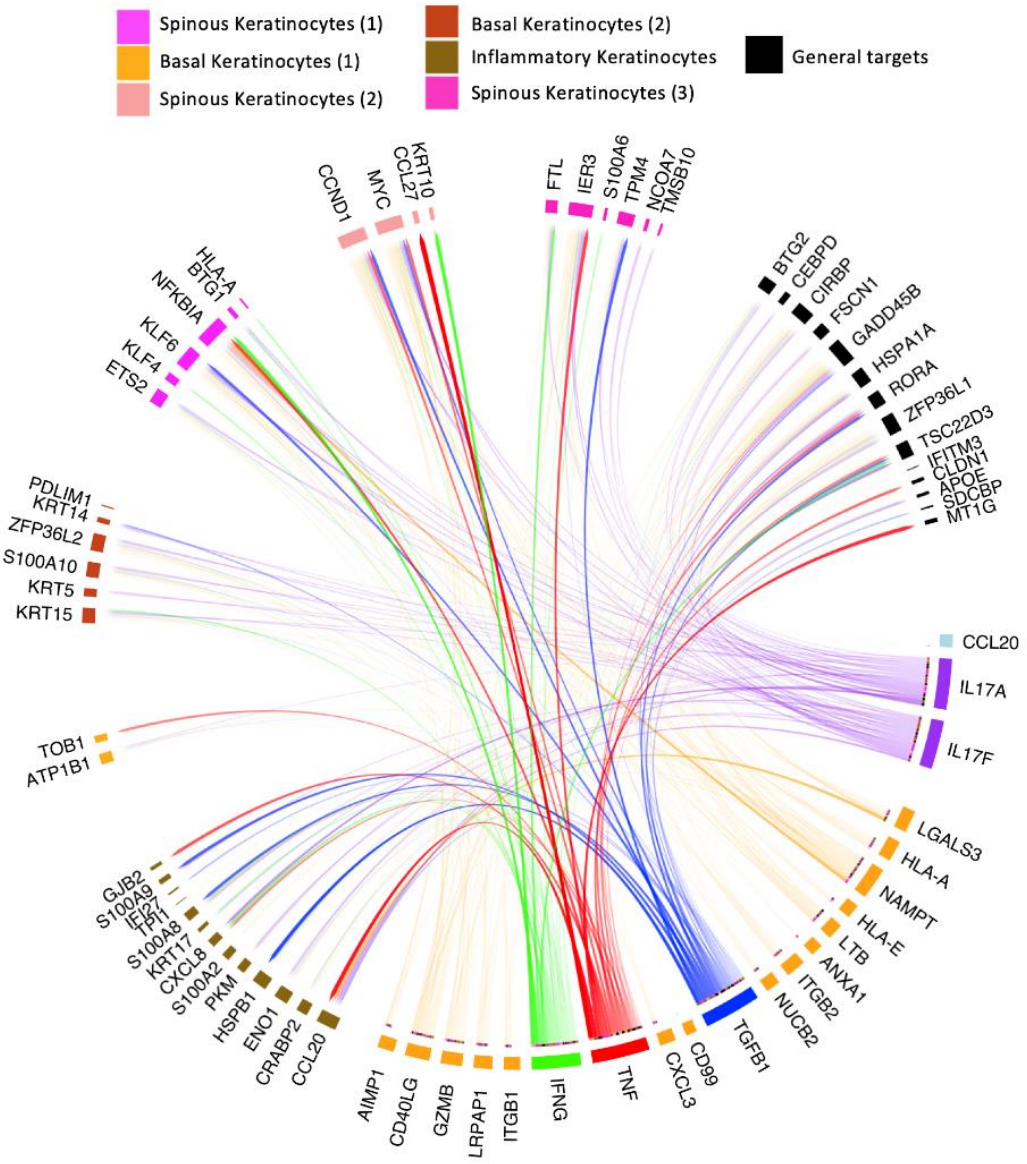

Figure 5.19 Th17 cells mediate the upregulation of proinflammatory genes in inflammatory keratinocytes. Circos plot displaying target genes of prioritised ligands from HS T cells. Target genes are grouped based on the cell population with the highest average expression of the target gene. Ligand:receptor analysis was performed using Nichenetr.

5.3.6 Characterisation of T cells used to generate HS T cell conditioned media

Next, in order to further examine interactions between T cells and keratinocytes or fibroblasts, skin 'crawl out' cultures were established to isolate skin-derived T cells (Clark *et al.*, 2006a). The cells isolated in this way were characterised using full-spectrum flow cytometry and then stimulated *in vitro* to generate T cell conditioned medium which was used to stimulate primary epidermal keratinocytes and dermal fibroblasts (**Section 5.3.7**).

To isolate skin T cells, biopsies of HS dermal tracts and healthy control skin were cultured for 10 days in IL-2 supplemented media which aided the survival and expansion of T cells (Clark *et al.*, 2006a). After 10 days, cells that migrated from HS and healthy control skin were harvested and stimulated with PMA and ionomycin and treated with Brefeldin for 4h at 37°C (**Section 2.2.9**). Samples were then stained for surface expression of CD45, CD3, CD4 and CD8, along with a viability stain, then fixed, permeabilised and stained for the intracellular cytokines IL-17A, IL-17F and IFN-γ. Samples were analysed by flow cytometry within 24 h.

Figure 5.20 displays a gating strategy for identifying CD4 and CD8 T cells from total cells which had emigrated from HS skin. Briefly, the ungated sample was plotted for Time vs Side Scatter Channel-Area (SSC-A) to ensure no fluidics/clumping issues (**Figure 5.20A**). Next, single cells were identified by a FSC-Area (FSC-A) vs FSC-Width (FSC-W) profile (**Figure 5.20B**). Single cells were then plotted for CD45 vs Fixable Viability dye eFluor506 (FixVia eFluor506) (**Figure 5.20C**), identifying live leukocytes. Lymphocytes were identified based on their characteristic FSC vs SSC profile (**Figure 5.20D**). Next, T cells were gated on FSC vs CD3 (**Figure 5.20E**) and CD4 vs CD8 was plotted to identify CD4 and CD8 T cells (**Figure 5.20F**).

Given that TRM cells were not clearly defined in the scRNA-seq dataset despite high expression of *CD69* by many T cell clusters (**Figure 5.6A**), cells that emigrated from HS and healthy control skin were gated on $CD45RO^+$ $CCR7^-$ cells and analysed for classical TRM markers (**Figure 5.21**-**Figure 5.22**). HS skin had relatively similar frequencies of both $CD69^-$ $CD103^+$ and $CD69^+$ $CD103^-$ CD4 T cells compared with healthy control skin (**Figure 5.21C-D**). Interestingly, there was a trend towards a reduction in the frequency of $CD69^+$ $CD103^+$ CD4 T cells in HS skin relative to healthy control skin, however this failed to reach significance

(**Figure 5.21E**). $CD69^+$ $CD103^-$ CD8 T cells also had a trend towards a reduction in HS skin relative to healthy controls (**Figure 5.22D**). In contrast, although it did not reach significance, there were trends towards an increase in both $CD69^-$ $CD103^+$ and $CD69^+$ $CD103^+$ CD8 T cells in HS relative to healthy controls (**Figure 5.22C, E**).

Next, the expression of inflammatory cytokines was evaluated within CD4 T cells in HS and healthy control skin. **Figure 5.23A** shows representative dot plots for IL-17A vs IFN-γ and **Figure 5.23B** displays IL-17A vs IL-17F expression on CD4 T cells from HS skin stimulated with PMA and ionomycin. There was a significant increase in the frequency of IL-17A producing CD4 T cells from HS skin relative to healthy control skin ($p < 0.05$) (**Figure 5.23C**). Interestingly, this increase was not replicated with IL-17F, as no difference in the frequency of IL-17F producing CD4 T cells between HS and healthy control skin was observed (**Figure 5.23D**). There was a trend towards an increase in IFN-γ^+ cells in HS CD4 T cells relative to healthy controls, however this failed to reach significance (**Figure 5.23E**). To determine if CD4 T cells express multiple cytokines simultaneously in HS skin, the frequency of cells co-expressing cytokines was evaluated. Interestingly, a large proportion of IL-17F producing CD4 T cells in HS lesions also co-expressed IL-17A and importantly there was a trend towards an increase in IL-17A and IL-17F co-expressing CD4 T cells in HS skin relative to healthy controls (**Figure 5.23F**). Similarly, there was an increase in the frequency of IL-17A and IFN-γ co-expressing CD4 T cells in HS skin compared with healthy controls ($p < 0.01$) (**Figure 5.23G**).

Cytokine expression from CD8 T cells in HS and healthy control skin is shown in **Figure 5.24**, displaying representative dot plots for IL-17A vs IFN-γ and IL-17A vs IL-17F (**Figure 5.24A-B**). There was no significant difference in the frequency of IL-17A or IL-17F producing CD8 T cells between HS and healthy controls (**Figure 5.24C-D**). While there was a trend towards an increase in IFN-γ^+ CD8 T cells in HS compared with healthy control skin, this failed to reach significance (**Figure 5.24E**). The frequency of CD8 T cells co-expressing IL-17A and IL-17F was similar in both HS and healthy control skin (**Figure 5.24F**), however there was a significant increase in the frequency of IL-17A and IFN-γ co-expressing CD8 T cells in HS skin relative to healthy controls ($p < 0.01$) (**Figure 5.24G**).

Next, the T cells which emigrated from HS and healthy control skin following 10-day culture in IL-2 supplemented media were stimulated for 5 days with anti-CD3/CD28 to generate HS T cell conditioned medium (HS-TCM) and the concentrations of inflammatory cytokines in the supernatants were evaluated (**Figure 5.25**). T cells derived from HS skin had elevated concentrations of IL-17A, IL-17F, TNF and IFN-γ cytokines in the cell supernatant, however the small number of donors precluded statistical analysis and limits the conclusions that can be drawn from this experiment (**Figure 5.25**).

Given IL-17A was predicted to regulate the expression of inflammatory genes in HS keratinocytes (**Figure 5.19**), the effect of IL-17A, TNF and HS-TCM on primary keratinocytes isolated from healthy skin was evaluated *in vitro* (**Figure 5.26**). Due to the low sample numbers available these results are preliminary. IL-17A increased the secretion of IL-8 by keratinocytes, while TNF had no effect. In addition, the combination of IL-17A and TNF did not enhance the production of IL-8 (**Figure 5.26**). To confirm the efficacy of each biologic used, each cytokine was blocked by its respective inhibitor. IL-17A was specifically inhibited with secukinumab and TNF was directly inhibited with adalimumab (**Figure 5.26**). Interestingly, HS-TCM (**Figure 5.25**) induced IL-8 secretion by keratinocytes (**Figure 5.26**). However, neither secukinumab or adalimumab inhibited this increase in IL-8, suggesting that multiple T cell-mediated pathways, beyond IL-17 and TNF cytokines, can promote IL-8 secretion by keratinocytes. These preliminary results warrant further investigation.

While TNF did not induce the expression of IL-8 in healthy control keratinocytes, keratinocytes from HS patients previously treated with TNF inhibitors had reduced expression of the *CXCL8*, *CXCL2* and *NFKBIA* (**Figure 5.27**). 791 genes were differentially expressed between keratinocytes derived from HS patients treated with anti-TNF therapy compared with those who were not on any biologic treatment (**Table 8.43Table 8.44**). A number of inflammatory pathways including IL-17, TNF and T cell receptor signaling were enriched from these DEGs (**Figure 5.28A**). Importantly, the genes involved in these inflammatory pathways were downregulated in keratinocytes from HS patients previously treated with anti-TNF therapies, demonstrating a broad dampening of keratinocyte inflammatory response following TNF inhibition in HS (**Figure 5.28B**).

In summary, this section identified T cells expressing TRM markers in HS and healthy control skin. Although there were no clear differences in the frequency of CD4 or CD8 T cell subsets expressing CD69 and/or CD103 within HS vs healthy skin, both CD4 and CD8 T cells had increased cytokine production in HS skin relative to healthy controls, with HS skin having increased frequencies of IL-17A$^+$ CD4 T cells and pathogenic CD4 and CD8 T cells which co-expressed IL-17A and IFN-γ. IL-17A, a combination of IL-17A and TNF, and HS-TCM derived from emigrated HS T cells elevated the expression of IL-8 in keratinocytes. Interestingly, in keratinocytes stimulated with both IL-17A and TNF, blocking IL-17A and not TNF reduced IL-8 secretion, highlighting the importance of IL-17A in promoting IL-8 from keratinocytes. Furthermore, keratinocytes derived from HS patients treated with TNF inhibitors had reduced expression of inflammatory mediators and downregulated inflammatory cytokine signaling relative to keratinocytes from untreated HS patients. However, as TNF did not induce the expression of IL-8 by keratinocytes *in vitro*, it is possible that the downregulation inflammatory mediators in HS keratinocytes following TNF inhibition may not be due to TNF blockade directly and may be due to the reduced frequency of Th17 cells in HS lesions following TNF inhibition.

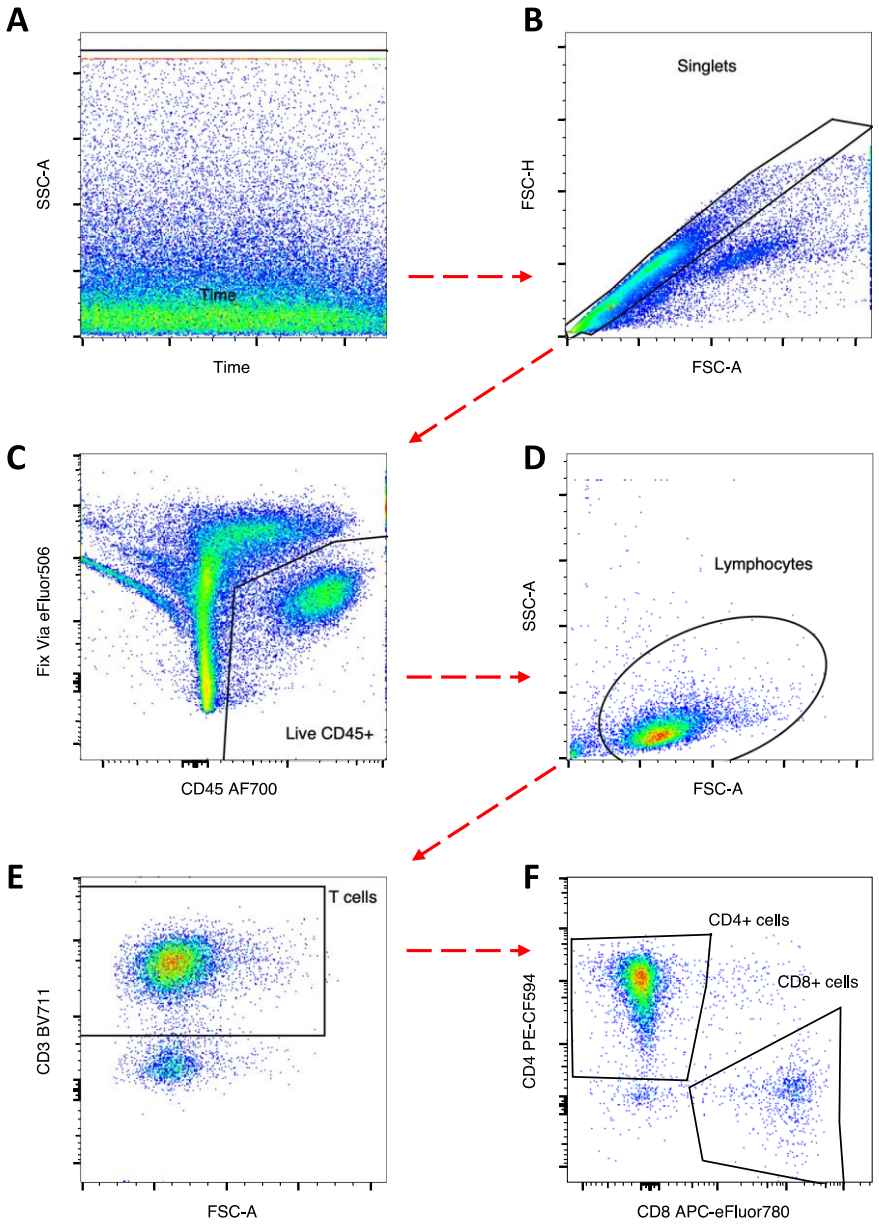

Figure 5.20 Plots illustrating the gating strategy to identify CD4 and CD8 T cells in HS and healthy control skin. Biopsies from the tracts of HS patients (n=6) and healthy control skin (n=13) were cultured for 10 days before the emigrated cells were stimulated with PMA and ionomycin and treated with Brefeldin A for 4h, stained for surface and intracellular markers, and analysed by flow cytometry. To identify CD4 and CD8 T cells, sequential gating was performed; Time vs Side Scatter Area (SSC-A) to identify a constant flow stream and remove data arising from potential clogs in the cytometer (A); Forward Scatter height (FSC-H) vs FSC-A to remove possible doublets (B); CD45 vs Fixable Viability Dye to identify viable immune cells (C); FSC-A vs SSC-A to identify lymphocytes (D); FSC-A vs CD3 to identify T cells (E); CD8 vs CD4 to identify CD4 and CD8 T cells (F).

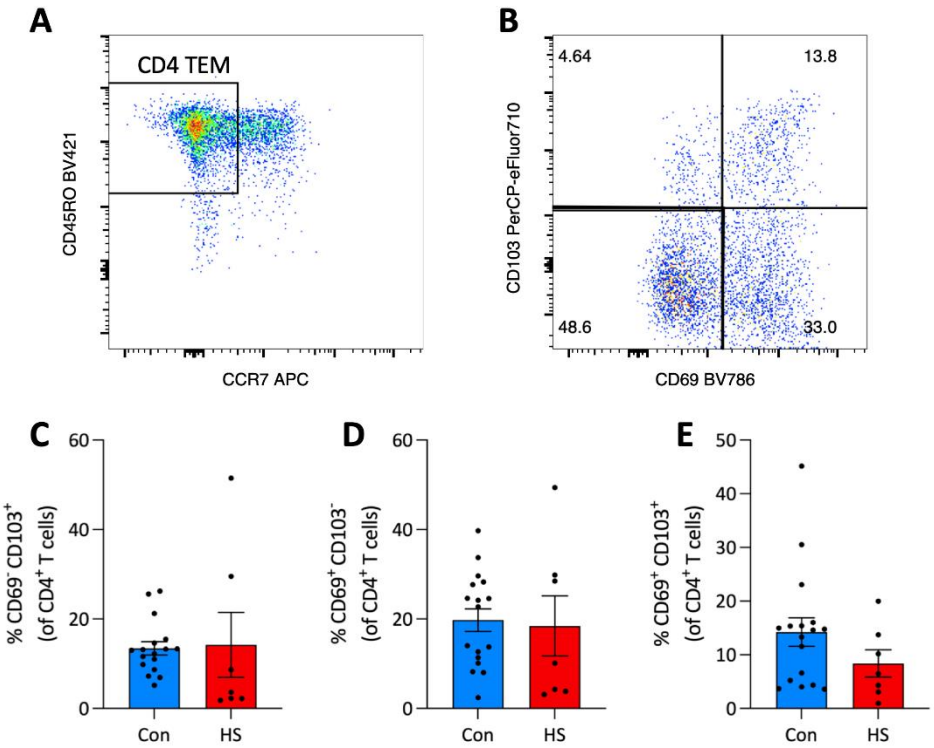

Figure 5.21 Frequency of CD4 T cells expressing TRM markers in HS and healthy control skin. Biopsies from the tracts of HS patients (n=6) and healthy control skin (n=8-13) were cultured for 10 days before the emigrated cells were stained for surface markers and analysed by flow cytometry. Representative dot plots for expression of CD45RO vs CCR7 (A), to identify central and effector memory CD4 T cells and CD69 vs CD103 (B) to identify CD4 TRM subsets. Plots were gated on single, live, $CD45^+$, $CD3^+$ $CD4^+$ lymphocytes. Graphs show the frequency of CD4 TRM subsets including $CD69^-CD103^+$ (C), $CD69^+CD103^-$ (D) and $CD69^+$ $CD103^+$ (E). Graphs represent individual samples with mean ± SEM for each group. Statistical significance was calculated by Mann-Whitney U test.

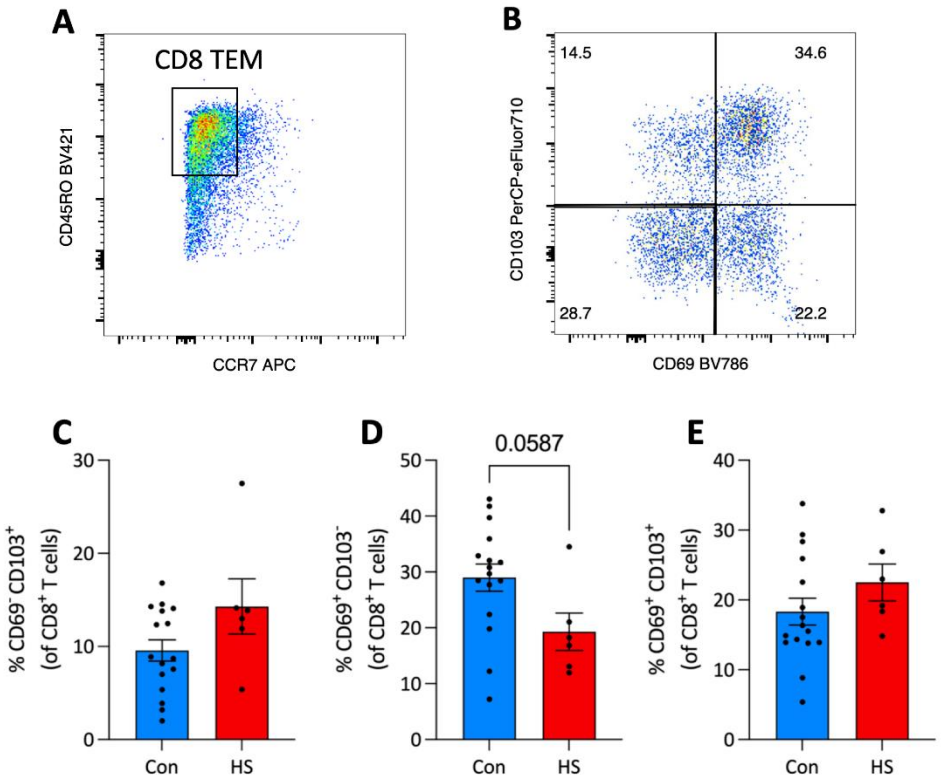

Figure 5.22 Frequency of CD8 resident memory T cells in HS and healthy control skin. Biopsies from the tracts of HS patients (n=6-7) and healthy control skin (n=16-17) were cultured for 10 days before the emigrated cells were stained for surface markers and analysed by flow cytometry. Representative dot plots for expression of CD45RO vs CCR7 (A), to identify central and effector memory CD4 T cells and CD69 vs CD103 (B) to identify CD8 TRM subsets. Plots were gated on single, live, $CD45^+$, $CD3^+$ $CD8^+$ lymphocytes. Graphs show the frequency of CD8 TRM subsets including $CD69^-$ $CD103^+$ (C), $CD69^+$ $CD103^-$ (D) and $CD69^+$ $CD103^+$ (E). Graphs represent individual samples with mean ± SEM for each group. Statistical significance was calculated by Mann-Whitney U test.

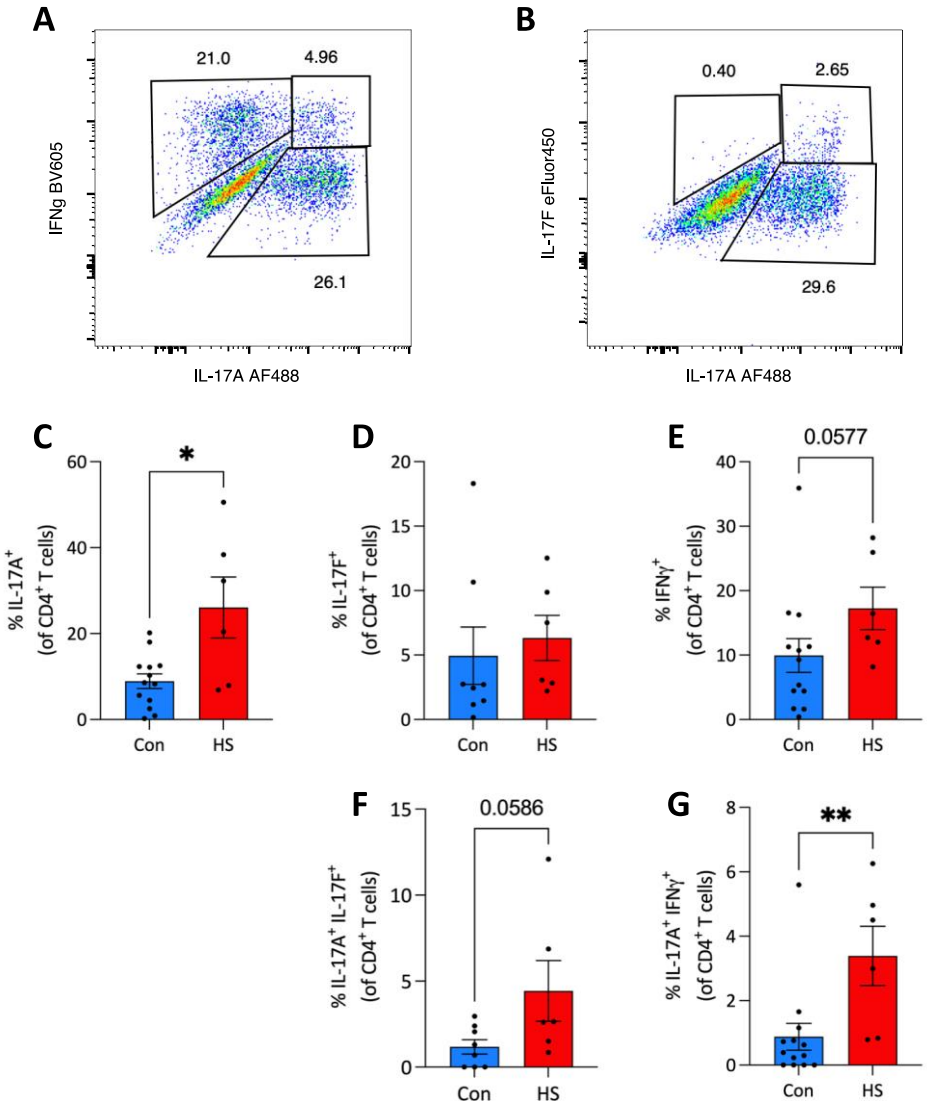

Figure 5.23 Increased secretion of IL-17A by CD4 T cells in HS skin. Biopsies from the tracts of HS patients (n=6) and healthy control skin (n=8-13) were cultured for 10 days before the emigrated cells were stimulated with PMA and ionomycin and treated with Brefeldin A for 4h, stained for surface and intracellular markers, and analysed by flow cytometry. Representative dot plots for expression of IL-17A vs IFN-γ (A) and IL-17A vs IL-17F (B) on CD4 T cells. Plots were gated on single, live, $CD45^+$, $CD3^+$ $CD4^+$ lymphocytes. Graphs show the frequency of CD4 T cells expressing IL-17A (C), IL-17F (D), IFN-γ (E), co-expression of IL-17A and IL-17F (F) and co-expression of IL-17A and IFN-γ (G). Graphs represent individual samples with mean ± SEM for each group. Statistical significance was calculated by Mann-Whitney U test, * $p < 0.05$, ** $p < 0.01$.

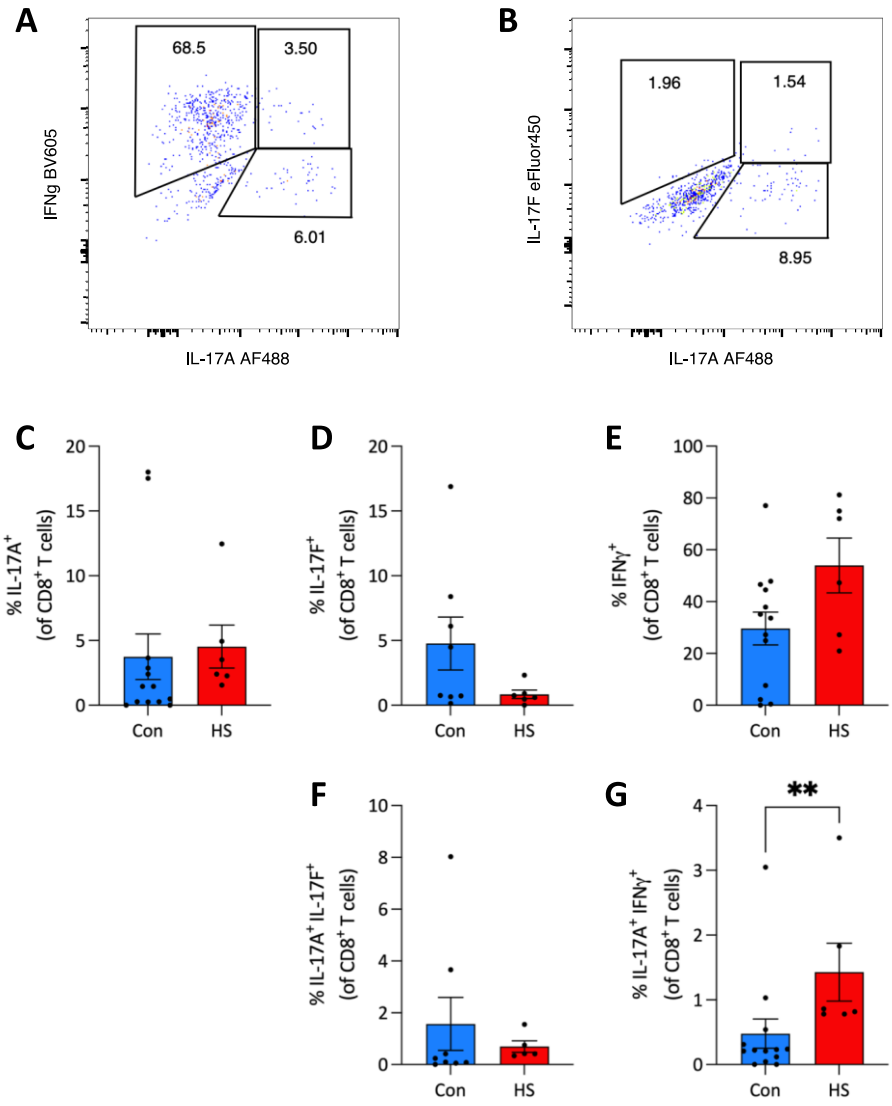

Figure 5.24 CD8 T cells in HS skin predominantly secrete IFN-γ. Biopsies from the tracts of HS patients (n=6) and healthy control skin (n=8-13) were cultured for 10 days before the emigrated cells were stimulated with PMA and ionomycin and treated with Brefeldin A for 4 hours, stained for surface and intracellular markers, and analysed by flow cytometry. Representative dot plots for expression of IL-17A vs IFN-γ (A) and IL-17A vs IL-17F (B) on CD8 T cells. Plots were gated on single, live, CD45$^+$, CD3$^+$ CD8$^+$ lymphocytes. Graphs show the frequency of CD8 T cells expressing IL-17A (C), IL-17F (D), IFN-γ (E), co-expression of IL-17A and IL-17F (F) and co-expression of IL-17A and IFN-γ (G). Graphs represent individual samples with mean ± SEM for each group. Statistical significance was calculated by Mann-Whitney U test, * $p < 0.05$, ** $p < 0.01$.

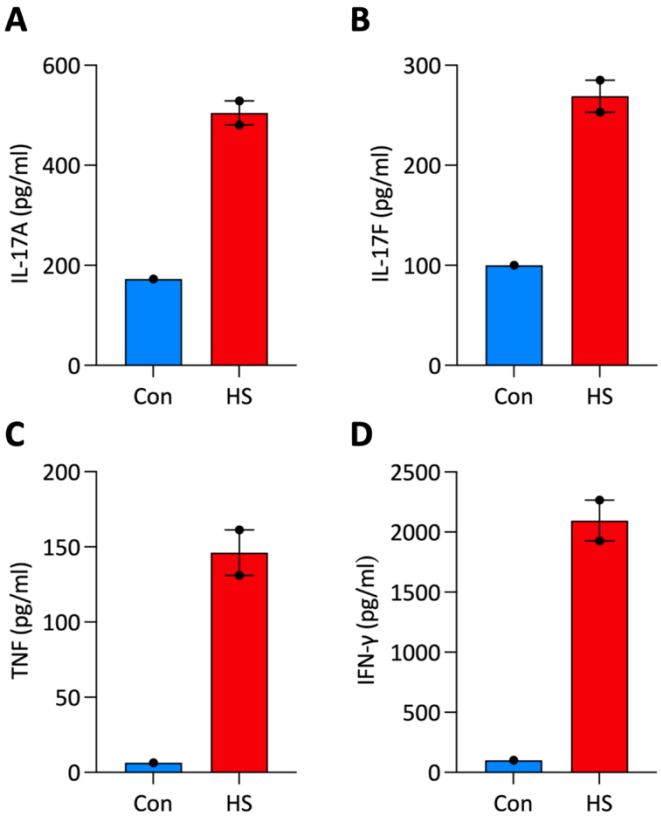

Figure 5.25 Concentrations of inflammatory cytokines in HS skin-derived T cell conditioned media. Biopsies from the tracts of HS patients (n=2) and healthy control skin (n=1) were cultured for 10 days before the emigrated cells were stimulated with anti-CD3/CD28 for 5 days. Concentrations of inflammatory cytokines IL-17A (A), IL-17F (B), TNF (C) and IFN-γ (C) secreted in the supernatant were evaluated by ELISA. Graphs represent individual samples with mean ± SEM for each group.

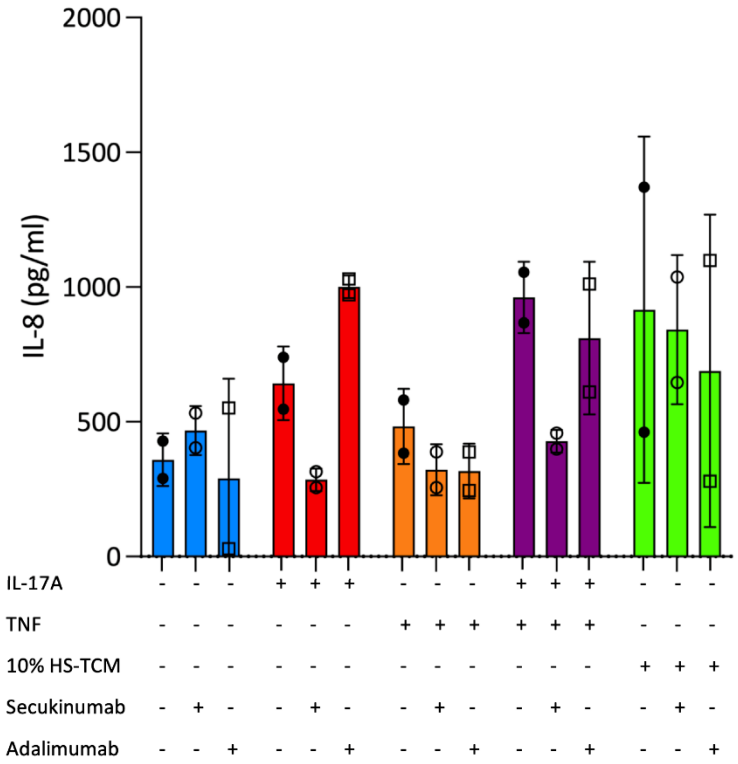

Figure 5.26 Preliminary data showing effect of IL-17A, TNF and HS-TCM on keratinocytes. Primary healthy control keratinocytes (n=2) were seeded in 96-well plates at a seeding density of 10,000 keratinocytes/well. Recombinant IL-17A (10 ng/ml), TNF (1 ng/ml) and 10% HS-TCM were applied to cells for 24 hours. 10 µg/ml of the IL-17A inhibitor secukinumab or the TNF inhibitor adalimumab were applied to the cytokines or HS-TCM for 30 minutes prior to stimulation. Concentrations of IL-8 in the supernatants were assessed by ELISA.

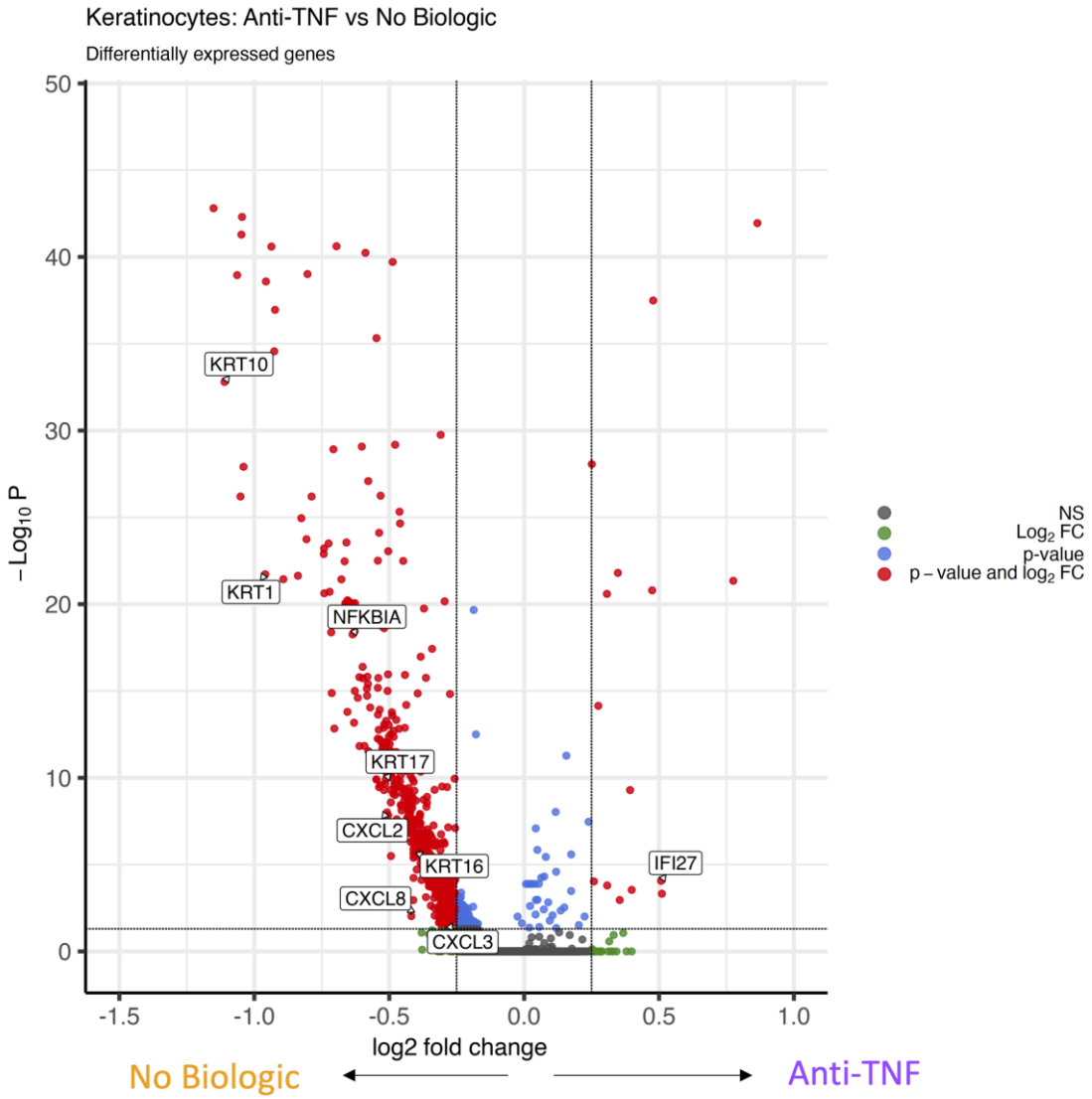

Figure 5.27 Differentially expressed genes between keratinocytes in HS patients treated with or without TNF inhibitors. Single cells isolated from HS lesional skin treated with (n=2) or without (n=4) TNF inhibitors were purified based on absence of CD45 expression, barcoded and sequenced by 10X Genomics scRNA-seq. Volcano plot visualises DEGs between keratinocytes derived from HS lesions treated with TNF inhibitors compared with those not treated with any biologics. Genes with a $log_2FC > 0$ are upregulated in anti-TNF derived keratinocytes and a $log_2FC < 0$ are downregulated in anti-TNF derived keratinocytes. The $-Log_{10}$ P Y-axis is a measure of significance.

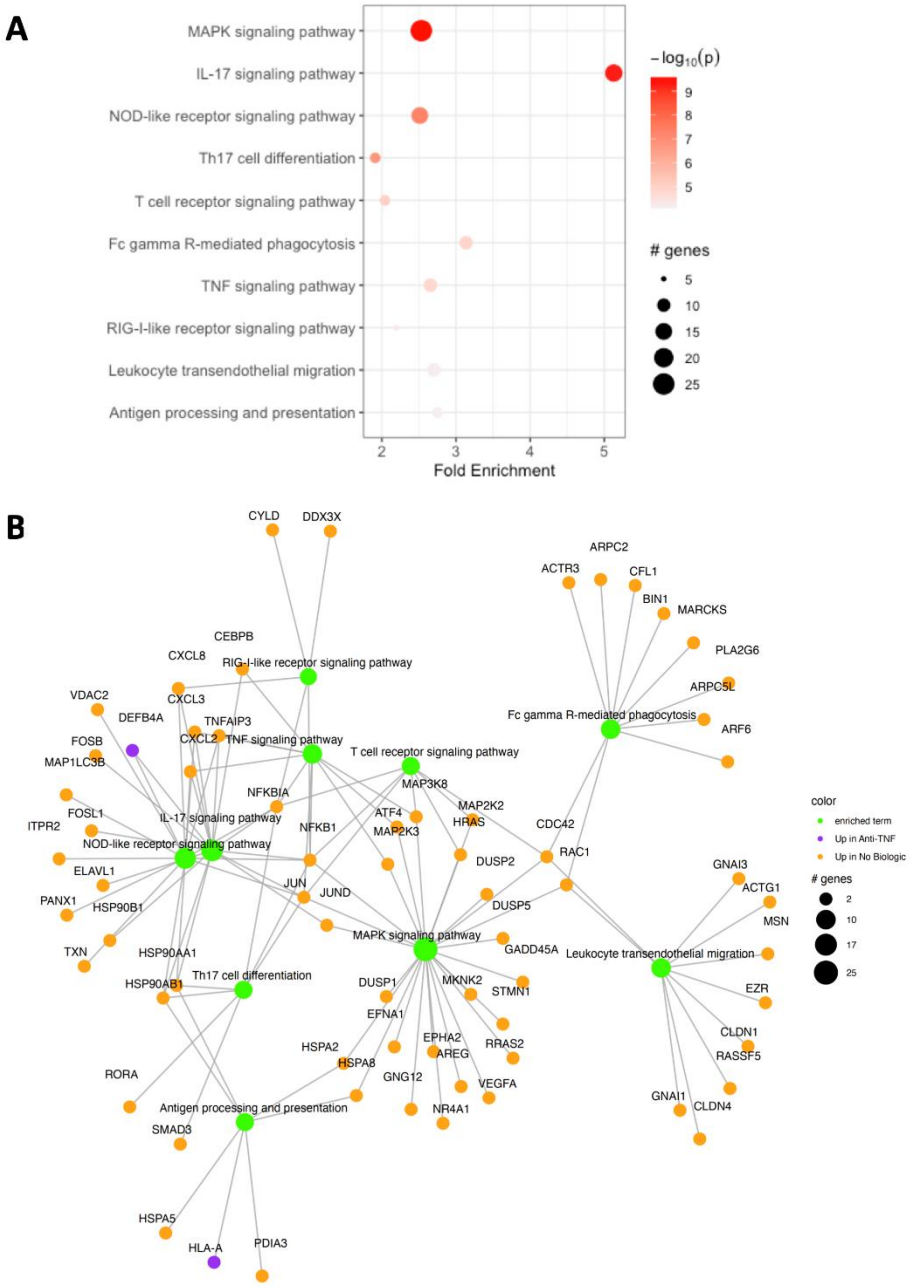

Figure 5.28 Immune pathways enriched in keratinocytes from HS patients treated with TNF inhibitors compared with those from untreated patients. Top 10 immune pathways enriched from the genes significantly differentially expressed between keratinocytes from HS patients with or without anti-TNF treatment (A). Gene-pathway network displaying the genes upregulated in TNF inhibitors treated HS keratinocytes (purple) or untreated (orange) HS keratinocytes in the top 5 immune pathways enriched from the differentially expressed genes between HS keratinocytes treated with or without TNF inhibitors (B).

5.3.7 HS inflammatory fibroblasts were regulated by T cell-mediated TNF signaling

This section delved deeper into the cellular interactions which may promote the inflammatory phenotype in HS fibroblasts. Considering the importance of T cells in HS inflammation the interactions between T cells and fibroblasts were evaluated.

TNF was deemed to be the T cell ligand with the highest potential to regulate the expression of DEGs in HS fibroblasts (**Figure 5.29A**). Other ligands with high Pearson correlation coefficients included *TGFB1*, *CCL20* and *IFNG*. *TNF* was primarily expressed by CD4 T cell clusters and Th17 cells (**Figure 5.29B**). Other ligands of note, including *CCL20* was expressed by Th17 cells, while *IFNG* was expressed by cytotoxic CD8 T cells and NK cell clusters (**Figure 5.29B**). *TNF* expression was relatively similar between HS and healthy controls in all T cell clusters (**Figure 5.29C**). Interestingly, there was a striking increase in *CCL20* expression in HS patients across a number of T cell clusters (**Figure 5.29C**). Given the regulatory potential of these ligands on downstream target genes expressed by fibroblasts, it is evident that *TGFB1* and *TNF* were likely major regulators of gene expression in HS fibroblasts (**Figure 5.30**). *TGFB1* and *TNF* regulate the expression of a number of DEGs in HS fibroblasts including *COL1A1*, *CXCL8*, *HIF1A* and MMPs (**Figure 5.30**). Importantly, IL-17 cytokines were not identified as potential regulators of gene expression in HS fibroblasts in this analysis. This was mainly due to the unexpected lack of IL-17 receptor expression by fibroblasts in this dataset. This is not to say fibroblasts do not express IL-17 receptors, but that expression was not detected at the time of sequencing, which may be due to certain proteins being stably expressed.

To understand the impact of T cell-derived ligands on the expression of inflammatory mediators in HS fibroblasts, a circos plot was generated (**Figure 5.31**). This plot illustrates the downstream target genes in each fibroblast cluster which were regulated by each of the T cell-derived ligands. *TNF* and *TGFB1* were important regulators of inflammatory gene expression in many of the fibroblast clusters (**Figure 5.31**). *TGFB1* regulated collagen expression in the reticular fibroblast (1) cluster, reticular fibroblast (2) activation and *CXCL8* and MMP expression in the inflammatory fibroblast (2) cluster. Additionally, TNF regulated the activation of the reticular fibroblast (2) cluster and *CXCL8, CXCL1* and MMP expression in the inflammatory fibroblast (2) cluster (**Figure 5.31**).

Ligand:receptor interaction analysis suggests that T cell-derived cytokines regulate the expression of inflammatory genes in HS fibroblasts. To estimate the effects of T cells on primary fibroblasts, healthy fibroblasts were stimulated with HS-TCM (**Figure 5.25**, **Figure 5.32**). Considering the prominent role of TNF and IL-17A in HS inflammation in addition to the ligand:receptor interaction analysis identifying TNF, but not IL-17A, as an important regulator of gene expression in HS fibroblasts (**Figure 5.31**), the differential effects of IL-17A and TNF on primary fibroblasts was also evaluated *in vitro* (**Figure 5.32**). HS-TCM, IL-17A, TNF and a combination of IL-17A and TNF significantly elevated the secretion of IL-6 by dermal fibroblasts; however IL-17A failed to induce IL-8 secretion, replicating the findings from the ligand:receptor interaction analysis. Interestingly, TNF and IL-17A synergistically acted on healthy dermal fibroblasts to elevate IL-8 secretion, but not IL-6 (**Figure 5.32A-B**). This indicated indirectly that fibroblasts indeed expressed the IL-17 receptor. Adalimumab significantly reduced IL-8 secretion from TNF stimulated fibroblasts. However, despite IL-17A not inducing IL-8 production, inhibiting IL-17A with secukinumab significantly reduced IL-8 secretion in the IL-17A plus TNF stimulated fibroblasts (**Figure 5.32B**). Adalimumab significantly reduced IL-8 to basal levels in HS-TCM stimulated fibroblasts, confirming the importance of T cell derived TNF on regulating IL-8 production in fibroblasts outlined by ligand:receptor interaction analysis (**Figure 5.32B**).

Fibroblasts isolated from HS patients treated with TNF inhibitors had reduced expression of MMPs, AMPs and chemokines which regulate immune cell recruitment to the site of inflammation (**Table 8.45Table 8.46**), illustrating the importance of TNF in regulating inflammatory gene expression in HS fibroblasts (**Figure 5.33**). TNF inhibition reduced cytokine signaling pathways and impacted metabolic processes in HS fibroblasts, reducing the expression of glycolytic genes and increasing the expression of oxidative phosphorylation associated genes (**Figure 5.34A-B**). While expression of *CXCL1*, *CXCL8*, S100s and MMPs in HS fibroblasts were reduced upon TNF inhibition in HS patients, expression of collagen genes was not affected, indicating an important role of TNF in promoting inflammatory fibroblasts in HS lesions (**Figure 5.35A-B**).

This section illustrates the role of *TGFB1, IL17A* and, in particular, *TNF* in regulating the expression of proinflammatory mediators in HS fibroblasts and highlights how the broad

inflammatory profile seen in HS lesions differentially activates specific fibroblast populations in HS lesions.

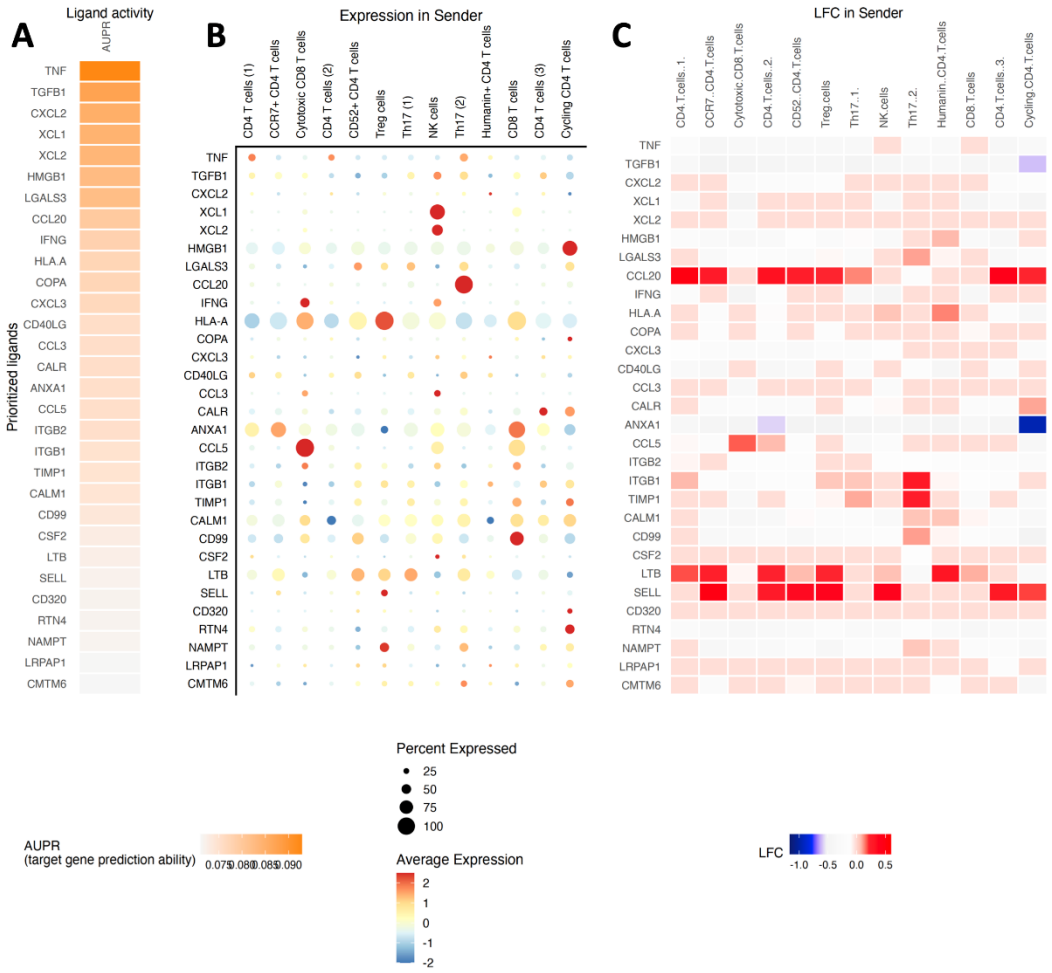

Figure 5.29 *TNF* and *TGFB1* drive the expression proinflammatory mediators in HS fibroblasts. Pearson correlation scores were generated using ligands expressed in T cells and DEGs in HS fibroblasts. A Pearson correlation score above 0.1 represents good capacity for inducing the DEGs seen in HS fibroblasts (A). Dotplot illustrating the expression of potential ligands in T cells (B). Heatmap displaying the relative change in expression of potential ligands in HS T cells compared with healthy control T cells (C).

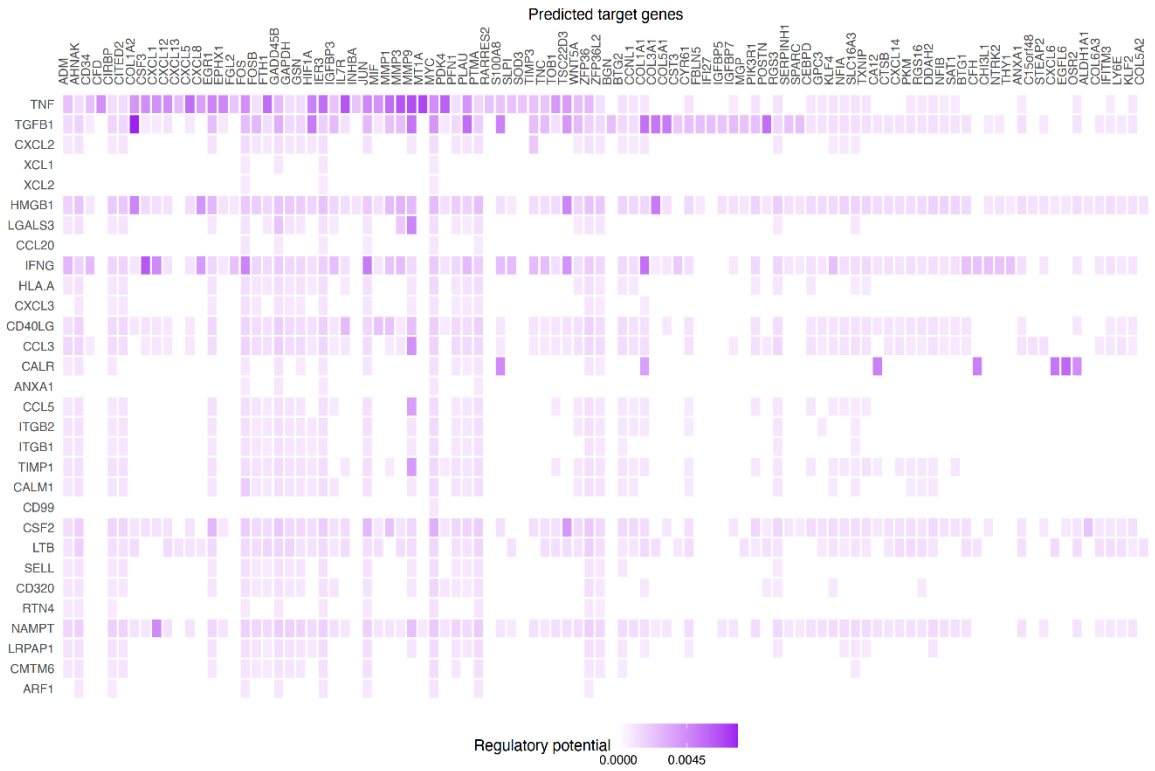

Figure 5.30 Heatmap displaying the regulatory potential of T cell ligands on HS fibroblast genes. Heatmap of the regulatory potential of potential ligands expressed by T cells on the downstream target genes expressed by HS fibroblasts.

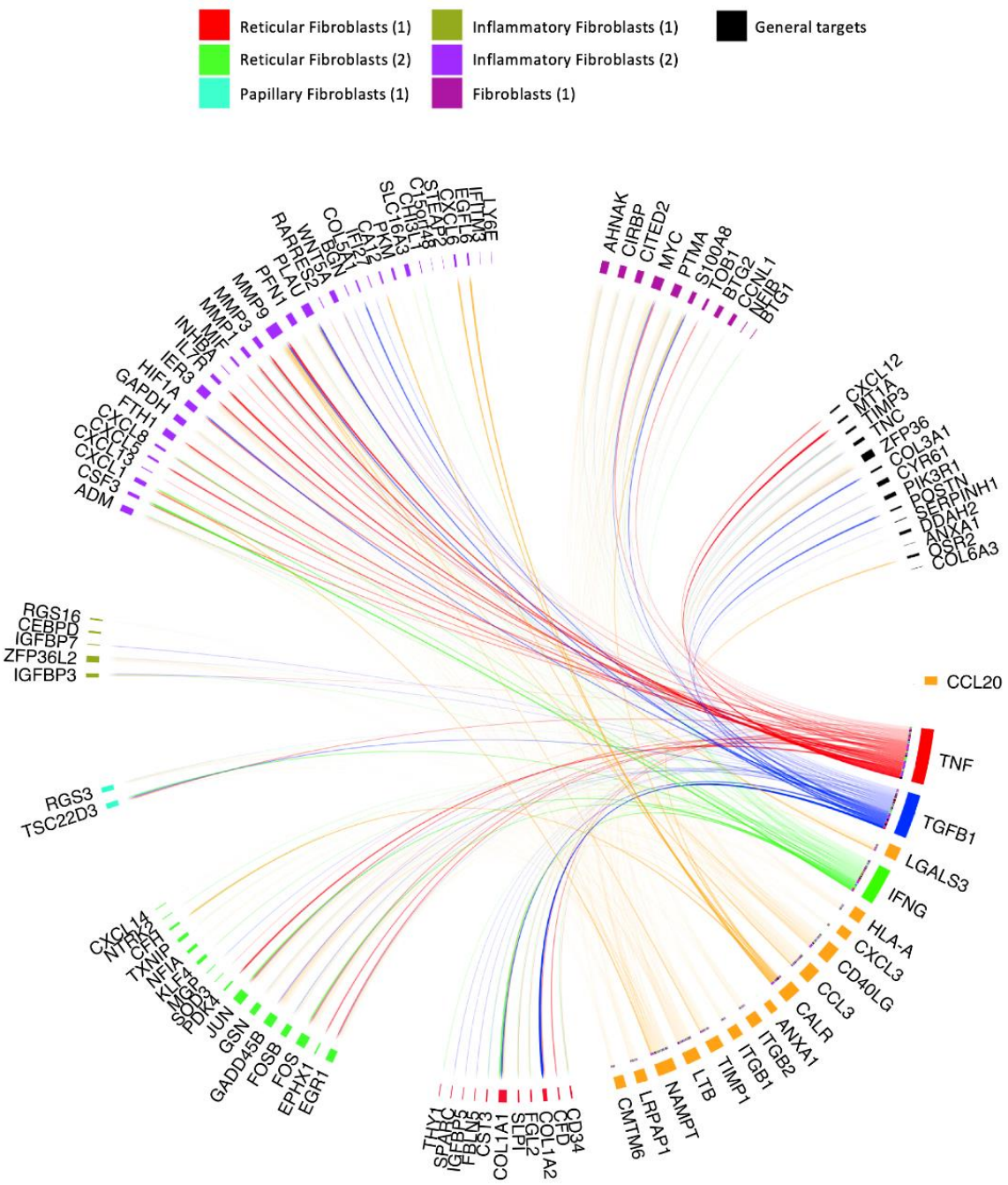

Figure 5.31 TNF and TGF-β predicted to drive activation of inflammatory fibroblasts. Circos plot displaying target genes of prioritised ligands from T cells. Target genes are grouped based on the fibroblast cluster that has the highest average expression of the downstream target gene. Ligand:receptor analysis was performed using Nichenetr.

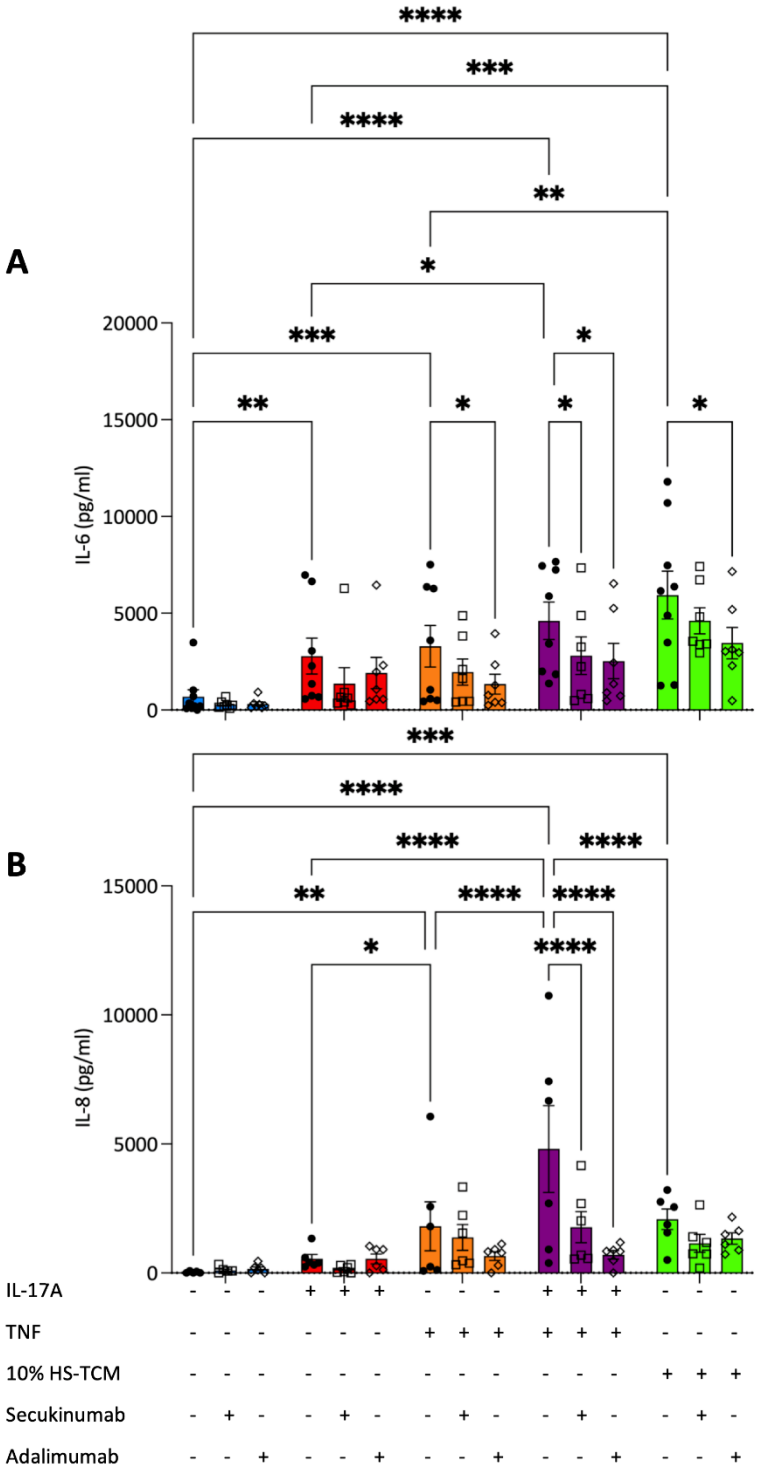

Figure 5.32 Induction of IL-8 and IL-6 in primary healthy dermal fibroblasts by IL-17, TNF and HS-TCM. Primary healthy control fibroblasts (n=6-9) were seeded in 96-well plates at a seeding density of 10,000 fibroblasts/well. Recombinant IL-17A (10 ng/ml), TNF (1 ng/ml) and 10% HS-TCM were applied to cells for 24 hours. 10 µg/ml of the IL-17A inhibitor secukinumab or the TNF inhibitor adalimumab were applied to the recombinant cytokines or HS-TCM for 30 minutes prior to stimulation. Concentrations of IL-6 (A) and IL-8 (B) in the supernatants were assessed by ELISA. Statistical differences were determined by Fisher's LSD test; * p <0.05, ** p <0.01, *** p <0.001, **** p <0.0001.

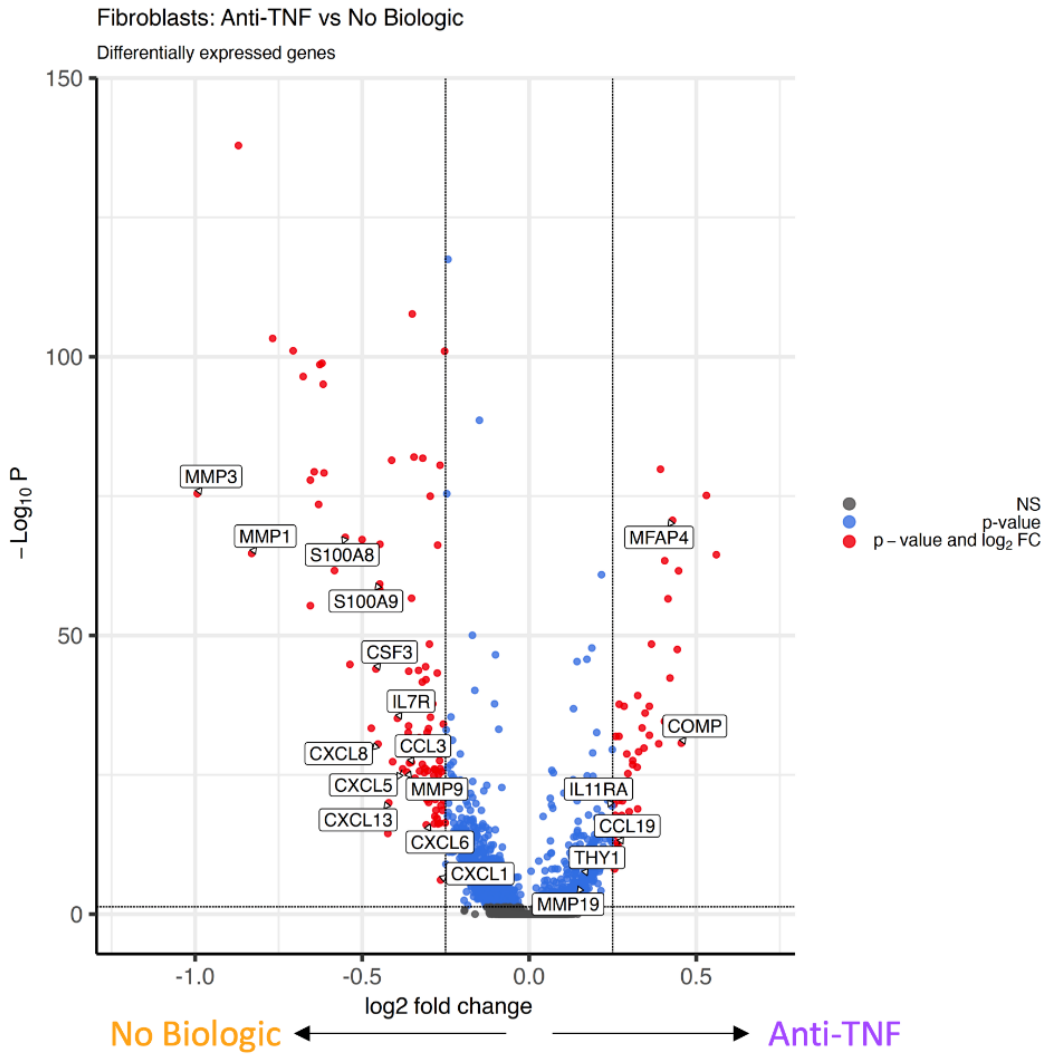

Figure 5.33 TNF inhibition reduced the expression of inflammatory mediators in HS fibroblasts. Single cells isolated from HS lesional skin treated with (n=2) or without (n=4) TNF inhibitors were purified based on absence of CD45 expression, barcoded and sequenced by 10X Genomics scRNA-seq. Volcano plot visualises DEGs from fibroblasts derived from the lesions of HS patients treated with TNF inhibitors compared with fibroblasts derived from untreated HS patients. Genes with a $log_2FC > 0$ are upregulated in anti-TNF treated fibroblasts and a $log_2FC < 0$ are downregulated in anti-TNF treated fibroblasts. The $-Log_{10}P$ Y-axis is a measure of significance.

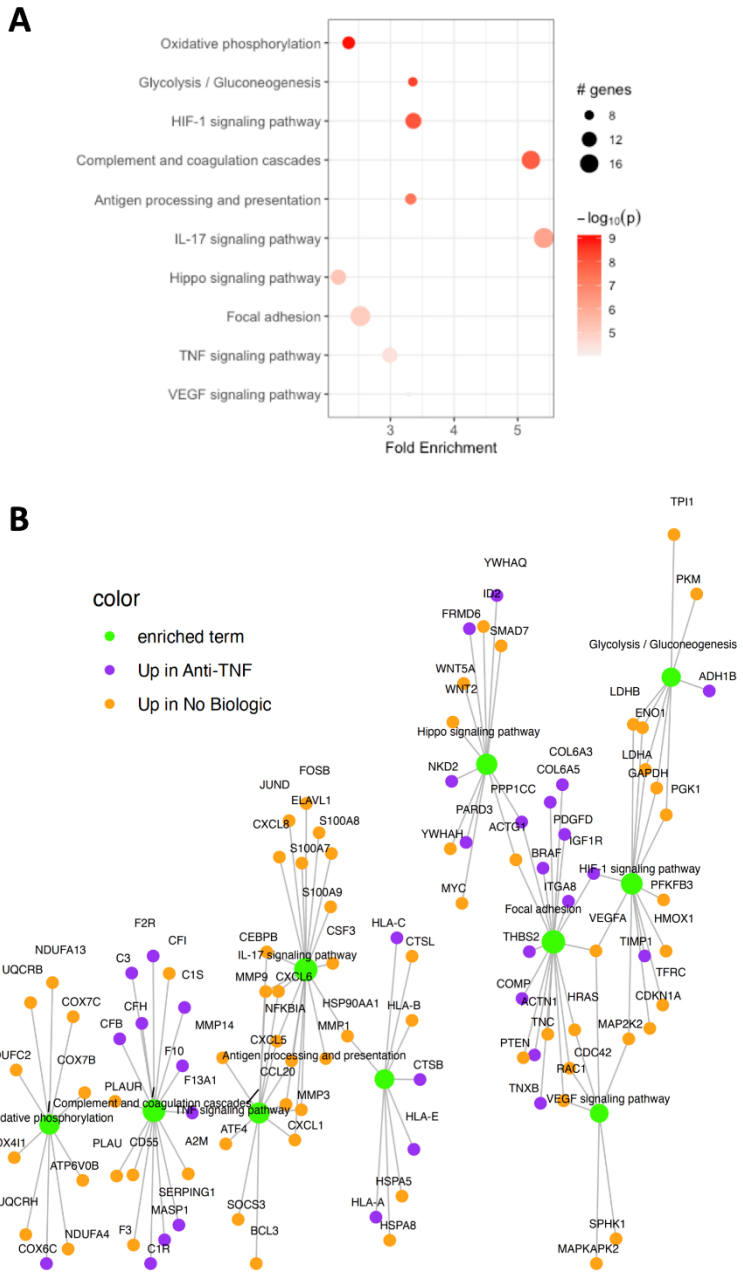

Figure 5.34 TNF inhibition reduced inflammatory cytokine signaling in HS fibroblasts. Single cells isolated from HS lesional skin treated with (n=2) or without (n=4) TNF inhibitors were purified based on CD45 expression, barcoded and sequenced by 10X Genomics scRNA-seq. Top 10 immune pathways enriched from the genes significantly differentially expressed between HS fibroblasts treated with or without TNF inhibitors (A). Gene-pathway network illustrating the genes upregulated in fibroblasts derived from HS patients treated with TNF inhibitors (purple) or fibroblasts derived from untreated (orange). HS patients in the top 5 immune pathways enriched from the differentially expressed genes between HS fibroblasts treated with or without TNF inhibitors (B).

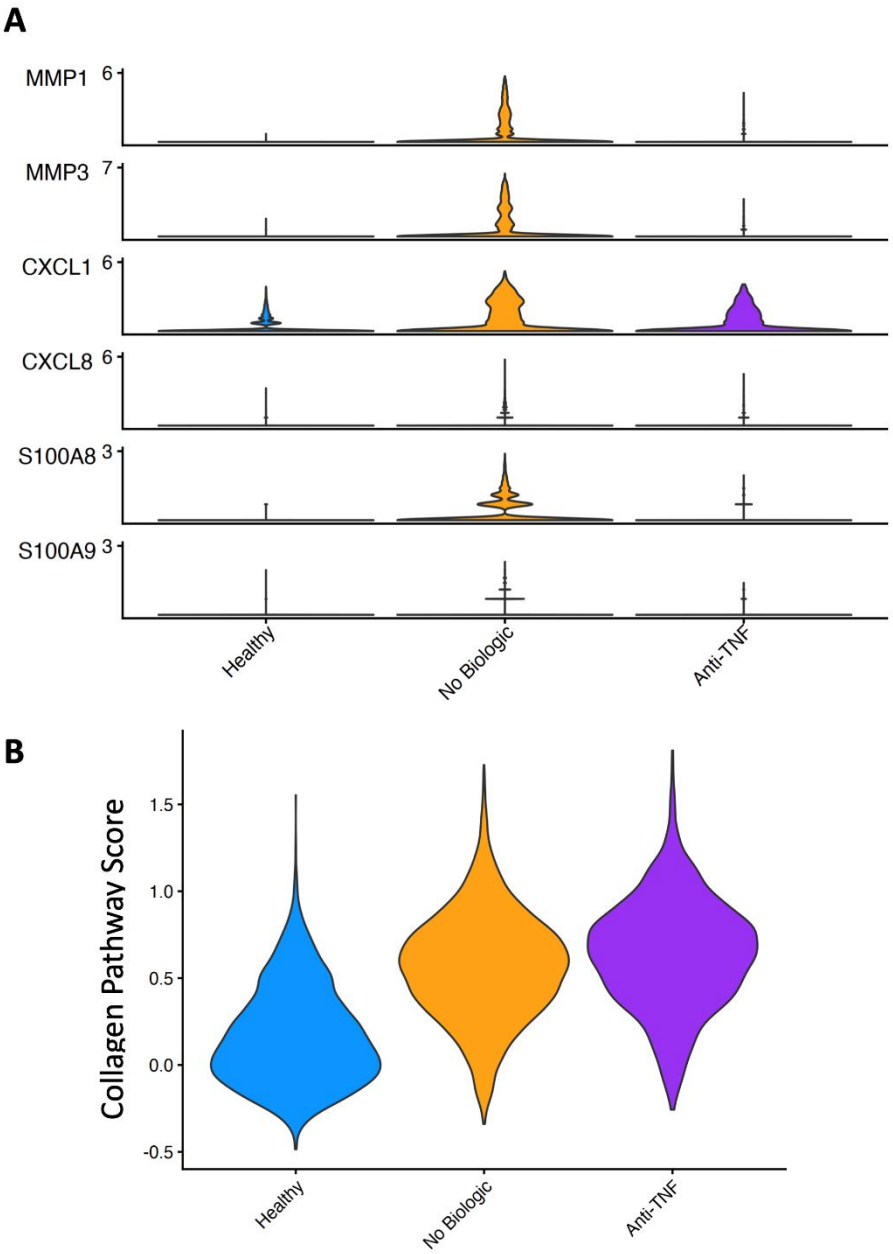

Figure 5.35 TNF inhibition reduces fibroblast MMP expression but not collagen production. Violin plot visualising the expression of MMPs (*MMP1*, *MMP3*), AMPs (*S100A8*, *S100A9*) and IL-17 regulated genes (*CXCL1, CXCL8*) in healthy control fibroblasts and HS fibroblasts treated with or without TNF inhibitors (A). Violin plot visualising the expression of collagen pathway score calculated using the AddModuleScore() function of all collagen genes (B).

5.4 Discussion

This study demonstrated that IL-17A and TNF are crucial T cell-derived cytokines which regulate inflammatory gene expression in HS keratinocytes and fibroblasts, respectively. Moreover, this study highlighted Th17 cells as a major source of both IL-17A and TNF in HS lesions, while also detailing the T cell subsets found in HS skin. It demonstrates, albeit in a small sample size, how TNF inhibition in HS patients can limit the dysregulated cytokine production which is characteristic of HS T cells, and reverse the inflammatory phenotypes in HS keratinocytes and fibroblasts, thus providing new insights into the broad anti-inflammatory effects of TNF inhibition in HS lesions.

T cells make up a large proportion of immune cells in HS lesions (Moran *et al.,* 2023). This study elaborates on this, identifying the specific CD4 and CD8 T cell subsets present in HS lesions. The CD4 T cells (1) and CD4 T cells (2) clusters had high expression of the activation markers *CD69*, *FOS* and *JUN*, suggesting that these clusters may contain activated T cells. CD4 T cells (1) and Th17 cells were the major sources of *TNF* expression in HS T cells, which was elevated in HS patients with a higher inflammatory load.

$CCR7^+$ T cells distinctly expressed the lymph node homing receptors *CCR7* and *SELL,* which are downregulated in effector memory T cells, and had elevated expression of *IL7R*. *IL7R* is constitutively expressed by naïve/early differentiated CD4 T cells and becomes downregulated upon T cell receptor (TCR) stimulation (Colpitts, Dalton and Scott, 2009). FACS data presented here indicates the majority of T cells emigrating from HS skin were effector memory T cells, however there were $CCR7^+$ T cells identified, specifically in the CD4 cohort which may represent central memory T cells. Together, this suggests that the $CCR7^+$ T cells may be primarily composed of less differentiated or central memory CD4 T cells. Interestingly, this cluster of $CCR7^+$ CD4 T cells was enriched following anti-TNF treatment. Adalimumab has been shown to skew the balance of memory and naïve T cells, upregulating the presence of naïve CD4 T cells (Povoleri *et al.,* 2020). A reduction in inflammatory cytokine-producing effector CD4 T cell subsets in favour of less differentiated CD4 T cells in HS lesions following TNF inhibition may explain the broad downregulation of inflammatory pathways following adalimumab treatment seen in this study.

Interestingly, Treg cells were marginally increased in HS lesions relative to healthy controls. This may be surprising given their role in suppressing effector T cell function, however elevated frequencies of Treg cells have previously been reported in HS skin (Moran *et al.,* 2017). Despite the increase of Treg cells, the ratio of Th17:Treg cells was still heavily skewed in favour of Th17 cells in HS lesions (Moran *et al.,* 2017). In this dataset, the Treg cell cluster had characteristic expression of *FOXP3*, CD25 (*IL2RA*), *ICOS* and *CTLA4*, while also having reduced expression of *CD69* and increased expression of *SELL*, indicating that these may be central Treg cells which can home to lymphoid tissue (Miragaia *et al.,* 2019). Following anti-TNF therapy, the imbalance of Th17:Treg cells was restored (Moran *et al.,* 2017). This data elaborates on these findings from Moran *et al.,* identifying *ICOS* as significantly downregulated following anti-TNF therapy. *ICOS* was primarily expressed by Treg cells in this dataset, and in mice, $ICOS^+$ Treg cells have been shown to have higher proliferative and suppressive capacity than $ICOS^-$ Treg cells (Kornete, Sgouroudis and Piccirillo, 2012). Interestingly, Treg cells also secreted different cytokines depending on the presence or absence of ICOS. $ICOS^+$ Treg cells secreted large amounts of IL-10 and moderate concentrations of TGF-β, while $ICOS^-$ Treg cells predominantly secreted TGF-β (Gogali *et al.,* 2012). Taken together, these data suggest that anti-TNF therapy not only changes the frequency of Treg cells in HS lesions but may also impact Treg function in HS lesions.

Treg cells had the highest expression of *IL32*, confirming findings from previous studies (Han *et al.,* 2021). Interestingly, the $CD52^+$ CD4 T cell cluster expressed similar levels of *IL32*, indicating a potential link between this cluster and the Treg cell cluster. CD4 T cells expressing high levels of CD52 have previously been found to play an important role in T cell regulation (Bandala-Sanchez *et al.,* 2013). These cells inhibit T cell activation through soluble CD52 release, which binds to Siglec-10 receptor and subsequently impairs the phosphorylation of the T cell receptor associated kinases Lck and Zap70 (Bandala-Sanchez *et al.,* 2013). TNF inhibition has previously been shown to induce Treg expansion in RA (Nguyen and Ehrenstein, 2016). Although an increase in the frequency of Treg cells in HS lesions following TNF inhibition was not observed in this study, there was an increase in $CD52^+$ CD4 T cells. This coupled with an increase in CD52 expression following adalimumab treatment, identifies an interesting feature of adalimumab treatment in HS lesions.

This chapter also examined for the first time, the presence of T cells expressing TRM markers in HS skin. TRM cells are transcriptionally and functionally distinct to both central memory and effector T cells. TRM cells are non-recirculating lymphocytes which permanently reside in peripheral tissue including the skin and gastrointestinal tract. TRM cells have distinct surface expression of CD49a, CD69 and CD103. TRM cells have potent effector functions making them important therapeutic targets in disease and infection. TRM cells have been reported to play an important role in psoriasis, with an enrichment of TRMs found at the sites of recurrent psoriatic plaques which had previously healed (Cheuk *et al.,* 2014). Psoriasis lesions with more TRM cells were found to have thicker psoriatic plaques and more severe psoriasis than those with fewer TRM cells (Kurihara *et al.,* 2019). Similar to psoriasis, HS is a recurrent disease, in which up to 27% of patients have recurrent lesions at the same site as a previous deroofing surgery (Mehdizadeh *et al.,* 2015). This coupled with the expression of *CD103* by IL-17A^{+} IL-17F^{+} HS T cells (Kim *et al.,* 2023) suggests an important role for TRM cells in HS.

CD69 was expressed by the majority of T cells in this scRNA-seq data. It is important to note that in addition to being a marker of TRM cells, CD69 is also expressed on recently activated T cells, making it difficult to definitively identify TRM cells in inflamed tissues in humans. Using flow cytometry, the proposed TRM subsets were defined in HS and healthy control skin. Although there were no significant differences in the frequency of TRMs between HS and healthy skin, the greatest reduction was seen in the CD69^{+} CD103^{-} CD8 TRMs. CD8 TRMs have been shown to infiltrate the epidermis, however CD103^{-} CD8 TRMs are enriched in the dermis (Watanabe *et al.,* 2015). Both CD4 and CD8 TRMs have been shown to make higher concentrations of inflammatory cytokines and CD103^{+} TRMs in particular have potent effector function but limited proliferative capacity (Watanabe *et al.,* 2015). CD103^{-} TRMs on the other hand can rapidly respond to secondary infection, have greater migratory potential and proliferative capacity (Fung *et al.,* 2022). Importantly, in the context of HS, CD4 TRMs have been shown to form clusters in the dermis along with APCs around the hair follicle (Collins *et al.,* 2016). Given hair follicle occlusion and subsequent rupture is a key initiating event of HS, the localisation of TRM/APC clusters around the hair follicle in HS skin may result in rapid recognition of released DAMPs and subsequent activation of HS TRMs. Future investigations into the potential role of TRM cells in HS would ideally focus

on non-lesional skin where the expression of CD69 on T cells is less likely to be confounded by activation.

IL-17 family cytokines have previously been described as potential key drivers of HS inflammation (Moran *et al.*, 2017; Kelly *et al.*, 2015). However, the source of IL-17 in HS has come under some debate. Neutrophils have previously been reported to be a major source of IL-17 in HS lesions (Lima *et al.,* 2016). However, the ability of neutrophils to make IL-17 has been questioned, with no evidence of IL-17A or IL-17F mRNA or protein detected in purified neutrophils (Tamassia *et al.,* 2018). Neutrophils express IL-17 receptors which may bind IL-17A and lead to false positive results. MAIT cells may also contribute to the increase in IL-17 cytokine found in HS lesions. IL-17A producing MAIT cells were found to be elevated in HS lesions relative to normal skin of HS patients (Gallagher *et al.,* 2023), however Th17 cells appeared to be the predominant source of IL-17 in HS lesions (Moran *et al.,* 2017). γδ T cells are another potential source of IL-17, however these have not yet been characterised in HS. Innate lymphoid cells (Montero-Vilchez *et al.* 2022) are enriched in non-lesional HS skin compared with lesional skin, with the frequencies of ILC2 and ILC3 subsets found particularly enriched in HS non-lesional skin (Petrasca *et al.*, 2023b). Following activation with IL-1β and IL-23, ILC3 have been shown to produce IL-17 (Teunissen *et al.,* 2014).

In this chapter, HS skin had elevated frequencies of IL-17A$^+$ CD4 T cells relative to healthy controls. HS skin also have elevated frequencies of CD4 T cells co-expressing IL-17A and both IL-17F and IFN-γ in HS CD4 T cells. Polyfunctional T cells have been reported to be highly pathogenic in RA (Basdeo *et al.,* 2015), while an enrichment of polyfunctional CD4 T cells has been described in HS lesions (Moran *et al.,* 2017). Expanding on this, two clusters of Th17 cells were identified by scRNA-seq, Th17 (2) had elevated *IL17A* and *IL17F* expression, and Th17 (1) had elevated expression of CD161 (*KLRB1*). As the Th17 (1) cluster expressed lower levels of IL-17 cytokines, these cells may be ex-Th17 cells. Unfortunately, given the limited expression observed of the chemokine receptors which distinguish ex-Th17 from Th17 cells, *CCR4* and *CXCR3* (Basdeo *et al.,* 2017), it is difficult to confidently identify ex-Th17 cells in this dataset. *IL17A* was identified as one of the most upregulated genes in HS lesional T cells relative to healthy control T cells. Interestingly, anti-TNF therapy reduced IL-17 expression and the frequency of IL-17 expressing T cells in HS lesions. This

coincides with previous reports which demonstrated TNF inhibition suppresses *IL17A* expression, Th17 differentiation (Ho *et al.*, 2021; Sugita *et al.*, 2012) and dramatically reduces the frequency of Th17 cells in HS lesions (Moran *et al.,* 2017).

IL-1β and IL-23 are pivotal for the development of Th17 cells (Wilson *et al.*, 2007; Acosta-Rodriguez *et al.*, 2007). Although there was limited expression of IL-1 and IL-23 receptors in this dataset, the expression of these receptors was nonetheless concentrated in Th17 cells. *IL1R1* has been shown to be elevated in HS IL-17$^+$ T cells in HS lesions relative to psoriasis, whereas *IL23R* has higher expression in psoriasis IL-17$^+$ T cells relative to HS. This suggests that the IL-1β-Th17 axis is dominant in HS, whereas Th17 cells in psoriasis are predominantly activated by IL-23 (Kim *et al.,* 2023).

IL-17 and TNF were identified as important regulators of inflammatory gene expression in HS keratinocytes and fibroblasts, respectively. In the previous chapter, HS keratinocytes were shown to have an altered differentiation program to keratinocytes from healthy skin. Basal keratinocytes either differentiated into spinous keratinocytes or into inflammatory keratinocytes (Ma, Jia and Zhang, 2016), likely in response to proinflammatory mediators found in the HS microenvironment. In the skin, Th17 cells have previously been reported to target keratinocytes primarily (Nograles *et al.,* 2008), and this was confirmed in this study which highlighted Th17 cells as a key regulator of inflammatory gene expression in HS keratinocytes. Th17 cell derived IL-17A and IL-17F regulated the expression of AMPs (*S100A8* and *S100A9*) and proinflammatory chemokines (*CCL20* and *CXCL8*) in HS inflammatory keratinocytes. While IL-17A induced the secretion of proinflammatory mediators by keratinocytes, anti-TNF treatment, albeit in a small sample number, proved to have a profound effect on the expression of inflammatory mediators in HS keratinocytes. Keratinocytes isolated from patients treated with anti-TNF therapies had significantly reduced expression of *KRT16*, *KRT17* and *CXCL8*, and reduced TNF and IL-17 signaling, demonstrating an overall dampening of keratinocyte activation. However, evidence suggests that rather than TNF inhibition preventing HS keratinocyte activation by preventing TNF stimulation, these effects may be as a result of the reduced Th17 frequency and function following anti-TNF treatment. Anti-TNF therapy could also have an impact on other inflammatory pathways not discussed here, including those mediated by innate immune cells.

While the importance of IL-17A has been well described in HS, little is known about the role of IL-17F in promoting HS inflammation. This study has shown HS lesions with a high inflammatory load had increased expression of both IL17A and IL17F relative to HS lesions with a low inflammatory load. Comparisons between the effects of IL-17A and IL-17F portray an interesting dynamic between these related cytokines and have important implication for therapeutic interventions. Removal of IL-17A led to a compensatory increase in IL-17F, although knockout mouse models of both IL-17A and IL-17F did not elicit the same effects (Chong *et al.,* 2020). Other studies indicate that while a high degree of overlap is seen in the genes regulated by IL-17A and IL-17F, there are also unique signaling pathways regulated by each cytokine (Crawford, Borcherding and Karandikar, 2023). Interestingly, the heterodimer of IL-17A/F was found to have a much greater regulatory effect on the expression of inflammatory genes than either IL-17A or IL-17F homodimers (Crawford, Borcherding and Karandikar, 2023). Unfortunately, FACS data presented here demonstrating the co-expression of IL-17A and IL-17F in HS T cells cannot determine if these cells are making the homodimers of IL-17A and IL-17F or the IL-17AF heterodimer.

Brodalumab, which blocks cytokine binding to the IL-17 receptor IL-17RA, has been shown to effectively reduce inflammatory pathways in HS lesional and perilesional skin (Navrazhina *et al.*, 2022a). Treatment with brodalumab was also shown to reduce epidermal thickening and immune cell infiltration into lesional and perilesional HS skin (Navrazhina *et al.*, 2022a). Moreover, treatment with brodalumab has proven to be effective in a small cohort of patients who failed to respond to other biologic therapies (Kearney, Hughes and Kirby, 2023). Bimekizumab, which blocks both IL-17A and IL-17F proved to be more effective than adalimumab in a phase 2 trial, with 46% of patients treated with bimekizumab having at least a 75% reduction in disease severity compared with 32% of adalimumab-treated patients (Glatt *et al.,* 2021). Initial reports from the phase 3 trial of bimekizumab are encouraging with over 55% of patients reported to have a 75% reduction in disease severity at 48 weeks (UCB, 2023), however full trial results have yet to be published.

IL-17 cytokines were found to be less important in driving the inflammatory phenotype of HS fibroblasts than keratinocytes. IL-17 receptors were not expressed at sufficient levels for IL-17 cytokines to be included in the ligand:receptor interaction analysis. Despite this, a

number of genes found downstream of IL-17 were upregulated in inflammatory fibroblasts, including *CXCL8*, *CXCL1* and *CCL20*. These genes can also be induced by *TNF* and *TGFB1* in HS fibroblasts. *TNF* regulated the activation of reticular fibroblasts and the expression of neutrophil chemoattractants, *CXCL8* and *CXCL1,* and MMPs in inflammatory fibroblasts. *TGFB1* regulated the expression of collagens in reticular fibroblasts and *MMP9* expression by inflammatory fibroblasts in HS lesions. TGF-β has previously been shown to interact with fibroblasts, stimulating extracellular matrix production to facilitate wound healing (Denton *et al.,* 2009). Continued TGF-β signaling induces fibrosis (Mauviel, 2005), which is supported by findings here highlighting *TGFB1* as an important regulator of collagen and MMP expression in HS fibroblasts. This dysregulated expression of collagen and MMPs driven by T cell derived cytokines provides a novel mechanism which may drive hypertrophic scarring in HS skin.

IFN-γ, predominantly expressed by NK cells and cytotoxic CD8 T cells in this dataset, was also identified as a potential regulator of inflammatory gene expression in HS keratinocytes. Levels of IFN-γ are elevated in chronic HS wounds (Banerjee, McNish and Shanmugam, 2017) and coupled with the fact that CD8 T cells have been found to migrate through the papillary dermis and into the epidermis, suggests that IFN-γ may promote an inflammatory phenotype in HS keratinocytes. IFN-γ has previously been found to induce the release of IL-1α, GM-CSF and TNF from the keratinocytes of AD patients (Pastore *et al.,* 1998).

Ligand:receptor interaction analysis demonstrated great overlap between the genes regulated by IL-17A and those regulated by TNF in HS fibroblasts. When used in combination, a synergistic induction of inflammatory mediators in dermal fibroblasts was observed, both in this study and elsewhere (Witte-Handel *et al.,* 2019). Interestingly, anti-TNF therapy significantly reduced inflammatory signaling in HS fibroblasts, reducing the expression of MMPs, *CXCL1*, *CXCL8* and *S100A8*. As with TNF inhibition in keratinocytes, it is difficult to decipher if the dampening of inflammatory gene expression observed was a direct effect of blocking the TNF cytokine directly or if it is due to the a secondary effect such as the reduction of Th17 cells as a result of TNF inhibition (Moran *et al.,* 2017). Importantly, the induction of IL-6 by HS-TCM was significantly reduced following TNF

inhibition, suggesting that TNF directly activated fibroblasts, driving them towards an inflammatory state in HS lesions.

Despite the limited number of samples and inflammatory mediators evaluated in the *in vitro* work here which limits the conclusions drawn from these experiments, they broadly support the scRNA-seq data highlighting the role of IL-17 in keratinocytes and TNF in dermal fibroblasts as potent regulators of inflammatory gene expression. Further, these findings are supported by previous studies which have detailed the regulation of numerous inflammatory mediators, including MMPs, IL-6 and CXCL6 in dermal fibroblasts and healthy keratinocytes by IL-17A and TNF (Witte-Handel *et al.,* 2019).

Overall, this chapter has added to our understanding of the interactions between immune and non-immune cells in HS lesions. This study has, for the first time, characterised TRM cells in HS skin, identifying the characteristic $CD69^{+/-}$ and $CD103^{+/-}$ populations. Th17 cells were identified as a major source of the cytokines IL-17 and TNF in HS lesional T cells and this chapter outlined IL-17A, IL-17F, TNF and TGF-β as important regulators of inflammatory gene expression in HS keratinocytes and fibroblasts. Perhaps most notably, this chapter identified Th17 cells as important drivers of keratinocyte differentiation into an inflammatory phenotype in HS lesions. Interestingly, TNF, but not IL-17, predominantly mediated the expression of inflammatory genes in HS fibroblasts, demonstrating the complexity of HS whereby different cells appear to be differentially regulated by inflammatory cytokines. Finally, the dysregulated cytokine signaling seen in HS T cells, keratinocytes, and fibroblasts, was dramatically reduced following TNF inhibition, demonstrating the broad effects of TNF blockade *in vivo*. Considering the dysregulated T cell profile in HS lesions presented here, the next chapter will focus on the upstream regulators of T cells and investigate potential novel therapeutic strategies which may correct the dysregulated cytokine production in HS.

Chapter 6

Myeloid cells and the NLRP3 inflammasome in HS

6 Myeloid cells and the NLRP3 inflammasome in HS

6.1 Introduction

Previous chapters have detailed the dysregulated transcriptomic profiles of keratinocytes, fibroblasts and T cells in HS lesions and indicate HS T cells promote the development of inflammatory phenotypes in HS keratinocytes and fibroblasts. IL-17 and TNF proved to be pivotal mediators of inflammatory gene expression in HS keratinocytes and HS fibroblasts. Myeloid cells appear to play a central role in HS pathogenesis, being major producers of IL-1β and TNF, both of which have been reported to promote HS inflammation (Lowe *et al.*, 2020). In order to further understand the role of myeloid cells in HS inflammation, myeloid cells in HS peripheral blood and HS skin were analysed for markers of inflammation and indicators of dysfunction.

Myeloid cells including monocytes, macrophages and DCs have previously been implicated in HS inflammation. Myeloid-derived cytokines IL-23A and IL-1β both of which are elevated in HS lesions, play an important role in Th17 cell development (Kelly *et al.,* 2015; Schlapbach *et al.,* 2011). IL-23A drives the differentiation of T cells into Th17 cells and IL-1β promotes the development of Th17 cells (Wilson *et al.*, 2007; Acosta-Rodriguez *et al.*, 2007). These upstream regulators of Th17 cells have previously been the subject of investigation for therapeutic inhibition in HS with moderate success. The IL-23A inhibitor guselkumab demonstrated moderate efficacy in a phase II trial in HS patients with 65% of HS patients reaching HiSCR (Dudink *et al.,* 2023), describing at least a 50% reduction in disease activity in disease activity, while in a phase II trial for the IL-1 receptor antagonist, anakinra, 78% of HS patients achieved HiSCR (Tzanetakou *et al.,* 2016). Targeting the IL-1 receptor has an additional effect of inhibiting the signaling of both IL-1α and IL-1β. The discontinuation of a phase II trial for the IL-1α inhibitor bermekimab in HS patients, suggests that the effects of anakinra in HS patients may have been due to IL-1β signaling blockade (NCT04988308).

Monocytes have previously been found to be elevated in the peripheral blood of severe HS patients, and HS PBMC exhibited reduced production of IL-1β and IL-6 in response to LPS, *Candida albicans* and *Staphylococcus aureus* relative to healthy PBMC, suggesting that HS monocytes may be dysfunctional (Kanni *et al.,* 2015). However, the latter study did not specifically evaluate the response of HS peripheral monocytes.

HS lesional skin also had an upregulation of myeloid cells relative to healthy control skin, with dermal macrophages and DCs increased in HS lesions (Dajnoki *et al.,* 2022). Myeloid cells were a primary source of IL-1 signaling in HS lesions, with cDC2 cells in particular, expressing relatively high levels of *IL1A*, *IL1B* and *IL18* (Lowe *et al.*, 2020). IL-1 signaling has previously been shown to be hyperactive in HS lesions, with *IL1A*, *IL1B*, *CASP1* and *NLRP3* elevated in HS lesions relative to healthy controls (Witte-Handel *et al.,* 2019). While IL-1β promotes the development of Th17 cells, IL-1β also upregulates the expression of MMPs and CXCL1 in healthy keratinocytes and dermal fibroblasts, potentially implicating myeloid cells in dermal scarring and neutrophil recruitment in HS (Witte-Handel *et al.,* 2019). Hyperactive IL-1 signaling and increased *NLRP3* expression in HS lesions suggests that NLRP3 inflammasome activation may be a crucial component of HS inflammation. Further evidence of myeloid dysregulation in HS comes from a scRNA-seq study which described increased M1 macrophage polarisation and increased expression of type I and type II interferon responsive genes in myeloid cells in HS skin (Mariottoni *et al.,* 2021).

Following the investigation of cellular signaling downstream of Th17 cells in HS keratinocytes and fibroblasts, characterisation of the upstream regulators of Th17 cells was evaluated in HS patients. A study evaluating the function of myeloid cells in HS lesions and peripheral blood would provide novel insight into immune dysregulation in HS. Additionally, a study evaluating the therapeutic potential of NLRP3 inflammasome inhibition would be invaluable to the field considering the limited therapeutic strategies available to HS patients.

6.2 Aims

The aims of the experiments in this chapter were to characterise myeloid cells in HS patients and identify potential therapeutic targets dysregulated in these cells.

Specifically, this chapter aimed to:

- Define monocyte subsets in HS peripheral blood by flow cytometry.
    - Evaluate the activation status and cytokine production by monocytes from HS patients.
- Characterise the transcriptomic profile of myeloid cells in HS lesions.
    - Identify myeloid cell subsets in HS lesional and healthy control skin.
    - Identify inflammatory mediators and inflammatory pathways dysregulated in HS myeloid cells.
- Evaluate the therapeutic potential of NLRP3 inflammasome inhibition in HS lesions.
    - Determine the concentration of inflammatory mediators secreted from HS lesional and healthy control skin.
    - Evaluate the effect of inhibiting the NLRP3 inflammasome on the secretion of inflammatory mediators from HS lesions.

6.3 Results

6.3.1 Clinical details

HS patients were recruited at dermatological consultations at St Vincent's Hospital, Dublin (**Table 6.1**). Healthy controls were donated by healthy volunteers from St Vincent's Hospital and Trinity Biomedical Sciences Institute, Dublin (**Table 6.2**). All samples were processed on the day of sampling as per **Section 2.2.19**.

The mean age of the HS patients was 34.1 y ± SD of 9.9 (n=22) and 29.7 y ± SD of 2.9 (n=9) for healthy controls (**Table 6.1**-**Table 6.2**). There were 73% females (n=16) in the HS group and 78% females (n=7) in the healthy control group. 86% of HS patients were classified as Hurley stage 2 and 14% were classified as Hurley stage 3. HS patients had a mean BMI of 35.8 kg/m^2 ± SD of 6.5, compared with a BMI of 22.2 kg/m^2 ± SD of 1.9 in healthy controls. All healthy controls were classified as non-smokers, while only 14% of HS patients were classified as non-smokers. 9% of HS patients were ex-smokers and 73% of HS patients were classified as current smokers.

Table 6.1 Clinical details for HS patients. Clinical details of HS patients at the time of sampling, including age, sex, Hurley stage, body mass index (BMI), smoking status and medication HS patients were on at the time of sampling. E-S: ex-smoker, F: female, M: male, Nrm: no relevant medications, N-S: non-smoker, S: smoker, n/a: data not available.

Patient ID	Age (y)	Sex	Hurley	BMI	Smoker	Medication	Analysis
BK083	27	F	2	35.6	S	Nrm	Monocyte isolation
BK084	n/a	F	3	39.9	n/a	Nrm	Monocyte isolation
BK085	24	M	2	43.8	S	Nrm	Monocyte isolation
BK086	27	F	2	34	N-S	Adalimumab, Metformin	Monocyte isolation
BK087	30	F	2	28.3	S	Nrm	Monocyte isolation
BK088	28	M	2	44	S	Nrm	Monocyte isolation
BK089	33	F	2	36.3	S	Nrm	Monocyte isolation
BK091	48	F	2	31.9	S	Nrm	Flow Cytometry, Monocyte isolation
BK092	45	F	2	34	S	Metformin	Flow Cytometry, Monocyte isolation
BK093	32	F	2	56	S	Nrm	Flow Cytometry, Monocyte isolation
BK094	19	M	2	36.9	E-S	Nrm	Flow Cytometry
BK095	38	F	3	30.8	S	Nrm	Flow Cytometry
BK096	63	M	2	31.2	S	Metformin	Flow Cytometry
BK097	24	M	2	32.9	N-S	Nrm	Flow Cytometry
BK098	40	F	2	33.3	S	Nrm	Inflammasome assay
BK100	31	F	2	30	S	Nrm	Inflammasome assay
BK101	34	M	2	25	S	Nrm	Inflammasome assay
BK102	39	F	2	43.3	S	Nrm	Inflammasome assay

Patient ID	Age (y)	Sex	Hurley	BMI	Smoker	Medication	Analysis
BK103	38	F	2	33.5	S	Nrm	Flow Cytometry, Monocyte isolation
BK104	n/a	F	2	38	S	Nrm	Flow Cytometry, Monocyte isolation
BK105	n/a	F	3	37.8	E-S	Rifampicin, Clindamycin	Flow Cytometry, Inflammasome assay
BK106	28	F	2	31.4	N-S	Nrm	Flow Cytometry, Inflammasome assay
	Mean 34.1 SD 9.9	73% F, 27% M	86% 2 14% 3	Mean 35.8 SD 6.5	73% S 9% E-S 14% N-S		

Table 6.2 Clinical details for healthy controls. Clinical details of healthy controls at the time of sampling, including age, sex, Hurley stage, body mass index (BMI), smoking status and medication HS patients were on at the time of sampling. F: female, M: male, Nrm: no relevant medications, N-S: non-smoker, n/a: data not available.

Patient ID	Age (y)	Sex	BMI	Smoker	Medication	Analysis
HC048	31	F	20.5	N-S	Nrm	Flow Cytometry, Monocyte isolation
HC049	28	F	21	N-S	Nrm	Flow Cytometry, Monocyte isolation
HC054	32	F	20.3	N-S	Nrm	Flow Cytometry
HC050	31	F	22.2	N-S	Nrm	Flow Cytometry, Monocyte isolation
HC051	29	F	21.5	N-S	Nrm	Flow Cytometry, Monocyte isolation
HC052	34	M	25.4	N-S	Nrm	Flow Cytometry, Monocyte isolation
HC053	32	M	24.9	N-S	Nrm	Flow Cytometry, Monocyte isolation
HC046	24	F	n/a	N-S	Nrm	Monocyte isolation
HC047	27	F	n/a	N-S	Nrm	Monocyte isolation
	Mean 29.7 SD 2.9	78% F, 22% M	Mean 22.2 SD 1.9	100% N-S		

6.3.2 Enumeration of monocyte populations in the peripheral blood of HS patients and healthy controls

In order to characterise monocytes in the blood of HS patients (**Table 6.1**) and healthy controls (**Table 6.2**), PBMC were isolated from whole blood as per **Section 2.1.5**. Cells were stained as per **Section 2.2.8** for surface expression of monocyte markers **Section 2.1.11**. A gating strategy for identifying $CD45^+$ immune cells is shown in **Figure 6.1**. Briefly, the ungated sample was plotted for FSC-area (FSC-A) vs Fixable Viability dye eFluor506 (FixVia eFluor506) to identify live cells (**Figure 6.1A**). Next, immune cells were identified as $CD45^+$ in the FSC-A vs CD45 plot (**Figure 6.1B**). Doublets were removed and single cells identified by FSC-A vs FSC-width (FSC-W) profile (**Figure 6.1C**). There was no significant difference between the absolute number of immune cells per ml of blood in HS patient and healthy control peripheral blood (**Figure 6.1D**).

Monocytes were identified using the gating strategy shown in **Figure 6.2**, which continues on from the identification of live, single, immune cells in **Figure 6.1**. Briefly, myeloid cells were gated based on their characteristic FSC vs SSC profile, which also excludes lymphocytes (**Figure 6.2A**). Lymphocytes potentially remaining from the previous gate were removed with HLA-DRA vs FSC due to their lack of HLA-DRA expression (**Figure 6.2B**); then monocytes were classified as $CD14^+$ and/or $CD16^+$ (**Figure 6.2C**). The lineage marker, which stains T cells (CD3), B cells (CD19, CD20) and NK cells (CD56), was used to validate the removal of lymphocytes in the myeloid cells gate (data not shown). Classical monocytes were classified as $CD14^+CD16^-$, intermediate monocytes were $CD14^+$ $CD16^+$ and non-classical monocytes were $CD14^-$ $CD16^+$ (**Figure 6.2D**). Having established a PBMC gating strategy, monocytes attributed to ~10% of immune cells in healthy controls and ~15% in HS patients, however this difference failed to reach significance (**Figure 6.2E**). Similarly, there was a trend towards an increase of monocytes per ml of blood in HS patients compared with healthy controls, but this failed to reach significance.

There were no differences in the frequency of classical or intermediate monocytes within the monocyte gate (**Figure 6.3A-B**). However, there was a trend towards an increase in the frequency of non-classical monocytes within the monocyte gate in healthy controls compared with HS patients (**Figure 6.3C**). The frequency of classical and intermediate monocytes within the single, $CD45^+$ cell gate relative to healthy controls, and the absolute

number of both classical and intermediate monocytes per ml of blood trended towards an increase in HS patients compared with healthy controls (**Figure 6.3D-E**, **G-H**). There were no differences in the frequency of non-classical monocytes within the single, $CD45^+$ cell gate, or in the absolute number of non-classical monocytes per ml of blood between HS patients and healthy controls (**Figure 6.3F**, **I**).

In summary, no significant differences in the frequency or absolute number of monocytes or monocyte subsets were observed in the PBMC of HS patients relative to healthy controls.

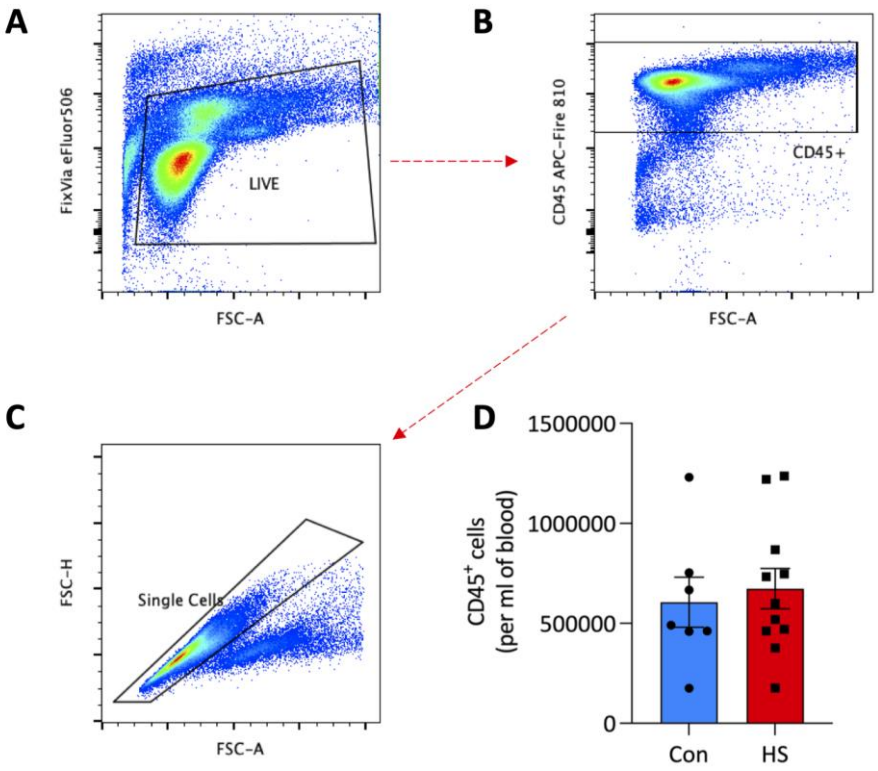

Figure 6.1 Plots representing the gating strategy to identify CD45$^+$ immune cells in the peripheral blood. PBMC from healthy controls (Con; n=7) or HS patients (n=11) were stained for surface markers and analysed by flow cytometry. To identify CD45$^+$ cells sequential gating was performed; Forward Scatter-Area (FSC-A) vs Fixable-Viability-Dye$^-$ to identify viable cells (A); FSC-A vs CD45 to identify immune cells (B); FSC-A vs FSC-Height (FSC-H) to exclude doublets (C). Plot shows the absolute number of live, single, CD45$^+$ cells per ml of blood in HS and healthy controls. Graphs represent individual samples with a mean ± SEM for each group. Statistical significance was calculated using Mann Whitney U test.

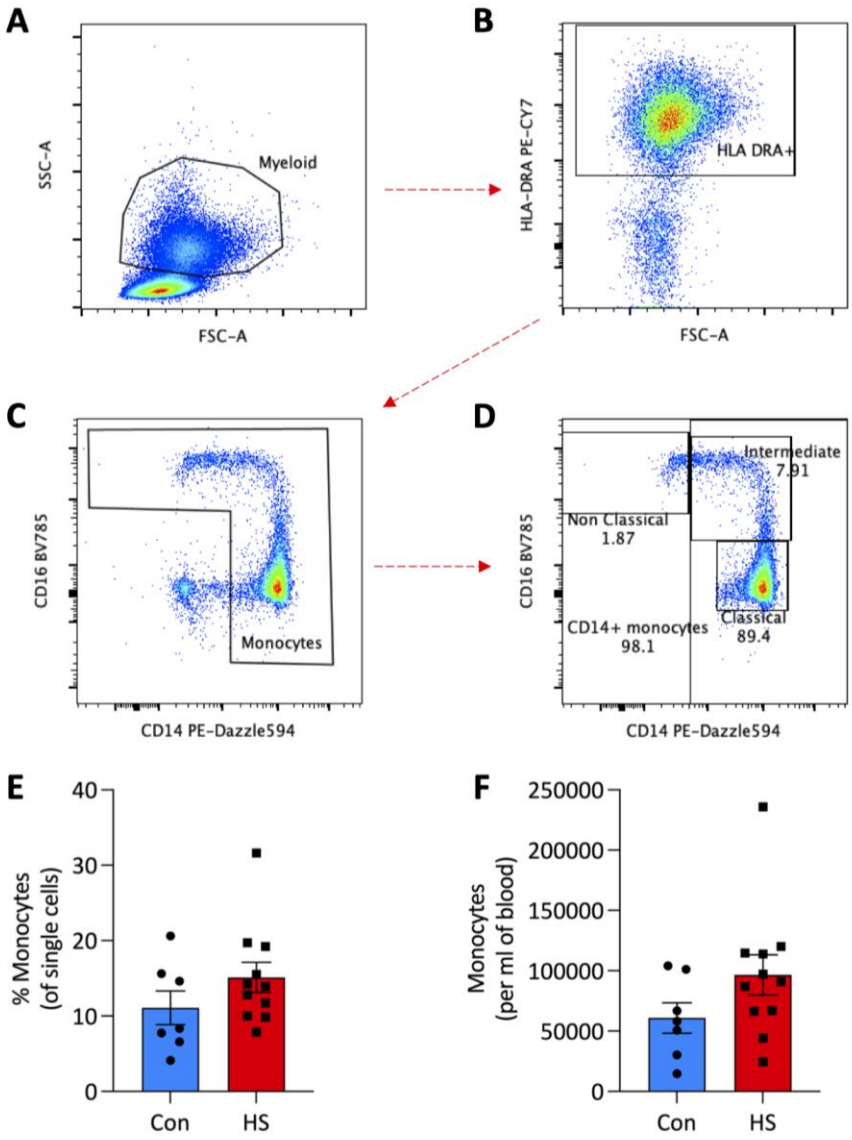

Figure 6.2 Plots representing the gating strategy to identify monocyte populations in peripheral blood. PBMC from healthy controls (Con; n=7) or HS patients (n=11) were stained for surface markers and analysed by flow cytometry. To identify classical, intermediate and non-classical monocyte populations cells were gated for live, single CD45$^+$ cells as per **Figure 6.1**. From there sequential gating was performed; Side Scatter-Area (SSC-A) vs FSC-A to exclude lymphocytes (A); FSC-A vs HLA-DRA to identify HLA$^+$ myeloid cells (B); CD14 vs CD16 to identify monocytes (C). Monocytes were gated into CD14$^+$ CD16$^-$ classical monocytes, CD14$^+$ CD16$^+$ intermediate monocytes or CD14$^-$ CD16$^+$ non classical monocytes (D). Plots show the frequency of total monocytes within the live, single, CD45$^+$ gate (E) and the absolute number of monocytes per ml of blood in HS and healthy controls (F). Graphs represent individual samples with a mean ± SEM for each group. Statistical significance was calculated using Mann Whitney U test.

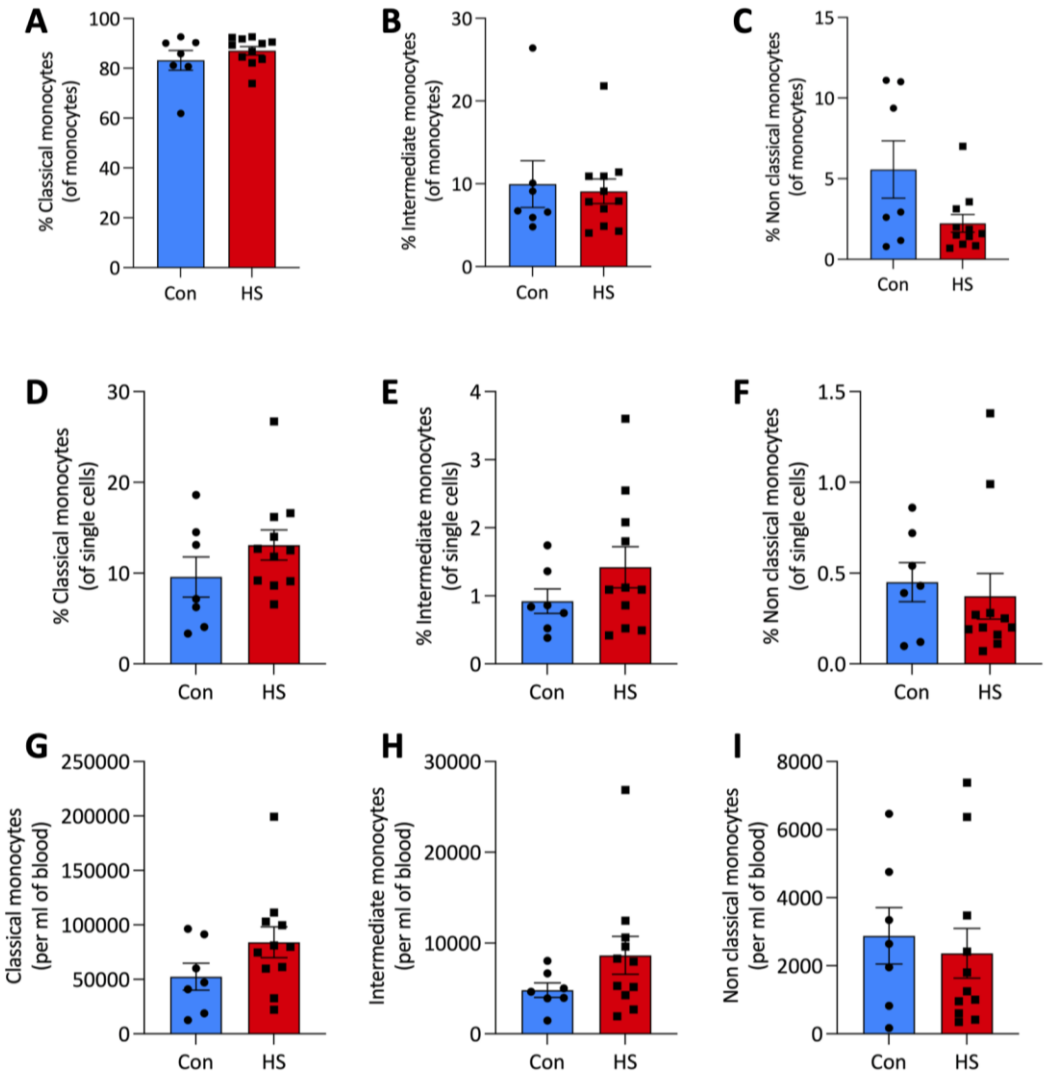

Figure 6.3 Frequency of classical and intermediate monocytes in HS and healthy control peripheral blood. PBMC from healthy controls (Con; n=7) or HS patients (n=11) were stained for surface markers, and analysed by flow cytometry. Graphs show the frequency of classical (A, D), intermediate (B, E) and non-classical (C, F) monocytes within the monocyte and single cell gate and the absolute number of classical (G), intermediate (H) and non-classical (I) monocytes per ml of blood. Graphs represent individual samples with a mean ± SEM for each group. Statistical significance was calculated using Mann Whitney U test.

6.3.3 Reduced activation of monocytes in HS patient peripheral blood

Having established that there were no significant differences in the frequency or absolute numbers of monocytes in HS patients vs healthy controls, next activation markers expressed by monocytes were assessed to ascertain if monocytes were differentially activated in HS compared with healthy controls. Markers typically involved in monocyte activation were investigated, including costimulatory molecules CD40, CD80 and CD86, HLA-DR, which is crucial for antigen presentation, CD14, loss of which is an indicator of monocyte activation, and CD64. CD64 is involved in a number of different immune processes, including phagocytosis, antibody-dependent cell mediated cytotoxicity and is also a marker for macrophage differentiation.

In order to investigate monocyte activation, the expression of activation markers was evaluated in each monocyte subset in both HS and healthy controls. Intermediate monocytes had elevated expression of CD40, CD80, CD86 and HLA-DR relative to both classical and non-classical monocytes in healthy controls (**Figure 6.4A-D**). In HS, intermediate monocytes had elevated expression of CD80, CD86 and HLA-DR, but not CD40 relative to classical and non-classical monocytes (**Figure 6.4A-D**). Interestingly, the expression of CD40 and CD86 markers were significantly decreased, while CD80 and HLA-DR trended towards a decrease in HS intermediate monocytes relative to healthy controls (**Figure 6.4A-D)**. Furthermore, classical monocytes had decreased CD40 expression and non-classical monocytes had decreased CD86 expression in HS patients relative to healthy controls (**Figure 6.4A, C)**. Overall, each monocyte subset had reduced expression of activation markers in HS peripheral blood compared with healthy controls.

There was also a trend towards an increase in CD64 expression in HS intermediate monocytes relative to healthy controls, indicating HS monocytes may be dysregulated (**Figure 6.5A**). Once monocytes become activated, the surface expression of CD14 decreases and soluble CD14 is released (Shive *et al.,* 2015). HS intermediate monocytes had a significant increase in CD14 expression relative to healthy control intermediate monocytes, suggesting reduced activation of HS intermediate monocytes (**Figure 6.5B**). Non-classical monocytes did not express CD64 or CD14.

Taken together, HS monocytes exhibited decreased expression of costimulatory markers CD40, CD80 and CD86, increased expression of CD14 suggesting decreased activation and reduced expression of HLA-DR required for antigen presentation. These data suggest that peripheral HS monocytes may be dysfunctional, with potentially reduced antigen presenting capacity and dampened activation.

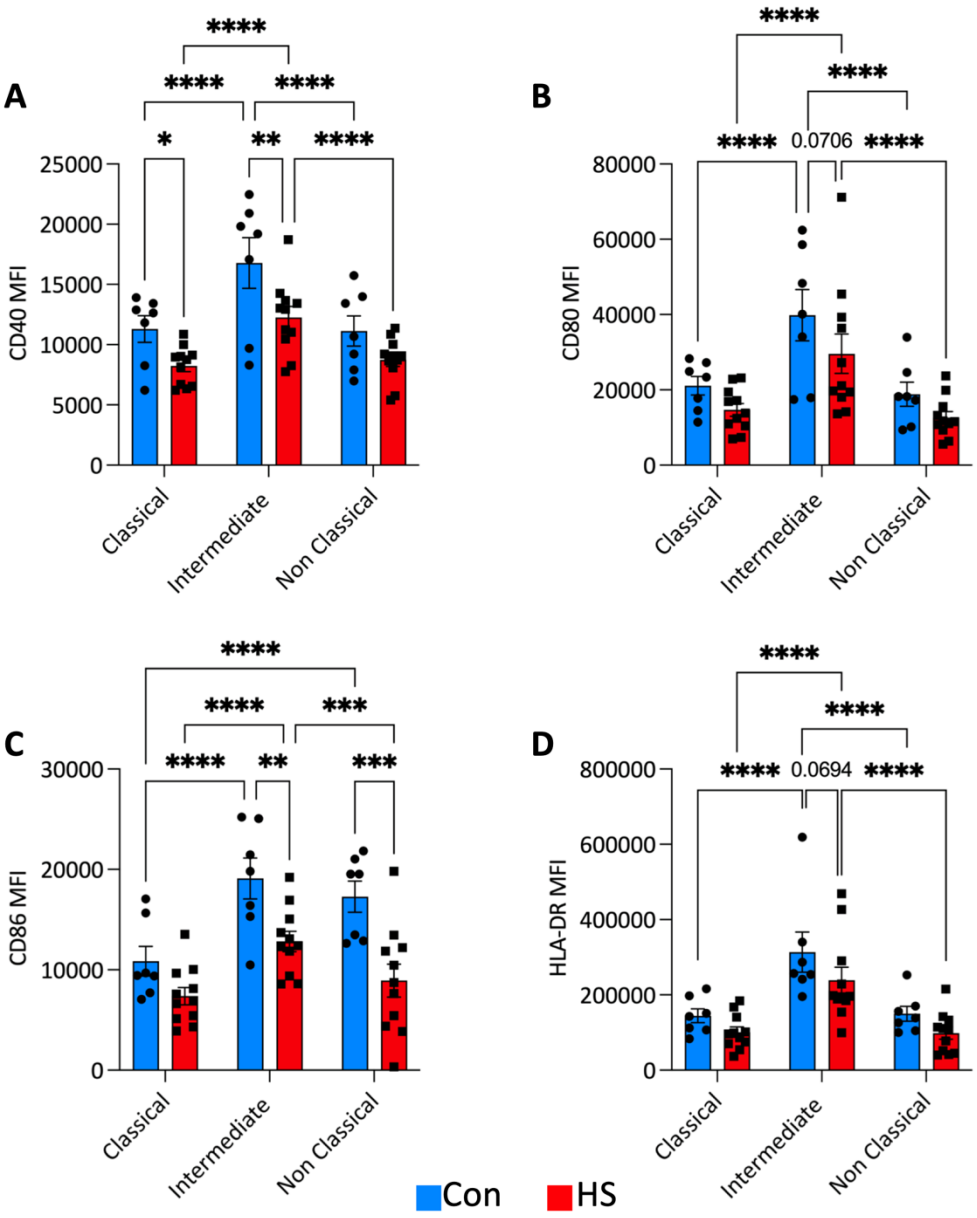

Figure 6.4 HS monocytes have reduced fluorescence intensity of activation markers compared with healthy control monocytes. PBMC from healthy controls (Con; n=7, blue) or HS patients (n=11, red) were stained for surface markers and analysed by flow cytometry. Graphs illustrate the mean fluorescence intensity (MFI) of CD40 (A), CD80 (B), CD86 (C) and HLA-DR (D) in classical, intermediate and non-classical monocytes in PBMC of HS patients and healthy controls. Graphs represent individual samples with a mean ± SEM for each group. Statistical significance was calculated using 2-way ANOVA with uncorrected Fisher's LSD test, * p <0.05, ** p <0.01, *** p <0.001, **** p <0.0001.

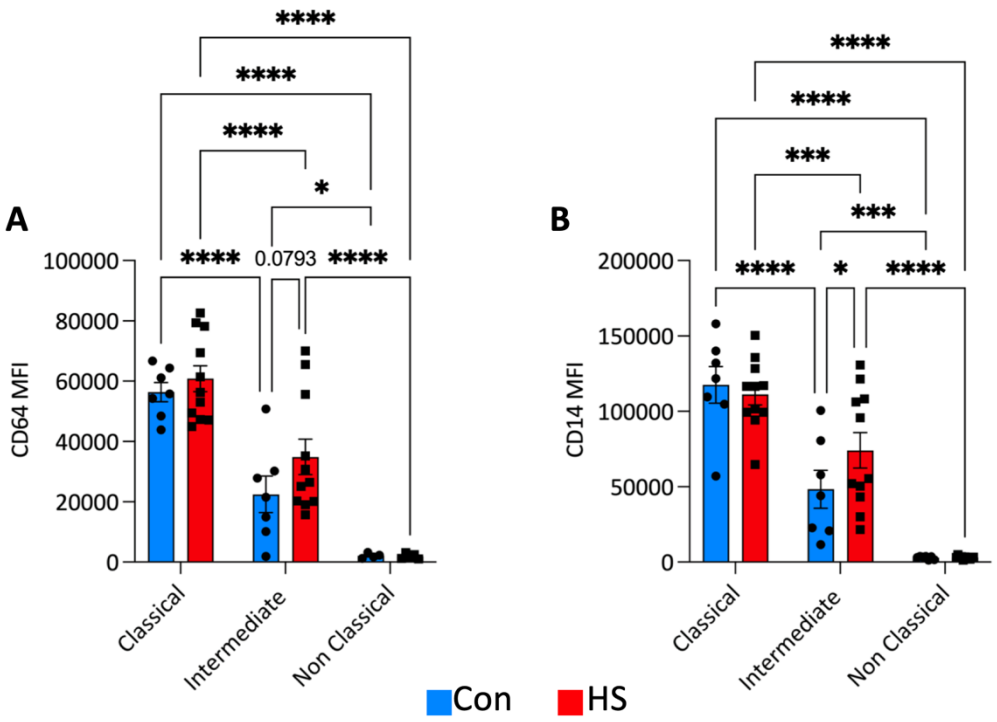

Figure 6.5 HS intermediate monocytes had increased fluorescence intensity of CD64 and CD14 compared with healthy control monocytes. PBMC from healthy controls (Con; n=7, blue) or HS patients (n=11, red) were stained for surface markers and analysed by flow cytometry. Graphs illustrate the mean fluorescence intensity (MFI) of CD64 (A), CD14 (B) in classical, intermediate and non-classical monocytes in PBMC of HS patients and healthy controls. Statistical significance was calculated using 2-way ANOVA with uncorrected Fisher's LSD test, * p <0.05, ** p <0.01, *** p <0.001, **** p <0.0001.

6.3.4 HS monocytes had an elevated TLR2/dectin response compared with healthy controls

While there was no significant difference in the frequency of monocytes in HS patients relative to healthy controls, the previous section suggested that HS monocytes may be dysfunctional. Reduced expression of costimulatory markers by HS monocytes, coupled with reduced HLA-DR and increased CD64 suggested that HS monocytes may be functionally impaired. The next experiments were designed to evaluate the ability of HS monocytes to respond to different TLR agonists, mimicking their role in fighting invading pathogens in the body.

PBMC were stimulated with the TLR4 agonist LPS or the TLR2/dectin agonist zymosan for 3 h and the expression of activation markers and cytokine production were evaluated by flow cytometry. Subsequent analysis was performed on gated $CD14^+$ monocytes, which grouped intermediate and classical monocytes together, to align with experiments isolating $CD14^+$ monocytes from peripheral blood. LPS did not induce the expression of CD40, CD80, CD86 and HLA-DR in HS or healthy control $CD14^+$ monocytes (**Figure 6.6A-D**). Interestingly, following LPS stimulation, HS monocytes had reduced expression of CD80 and HLA-DR and a trend towards a reduction in CD86 expression relative to healthy controls, supporting the idea that HS monocytes may be dysfunctional (**Figure 6.6A-D**). Upon zymosan stimulation, monocytes had increased expression of CD40 and CD86, and reduced CD80 and HLA-DR expression relative to unstimulated monocytes, in both HS and healthy donors (**Figure 6.6A- D**).

Stimulation with LPS induced the expression of CD64 in both HS and healthy control $CD14^+$ monocytes, suggesting that LPS stimulation may promote differentiation of monocytes into macrophages or DCs (**Figure 6.7A-B**). Upon stimulation with zymosan, HS $CD14^+$ monocytes had elevated expression of CD64 relative to healthy controls, suggesting that HS monocytes may be primed to differentiate upon TLR2 stimulation (**Figure 6.7A**). Similar CD14 expression was seen between both HS and healthy controls in the unstimulated and LPS stimulated $CD14^+$ monocytes, while zymosan treated $CD14^+$ monocytes had reduced expression of CD14 (**Figure 6.7B**).

Next, cytokine production was evaluated in HS and healthy control monocytes to determine if HS monocytes had an altered inflammatory response. Representative plots display the expression of TNF vs IL-12 (p40/p70), IL-1β vs IL-6 and IL-1β vs TNF on $CD14^+$ monocytes in HS patient peripheral blood (**Figure 6.8A-C**). Due to the negligible IL-12 (p40/p70) expression in stimulated monocytes, the frequency of IL-12 (p40/p70) producing monocytes was not shown.

Upon stimulation with LPS the frequency of IL-1β producing monocytes increased within the $CD14^+$ monocyte and the single, $CD45^+$ cell gate in both HS and healthy controls relative to unstimulated $CD14^+$ monocytes (**Figure 6.9A-B**). Interestingly, there was a trend towards an increase in the frequency of IL-$1\beta^+$ monocytes in HS relative to healthy controls following zymosan stimulation (p=0.067)(**Figure 6.9B**). LPS induced IL-6 expression in $CD14^+$ monocytes and interestingly, the frequency of IL-6^+ $CD14^+$ monocytes trended towards an increase in HS patients relative to healthy controls (p=0.069)(**Figure 6.9C-D**). Although zymosan did not induce IL-6 production to the same extent as LPS stimulation, there was a significant increase in the frequency of IL-6 producing $CD14^+$ monocytes in HS patients relative to healthy controls (**Figure 6.9C-D**). Similarly, while LPS induced TNF expression in both healthy and HS $CD14^+$ monocytes, the frequency of TNF^+ $CD14^+$ monocytes following zymosan stimulation was significantly elevated in HS compared with healthy controls (**Figure 6.9E-F**).

Considering the increased frequency of cytokine-producing monocytes in HS patients following zymosan stimulation relative to healthy controls, the concentration of inflammatory mediators secreted from HS and healthy control $CD14^+$ monocytes was assessed. $CD14^+$ monocytes were purified from PBMC by CD14 positive selection MACS and stimulated with LPS or zymosan for 24 h. While cytometric analysis facilitates analysis of monocytes from PBMC, using purified monocytes may overcome some limitations associated with using PBMC. Stimulating PBMC with TLR agonists may activate other cells within the cellular milieu of PBMC to produce inflammatory cytokines which can then promote monocyte activation. Using purified monocytes would circumvent any indirect activation from other cell populations and account for TLR stimulation alone. Concentrations of IL-1β, TNF, and IL-6 in the supernatants were assessed by ELISA (**Figure**

6.10A-C). LPS induced the secretion of IL-1β, TNF and IL-6 in both healthy and HS $CD14^+$ monocytes (**Figure 6.10A-C**). Similar levels of IL-1β and TNF was seen in both HS and healthy control $CD14^+$ monocytes following LPS stimulation, while HS $CD14^+$ monocytes secreted significantly higher concentrations of IL-6 relative to healthy control $CD14^+$ monocytes (**Figure 6.10A-C**). Surprisingly, upon stimulation with zymosan, HS $CD14^+$ monocytes secreted elevated concentrations of IL-1β, TNF and IL-6 relative to healthy control $CD14^+$ monocytes (**Figure 6.10A-C**). Importantly, zymosan stimulation induced significantly elevated secretion of IL-1β and TNF in HS monocytes compared to LPS stimulated monocytes, indicating a specifically heightened response to TLR2/dectin stimulation (**Figure 6.10A-C**).

Taken together, these data suggest that HS monocytes may be dysregulated compared with healthy control monocytes. HS monocytes appear to be primed to differentiate and exhibited an increased inflammatory response relative to healthy control monocytes in response to a TLR2/dectin agonist.

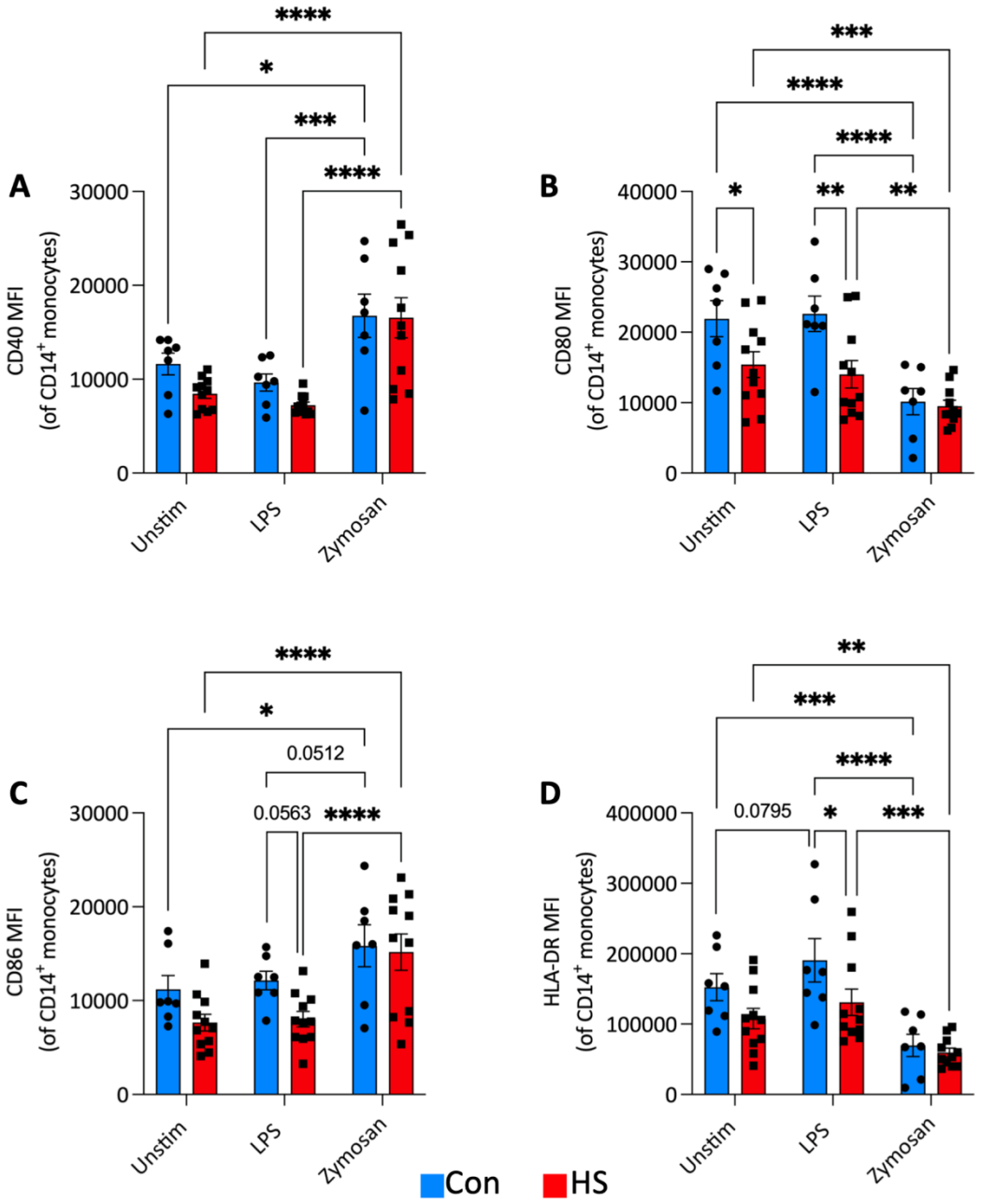

Figure 6.6 Zymosan induced the expression of activation markers in CD14+ monocytes. PBMC from healthy controls (Con; n=7) or HS patients (n=11) were stimulated with LPS (100 ng/ml) or zymosan (1 μg/ml) and treated with Brefeldin A for 3 h, stained for surface and intracellular markers, and analysed by flow cytometry. Graphs illustrate the mean fluorescence intensity (MFI) of CD40 (A), CD80 (B), CD86 (C), HLA-DR (D) in $CD14^+$ monocytes (classical and intermediate monocytes) in PBMC of HS patients and healthy controls. Graphs represent individual samples with a mean ± SEM for each group. Statistical significance was calculated using 2-way ANOVA with uncorrected Fisher's LSD test, * $p < 0.05$, ** $p < 0.01$, *** $p < 0.001$, **** $p < 0.0001$.

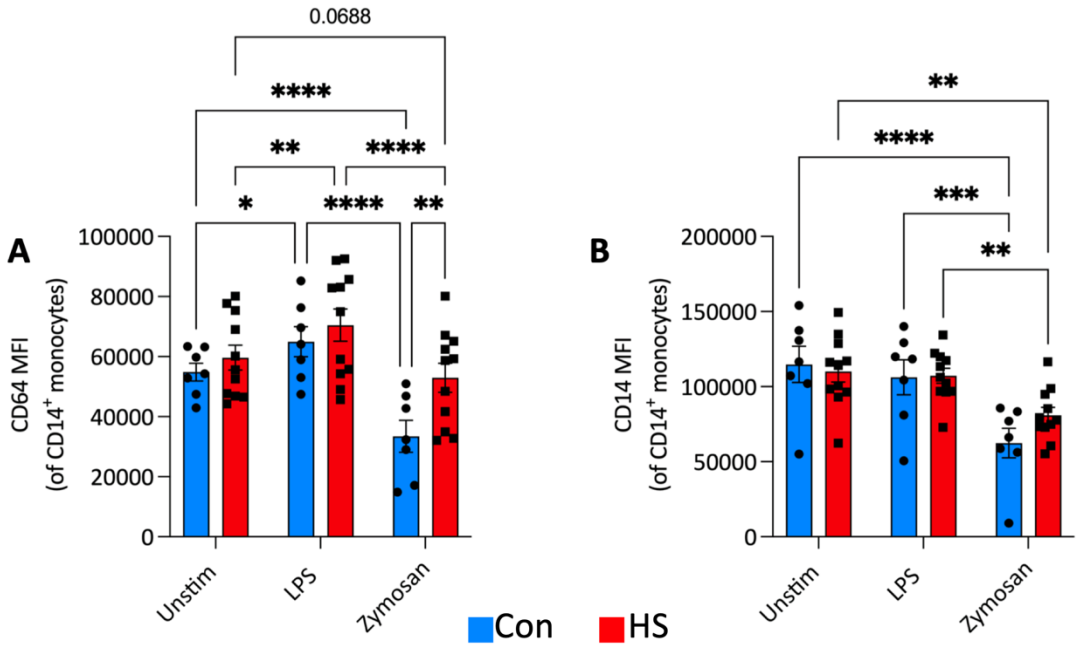

Figure 6.7 Zymosan induces the expression of CD64 in CD14+ monocytes. PBMC from healthy controls (Con; n=7) or HS patients (n=11) were stimulated with LPS (100 ng/ml) or zymosan (1 μg/ml) and treated with Brefeldin A for 3 h, stained for surface and intracellular markers, and analysed by flow cytometry. Graphs illustrate the mean fluorescence intensity (MFI) of CD64 (A), CD14 (B) in $CD14^+$ monocytes (classical and intermediate monocytes) in PBMC of HS patients and healthy controls. Graphs represent individual samples with a mean ± SEM for each group. Statistical significance was calculated using 2-way ANOVA with uncorrected Fisher's LSD test, * $p < 0.05$, ** $p < 0.01$, *** $p < 0.001$, **** $p < 0.0001$.

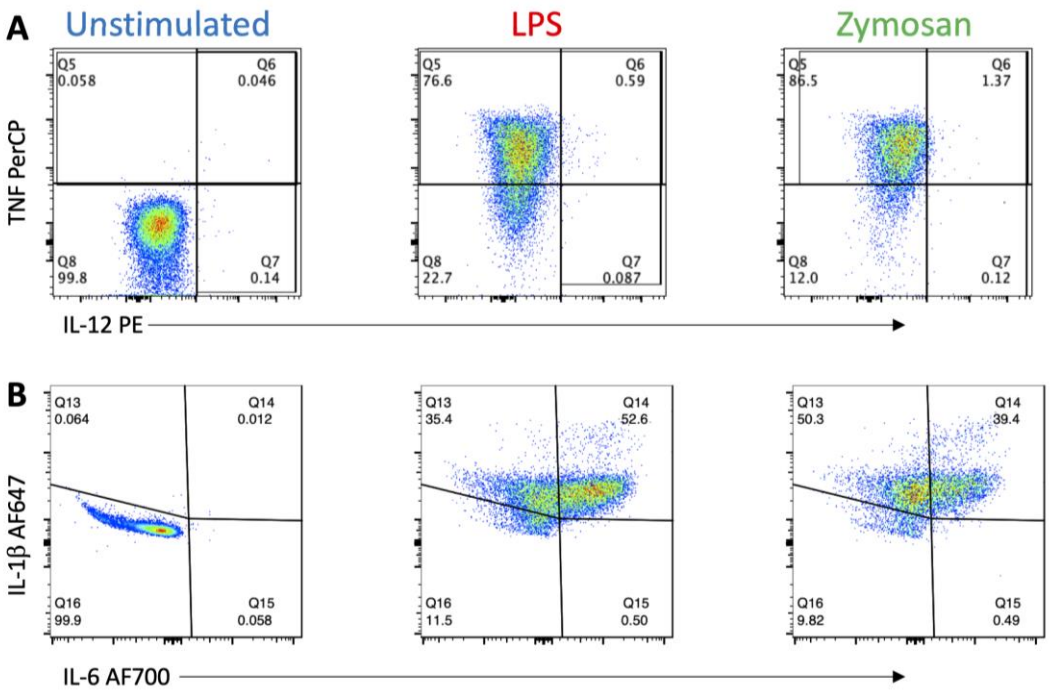

Figure 6.8 Plots representing the gating strategy to identify monocyte populations in the peripheral blood. PBMC from healthy controls (Con; n=7) or HS patients (n=11) were stimulated with LPS (100 ng/ml, centre) or zymosan (1 μg/ml, right) and treated with Brefeldin A for 3 h, stained for surface and intracellular markers, and analysed by flow cytometry. Representative dot plots display expression of cytokines TNF vs IL-12 (p40/p70) (A), IL-1β vs IL-6 (B) and IL-1β vs TNF (C) in HS peripheral blood.

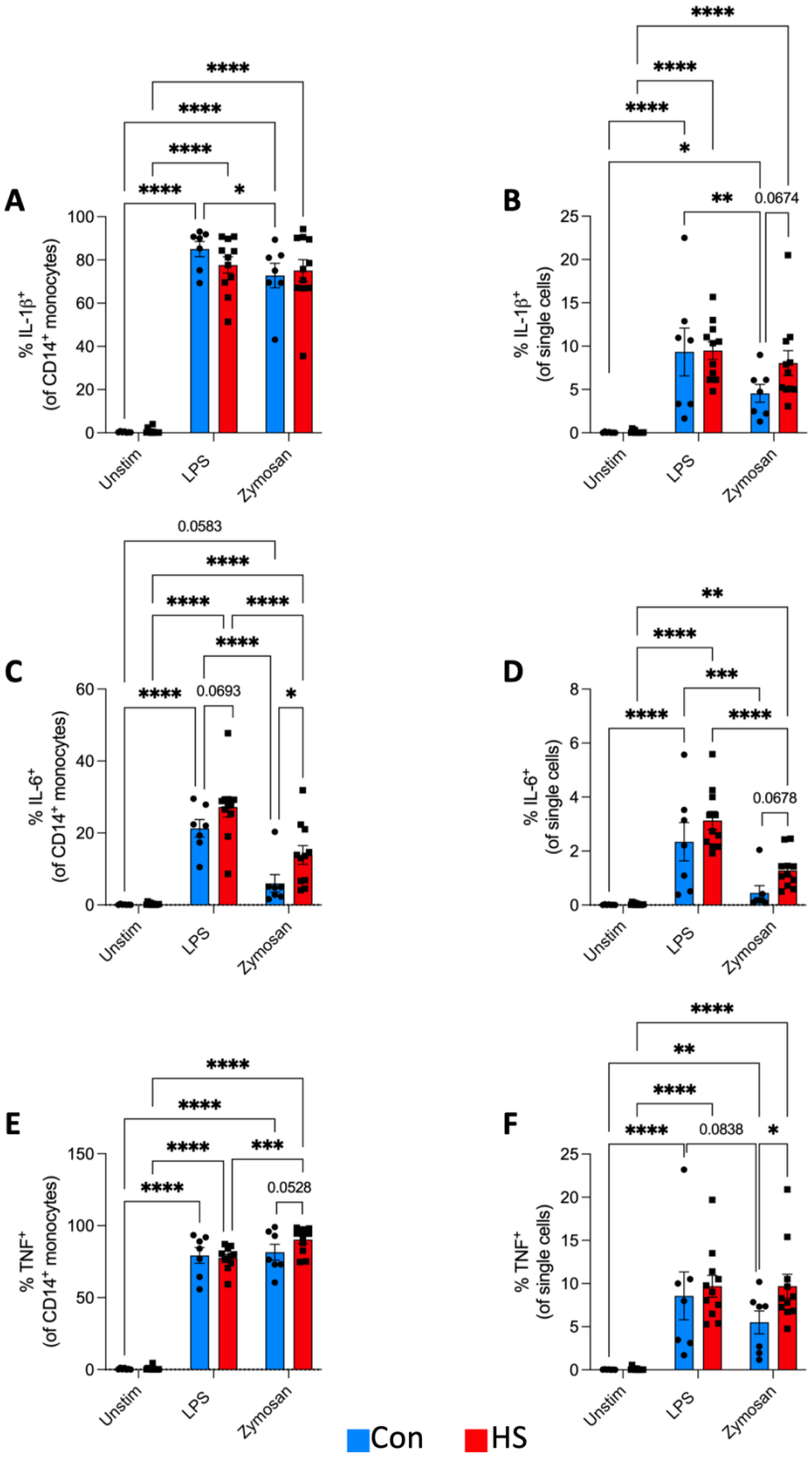

Figure 6.9 increased cytokine production following TLR2/dectin agonism in HS monocytes compared with healthy control monocytes. PBMC from healthy controls (Con; n=7) or HS patients (n=11) were stimulated with LPS (100 ng/ml) or zymosan (1 μg/ml) and treated with Brefeldin A for 3 h, stained for surface and intracellular markers, and analysed by flow cytometry. Graphs show the frequency of IL-1β+ (A, B), IL-6+ (C, D) and TNF+ (E, F) monocytes within CD14+ monocytes and the single cell gate. Graphs represent individual samples with a mean ± SEM for each group. Statistical significance was calculated using 2-way ANOVA with uncorrected Fisher's LSD test, * p <0.05, ** p <0.01, *** p <0.001, **** p <0.0001.

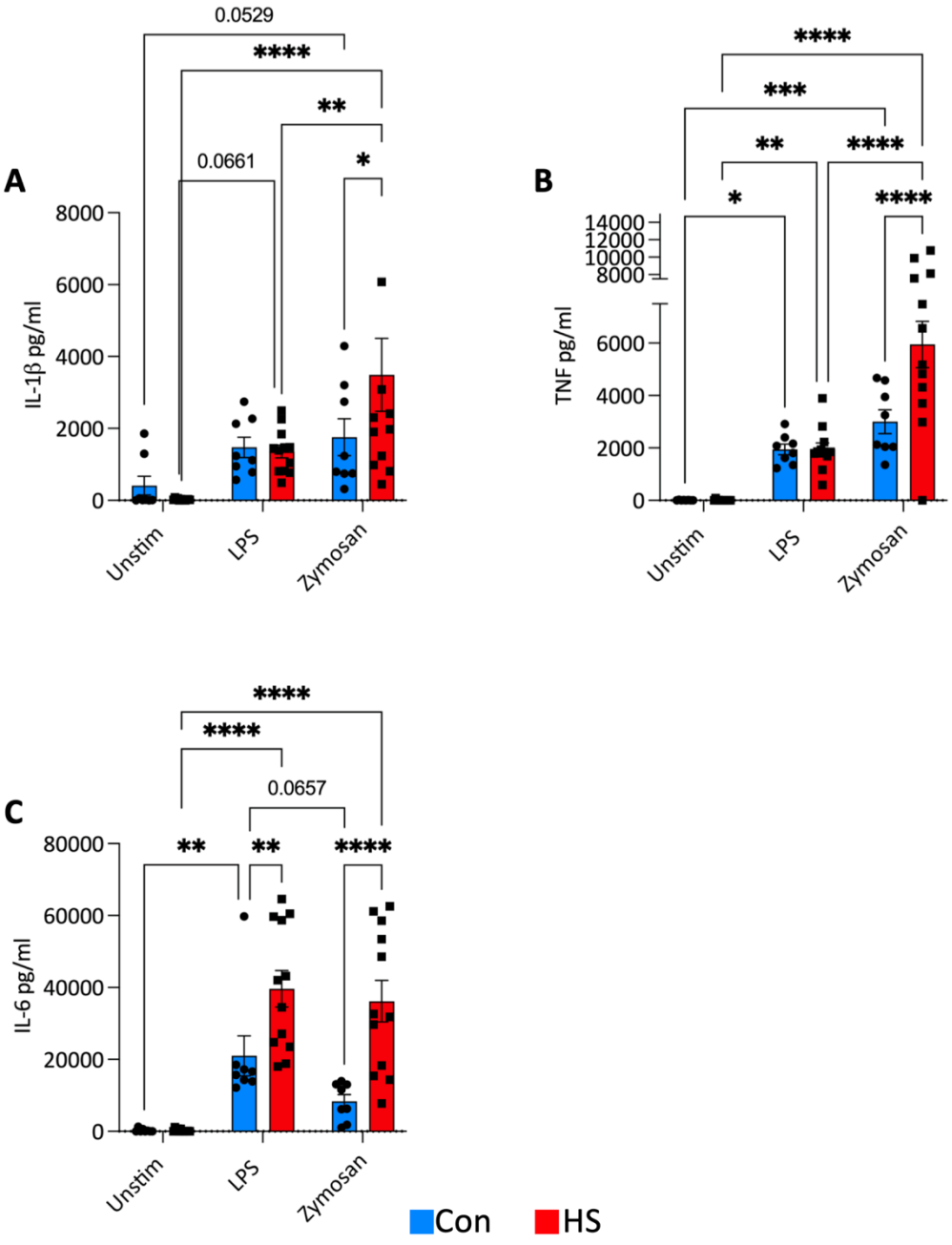

Figure 6.10 HS CD14$^+$ monocytes have elevated cytokine secretion in response to TLR2/dectin agonist. CD14$^+$ cells were purified from PBMC of healthy controls (Con; n=8) or HS patients (n=12) by MACS. Purified CD14$^+$ cells were stimulated with LPS (100 ng/ml, centre) or zymosan (1 μg/ml) for 24 h. The concentrations of IL-1β (A), TNF (B) and IL-6 (C) in the supernatants were assessed by ELISA. Graphs represent individual samples with a mean ± SEM for each group. Statistical significance was calculated using 2-way ANOVA with uncorrected Fisher's LSD test, * p <0.05, ** p <0.01, *** p <0.001, **** p <0.0001.

6.3.5 scRNA-seq identifies 8 distinct myeloid clusters in HS lesional and healthy control skin

Given the apparent dysregulation of monocytes in HS patient peripheral blood, the role of myeloid cells in HS skin was examined. scRNA-seq analysis was performed on $CD45^+$ immune cells. Skin biopsies were processed, and cells sequenced as per **Section 2.2.19**. Raw sequencing data was processed and analysed primarily using Cell Ranger and Seurat (Zheng *et al.*, 2017; Stuart *et al.*, 2019). Once annotated (**Figure 8.1**), cells with macrophage and DC signatures were isolated and reprocessed to generate a specific myeloid cell analysis.

8 distinct cell clusters were identified on the myeloid UMAP, including populations of Langerhans cells, dermal macrophages and DCs (**Figure 6.11A**). **Figure 6.11B** displays the generally similar frequency of each cell cluster relative to total myeloid cells in each sample. Cell clusters were annotated based on the presence or absence of classical cell markers. Typically, 10-20 cell markers were used in combination to identify each particular cell cluster. Dermal macrophages were identified by high expression of *MARCO* (**Figure 6.12A**), *MRC1* (CD206, **Figure 6.12B**) and *CD163* (**Figure 6.12C**). Langerhans cells were identified by elevated expression of *CD1C* (**Figure 6.12D**), *CD1A* (**Figure 6.12E**) and *MNDA* (**Figure 6.12F**). cDC2 cells had characteristic expression of *CD1C* and *ITGAX* (CD11c, **Figure 6.12G**) and cDC1 cells had unique expression of *CLEC9A* (**Figure 6.12H**).

To determine specific markers for each cell cluster, Wilcoxon Rank Sum test was performed (**Figure 6.13**). Dermal macrophages had uniquely high expression of complement genes (*C1QB*, *C1QC*, *C1QA*), implicating dermal macrophages in complement-dependent tissue immunity (**Figure 6.13**). cDC2 clusters had elevated expression of the inflammatory mediators *IL1B*, *CCL20*, *CXCL2* and *CXCL3* (**Figure 6.13**). *CXCL2* has previous been linked with inflammasome activation and IL-1β production (Boro and Balaji, 2017), while *CXCL3* regulates neutrophil recruitment (Metzemaekers, Gouwy and Proost, 2020), indicating that cDC2 cells have an essential role in promoting HS inflammation. Interestingly, the cDC2 (1) cluster had elevated expression of *IL1R2* which has been found to negatively regulate IL-1β signaling by competing with IL-1R1 for IL-1β (McMahan *et al.,* 1991). This cDC2 (1) cluster was enriched in healthy controls and in HS4 and HS6, which constituted the HS-lo cohort

of samples. Langerhans cells also expressed *IL1B*, *CXCL2* and *CXCL3* (**Figure 6.13**), however to a lesser extent to the cDC (2) cluster, which appeared to be the most inflammatory cluster found in HS lesions. No inflammatory mediators were identified as the cluster markers of cDC1 cells, suggesting that these cells may not play a role in promoting HS inflammation.

In summary, 8 distinct myeloid clusters were identified in HS lesional and healthy control skin. Dermal macrophages, Langerhans cells, cDC1 and cDC2 cell clusters were identified as the major cell clusters in HS lesional and healthy control skin. Dermal macrophages appeared to regulate complement-dependent tissue immunity, while cDC2 and Langerhans cells likely to play an active role in promoting HS inflammation.

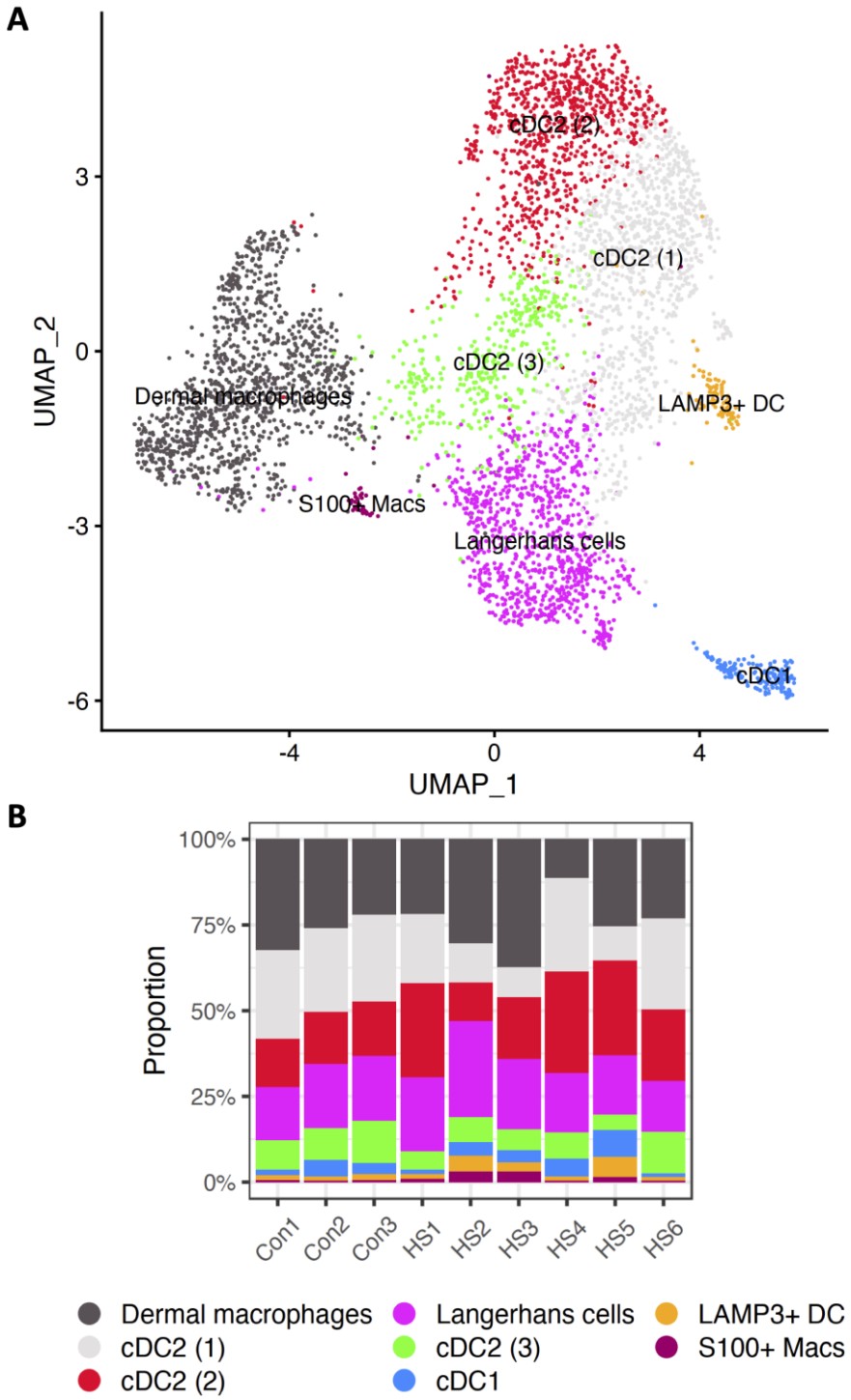

Figure 6.11 8 distinct myeloid clusters identified within HS patient lesions and healthy control skin. Cells isolated from healthy control skin (Con, n=3) or HS lesional skin (HS, n=6) were purified based on CD45 expression, barcoded and their gene expression determined by 10X Genomic scRNA-seq. T cells, NK cells, B cells, plasma cells and mast cells were identified and removed from further analysis. Myeloid cells were identified and subclustered into 8 unique clusters generated by unsupervised classification (A). Bar plot displays the frequency of each cluster in each healthy control and HS patient sample (B).

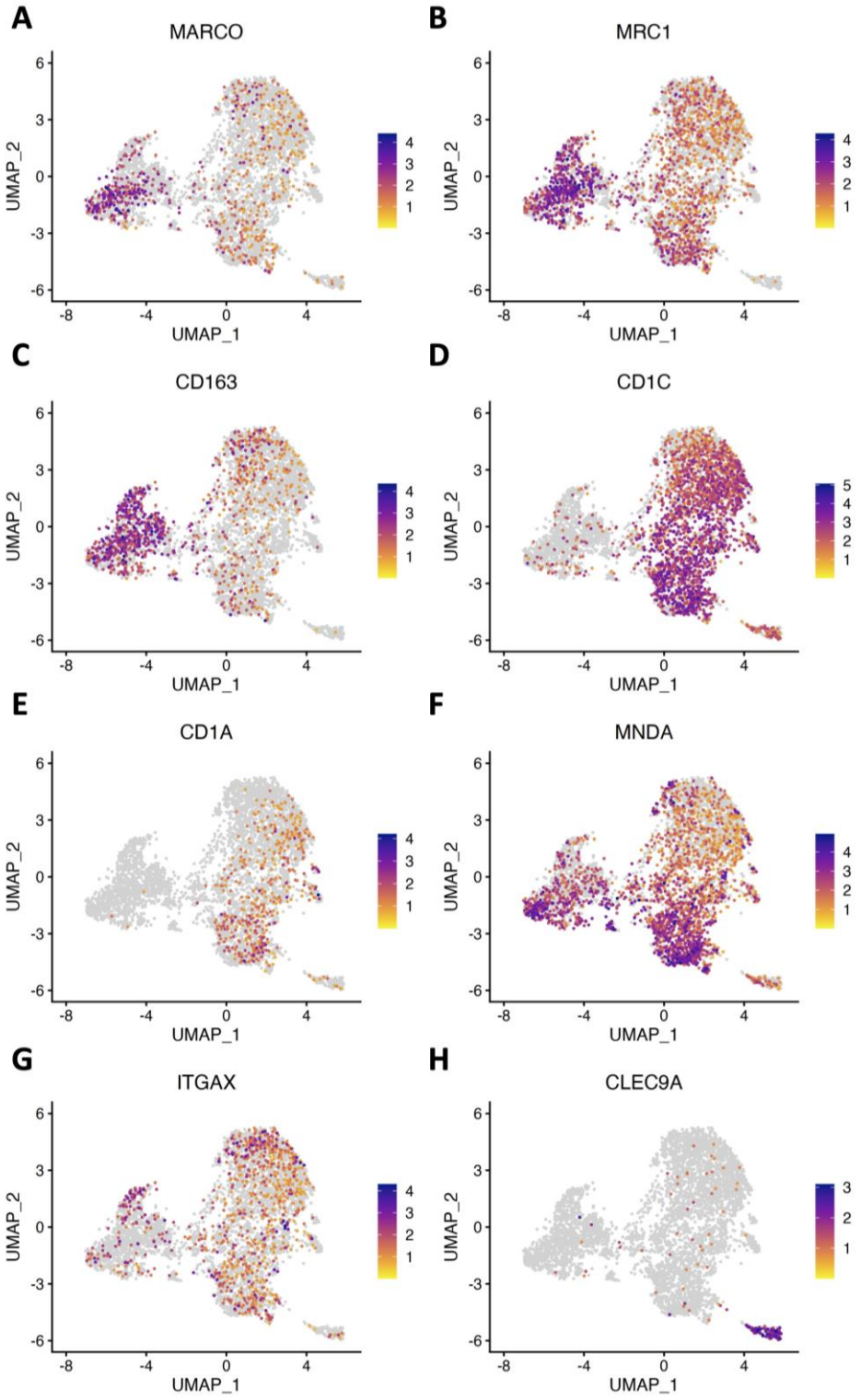

Figure 6.12 Characterisation of myeloid cell clusters. Cells isolated from healthy control skin (Con, n=3) or HS lesional skin (HS, n=6) were purified based on CD45 expression, barcoded and their gene expression determined by 10X Genomics scRNA-seq. UMAPs display gene expression of *MARCO* (A), *MRC1* (CD206; B), *CD163* (C), *CD1C* (D), *CD1A* (E), *MNDA* (F), *ITGAX* (CD11C; G) and *CLEC9A* (H) in myeloid cell clusters.

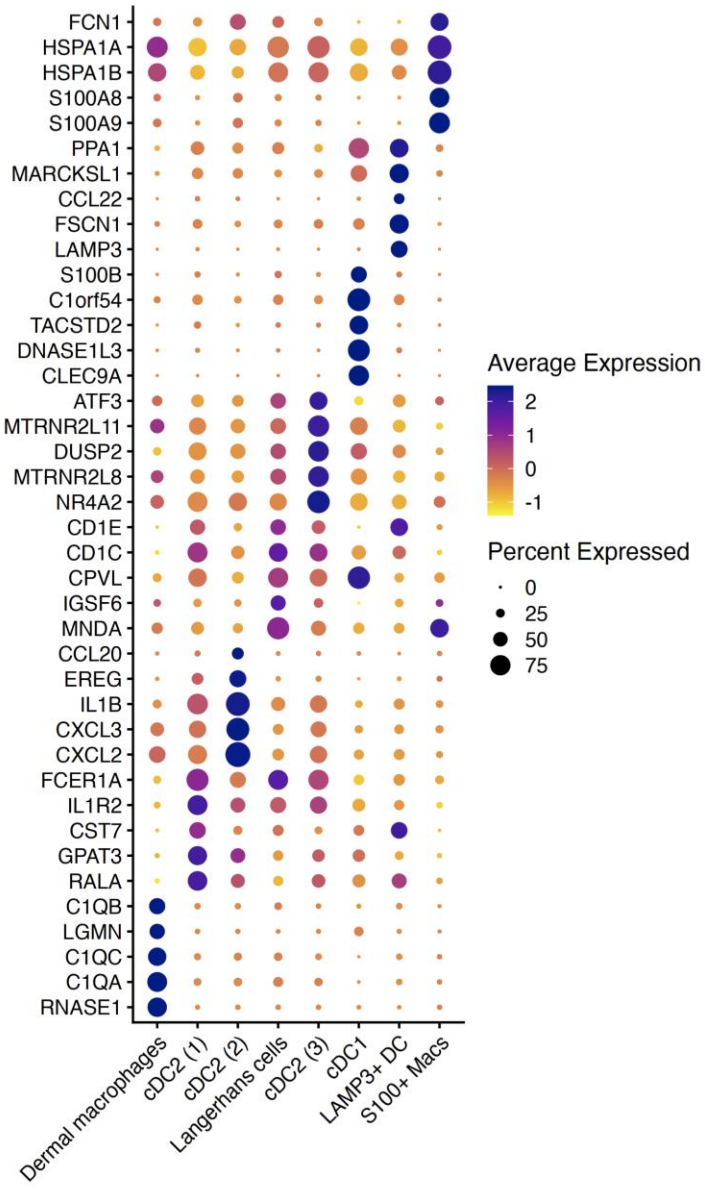

Figure 6.13 Identification of specific myeloid cell cluster markers. Cells isolated from healthy control skin (Con, n=3) or HS lesional skin (HS, n=6) were purified based on CD45 expression, barcoded and their gene expression determined by 10X Genomics scRNA-seq. Dotplot displayed cluster-specific genes identified by Wilcoxon Rank Sum test.

6.3.6 HS myeloid cells displayed elevated cytokine signaling and inflammasome activation

As myeloid cells appeared to play an important role in promoting HS skin inflammation, the transcriptomic differences between HS and healthy control myeloid cells were evaluated. To estimate the overall transcriptomic differences between myeloid cells in HS lesions and healthy control skin, PCA was performed on individual patient samples (**Figure 6.14**). Healthy control myeloid cells had similar transcriptomes and grouped closely together, while greater heterogeneity existed among HS samples. HS samples could be grouped into a HS-hi cohort which were transcriptionally distinct to healthy control myeloid cells, and a HS-lo cohort which were more transcriptionally similar to healthy control myeloid cells. Importantly, the same patients were also categorised as HS-hi and HS-lo in the previous chapters.

Considering the downregulation of activation markers in peripheral HS monocytes (**Section 6.3.3**), the expression of CD40 signaling was evaluated in HS and healthy control myeloid cells (**Figure 6.15**). The CD40 signaling module included a number of genes including *CD80*, *CD86*, *CD40* and *HLA-DRA* which were downregulated in HS peripheral monocytes. Interestingly, the CD40 signature score in each cluster was lower in HS lesional skin relative to healthy control skin. This suggested that the dysregulation of HS monocytes continues as these cells progress into the skin and differentiate in macrophages or DCs.

In order to understand the dysregulation of myeloid cells in HS lesions, Wilcoxon Rank Sum test was performed to identify DEGs between HS and healthy control cells in each myeloid cell cluster. Pathway analysis was then performed on the DEGs between HS and healthy control cells in each cluster (**Figure 6.16A-G, Table 8.47-Table 8.58**). A high degree of overlap was seen in the most enriched immune pathways enriched across each of the myeloid cell clusters, with IL-17, TNF and NLR signaling featuring prominently among the most enriched pathways in many of the myeloid cell clusters. Interestingly, the cDC2 (1) cluster may be metabolically dysregulated as oxidative phosphorylation was enriched among the DEGs between HS and healthy control cells in this cluster (**Figure 6.16B**). Additionally, antigen presentation was significantly enriched among the DEGs in HS vs healthy controls in the cDC2 (2) cluster (**Figure 6.16C**). Upon further investigation, HS cDC2

(2) cells appeared to have reduced antigen presenting capacity, with reduced expression of antigen presentation related genes relative to healthy controls (**Figure 6.17**).

Considering the important role of IL-1β signaling in promoting HS inflammation, the potential role of the NLRP3 inflammasome was investigated in HS and healthy control myeloid cells. Genes involved in NLRP3 inflammasome signaling were elevated in HS cDC2 (2) cells compared with healthy control and relative to other myeloid clusters (**Figure 6.18**). This suggested that the NLRP3 inflammasome was primarily activated in the cDC2 (2) cluster in HS patients. Although *IL1B* appeared to be expressed by multiple myeloid clusters, highest expression was concentrated in the cDC2 (2) cluster (**Figure 6.19A**). This coincided with *NLRP3* expression which again was expressed by every myeloid cell cluster, but predominantly found in the cDC2 (2) cluster (**Figure 6.19B**). *CASP1*, another inflammasome component, was most highly expressed by Langerhans cells, while *IL18* expression was scattered across all myeloid clusters (**Figure 6.19C-D**). Additionally, cDC2 cells also appeared to be the main source of *IL23A*, an important cytokine in the development of Th17 cells (**Figure 6.19E**).

As the frequency of cDC2 cell clusters differed across HS-hi and HS-lo cohorts, next the expression of inflammasome components and inflammatory mediators were evaluated in HS-hi, HS-lo and healthy control myeloid cells. Myeloid cells from HS patients in the HS-hi cohort had significantly elevated expression of NLRP3 inflammasome components, including *NLRP3* and *CASP1* (**Figure 6.20A-B**), increased expression of downstream cytokines *IL1B* and *IL18* (**Figure 6.20C-D**) and elevated expression of inflammatory mediators *IL23A*, *IL6*, *CCL20*, *TNF* and *TGFB1* (**Figure 6.20E-F**). Interestingly, at a cluster level, *NLRP3, IL1B* and *IL18* expression was only significantly elevated in HS-hi patients in cDC2 clusters, highlighting cDC2 cells as a key source of the NLRP3 inflammasome and inflammasome-associated cytokines (**Figure 6.21A,C,D**). *CASP1* expression was elevated in HS-hi patients in cDC2 clusters, dermal macrophages and Langerhans cells (**Figure 6.21B**).

cDC2 cells were the predominant source of the proinflammatory mediators *IL23A*, *IL6*, *CCL20* and *TNF*, and each of these inflammatory mediators were significantly elevated in HS-hi patients in the cDC2 (2) cluster (**Figure 6.22A-D**). Contrastingly, *TGFB1* was expressed

by cDC1, cDC2, dermal macrophages and Langerhans cell clusters and was significantly elevated in HS-hi patients in each of these cell clusters (**Figure 6.22E**).

Taken together, these data suggested that HS myeloid cells may be dysregulated in HS lesional skin relative to healthy control skin. cDC2 cells had a reduced CD40 signature and potentially reduced antigen presenting capacity in HS lesions. cDC2 cells were also a major source of the NLRP3 inflammasome and had increased expression of proinflammatory mediators in HS-hi patients, highlighting these cells as an important regulator of inflammation in HS.

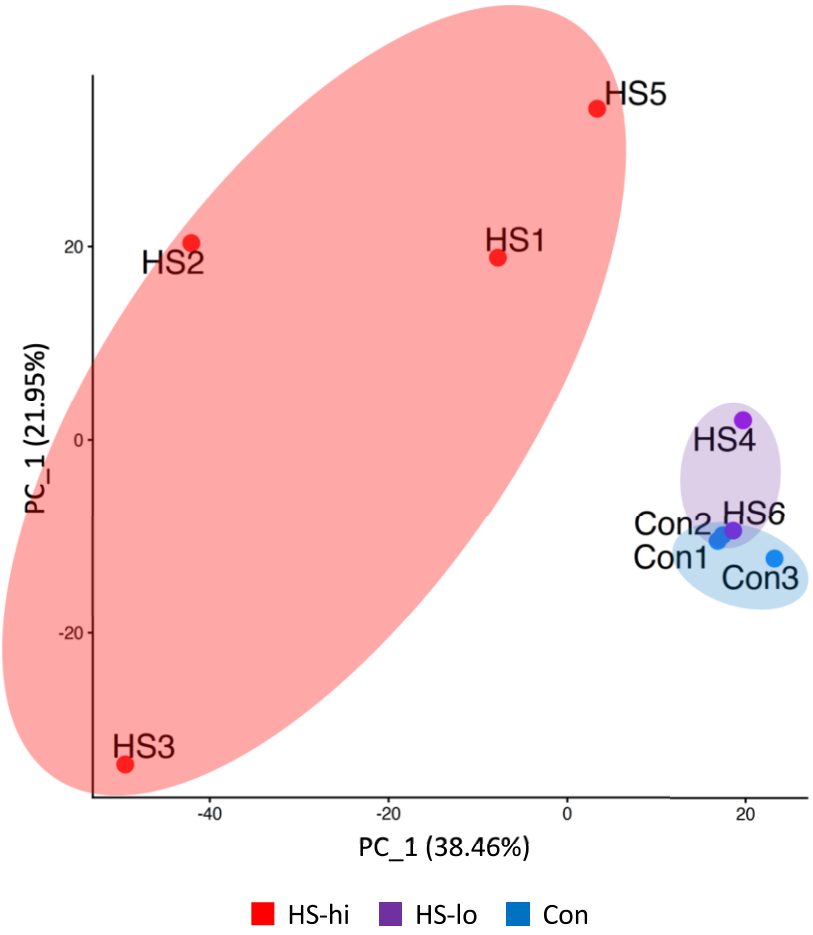

Figure 6.14 Principal component analysis of myeloid cells from HS patient lesions and healthy control skin. Cells isolated from healthy control skin (Con, n=3) or HS lesional skin (HS, n=6) were purified based on CD45 expression, barcoded and their gene expression determined by 10X Genomics scRNA-seq. PCA illustrates the homogenous healthy control (blue) myeloid cells and the heterogenous HS myeloid cells which were grouped into HS-hi samples (red) and HS-lo samples (purple) which grouped closely to healthy controls.

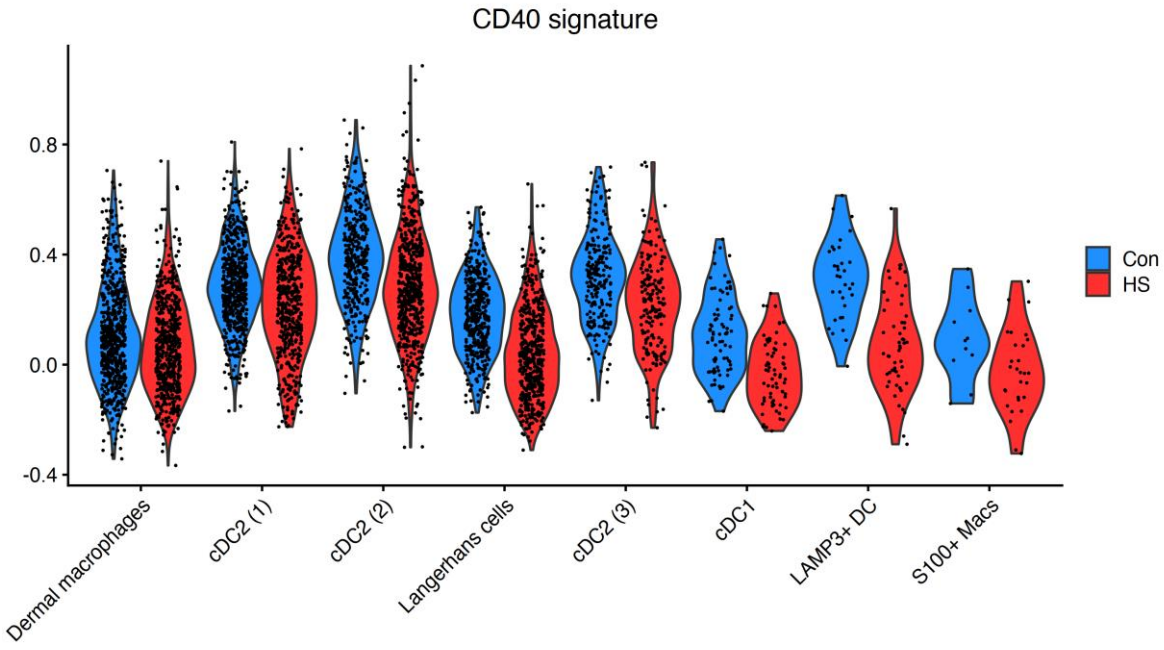

Figure 6.15 HS myeloid cells have reduced CD40 signaling compared with healthy controls. Cells isolated from healthy control skin (Con, n=3) or HS lesional skin (HS, n=6) were purified based on CD45 expression, barcoded and their gene expression determined by 10X Genomics scRNA-seq. Pathway activity scores were estimated for CD40 activation using the AddModuleScore function in Seurat.

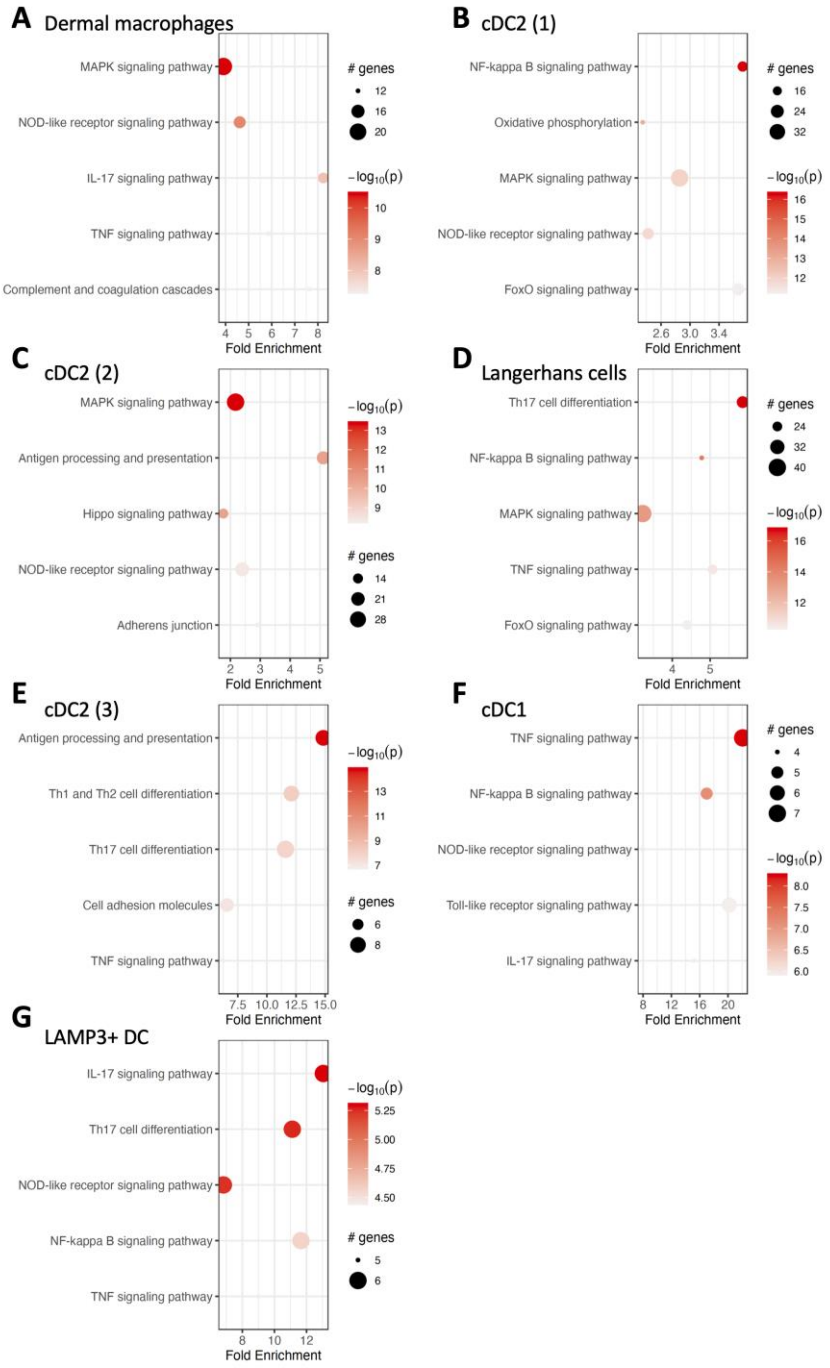

Figure 6.16 IL-17, TNF and NLR signaling were dysregulated in HS myeloid cells. Cells isolated from healthy control skin (Con, n=3) or HS lesional skin (HS, n=6) were purified based on CD45 expression, barcoded and their gene expression determined by 10X Genomics scRNA-seq. The top 5 immune related pathways enriched from DEGs between HS and healthy control cells in each individual cluster were displayed by dotplot. DEGs were calculated by Wilcoxon Rank Sum test in each cluster between HS and healthy control cells. Kegg pathways enriched from these DEGs in dermal macrophages (A), cDC2 (1) (B), cDC2 (2) (C), Langerhans cells (D), cDC2 (3) (E), cDC1 (F) and LAMP3+ DC (G) were displayed.

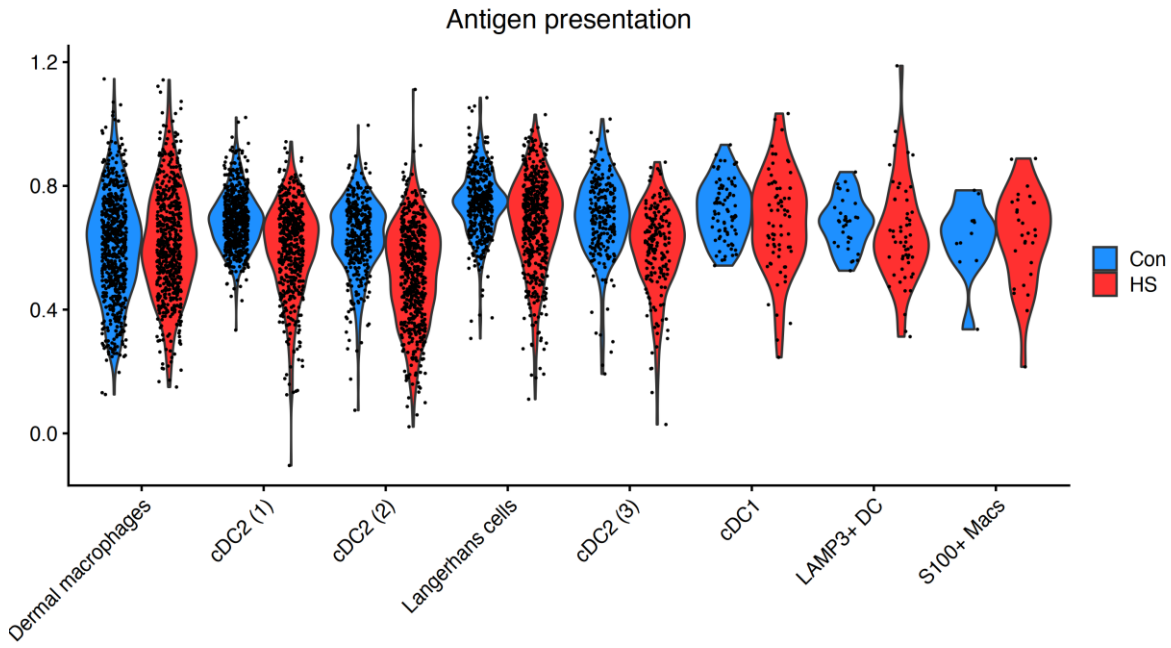

Figure 6.17 HS cDC2 (2) cluster had reduced antigen presentation capacity. Cells isolated from healthy control skin (Con, n=3) or HS lesional skin (HS, n=6) were purified based on CD45 expression, barcoded and their gene expression determined by 10X Genomics scRNA-seq. Pathway activity scores were estimated for antigen presentation was calculated using the AddModuleScore function in Seurat.

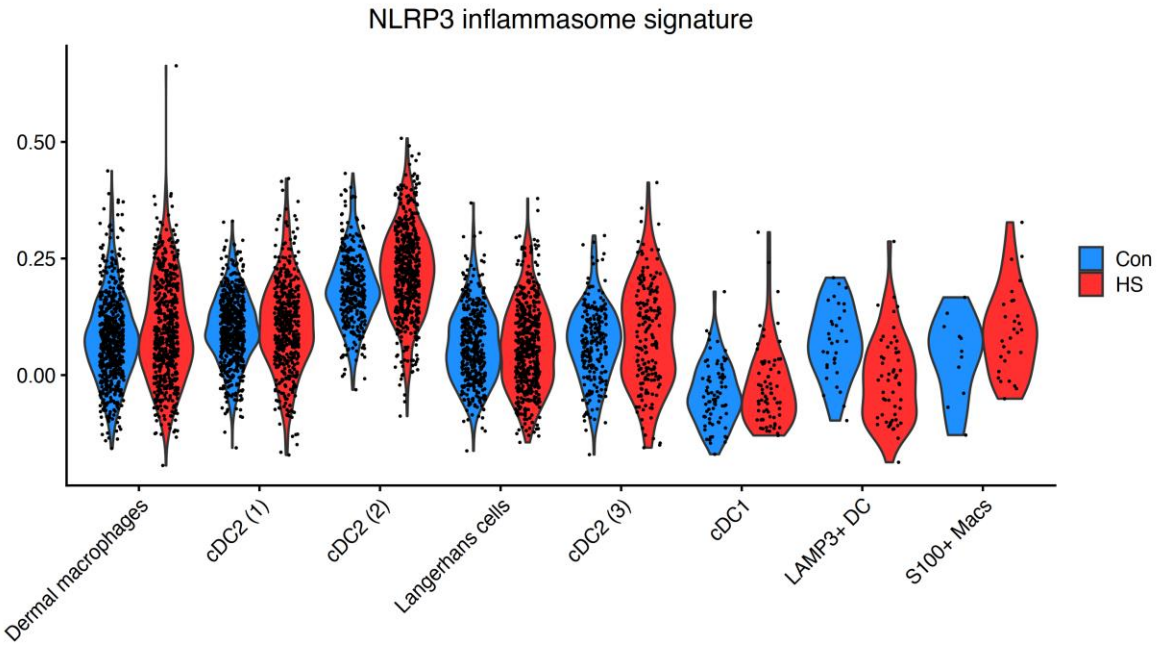

Figure 6.18 HS cDC2 (2) cluster had increased NLRP3 inflammasome signaling. Cells isolated from healthy control skin (Con, n=3) or HS lesional skin (HS, n=6) were purified based on CD45 expression, barcoded and their gene expression determined by 10X Genomics scRNA-seq. Pathway activity scores were estimated for the NLRP3 inflammasome using the AddModuleScore function in Seurat.

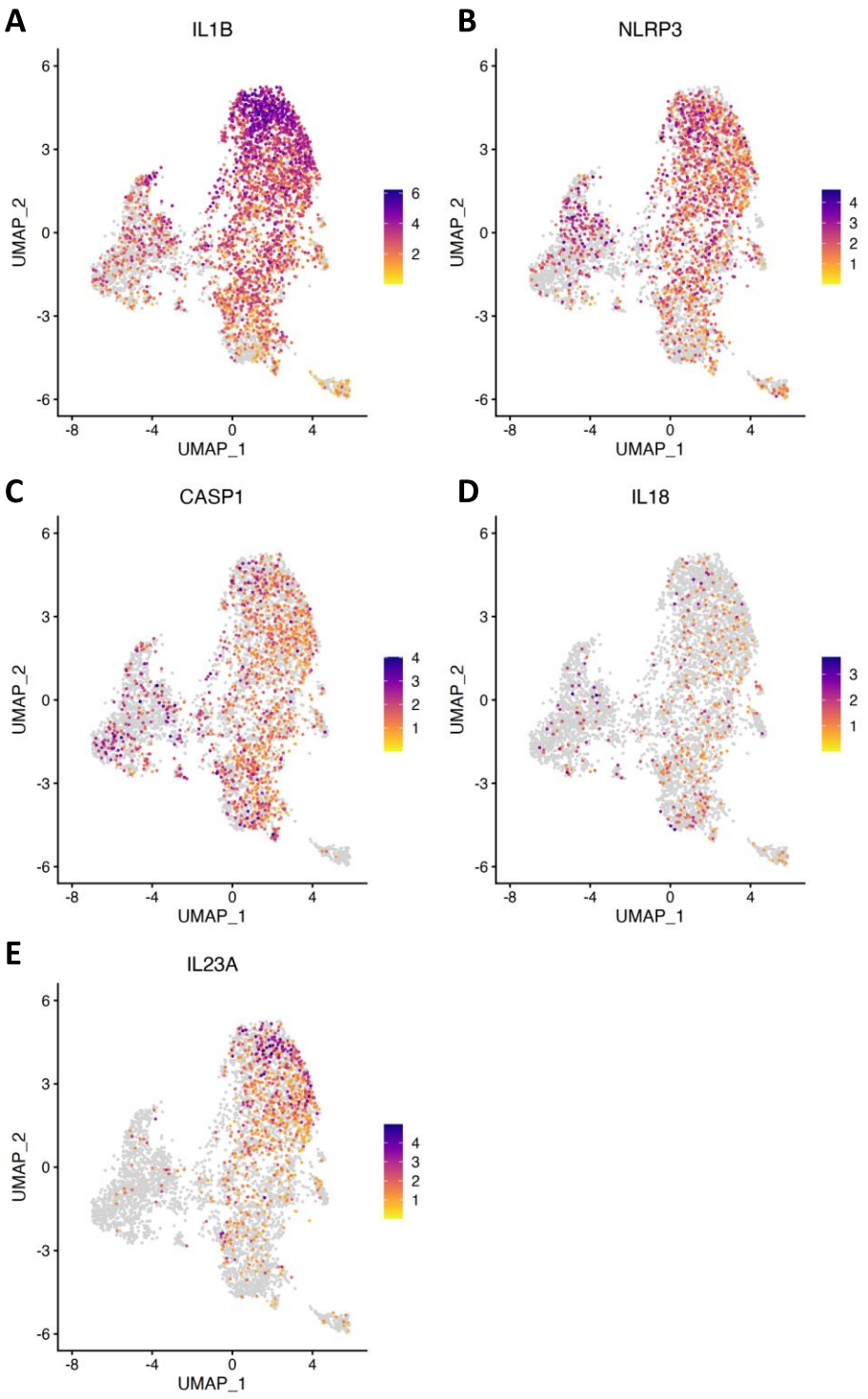

Figure 6.19 cDC2 cells had elevated expression of NLRP3 inflammasome components. Cells isolated from healthy control skin (Con, n=3) or HS lesional skin (HS, n=6) were purified based on CD45 expression, barcoded and their gene expression determined by 10X Genomics scRNA-seq. UMAPs display gene expression of *IL1B* (A), *NLRP3* (B), *CASP1* (C), *IL18* (D) and *IL23A* (E) in myeloid cell clusters.

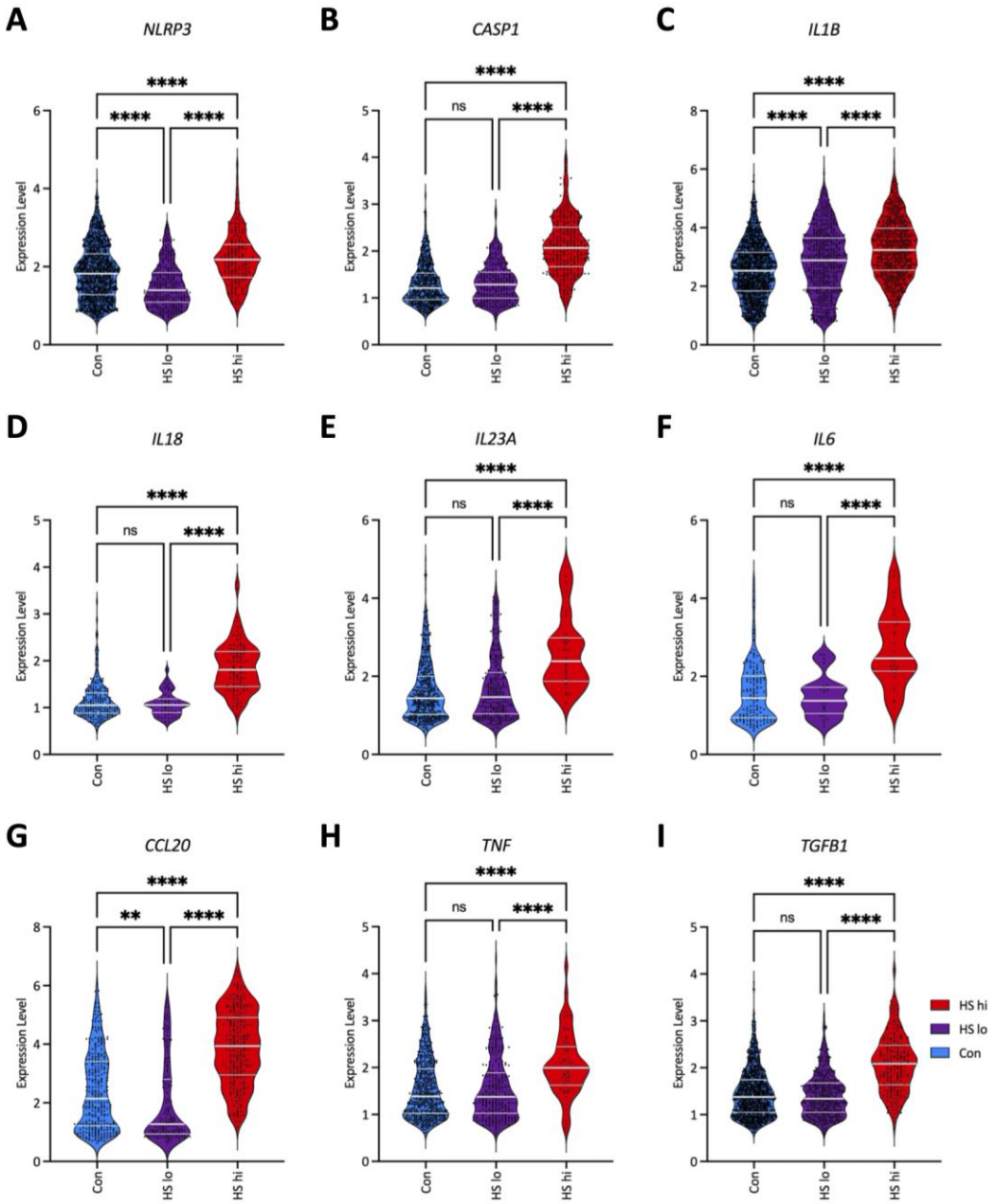

Figure 6.20 Upregulation of NLRP3 inflammasome-related genes in myeloid cells from HS skin. Cells isolated from healthy control skin (Con, n=3) or HS lesional skin (HS, n=6) were purified based on CD45 expression, barcoded and their gene expression determined by 10X Genomics scRNA-seq. Violin plots display the relative expression of *NLRP3* (A), *CASP1* (B), *IL1B* (C), *IL18* (D), *IL23A* (E), *IL6* (F), *CCL20* (G), *TNF* (H), *TGFB1* (I), where present, within myeloid cells from healthy control (Con), HS-lo and HS-hi samples. Statistical significance was calculated using Kruskal–Wallis test with Dunn's multiple comparisons, * p <0.05, ** p <0.01, *** p <0.001, **** p <0.0001.

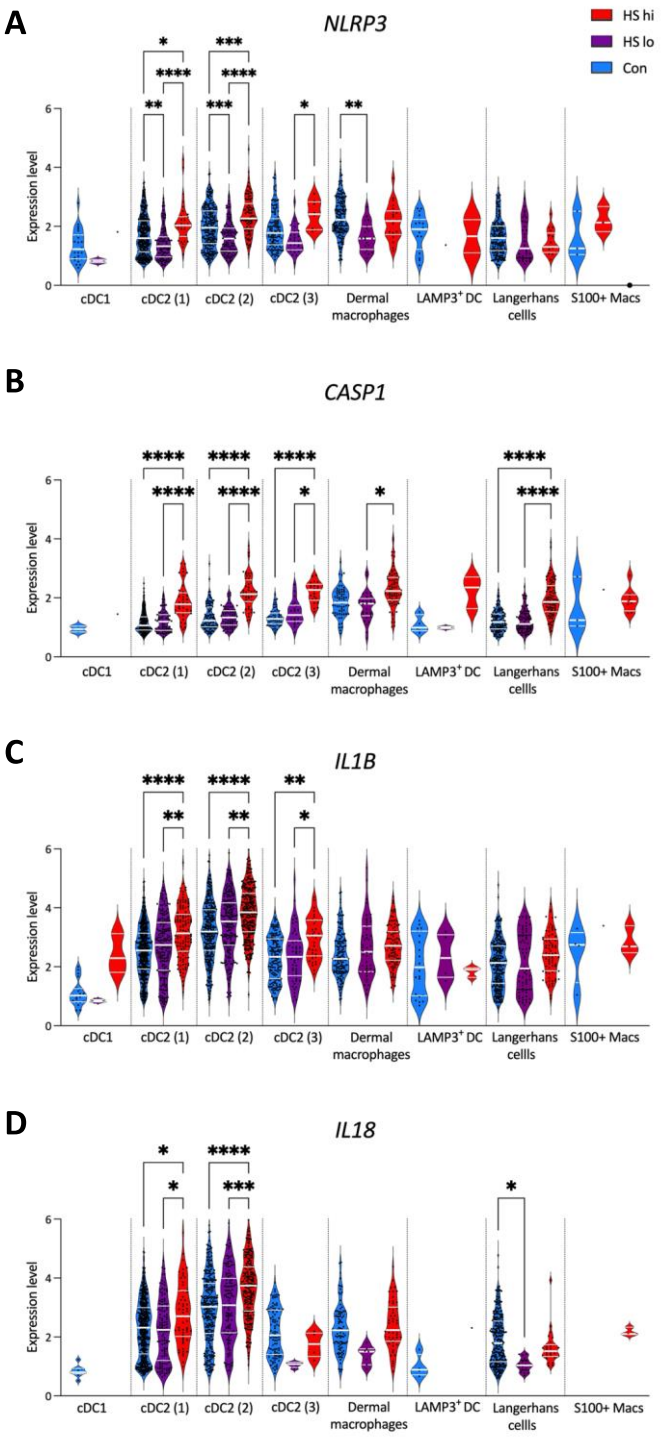

Figure 6.21 Relative expression of inflammasome related genes in specific myeloid cell clusters of healthy controls, HS-lo and HS-hi skin. Cells isolated from healthy control skin (Con, n=3) or HS lesional skin (HS, n=6) were purified based on CD45 expression, barcoded and their gene expression determined by 10X Genomics scRNA-seq. Violin plots display the relative expression of *NLRP3* (A), *CASP1* (B), *IL1B* (C), *IL18* (D), where present, within myeloid cells from healthy control (Con), HS-lo and HS-hi samples. Statistical significance was calculated using Kruskal–Wallis test with Dunn's multiple comparisons, * p <0.05, ** p <0.01, *** p <0.001, **** p <0.0001.

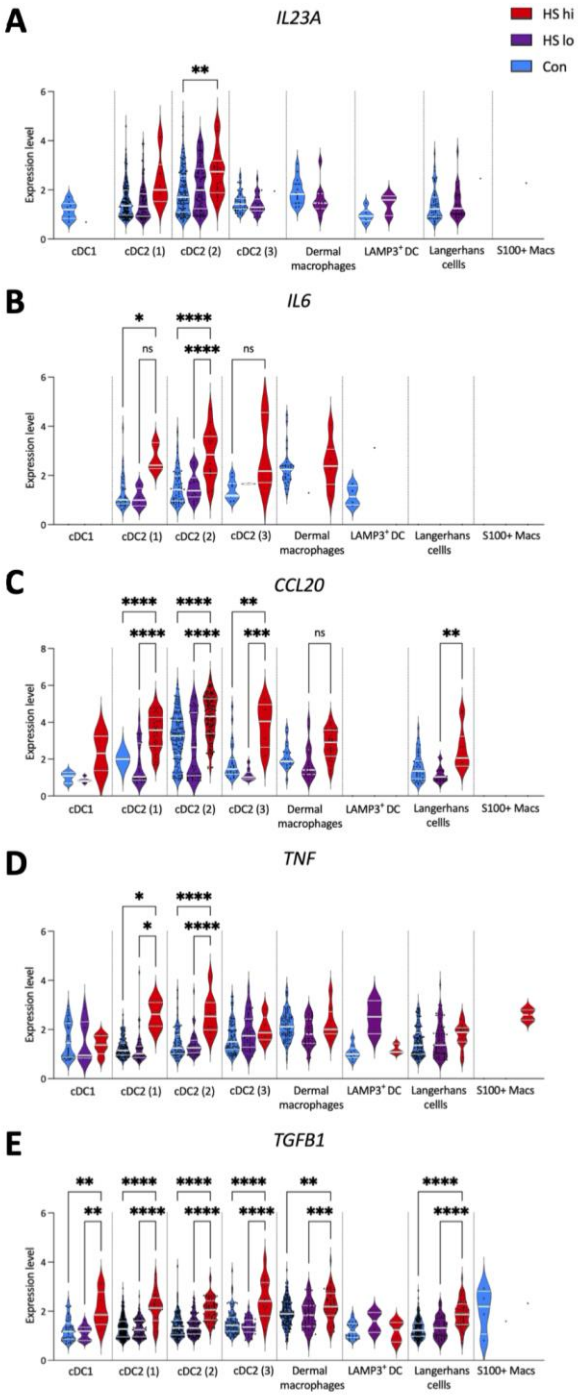

Figure 6.22 Relative expression of inflammatory cytokines and chemokines in specific myeloid cell clusters of healthy controls, HS-lo and HS-hi skin. Cells isolated from healthy control skin (Con, n=3) or HS lesional skin (HS, n=6) were purified based on CD45 expression, barcoded and their gene expression determined by 10X Genomics scRNA-seq. Violin plots display the relative expression of *NLRP3* (A), *CASP1* (B), *IL1B* (C), *IL18* (D), where present, within myeloid cells from healthy control (Con), HS-lo and HS-hi samples. Statistical significance was calculated using Kruskal–Wallis test with Dunn's multiple comparisons, * p <0.05, ** p <0.01, *** p <0.001, **** p <0.0001.

6.3.7 TNF inhibition reduces TNF and IL-17 signaling but not IL-1β or NLRP3 inflammasome signaling

Increased inflammatory cytokine production in HS myeloid cells indicates severe dysfunction of myeloid cells in HS lesions. TNF was identified as significantly elevated in HS lesions with high inflammatory loads and TNF signaling was found to be dysregulated in many myeloid clusters. This suggests TNF inhibition would have a profound impact on the inflammatory output of HS myeloid cells. 3,342 genes were downregulated upon TNF inhibition, including *TNF*, *IL23A*, *CXCL8* and *TGFB1* (**Figure 6.23**). Interestingly, *S100A8*, *S100A9* and *HIF1A* continued to be upregulated in HS lesions following TNF inhibition.

To evaluate the effect these 3,342 DEGs had on inflammatory signaling in HS myeloid cells, pathway analysis was performed. Of note, TNF, IL-17 and NLR signaling were found to be enriched among the DEGs (**Figure 6.24A**). Interestingly, anti-TNF therapy skewed the frequencies of myeloid cells in HS lesions, increasing the frequency of Langerhans cells while decreasing the frequency of cDC2 cells, however the small number of samples prohibits statistical analysis (**Figure 6.24B**).

Previous sections identified myeloid cells, and in particular cDC2 cells as important sources of *IL1B* expression. Interestingly, despite a reduction in the frequency of cDC2 cells, the expression of *IL1B* was similar in HS myeloid cells treated with or without anti-TNF therapy (**Figure 6.25A**). Similarly, TNF inhibition did not reduce the NLRP3 inflammasome signature found in HS myeloid cells, in fact, cDC2 cells treated with anti-TNF therapy had an elevated NLRP3 inflammasome signature compared with their untreated counterparts (**Figure 6.25A**). This importantly demonstrates a key inflammatory pathway which remains unaffected by anti-TNF therapy in HS lesions.

Taken together, these data demonstrate TNF inhibition alters the myeloid cell landscape in HS lesions and reduces the expression of many inflammatory mediators. However, TNF inhibition does not impact *IL1B* expression or the NLRP3 inflammasome signature of myeloid cells in HS lesions.

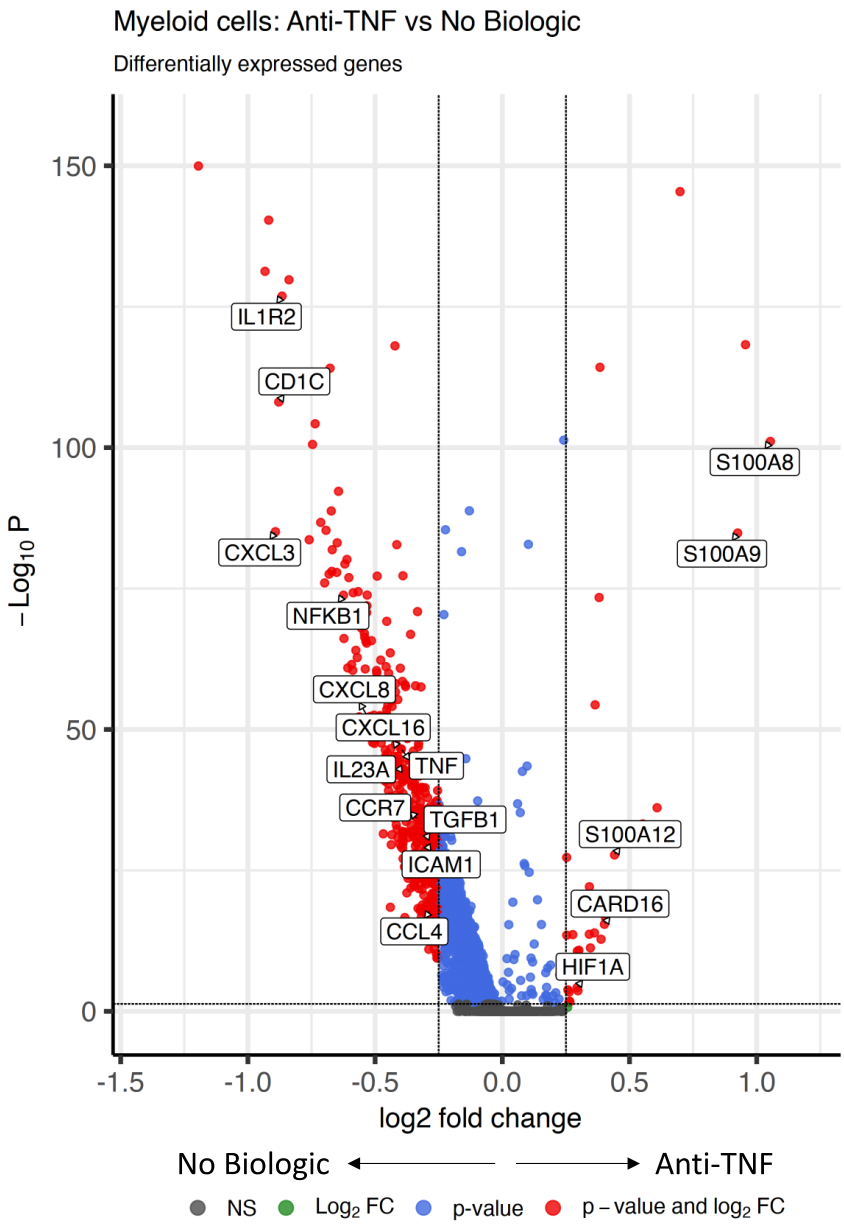

Figure 6.23 Volcano plot visualising differentially expressed genes between myeloid cells derived from HS patients treated with or without anti-TNF therapies. Single cells isolated from healthy controls (Con; n=3) or HS lesional skin (HS; n=6) were purified based on CD45 expression, barcoded and sequenced by 10X Genomics scRNA-seq. Volcano plot visualises DEGs in anti-TNF treated compared with untreated HS myeloid cells. Genes with a $log_2FC > 0$ are upregulated in anti-TNF treated HS myeloid cells and a $log_2FC < 0$ are downregulated in anti-TNF treated HS myeloid cells. The $-Log_{10}P$ Y-axis is a measure of significance.

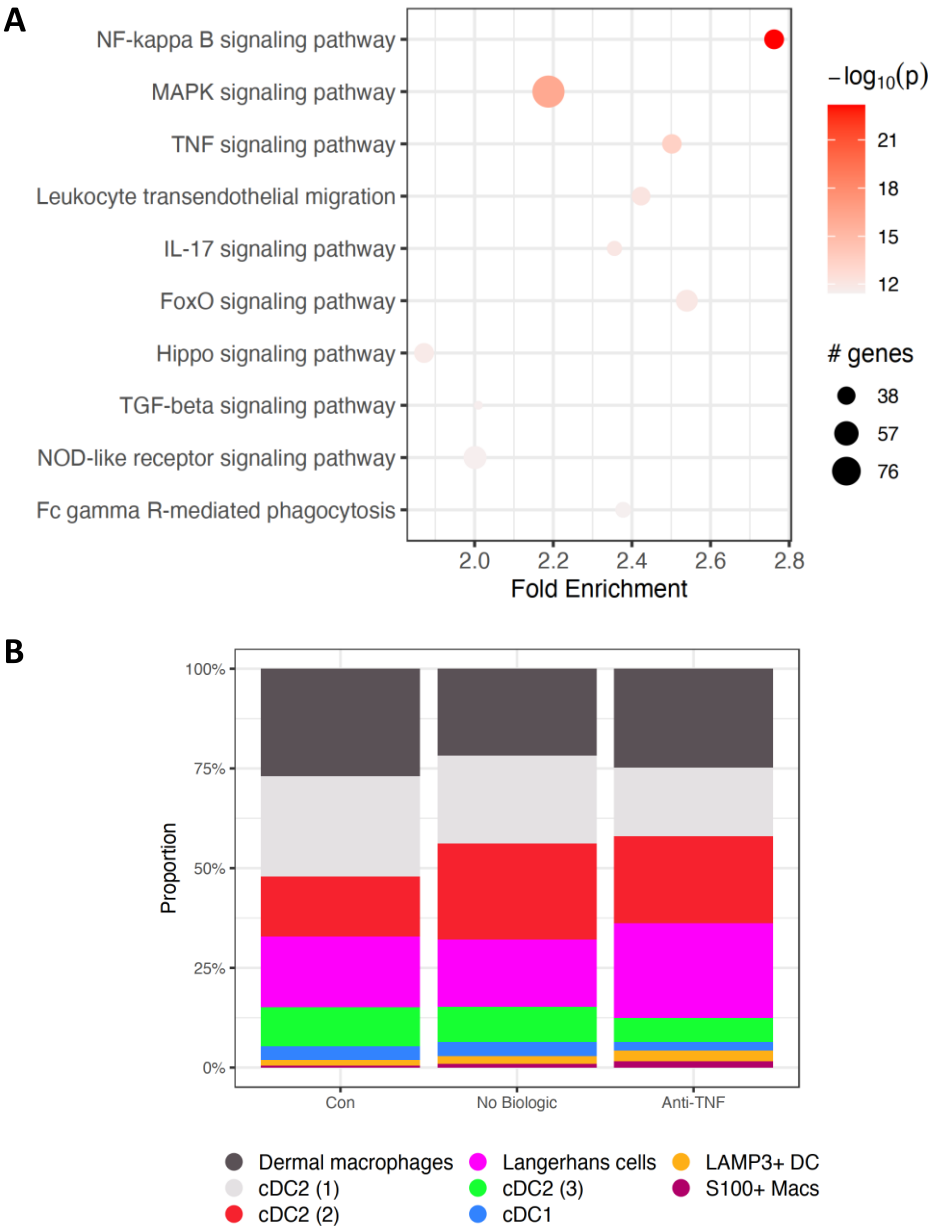

Figure 6.24 TNF therapy reduces the inflammatory output from myeloid cells in HS lesions. Top 10 immune pathways enriched from the genes significantly differentially expressed between treated the myeloid cells of anti-TNF treated and untreated HS patients ($p < 0.05$ and $\log_2FC > 0.1$) (A). Bar chart showing the proportion of each myeloid cell cluster relative to myeloid cells in the $CD45^-$ dataset (B).

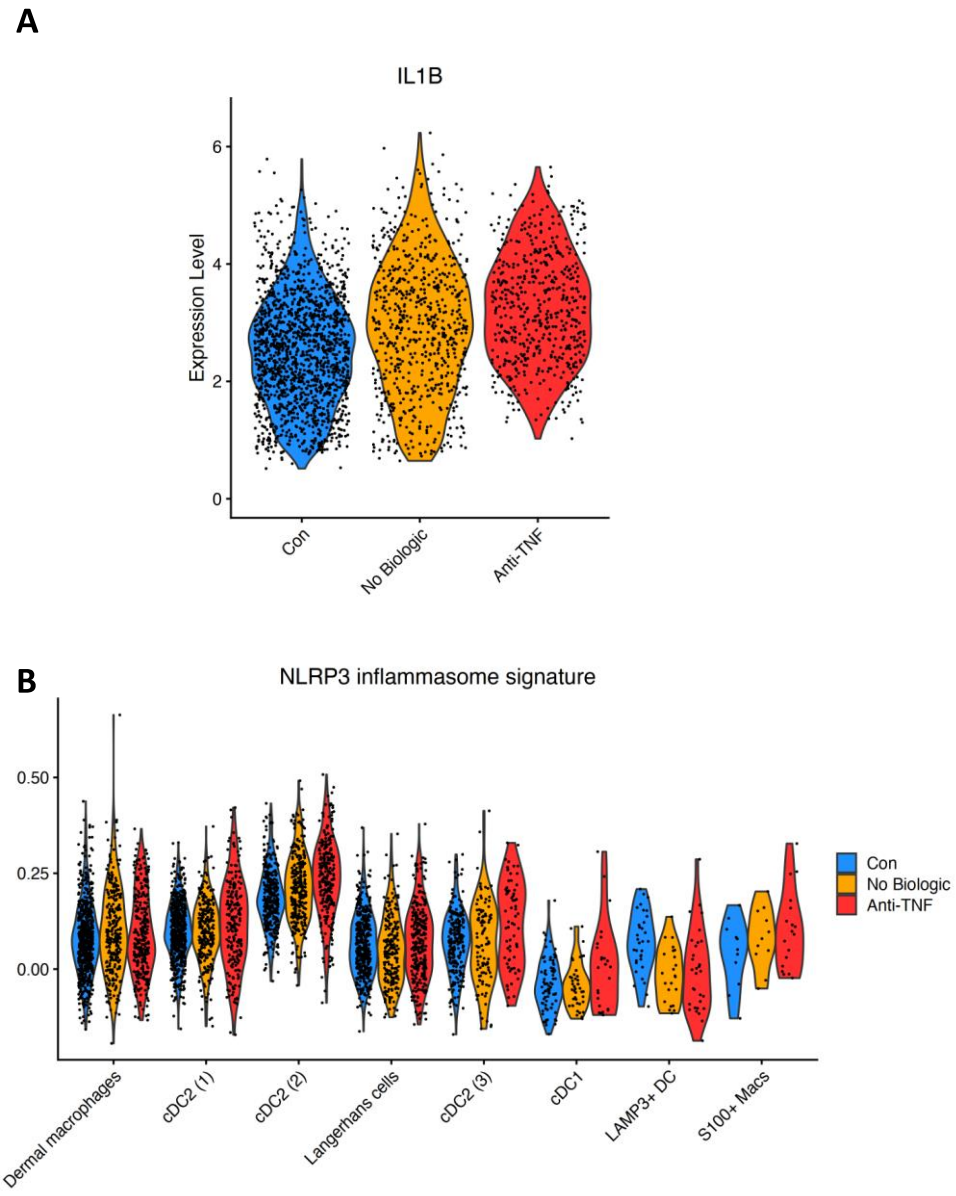

Figure 6.25 TNF inhibition has no effect on *IL1B* expression or NLRP3 inflammasome signaling in HS lesions. Single cells isolated from healthy controls (Con; n=3) or HS lesional skin (HS; n=6) were purified based on CD45 expression, barcoded and sequenced by 10X Genomics scRNA-seq. Violin plot visualises the expression of *IL1B* by myeloid cells in healthy control and HS patients treated with or without anti-TNF therapy. The NLRP3 inflammasome signature was estimated were estimated in myeloid cells of healthy controls and HS patients treated with or with anti-TNF therapy, using the AddModuleScore function in Seurat.

6.3.8 Blocking the NLRP3 inflammasome reduced inflammatory cytokine secretion in HS skin

Having demonstrated increased expression of the NLRP3 inflammasome in cDC2 cells in HS patients, the next question addressed was whether therapeutically targeting the NLRP3 inflammasome could reduce inflammatory mediator production in HS patients. Monocytes are a primary source of the NLRP3 inflammasome in peripheral blood (Netea *et al.,* 2009), and considering HS monocytes have been shown to be dysfunctional (**Section 6.3.4**), first the effect of NLRP3 inflammasome inhibition was evaluated in PBMC. Interestingly, HS monocytes had reduced IL-1β production relative to healthy controls following NLRP3 inflammasome activation (**Figure 6.26A**). Importantly, blocking inflammasome activation using MCC950 significantly reduced IL-1β production in both HS and healthy monocytes. Demonstrating the specificity of inflammasome inhibition, MCC950 had no effect on TNF production (**Figure 6.26B**).

As NLRP3 inflammasome inhibition successfully reduced IL-1β production in HS monocytes, next the effect of MCC950 was evaluated in HS skin. HS lesional and healthy control skin was cultured *ex vivo* for 24 h in the presence or absence of MCC950. The concentration of inflammatory mediators in the supernatant was evaluated by MSD and ELISA. HS lesions had significantly increased secretion of IL-1β (**Figure 6.27A**), IL-18 (**Figure 6.27B**), IL-17A (**Figure 6.27E**), IFN-γ (**Figure 6.27F**) and IL-36γ (**Figure 6.27K**) relative to healthy controls. There was also a trend towards an increase in the release of TNF (**Figure 6.27D**), CCL20 (**Figure 6.27G**), IL-17C (**Figure 6.27H**), CXCL1 (**Figure 6.27I**), IL-8 (**Figure 6.27J**), MMP3 (**Figure 6.27L**) and S100A8 (**Figure 6.27M**) from HS lesions relative to healthy controls. Interestingly, significant correlations was observed between multiple inflammatory mediators (**Figure 6.28**). Importantly, IL-1β significantly correlated with the secretion of IL-8, IFN-γ, IL17A, CXCL1, and IL-1α, demonstrating a potentially crucial role for IL-1β in promoting HS inflammation.

To evaluate the overall relationship between cytokines in HS and healthy control skin, a biplot was constructed, coupling information of a PCA and loadings plots (**Figure 6.29**). The length of the arrow in the biplot indicates the contribution of that particular analyte to the PCA coordinates. The angle of the arrows outline the correlations between analytes. Acute

angles between arrows indicate positive correlations between analytes, arrows at 90° to another arrow indicates no correlation exists between analytes and arrows at 180° to another arrow indicates a negative correlation between analytes. This biplot highlights the homogenous nature of healthy control skin, outlined by the small ellipse encompassing the healthy control samples (**Figure 6.29**). Contrastingly, HS samples were diverse and exhibited a higher inflammatory output compared with healthy controls, detailed by the large ellipse (**Figure 6.29**).

Following NLRP3 inflammasome inhibition, HS lesions had significantly reduced secretion of IL-1β (**Figure 6.30A**), TNF (**Figure 6.30D**), IL-17A (**Figure 6.30E**), IFN-γ (**Figure 6.30F**), CCL20 (**Figure 6.30G**), CXCL1 (**Figure 6.30I**), IL-8 (**Figure 6.30J**) and IL-36γ (**Figure 6.30K**). Conversely, there were no significant changes in the secretion of IL-18 (**Figure 6.30B**), IL-1α (**Figure 6.30C**), IL-17C (**Figure 6.30H**), MMP3 (**Figure 6.30L**) or S100A8 (**Figure 6.30M**) following treatment with MCC950 in HS lesions. Looking at the overall secretome of HS lesions using the biplot, MCC950 globally reduced the total inflammatory output of HS lesions as indicated by the smaller ellipse relative to the larger ellipse representing untreated HS lesions (**Figure 6.31**).

In summary, HS lesional skin had an increased release of inflammatory mediators, including IL-1β and IL-17A, which were reduced following NLRP3 inflammasome inhibition. These data provided proof of concept that targeting NLRP3 inflammasome activation effectively inhibits the secretion of proinflammatory mediators and indicates that NLRP3 inflammasome inhibitors may be a potential novel therapeutic target in HS.

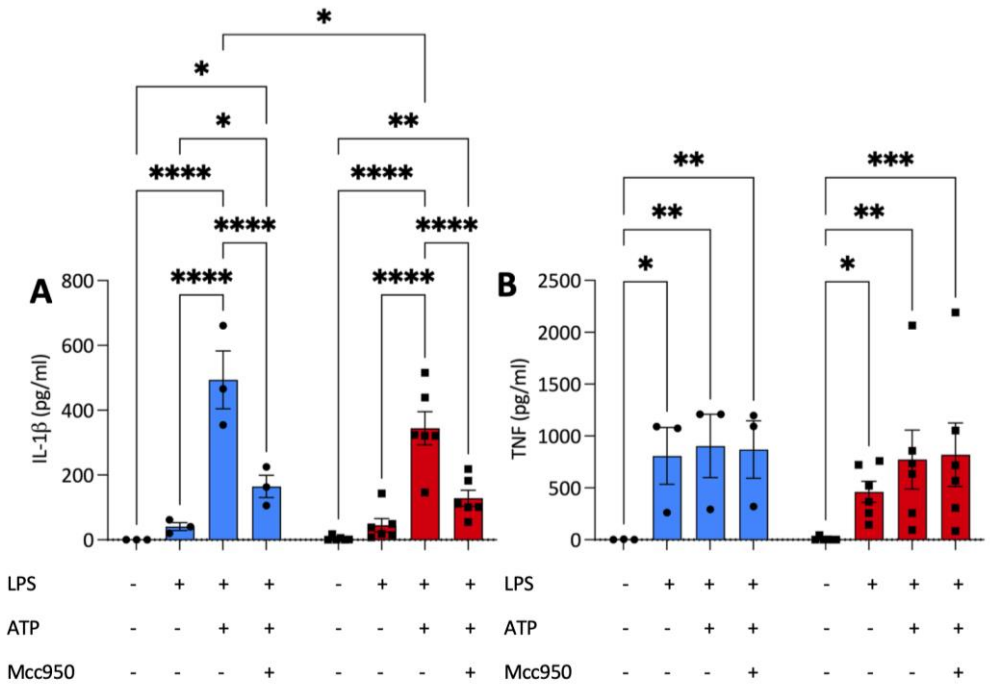

Figure 6.26 MCC950 inhibits inflammasome activation in HS PBMC. PBMC from healthy controls (Con; n=7) or HS patients (n=11) were stimulated with LPS (100 ng/ml) for 3 h before treating with ATP (5 mM) for 1 h; MCC950 (100 nM) were added 30 mins prior to ATP. The concentrations of IL-1β (A) and TNF (B) in the supernatants were assessed by ELISA. Graphs represent individual samples with a mean ± SEM for each group. Statistical significance was calculated using 2-way ANOVA with uncorrected Fisher's LSD test, * p <0.05, ** p <0.01, *** p <0.001, **** p <0.0001.

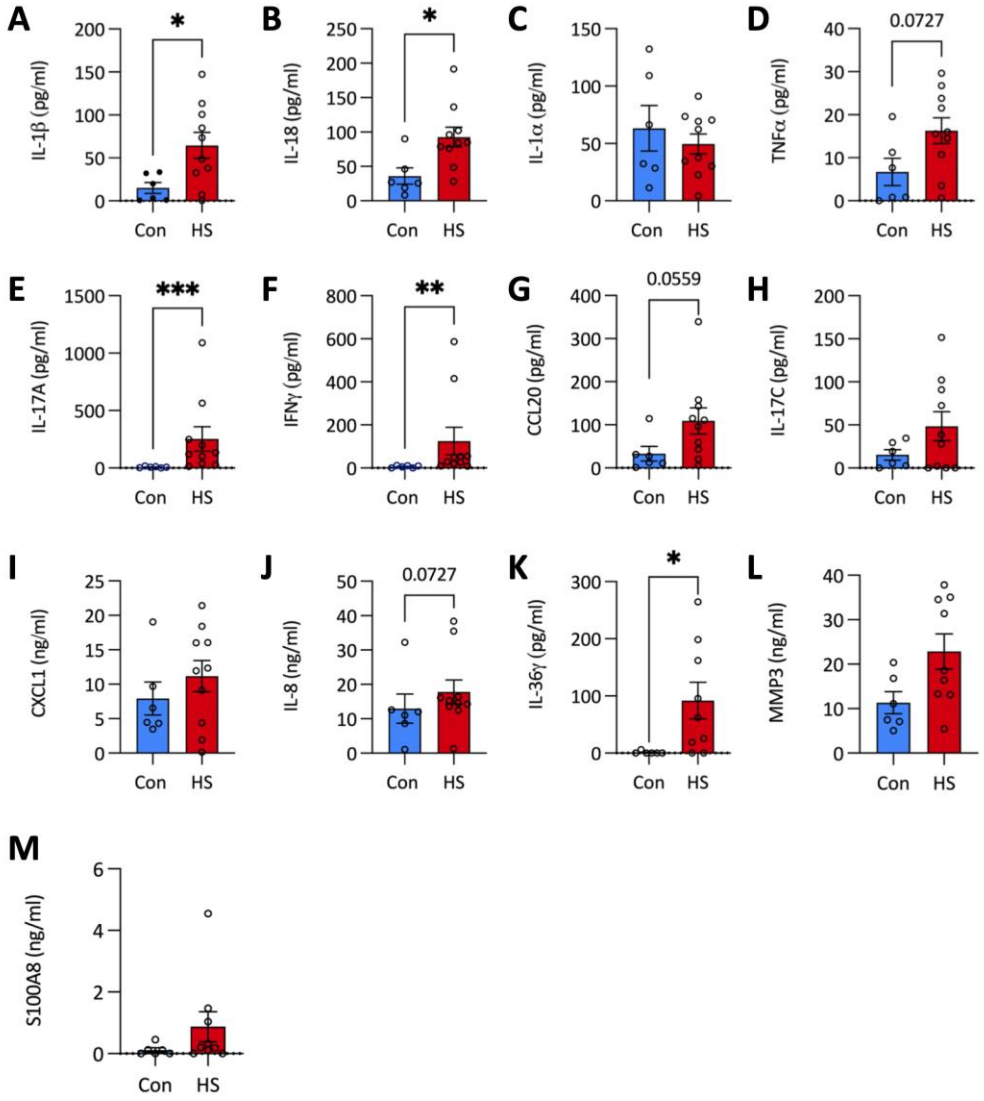

Figure 6.27 Increased release of inflammatory mediators from HS lesions relative to healthy control skin. Explants of healthy control (Con; n=6) or HS skin (n=9-10) were cultured for 24 h. The concentrations of IL-1β (A), IL-18 (B), IL-1α (C), TNF-α (D), IL-17A (E), IFN-γ (F), CCL20 (G), IL-17C (H), CXCL1 (I), IL-8 (J), IL-36γ (K), MMP3 (L), S100A8 (M) in the supernatants were assessed by MSD or ELISA. Graphs represent individual samples with a mean ± SEM for each group. Statistical significance was calculated using Mann Whitney U test, * p <0.05, ** p <0.01, *** p <0.001.

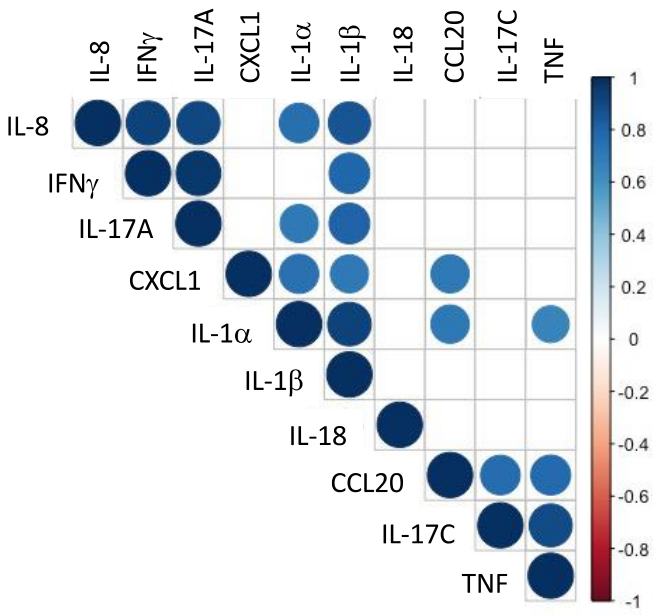

Figure 6.28 Correlation of inflammatory mediators secreted from HS skin. Explants of healthy control (Con; n=6) or HS skin (n=9-10) were cultured for 24 h. Pearson correlation scores were calculated between analytes measured by MSD in HS skin only.

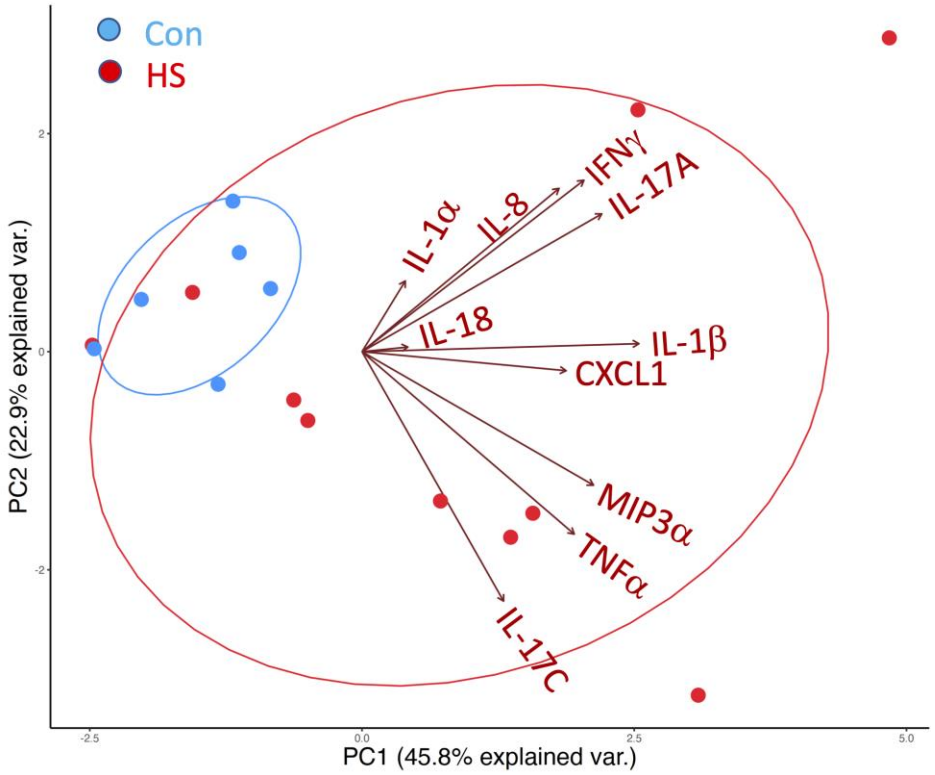

Figure 6.29 HS lesions had heterogenous inflammatory cytokine secretion. Explants of healthy control (Con; n=6) or HS skin (n=9-10) were cultured for 24 h. PCA plot displays the variance between individual healthy control and HS samples. An overlayed loadings plot displays the effect each analyte measured by MSD has on the PCA coordinance. The longer the arrow the greater effect that particular analyte has on pushing a sample towards that direction in the PCA plot.

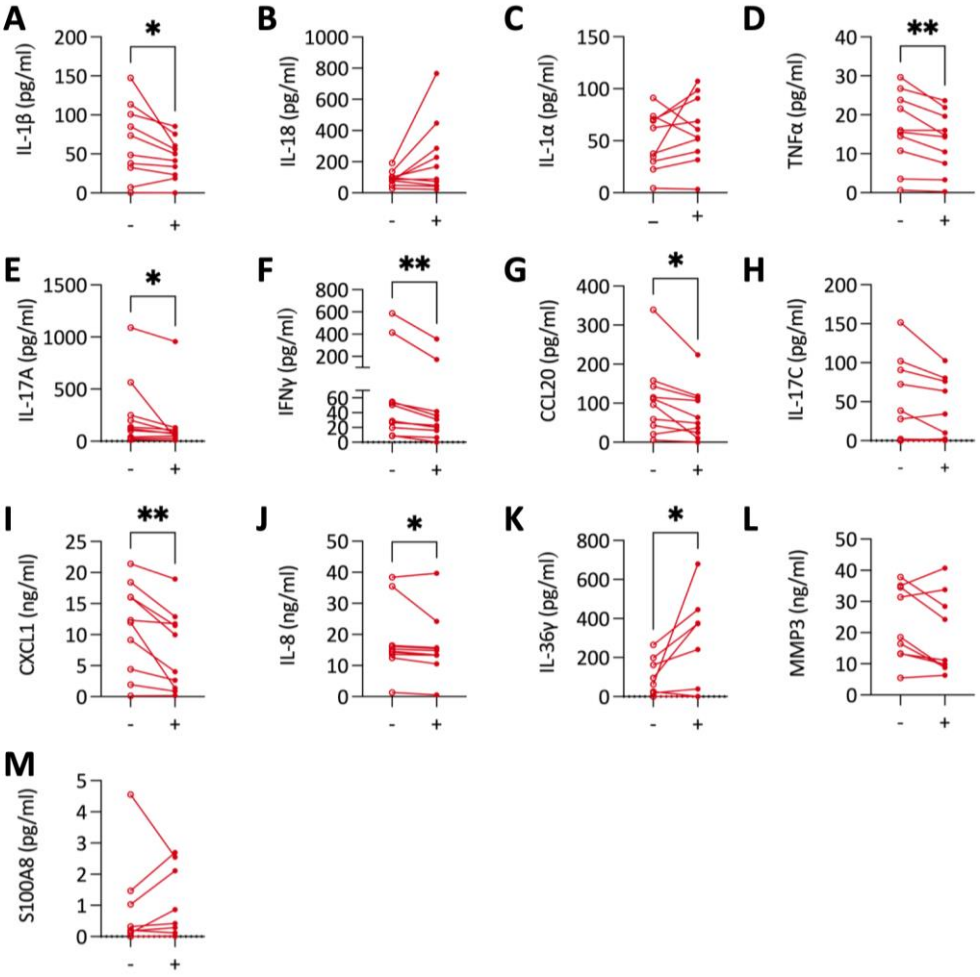

Figure 6.30 NLRP3 inflammasome inhibition reduced the inflammatory cytokine production in HS skin. Explants of healthy control (Con; n=6) or HS skin (n=9-10) were cultured for 24 h in the presence or absence of MCC950 (100 nM). The concentrations of IL-1β (A), IL-18 (B), IL-1α (C), TNF-α (D), IL-17A (E), IFN-γ (F), CCL20 (G), IL-17C (H), CXCL1 (I), IL-8 (J), IL-36γ (K), MMP3 (L), S100A8 (M) in the supernatants were assessed by MSD or ELISA. Graphs represent individual samples with a mean ± SEM for each group. Statistical significance was calculated using Mann Whitney U test, * $p < 0.05$, ** $p < 0.01$.

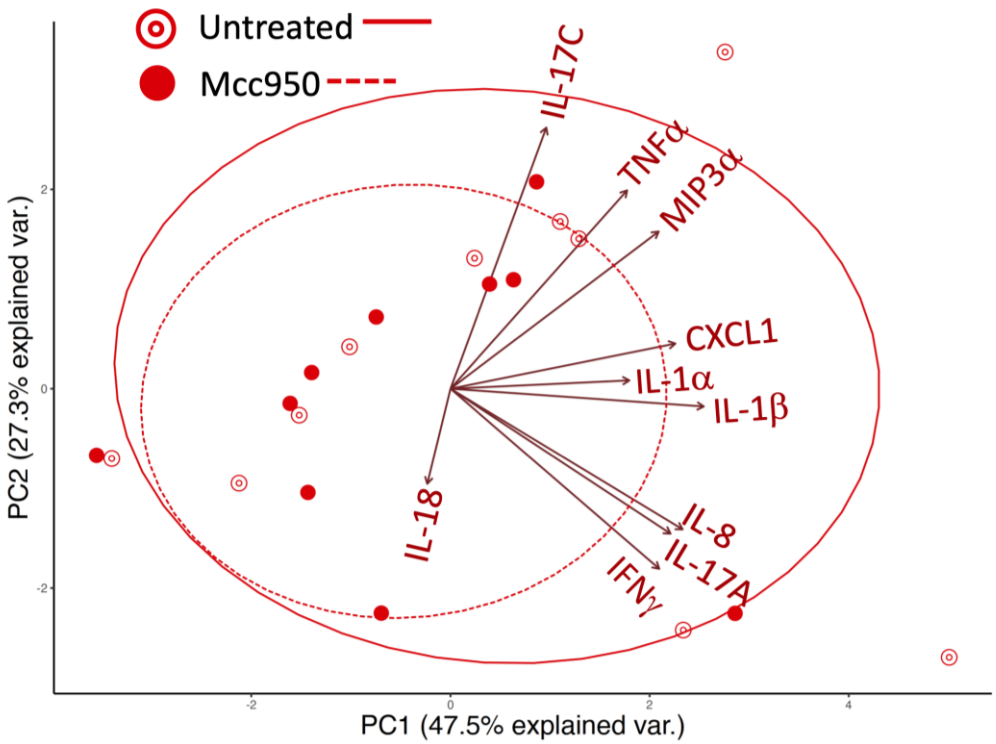

Figure 6.31 NLRP3 inflammasome inhibition reduced the overall inflammatory burden in HS skin. Explants of healthy control (Con; n=6) or HS skin (n=9-10) were cultured for 24 h in the presence or absence of MCC950 (100 nM). The concentrations of IL-1β (A), IL-18 (B), IL-1α (C), TNF-α (D), IL-17A (E), IFN-γ (F), CCL20 (G), IL-17C (H), CXCL1 (I), IL-8 (J), IL-36γ (K), MMP3 (L), S100A8 (M) in the supernatants were assessed by MSD or ELISA.

6.4 Discussion

This chapter uncovered novel insights into how dysregulated myeloid cells contribute to HS inflammation by providing detailed characterisation of myeloid cells in HS lesions and peripheral blood using high parameter flow cytometry and scRNA-seq. Firstly, it uncovered differences in the functional profiles between healthy control and HS monocytes in peripheral blood. HS monocytes had reduced expression of costimulatory molecules and increased production of inflammatory cytokines in response to a TLR2/dectin agonist. Additionally, myeloid cells in HS lesions were found to be dysregulated, with reduced expression of genes associated with antigen presentation, activation markers and increased inflammatory signaling. Moreover, cDC2 cells were found to be a major source of inflammatory mediators, including the NLRP3 inflammasome and *IL23A* in HS lesions. Elevated expression of NLRP3 inflammasome components in HS lesions, including increased expression of *NLRP3*, *IL1B* and *CASP1* in HS lesions highlighted the NLRP3 inflammasome as a potential therapeutic target of interest. While HS lesions had increased secretion of inflammatory mediators, NLRP3 inflammasome inhibition dramatically reduced the overall inflammatory output of HS lesions, indicating a central role of the NLRP3 inflammasome in promoting HS inflammation. Importantly, this study demonstrated proof of concept that inhibition of NLRP3 inflammasome activation in HS skin effectively reduces the secretion of important inflammatory cytokines which drive HS inflammation, including IL-1β, IL-17A, TNF and IFN-γ.

Dysregulated TLR signaling has previously been described in HS. TLRs are essential for the recognition of a broad range of PAMPs and DAMPs by innate immune cells. TLR2, which amongst other receptors (TLR6, dectin-2, complement receptor 3), senses zymosan (Ozinsky *et al.*, 2000; Xia *et al.*, 1999; Brown *et al.*, 2002), was found to be elevated in HS lesions (Hunger *et al.,* 2008). $CD68^+$ macrophages and $CD209^+$ DC were identified as the main source of TLR2 expression in HS lesions (Hunger *et al.,* 2008). More recent transcriptomic analysis identified TLR3, 4 and 9 to be elevated in HS lesional skin relative to healthy skin (Lowe *et al.*, 2020), however relatively little is known about the expression of TLRs by monocytes in HS peripheral blood.

This chapter builds on previous findings which detailed a stepwise increase in the number of monocytes in HS peripheral blood with increasing disease severity (Kanni *et al.,* 2015).

These differences between HS patients and healthy controls were primarily attributed to elevated intermediate and non-classical monocytes in HS patients (Kanni *et al.,* 2015). However, the data in this chapter failed to identify a significant difference in the absolute number of monocytes between HS patients and healthy controls. This discrepancy may have been due to the limited number of patients recruited into this study. Nonetheless, HS monocytes had reduced expression of costimulatory molecules CD40, CD80 and CD86 and HLA-DR relative to healthy controls.

Data presented here replicates previous findings which detailed a dampened cytokine response to LPS in HS PBMC (Kanni *et al.,* 2015). Contrary to this, in purified monocytes no difference was observed in the secretion of IL-1β or TNF between HS and healthy controls following 24 h LPS stimulation. Interestingly, purified HS monocytes had a heightened response to the TLR2 agonist, zymosan, secreting elevated levels of inflammatory cytokines compared with those from healthy controls, suggesting HS monocytes may be primed to respond to TLR2 agonists. The original stimuli which may have primed HS monocytes to have this elevated response to zymosan is unknown but may come in the form of AMPs such as S100A9 or β-defensin-2. Previous chapters highlighted *S100A9* expression as significantly elevated in HS lesions, while others have described elevated levels in HS serum relative to healthy controls (Wieland *et al.,* 2013). S100A9 and β-defensin-2 have been shown to activate TLR2 (Choudhary *et al.,* 2019), and may provide an initial signal which primes HS monocytes to have an elevated cytokine response. Bacteria may also prime this TLR2 response in HS peripheral monocytes, with lipoteichoic acid on gram-negative bacteria (Jimenez-Dalmaroni *et al.*, 2009), or peptidoglycan on *Staphylococcus* known to activate TLR2 (Natsuka *et al.*, 2008), however it is not clear where peripheral monocytes would encounter them.

As a number of HS patients could be considered immunocompromised due to anti-TNF and anti-IL-17 therapies, raising concerns that infections such as COVID-19 might endanger HS patients with more severe infection. However, a surprisingly low incidence of COVID-19 infection has been reported in HS patients. This contrasts with psoriasis patients who had similar infection rates to the general population (Dewigne *et al.,* 2022; Piaserico *et al.,* 2020). The difference in COVID-19 incidence between HS and psoriasis patients is even more striking considering the similar biological pathways involved in both inflammatory

dermatoses (Fletcher *et al.,* 2020). Importantly, the COVID-19 envelope protein is sensed by TLR2, perhaps explaining why HS patients have more effective clearance of COVID-19 and lower incidence of COVID-19 infection (Zheng *et al.,* 2021).

Lowe *et al.,* previously attributed the elevated IL-1 signaling in HS lesions to cDC2 cells (Lowe *et al.*, 2020), this chapter has further expanded on this, highlighting cDC2 cells as a major source of the NLRP3 inflammasome. 8 myeloid clusters were identified in this scRNA-seq dataset, including dermal macrophages, Langerhans cells, cDC2s, cDC1s, LAMP3+ DCs and S100+ macrophages. Dermal macrophages presented here, have previously been characterised by Lowe *et al.,* who described $CD163^+$ macrophages as the largest myeloid population in HS lesions. Corresponding to the dermal macrophages described in this chapter, $CD163^+$ macrophages are known to suppress inflammation in cancer (Kubota *et al.,* 2017), however, may contribute to fibrosis in HS. $CD163^+$ macrophages have been detected in the dermis of HS lesions and mediate excess collagen deposition via CCL18 production (Byrd *et al.,* 2018).

This study has described reduced antigen presenting capacity, decreased CD40 signaling and increased expression of the NLRP3 inflammasome in HS cDC2 cells, suggesting that cDC2 cells may be dysfunctional in HS lesions. Expression of *IL1B*, *NLRP3* and *CASP1* were particularly elevated in HS-hi myeloid cells, outlining a clear association between *IL1B* and inflammation. Furthermore, cDC2 cells were found to be a major source of inflammatory mediators previously shown to be upregulated in HS lesions, including *IL23A*, *IL6*, *CCL20*, *TNF* and *TGFB1*, especially in HS patients with a higher inflammatory load. IL-1β and IL-23A are potent inducers of Th17 cells, while IL-17A has been shown to recruit IL-1β producing myeloid cells in the early stages of autoimmunity, implicating Th17 cells and cDC2 cells in a feedforward inflammatory loop (Acosta-Rodriguez *et al.*, 2007; Manel, Unutmaz and Littman, 2008; McGinley *et al.*, 2020). These data suggest an important role for myeloid cells and cDC2 cells in particular, in promoting HS inflammation.

TNF inhibition has previously been shown to polarise macrophages, reducing expression of the costimulatory markers CD40 and CD80, inhibiting the production of TNF, IL-6 and IL-12 and increasing phagocytosis (Degboé *et al.,* 2019). In Crohn's disease, high IL-1β expression has been proposed as a potential biomarker to identify patients who failed to respond to

adalimumab (Gole *et al.,* 2023). Contrastingly, adalimumab treatment was found to have minimal effects on IL-1 signaling in HS patients (Lowe *et al.*, 2020), supporting findings presented here that TNF inhibition did not impact IL-1β expression or NLRP3 inflammasome signaling in HS lesions. Unfortunately, a limitation of this study is the low number of patients recruited into this scRNA-seq study treated with TNF blockade.

This study supports previous findings of elevated levels of inflammatory mediators in HS lesions, including IL-1β, IL-18, IL-17A, IFN-γ and IL36γ (Kelly *et al.*, 2015; Banerjee, McNish and Shanmugam, 2017; Thomi *et al.*, 2017). Th17 cells have been shown to express *IL1R1* and clear associations were found between the concentrations of IL-17A and IL-1β in HS lesions, suggesting that IL-1β may promote HS inflammation, in part, through promoting the development of Th17 cells (Chung *et al.*, 2009; Gulen *et al.*, 2010). Interestingly, IL-1β was shown to induce the expression of IL-17A, IL-6 and TNF in normal skin, however cytokine concentrations did not reach levels seen in HS lesions (Vossen *et al.,* 2020). The potential value of potentially blocking IL-1 signaling is supported by the phase II trial of anakinra, where 78% of HS patients experienced a 50% reduction in disease activity (Tzanetakou *et al.,* 2016).

Considering the elevated IL-1 signaling and increased expression of *NLRP3* reported here and by others (Witte-Handel *et al.,* 2019), targeting NLRP3 inflammasome activation may prove to be a potential future therapeutic strategy for HS patients. Blocking NLRP3 inflammasome activation with MCC950 expectedly reduced IL-1β levels in HS lesional skin, however, IL-17A, TNF, IFN-γ, IL-8, CCL20 and CXCL1, all of which have been implicated in HS pathogenesis, were also reduced. While this data supports previous findings of increased IL-36γ expression in HS lesions (Di Caprio *et al.,* 2017), interestingly, upon inhibition of NLRP3 inflammasome activation, increased concentrations of IL-36γ were detected. The reason for this is unknown but may be due to a feedback mechanism. IL-36γ has been shown to promote the activation of the NLRP3 inflammasome (Chi *et al.,* 2017) and IL-36R antagonists have been shown to inhibit NLRP3 inflammasome activation (Tian *et al.,* 2020), indicating that this anomaly may be due to an interaction between IL-36γ and the NLRP3 inflammasome. Interestingly, MCC950 also did not reduce the secretion of IL-18 in this skin explant model, despite being processed via NLRP3. This anomaly could be explained by

caspase-independent cleavage of IL-18 by neutrophil serine proteases (Robertson *et al.,* 2006).

Currently, a number of phase I and phase II trials are underway assessing the safety and efficacy of NLRP3 inflammasome inhibition (Schwaid and Spencer, 2021). A range of diseases, including CAPS, heart failure, gout, melanoma, lung fibrosis and neurodegenerative diseases have been targeted in these clinical trials with NLRP3 inflammasome inhibitors (Schwaid and Spencer, 2021). This study provides proof of concept that NLRP3 inflammasome inhibitors may be effective in HS and suggests that in future HS could potentially be added to this list.

The major limitation of this study is the relatively small numbers of HS patients recruited, particularly considering the heterogenous nature of HS. Increased recruitment of HS patients into this study would facilitate patient stratification based on disease severity. Similarly, with the scRNA-seq analysis, two HS patients were being treated with anti-TNF therapies at the time of sampling and the heterogenous nature of HS highlights the importance of further validation with a larger cohort of HS patients.

Overall, this chapter has added substantially to our understanding of myeloid cells in HS peripheral blood and lesions and the role of the NLRP3 inflammasome in promoting HS inflammation. This chapter detailed the dysregulation of monocytes in HS peripheral blood, characterised myeloid cells in HS lesional skin and identified cDC2 cells as major sources of *IL23A, IL1B* and the NLRP3 inflammasome. This is also the first proof of concept study that targeting NLRP3 inflammasome activation in HS skin reduced the overall inflammatory output in HS lesions and may be a potential future therapeutic strategy for HS patients.

Chapter 7

General Discussion

7 General Discussion

7.1 Discussion

HS is a highly distressing disease which frequently goes undiagnosed for years, and once diagnosed, current treatments are generally unsatisfactory and disease relapse is frequent. Therefore, studies to elucidate the pathogenesis of HS are important to understand the complex nature of HS which may lead to the development of improved therapeutics.

With the general hypothesis of a dysregulated immune response driving inflammation in HS lesions, this study sought to analyse the role of keratinocytes and fibroblasts in greater detail than has previously been undertaken. It highlighted, for the first time, multiple keratinocyte and fibroblast cell subsets which were dysregulated in HS lesional skin. It outlined B cells and elevated immunoglobulins as key features of HS which differentiates HS from other inflammatory dermatoses. Further, research findings here suggested that targeting the NLRP3 inflammasome, which is upregulated in cDC2 cells in HS lesions, may be a future therapeutic strategy in HS.

The data presented herein, utilised primary human tissue from healthy control donors and importantly, lesional, tract and normal skin from HS patients, employing technologies such as RNA-seq and multiparameter flow cytometry to maximise outputs. The small biopsy size often limits the experimental approaches however, primary tissue is the best representation of HS disease due to the lack of suitable mouse models for HS. Although $PSEN^{-}$, $PESEN1^{-}/PSEN2^{-}$ and $NCSTN^{+/-}$ mouse models have been developed, and replicate some histological features of HS lesions (Pan *et al.*, 2004; Li *et al.*, 2007), only a minority of HS patients have been found with genetic variants in these genes (Nomura, 2020). Importantly, whether the immune cell profiles of these mouse models replicate the immune cell profile in HS lesions has yet to be elucidated. This emphasises the importance of using primary tissue from HS patients, which although limited in size, provides the best representation of HS disease.

This study demonstrated the complex inflammatory milieu which distinguishes HS from other inflammatory dermatoses. While AD can be generally considered a Th2-mediated disease, and psoriasis a Th17-mediated disease, the data presented here implicated B cells,

plasma cells, keratinocytes, fibroblasts, T cells and myeloid cells in HS inflammation. The data presented in **Chapter 3** clearly identified B cells and plasma cells as a distinguishing feature of HS, which is supported by previous findings identifying B cells and plasma cells in HS lesions (Gudjonsson *et al.*, 2020). This elevated B cell signature is an important feature of HS lesions, and interestingly, HS patients with an elevated B cell signature were found to be less likely to respond to adalimumab treatment (Hambly *et al.*, 2023). The increased expression of immunoglobulin genes in HS lesions presented here, may play an active role in promoting inflammation by activating dermal macrophages in HS lesions (Carmona-Rivera *et al.*, 2022).

HS lesions have a number of distinct dermatological features including epidermal hyperplasia, dermal tunnel formation and hypertrophic scarring which suggest an important role for both keratinocytes and fibroblasts in HS pathogenesis. The data presented here characterised an inflammatory phenotype in both HS keratinocytes and fibroblasts. HS keratinocytes appeared to have aberrant differentiation, with increased expression of inflammatory keratins, AMPs and chemokines which is likely driven by Th17 cells. While Th17-driven epidermal hyperplasia is a prominent feature of psoriasis lesions, data presented here outlines a similar process occurs in HS. While IL-17 cytokines evidently play a role in both HS and psoriasis, keratinocytes behave differently in both dermatoses. In psoriasis, upon IL-17 stimulation, keratinocytes have unregulated proliferation to form the scaly plaques characteristic of psoriasis lesions, whereas in HS, keratinocytes contribute to inflammation by producing chemokines and cytokines but do not have unregulated proliferation, as seen with the moderate thickening of the epidermal layer, suggesting that unique molecular mechanisms regulate keratinocyte proliferation in HS and psoriasis.

Dermal tunnels have recently been identified as a hotspot of immune activity within HS lesions. How dermal tunnels form in HS has yet to be fully elucidated, however it likely involves fibroblast activity (Frew *et al.*, 2019). The scRNA-seq analysis of fibroblasts presented herein, provides the first detailed characterisation of HS lesional fibroblasts, providing novel insights into their role in promoting HS inflammation. Increased expression of the neutrophil chemoattractants, *CXCL1*, *CXCL5* and *CXCL8* coupled with pronounced antimicrobial activity in inflammatory fibroblasts suggests a potential role in dermal tunnel formation. While an influx of neutrophils have been shown to enter HS lesions, dramatic

neutrophil infiltrate has been detected in HS dermal tunnels (Navrazhina *et al.*, 2021a). Dermal tunnels have also been shown to have a luminal biofilm which may trigger an antimicrobial response in HS fibroblasts (Ring *et al.*, 2017a). Evidence suggests that HS fibroblasts may also be implicated in the development of hypertrophic scarring in HS. Dysregulated expression of collagen and MMP genes are key features in the formation of hypertrophic scars which are present in HS inflammatory fibroblasts. Unfortunately, lack of histological examination means the presence of dermal tunnels or hypertrophic scarring in these patients cannot be confirmed.

This study suggests the dysregulated expression of inflammatory, and scarring-associated genes in HS fibroblasts is likely driven by TNF and TGF-β. TGF-β has previously been implicated in the development of scarring (Liu *et al.*, 2016), while TNF regulated the expression of neutrophil chemoattractants, collagen genes and MMPs in HS fibroblasts. Further, the increased expression of *CSF3*, also driven by TNF, has previously been shown to promote neutrophil activity in HS lesions (Gamell *et al.*, 2023). Coinciding with this, HS patients treated with TNF blockade had an overall reduction in expression of inflammatory mediators, and importantly, a reduction in the expression of neutrophil attractants, *CSF3* and AMPs, indicating that TNF inhibition can reduce neutrophil activity and potentially dermal tunnel development in HS lesions. Adalimumab trials in HS suggested that dermal tunnels prolong time to achieve HiSCR and tunnels cannot be completely resolved with adalimumab treatment (Frew *et al.*, 2021a). However, reports suggest different types of dermal tunnels respond differently to adalimumab (Martorell *et al.*, 2019). Dermal and dermoepidermal fistulas have been found to respond well to adalimumab treatment, while complex and subcutaneous tunnels did not respond to TNF blockade and required surgical removal (Martorell *et al.*, 2019).

While T cell dysregulation has been identified in HS for some time now, detailed examination of T cell subsets in HS lesions by scRNA-seq has been lacking. Findings here replicate previous studies identifying increased IL-17A^{+} T cells (Moran *et al.*, 2017), while also detailing a potential novel regulatory subset in CD52^{+} CD4 T cells which has not previously been defined in HS lesions. The majority of cells in this scRNA-seq dataset expressed the TRM marker *CD69*, however, it is difficult to determine if these cells are truly resident as CD69 expression is also increased upon activation. Characterisation of

emigrated T cells from HS sinus tracts identified resident memory populations expressing CD69 and/or CD103. While further investigation is required, the characterisation TRM cells in HS lesions may be important for understanding HS pathogenesis considering their highly pathogenic nature in other disease settings, and their tendency to locate around hair follicles in HS skin (Collins *et al.*, 2016).

Myeloid cells are crucial for the development of Th17 cells and dysfunction of which may encourage the development of Th17 cells in HS lesions. In peripheral blood, HS monocytes have previously been shown to be elevated in HS patients and had a dampened response to LPS (Kanni *et al.*, 2015). Elaborating on this suggestion of monocyte dysfunction, findings presented herein suggested that HS monocytes had reduced expression of costimulatory molecules relative to healthy controls, while an elevated response to the TLR2/dectin agonist zymosan, suggested that HS monocytes may be primed to respond to specific stimuli. This elevated response to TLR2/dectin stimulation with zymosan, coupled with the metabolic reprogramming of HS PBMC (Petrasca *et al.*, 2023a), increased myelopoiesis found in HS blood (Kearney *et al.*, 2023) and potential epigenetic changes as indicated by altered hydroxy-methylation in HS lesions (Hessam *et al.*, 2017) may be indicative that aberrant trained immunity may be implicated in HS inflammation. Importantly, this elevated response may contribute to the effective clearance of COVID-19 infection and result in the reduced COVID-19 incidence seen in HS patients relative to the general population.

Dysregulated myeloid cell function continues in HS lesional skin, data presented here suggests cDC2 cells are also the main source of the NLRP3 inflammasome, *IL1B* and *IL23A* in HS lesions, replicating previous findings (Lowe *et al.*, 2020). Importantly, while TNF inhibition in HS patients reduced the expression of *IL23A*, *TNF* and *CXCL8* in myeloid cells, it did not affect the expression of NLRP3 inflammasome components or *IL1B*. This may explain why some HS patients do not respond to adalimumab treatment, with potentially a greater role for NLRP3 inflammasome mediated IL-1 signaling in these patients.

Importantly, this study demonstrated proof of principle that inhibition of NLRP3 inflammasome activation may be an effective therapeutic strategy in HS. *Ex vivo* analysis presented here replicated increased levels of inflammatory cytokine release from HS skin

detailed by others. Upon inhibition of the NLRP3 inflammasome, significant reductions in IL-1β were found in HS lesions. Interestingly, NLRP3 inflammasome inhibition also reduced the secretion of IL-17A, CXCL1, and CCL20, indicating an intrinsic link between NLRP3 inflammasome activation and IL-17 signaling. Importantly, inhibition of the NLRP3 inflammasome can reduce levels of inflammatory cytokines including IL-1β, TNF and IL-17, which have previously been implicated as key drivers of HS. What activates the NLRP3 inflammasome in HS skin has yet to be elucidated, however studies have previously demonstrated that AMPs including S100A8 and S100A9, which are highly elevated in HS lesions, can be a priming signal for the NLRP3 inflammasome (Choudhary *et al.*, 2019). The rupture of hair follicle likely releases a range of DAMPs which may trigger NLRP3 inflammasome activation, including keratins fibres, bacteria and sebum components.

7.2 Implications for HS therapy

The findings within this thesis highlighted the complex nature of HS (**Figure 7.1A**) and reinforce the need for a larger arsenal of targeted therapeutics or treatments which have a broad inhibitory effect on multiple inflammatory pathways. This study has also emphasised the need to find ways to stratify patients for specific targeted therapies based on their inflammatory profile.

The profound success of IL-17 targeted therapies in psoriasis, and the prominence of Th17 cells and IL-17 signaling in HS suggested that anti-IL-17 therapy would be effective in HS. However, while IL-17 inhibitors, have revolutionised the treatment of severe psoriasis, secukinumab was recently approved by the EMA for treatment in HS, with <50% of HS patients achieving HiSCR (Kimball *et al.*, 2023a). Dual cytokine blockade of IL-17A and IL-17F with bimekizumab proved to be effective in a small cohort of psoriasis patients (Oliver *et al.*, 2022). Phase 2 trials of bimekizumab in HS proved to be more effective than adalimumab, demonstrating dual IL-17 cytokine inhibition as an effective treatment strategy in HS (Glatt *et al.*, 2021). Similarly, brodalumab treatment has been found to be extremely effective in open label trials in HS (Navrazhina *et al.*, 2022a; Frew *et al.*, 2020), however larger trials are required to evaluate the true efficacy of IL-17 receptor blockade. Unfortunately, the elevated complexity of HS pathogenesis relative to psoriasis displayed

in this study suggests therapies targeting IL-17 signaling alone may not be as effective in HS as they are in psoriasis.

In addition to targeting IL-17 cytokines or their receptor, therapies which act upstream of IL-17 cytokine generation present another therapeutic opportunity. cDC2 cells were the primary source of both *IL1B* and *IL23A* expression in HS lesions, which are thought to be crucial for the development of Th17 cells, and so are attractive potential therapeutic targets in HS. IL-23 inhibition proved highly successful in psoriasis (Reich *et al.*, 2019) and achieved promising results In a phase 2 trial of 20 HS patients in which 65% had at least a 50% improvement in disease activity (Dudink *et al.*, 2023). However, in the larger phase 2b NOVA trial for guselkumab (NCT03628924), IL-23 inhibition was only effective in a cohort of HS patients, indicating that IL-23 may not be central to HS. Direct inhibition of IL-1β has shown both positive and negative results in individual case reports (Houriet *et al.*, 2017; Sun *et al.*, 2017). More comprehensive trials have been performed on anakinra in HS, which competitively inhibits the interaction between IL-1α and IL-1β with their receptor, demonstrating moderate efficacy in HS (Tzanetakou *et al.*, 2016). However, IL-1β has been shown to have broad effect on a range of immune cells in HS. IL-1β was shown to regulate the expression of multiple cytokines, chemokines and MMPs in HS fibroblasts which promote neutrophil recruitment and scar formation, while IL-1β also induces the expression of neutrophil chemoattractants in keratinocytes (Witte-Handel *et al.*, 2019). Neutrophils, shown to be elevated in severe HS (Lima *et al.*, 2016), can also produce IL-1β, and in turn, exogenous IL-1β induces NET formation (Mitroulis *et al.*, 2011). Together, this suggests targeting IL-1β signaling may be a promising therapeutic strategy in HS, however efficacy may depend on HS disease severity.

Until recently, TNF inhibition with adalimumab was the only biologic approved for the treatment of HS (Kimball *et al.*, 2012). Data presented here demonstrated the impact of anti-TNF treatment on the expression of inflammatory mediators in keratinocytes, fibroblasts, T cells and myeloid cells in HS lesions. TNF inhibition reduced the expression of various inflammatory mediators (**Figure 7.1B**), beyond downregulation of TNF, demonstrating the immune-modulating potential of anti-TNF therapies in HS. Despite this, some inflammatory pathways were not affected by TNF inhibition. Notably, NLRP3

inflammasome and IL-1 signaling were not downregulated in HS patients treated with TNF blockade, identifying a key inflammatory pathway which remained active in these HS patients treated with anti-TNF therapies. Elevated NLRP3 inflammasome signaling in some HS patients may explain why some patients fail to respond to anti-TNF therapy.

This study also highlighted B cells as a distinguishing feature of HS lesions. While *ex vivo* studies and single case reports suggest B cell depletion with rituximab may be effective in HS (Takahashi *et al.*, 2018; Vossen *et al.*, 2019a), the potential severe adverse side effects of B cell depletion mean specific therapies may be more beneficial. The use of fostamatinib, a spleen tyrosine kinase inhibitor targeting B cells and plasma cells has been trialled in a small cohort of patients, yielding promising results, however larger studies are required (Jepsen *et al.*, 2023).

This study has emphasised the heterogeneous nature of HS inflammation which may have important therapeutic implications. **Chapter 3** described an increased B cell and immunoglobulin signature in a cohort of HS patients, while subsequent chapters illustrated the potential to stratify patients based on lesions with a high and low inflammatory load. Importantly, this stratification was replicated in HS fibroblasts, T cells and myeloid cells but not HS keratinocytes. This adds an extra layer onto the complexity of HS, indicating that in HS the activation of keratinocytes may not fully reflect the inflammation in the HS dermis. Identifying key characteristics in HS lesions in order to stratify HS into subgroups could improve patient responses to therapy, aligning patients with more suitable treatment options.

The data presented here, suggests NLRP3 inflammasome inhibitors may be an effective therapeutic strategy in HS. Blocking inflammasome activation induces widespread inhibitory effects, reducing the levels of IL-1β, IL-17A and TNF in this HS lesional skin explant model (**Figure 7.1C**). NLRP3 inflammasome inhibition is currently being trialled in a phase 3 trial for small cell lung cancer (NCT05566041) and phase 2 trials for osteoarthritis, gout and CAPS (NCT01768975)(Klück *et al.*, 2020; Lonnemann *et al.*, 2020). Further investigation into the efficacy of NLRP3 inflammasome inhibition in HS is required, however this study opens a novel potential therapeutic avenue for HS patients.

This complexity in HS inflammation incorporates elements of both autoinflammation, with elevated inflammasome and IL-1 signaling, and autoimmunity, as seen with the presence of autoreactive B cells and autoantibodies in HS lesions (Carmona-Rivera *et al.*, 2022). Due to the presence of a B cell and immunoglobulin signature in only a cohort of HS patients, it is possible that autoinflammation occurs first, which then promotes an autoimmune response in HS patients. It may therefore be beneficial to treat HS patients early with inflammasome inhibitors before the initiation of an autoimmune response.

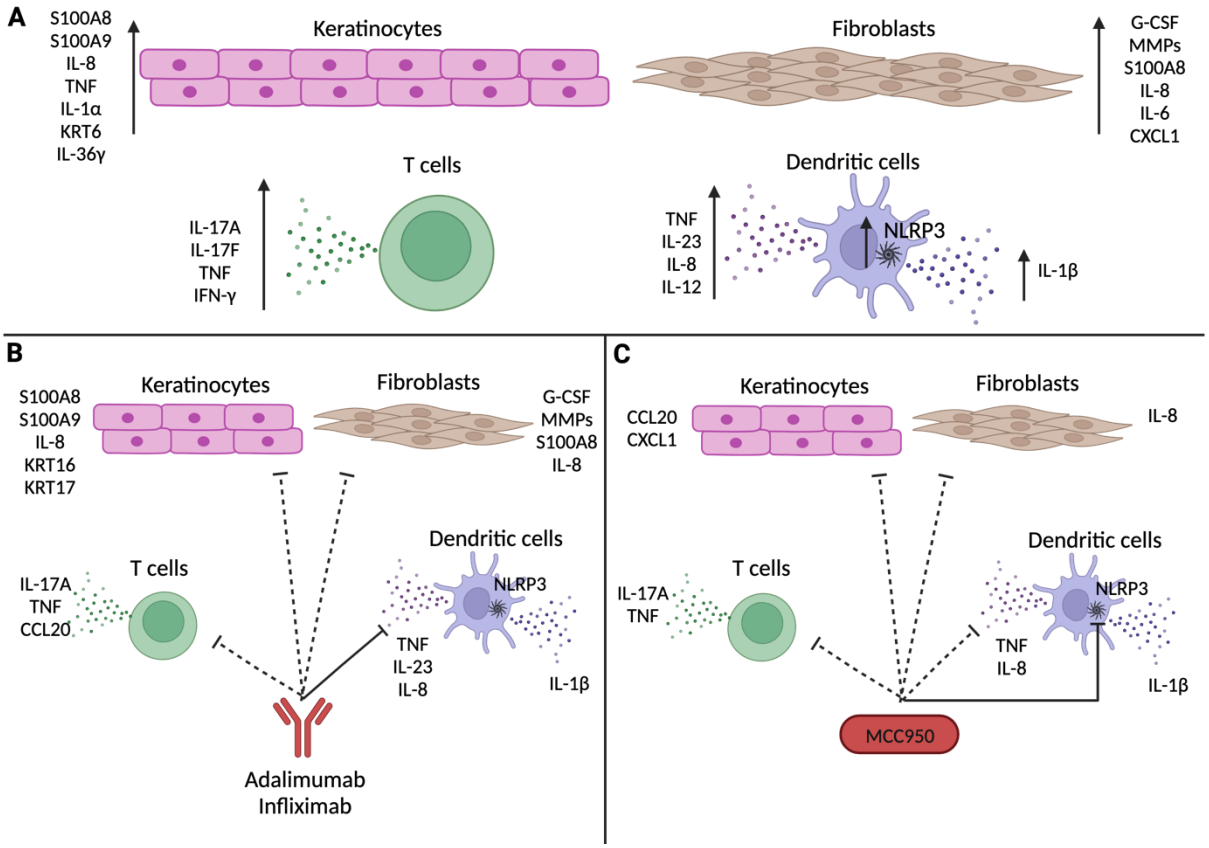

Figure 7.1 Effects of anti-TNF and MCC950 on dysregulated cellular responses in HS. The data presented in this thesis suggests multiple cell types become dysregulated during the course of HS disease. Keratinocytes have an increased inflammatory phenotype expressing KRT6 and elevated expression of the inflammatory mediators S100A8, S100A9 and IL-8. HS keratinocytes have also been shown to produce the inflammatory cytokines TNF, IL-1α and IL-36γ. Fibroblasts similarly have increased expression of inflammatory cytokines (IL-6 and G-CSF), neutrophil chemoattractants (CXCL1 and IL-8), as well as dysregulated MMP and AMP production. T cells in HS lesions have elevated expression of inflammatory cytokines IL-17A, IL-17F, IFN-γ and TNF. HS DCs have increased TNF, IL-23 and IL-8 expression and pronounced IL-1β expression relative to healthy controls (A). Following TNF blockade, there were dramatic reductions in the expression of inflammatory mediators in keratinocytes, fibroblasts, T cells and DC. Importantly, TNF inhibition did not impact IL-1β expression or NLRP3 inflammasome expression in HS DCs (B). Treatment with the NLRP3 inflammasome inhibitor, MCC950, directly inhibited the secretion of IL-1β in HS lesions, and indirectly reduced the secretion of TNF, IL-17A, CCL20, CXCL1 and IL-8 (C).

7.3 Limitations

While this project has provided novel insight into HS pathogenesis, there were inevitably some limitations in this project. Relatively small sample sizes have limited the conclusions which can be generated in some experiments, and increased sample sizes would facilitate stratification of HS patients based on clinical data such as disease severity. Successful collaboration with leading clinicians and surgeons provided access to primary tissue and blood to effectively study HS immunopathogenesis. Unfortunately, it was impossible to match the locations of HS lesional and healthy control skin samples. HS lesions were mostly from the axilla and groin, whereas the healthy control skin samples came from excess skin from the breast of reduction mammoplasty surgeries or from the abdomen of reduction abdominoplasty surgery. Similarly, healthy blood came from anonymous donors in TCD and staff from SVUH which did not have matched BMI or smoking status to the HS patients. A compounding factor which must also be considered is the high BMI and obesity of HS patients included in these studies. While some of the healthy controls included in these studies came from abdominoplasty surgeries and likely had high BMI and obesity, many healthy donors did not have matched BMI to HS patients, and so the background inflammation associated with obesity must be considered.

While scRNA-seq is an exceptional research tool, like all techniques, there are limitations to its findings. Importantly, it identifies the levels of mRNA at a snapshot in time rather than protein translation, meaning proteomic techniques are required to validate findings here. Further detailed proteomic analysis of HS lesional skin should be used to validate findings here and confirm transcriptomic alterations identified in HS skin extend to alterations at the protein level. In addition, expression of certain genes, expected to be present in the data seem to be absent, including *IL17RA* in fibroblasts. This is not to say these genes are not expressed, but merely not transcribed at that moment in time. This may reflect a technical artifact of scRNA-seq in which certain genes are not captured optimally, or a biological artifact in which certain proteins are stably expressed and so do not have a high turnover of mRNA. While scRNA-seq is a state-of-the-art technique, it lacks the sequencing depth which can be routinely achieved in bulk RNA-seq. Conversely, bulk RNA-seq loses the ability to pinpoint the specific cell populations responsible for transcriptomic alterations. Importantly, samples used for bulk RNA-seq and scRNA-seq analysis were previously cryopreserved. Unfortunately, considering the important role of neutrophils in HS

inflammation, cryopreservation means neutrophil populations were lost for this transcriptomic analysis in both the bulk and scRNA-seq datasets.

Characterisation of T cells by flow cytometry was performed on emigrating T cells from HS tracts and healthy control skin. This process required a 10-day culture in IL-2 supplemented media which may not exactly reflect T cells in HS lesions. Unfortunately, the limited number of cells recovered from skin digestions made it difficult for extensive analysis of TRM cells in particular. TRM cells are difficult to confidently identify in active HS lesions. CD69 is expressed by both TRM cells and activated T cells. A better reflection of potentially skewed TRM cell profiles may come from unaffected HS skin where local T cells would not be activated by the inflammatory microenvironment. Also, the lack of histological analysis limits some of the conclusion which can be made about the formation of dermal tunnels and hypertrophic scarring in this dataset.

7.4 Future directions

This study gave a global overview of the complex immune landscape within HS lesions. It has implicated B cells, plasma cells, Th17 cells, keratinocytes, fibroblasts and cDC2 cells in HS pathogenesis and identified the NLRP3 inflammasome as a potential novel therapeutic strategy in HS.

Findings here, and by others, have implicated B cells in HS inflammation (Gudjonsson *et al.*, 2020). Further investigation into B cell function and B cell receptor specificity would provide further insight into the pathogenic role B cells may have in HS lesions. This may be particularly interesting in HS patients treated with adalimumab, with elevated B cell signature identified in HS patients who failed to respond to adalimumab (Hambly *et al.*, 2023). Considering the increase of B cells in HS peripheral blood, evaluation of B cells in the periphery may provide a potential biomarker to stratify potential responders and non-responders to adalimumab treatment.

Interestingly, an altered differentiation program was identified in HS keratinocytes relative to healthy keratinocytes. This altered differentiation, characterised by increased expression of *KRT6*, *KRT16* and *KRT17* likely contributes to the epidermal hyperplasia seen

in HS. Detailed investigation into the molecular mechanisms which regulate keratinocyte proliferation in HS and psoriasis lesions could provide insight into why psoriasis patients develop the scaly plaques and provide additional insight into the contribution of keratinocytes to HS inflammation. The functional differences between HS and psoriasis keratinocytes should also be evaluated. Data presented here demonstrated elevated expression of *CXCL8, CXCL2 and CCL27* by HS keratinocytes relative to psoriasis, indicating functional differences between HS and psoriasis keratinocytes.

As dermal tunnels and hypertrophic scarring are distinctive features of HS, more detailed characterisation of the specific cells present here would be invaluable to the field. Highly multiplex tissue imaging, such as ChipCytometry (Jarosch *et al.*, 2022), which uses iterative cycles of staining with fluorophore-conjugated antibodies, would allow the localisation of cell populations in HS dermal tunnels. Further, it is important to identify what drives the development of hypertrophic scarring in HS patients. scRNA-seq of fibroblasts from HS hypertrophic scars and fibroblasts from HS patients with Hurley stage 1, 2 and 3 disease would provide insight into the transcriptional changes which promote the development of hypertrophic scars in HS. Considering the impact of hypertrophic scarring on patients' quality of life (Krakowski *et al.*, 2014), further investigation into what drives this process would be invaluable.

While this study identified the presence of TRM markers in HS tracts, further investigation is required to confidently identify TRM cells in HS skin. To do this, a larger flow cytometry panel incorporating both central and resident memory markers in peri-lesional and uninvolved HS skin would be beneficial. Further, identifying where these cells localise in HS lesions would also be beneficial. This study identified $CD52^{+}$ CD4 T cells not previously identified in HS lesions. Further characterisation of these cells is required to determine if these cells have a regulatory function in HS skin. While this study demonstrated that anti-TNF therapy downregulated the expression of many inflammatory mediators in various cell types in HS lesions, the small number of HS patients treated with anti-TNF therapies (n=2) makes it difficult to make confident conclusions from these data. A study involving a larger cohort of patients is required to validate some of the findings presented here.

Th17 cells have been implicated in HS pathogenesis, and IL-23A and IL-1β, which are essential for Th17 development, have been postulated as potential therapeutic targets in HS. Despite this, IL-23 inhibition was only successful in a cohort of HS patients, indicating IL-23 may not be central to HS. Recent studies suggest that this may be due to reduced expression of *IL23R* and increased *IL1R1* in HS Th17 cells relative to psoriasis, suggesting that the IL-1β:Th17 axis is likely dominant in HS. Further characterisation of Th17 cells is required to confirm these findings, including evaluating the expression of IL-23R and IL-1R1 on the surface of HS Th17 cells.

An interesting feature of HS was identified in **Chapter 6** as HS monocytes had reduced expression of costimulatory molecules and an increased response to the TLR2/dectin agonist, zymosan. To further elaborate on this, TLR expression should be evaluated on HS monocytes to determine if there is an increase in TLR2 expression relative to healthy monocytes. The increased expression of CD64 and HLA-DR indicated a potential dysregulation in phagocytosis and antigen presentation. Assays evaluating the phagocytic and antigen presenting capacity of HS monocytes would provide additional insight into monocyte dysregulation in HS patients. An important question arising from this study is whether HS monocytes continue to be dysfunctional as they migrate into the skin. Further investigation into monocyte differentiation in HS lesions may provide further insight into myeloid cell dysregulation presented in this study.

Inhibiting the NLRP3 inflammasome proved to be effective at reducing inflammatory mediators in this *ex vivo* model, however what activates the NLRP3 inflammasome in HS lesions has yet to be elucidated. While there may be numerous activators of the NLRP3 inflammasome in HS lesions, the components of a ruptured hair follicle which likely initiates HS disease are prime candidates. Inflammasome assays evaluating the ability of keratin fibres and DAMPs including S100A8 and S100A9 to activate the inflammasome could provide insight into the key initiating events of HS.

Overall, this study has added to our understanding of HS inflammation. This study has demonstrated the highly complex nature of HS relative to other inflammatory dermatoses, while also identifying potential novel therapeutic strategies in HS.

Chapter 8

Appendix

8 Appendix

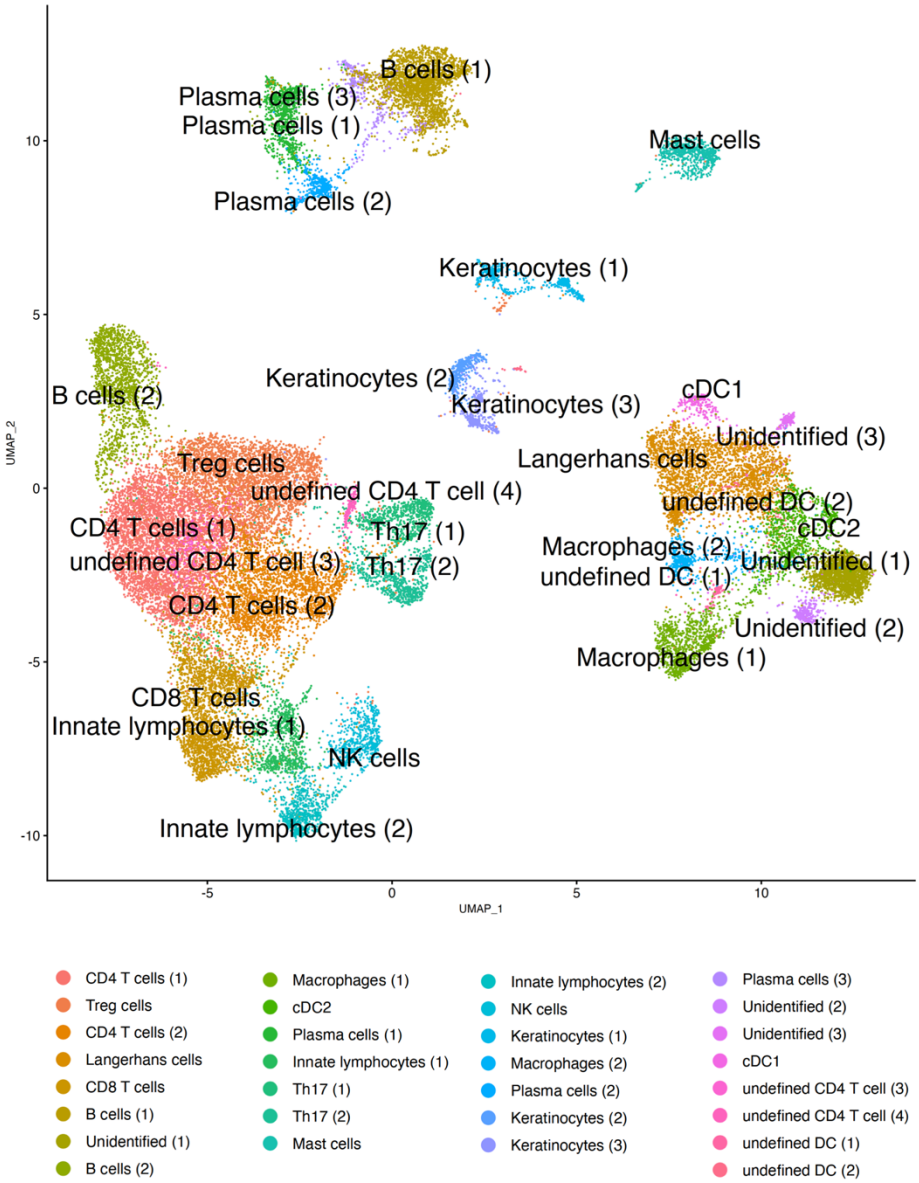

Figure 8.1 UMAP displaying 30 unique cell clusters in the CD45⁺ dataset. Single cells isolated from healthy controls (Con; n=3) or HS lesional skin (HS; n=6) were purified based on CD45 expression, barcoded and sequenced by 10X Genomics scRNA-seq. UMAP displays the individual cells isolated from HS lesional skin and healthy control skin integrated together following unsupervised classification of CD45⁺ cells.

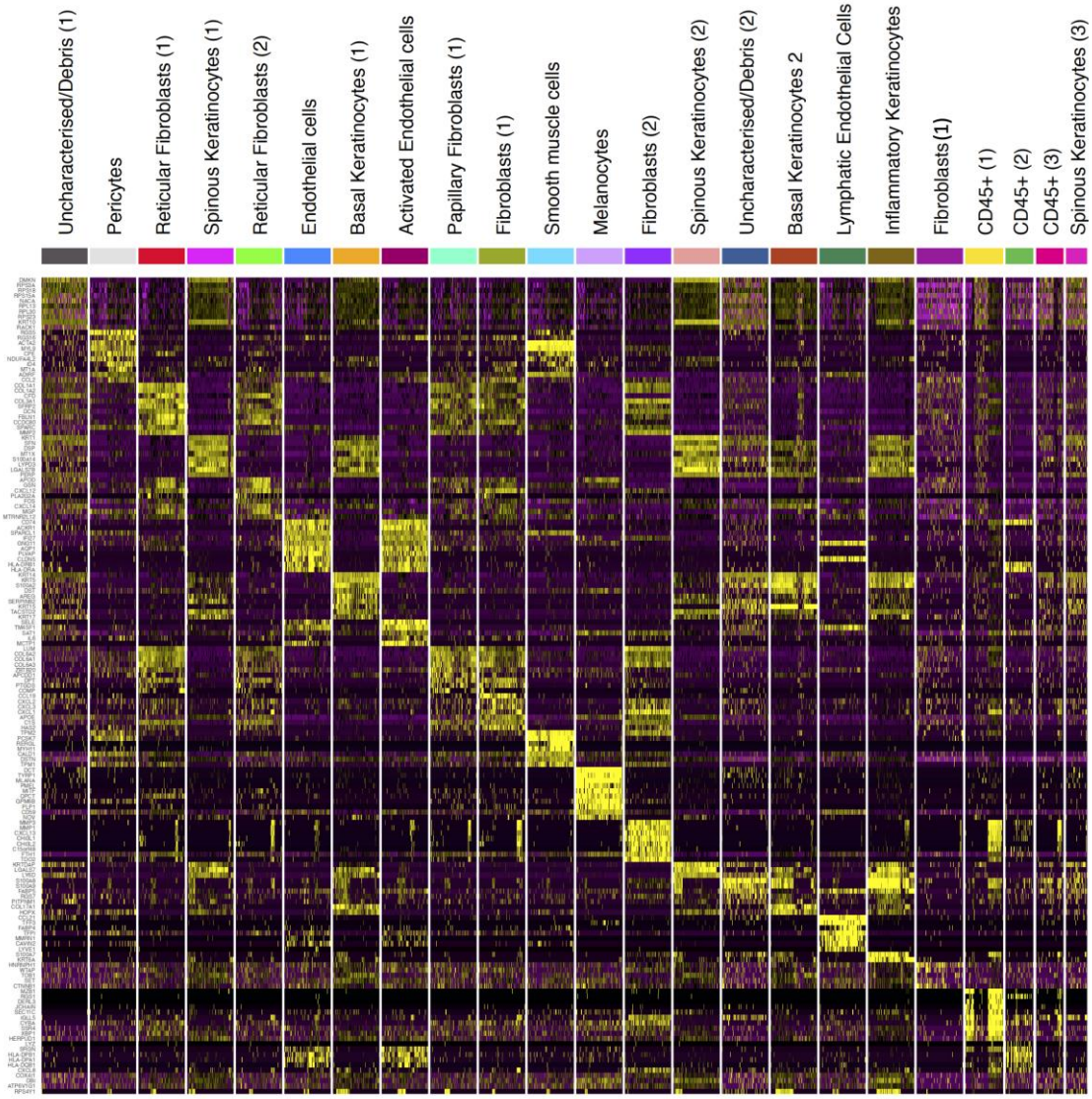

Figure 8.2 Heatmap of cluster-specific markers. Single cells isolated from healthy controls (Con; n=3) or HS lesional skin (HS; n=6) were purified based on absence of CD45 expression, barcoded and sequenced by 10X Genomics scRNA-seq. Heatmap visualised cluster-specific genes identified by Wilcoxon Rank Sum test.

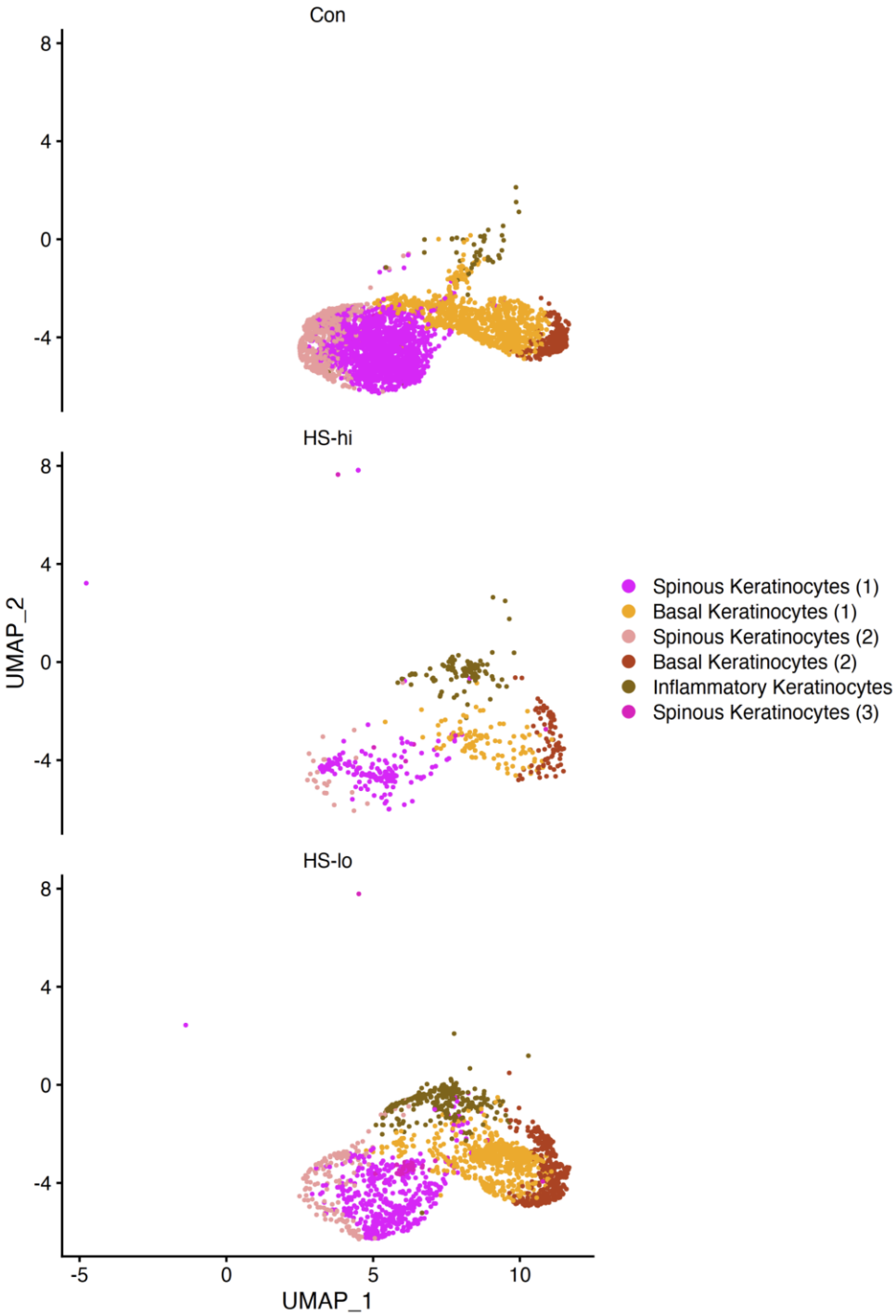

Figure 8.3 UMAP displaying keratinocytes in HS-hi lesions, HS-lo lesions and healthy control skin. Single cells isolated from healthy controls (Con; n=3) or HS lesional skin (HS; n=6) were purified based on absence of CD45 expression, barcoded and sequenced by 10X Genomics scRNA-seq. UMAP displays the individual cells isolated from HS-hi lesional skin (n=4), HS-lo (n=2) lesional skin and healthy control skin integrated together after unsupervised classification of $CD45^-$ cells.

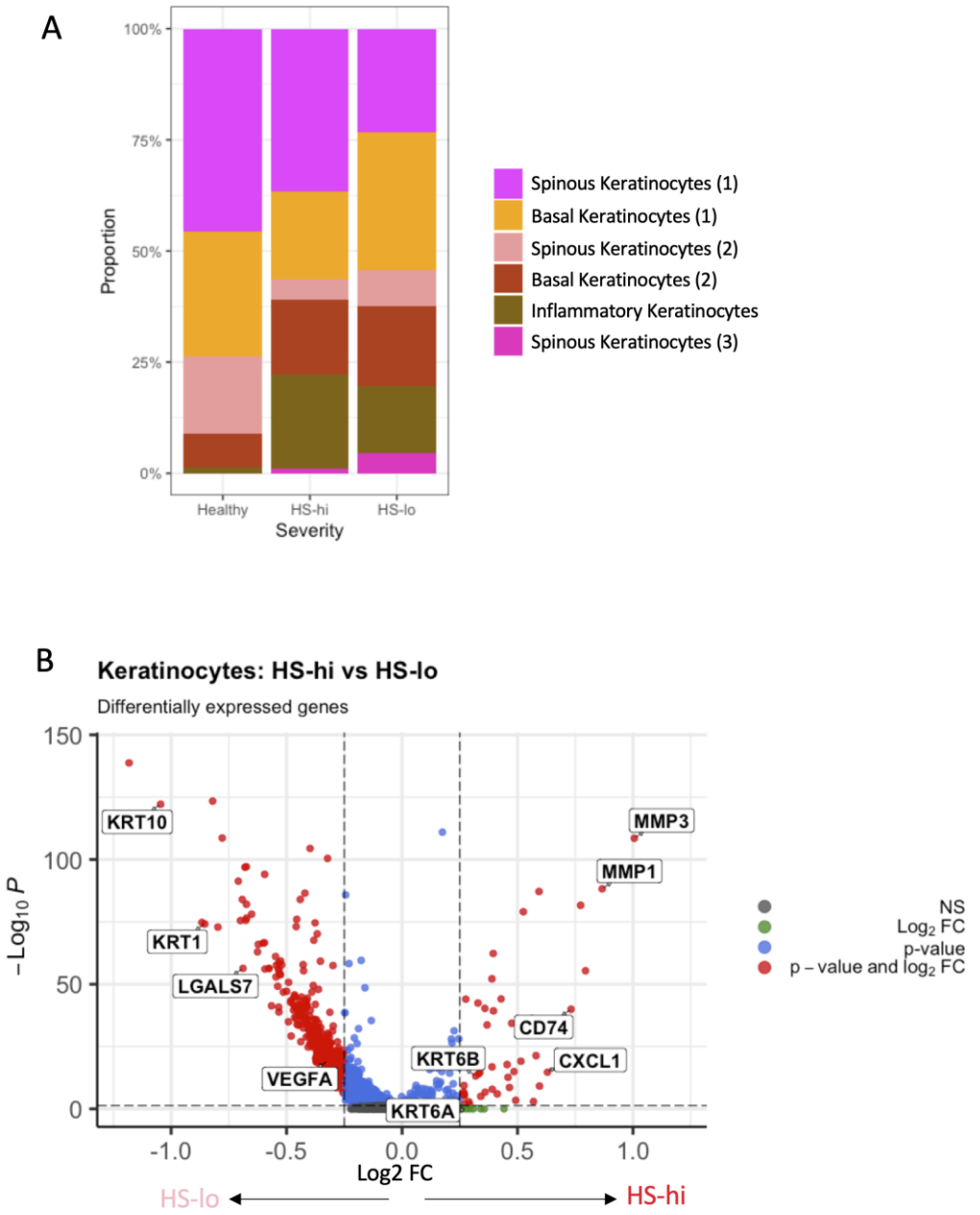

Figure 8.4 Cellular frequencies and transcriptomic differences between HS-hi and HS-lo keratinocytes. Single cells isolated from healthy controls (Con; n=3) or HS lesional skin (HS; n=6) were purified based on absence of CD45 expression, barcoded and sequenced by 10X Genomics scRNA-seq. Bar chart showing the proportion of each keratinocyte cluster relative to all keratinocytes in healthy control, HS-hi (n=4) and HS-lo (n=2) lesional skin (A). Volcano plot visualises DEGs in papillary fibroblasts (1) from HS lesions compared with those in healthy control skin. Genes with a $log_2FC > 0$ are upregulated in HS and a $log_2FC < 0$ are downregulated in HS. The $-Log_{10}P$ Y-axis is a measure of significance (B).

A

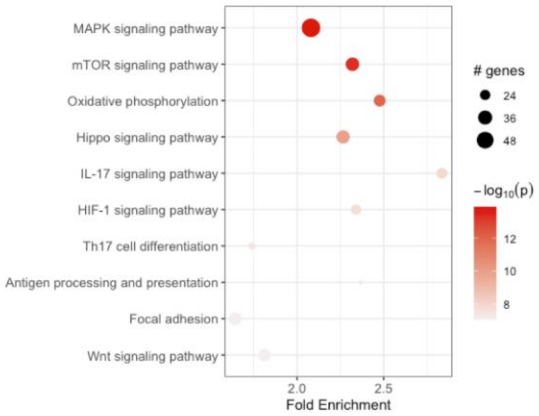

B

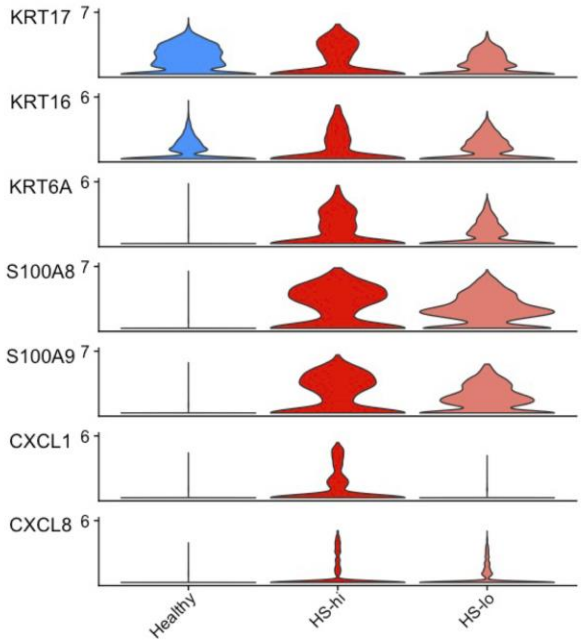

Figure 8.5 IL-17-regulated genes are elevated in HS-hi lesions relative HS-lo lesions and healthy control skin. Top 10 immune pathways enriched from the genes significantly differentially expressed between HS-lo (n=2) and HS-hi (n=4) lesions ($p < 0.05$ and $\log_2FC > 0.1$) (A). Violin plot visualising the expression of inflammatory keratins (KRT6A, KRT16, KRT17), AMPs (S100A8, S100A9) and IL-17 regulated genes (CXCL1, CXCL8) (B).

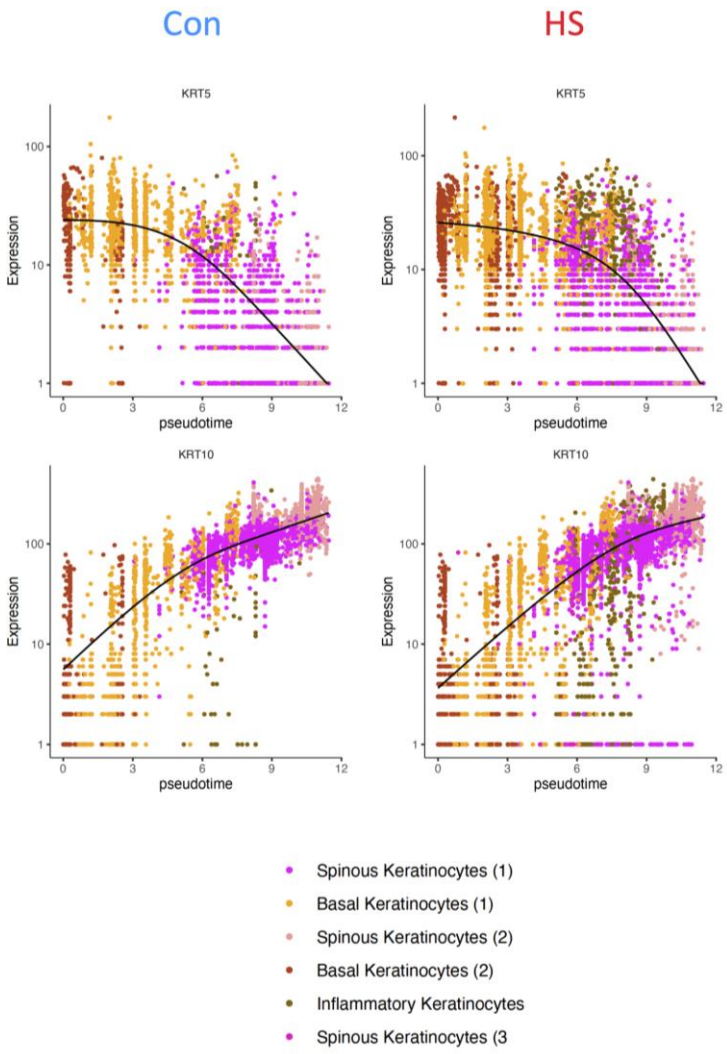

Figure 8.6 Expression of KRT5 and KRT10 across pseudotime trajectory. Single cells isolated from healthy controls (Con; n=3) or HS lesional skin (HS; n=6) were purified based on absence of CD45 expression, barcoded and sequenced by 10X Genomics scRNA-seq. Pseudotime trajectory analysis performed using Monocle3 on the keratinocyte clusters to identify how cells choose between different cellular states. Scatter plot tracking the expression of *KRT5* and *KRT10* across pseudotime in healthy control and HS keratinocytes (B).

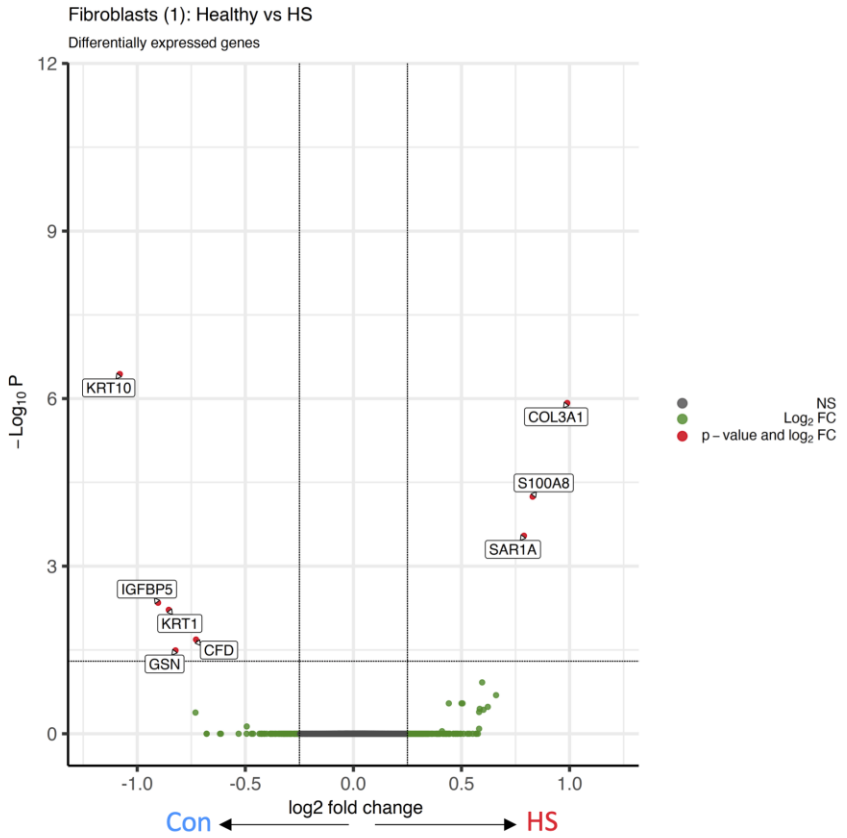

Figure 8.7 Differentially expressed genes in the fibroblast (1) cluster between HS lesional and healthy control skin. Single cells isolated from healthy controls (Con; n=3) or HS lesional skin (HS; n=6) were purified based on the absence CD45 expression, barcoded and sequenced by 10X Genomics scRNA-seq. Volcano plot visualises DEGs in fibroblasts (1) from HS lesions compared with those in healthy control skin. Genes with a $log_2FC >0$ are upregulated in HS and a $log_2FC <0$ are downregulated in HS. The $-Log_{10}P$ Y-axis is a measure of significance.

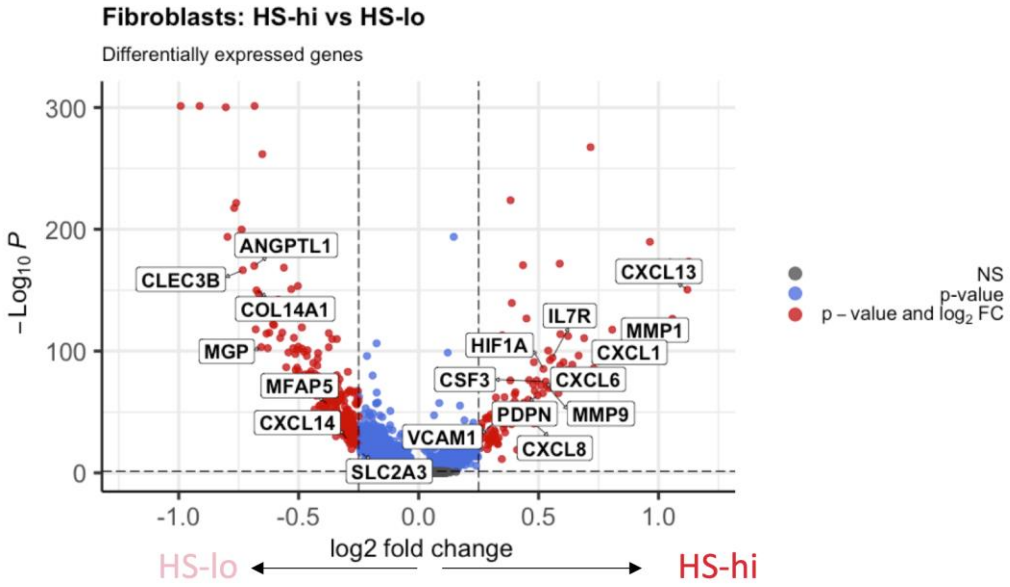

Figure 8.8 Differentially expressed genes between HS-hi and HS-lo fibroblasts. Single cells isolated from healthy controls (Con; n=3) or HS lesional skin (HS; n=6) were purified based on the absence CD45 expression, barcoded and sequenced by 10X Genomics scRNA-seq. Volcano plot visualises

DEGs in fibroblasts from HS-hi lesions compared with those in HS-lo lesional skin. Genes with a $log_2FC > 0$ are upregulated in HS and a $log_2FC < 0$ are downregulated in HS. The $-Log_{10}$ P Y-axis is a measure of significance.

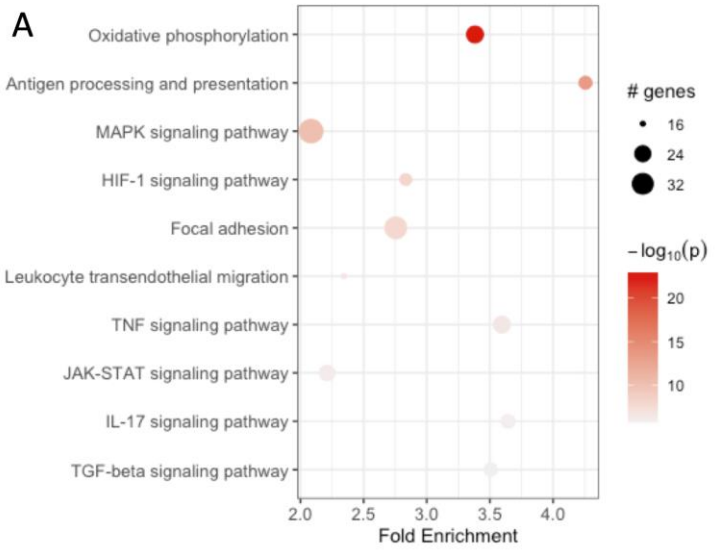

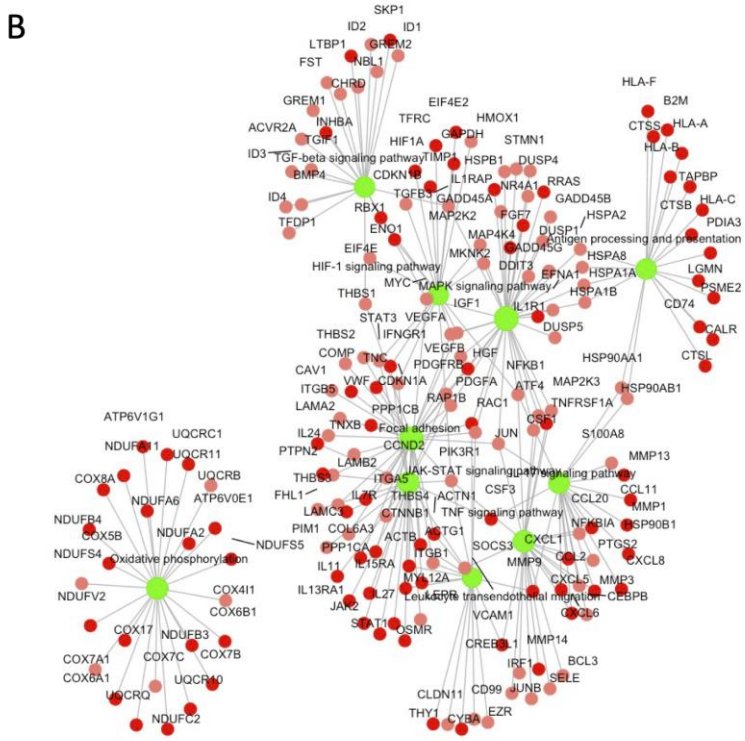

Figure 8.9 Immune pathways enriched in HS-hi fibroblasts relative to HS-lo fibroblasts. Top 10 immune pathways enriched from the genes significantly differentially expressed between HS-lo and HS-hi lesions ($p < 0.05$ and $log_2FC > 0.1$) (A). Gene-pathway network visualising the genes upregulated in HS-hi (red) or HS-lo (pink) lesions in the top 5 immune pathways enriched from the differentially expressed genes between healthy control and HS lesional fibroblasts in the fibroblasts (B).

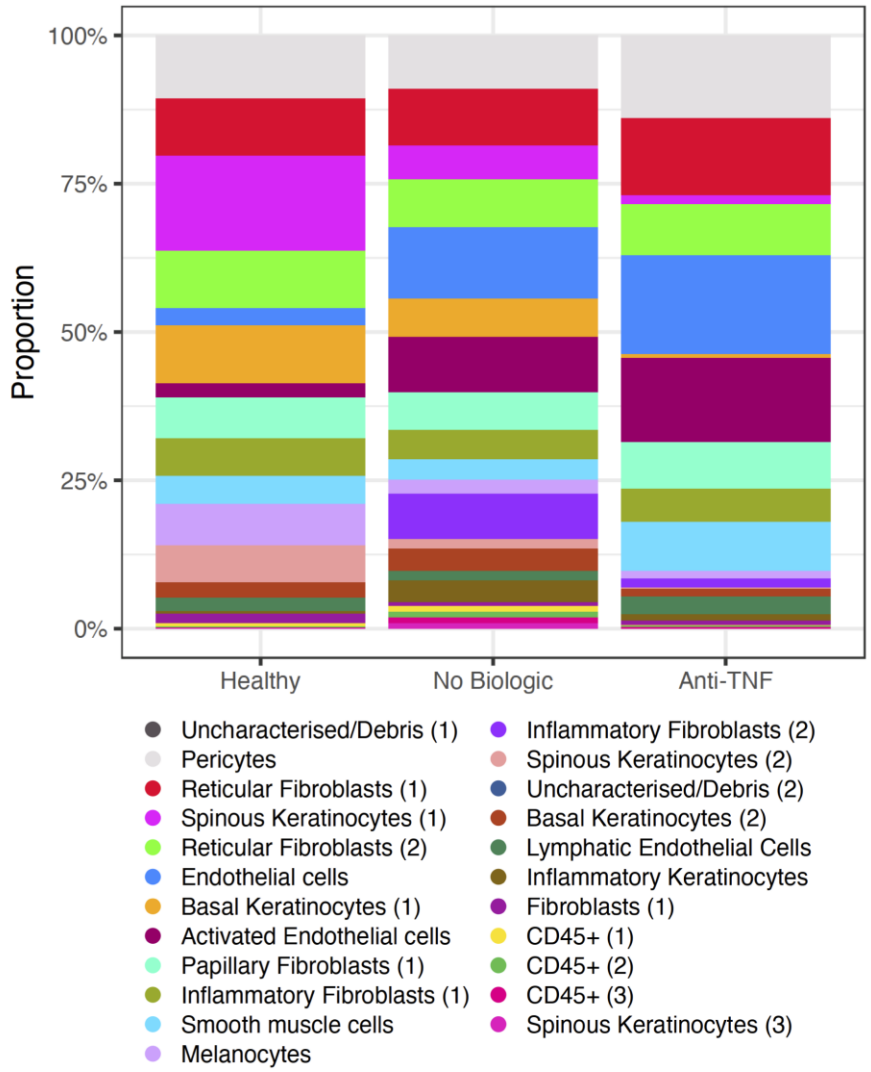

Figure 8.10 Cell frequencies in healthy control and HS lesional skin treated with or without TNF inhibitors. Single cells isolated from healthy controls (Con; n=3) or HS lesional skin (HS; n=6) were purified based on the absence of CD45 expression, barcoded and sequenced by 10X Genomics scRNA-seq. Bar chart showing the proportion of each cluster relative to all cells in healthy control, HS lesional skin treated with or without TNF inhibitors.

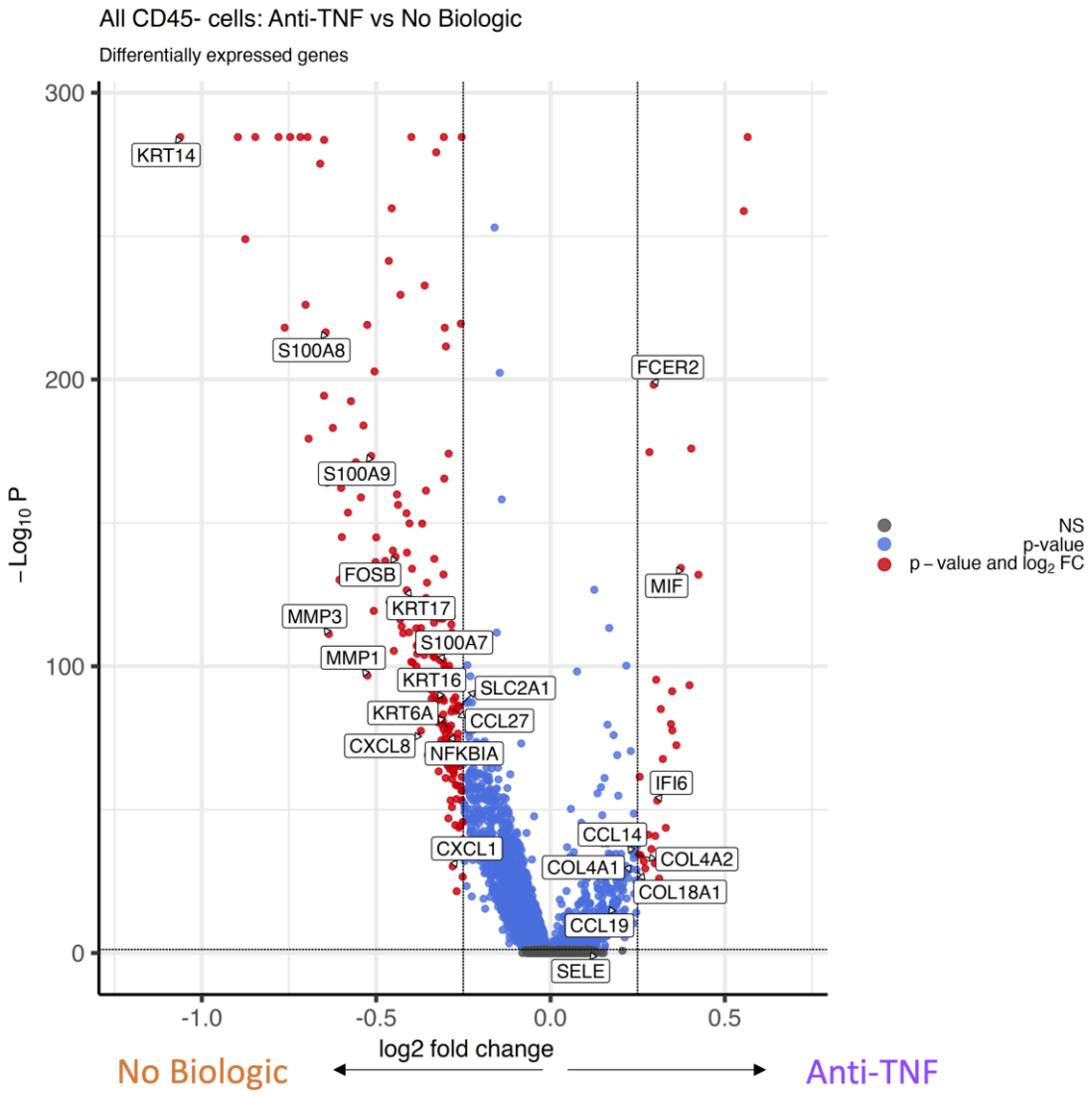

Figure 8.11 Differentially expressed genes between HS lesions treated with or without TNF inhibitors. Single cells isolated from HS lesional skin treated with (n=2) or without (n=4) TNF inhibitors were purified based on the absence CD45 expression, barcoded and sequenced by 10X Genomics scRNA-seq. Volcano plot visualises DEGs from HS lesions treated with TNF inhibitors compared with HS lesional skin not treated with any biologics. Genes with a $log_2FC > 0$ are upregulated in HS and a $log_2FC < 0$ are downregulated in HS. The $-Log_{10}$ P Y-axis is a measure of significance.

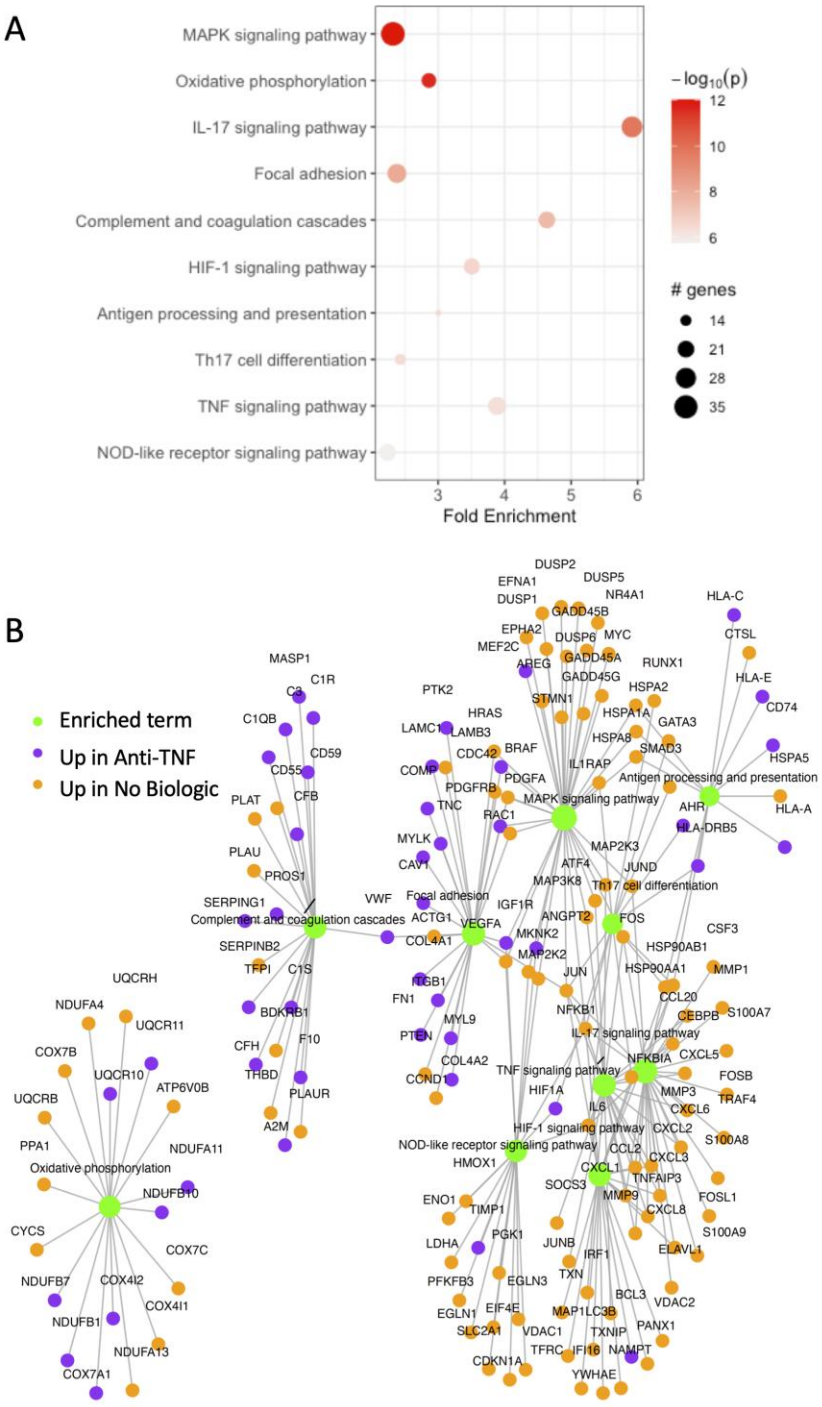

Figure 8.12 Immune pathways enriched in HS lesions treated with TNF inhibitors compared with HS lesions not treated with any biologic. Top 10 immune pathways enriched from the genes significantly differentially expressed between HS lesions treated with or without TNF inhibitors ($p < 0.05$ and $\log_2FC > 0.1$) (A). Gene-pathway network visualising the genes upregulated in TNF inhibitors treated HS lesions (purple) or untreated (orange) HS lesions in the top 5 immune pathways enriched from the differentially expressed genes between HS lesions treated with or without TNF inhibitors (B).

Table 8.1 Top 50 genes upregulated in HC skin relative to HS lesions determined by bulk RNA-seq

LYRM9	*S100A5*	*C10orf71*	*FAT3*	*CENPV*
PIGL	*STK31*	*GRM2*	*PKP2*	*MYLK4*
KCNH8	*TMEM108*	*CCDC113*	*SLC16A12*	*CAMK2B*
AGBL4	*UNC13C*	*SLC4A5*	*KATNAL2*	*IGSF11*
SNRNP200	*NELL2*	*FAM120C*	*SPG7*	*MAILR*
PEBP4	*MROH8*	*CCKBR*	*CDH12*	*ARSG*
TMPRSS5	*DOCK3*	*LOC101929128*	*NRXN3*	*PTN*
CRABP1	*LOC101928728*	*LOC101927787*	*SH3D21*	*SAXO1*
LINC01159	*HSF2BP*	*EMC3-AS1*	*POU3F3*	*RFX3-DT*
MYOC	*GJC3*	*RBM3*	*PARP2*	*EPB41L4A-AS1*

Table 8.2 Top 50 genes upregulated in HS lesional skin relative to HC skin determined by bulk RNA-seq

DLEU2	*IL23R*	*HELB*	*PPM1D*	*ZC3HAV1*
TMEM14EP	*PARP15*	*SLC23A3*	*AKR1B10*	*CARD6*
LINC02687	*IGHG4*	*CHORDC1*	*TMPRSS11GP*	*RAC2*
EDEM3	*SHOC1*	*SLC4A10*	*TRA2A*	*SAMD9*
TPBG	*ATG4C*	*BDKRB2*	*TBCK*	*UBE2L6*
CCR5	*APOL1*	*TRABD2A*	*LY96*	*CEP192*
IGHG1	*ODF3B*	*CFAP54*	*PLAAT4*	*PRKCA-AS1*
IGHG2	*TOR1B*	*TYMP*	*LINC02860*	*ST8SIA4*
CHST11	*IGKV1-32*	*LOC100419583*	*IKZF3*	*GPR15*
SAMSN1	*CD83*	*ZDBF2*	*VAV1*	*ITGAL*

Table 8.3 Top 50 genes upregulated in psoriasis lesional skin relative to HS lesional skin determined by bulk RNA-seq

TCN1	*ABCG4*	*DEFB103A*	*CCNE1*	*PGAM1*
GJB2	*KLK13*	*PRSS27*	*FAAHP1*	*ACP7*
SERPINB4	*HK2*	*CDK5R1*	*SPRR2F*	*LCE3A*
GJB6	*HRH2*	*SH2D4A*	*ZNF662*	*HMGB3*
SERPINB3	*S100A8*	*DEFB4B*	*S100A2*	*KRT6A*
FABP5	*HEPHL1*	*CRABP2*	*CIB2*	*MAP4K4*
S100A7A	*DEFB103B*	*IL36A*	*PRSS3*	*SLC6A14*
DEFB4A	*S100A9*	*INA*	*TNIP3*	*KRT16*
SPRR2C	*S100A12*	*LCE3E*	*S100A7*	*OASL*
PLA2G4D	*PI3*	*KLK6*	*ATP12A*	*SERPINB13*

Table 8.4 Top 50 genes upregulated in HS lesional skin relative to psoriasis lesional skin determined by bulk RNA-seq

ADRB2	*ZSCAN18*	*PCDHGA7*	*ZNF577*	*TAPT1-AS1*
CMAHP	*ST7L*	*PCDHGA11*	*TMEM132B*	*MMP28*
ZNF204P	*CYP39A1*	*TGFBI*	*PCDHGA6*	*ZNF347*
PCDHGB8P	*NAB1*	*DNAH11*	*PCDHGA9*	*ZNF573*
CLDN18	*EIF4A2*	*TMEM43*	*ZNF471*	*C10orf67*
PCDHGA8	*SLC25A27*	*ZNF852*	*MYO9A*	*CRELD1*
PPIL6	*ZNF862*	*ANKDD1B*	*POGZ*	*PCDHGB3*
TNNT3	*PCDHGB4*	*UBN2*	*ZNF793*	*GAL3ST1*
LOC101929653	*ZNF135*	*MAB21L1*	*APLF*	*PCDHGA5*
LOC728392	*EOLA2-DT*	*ADCY10P1*	*TTLL11*	*FAM221A*

Table 8.5 Top 50 genes upregulated in HS lesional skin relative to AD lesional skin determined by bulk RNA-seq

ZNF544	*BTG2-DT*	*MAB21L1*	*ZNF135*	*FRMD4A*
SLC23A3	*MEIS1*	*ZNF675*	*INTU*	*CDH4*
ZNF334	*ADCY10P1*	*TAPT1-AS1*	*RYR1*	*HEMK1*
IGHA2	*GPR162*	*CDH23*	*EWSAT1*	*SSPOP*
ZNF728	*TTLL11*	*ZNF221*	*EOLA2-DT*	*OR10AD1*
LOC728392	*ZNF667*	*PNMA8B*	*TBCK*	*ZNF132*
NR2F1	*ZNF862*	*ZNF681*	*CYP39A1*	*SMO*
PRDM6	*PHYHIP*	*MACROD1*	*C11orf80*	*GRM6*
DNASE1	*C5*	*FLRT1*	*UBE3B*	*LOC441239*
ZSCAN18	*LOC100506076*	*IGHA1*	*GSTM2*	*FLRT2*

Table 8.6 Top 50 genes upregulated in AD lesional skin relative to HS lesional skin determined by bulk RNA-seq

NELL2	*MMP1*	*NRIP3*	*TPMT*	*SERPINB13*
RBM3	*KRT6C*	*KRT6B*	*DNAJB5*	*CTNNA1*
KDM7A-DT	*SCG2*	*SH2D5*	*KRT6A*	*SERPINB4*
RGS20	*RNASEH1*	*ETV6*	*GPRIN1*	*MTCH2*
MMP3	*PRSS53*	*BECN1*	*KRT16*	*INA*
EPGN	*ACTC1*	*PRSS3*	*COX6C*	*SLC5A5*
FAT1	*BHLHE40*	*IL13RA2*	*EAF1*	*RRAS2*
TNC	*SORCS3*	*CDYL2*	*SNHG16*	*SNAP25*
DEFB103A	*HMGA2*	*TUBGCP5*	*UFD1*	*SIAH1*
DEFB103B	*CAPN2*	*PGF*	*CXCL8*	*DAZAP2*

Table 8.7 Top 50 genes upregulated in HS lesional skin relative to healthy control skin in all CD45$^-$ cells determined by scRNA-seq

SERF2	*IFITM3*	*PLVAP*	*COL5A2*	*VWF*
MMP3	*S100A8*	*RNASE1*	*PFN1*	*COL1A1*
IGLL5	*GAPDH*	*ENG*	*AQP1*	*IER3*
IFI27	*CXCL13*	*CD74*	*CHN1*	*ATP5F1E*
RPS4Y1	*S100A7*	*IFITM2*	*FOXP1*	*PECAM1*
IFITM1	*S100A9*	*CHI3L2*	*HIF1A*	*C15orf48*
SPARC	*MMP1*	*CTSB*	*TMSB4X*	*PNPLA6*
COL3A1	*TMSB10*	*LUM*	*TIMP1*	*PDPN*
TDO2	*SELE*	*ACKR1*	*TPM4*	*WNT5A*
CHI3L1	*COMP*	*FTL*	*DCLK2*	*LY6E*

Table 8.8 Top 50 genes downregulated in HS lesional skin relative to healthy control skin in all CD45$^-$ cells determined by scRNA-seq

RPL5	*H3F3B*	*MT1E*	*PNRC1*	*MT2A*
MYC	*RAC1*	*POLE2*	*BTG1*	*RPS8*
YBX3	*RPL7*	*RPL4*	*IGFBP5*	*ZNF185*
CIRBP	*NTRK2*	*CLDN1*	*MFSD2A*	*NFKBIA*
TOB1	*TSC22D3*	*RPL9*	*GAS6*	*CCL27*
RPS27A	*PCDH15*	*RPS18*	*LGALS7*	*KLF5*
DMKN	*LGALS7B*	*PI16*	*CFD*	*CEBPD*
RHOB	*NCL*	*SCN1A*	*RPL21*	*BTG2*
RPL7A	*DSP*	*RPS10*	*CXCL14*	*APOD*
ADH1B	*TRIM29*	*ZBTB16*	*RPL8*	*RPS6*

Table 8.9 Top 50 genes upregulated in HS-hi lesional skin relative to HS-lo lesional skin in all CD45$^-$ cells determined by scRNA-seq

SERF2	*IFITM3*	*LUM*	*CLU*	*C1S*
CHI3L2	*CXCL13*	*STEAP1*	*CXCL1*	*FSTL1*
RARRES2	*B2M*	*C3*	*IL7R*	*PPIB*
RPS26	*MMP1*	*TMSB10*	*TPM2*	*INHBA*
LGALS1	*TIMP1*	*C15orf48*	*IFITM2*	*CXCL6*
HLA-A	*S100A6*	*BGN*	*THY1*	*GGT5*
SELENOM	*MIF*	*HLA-C*	*MMP9*	*EGFL6*
MMP3	*TDO2*	*C1R*	*COL5A2*	*CCL3*
IFITM1	*NNMT*	*PCOLCE*	*SERPING1*	*SLC16A3*
CHI3L1	*MT1F*	*STEAP2*	*CXCL5*	*LAPTM4A*

Table 8.10 Top 50 genes upregulated in HS-lo lesional skin relative to HS-hi lesional skin in all CD45$^-$ cells determined by scRNA-seq

KRT5	*RAC1*	*FAU*	*CDKN1A*	*C19orf33*
YBX3	*LGALS7B*	*RPS18*	*RPS4Y1*	*SERPINB5*
RPLP2	*RPL13A*	*AMD1*	*MTRNR2L1*	*PMAIP1*
RPS27A	*AQP3*	*RPL13*	*GADD45B*	*KRT15*
DMKN	*DSP*	*RPL27A*	*GAS6*	*S100A14*
LY6D	*PLA2G6*	*RPS15A*	*LGALS7*	*KLF5*
MIB2	*RPL4*	*S100A2*	*RPS20*	*CEBPD*
SLC38A2	*EHF*	*RPS23*	*ZBTB7A*	*LYPD3*
EFNA1	*RPS3A*	*PITPNM1*	*GADD45A*	*RPL30*
DNAJB1	*RPL9*	*EZR*	*SPINT2*	*SERPINB2*

Table 8.11 Top 50 genes upregulated in HS lesional skin relative to healthy control skin in all keratinocytes determined by scRNA-seq

RPS4Y1	*DACH2*	*PNPLA6*	*ECE1*	*CLEC7A*
GJB2	*FABP5*	*HSPB1*	*ATP1B1*	*TIRAP*
S100A8	*FTL*	*PLAT*	*RGS7*	*VSNL1*
S100A7	*DDX3Y*	*EIF1AY*	*NCOA7*	*CALML3*
S100A9	*S100A6*	*KRT14*	*EFEMP2*	*KYNU*
KRT6A	*KRT15*	*PKM*	*TXNDC17*	*GJB6*
S100A2	*MT-CO2*	*SLC25A17*	*C12orf75*	*SLC7A8*
DCLK2	*WRB*	*IER3*	*TMSB10*	*TNFSF10*
IFITM3	*PLAU*	*SERPINB4*	*CTSC*	*SERF2*
IGLL5	*MT-CO1*	*SLC1A5*	*AKR1B10*	*EREG*

Table 8.12 Top 50 genes downregulated in HS lesional skin relative to healthy control skin in all keratinocytes determined by scRNA-seq

MYC	*MT1E*	*PNRC1*	*RPL32*	*RPL8*
MT2A	*RPS12*	*RPS24*	*TUBB2A*	*UBR4*
RPS6	*ZFP36L1*	*RPL21*	*TOB1*	*HLA-A*
RPS4X	*DSP*	*LGALS3*	*AHNAK2*	*RPL34*
MT1X	*CFD*	*ADRB2*	*MFSD2A*	*RPL10A*
RPS10	*KLF4*	*DMKN*	*RPL35*	*ZFP36L2*
CCL27	*RPS8*	*RPL3*	*TSC22D3*	*PCDH15*
NFKBIA	*RSRP1*	*RPS29*	*CEBPD*	*CACTIN*
H3F3B	*RPL36A*	*BTG1*	*CCND1*	*SIK1*
RPLP1	*APOE*	*CIRBP*	*KLF6*	*RPL5*

Table 8.13 Top 50 genes upregulated in HS lesional skin relative to healthy control skin in the spinous keratinocytes (1) cluster determined by scRNA-seq

S100A8	*DACH2*	*MMP1*	*EREG*	*ATP1B1*
RPS4Y1	*FTL*	*SLC1A5*	*CXCL8*	*TIRAP*
S100A9	*TMSB10*	*MMP3*	*AKR1B10*	*ACTB*
GJB2	*S100A6*	*IER3*	*NCOA7*	*CLEC7A*
S100A7	*CXCR4*	*TM4SF1*	*KRT15*	*SERPINB4*
DDX3Y	*PLAU*	*PNPLA6*	*SLC25A17*	*KYNU*
IGLL5	*KRT14*	*LUM*	*IFITM3*	*CTSC*
FABP5	*EIF1AY*	*WRB*	*PRR29*	*SELE*
KRT6A	*EFEMP2*	*S100A2*	*CRABP2*	*RGS7*
DCLK2	*PLAT*	*CXCL1*	*CXCL13*	*LIMA1*

Table 8.14 Top 50 genes downregulated in HS lesional skin relative to healthy control skin in the spinous keratinocytes (1) cluster determined by scRNA-seq

MT1X	*NFKBIA*	*RPL36A*	*RPL10A*	*KRT1*
RPS4X	*RPS12*	*RPS29*	*DMKN*	*KLF4*
RPS6	*CIRBP*	*RPL35*	*PNRC1*	*RPL11*
MT1E	*RPS10*	*CCL27*	*AHNAK2*	*KRT10*
MYC	*RSRP1*	*RPL32*	*RPL3*	*RPL21*
MT2A	*RPL34*	*LGALS3*	*RPL36*	*RPS2*
RPS8	*TOB1*	*ZFP36L2*	*BTG1*	*LGALS7B*
RPLP1	*CFD*	*CCND1*	*MFSD2A*	*RPL7*
CXCL14	*DSP*	*RPS24*	*TSC22D3*	*HLA-C*
ZFP36L1	*LGALS7*	*H3F3B*	*ADRB2*	*CEBPD*

Table 8.15 Top 50 genes upregulated in HS lesional skin relative to healthy control skin in the basal keratinocytes (1) cluster determined by scRNA-seq

S100A8	*EHF*	*EIF1AY*	*PKM*	*ALDH3A1*
RPS4Y1	*KRT6A*	*IFITM3*	*BTF3*	*LPAR6*
S100A9	*DACH2*	*HSPB1*	*TPM4*	*SLC25A6*
GJB2	*WRB*	*SLC25A17*	*FABP5*	*PTGS2*
S100A2	*KRT15*	*NCOA7*	*PFN1*	*PDLIM1*
FTL	*TMSB10*	*ATP1B1*	*RGS7*	*FSCN1*
MT-CO1	*MT-CO2*	*PLAU*	*TXNRD1*	*PITPNM1*
DDX3Y	*IGLL5*	*ECE1*	*SLC1A5*	*VSNL1*
S100A7	*IER3*	*PNPLA6*	*TXNDC17*	*ANKRD10*
DCLK2	*S100A6*	*EREG*	*PHLDA1*	*CCL20*

Table 8.16 Top 50 genes downregulated in HS lesional skin relative to healthy control skin in the basal keratinocytes (1) cluster determined by scRNA-seq

MT1X	*DMKN*	*RPS24*	*LGALS3*	*CACTIN*
MT2A	*RPS12*	*RPL36A*	*TOB1*	*APOE*
MYC	*RSRP1*	*UBR4*	*BCL2L11*	*TXNIP*
MT1E	*H3F3B*	*ZFP36L2*	*ZFP36L1*	*B2M*
RPS4X	*CFD*	*RPL3*	*RPS26*	*RPS29*
CCL27	*CIRBP*	*HLA-A*	*SIK1*	*RPL35*
TSC22D3	*CEBPD*	*RPS8*	*HLA-C*	*RPL7A*
RPS6	*NFKBIA*	*DSP*	*KRT1*	*RPL32*
RPS10	*RPL21*	*PCDH15*	*RPL5*	*PRDM10*
KLF4	*RPLP1*	*ADRB2*	*KLF6*	*MT1G*

Table 8.17 Top 50 genes upregulated in HS lesional skin relative to healthy control skin in the spinous keratinocytes (2) cluster determined by scRNA-seq

S100A8	*DACH2*	*GJB6*	*S100A2*	*IFITM3*
RPS4Y1	*CRABP2*	*MT-CO1*	*PKM*	*ATP1B1*
S100A9	*HSPB1*	*SLC1A5*	*AQP3*	*KYNU*
S100A7	*PNPLA6*	*CLEC7A*	*IGLL5*	*MPZL2*
SERPINB4	*KRT14*	*PLAU*	*DBI*	*C12orf75*
FABP5	*DDX3Y*	*SLC25A17*	*IER3*	*S100A14*
KRT6A	*CALML3*	*TIRAP*	*ZNF589*	*SOSTDC1*
DCLK2	*MT-CO2*	*CTSC*	*SERPINB3*	*EREG*
AKR1B10	*EIF1AY*	*ECE1*	*EFEMP2*	*MID1IP1*
GJB2	*C10orf99*	*CXCR4*	*WRB*	*AC087632.1*

Table 8.18 Top 50 genes downregulated in HS lesional skin relative to healthy control skin in the spinous keratinocytes (2) cluster determined by scRNA-seq

MT2A	*DSP*	*AHNAK2*	*CCL27*	*NR4A1*
MT1X	*RPS26*	*CCND1*	*ZFP36*	*CIRBP*
MT1E	*CFD*	*RPS6*	*B2M*	*SRSF5*
MYC	*NFKBIA*	*ADRB2*	*ZFP36L2*	*PNRC1*
ZFP36L1	*LGALS3*	*RPL34*	*H1FX*	*RPL36A*
RPS4X	*H3F3B*	*TSC22D3*	*RPLP1*	*RPS24*
APOE	*CXCL14*	*LGALS7*	*TXNIP*	*SOCS3*
HLA-C	*KLF4*	*TUBB2A*	*PLLP*	*RPL32*
HLA-A	*RPS10*	*MFSD2A*	*CACTIN*	*SIK1*
TOB1	*RSRP1*	*UBR4*	*KLF6*	*DUSP2*

Table 8.19 Top 50 genes upregulated in HS lesional skin relative to healthy control skin in the basal keratinocytes (2) cluster determined by scRNA-seq

S100A8	*DAPL1*	*DBI*	*SERF2*	*MT-CO2*
S100A9	*SLC25A6*	*BRD8*	*UQCRH*	*UQCR10*
S100A2	*CLCA2*	*TXNDC17*	*S100A16*	*PLAT*
RPS4Y1	*DDIT3*	*TMA7*	*ENO1*	*SLC25A17*
GJB2	*ATP1B3*	*ALDH3A1*	*RNF7*	*ATP6V0E1*
IFITM3	*MT-CO1*	*FABP5*	*DACH2*	*UQCR11*
TNFSF10	*IGLL5*	*PRXL2A*	*BCL11A*	*IMPA2*
LPAR6	*HSPB1*	*VSNL1*	*PNPLA6*	*C9orf3*
EHF	*KRT6A*	*TAX1BP3*	*KRT15*	*PYCARD*
S100A7	*PHGDH*	*ATP5MPL*	*DCLK2*	*MTRNR2L12*

Table 8.20 Top 50 genes downregulated in HS lesional skin relative to healthy control skin in the basal keratinocytes (2) cluster determined by scRNA-seq

H3F3B	*DMKN*	*B2M*	*MGP*	*MYC*
CFD	*UBR4*	*CACTIN*	*PNRC1*	*KRT10*
MT1X	*KLF4*	*BCL2L11*	*RPS18*	*CLEC3B*
NFKBIA	*PCDH15*	*HSP90AB1*	*GSN*	*ZFP36*
POSTN	*EIF1*	*CRYAB*	*SCGB2A2*	*MUCL1*
MT2A	*CALM2*	*PI16*	*TOB1*	*ERRFI1*
DDX5	*SERPINB7*	*LGALS3*	*CXCL12*	*ITGA7*
APOD	*PRDM10*	*DNAJA1*	*RPL9*	*ACTB*
SERPINB2	*CXCL14*	*BTG1*	*TUBB2A*	*CACNA2D2*
RPS4X	*DCN*	*LDHA*	*H2AFZ*	*UMOD*

Table 8.21 Top 50 genes upregulated in HS lesional skin relative to healthy control skin in the inflammatory keratinocytes cluster determined by scRNA-seq

S100A8	*ENSA*	*FOS*	*TIMM13*	*PARK7*
PRXL2A	*C1orf21*	*PNPLA6*	*ARPC2*	*ATP5MPL*
S100A9	*SERPINB4*	*MRPL27*	*PPIA*	*SDC1*
IER2	*S100A16*	*CTSD*	*HSBP1*	*SEM1*
TAX1BP3	*DEGS1*	*AKR1B10*	*DCLK2*	*ATP5PB*
RPS4Y1	*ID1*	*GRN*	*DBI*	*LSP1*
PSMA7	*CAPG*	*CBR1*	*HSPA1B*	*P4HB*
PDZK1IP1	*GSTA4*	*CA2*	*NSG1*	*KRT1*
PYCARD	*LY6D*	*UPF3B*	*MRPL51*	*S100A7*
IFITM3	*CLEC2B*	*WRB*	*UBE2L3*	*MIB2*

Table 8.22 28 genes downregulated in HS lesional skin relative to healthy control skin in the inflammatory keratinocytes cluster determined by scRNA-seq

RPS4X	*LBH*	*SCGB2A2*	*NTRK2*
S100P	*RPL8*	*HMGCS2*	*KRT23*
POLE2	*MUCL1*	*PDK4*	*MT1A*
KRT17	*FRRS1L*	*CFD*	*TOB1*
DCD	*C1QTNF12*	*PTN*	*IFFO2*
FA2H	*MT2A*	*PI16*	*ISM1*
SCGB1D2	*PNLIPRP3*	*RPS9*	*NPAS2*

Table 8.23 Top 50 genes downregulated in HS-hi lesional skin relative to HS-lo skin in all keratinocytes determined by scRNA-seq

RPS4Y1	*LGALS7*	*PLA2G6*	*HOPX*	*SERPINB5*
KRT10	*MTRNR2L1*	*WRB*	*AQP3*	*H1FX*
KRTDAP	*CEBPD*	*MTRNR2L12*	*TPPP3*	*HES1*
KRT1	*SERPINB2*	*GSPT1*	*NCL*	*GAS6*
KLF5	*DSP*	*DSG1*	*MIB2*	*BAZ1A*
DMKN	*RAC1*	*CEBPA*	*FGFBP1*	*LSP1*
YBX3	*ZFP36L2*	*FABP5*	*HDGF*	*ERRFI1*
PITPNM1	*MT-ND4L*	*ZNF706*	*GOLGA4*	*CSTA*
CEBPB	*RND3*	*HSPA2*	*KIAA0895*	*LAMP1*
MTRNR2L11	*DUSP1*	*IER5*	*FERMT2*	*EHF*

Table 8.24 Top 50 genes upregulated in HS-hi lesional skin relative to HS-lo skin in all keratinocytes determined by scRNA-seq

MMP3	*LGALS1*	*IGLL5*	*RPS26*	*SPARC*
MMP1	*RARRES2*	*HLA-A*	*COL1A2*	*CXCL12*
IFI27	*CHI3L1*	*SERPINF1*	*COL1A1*	*PCOLCE*
LTF	*C1R*	*CACTIN*	*SELENOM*	*KRT6A*
LUM	*DCN*	*CHI3L2*	*TPM2*	*SAA1*
CD74	*CTGF*	*NNMT*	*SERPINB3*	*TYMP*
CXCL1	*IFITM1*	*IFITM3*	*TDO2*	*FSTL1*
COL3A1	*CLU*	*HBB*	*HLA-DRB1*	*HLA-C*
CXCL13	*C1S*	*C15orf48*	*KRT6B*	*IFI6*
TIMP1	*BGN*	*SERPINB4*	*MMP2*	*HLA-DRA*

Table 8.25 Top 50 genes upregulated in HS lesional skin relative to psoriasis lesional skin in all keratinocytes determined by scRNA-seq

RPL5	*RSL24D1*	*SEPT7*	*RPL36A*	*RPLP0*
H2AFY	*C9orf3*	*RPS29*	*ANXA2*	*TSC22D1*
RPS2	*RPL18A*	*CD99*	*PGLS*	*RPS3*
RPL6	*TROVE2*	*CNOT2*	*C6orf48*	*WRB*
QARS	*RPS19*	*BTF3*	*H3F3B*	*CYCS*
SEPT2	*DSTN*	*MARCH6*	*RPL10*	*RPS13*
TSPAN31	*AES*	*TPPP3*	*RPL3*	*RPL35*
TUBA1B	*EEF1A1*	*RPL31*	*HNRNPL*	*RPL13A*
ASNA1	*RPS27A*	*H2AFV*	*RPL7*	*RPL36*
PTMA	*DARS*	*RPL35A*	*PPP2CA*	*SEPT9*

Table 8.26 Top 50 genes downregulated in HS lesional skin relative to psoriasis lesional skin in all keratinocytes determined by scRNA-seq

RAPGEF2	*MAGI1*	*CLASP2*	*TBC1D5*	*MACF1*
ATP9B	*CAPN12*	*AGAP1*	*TYMP*	*NUMA1*
FTO	*MLLT3*	*EVPL*	*TMCC1*	*ARHGEF4*
XPO6	*RREB1*	*ASAP1*	*PCCA*	*VPS13D*
AHCYL2	*RABGAP1L*	*CUX1*	*ARID1B*	*ZFAND3*
SPPL3	*WDFY3*	*PPP6R3*	*MRTFA*	*NCOA1*
EXOC4	*EFHC2*	*TCF12*	*KANK1*	*MAP4K3*
WWOX	*SLC22A23*	*PDE8A*	*AMBRA1*	*SBNO2*
JARID2	*EFNA5*	*KANSL1*	*CCNY*	*PHLPP1*
QKI	*C11orf49*	*VTI1A*	*CBWD5*	*USP34*

Table 8.27 Top 50 genes upregulated in HS lesional skin relative to healthy control skin in all fibroblasts determined by scRNA-seq

SERF2	*S100A8*	*GAPDH*	*MT1F*	*TMEM45A*
BGN	*IGLL5*	*PTMA*	*CTSB*	*SFRP2*
LGALS1	*B2M*	*EGFL6*	*S100A9*	*MT-CO1*
LUM	*CHI3L1*	*COL1A2*	*TNC*	*DIO2*
COL1A1	*IFITM3*	*COL6A2*	*WNT5A*	*STEAP2*
COL3A1	*MMP1*	*PDPN*	*C15orf48*	*POSTN*
TDO2	*MMP3*	*FTL*	*SLC16A3*	*C4orf48*
COL6A3	*COMP*	*STEAP1*	*COL5A1*	*RARRES2*
COL5A2	*CHI3L2*	*HIF1A*	*CHN1*	*CA12*
COL6A1	*CXCL13*	*SPARC*	*INHBA*	*RGS3*

Table 8.28 Top 50 genes downregulated in HS lesional skin relative to healthy control skin in all fibroblasts determined by scRNA-seq

ABI3BP	*TXNIP*	*MAP1B*	*C7*	*CIRBP*
GSN	*ITM2A*	*JUN*	*ALDH1A1*	*IGFBP3*
ADH1B	*CEBPD*	*NFIA*	*DMKN*	*PNRC1*
GPX3	*APOD*	*PI16*	*CD34*	*IGFBP6*
NTRK2	*MGP*	*MYC*	*ANGPTL5*	*BTG2*
CCDC80	*KLF4*	*FBLN1*	*NFIB*	*MTRNR2L1*
IGFBP5	*CHRDL1*	*SOD3*	*SLPI*	*KLF2*
PDK4	*CLEC3B*	*TSPAN8*	*GAS6*	*PIK3R1*
CFD	*TIMP3*	*KRT1*	*ZBTB16*	*TSC22D3*
CXCL14	*ZFP36L2*	*FGL2*	*CD81*	*MT1A*

Table 8.29 Top 50 genes upregulated in HS lesional skin relative to healthy control skin in the reticular fibroblast (1) cluster determined by scRNA-seq

LUM	*MT-CO2*	*RPS19*	*ENAH*	*ITM2C*
BGN	*COL5A2*	*CHN1*	*EGFL6*	*POSTN*
COMP	*COL18A1*	*PTGDS*	*MT-ND3*	*RPL28*
COL3A1	*MT-CO3*	*COL1A2*	*S100A8*	*APCDD1*
COL6A1	*COL1A1*	*LGALS1*	*TPM2*	*TYMP*
MT-CO1	*THY1*	*SFRP2*	*GAPDH*	*RGS3*
COL6A2	*SERF2*	*HIF1A*	*RPL41*	*CHI3L1*
COL6A3	*TDO2*	*COL5A1*	*STEAP1*	*GUCY1A1*
PTMA	*B2M*	*IFITM3*	*MT-ATP6*	*DIO2*
TNC	*MT1F*	*PTK7*	*CTSC*	*MT-ND4*

Table 8.30 Top 50 genes downregulated in HS lesional skin relative to healthy control skin in the reticular fibroblast (1) cluster determined by scRNA-seq

GSN	*PI16*	*CD34*	*CXCL14*	*FCGRT*
APOD	*DCN*	*MATN4*	*ZFP36L2*	*JUN*
CFD	*TIMP3*	*FAM180B*	*KLF4*	*LAMP1*
CPE	*TSPAN8*	*ABI3BP*	*FGL2*	*LGALS3*
SLPI	*NTRK2*	*MAP1B*	*CD81*	*C1QTNF4*
CHRDL1	*CCDC80*	*IGFBP5*	*ITM2A*	*CD55*
MGP	*MFAP5*	*SOD3*	*LOX*	*MGST1*
FBLN1	*SCARA5*	*IGFBP6*	*CST3*	*KLF2*
CLEC3B	*ANGPTL5*	*PDK4*	*CPVL*	*AHNAK2*
GPX3	*ADH1B*	*TSC22D3*	*ANXA2*	*PCOLCE2*

Table 8.31 Top 50 genes upregulated in HS lesional skin relative to healthy control skin in the reticular fibroblast (2) cluster determined by scRNA-seq

COL1A1	*S100A8*	*CHI3L1*	*CXCL13*	*RPS4Y1*
COL3A1	*COMP*	*BGN*	*FTL*	*TNC*
MT-CO1	*MT-CO2*	*S100A9*	*MT-CYB*	*S100A7*
B2M	*IGLL5*	*CHI3L2*	*C15orf48*	*HSPA1A*
PTMA	*TMSB10*	*GAPDH*	*MT-ATP6*	*MT-ND3*
LGALS1	*SPARC*	*TCIM*	*CLDN11*	*POSTN*
COL1A2	*COL6A1*	*TDO2*	*IER3*	*COL5A2*
SERF2	*MT-CO3*	*APCDD1*	*COL6A2*	*EGFL6*
LUM	*MMP3*	*PDPN*	*TIMP1*	*CXCL8*
SFRP2	*MMP1*	*MT-ND4*	*MT1F*	*IFITM3*

Table 8.32 Top 50 genes downregulated in HS lesional skin relative to healthy control skin in the reticular fibroblast (2) cluster determined by scRNA-seq

GSN	*ADH1B*	*NTRK2*	*EPHX1*	*CFH*
APOD	*TXNIP*	*NFIA*	*MAP1B*	*CPE*
CFD	*GPX3*	*ABI3BP*	*IGFBP6*	*CIRBP*
CXCL14	*FBLN1*	*CEBPD*	*PLPP3*	*RPL21*
MGP	*PDK4*	*GPC3*	*PID1*	*CCNI*
TIMP3	*NFIB*	*SOD3*	*CXCL12*	*EFEMP1*
ITM2A	*C7*	*JUN*	*ALDH1A1*	*PI16*
IGFBP5	*IGFBP3*	*PIK3R1*	*YBX3*	*PNRC1*
ZFP36L2	*KLF4*	*EGR1*	*PODN*	*RPS8*
CCDC80	*CHRDL1*	*MYC*	*CYGB*	*GAS6*

Table 8.33 Top 50 genes upregulated in HS lesional skin relative to healthy control skin in the papillary fibroblast (1) cluster determined by scRNA-seq

LUM	*SERF2*	*B2M*	*STEAP2*	*MMP3*
COL3A1	*BGN*	*SFRP2*	*IFITM1*	*ATP5F1E*
COL1A1	*DIO2*	*TMEM45A*	*POLR2L*	*HIF1A*
COMP	*IFITM3*	*FTL*	*MMP1*	*TNFRSF21*
COL6A3	*CTSB*	*IGLL5*	*WNT5A*	*PDPN*
COL1A2	*S100A8*	*LY6E*	*IL24*	*SGIP1*
COL6A2	*TNC*	*S100A9*	*CXCL13*	*RCN3*
SPARC	*RARRES2*	*COL5A2*	*CHI3L2*	*ATP6V0E1*
COL6A1	*STEAP1*	*THY1*	*CHN1*	*CHI3L1*
LGALS1	*TDO2*	*RGS3*	*RPS4Y1*	*MT1F*

Table 8.34 Top 50 genes downregulated in HS lesional skin relative to healthy control skin in the papillary fibroblast (1) cluster determined by scRNA-seq

ZFP36L2	*MGP*	*PI16*	*CYR61*	*MT-ND1*
IGFBP5	*TSC22D3*	*EIF1*	*BTG1*	*RPL9*
CXCL14	*JUN*	*MTRNR2L11*	*MT-ND4L*	*MT1A*
GSN	*PNRC1*	*CCDC80*	*RPS18*	*RPLP2*
MTRNR2L12	*MYC*	*KRT1*	*TIMP3*	*CLEC3B*
MTRNR2L1	*FBLN1*	*ADH1B*	*WIF1*	*RAC1*
CFD	*ABI3BP*	*TXNIP*	*KLF2*	*PCDH15*
KLF4	*NFKBIA*	*CD81*	*BTG2*	*GAS6*
APOD	*RPS27A*	*MTRNR2L8*	*RHOB*	*SRSF5*
CEBPD	*DMKN*	*ZFP36*	*ZBTB16*	*DUSP1*

Table 8.35 Top 50 genes upregulated in HS lesional skin relative to healthy control skin in the inflammatory fibroblast (1) cluster determined by scRNA-seq

LUM	*CTSB*	*GAPDH*	*S100A9*	*PDPN*
COL3A1	*SFRP2*	*STEAP1*	*RCN3*	*BGN*
COL1A1	*COL6A1*	*IFITM3*	*IL24*	*COMP*
LGALS1	*COL6A2*	*TIMP1*	*CA12*	*DCN*
COL1A2	*TDO2*	*CXCL13*	*CXCL8*	*HIF1A*
SERF2	*IGLL5*	*COL5A2*	*STEAP2*	*PRSS23*
FTL	*MMP1*	*MMP3*	*RARRES2*	*PFN1*
COL6A3	*S100A8*	*MMP2*	*PTMA*	*C4orf48*
SPARC	*CHI3L2*	*CXCL1*	*INHBA*	*FSTL1*
CHI3L1	*CTHRC1*	*PLA2G2A*	*TMEM45A*	*DIO2*

Table 8.36 Top 50 genes downregulated in HS lesional skin relative to healthy control skin in the inflammatory fibroblast (1) cluster determined by scRNA-seq

ZFP36L2	*GSN*	*DPT*	*RPL7*	*MTRNR2L1*
IGFBP5	*MYC*	*RPL21*	*APOD*	*MT-ND4L*
ADH1B	*RPS27A*	*RPS8*	*EEF1A1*	*ADIRF*
CCDC80	*ABI3BP*	*CIRBP*	*YBX3*	*RPS6*
CEBPD	*CXCL14*	*RPL5*	*ITM2A*	*RPL11*
MT1M	*RPS4X*	*MT1A*	*RPL32*	*CFD*
IGFBP3	*C7*	*PTN*	*VIM*	*CXCL12*
IGFBP7	*KLF4*	*RPL34*	*RPL8*	*RGS16*
MGP	*TXNIP*	*RPL9*	*TNFSF13B*	*CD81*
PNRC1	*BTG1*	*RPL35A*	*NFIA*	*BTG2*

Table 8.37 Top 50 genes upregulated in HS-hi lesional skin relative to HS-lo lesional skin in all fibroblast cluster determined by scRNA-seq

RPS26	*HLA-B*	*RPS4X*	*HIF1A*	*CXCL6*
IFITM3	*MT2A*	*EGFL6*	*CA12*	*MMP9*
B2M	*MMP1*	*IL7R*	*MT1E*	*CCL3*
CLU	*TDO2*	*STEAP2*	*NNMT*	*WFDC2*
CHI3L1	*IFITM1*	*CXCL1*	*GGT5*	*IGLL5*
CHI3L2	*SELENOM*	*C3*	*CSF3*	*FMO1*
RARRES2	*STEAP1*	*HLA-C*	*SLC16A3*	*RUNX2*
HLA-A	*MT1F*	*PLAU*	*S100A11*	*PDPN*
CXCL13	*LUM*	*CXCL5*	*LGALS1*	*WNT2*
MMP3	*MIF*	*C15orf48*	*WNT5A*	*ALPL*

Table 8.38 Top 50 genes downregulated in HS-hi lesional skin relative to HS-lo lesional skin in all fibroblast cluster determined by scRNA-seq

MTRNR2L1	*GAS6*	*SFN*	*VIM*	*ADIRF*
MTRNR2L11	*CLEC3B*	*GEM*	*CLDN11*	*CCDC80*
MTRNR2L12	*DMKN*	*CEBPB*	*MGP*	*RND3*
RPS4Y1	*KLF2*	*HES1*	*SFRP2*	*GADD45B*
KRT1	*COL14A1*	*HSPB1*	*IGFBP5*	*EIF1*
HTRA1	*ID3*	*ELN*	*PDGFRL*	*KRT10*
ZFP36L2	*MTRNR2L6*	*SLC38A2*	*MT-ND4L*	*PPP1R10*
MTRNR2L8	*RGS16*	*SOX4*	*FBLN1*	*NFIX*
CEBPD	*DNAJB1*	*KRTDAP*	*CD81*	*COMP*
ANGPTL1	*KRT14*	*PLA2G6*	*NBL1*	*KLF4*

Table 8.39 Top 50 genes upregulated in HS lesional skin relative to healthy control skin in all T cells determined by scRNA-seq

TMSB4X	*TMA7*	*SH3BGRL3*	*RPS3*	*MT-CO1*
IGLL5	*KLRB1*	*RPS19*	*DDX3Y*	*RPS25*
ACTB	*SERF2*	*CORO1A*	*TLL1*	*PASK*
RPS14	*JCHAIN*	*IL17A*	*IL17F*	*ARPC1B*
RPLP1	*GIMAP7*	*RPS8*	*AC087632.1*	*UQCR10*
RPS4Y1	*RPL26*	*UBA52*	*RPS18*	*UCP2*
RPL23A	*GIMAP4*	*LRMDA*	*CD3D*	*CD7*
PFN1	*RPS5*	*ATP5F1E*	*UQCR11*	*N4BP2L2*
RPL18A	*KIAA0895*	*LIMD2*	*SRP9*	*RPS27*
B2M	*SELL*	*RPS15*	*CCL20*	*RPS28*

Table 8.40 Top 50 genes downregulated in HS lesional skin relative to healthy control skin in all T cells determined by scRNA-seq

CHD2	*TSC22D3*	*BTG1*	*DUSP5*	*TUBA1B*
FOS	*SRSF7*	*NR4A2*	*UBE2S*	*HSPA5*
TOB1	*CRYBG1*	*TNFAIP3*	*CITED2*	*GADD45B*
CXCR4	*LGALS1*	*PTGER4*	*DUSP1*	*FTH1*
LMNA	*ZNF331*	*BRD2*	*ZFP36L2*	*TUBB4B*
RGCC	*DUSP2*	*TXNIP*	*JUNB*	*CST3*
ANKRD28	*ZC3HAV1*	*ID2*	*ZFAND5*	*SRGN*
DNAJA1	*PRDM1*	*TSPYL2*	*ETS1*	*TUBB2A*
H3F3B	*EZR*	*EIF1*	*SOCS1*	*HNRNPL*
ZFP36	*ANXA1*	*KLF6*	*HSPA8*	*DDX3X*

Table 8.41 Top 50 genes upregulated in anti-TNF treated relative to untreated T cells in HS lesions determined by scRNA-seq

RPS26	*RPS15*	*LIMD2*	*RPS18*	*TMSB4X*
RPS14	*NT5M*	*RPS6*	*RPL41*	*CORO1A*
RPL23A	*RPL26*	*N4BP2L2*	*RPS3*	*RPL34*
RPS27	*RPL3*	*RGS7*	*RPL35*	*RPL12*
RPS4X	*RPS28*	*RPL36*	*RPS2*	*RPL28*
GIMAP7	*RPS29*	*HSPA1B*	*SELL*	*HSPE1*
RPL18A	*RPS5*	*TMA7*	*RPL39*	*UBA52*
C1QB	*ACTB*	*RNF146*	*RPL11*	*S1PR4*
GIMAP4	*CD52*	*RPL31*	*RPS9*	*UCP2*
RPS19	*LIG1*	*GPX8*	*ATP5F1E*	*PSMB10*

Table 8.42 Top 50 genes downregulated in anti-TNF treated relative to untreated T cells in HS lesions determined by scRNA-seq

LMNA	*UBC*	*CREM*	*MT-CO2*	*TUBB4B*
DUSP2	*PNRC1*	*COTL1*	*PTP4A2*	*SIAH2*
RPS4Y1	*KLF6*	*CITED2*	*GADD45A*	*RGS1*
EIF1	*CXCL8*	*H3F3B*	*MT-ATP6*	*CNOT6L*
ZFP36L2	*ZFP36*	*NR4A2*	*DUSP5*	*JUNB*
BTG1	*MT-CO1*	*MT-ND2*	*STMN1*	*CXCR4*
RGCC	*DUSP1*	*ANKRD28*	*TNFAIP3*	*CSRNP1*
NFKBIA	*LGALS1*	*HSPA5*	*HLA-B*	*DNAJA1*
MT-CO3	*VIM*	*SRGN*	*CD69*	*BIRC3*
MT-CYB	*HLA-DRA*	*EZR*	*MT-ND1*	*HSPA8*

Table 8.43 Top 50 genes downregulated in TNF treated relative to untreated HS lesional skin in all keratinocytes determined by scRNA-seq

CEBPB	*MTRNR2L11*	*GSPT1*	*DSP*	*IGLL5*
KRT10	*DUSP1*	*IER3*	*PLA2G6*	*HDGF*
CEBPD	*DMKN*	*EZR*	*SERPINB5*	*KPNA2*
SERPINB2	*PHLDA2*	*TPPP3*	*LMNA*	*HSPA8*
KLF5	*H1FX*	*ERRFI1*	*LYPD3*	*RND3*
YBX3	*GADD45A*	*PNRC1*	*PTP4A2*	*TACSTD2*
RPS4Y1	*MTRNR2L12*	*KRTDAP*	*PCBP1*	*FGFBP1*
KRT1	*IER5*	*RPS23*	*HSPA5*	*FAU*
RAC1	*ZFP36L2*	*AMD1*	*NFKBIA*	*SOX15*
MTRNR2L1	*PITPNM1*	*ZNF706*	*AQP3*	*H2AFZ*

Table 8.44 Top 50 genes upregulated in TNF treated relative to untreated HS lesional skin in all keratinocytes determined by scRNA-seq

LTF	*C2orf68*	*HIST1H2AE*	*SAA2*	*CLIC6*
IFITM1	*SAA1*	*PSMB10*	*SERF2*	*CCL7*
C1R	*HIST1H2AC*	*SHBG*	*CEP19*	*PNLDC1*
IFI27	*KSR1*	*TMSB10*	*SHISA2*	*BMX*
FCER2	*C1QB*	*NEURL4*	*Z84492.1*	*B2M*
RPS26	*CTSH*	*TCF7*	*HIST1H4H*	*HOXC11*
MIF	*MLPH*	*DEFB4A*	*OSCAR*	*DEFB4B*
C2orf68	*HIST1H2AE*	*TINAGL1*	*HOXC4*	*ARMH1*

Table 8.45 Top 50 genes downregulated in TNF treated relative to untreated HS lesional skin in all fibroblasts determined by scRNA-seq

MMP3	*RAC1*	*CSF3*	*S100A2*	*RPS4Y1*
CEBPB	*BRI3*	*CXCL8*	*CA12*	*CDK2AP1*
MMP1	*YBX3*	*PTMS*	*CD81*	*CCL3*
CEBPD	*C11orf96*	*S100A9*	*HTRA3*	*SAT1*
KRT14	*CTGF*	*NENF*	*IL7R*	*TIMP3*
H1FX	*S100A8*	*DUSP1*	*SFN*	*FAU*
C15orf48	*INHBA*	*CHI3L1*	*BASP1*	*RPS3A*
TMEM158	*NBL1*	*CXCL13*	*CXCL5*	*RPS23*
MTRNR2L11	*MTRNR2L1*	*RRAD*	*MMP9*	*TGFBI*
IGLL5	*PLAU*	*RPS20*	*FBLN1*	*PTP4A2*

Table 8.46 Top 50 genes upregulated in TNF treated relative to untreated HS lesional skin in all fibroblasts determined by scRNA-seq

PTGDS	*C3*	*MIF*	*PCSK1N*	*RARRES2*
MT1F	*RPS26*	*PLA2G2A*	*NFIA*	*F10*
COMP	*TNC*	*PLAGL1*	*MASP1*	*EMX2*
RBMS3	*IFITM1*	*OLFML3*	*TCF4*	*DIO2*
APCDD1	*ARRDC3*	*CD9*	*SFRP2*	*PHACTR2*
MFAP4	*TXNIP*	*RIN2*	*ACKR4*	*ARL6IP5*
ZBTB20	*ABCA6*	*MT1X*	*AL163636.2*	*PLAC9*
COL18A1	*PLEKHH2*	*SCPEP1*	*CCL19*	*FXYD1*
PPIB	*C2orf68*	*LEPR*	*IFI6*	*APELA*
CFB	*ENPP2*	*HMGN3*	*TMEM176B*	*IL11RA*

Table 8.47 Top 50 genes upregulated in HS lesions relative healthy control skin in the dermal macrophage cluster determined by scRNA-seq

IGLL5	*NRG1*	*LGALS1*	*SERF2*	*RPL39*
LYZ	*CSTA*	*LIMD2*	*HLA-DPB1*	*TNFSF13B*
FCN1	*S100A12*	*RPS2*	*HLA-DRA*	*S100A11*
S100A8	*SH3BGRL3*	*CD48*	*ASGR1*	*CTSS*
S100A9	*RPL28*	*C15orf48*	*JCHAIN*	*B2M*
SERPINA1	*VCAN*	*FPR1*	*MT-CO1*	*CD52*
RPL41	*TYROBP*	*RPL18A*	*CLEC7A*	*AQP9*
LGALS2	*ACTB*	*RPS28*	*CARD16*	*RNASE2*
RPS19	*LST1*	*GAPDH*	*OLR1*	*RPS27*
CAPG	*RPS15*	*PPA1*	*CLEC4A*	*RPS4Y1*

Table 8.48 Top 50 genes downregulated in HS lesions relative healthy control skin in the dermal macrophage cluster determined by scRNA-seq

RNASE1	*LMNA*	*MAFB*	*ZFAND5*	*FILIP1L*
CEBPD	*MTRNR2L12*	*DAB2*	*FUS*	*GADD45B*
PDK4	*KLF4*	*SELENOP*	*KLF9*	*EMB*
RHOB	*C1QC*	*CEBPB*	*CCL4*	*CPEB4*
KLF6	*KLF2*	*JUN*	*C1QB*	*HPGDS*
C1QA	*LYVE1*	*ARRDC3*	*ABCA6*	*FGL2*
TSC22D3	*MTRNR2L1*	*TPT1*	*MRC1*	*MAF*
EMP1	*FOSB*	*JUND*	*ANXA1*	*CD99*
FOLR2	*ZFP36L2*	*LGMN*	*AHNAK*	*CH25H*
CST3	*TNFAIP3*	*PELI1*	*MS4A4A*	*MT2A*

Table 8.49 Top 42 genes upregulated in HS lesions relative healthy control skin in the cDC2 (1) cluster determined by scRNA-seq

IGLL5	*JCHAIN*	*MT-ND3*	*IL17A*	*EIF1AY*
RPS4Y1	*FTL*	*TMSB4X*	*OLR1*	*CD14*
S100A8	*CYBB*	*TMEM52B*	*TMEM176B*	
LYZ	*TLL1*	*HLA-DQA2*	*PTMA*	
SERF2	*OAZ1*	*SLC39A9*	*ACTB*	
TYROBP	*DDX3Y*	*S100A12*	*KIAA0895*	
S100A9	*NRG1*	*RPL41*	*TMEM176A*	
MT-CO1	*SRGN*	*PRKACB*	*TIMP1*	
AC087632.1	*CYCS*	*B2M*	*SH3BGRL3*	
FCN1	*THBS1*	*WDR17*	*MS4A6A*	

Table 8.50 Top 50 genes downregulated in HS lesions relative healthy control skin in the cDC2 (1) cluster determined by scRNA-seq

CEBPD	*RAC1*	*CRYBG1*	*RPS29*	*REL*
MT2A	*KLF6*	*ANXA1*	*BIN1*	*RHOB*
HLA-DQA1	*ZFP36L2*	*USP12*	*CLIC2*	*MT-ND4L*
HLA-DRB5	*VIM*	*RBM3*	*RPS6*	*RGCC*
TOB1	*PMAIP1*	*RNF144B*	*RPS4X*	*MTRNR2L12*
IL1R2	*AKAP13*	*ANKRD28*	*SH3BP5*	*RGS1*
TSC22D3	*BASP1*	*ZFAND5*	*RAB11FIP1*	*RPS2*
FILIP1L	*LMNA*	*IL1RAP*	*DSTN*	*CST7*
HLA-DQB2	*B3GNT5*	*PELI1*	*MAP4K4*	*SYAP1*
DUSP5	*MAP2K1*	*DNAJA1*	*ALOX5AP*	*ARL4C*

Table 8.51 Top 49 genes upregulated in HS lesions relative healthy control skin in the cDC2 (2) cluster determined by scRNA-seq

IGLL5	*MT-CO2*	*ACTB*	*S100A12*	*B2M*
TYROBP	*SERF2*	*MT-CO3*	*CTSD*	*NAMPT*
MT-CO1	*CXCL2*	*MT-ATP6*	*DDX3Y*	*HIF1A*
FTL	*SLC2A3*	*CYBB*	*PTGS2*	*CYCS*
LYZ	*RPS4Y1*	*S100A4*	*TMSB4X*	*SRGN*
S100A9	*SH3BGRL3*	*VMP1*	*H3F3A*	*GAPDH*
S100A8	*IER3*	*NRG1*	*MT-ND2*	*PLAUR*
MT-ND3	*JCHAIN*	*SOD2*	*SERPINA1*	*EREG*
FCN1	*TIMP1*	*BCL2A1*	*TMEM52B*	*OLR1*
MT-ND4	*OAZ1*	*CYBA*	*BLVRB*	

Table 8.52 Top 50 genes downregulated in HS lesions relative healthy control skin in the cDC2 (2) cluster determined by scRNA-seq

CEBPD	*RGS1*	*HLA-DPB1*	*CLIC2*	*C1QA*
HLA-DQA1	*ZFP36L2*	*RNF144B*	*HLA-DRB1*	*SIAH1*
FILIP1L	*CRYBG1*	*RAC1*	*PELI1*	*EEF1A1*
IL1R2	*CCR7*	*B3GNT5*	*TSC22D3*	*RPL4*
HLA-DRB5	*RPS4X*	*RPS6*	*RHOB*	*HSPA8*
MT2A	*DUSP5*	*HLA-DQB2*	*C1QC*	*RPL5*
TOB1	*REL*	*LPAR6*	*CD1C*	*MAP4K4*
FCER1A	*CH25H*	*DNAJB14*	*HLA-DPA1*	*GNAS*
LMNA	*MAP2K1*	*AKAP13*	*IL1RAP*	*BIN1*
ANKRD28	*PABPC4*	*PMAIP1*	*PTTG1*	*CCND2*

Table 8.53 Top 48 genes upregulated in HS lesions relative healthy control skin in the Langerhans cells cluster determined by scRNA-seq

IGLL5	*ACTB*	*ATP5MPL*	*TMEM176A*	*MNDA*
LYZ	*SH3BGRL3*	*TMEM176B*	*ABI3*	*FTL*
FCN1	*H3F3A*	*S100A12*	*ATP5MC2*	*SERPINA1*
TYROBP	*TMSB4X*	*OAZ1*	*AC087632.1*	*UQCR10*
S100A8	*B2M*	*AIF1*	*FKBP1A*	*JCHAIN*
S100A9	*S100A11*	*FPR1*	*RPS28*	*RPS19*
SERF2	*ATP5F1E*	*RPL41*	*UBA52*	
VAMP8	*RPS4Y1*	*VCAN*	*TLL1*	
CYBB	*MS4A6A*	*RPS14*	*CYBA*	
NRG1	*CALM2*	*CFL1*	*ATP5ME*	

Table 8.54 Top 50 genes downregulated in HS lesions relative healthy control skin in the Langerhans cells cluster determined by scRNA-seq

CEBPD	*TSC22D3*	*DUSP2*	*MAP3K8*	*BTG1*
TOB1	*DUSP5*	*KLF4*	*ALCAM*	*FCGR2B*
IL1R2	*MTRNR2L1*	*ZFP36L2*	*MT2A*	*ID2*
KLF6	*LMNA*	*CXCL8*	*NFKB1*	*CST3*
MTRNR2L12	*HLA-DQA1*	*PMAIP1*	*ANKRD28*	*HLA-DRB1*
RGCC	*FILIP1L*	*CD1C*	*NLRP3*	*RHOB*
HLA-DRB5	*HLA-DQB2*	*RAC1*	*BIRC3*	*CD69*
TNFAIP3	*SGK1*	*FCER1A*	*CD83*	*CPVL*
RGS1	*MTRNR2L8*	*VIM*	*AKAP13*	*CD1E*
MTRNR2L11	*ZFAND5*	*SLC38A2*	*B3GNT5*	*NFKBIA*

Table 8.55 16 genes upregulated in HS lesions relative healthy control skin in the cDC2 (3) cluster determined by scRNA-seq

IGLL5	*FTL*	*FCN1*	*CYBB*	*TYROBP*
S100A9	*H3F3A*	*ACTB*	*SERF2*	*TMSB4X*
S100A8	*NRG1*	*OAZ1*	*SH3BGRL3*	*LYZ*
RPS4Y1				

Table 8.56 Top 50 genes downregulated in HS lesions relative healthy control skin in the cDC2 (3) cluster determined by scRNA-seq

HLA-DRB5	*MTRNR2L1*	*RGCC*	*AHNAK*	*CA2*
HLA-DQA1	*HLA-DQB2*	*MT2A*	*KLF4*	*FCER1A*
TOB1	*ZFP36L2*	*RAB11FIP1*	*DDX24*	*SGK1*
FILIP1L	*RPS29*	*RGS1*	*AREG*	*FCGR2B*
HLA-DRB1	*DUSP5*	*TSC22D3*	*BRD8*	*LPAR6*
LMNA	*MTRNR2L8*	*KLF2*	*RNF144B*	*NFKB1*
MTRNR2L12	*RHOB*	*RPS6*	*NLRP3*	*ANXA1*
CEBPD	*VIM*	*ANKRD28*	*PMAIP1*	*CIRBP*
IL1R2	*AKAP13*	*SLC38A2*	*SH3BP5*	*CHD2*
KLF6	*REL*	*MTRNR2L11*	*ZFAND5*	*AVPI1*

Table 8.57 Top 50 genes downregulated in HS lesions relative healthy control skin in the cDC1 cluster determined by scRNA-seq. * Only *IGLL5*, *RPS4Y1* and *HLA-DQB1* were upregulated in HS lesions.

ZFP36L2	*KLF6*	*ID2*	*GADD45B*	*B3GNT5*
CEBPD	*PPP1R15A*	*TOB1*	*ZFP36*	*TSC22D3*
RGS1	*DUSP2*	*DDIT4*	*INTS6*	*BIN1*
RAC1	*FNBP1*	*AKAP13*	*MAP2K1*	*MT2A*
DUSP1	*DUSP5*	*MTRNR2L8*	*SLC38A2*	*RPL36A*
KLF4	*IL1RAP*	*BIRC3*	*FOS*	*NFKBID*
BASP1	*IER5*	*MAFF*	*RPS6*	*PNRC1*
BRI3	*RPS4X*	*TNFAIP3*	*CD83*	*TGFBI*
CD1C	*NINJ1*	*NFKB1*	*SPAG9*	*CDC42EP3*
IL1R2	*NFKBIA*	*AHNAK*	*MAP3K8*	*YBX3*

Table 8.58 Top 50 genes downregulated in HS lesions relative healthy control skin in the LAMP3+ cluster determined by scRNA-seq. * Only *IGLL5* was upregulated in HS lesions.

TNFAIP3	*RASGEF1B*	*ETS2*	*FOSB*	*LDLRAD4*
ELF1	*FCER1A*	*RAB11FIP1*	*ARGLU1*	*USP12*
PMAIP1	*CD55*	*IL1RAP*	*VEGFA*	*ATP1B1*
DUSP5	*FILIP1L*	*TTC3*	*CKS2*	*BCAT1*
CXCL8	*IL1R2*	*LMNA*	*NLRP3*	*ALCAM*
DNAJB14	*ANKRD28*	*MAP4K4*	*PLAUR*	*GLRX*
DUSP2	*KLF4*	*ZC3H12A*	*LRRFIP1*	*KLF10*
TOB1	*NFKBIA*	*GNA13*	*ATP2B1*	*DOK2*
CREM	*REL*	*RGCC*	*SLC38A2*	*NFE2L2*
LAPTM5	*PTGER4*	*NR4A2*	*ABL2*	*CHML*

Table 8.59 Number of cells sequenced by 10X Genomics scRNA-seq.

Patients	CD45+ (no. of cells)	CD45- (no. of cells)
HS1	2850	2130
HS2	4390	861
HS3	3332	2363
HS4	3976	3935
HS5	4159	2249
HS6	2502	2649
Con1	4252	4803
Con2	3265	4606
Con3	3944	4069

References

Abdou, A. G., Maraee, A. H., Al-Bara, A. M. and Diab, W. M. (2011) 'Immunohistochemical expression of TGF-β1 in keloids and hypertrophic scars', *Am J Dermatopathol,* 33(1), pp. 84-91.10.1097/DAD.0b013e3181d0c3ad

Abergel, R. P., Chu, M. L., Bauer, E. A. and Uitto, J. (1987) 'Regulation of collagen gene expression in cutaneous diseases with dermal fibrosis: evidence for pretranslational control', *J Invest Dermatol,* 88(6), pp. 727-31.10.1111/1523-1747.ep12470397

Acosta-Rodriguez, E. V., Napolitani, G., Lanzavecchia, A. and Sallusto, F. (2007) 'Interleukins 1beta and 6 but not transforming growth factor-beta are essential for the differentiation of interleukin 17-producing human T helper cells', *Nat Immunol,* 8(9), pp. 942-9.10.1038/ni1496

Akimzhanov, A. M., Yang, X. O. and Dong, C. (2007) 'Chromatin remodeling of interleukin-17 (IL-17)-IL-17F cytokine gene locus during inflammatory helper T cell differentiation', *J Biol Chem,* 282(9), pp. 5969-72.10.1074/jbc.C600322200

Alavi, A., Hamzavi, I., Brown, K., Santos, L. L., Zhu, Z., Liu, H., Howell, M. D. and Kirby, J. S. (2022) 'Janus kinase 1 inhibitor INCB054707 for patients with moderate-to-severe hidradenitis suppurativa: results from two phase II studies', *Br J Dermatol,* 186(5), pp. 803-813.10.1111/bjd.20969

Albanesi, C., Scarponi, C., Giustizieri, M. L. and Girolomoni, G. (2005) 'Keratinocytes in inflammatory skin diseases', *Curr Drug Targets Inflamm Allergy,* 4(3), pp. 329-34.10.2174/1568010054022033

Alharbi, Z., Kauczok, J. and Pallua, N. (2012) 'A review of wide surgical excision of hidradenitis suppurativa', *BMC Dermatol,* 12, pp. 9.10.1186/1471-5945-12-9

Alikhan, A., Lynch, P. J. and Eisen, D. B. (2009) 'Hidradenitis suppurativa: a comprehensive review', *J Am Acad Dermatol,* 60(4), pp. 539-61; quiz 562-3.10.1016/j.jaad.2008.11.911

Alquicira-Hernandez, J. and Powell, J. E. (2021) 'Nebulosa recovers single-cell gene expression signals by kernel density estimation', *Bioinformatics,* 37(16), pp. 2485-2487.10.1093/bioinformatics/btab003

Alvarez, M. J., Shen, Y., Giorgi, F. M., Lachmann, A., Ding, B. B., Ye, B. H. and Califano, A. (2016) 'Functional characterization of somatic mutations in cancer using network-based inference of protein activity', *Nat Genet,* 48(8), pp. 838-47.10.1038/ng.3593

André, R., Marescassier, H., Gabay, C., Pittet, B. and Laffitte, E. (2019) 'Long-term therapy with anakinra in hidradenitis suppurativa in three patients', *Int J Dermatol,* 58(11), pp. e208-e209.10.1111/ijd.14596

Annunziato, F., Cosmi, L., Santarlasci, V., Maggi, L., Liotta, F., Mazzinghi, B., Parente, E., Filì, L., Ferri, S., Frosali, F., Giudici, F., Romagnani, P., Parronchi, P., Tonelli, F., Maggi, E. and Romagnani, S. (2007) 'Phenotypic and functional features of human Th17 cells', *J Exp Med,* 204(8), pp. 1849-61.10.1084/jem.20070663

Aran, D., Hu, Z. and Butte, A. J. (2017) 'xCell: digitally portraying the tissue cellular heterogeneity landscape', *Genome Biol,* 18(1), pp. 220.10.1186/s13059-017-1349-1

Aran, D., Looney, A. P., Liu, L., Wu, E., Fong, V., Hsu, A., Chak, S., Naikawadi, R. P., Wolters, P. J., Abate, A. R., Butte, A. J. and Bhattacharya, M. (2019) 'Reference-based analysis of lung single-cell sequencing reveals a transitional profibrotic macrophage', *Nat Immunol,* 20(2), pp. 163-172.10.1038/s41590-018-0276-y

Avniel, S., Arik, Z., Maly, A., Sagie, A., Basst, H. B., Yahana, M. D., Weiss, I. D., Pal, B., Wald, O., Ad-El, D., Fujii, N., Arenzana-Seisdedos, F., Jung, S., Galun, E., Gur, E. and Peled, A. (2006) 'Involvement of the CXCL12/CXCR4 pathway in the recovery of skin following burns', *J Invest Dermatol,* 126(2), pp. 468-76.10.1038/sj.jid.5700069

Banchereau, J. and Steinman, R. M. (1998) 'Dendritic cells and the control of immunity', *Nature,* 392(6673), pp. 245-52.10.1038/32588

Bandala-Sanchez, E., Zhang, Y., Reinwald, S., Dromey, J. A., Lee, B. H., Qian, J., Böhmer, R. M. and Harrison, L. C. (2013) 'T cell regulation mediated by interaction of soluble CD52 with the inhibitory receptor Siglec-10', *Nat Immunol,* 14(7), pp. 741-8.10.1038/ni.2610

Banerjee, A., McNish, S. and Shanmugam, V. K. (2017) 'Interferon-gamma (IFN-gamma) is Elevated in Wound Exudate from Hidradenitis Suppurativa', *Immunol Invest,* 46(2), pp. 149-158.10.1080/08820139.2016.1230867

Baranzini, S. E. (2014) 'The role of antiproliferative gene Tob1 in the immune system', *Clin Exp Neuroimmunol,* 5(2), pp. 132-136.10.1111/cen3.12125

Baroni, A., Buommino, E., De Gregorio, V., Ruocco, E., Ruocco, V. and Wolf, R. (2012) 'Structure and function of the epidermis related to barrier properties', *Clin Dermatol,* 30(3), pp. 257-62.10.1016/j.clindermatol.2011.08.007

Basdeo, S. A., Cluxton, D., Sulaimani, J., Moran, B., Canavan, M., Orr, C., Veale, D. J., Fearon, U. and Fletcher, J. M. (2017) 'Ex-Th17 (Nonclassical Th1) Cells Are Functionally Distinct from Classical Th1 and Th17 Cells and Are Not Constrained by Regulatory T Cells', *J Immunol,* 198(6), pp. 2249-2259.10.4049/jimmunol.1600737

Basdeo, S. A., Moran, B., Cluxton, D., Canavan, M., McCormick, J., Connolly, M., Orr, C., Mills, K. H., Veale, D. J., Fearon, U. and Fletcher, J. M. (2015) 'Polyfunctional, Pathogenic CD161+ Th17 Lineage Cells Are Resistant to Regulatory T Cell-Mediated Suppression in the Context of Autoimmunity', *J Immunol,* 195(2), pp. 528-40.10.4049/jimmunol.1402990

Bautista-Hernández, L. A., Gómez-Olivares, J. L., Buentello-Volante, B. and Bautista-de Lucio, V. M. (2017) 'Fibroblasts: The Unknown Sentinels Eliciting Immune Responses Against Microorganisms', *Eur J Microbiol Immunol (Bp),* 7(3), pp. 151-157.10.1556/1886.2017.00009

Bedoui, S., Whitney, P. G., Waithman, J., Eidsmo, L., Wakim, L., Caminschi, I., Allan, R. S., Wojtasiak, M., Shortman, K., Carbone, F. R., Brooks, A. G. and Heath, W. R. (2009) 'Cross-presentation of viral and self antigens by skin-derived CD103+ dendritic cells', *Nat Immunol,* 10(5), pp. 488-95.10.1038/ni.1724

Bettelli, E., Carrier, Y., Gao, W., Korn, T., Strom, T. B., Oukka, M., Weiner, H. L. and Kuchroo, V. K. (2006) 'Reciprocal developmental pathways for the generation of pathogenic effector TH17 and regulatory T cells', *Nature,* 441(7090), pp. 235-8.10.1038/nature04753

Blok, J. L., Li, K., Brodmerkel, C., Horvátovich, P., Jonkman, M. F. and Horváth, B. (2016) 'Ustekinumab in hidradenitis suppurativa: clinical results and a search for potential biomarkers in serum', *Br J Dermatol,* 174(4), pp. 839-46.10.1111/bjd.14338

Boro, M. and Balaji, K. N. (2017) 'CXCL1 and CXCL2 Regulate NLRP3 Inflammasome Activation via G-Protein-Coupled Receptor CXCR2', *J Immunol,* 199(5), pp. 1660-1671.10.4049/jimmunol.1700129

Brand, S. (2009) 'Crohn's disease: Th1, Th17 or both? The change of a paradigm: new immunological and genetic insights implicate Th17 cells in the pathogenesis of Crohn's disease', *Gut,* 58(8), pp. 1152-67.10.1136/gut.2008.163667

Brinkmann, V., Reichard, U., Goosmann, C., Fauler, B., Uhlemann, Y., Weiss, D. S., Weinrauch, Y. and Zychlinsky, A. (2004) 'Neutrophil extracellular traps kill bacteria', *Science,* 303(5663), pp. 1532-5.10.1126/science.1092385

Browaeys, R., Saelens, W. and Saeys, Y. (2020) 'NicheNet: modeling intercellular communication by linking ligands to target genes', *Nat Methods,* 17(2), pp. 159-162.10.1038/s41592-019-0667-5

Brown, G. D., Taylor, P. R., Reid, D. M., Willment, J. A., Williams, D. L., Martinez-Pomares, L., Wong, S. Y. and Gordon, S. (2002) 'Dectin-1 is a major beta-glucan receptor on macrophages', *J Exp Med,* 196(3), pp. 407-12.10.1084/jem.20020470

Byrd, A. S., Carmona-Rivera, C., O'Neil, L. J., Carlucci, P. M., Cisar, C., Rosenberg, A. Z., Kerns, M. L., Caffrey, J. A., Milner, S. M., Sacks, J. M., Aliu, O., Broderick, K. P., Reichner, J. S., Miller, L. S., Kang, S., Robinson, W. H., Okoye, G. A. and Kaplan, M. J. (2019) 'Neutrophil extracellular traps, B cells, and type I interferons contribute to immune dysregulation in hidradenitis suppurativa', *Sci Transl Med,* 11(508).10.1126/scitranslmed.aav5908

Byrd, A. S., Kerns, M. L., Williams, D. W., Zarif, J. C., Rosenberg, A. Z., Delsante, M., Liu, H., Dillen, C. A., Maynard, J. P., Caffrey, J. A., Sacks, J. M., Milner, S. M., Aliu, O., Broderick, K. P., Lew, L. S., Miller, L. S., Kang, S. and Okoye, G. A. (2018) 'Collagen deposition in chronic hidradenitis suppurativa: potential role for CD163', *Br J Dermatol,* 179(3), pp. 792-794.10.1111/bjd.16600

Calao, M., Wilson, J. L., Spelman, L., Billot, L., Rubel, D., Watts, A. D. and Jemec, G. B. E. (2018) 'Hidradenitis Suppurativa (HS) prevalence, demographics and management pathways in Australia: A population-based cross-sectional study', *PLoS One,* 13(7), pp. e0200683.10.1371/journal.pone.0200683

Canoui-Poitrine, F., Revuz, J. E., Wolkenstein, P., Viallette, C., Gabison, G., Pouget, F., Poli, F., Faye, O. and Bastuji-Garin, S. (2009) 'Clinical characteristics of a series of 302 French patients with hidradenitis suppurativa, with an analysis of factors associated with disease severity', *J Am Acad Dermatol,* 61(1), pp. 51-7.10.1016/j.jaad.2009.02.013

Cao, J., Packer, J. S., Ramani, V., Cusanovich, D. A., Huynh, C., Daza, R., Qiu, X., Lee, C., Furlan, S. N., Steemers, F. J., Adey, A., Waterston, R. H., Trapnell, C. and Shendure, J. (2017) 'Comprehensive single-cell transcriptional profiling of a multicellular organism', *Science,* 357(6352), pp. 661-667.10.1126/science.aam8940

Cao, J., Spielmann, M., Qiu, X., Huang, X., Ibrahim, D. M., Hill, A. J., Zhang, F., Mundlos, S., Christiansen, L., Steemers, F. J., Trapnell, C. and Shendure, J. (2019) 'The single-cell transcriptional landscape of mammalian organogenesis', *Nature,* 566(7745), pp. 496-502.10.1038/s41586-019-0969-x

Caproni, M., Antiga, E., Volpi, W., Verdelli, A., Venegoni, L., Quaglino, P., Fabbri, P. and Marzano, A. V. (2015) 'The Treg/Th17 cell ratio is reduced in the skin lesions of patients with pyoderma gangrenosum', *Br J Dermatol,* 173(1), pp. 275-8.10.1111/bjd.13670

Carmona-Rivera, C., Carlucci, P. M., Moore, E., Lingampalli, N., Uchtenhagen, H., James, E., Liu, Y., Bicker, K. L., Wahamaa, H., Hoffmann, V., Catrina, A. I., Thompson, P., Buckner, J. H., Robinson, W. H., Fox, D. A. and Kaplan, M. J. (2017) 'Synovial fibroblast-neutrophil interactions promote pathogenic adaptive immunity in rheumatoid arthritis', *Sci Immunol,* 2(10).10.1126/sciimmunol.aag3358

Carmona-Rivera, C., O'Neil, L. J., Patino-Martinez, E., Shipman, W. D., Zhu, C., Li, Q. Z., Kerns, M. L., Barnes, L. A., Caffrey, J. A., Kang, S., Kaplan, M. J., Okoye, G. A. and Byrd, A. S. (2022) 'Autoantibodies Present in Hidradenitis Suppurativa Correlate with Disease Severity and Promote the Release of Proinflammatory Cytokines in Macrophages', *J Invest Dermatol,* 142(3 Pt B), pp. 924-935.10.1016/j.jid.2021.07.187

Chang, S. H., Reynolds, J. M., Pappu, B. P., Chen, G., Martinez, G. J. and Dong, C. (2011) 'Interleukin-17C promotes Th17 cell responses and autoimmune disease via interleukin-17 receptor E', *Immunity,* 35(4), pp. 611-21.10.1016/j.immuni.2011.09.010

Chen, G. Y. and Nuñez, G. (2010) 'Sterile inflammation: sensing and reacting to damage', *Nat Rev Immunol,* 10(12), pp. 826-37.10.1038/nri2873

Cheuk, S., Wikén, M., Blomqvist, L., Nylén, S., Talme, T., Ståhle, M. and Eidsmo, L. (2014) 'Epidermal Th22 and Tc17 cells form a localized disease memory in clinically healed psoriasis', *J Immunol,* 192(7), pp. 3111-20.10.4049/jimmunol.1302313

Chi, H. H., Hua, K. F., Lin, Y. C., Chu, C. L., Hsieh, C. Y., Hsu, Y. J., Ka, S. M., Tsai, Y. L., Liu, F. C. and Chen, A. (2017) 'IL-36 Signaling Facilitates Activation of the NLRP3 Inflammasome and IL-23/IL-17 Axis in Renal Inflammation and Fibrosis', *J Am Soc Nephrol,* 28(7), pp. 2022-2037.10.1681/ASN.2016080840

Chieosilapatham, P., Kiatsurayanon, C., Umehara, Y., Trujillo-Paez, J. V., Peng, G., Yue, H., Nguyen, L. T. H. and Niyonsaba, F. (2021) 'Keratinocytes: innate immune cells in atopic dermatitis', *Clin Exp Immunol,* 204(3), pp. 296-309.10.1111/cei.13575

Chong, W. P., Mattapallil, M. J., Raychaudhuri, K., Bing, S. J., Wu, S., Zhong, Y., Wang, W., Chen, Z., Silver, P. B., Jittayasothorn, Y., Chan, C. C., Chen, J., Horai, R. and Caspi, R. R. (2020) 'The Cytokine IL-17A Limits Th17 Pathogenicity via a Negative Feedback Loop Driven by Autocrine Induction of IL-24', *Immunity,* 53(2), pp. 384-397.e5.10.1016/j.immuni.2020.06.022

Chou, Y. T., Lai, F. J., Chang, N. S. and Hsu, L. J. (2020) 'Deficiency Causes Downregulation of Prosurvival ERK Signaling and Abnormal Homeostatic Responses in Mouse Skin', *Front Cell Dev Biol,* 8, pp. 558432.10.3389/fcell.2020.558432

Choudhary, V., Uaratanawong, R., Patel, R. R., Patel, H., Bao, W., Hartney, B., Cohen, E., Chen, X., Zhong, Q., Isales, C. M. and Bollag, W. B. (2019) 'Phosphatidylglycerol Inhibits Toll-Like Receptor-Mediated Inflammation by Danger-Associated Molecular Patterns', *J Invest Dermatol,* 139(4), pp. 868-877.10.1016/j.jid.2018.10.021

Chu, H. and Mazmanian, S. K. (2013) 'Innate immune recognition of the microbiota promotes host-microbial symbiosis', *Nat Immunol,* 14(7), pp. 668-75.10.1038/ni.2635

Chung, Y., Chang, S. H., Martinez, G. J., Yang, X. O., Nurieva, R., Kang, H. S., Ma, L., Watowich, S. S., Jetten, A. M., Tian, Q. and Dong, C. (2009) 'Critical regulation of early Th17 cell differentiation by interleukin-1 signaling', *Immunity,* 30(4), pp. 576-87.10.1016/j.immuni.2009.02.007

Cibrian, D. and Sanchez-Madrid, F. (2017) 'CD69: from activation marker to metabolic gatekeeper', *Eur J Immunol,* 47(6), pp. 946-953.10.1002/eji.201646837

Clark, R. A. (2015) 'Resident memory T cells in human health and disease', *Sci Transl Med,* 7(269), pp. 269rv1.10.1126/scitranslmed.3010641

Clark, R. A., Chong, B., Mirchandani, N., Brinster, N. K., Yamanaka, K., Dowgiert, R. K. and Kupper, T. S. (2006a) 'The vast majority of CLA+ T cells are resident in normal skin', *J Immunol,* 176(7), pp. 4431-9.10.4049/jimmunol.176.7.4431

Clark, R. A., Chong, B. F., Mirchandani, N., Yamanaka, K., Murphy, G. F., Dowgiert, R. K. and Kupper, T. S. (2006b) 'A novel method for the isolation of skin resident T cells from normal and diseased human skin', *J Invest Dermatol,* 126(5), pp. 1059-70.10.1038/sj.jid.5700199

Coates, M., Mariottoni, P., Corcoran, D. L., Kirshner, H. F., Jaleel, T., Brown, D. A., Brooks, S. R., Murray, J., Morasso, M. I. and MacLeod, A. S. (2019) 'The skin transcriptome in hidradenitis suppurativa uncovers an antimicrobial and sweat gland gene signature which has distinct overlap with wounded skin', *PLoS One,* 14(5), pp. e0216249.10.1371/journal.pone.0216249

Cohen, K. W. and Frahm, N. (2017) 'Current views on the potential for development of a HIV vaccine', *Expert Opin Biol Ther,* 17(3), pp. 295-303.10.1080/14712598.2017.1282457

Coll, R. C., Hill, J. R., Day, C. J., Zamoshnikova, A., Boucher, D., Massey, N. L., Chitty, J. L., Fraser, J. A., Jennings, M. P., Robertson, A. A. B. and Schroder, K. (2019) 'MCC950 directly targets the NLRP3 ATP-hydrolysis motif for inflammasome inhibition', *Nat Chem Biol,* 15(6), pp. 556-559.10.1038/s41589-019-0277-7

Collins, N., Jiang, X., Zaid, A., Macleod, B. L., Li, J., Park, C. O., Haque, A., Bedoui, S., Heath, W. R., Mueller, S. N., Kupper, T. S., Gebhardt, T. and Carbone, F. R. (2016) 'Skin CD4(+) memory T cells exhibit combined cluster-mediated retention and equilibration with the circulation', *Nat Commun,* 7, pp. 11514.10.1038/ncomms11514

Colpitts, S. L., Dalton, N. M. and Scott, P. (2009) 'IL-7 receptor expression provides the potential for long-term survival of both CD62Lhigh central memory T cells and Th1 effector cells during Leishmania major infection', *J Immunol,* 182(9), pp. 5702-11.10.4049/jimmunol.0803450

Cosmi, L., De Palma, R., Santarlasci, V., Maggi, L., Capone, M., Frosali, F., Rodolico, G., Querci, V., Abbate, G., Angeli, R., Berrino, L., Fambrini, M., Caproni, M., Tonelli, F., Lazzeri, E., Parronchi, P., Liotta, F., Maggi, E., Romagnani, S. and Annunziato, F. (2008) 'Human interleukin 17-producing cells originate from a CD161+CD4+ T cell precursor', *J Exp Med,* 205(8), pp. 1903-16.10.1084/jem.20080397

Crawford, M. P., Borcherding, N. and Karandikar, N. J. (2023) 'IL-17 cytokines preferentially act on naïve CD4+ T cells with the IL-17AF heterodimer inducing the greatest functional changes', *PLoS One,* 18(4), pp. e0285166.10.1371/journal.pone.0285166

Dai, X., Tohyama, M., Murakami, M. and Sayama, K. (2017) 'Epidermal keratinocytes sense dsRNA via the NLRP3 inflammasome, mediating interleukin (IL)-1β and IL-18 release', *Exp Dermatol,* 26(10), pp. 904-911.10.1111/exd.13334

Dajnoki, Z., Somogyi, O., Medgyesi, B., Jenei, A., Szabó, L., Gáspár, K., Hendrik, Z., Gergely, P., Imre, D., Póliska, S., Törőcsik, D., Zouboulis, C. C., Prens, E. P., Kapitány, A. and Szegedi, A. (2022) 'Primary alterations during the development of hidradenitis suppurativa', *J Eur Acad Dermatol Venereol,* 36(3), pp. 462-471.10.1111/jdv.17779

Dan Lu, Liu, L., Sun, Y., Song, J., Yin, Q., Zhang, G., Qi, F., Hu, Z., Yang, Z., Zhou, Z., Hu, Y., Zhang, L., Ji, J., Zhao, X., Jin, Y., McNutt, M. A. and Yin, Y. (2020) 'The phosphatase PAC1 acts as a T cell suppressor and attenuates host antitumor immunity', *Nat Immunol,* 21(3), pp. 287-297.10.1038/s41590-019-0577-9

Davila, M. L., Xu, M., Huang, C., Gaddes, E. R., Winter, L., Cantorna, M. T., Wang, Y. and Xiong, N. (2022) 'CCL27 is a crucial regulator of immune homeostasis of the skin and mucosal tissues', *iScience,* 25(6), pp. 104426.10.1016/j.isci.2022.104426

de Winter, K., van der Zee, H. H. and Prens, E. P. (2012) 'Is mechanical stress an important pathogenic factor in hidradenitis suppurativa?', *Exp Dermatol,* 21(3), pp. 176-7.10.1111/j.1600-0625.2012.01443.x

Degboé, Y., Rauwel, B., Baron, M., Boyer, J. F., Ruyssen-Witrand, A., Constantin, A. and Davignon, J. L. (2019) 'Polarization of Rheumatoid Macrophages by TNF Targeting Through an IL-10/STAT3 Mechanism', *Front Immunol,* 10, pp. 3.10.3389/fimmu.2019.00003

Del Duca, E., Morelli, P., Bennardo, L., Di Raimondo, C. and Nisticò, S. P. (2020) 'Cytokine Pathways and Investigational Target Therapies in Hidradenitis Suppurativa', *Int J Mol Sci,* 21(22).10.3390/ijms21228436

Denton, C. P., Khan, K., Hoyles, R. K., Shiwen, X., Leoni, P., Chen, Y., Eastwood, M. and Abraham, D. J. (2009) 'Inducible lineage-specific deletion of TbetaRII in fibroblasts defines a pivotal regulatory role during adult skin wound healing', *J Invest Dermatol,* 129(1), pp. 194-204.10.1038/jid.2008.171

Dewigne, M., Orte Cano, C., Daoud, M., Del Marmol, V. and Benhadou, F. (2022) 'Low incidence of COVID-19 in hidradenitis suppurativa: How to interpret it?', *Exp Dermatol,* 31(3), pp. 435-436.10.1111/exd.14475

Di Caprio, R., Balato, A., Caiazzo, G., Lembo, S., Raimondo, A., Fabbrocini, G. and Monfrecola, G. (2017) 'IL-36 cytokines are increased in acne and hidradenitis suppurativa', *Arch Dermatol Res,* 309(8), pp. 673-678.10.1007/s00403-017-1769-5

Dudink, K., Bouwman, K., Chen, Y., DePrimo, S. E., Munoz-Elias, E. J., Aarts, P., Schappin, R., Florencia, E. F., van Heeswijk, B., Prens, L. M., van der Zee, H. H., Prens, E. P., van Straalen, K. R. and Horváth, B. (2023) 'Guselkumab for hidradenitis suppurativa: a phase II, open-label, mode-of-action study', *Br J Dermatol,* 188(5), pp. 601-609.10.1093/bjd/ljad010

Dutertre, C. A., Becht, E., Irac, S. E., Khalilnezhad, A., Narang, V., Khalilnezhad, S., Ng, P. Y., van den Hoogen, L. L., Leong, J. Y., Lee, B., Chevrier, M., Zhang, X. M., Yong, P. J. A., Koh, G., Lum, J., Howland, S. W., Mok, E., Chen, J., Larbi, A., Tan, H. K. K., Lim, T. K. H., Karagianni, P., Tzioufas, A. G., Malleret, B., Brody, J., Albani, S., van Roon, J., Radstake, T., Newell, E. W. and Ginhoux, F. (2019) 'Single-Cell Analysis of Human Mononuclear Phagocytes Reveals Subset-Defining Markers and Identifies Circulating Inflammatory Dendritic Cells', *Immunity,* 51(3), pp. 573-589.e8.10.1016/j.immuni.2019.08.008

Ershaid, N., Sharon, Y., Doron, H., Raz, Y., Shani, O., Cohen, N., Monteran, L., Leider-Trejo, L., Ben-Shmuel, A., Yassin, M., Gerlic, M., Ben-Baruch, A., Pasmanik-Chor, M., Apte, R. and Erez, N. (2019) 'NLRP3 inflammasome in fibroblasts links tissue damage with inflammation in breast cancer progression and metastasis', *Nat Commun,* 10(1), pp. 4375.10.1038/s41467-019-12370-8

Esmann, S. and Jemec, G. B. (2016) 'Assessing the quality of life over longer periods', *J Eur Acad Dermatol Venereol,* 30(1), pp. 189-90.10.1111/jdv.12700

Eyerich, S., Eyerich, K., Pennino, D., Carbone, T., Nasorri, F., Pallotta, S., Cianfarani, F., Odorisio, T., Traidl-Hoffmann, C., Behrendt, H., Durham, S. R., Schmidt-Weber, C. B. and Cavani, A. (2009) 'Th22 cells represent a distinct human T cell subset involved in epidermal immunity and remodeling', *J Clin Invest,* 119(12), pp. 3573-85.10.1172/JCI40202

Fenini, G., Karakaya, T., Hennig, P., Di Filippo, M. and Beer, H. D. (2020) 'The NLRP1 Inflammasome in Human Skin and Beyond', *Int J Mol Sci,* 21(13).10.3390/ijms21134788

Fisher, B. A. (2020) 'Assessment of the anti-CD40 antibody iscalimab in patients with primary Sjögren's syndrome: a multicentre, randomised, double-blind, placebo-controlled, proof-of-concept study', *Lancet Rheumatol.*10.1016/S2665-9913(19)30135-3

Fletcher, J. M., Moran, B., Petrasca, A. and Smith, C. M. (2020) 'IL-17 in inflammatory skin diseases psoriasis and hidradenitis suppurativa', *Clin Exp Immunol,* 201(2), pp. 121-134.10.1111/cei.13449

Freedberg, I. M., Tomic-Canic, M., Komine, M. and Blumenberg, M. (2001) 'Keratins and the keratinocyte activation cycle', *J Invest Dermatol,* 116(5), pp. 633-40.10.1046/j.1523-1747.2001.01327.x

Frew, J. W., Hawkes, J. E. and Krueger, J. G. (2018) 'A systematic review and critical evaluation of inflammatory cytokine associations in hidradenitis suppurativa', *F1000Res,* 7, pp. 1930.10.12688/f1000research.17267.1

Frew, J. W., Jiang, C. S., Singh, N., Grand, D., Navrazhina, K., Vaughan, R. and Krueger, J. G. (2021a) 'Dermal tunnels influence time to clinical response and family history influences time to loss of clinical response in patients with hidradenitis suppurativa treated with adalimumab', *Clin Exp Dermatol,* 46(2), pp. 306-313.10.1111/ced.14448

Frew, J. W., Navrazhina, K., Grand, D., Sullivan-Whalen, M., Gilleaudeau, P., Garcet, S., Ungar, J. and Krueger, J. G. (2020) 'The effect of subcutaneous brodalumab on clinical disease activity in hidradenitis suppurativa: An open-label cohort study', *J Am Acad Dermatol,* 83(5), pp. 1341-1348.10.1016/j.jaad.2020.05.007

Frew, J. W., Navrazhina, K., Marohn, M., Lu, P. C. and Krueger, J. G. (2019) 'Contribution of fibroblasts to tunnel formation and inflammation in hidradenitis suppurativa/ acne inversa', *Exp Dermatol,* 28(8), pp. 886-891.10.1111/exd.13978

Frew, J. W., Navrazhina, K., Sullivan-Whalen, M., Gilleaudeau, P., Garcet, S. and Krueger, J. G. (2021b) 'Weekly administration of brodalumab in hidradenitis suppurativa: an open-label cohort study', *Br J Dermatol,* 184(2), pp. 350-352.10.1111/bjd.19478

Frings, V. G., Jopp, L., Srivastava, M., Presser, D., Goebeler, M. and Schmidt, M. (2022) 'Stress signalling and STAT1 activation characterize the keratinocytic gene expression pattern in Hidradenitis suppurativa', *J Eur Acad Dermatol Venereol,* 36(12), pp. 2488-2498.10.1111/jdv.18465

Fung, H. Y., Teryek, M., Lemenze, A. D. and Bergsbaken, T. (2022) 'CD103 fate mapping reveals that intestinal CD103', *Sci Immunol,* 7(77), pp. eabl9925.10.1126/sciimmunol.abl9925

Furue, M., Furue, K., Tsuji, G. and Nakahara, T. (2020) 'Interleukin-17A and Keratinocytes in Psoriasis', *Int J Mol Sci,* 21(4).10.3390/ijms21041275

Gaffen, S. L. (2009) 'Structure and signalling in the IL-17 receptor family', *Nat Rev Immunol,* 9(8), pp. 556-67.10.1038/nri2586

Gallagher, C., Mahon, J. M., O'Neill, C., Cassidy, F. C., Dunbar, H., De Barra, C., Cadden, C., Pisarska, M. M., Wood, N. A. W., Masterson, J. C., McNamee, E. N., Schrumpf, E., English, K., O'Shea, D., Tobin, A. M. and Hogan, A. E. (2023) 'Mucosal-Associated Invariant T Cells Are Altered in Patients with Hidradenitis Suppurativa and Contribute to the Inflammatory Milieu', *J Invest Dermatol,* 143(6), pp. 1094-1097.e2.10.1016/j.jid.2022.11.011

Gallais Serezal, I., Hoffer, E., Ignatov, B., Martini, E., Zitti, B., Ehrstrom, M. and Eidsmo, L. (2019) 'A skewed pool of resident T cells triggers psoriasis-associated tissue responses in never-lesional skin from patients with psoriasis', *J Allergy Clin Immunol,* 143(4), pp. 1444-1454.10.1016/j.jaci.2018.08.048

Gamell, C., Bankovacki, A., Scalzo-Inguanti, K., Sedgmen, B., Alhamdoosh, M., Gail, E., Turkovic, L., Millar, C., Johnson, L., Wahlsten, M., Richter, J., Schuster, J., Dyson, A., Nicolopoulos, J., Varigos, G., Ng, M., Wilson, N., Field, J., Kern, J. S. and Lindqvist, L. M. (2023) 'CSL324, a granulocyte colony-stimulating factor receptor antagonist, blocks neutrophil migration markers that are upregulated in hidradenitis suppurativa', *Br J Dermatol,* 188(5), pp. 636-648.10.1093/bjd/ljad013

Gao, Y., Yao, X., Zhai, Y., Li, L., Li, H., Sun, X., Yu, P., Xue, T., Li, Y. and Hu, Y. (2021) 'Single cell transcriptional zonation of human psoriasis skin identifies an alternative immunoregulatory axis conducted by skin resident cells', *Cell Death Dis,* 12(5), pp. 450.10.1038/s41419-021-03724-6

Gao, Y., Yi, X. and Ding, Y. (2017) 'Combined Transcriptomic Analysis Revealed AKR1B10 Played an Important Role in Psoriasis through the Dysregulated Lipid Pathway and Overproliferation of Keratinocyte', *Biomed Res Int,* 2017, pp. 8717369.10.1155/2017/8717369

Garcia-Alonso, L., Holland, C. H., Ibrahim, M. M., Turei, D. and Saez-Rodriguez, J. (2019) 'Benchmark and integration of resources for the estimation of human transcription factor activities', *Genome Res,* 29(8), pp. 1363-1375.10.1101/gr.240663.118

Garg, A., Kirby, J. S., Lavian, J., Lin, G. and Strunk, A. (2017) 'Sex- and Age-Adjusted Population Analysis of Prevalence Estimates for Hidradenitis Suppurativa in the United States', *JAMA Dermatol,* 153(8), pp. 760-764.10.1001/jamadermatol.2017.0201

Garg, A., Papagermanos, V., Midura, M. and Strunk, A. (2018) 'Incidence of hidradenitis suppurativa among tobacco smokers: a population-based retrospective analysis in the U.S.A', *Br J Dermatol,* 178(3), pp. 709-714.10.1111/bjd.15939

Gerdes, S., Staubach, P., Dirschka, T., Wetzel, D., Weirich, O., Niesmann, J., da Mota, R., Rothhaar, A., Ardabili, M., Vlasitz, G., Feldwisch, J., Osterling Koskinen, L., Ohlman, S., Peloso, P. M., Brun, N. C. and Frejd, F. Y. (2023) 'Izokibep for the treatment of moderate-to-severe plaque psoriasis: a phase II, randomized, placebo-controlled, double-blind, dose-finding multicentre study including long-term treatment', *Br J Dermatol,* 189(4), pp. 381-391.10.1093/bjd/ljad186

Ginhoux, F., Tacke, F., Angeli, V., Bogunovic, M., Loubeau, M., Dai, X. M., Stanley, E. R., Randolph, G. J. and Merad, M. (2006) 'Langerhans cells arise from monocytes in vivo', *Nat Immunol,* 7(3), pp. 265-73.10.1038/ni1307

Giustizieri, M. L., Mascia, F., Frezzolini, A., De Pità, O., Chinni, L. M., Giannetti, A., Girolomoni, G. and Pastore, S. (2001) 'Keratinocytes from patients with atopic dermatitis and psoriasis show a distinct chemokine production profile in response to T cell-derived cytokines', *J Allergy Clin Immunol,* 107(5), pp. 871-7.10.1067/mai.2001.114707

Gkini, M. A. and Bewley, A. P. (2018) 'Development of hidradenitis suppurativa in a patient treated with ustekinumab for her psoriasis: A potential paradoxical reaction?', *Dermatol Ther,* 31(6), pp. e12742.10.1111/dth.12742

Glatt, S., Jemec, G. B. E., Forman, S., Sayed, C., Schmieder, G., Weisman, J., Rolleri, R., Seegobin, S., Baeten, D., Ionescu, L., Zouboulis, C. C. and Shaw, S. (2021) 'Efficacy and Safety of Bimekizumab in Moderate to Severe Hidradenitis Suppurativa: A Phase 2, Double-blind, Placebo-Controlled Randomized Clinical Trial', *JAMA Dermatol,* 157(11), pp. 1279-1288.10.1001/jamadermatol.2021.2905

Gogali, F., Paterakis, G., Rassidakis, G. Z., Kaltsas, G., Liakou, C. I., Gousis, P., Neonakis, E., Manoussakis, M. N. and Liapi, C. (2012) 'Phenotypical analysis of lymphocytes with suppressive and regulatory properties (Tregs) and NK cells in the papillary carcinoma of thyroid', *J Clin Endocrinol Metab,* 97(5), pp. 1474-82.10.1210/jc.2011-1838

Goldburg, S. R., Strober, B. E. and Payette, M. J. (2019) 'Part I. Hidradenitis Suppurativa: Epidemiology, clinical presentation, and pathogenesis', *J Am Acad Dermatol*.10.1016/j.jaad.2019.08.090

Gole, B., Pernat, C., Jezernik, G. and Potočnik, U. (2023) 'The expression IL1B correlates negatively with the clinical response to adalimumab in Crohn's disease patients: An ex vivo approach using peripheral blood mononuclear cells', *Life Sci,* 326, pp. 121822.10.1016/j.lfs.2023.121822

Gordon, K. B., Langley, R. G., Leonardi, C., Toth, D., Menter, M. A., Kang, S., Heffernan, M., Miller, B., Hamlin, R., Lim, L., Zhong, J., Hoffman, R. and Okun, M. M. (2006) 'Clinical response to adalimumab treatment in patients with moderate to severe psoriasis: double-blind, randomized controlled trial and open-label extension study', *J Am Acad Dermatol,* 55(4), pp. 598-606.10.1016/j.jaad.2006.05.027

Gottlieb, A., Natsis, N. E., Kerdel, F., Forman, S., Gonzalez, E., Jimenez, G., Hernandez, L., Kaffenberger, J., Guido, G., Lucas, K., Montes, D., Gold, M., Babcock, C. and Simard, J. (2020) 'A Phase II Open-Label Study of Bermekimab in Patients with Hidradenitis Suppurativa Shows Resolution of Inflammatory Lesions and Pain', *J Invest Dermatol,* 140(8), pp. 1538-1545.e2.10.1016/j.jid.2019.10.024

Grant, A., Gonzalez, T., Montgomery, M. O., Cardenas, V. and Kerdel, F. A. (2010) 'Infliximab therapy for patients with moderate to severe hidradenitis suppurativa: a randomized, double-blind, placebo-controlled crossover trial', *J Am Acad Dermatol,* 62(2), pp. 205-17.10.1016/j.jaad.2009.06.050

Grewal, I. S., Foellmer, H. G., Grewal, K. D., Xu, J., Hardardottir, F., Baron, J. L., Janeway, C. A. and Flavell, R. A. (1996) 'Requirement for CD40 ligand in costimulation induction, T cell activation, and experimental allergic encephalomyelitis', *Science,* 273(5283), pp. 1864-7.10.1126/science.273.5283.1864

Grice, E. A. and Segre, J. A. (2011) 'The skin microbiome', *Nat Rev Microbiol,* 9(4), pp. 244-53.10.1038/nrmicro2537

Griffin, G. K., Newton, G., Tarrio, M. L., Bu, D. X., Maganto-Garcia, E., Azcutia, V., Alcaide, P., Grabie, N., Luscinskas, F. W., Croce, K. J. and Lichtman, A. H. (2012) 'IL-17 and TNF-alpha sustain neutrophil recruitment during inflammation through synergistic effects on endothelial activation', *J Immunol,* 188(12), pp. 6287-99.10.4049/jimmunol.1200385

Griffin, M. O., Ceballos, G. and Villarreal, F. J. (2011) 'Tetracycline compounds with non-antimicrobial organ protective properties: possible mechanisms of action', *Pharmacol Res,* 63(2), pp. 102-7.10.1016/j.phrs.2010.10.004

Gudjonsson, J. E., Tsoi, L. C., Ma, F., Billi, A. C., van Straalen, K. R., Vossen, A., van der Zee, H. H., Harms, P. W., Wasikowski, R., Yee, C. M., Rizvi, S. M., Xing, X., Xing, E., Plazyo, O., Zeng, C., Patrick, M. T., Lowe, M. M., Burney, R. E., Kozlow, J. H., Cherry-Bukowiec, J. R., Jiang, Y., Kirma, J., Weidinger, S., Cushing, K. C., Rosenblum, M. D., Berthier, C., MacLeod, A. S., Voorhees, J. J., Wen, F., Kahlenberg, J. M., Maverakis, E., Modlin, R. L. and Prens, E. P. (2020) 'Contribution of plasma cells and B cells to hidradenitis suppurativa pathogenesis', *JCI Insight,* 5(19).10.1172/jci.insight.139930

Guet-Revillet, H., Coignard-Biehler, H., Jais, J. P., Quesne, G., Frapy, E., Poirée, S., Le Guern, A. S., Le Flèche-Matéos, A., Hovnanian, A., Consigny, P. H., Lortholary, O., Nassif, X., Nassif, A. and Join-Lambert, O. (2014) 'Bacterial pathogens associated with hidradenitis suppurativa, France', *Emerg Infect Dis,* 20(12), pp. 1990-8.10.3201/eid2012.140064

Gulen, M. F., Kang, Z., Bulek, K., Youzhong, W., Kim, T. W., Chen, Y., Altuntas, C. Z., Sass Bak-Jensen, K., McGeachy, M. J., Do, J. S., Xiao, H., Delgoffe, G. M., Min, B., Powell, J. D., Tuohy, V. K., Cua, D. J. and Li, X. (2010) 'The receptor SIGIRR suppresses Th17 cell proliferation via inhibition of the interleukin-1 receptor pathway and mTOR kinase activation', *Immunity,* 32(1), pp. 54-66.10.1016/j.immuni.2009.12.003

Guo, H., Wang, M., Wang, B., Guo, L., Cheng, Y., Wang, Z., Sun, Y. Q., Wang, Y., Chang, Y. J. and Huang, X. J. (2022) 'PRDM1 Drives Human Primary T Cell Hyporesponsiveness by Altering the T Cell Transcriptome and Epigenome', *Front Immunol,* 13, pp. 879501.10.3389/fimmu.2022.879501

Gupta, R. K., Gracias, D. T., Figueroa, D. S., Miki, H., Miller, J., Fung, K., Ay, F., Burkly, L. and Croft, M. (2021) 'TWEAK functions with TNF and IL-17 on keratinocytes and is a potential target for psoriasis therapy', *Sci Immunol,* 6(65), pp. eabi8823.10.1126/sciimmunol.abi8823

Guttman-Yassky, E. and Krueger, J. G. (2018) 'IL-17C: A Unique Epithelial Cytokine with Potential for Targeting across the Spectrum of Atopic Dermatitis and Psoriasis', *J Invest Dermatol,* 138(7), pp. 1467-1469.10.1016/j.jid.2018.02.037

Hafemeister, C. and Satija, R. (2019) 'Normalization and variance stabilization of single-cell RNA-seq data using regularized negative binomial regression', *Genome Biol,* 20(1), pp. 296.10.1186/s13059-019-1874-1

Hambly, R., Gatault, S., Smith, C. M., Iglesias-Martinez, L. F., Kearns, S., Rea, H., Marasigan, V., Lynam-Loane, K., Kirthi, S., Hughes, R., Fletcher, J. M., Kolch, W. and Kirby, B. (2023) 'B-cell and complement signature in severe hidradenitis suppurativa that does not respond to adalimumab', *Br J Dermatol,* 188(1), pp. 52-63.10.1093/bjd/ljac007

Han, L., Chen, S., Chen, Z., Zhou, B., Zheng, Y. and Shen, L. (2021) 'Interleukin 32 Promotes Foxp3', *Front Cell Dev Biol,* 9, pp. 704853.10.3389/fcell.2021.704853

Hana, A., Booken, D., Henrich, C., Gratchev, A., Maas-Szabowski, N., Goerdt, S. and Kurzen, H. (2007) 'Functional significance of non-neuronal acetylcholine in skin epithelia', *Life Sci,* 80(24-25), pp. 2214-20.10.1016/j.lfs.2007.02.007

Haniffa, M., Gunawan, M. and Jardine, L. (2015) 'Human skin dendritic cells in health and disease', *J Dermatol Sci,* 77(2), pp. 85-92.10.1016/j.jdermsci.2014.08.012

He, H., Suryawanshi, H., Morozov, P., Gay-Mimbrera, J., Del Duca, E., Kim, H. J., Kameyama, N., Estrada, Y., Der, E., Krueger, J. G., Ruano, J., Tuschl, T. and Guttman-Yassky, E. (2020) 'Single-cell transcriptome analysis of human skin identifies novel fibroblast subpopulation and enrichment of immune subsets in atopic dermatitis', *J Allergy Clin Immunol*.10.1016/j.jaci.2020.01.042

Henri, S., Poulin, L. F., Tamoutounour, S., Ardouin, L., Guilliams, M., de Bovis, B., Devilard, E., Viret, C., Azukizawa, H., Kissenpfennig, A. and Malissen, B. (2010) 'CD207+ CD103+ dermal dendritic cells cross-present keratinocyte-derived antigens irrespective of the presence of Langerhans cells', *J Exp Med,* 207(1), pp. 189-206.10.1084/jem.20091964

Hessam, S., Sand, M., Lang, K., Käfferlein, H. U., Scholl, L., Gambichler, T., Skrygan, M., Brüning, T., Stockfleth, E. and Bechara, F. G. (2017) 'Altered Global 5-Hydroxymethylation Status in Hidradenitis Suppurativa: Support for an Epigenetic Background', *Dermatology,* 233(2-3), pp. 129-135.10.1159/000478043

Ho, C. H., Silva, A. A., Tomita, B., Weng, H. Y. and Ho, I. C. (2021) 'Differential impacts of TNFα inhibitors on the transcriptome of Th cells', *Arthritis Res Ther,* 23(1), pp. 199.10.1186/s13075-021-02558-z

Hoffman, H. M., Mueller, J. L., Broide, D. H., Wanderer, A. A. and Kolodner, R. D. (2001) 'Mutation of a new gene encoding a putative pyrin-like protein causes familial cold autoinflammatory syndrome and Muckle-Wells syndrome', *Nat Genet,* 29(3), pp. 301-5.10.1038/ng756

Hoffman, L. K., Ghias, M. H. and Lowes, M. A. (2017) 'Pathophysiology of hidradenitis suppurativa', *Semin Cutan Med Surg,* 36(2), pp. 47-54.10.12788/j.sder.2017.017

Homey, B., Alenius, H., Müller, A., Soto, H., Bowman, E. P., Yuan, W., McEvoy, L., Lauerma, A. I., Assmann, T., Bünemann, E., Lehto, M., Wolff, H., Yen, D., Marxhausen, H., To, W., Sedgwick, J., Ruzicka, T., Lehmann, P. and Zlotnik, A. (2002) 'CCL27-CCR10 interactions regulate T cell-mediated skin inflammation', *Nat Med,* 8(2), pp. 157-65.10.1038/nm0202-157

Honardoust, D., Varkey, M., Marcoux, Y., Shankowsky, H. A. and Tredget, E. E. (2012) 'Reduced decorin, fibromodulin, and transforming growth factor-β3 in deep dermis leads to hypertrophic scarring', *J Burn Care Res,* 33(2), pp. 218-27.10.1097/BCR.0b013e3182335980

Hornum, L., Hansen, A. J., Tornehave, D., Fjording, M. S., Colmenero, P., Wätjen, I. F., Søe Nielsen, N. H., Bliddal, H. and Bartels, E. M. (2017) 'C5a and C5aR are elevated in joints of rheumatoid and psoriatic arthritis patients, and C5aR blockade attenuates leukocyte migration to synovial fluid', *PLoS One,* 12(12), pp. e0189017.10.1371/journal.pone.0189017

Horváth, B., Janse, I. C., Blok, J. L., Driessen, R. J., Boer, J., Mekkes, J. R., Prens, E. P. and van der Zee, H. H. (2017) 'Hurley Staging Refined: A Proposal by the Dutch Hidradenitis Suppurativa Expert Group', *Acta Derm Venereol,* 97(3), pp. 412-413.10.2340/00015555-2513

Hotz, C., Boniotto, M., Guguin, A., Surenaud, M., Jean-Louis, F., Tisserand, P., Ortonne, N., Hersant, B., Bosc, R., Poli, F., Bonnabau, H., Thiebaut, R., Godot, V., Wolkenstein, P., Hocini, H., Levy, Y. and Hue, S. (2016) 'Intrinsic Defect in Keratinocyte Function Leads to Inflammation in Hidradenitis Suppurativa', *J Invest Dermatol,* 136(9), pp. 1768-1780.10.1016/j.jid.2016.04.036

Houriet, C., Seyed Jafari, S. M., Thomi, R., Schlapbach, C., Borradori, L., Yawalkar, N. and Hunger, R. E. (2017) 'Canakinumab for Severe Hidradenitis Suppurativa: Preliminary Experience in 2 Cases', *JAMA Dermatol,* 153(11), pp. 1195-1197.10.1001/jamadermatol.2017.2392

Hu, X., Chakravarty, S. D. and Ivashkiv, L. B. (2008) 'Regulation of interferon and Toll-like receptor signaling during macrophage activation by opposing feedforward and feedback inhibition mechanisms', *Immunol Rev,* 226, pp. 41-56.10.1111/j.1600-065X.2008.00707.x

Huang, Y., Tang, J., Cai, Z., Zhou, K., Chang, L., Bai, Y. and Ma, Y. (2020) 'Induces the Production of Th17 Cells in the Colon of Mice', *J Immunol Res,* 2020, pp. 9607328.10.1155/2020/9607328

Hunger, R. E., Surovy, A. M., Hassan, A. S., Braathen, L. R. and Yawalkar, N. (2008) 'Toll-like receptor 2 is highly expressed in lesions of acne inversa and colocalizes with C-type lectin receptor', *Br J Dermatol,* 158(4), pp. 691-7.10.1111/j.1365-2133.2007.08425.x

Huse, K., Bai, B., Hilden, V. I., Bollum, L. K., Våtsveen, T. K., Munthe, L. A., Smeland, E. B., Irish, J. M., Wälchli, S. and Myklebust, J. H. (2022) 'Mechanism of CD79A and CD79B Support for IgM+ B Cell Fitness through B Cell Receptor Surface Expression', *J Immunol,* 209(10), pp. 2042-2053.10.4049/jimmunol.2200144

Jang, S., Park, J. S., Won, Y. H., Yun, S. J. and Kim, S. J. (2012) 'The Expression of Toll-Like Receptors (TLRs) in Cultured Human Skin Fibroblast is Modulated by Histamine', *Chonnam Med J,* 48(1), pp. 7-14.10.4068/cmj.2012.48.1.7

Jarosch, S., Köhlen, J., Wagner, S., D'Ippolito, E. and Busch, D. H. (2022) 'ChipCytometry for multiplexed detection of protein and mRNA markers on human FFPE tissue samples', *STAR Protoc,* 3(2), pp. 101374.10.1016/j.xpro.2022.101374

Jemec, G. B. (2012) 'Clinical practice. Hidradenitis suppurativa', *N Engl J Med,* 366(2), pp. 158-64.10.1056/NEJMcp1014163

Jennings, L., Hambly, R., Hughes, R., Moriarty, B. and Kirby, B. (2020) 'Metformin use in hidradenitis suppurativa', *J Dermatolog Treat,* 31(3), pp. 261-263.10.1080/09546634.2019.1592100

Jepsen, R., Edwards, C., Flora, A., Kozera, E. and Frew, J. W. (2023) 'A proof-of-concept open-label clinical trial of spleen tyrosine kinase antagonism using fostamatinib in moderate-to-severe hidradenitis suppurativa', *J Am Acad Dermatol,* 89(4), pp. 694-702.10.1016/j.jaad.2023.05.076

Jiang, D. and Rinkevich, Y. (2020) 'Scars or Regeneration?-Dermal Fibroblasts as Drivers of Diverse Skin Wound Responses', *Int J Mol Sci,* 21(2).10.3390/ijms21020617

Jimenez-Dalmaroni, M. J., Xiao, N., Corper, A. L., Verdino, P., Ainge, G. D., Larsen, D. S., Painter, G. F., Rudd, P. M., Dwek, R. A., Hoebe, K., Beutler, B. and Wilson, I. A. (2009) 'Soluble CD36 ectodomain binds negatively charged diacylglycerol ligands and acts as a co-receptor for TLR2', *PLoS One,* 4(10), pp. e7411.10.1371/journal.pone.0007411

Jo, E. K., Kim, J. K., Shin, D. M. and Sasakawa, C. (2016) 'Molecular mechanisms regulating NLRP3 inflammasome activation', *Cell Mol Immunol,* 13(2), pp. 148-59.10.1038/cmi.2015.95

Jones, A., Ciurtin, C., Ismajli, M., Leandro, M., Sengupta, R. and Machado, P. M. (2018) 'Biologics for treating axial spondyloarthritis', *Expert Opin Biol Ther,* 18(6), pp. 641-652.10.1080/14712598.2018.1468884

Jongbloed, S. L., Kassianos, A. J., McDonald, K. J., Clark, G. J., Ju, X., Angel, C. E., Chen, C. J., Dunbar, P. R., Wadley, R. B., Jeet, V., Vulink, A. J., Hart, D. N. and Radford, K. J. (2010) 'Human CD141+ (BDCA-3)+ dendritic cells (DCs) represent a unique myeloid DC subset that cross-presents necrotic cell antigens', *J Exp Med,* 207(6), pp. 1247-60.10.1084/jem.20092140

Kahaly, G. J., Stan, M. N., Frommer, L., Gergely, P., Colin, L., Amer, A., Schuhmann, I., Espie, P., Rush, J. S., Basson, C. and He, Y. (2020) 'A Novel Anti-CD40 Monoclonal Antibody, Iscalimab, for Control of Graves Hyperthyroidism-A Proof-of-Concept Trial', *J Clin Endocrinol Metab,* 105(3).10.1210/clinem/dgz013

Kahl, C. R. and Means, A. R. (2003) 'Regulation of cell cycle progression by calcium/calmodulin-dependent pathways', *Endocr Rev,* 24(6), pp. 719-36.10.1210/er.2003-0008

Kanni, T., Tzanetakou, V., Savva, A., Kersten, B., Pistiki, A., van de Veerdonk, F. L., Netea, M. G., van der Meer, J. W. and Giamarellos-Bourboulis, E. J. (2015) 'Compartmentalized Cytokine Responses in Hidradenitis Suppurativa', *PLoS One,* 10(6), pp. e0130522.10.1371/journal.pone.0130522

Karmakar, M., Katsnelson, M. A., Dubyak, G. R. and Pearlman, E. (2016) 'Neutrophil P2X7 receptors mediate NLRP3 inflammasome-dependent IL-1β secretion in response to ATP', *Nat Commun,* 7, pp. 10555.10.1038/ncomms10555

Kashem, S. W., Haniffa, M. and Kaplan, D. H. (2017) 'Antigen-Presenting Cells in the Skin', *Annu Rev Immunol,* 35, pp. 469-499.10.1146/annurev-immunol-051116-052215

Katsanos, K. H., Christodoulou, D. K. and Tsianos, E. V. (2002) 'Axillary hidradenitis suppurativa successfully treated with infliximab in a Crohn's disease patient', *Am J Gastroenterol,* 97(8), pp. 2155-6.10.1111/j.1572-0241.2002.05950.x

Kearney, N., Hughes, R. and Kirby, B. (2023) 'Treatment of hidradenitis suppurativa with brodalumab in biologic treatment failures: experiences from a specialty clinic', *Clin Exp Dermatol,* 48(7), pp. 790-792.10.1093/ced/llad130

Kearney, N., McCourt, C., Hambly, R., Hughes, R., O'Kane, D. and Kirby, B. (2023) 'Association of Biologic Treatment in Hidradenitis Suppurativa With Reduced Neutrophil-Lymphocyte Ratio and Platelet-Lymphocyte Ratio', *JAMA Dermatol,* 159(2), pp. 222-224.10.1001/jamadermatol.2022.5710

Keary, E., Hevey, D. and Tobin, A. M. (2020) 'A qualitative analysis of psychological distress in hidradenitis suppurativa', *Br J Dermatol,* 182(2), pp. 342-347.10.1111/bjd.18135

Kelly, G., Hughes, R., McGarry, T., van den Born, M., Adamzik, K., Fitzgerald, R., Lawlor, C., Tobin, A. M., Sweeney, C. M. and Kirby, B. (2015) 'Dysregulated cytokine expression in lesional and nonlesional skin in hidradenitis suppurativa', *Br J Dermatol,* 173(6), pp. 1431-9.10.1111/bjd.14075

Kelly, M. E., Heneghan, H. M., McDermott, F. D., Nason, G. J., Freeman, C., Martin, S. T. and Winter, D. C. (2014) 'The role of loose seton in the management of anal fistula: a multicenter study of 200 patients', *Tech Coloproctol,* 18(10), pp. 915-9.10.1007/s10151-014-1186-0

Kim, J., Lee, J., Li, X., Lee, H. S., Kim, K., Chaparala, V., Murphy, W., Zhou, W., Cao, J., Lowes, M. A. and Krueger, J. G. (2023) 'Single-cell transcriptomics suggest distinct upstream drivers of IL-17A/F in hidradenitis versus psoriasis', *J Allergy Clin Immunol,* 152(3), pp. 656-666.10.1016/j.jaci.2023.05.012

Kim, J. W. and Kim, S. Y. (2021) 'The Era of Janus Kinase Inhibitors for Inflammatory Bowel Disease Treatment', *Int J Mol Sci,* 22(21).10.3390/ijms222111322

Kimball, A. B., Jemec, G. B., Yang, M., Kageleiry, A., Signorovitch, J. E., Okun, M. M., Gu, Y., Wang, K., Mulani, P. and Sundaram, M. (2014) 'Assessing the validity, responsiveness and meaningfulness of the Hidradenitis Suppurativa Clinical Response (HiSCR) as the clinical endpoint for hidradenitis suppurativa treatment', *Br J Dermatol,* 171(6), pp. 1434-42.10.1111/bjd.13270

Kimball, A. B., Jemec, G. B. E., Alavi, A., Reguiai, Z., Gottlieb, A. B., Bechara, F. G., Paul, C., Giamarellos Bourboulis, E. J., Villani, A. P., Schwinn, A., Ruëff, F., Pillay Ramaya, L., Reich, A., Lobo, I., Sinclair, R., Passeron, T., Martorell, A., Mendes-Bastos, P., Kokolakis, G., Becherel, P. A., Wozniak, M. B., Martinez, A. L., Wei, X., Uhlmann, L., Passera, A., Keefe, D., Martin, R., Field, C., Chen, L., Vandemeulebroecke, M., Ravichandran, S. and Muscianisi, E. (2023a) 'Secukinumab in moderate-to-severe hidradenitis suppurativa (SUNSHINE and SUNRISE): week 16 and week 52 results of two identical, multicentre, randomised, placebo-controlled, double-blind phase 3 trials', *Lancet*.10.1016/S0140-6736(23)00022-3

Kimball, A. B., Kerdel, F., Adams, D., Mrowietz, U., Gelfand, J. M., Gniadecki, R., Prens, E. P., Schlessinger, J., Zouboulis, C. C., van der Zee, H. H., Rosenfeld, M., Mulani, P., Gu, Y., Paulson, S., Okun, M. and Jemec, G. B. (2012) 'Adalimumab for the treatment of moderate to severe Hidradenitis suppurativa: a parallel randomized trial', *Ann Intern Med,* 157(12), pp. 846-55.10.7326/0003-4819-157-12-201212180-00004

Kimball, A. B., Okun, M. M., Williams, D. A., Gottlieb, A. B., Papp, K. A., Zouboulis, C. C., Armstrong, A. W., Kerdel, F., Gold, M. H., Forman, S. B., Korman, N. J., Giamarellos-Bourboulis, E. J., Crowley, J. J., Lynde, C., Reguiai, Z., Prens, E. P., Alwawi, E., Mostafa, N. M., Pinsky, B., Sundaram, M., Gu, Y., Carlson, D. M. and Jemec, G. B. (2016) 'Two Phase 3 Trials of Adalimumab for Hidradenitis Suppurativa', *N Engl J Med,* 375(5), pp. 422-34.10.1056/NEJMoa1504370

Kimball, A. B., Prens, E. P., Passeron, T., Maverakis, E., Turchin, I., Beeck, S., Drogaris, L., Geng, Z., Zhan, T., Messina, I. and Bechara, F. G. (2023b) 'Efficacy and Safety of Risankizumab for the Treatment of Hidradenitis Suppurativa: A Phase 2, Randomized, Placebo-Controlled Trial', *Dermatol Ther (Heidelb),* 13(5), pp. 1099-1111.10.1007/s13555-023-00913-3

Kirby, J. S. (2021) 'Unraveling the Heterogeneity of Hidradenitis Suppurativa with Phenotype Schema', *J Invest Dermatol,* 141(5), pp. 1136-1138.10.1016/j.jid.2020.10.014

Kirk, T., Ahmed, A. and Rognoni, E. (2021) 'Fibroblast Memory in Development, Homeostasis and Disease', *Cells,* 10(11).10.3390/cells10112840

Klint, S., Feldwisch, J., Gudmundsdotter, L., Dillner Bergstedt, K., Gunneriusson, E., Höidén Guthenberg, I., Wennborg, A., Nyborg, A. C., Kamboj, A. P., Peloso, P. M., Bejker, D. and Frejd, F. Y. (2023) 'Izokibep: Preclinical development and first-in-human study of a novel IL-17A neutralizing Affibody molecule in patients with plaque psoriasis', *MAbs,* 15(1), pp. 2209920.10.1080/19420862.2023.2209920

Klück, V., Jansen, T. L. T. A., Janssen, M., Comarniceanu, A., Efdé, M., Tengesdal, I. W., Schraa, K., Cleophas, M. C. P., Scribner, C. L., Skouras, D. B., Marchetti, C., Dinarello, C. A. and Joosten, L. A. B. (2020) 'Dapansutrile, an oral selective NLRP3 inflammasome inhibitor, for treatment of gout flares: an open-label, dose-adaptive, proof-of-concept, phase 2a trial', *Lancet Rheumatol,* 2(5), pp. e270-e280.10.1016/s2665-9913(20)30065-5

Kokolakis, G., Wolk, K., Schneider-Burrus, S., Kalus, S., Barbus, S., Gomis-Kleindienst, S. and Sabat, R. (2020) 'Delayed Diagnosis of Hidradenitis Suppurativa and Its Effect on Patients and Healthcare System', *Dermatology,* 236(5), pp. 421-430.10.1159/000508787

Kornete, M., Sgouroudis, E. and Piccirillo, C. A. (2012) 'ICOS-dependent homeostasis and function of Foxp3+ regulatory T cells in islets of nonobese diabetic mice', *J Immunol,* 188(3), pp. 1064-74.10.4049/jimmunol.1101303

Korsunsky, I., Millard, N., Fan, J., Slowikowski, K., Zhang, F., Wei, K., Baglaenko, Y., Brenner, M., Loh, P. R. and Raychaudhuri, S. (2019) 'Fast, sensitive and accurate integration of single-cell data with Harmony', *Nat Methods,* 16(12), pp. 1289-1296.10.1038/s41592-019-0619-0

Kozera, E., Flora, A. and Frew, J. W. (2022) 'Real-world safety and clinical response of Janus kinase inhibitor upadacitinib in the treatment of hidradenitis suppurativa: A retrospective cohort study', *J Am Acad Dermatol,* 87(6), pp. 1440-1442.10.1016/j.jaad.2022.07.047

Krakowski, A. C., Admani, S., Uebelhoer, N. S., Eichenfield, L. F. and Shumaker, P. R. (2014) 'Residual scarring from hidradenitis suppurativa: fractionated CO2 laser as a novel and noninvasive approach', *Pediatrics,* 133(1), pp. e248-51.10.1542/peds.2012-3356

Kromann, C. B., Ibler, K. S., Kristiansen, V. B. and Jemec, G. B. (2014) 'The influence of body weight on the prevalence and severity of hidradenitis suppurativa', *Acta Derm Venereol,* 94(5), pp. 553-7.10.2340/00015555-1800

Kryczek, I., Zhao, E., Liu, Y., Wang, Y., Vatan, L., Szeliga, W., Moyer, J., Klimczak, A., Lange, A. and Zou, W. (2011) 'Human TH17 cells are long-lived effector memory cells', *Sci Transl Med,* 3(104), pp. 104ra100.10.1126/scitranslmed.3002949

Kubo, A., Ishizaki, I., Kawasaki, H., Nagao, K., Ohashi, Y. and Amagai, M. (2013) 'The stratum corneum comprises three layers with distinct metal-ion barrier properties', *Sci Rep,* 3, pp. 1731.10.1038/srep01731

Kubota, K., Moriyama, M., Furukawa, S., Rafiul, H. A. S. M., Maruse, Y., Jinno, T., Tanaka, A., Ohta, M., Ishiguro, N., Yamauchi, M., Sakamoto, M., Maehara, T., Hayashida, J. N., Kawano, S., Kiyoshima, T. and Nakamura, S. (2017) 'CD163', *Sci Rep,* 7(1), pp. 1755.10.1038/s41598-017-01661-z

Kupper, T. S. and Groves, R. W. (1995) 'The interleukin-1 axis and cutaneous inflammation', *J Invest Dermatol,* 105(1 Suppl), pp. 62S-66S.10.1111/1523-1747.ep12316087

Kurihara, K., Fujiyama, T., Phadungsaksawasdi, P., Ito, T. and Tokura, Y. (2019) 'Significance of IL-17A-producing CD8', *J Dermatol Sci,* 95(1), pp. 21-27.10.1016/j.jdermsci.2019.06.002

Kurokawa, I., Nishijima, S., Kusumoto, K., Senzaki, H., Shikata, N. and Tsubura, A. (2002) 'Immunohistochemical study of cytokeratins in hidradenitis suppurativa (acne inversa)', *J Int Med Res,* 30(2), pp. 131-6.10.1177/147323000203000205

Lajevardi, S. S. and Abeysinghe, J. (2015) 'Novel Technique for Management of Axillary Hidradenitis Suppurativa Using Setons', *Case Rep Surg,* 2015, pp. 369657.10.1155/2015/369657

Lalor, S. J., Dungan, L. S., Sutton, C. E., Basdeo, S. A., Fletcher, J. M. and Mills, K. H. (2011) 'Caspase-1-processed cytokines IL-1beta and IL-18 promote IL-17 production by gammadelta and CD4 T cells that mediate autoimmunity', *J Immunol,* 186(10), pp. 5738-48.10.4049/jimmunol.1003597

Lande, R., Ganguly, D., Facchinetti, V., Frasca, L., Conrad, C., Gregorio, J., Meller, S., Chamilos, G., Sebasigari, R., Riccieri, V., Bassett, R., Amuro, H., Fukuhara, S., Ito, T., Liu, Y. J. and Gilliet, M. (2011) 'Neutrophils activate plasmacytoid dendritic cells by releasing self-DNA-peptide complexes in systemic lupus erythematosus', *Sci Transl Med,* 3(73), pp. 73ra19.10.1126/scitranslmed.3001180

Langfelder, P. and Horvath, S. (2008) 'WGCNA: an R package for weighted correlation network analysis', *BMC Bioinformatics,* 9, pp. 559.10.1186/1471-2105-9-559

Langley, R. G., Elewski, B. E., Lebwohl, M., Reich, K., Griffiths, C. E., Papp, K., Puig, L., Nakagawa, H., Spelman, L., Sigurgeirsson, B., Rivas, E., Tsai, T. F., Wasel, N., Tyring, S., Salko, T., Hampele, I., Notter, M., Karpov, A., Helou, S., Papavassilis, C., Group, E. S. and Group, F. S. (2014) 'Secukinumab in plaque psoriasis--results of two phase 3 trials', *N Engl J Med,* 371(4), pp. 326-38.10.1056/NEJMoa1314258

Latz, E., Xiao, T. S. and Stutz, A. (2013) 'Activation and regulation of the inflammasomes', *Nat Rev Immunol,* 13(6), pp. 397-411.10.1038/nri3452

Leal Rojas, I. M., Mok, W. H., Pearson, F. E., Minoda, Y., Kenna, T. J., Barnard, R. T. and Radford, K. J. (2017) 'Human Blood CD1c', *Front Immunol,* 8, pp. 971.10.3389/fimmu.2017.00971

Lee, K. H., Lee, C. H., Jeong, J., Jang, A. H. and Yoo, C. G. (2015) 'Neutrophil Elastase Differentially Regulates Interleukin 8 (IL-8) and Vascular Endothelial Growth Factor (VEGF) Production by Cigarette Smoke Extract', *J Biol Chem,* 290(47), pp. 28438-28445.10.1074/jbc.M115.663567

Leffler, J., Martin, M., Gullstrand, B., Tydén, H., Lood, C., Truedsson, L., Bengtsson, A. A. and Blom, A. M. (2012) 'Neutrophil extracellular traps that are not degraded in systemic lupus erythematosus activate complement exacerbating the disease', *J Immunol,* 188(7), pp. 3522-31.10.4049/jimmunol.1102404

Leslie, K. S., Tripathi, S. V., Nguyen, T. V., Pauli, M. and Rosenblum, M. D. (2014) 'An open-label study of anakinra for the treatment of moderate to severe hidradenitis suppurativa', *J Am Acad Dermatol,* 70(2), pp. 243-51.10.1016/j.jaad.2013.09.044

Lexberg, M. H., Taubner, A., Albrecht, I., Lepenies, I., Richter, A., Kamradt, T., Radbruch, A. and Chang, H. D. (2010) 'IFN-γ and IL-12 synergize to convert in vivo generated Th17 into Th1/Th17 cells', *Eur J Immunol,* 40(11), pp. 3017-27.10.1002/eji.201040539

Li, N., Yamasaki, K., Saito, R., Fukushi-Takahashi, S., Shimada-Omori, R., Asano, M. and Aiba, S. (2014) 'Alarmin function of cathelicidin antimicrobial peptide LL37 through IL-36γ induction in human epidermal keratinocytes', *J Immunol,* 193(10), pp. 5140-8.10.4049/jimmunol.1302574

Li, T., Wen, H., Brayton, C., Das, P., Smithson, L. A., Fauq, A., Fan, X., Crain, B. J., Price, D. L., Golde, T. E., Eberhart, C. G. and Wong, P. C. (2007) 'Epidermal growth factor receptor and notch pathways participate in the tumor suppressor function of gamma-secretase', *J Biol Chem,* 282(44), pp. 32264-73.10.1074/jbc.M703649200

Liao, Y., Smyth, G. K. and Shi, W. (2019) 'The R package Rsubread is easier, faster, cheaper and better for alignment and quantification of RNA sequencing reads', *Nucleic Acids Res,* 47(8), pp. e47.10.1093/nar/gkz114

Lima, A. L., Karl, I., Giner, T., Poppe, H., Schmidt, M., Presser, D., Goebeler, M. and Bauer, B. (2016) 'Keratinocytes and neutrophils are important sources of proinflammatory molecules in hidradenitis suppurativa', *Br J Dermatol,* 174(3), pp. 514-21.10.1111/bjd.14214

List, E. K., Pascual, J. C., Zarchi, K., Nurnberg, B. M. and Jemec, G. B. E. (2019) 'Mast cells in hidradenitis suppurativa: a clinicopathological study', *Arch Dermatol Res,* 311(4), pp. 331-335.10.1007/s00403-019-01910-3

Liu, F. L., Chen, C. H., Chu, S. J., Chen, J. H., Lai, J. H., Sytwu, H. K. and Chang, D. M. (2007) 'Interleukin (IL)-23 p19 expression induced by IL-1beta in human fibroblast-like synoviocytes with rheumatoid arthritis via active nuclear factor-kappaB and AP-1 dependent pathway', *Rheumatology (Oxford),* 46(8), pp. 1266-73.10.1093/rheumatology/kem055

Liu, J., Zhang, X., Cheng, Y. and Cao, X. (2021) 'Dendritic cell migration in inflammation and immunity', *Cell Mol Immunol,* 18(11), pp. 2461-2471.10.1038/s41423-021-00726-4

Liu, Y., Li, Y., Li, N., Teng, W., Wang, M., Zhang, Y. and Xiao, Z. (2016) 'TGF-β1 promotes scar fibroblasts proliferation and transdifferentiation via up-regulating MicroRNA-21', *Sci Rep,* 6, pp. 32231.10.1038/srep32231

Lonnemann, N., Hosseini, S., Marchetti, C., Skouras, D. B., Stefanoni, D., D'Alessandro, A., Dinarello, C. A. and Korte, M. (2020) 'The NLRP3 inflammasome inhibitor OLT1177 rescues cognitive impairment in a mouse model of Alzheimer's disease', *Proc Natl Acad Sci U S A,* 117(50), pp. 32145-32154.10.1073/pnas.2009680117

Love, M. I., Huber, W. and Anders, S. (2014) 'Moderated estimation of fold change and dispersion for RNA-seq data with DESeq2', *Genome Biol,* 15(12), pp. 550.10.1186/s13059-014-0550-8

Lowe, M. M., Naik, H. B., Clancy, S., Pauli, M., Smith, K. M., Bi, Y., Dunstan, R., Gudjonsson, J. E., Paul, M., Harris, H., Kim, E., Shin, U. S., Ahn, R., Liao, W., Hansen, S. L. and Rosenblum, M. D. (2020) 'Immunopathogenesis of hidradenitis suppurativa and response to anti-TNF-alpha therapy', *JCI Insight,* 5(19).10.1172/jci.insight.139932

Lun, A. T. L., Riesenfeld, S., Andrews, T., Dao, T. P., Gomes, T., participants in the 1st Human Cell Atlas, J. and Marioni, J. C. (2019) 'EmptyDrops: distinguishing cells from empty droplets in droplet-based single-cell RNA sequencing data', *Genome Biol,* 20(1), pp. 63.10.1186/s13059-019-1662-y

Lynch, L., Nowak, M., Varghese, B., Clark, J., Hogan, A. E., Toxavidis, V., Balk, S. P., O'Shea, D., O'Farrelly, C. and Exley, M. A. (2012) 'Adipose tissue invariant NKT cells protect against diet-induced obesity and metabolic disorder through regulatory cytokine production', *Immunity,* 37(3), pp. 574-87.10.1016/j.immuni.2012.06.016

Ma, W. Y., Jia, K. and Zhang, Y. (2016) 'IL-17 promotes keratinocyte proliferation via the downregulation of C/EBPα', *Exp Ther Med,* 11(2), pp. 631-636.10.3892/etm.2015.2939

Madison, K. C. (2003) 'Barrier function of the skin: "la raison d'être" of the epidermis', *J Invest Dermatol,* 121(2), pp. 231-41.10.1046/j.1523-1747.2003.12359.x

Maeda, S., Osaga, S., Maeda, T., Takeda, N., Tamechika, S. Y., Naniwa, T. and Niimi, A. (2019) 'Circulating Th17.1 cells as candidate for the prediction of therapeutic response to abatacept in patients with rheumatoid arthritis: An exploratory research', *PLoS One,* 14(11), pp. e0215192.10.1371/journal.pone.0215192

Maeda, Y., Kurakawa, T., Umemoto, E., Motooka, D., Ito, Y., Gotoh, K., Hirota, K., Matsushita, M., Furuta, Y., Narazaki, M., Sakaguchi, N., Kayama, H., Nakamura, S., Iida, T., Saeki, Y., Kumanogoh, A., Sakaguchi, S. and Takeda, K. (2016) 'Dysbiosis Contributes to Arthritis Development via Activation of Autoreactive T Cells in the Intestine', *Arthritis Rheumatol,* 68(11), pp. 2646-2661.10.1002/art.39783

Malara, A., Hughes, R., Jennings, L., Sweeney, C. M., Lynch, M., Awdeh, F., Timoney, I., Tobin, A. M., Lynam-Loane, K., Tobin, L., Hogan, A., O'Shea, D. and Kirby, B. (2018) 'Adipokines are dysregulated in patients with hidradenitis suppurativa', *Br J Dermatol,* 178(3), pp. 792-793.10.1111/bjd.15904

Malissen, B., Tamoutounour, S. and Henri, S. (2014) 'The origins and functions of dendritic cells and macrophages in the skin', *Nat Rev Immunol,* 14(6), pp. 417-28.10.1038/nri3683

Manel, N., Unutmaz, D. and Littman, D. R. (2008) 'The differentiation of human T(H)-17 cells requires transforming growth factor-beta and induction of the nuclear receptor RORgammat', *Nat Immunol,* 9(6), pp. 641-9.10.1038/ni.1610

Mangan, P. R., Harrington, L. E., O'Quinn, D. B., Helms, W. S., Bullard, D. C., Elson, C. O., Hatton, R. D., Wahl, S. M., Schoeb, T. R. and Weaver, C. T. (2006) 'Transforming growth factor-beta induces development of the T(H)17 lineage', *Nature,* 441(7090), pp. 231-4.10.1038/nature04754

Mariottoni, P., Jiang, S. W., Prestwood, C. A., Jain, V., Suwanpradid, J., Whitley, M. J., Coates, M., Brown, D. A., Erdmann, D., Corcoran, D. L., Gregory, S. G., Jaleel, T., Zhang, J. Y., Harris-Tryon, T. A. and MacLeod, A. S. (2021) 'Single-Cell RNA Sequencing Reveals Cellular and Transcriptional Changes Associated With M1 Macrophage Polarization in Hidradenitis Suppurativa', *Front Med (Lausanne),* 8, pp. 665873.10.3389/fmed.2021.665873

Martínez, F., Nos, P., Benlloch, S. and Ponce, J. (2001) 'Hidradenitis suppurativa and Crohn's disease: response to treatment with infliximab', *Inflamm Bowel Dis,* 7(4), pp. 323-6.10.1097/00054725-200111000-00008

Martorell, A., Garcia-Martinez, F. J., Jimenez-Gallo, D., Pascual, J. C., Pereyra-Rodriguez, J., Salgado, L. and Vilarrasa, E. (2015) 'An Update on Hidradenitis Suppurativa (Part I): Epidemiology, Clinical Aspects, and Definition of Disease Severity', *Actas Dermosifiliogr,* 106(9), pp. 703-15.10.1016/j.ad.2015.06.004

Martorell, A., Giovanardi, G., Gomez-Palencia, P. and Sanz-Motilva, V. (2019) 'Defining Fistular Patterns in Hidradenitis Suppurativa: Impact on the Management', *Dermatol Surg,* 45(10), pp. 1237-1244.10.1097/DSS.0000000000001916

Martorell, A., Jfri, A., Koster, S. B. L., Gomez-Palencia, P., Solera, M., Alfaro-Rubio, A., Hueso, L. and Sanz-Motilva, V. (2020) 'Defining hidradenitis suppurativa phenotypes based on the elementary lesion pattern: results of a prospective study', *J Eur Acad Dermatol Venereol,* 34(6), pp. 1309-1318.10.1111/jdv.16183

Mauviel, A. (2005) 'Transforming growth factor-beta: a key mediator of fibrosis', *Methods Mol Med,* 117, pp. 69-80.10.1385/1-59259-940-0:069

Maya-Mendoza, A., Moudry, P., Merchut-Maya, J. M., Lee, M., Strauss, R. and Bartek, J. (2018) 'High speed of fork progression induces DNA replication stress and genomic instability', *Nature,* 559(7713), pp. 279-284.10.1038/s41586-018-0261-5

McCarthy, S., Barrett, M., Kirthi, S., Pellanda, P., Vlckova, K., Tobin, A. M., Murphy, M., Shanahan, F. and O'Toole, P. W. (2022) 'Altered Skin and Gut Microbiome in Hidradenitis Suppurativa', *J Invest Dermatol,* 142(2), pp. 459-468.e15.10.1016/j.jid.2021.05.036

McGinley, A. M., Sutton, C. E., Edwards, S. C., Leane, C. M., DeCourcey, J., Teijeiro, A., Hamilton, J. A., Boon, L., Djouder, N. and Mills, K. H. G. (2020) 'Interleukin-17A Serves a Priming Role in Autoimmunity by Recruiting IL-1beta-Producing Myeloid Cells that Promote Pathogenic T Cells', *Immunity,* 52(2), pp. 342-356 e6.10.1016/j.immuni.2020.01.002

McGinnis, C. S., Murrow, L. M. and Gartner, Z. J. (2019) 'DoubletFinder: Doublet Detection in Single-Cell RNA Sequencing Data Using Artificial Nearest Neighbors', *Cell Syst,* 8(4), pp. 329-337 e4.10.1016/j.cels.2019.03.003

McMahan, C. J., Slack, J. L., Mosley, B., Cosman, D., Lupton, S. D., Brunton, L. L., Grubin, C. E., Wignall, J. M., Jenkins, N. A. and Brannan, C. I. (1991) 'A novel IL-1 receptor, cloned from B cells by mammalian expression, is expressed in many cell types', *EMBO J,* 10(10), pp. 2821-32.10.1002/j.1460-2075.1991.tb07831.x

Mehdizadeh, A., Hazen, P. G., Bechara, F. G., Zwingerman, N., Moazenzadeh, M., Bashash, M., Sibbald, R. G. and Alavi, A. (2015) 'Recurrence of hidradenitis suppurativa after surgical management: A systematic review and meta-analysis', *J Am Acad Dermatol,* 73(5 Suppl 1), pp. S70-7.10.1016/j.jaad.2015.07.044

Méhul, B., Bernard, D. and Schmidt, R. (2001) 'Calmodulin-like skin protein: a new marker of keratinocyte differentiation', *J Invest Dermatol,* 116(6), pp. 905-9.10.1046/j.0022-202x.2001.01376.x

Melnik, B. C. and Plewig, G. (2013) 'Impaired Notch signalling: the unifying mechanism explaining the pathogenesis of hidradenitis suppurativa (acne inversa)', *Br J Dermatol,* 168(4), pp. 876-8.10.1111/bjd.12068

Menis, D., Maroñas-Jiménez, L., Delgado-Marquez, A. M., Postigo-Llorente, C. and Vanaclocha-Sebastián, F. (2015) 'Two cases of severe hidradenitis suppurativa with failure of anakinra therapy', *Br J Dermatol,* 172(3), pp. 810-1.10.1111/bjd.13292

Metzemaekers, M., Gouwy, M. and Proost, P. (2020) 'Neutrophil chemoattractant receptors in health and disease: double-edged swords', *Cell Mol Immunol,* 17(5), pp. 433-450.10.1038/s41423-020-0412-0

Miller, I. M., Ellervik, C., Vinding, G. R., Zarchi, K., Ibler, K. S., Knudsen, K. M. and Jemec, G. B. (2014) 'Association of metabolic syndrome and hidradenitis suppurativa', *JAMA Dermatol,* 150(12), pp. 1273-80.10.1001/jamadermatol.2014.1165

Miller, I. M., McAndrew, R. J. and Hamzavi, I. (2016) 'Prevalence, Risk Factors, and Comorbidities of Hidradenitis Suppurativa', *Dermatol Clin,* 34(1), pp. 7-16.10.1016/j.det.2015.08.002

Miller, I. M., Ring, H. C., Prens, E. P., Rytgaard, H., Mogensen, U. B., Ellervik, C. and Jemec, G. B. (2016) 'Leukocyte Profile in Peripheral Blood and Neutrophil-Lymphocyte Ratio in Hidradenitis Suppurativa: A Comparative Cross-Sectional Study of 462 Cases', *Dermatology,* 232(4), pp. 511-9.10.1159/000446021

Miragaia, R. J., Gomes, T., Chomka, A., Jardine, L., Riedel, A., Hegazy, A. N., Whibley, N., Tucci, A., Chen, X., Lindeman, I., Emerton, G., Krausgruber, T., Shields, J., Haniffa, M., Powrie, F. and Teichmann, S. A. (2019) 'Single-Cell Transcriptomics of Regulatory T Cells Reveals Trajectories of Tissue Adaptation', *Immunity,* 50(2), pp. 493-504.e7.10.1016/j.immuni.2019.01.001

Mitroulis, I., Kambas, K., Chrysanthopoulou, A., Skendros, P., Apostolidou, E., Kourtzelis, I., Drosos, G. I., Boumpas, D. T. and Ritis, K. (2011) 'Neutrophil extracellular trap formation is associated with IL-1β and autophagy-related signaling in gout', *PLoS One,* 6(12), pp. e29318.10.1371/journal.pone.0029318

Miyara, M. and Sakaguchi, S. (2007) 'Natural regulatory T cells: mechanisms of suppression', *Trends Mol Med,* 13(3), pp. 108-16.10.1016/j.molmed.2007.01.003

Molinelli, E., De Simoni, E., Candelora, M., Sapigni, C., Brisigotti, V., Rizzetto, G., Offidani, A. and Simonetti, O. (2023) 'Systemic Antibiotic Therapy in Hidradenitis Suppurativa: A Review on Treatment Landscape and Current Issues', *Antibiotics (Basel),* 12(6).10.3390/antibiotics12060978

Mommers, J. M., van Rossum, M. M., van Erp, P. E. and van De Kerkhof, P. C. (2000) 'Changes in keratin 6 and keratin 10 (co-)expression in lesional and symptomless skin of spreading psoriasis', *Dermatology,* 201(1), pp. 15-20.10.1159/000018422

Montero-Vilchez, T., Pozo-Román, T., Sánchez-Velicia, L., Vega-Gutiérrez, J., Arias-Santiago, S. and Molina-Leyva, A. (2022) 'Ustekinumab in the treatment of patients with hidradenitis suppurativa: multicenter case series and systematic review', *J Dermatolog Treat,* 33(1), pp. 348-353.10.1080/09546634.2020.1755008

Moran, B., Smith, C. M., Zabarowski, A., Ryan, M., Karman, J., Dunstan, R. W., Smith, K. M., Hambly, R., Musilova, J., Petrasca, A., Fabre, A., O'Donnell, M., Hokamp, K., Mills, K. H. G., Housley, W. J., Winter, D. C., Kirby, B. and Fletcher, J. M. (2023) 'Targeting the NLRP3 inflammasome reduces inflammation in hidradenitis suppurativa skin', *Br J Dermatol,* 189(4), pp. 447-458.10.1093/bjd/ljad184

Moran, B., Sweeney, C. M., Hughes, R., Malara, A., Kirthi, S., Tobin, A. M., Kirby, B. and Fletcher, J. M. (2017) 'Hidradenitis Suppurativa Is Characterized by Dysregulation of the Th17:Treg Cell Axis, Which Is Corrected by Anti-TNF Therapy', *J Invest Dermatol,* 137(11), pp. 2389-2395.10.1016/j.jid.2017.05.033

Murphrey, M. B. M., J; Zito, P (2023) 'StatPearls'.

Murphy, A. J., Kraakman, M. J., Kammoun, H. L., Dragoljevic, D., Lee, M. K., Lawlor, K. E., Wentworth, J. M., Vasanthakumar, A., Gerlic, M., Whitehead, L. W., DiRago, L., Cengia, L., Lane, R. M., Metcalf, D., Vince, J. E., Harrison, L. C., Kallies, A., Kile, B. T., Croker, B. A., Febbraio, M. A. and Masters, S. L. (2016) 'IL-18 Production from the NLRP1 Inflammasome Prevents Obesity and Metabolic Syndrome', *Cell Metab,* 23(1), pp. 155-64.10.1016/j.cmet.2015.09.024

Murphy, K. and Weaver, C. (2017) 'Janeway's Immunobiology, 9th Edition', *Janeway's Immunobiology, 9th Edition*, pp. 1-904

Musilova, J., Moran, B., Sweeney, C. M., Malara, A., Zaborowski, A., Hughes, R., Winter, D. C., Fletcher, J. M. and Kirby, B. (2020) 'Enrichment of Plasma Cells in the Peripheral Blood and Skin of Patients with Hidradenitis Suppurativa', *J Invest Dermatol,* 140(5), pp. 1091-1094.e2.10.1016/j.jid.2019.08.453

Nathan, C. F., Murray, H. W., Wiebe, M. E. and Rubin, B. Y. (1983) 'Identification of interferon-gamma as the lymphokine that activates human macrophage oxidative metabolism and antimicrobial activity', *J Exp Med,* 158(3), pp. 670-89.10.1084/jem.158.3.670

Natsuka, M., Uehara, A., Yang, S., Echigo, S. and Takada, H. (2008) 'A polymer-type water-soluble peptidoglycan exhibited both Toll-like receptor 2- and NOD2-agonistic activities, resulting in synergistic activation of human monocytic cells', *Innate Immun,* 14(5), pp. 298-308.10.1177/1753425908096518

Navrazhina, K., Frew, J. W., Gilleaudeau, P., Sullivan-Whalen, M., Garcet, S. and Krueger, J. G. (2021a) 'Epithelialized tunnels are a source of inflammation in hidradenitis suppurativa', *J Allergy Clin Immunol*.10.1016/j.jaci.2020.12.651

Navrazhina, K., Frew, J. W., Grand, D., Williams, S. C., Hur, H., Gonzalez, J., Garcet, S. and Krueger, J. G. (2022a) 'Interleukin-17RA blockade by brodalumab decreases inflammatory pathways in hidradenitis suppurativa skin and serum', *Br J Dermatol,* 187(2), pp. 223-233.10.1111/bjd.21060

Navrazhina, K., Frew, J. W. and Krueger, J. G. (2020) 'Interleukin 17C is elevated in lesional tissue of hidradenitis suppurativa', *Br J Dermatol,* 182(4), pp. 1045-1047.10.1111/bjd.18556

Navrazhina, K., Garcet, S., Frew, J. W., Zheng, X., Coats, I., Guttman-Yassky, E. and Krueger, J. G. (2022b) 'The inflammatory proteome of hidradenitis suppurativa skin is more expansive than that of psoriasis vulgaris', *J Am Acad Dermatol,* 86(2), pp. 322-330.10.1016/j.jaad.2021.07.035

Navrazhina, K., Garcet, S., Gonzalez, J., Grand, D., Frew, J. W. and Krueger, J. G. (2021b) 'In-Depth Analysis of the Hidradenitis Suppurativa Serum Proteome Identifies Distinct Inflammatory Subtypes', *J Invest Dermatol,* 141(9), pp. 2197-2207.10.1016/j.jid.2021.02.742

Nestle, F. O., Zheng, X. G., Thompson, C. B., Turka, L. A. and Nickoloff, B. J. (1993) 'Characterization of dermal dendritic cells obtained from normal human skin reveals phenotypic and functionally distinctive subsets', *J Immunol,* 151(11), pp. 6535-45. Available at: https://www.ncbi.nlm.nih.gov/pubmed/7504023

Netea, M. G., Nold-Petry, C. A., Nold, M. F., Joosten, L. A., Opitz, B., van der Meer, J. H., van de Veerdonk, F. L., Ferwerda, G., Heinhuis, B., Devesa, I., Funk, C. J., Mason, R. J., Kullberg, B. J., Rubartelli, A., van der Meer, J. W. and Dinarello, C. A. (2009) 'Differential requirement for the activation of the inflammasome for processing and release of IL-1beta in monocytes and macrophages', *Blood,* 113(10), pp. 2324-35.10.1182/blood-2008-03-146720

Neumann, A., Björck, L. and Frick, I. M. (2020) ', an Anaerobic Gram-Positive Bacterium of the Normal Human Microbiota, Induces Inflammation by Activating Neutrophils', *Front Microbiol,* 11, pp. 65.10.3389/fmicb.2020.00065

Nguyen, A. V. and Soulika, A. M. (2019) 'The Dynamics of the Skin's Immune System', *Int J Mol Sci,* 20(8).10.3390/ijms20081811

Nguyen, D. X. and Ehrenstein, M. R. (2016) 'Anti-TNF drives regulatory T cell expansion by paradoxically promoting membrane TNF-TNF-RII binding in rheumatoid arthritis', *J Exp Med,* 213(7), pp. 1241-53.10.1084/jem.20151255

Nisar, S., Roberson, J. L., Carney, B. C., Alkhalil, A., Moffatt, L. T. and Shupp, J. W. (2019) 'Further Histological and Cellular Characterization of Hidradenitis Suppurativa in 11 Patients', *Eplasty,* 19, pp. e21. Available at: https://www.ncbi.nlm.nih.gov/pubmed/31885764

Nograles, K. E., Zaba, L. C., Guttman-Yassky, E., Fuentes-Duculan, J., Suarez-Farinas, M., Cardinale, I., Khatcherian, A., Gonzalez, J., Pierson, K. C., White, T. R., Pensabene, C., Coats, I., Novitskaya, I., Lowes, M. A. and Krueger, J. G. (2008) 'Th17 cytokines interleukin (IL)-17 and IL-22 modulate distinct inflammatory and keratinocyte-response pathways', *Br J Dermatol,* 159(5), pp. 1092-102.10.1111/j.1365-2133.2008.08769.x

Nomura, T. (2020) 'Hidradenitis Suppurativa as a Potential Subtype of Autoinflammatory Keratinization Disease', *Front Immunol,* 11, pp. 847.10.3389/fimmu.2020.00847

Ogawa, E., Owada, Y., Ikawa, S., Adachi, Y., Egawa, T., Nemoto, K., Suzuki, K., Hishinuma, T., Kawashima, H., Kondo, H., Muto, M., Aiba, S. and Okuyama, R. (2011) 'Epidermal FABP (FABP5) regulates keratinocyte differentiation by 13(S)-HODE-mediated activation of the NF-kappaB signaling pathway', *J Invest Dermatol,* 131(3), pp. 604-12.10.1038/jid.2010.342

Oliveira, C. B., Byrd, A. S., Okoye, G. A., Kaplan, M. J. and Carmona-Rivera, C. (2023) 'Neutralizing Anti–DNase 1 and –DNase 1L3 Antibodies Impair Neutrophil Extracellular Traps Degradation in Hidradenitis Suppurativa', *J Invest Dermatol,* 143(1), pp. 57-66.10.1016/j.jid.2022.06.024

Oliver, R., Krueger, J. G., Glatt, S., Vajjah, P., Mistry, C., Page, M., Edwards, H., Garcet, S., Li, X., Dizier, B., Maroof, A., Watling, M., El Baghdady, A., Baeten, D., Ionescu, L. and Shaw, S. (2022) 'Bimekizumab for the treatment of moderate-to-severe plaque psoriasis: efficacy, safety, pharmacokinetics, pharmacodynamics and transcriptomics from a phase IIa, randomized, double-blind multicentre study', *Br J Dermatol,* 186(4), pp. 652-663.10.1111/bjd.20827

Onderdijk, A. J., van der Zee, H. H., Esmann, S., Lophaven, S., Dufour, D. N., Jemec, G. B. and Boer, J. (2013) 'Depression in patients with hidradenitis suppurativa', *J Eur Acad Dermatol Venereol,* 27(4), pp. 473-8.10.1111/j.1468-3083.2012.04468.x

Ortiz-Lopez, L. I., Choudhary, V. and Bollag, W. B. (2022) 'Updated Perspectives on Keratinocytes and Psoriasis: Keratinocytes are More Than Innocent Bystanders', *Psoriasis (Auckl),* 12, pp. 73-87.10.2147/PTT.S327310

Orvain, C., Lin, Y. L., Jean-Louis, F., Hocini, H., Hersant, B., Bennasser, Y., Ortonne, N., Hotz, C., Wolkenstein, P., Boniotto, M., Tisserand, P., Lefebvre, C., Lelièvre, J. D., Benkirane, M., Pasero, P., Lévy, Y. and Hüe, S. (2020) 'Hair follicle stem cell replication stress drives IFI16/STING-dependent inflammation in hidradenitis suppurativa', *J Clin Invest,* 130(7), pp. 3777-3790.10.1172/JCI131180

Ouchi, T., Kubo, A., Yokouchi, M., Adachi, T., Kobayashi, T., Kitashima, D. Y., Fujii, H., Clausen, B. E., Koyasu, S., Amagai, M. and Nagao, K. (2011) 'Langerhans cell antigen capture through tight junctions confers preemptive immunity in experimental staphylococcal scalded skin syndrome', *J Exp Med,* 208(13), pp. 2607-13.10.1084/jem.20111718

Ozinsky, A., Underhill, D. M., Fontenot, J. D., Hajjar, A. M., Smith, K. D., Wilson, C. B., Schroeder, L. and Aderem, A. (2000) 'The repertoire for pattern recognition of pathogens by the innate immune system is defined by cooperation between toll-like receptors', *Proc Natl Acad Sci U S A,* 97(25), pp. 13766-71.10.1073/pnas.250476497

Pan, Y., Lin, M. H., Tian, X., Cheng, H. T., Gridley, T., Shen, J. and Kopan, R. (2004) 'gamma-secretase functions through Notch signaling to maintain skin appendages but is not required for their patterning or initial morphogenesis', *Dev Cell,* 7(5), pp. 731-43.10.1016/j.devcel.2004.09.014

Papp, K. A., Reich, K., Paul, C., Blauvelt, A., Baran, W., Bolduc, C., Toth, D., Langley, R. G., Cather, J., Gottlieb, A. B., Thaçi, D., Krueger, J. G., Russell, C. B., Milmont, C. E., Li, J., Klekotka, P. A., Kricorian, G. and Nirula, A. (2016) 'A prospective phase III, randomized, double-blind, placebo-controlled study of brodalumab in patients with moderate-to-severe plaque psoriasis', *Br J Dermatol,* 175(2), pp. 273-86.10.1111/bjd.14493

Papp, K. A., Weinberg, M. A., Morris, A. and Reich, K. (2021) 'IL17A/F nanobody sonelokimab in patients with plaque psoriasis: a multicentre, randomised, placebo-controlled, phase 2b study', *Lancet,* 397(10284), pp. 1564-1575.10.1016/S0140-6736(21)00440-2

Park, G. T., Seo, E. Y., Lee, K. M., Lee, D. Y. and Yang, J. M. (2006) 'Tob is a potential marker gene for the basal layer of the epidermis and is stably expressed in human primary keratinocytes', *Br J Dermatol,* 154(3), pp. 411-8.10.1111/j.1365-2133.2005.07037.x

Parker, H. and Winterbourn, C. C. (2012) 'Reactive oxidants and myeloperoxidase and their involvement in neutrophil extracellular traps', *Front Immunol,* 3, pp. 424.10.3389/fimmu.2012.00424

Parkes, G. C., Whelan, K. and Lindsay, J. O. (2014) 'Smoking in inflammatory bowel disease: impact on disease course and insights into the aetiology of its effect', *J Crohns Colitis,* 8(8), pp. 717-25.10.1016/j.crohns.2014.02.002

Pasparakis, M., Haase, I. and Nestle, F. O. (2014) 'Mechanisms regulating skin immunity and inflammation', *Nat Rev Immunol,* 14(5), pp. 289-301.10.1038/nri3646

Pastore, S., Corinti, S., La Placa, M., Didona, B. and Girolomoni, G. (1998) 'Interferon-gamma promotes exaggerated cytokine production in keratinocytes cultured from patients with atopic dermatitis', *J Allergy Clin Immunol,* 101(4 Pt 1), pp. 538-44.10.1016/S0091-6749(98)70361-6

Perret, L. J. and Tait, C. P. (2014) 'Non-antibiotic properties of tetracyclines and their clinical application in dermatology', *Australas J Dermatol,* 55(2), pp. 111-8.10.1111/ajd.12075

Petrasca, A., Hambly, R., Kearney, N., Smith, C. M., Pender, E. K., Mac Mahon, J., O'Rourke, A. M., Ismaiel, M., Boland, P. A., Almeida, J. P., Kennedy, C., Zaborowski, A., Murphy, S., Winter, D., Kirby, B. and Fletcher, J. M.

(2023a) 'Metformin has anti-inflammatory effects and induces immunometabolic reprogramming in hidradenitis suppurativa via multiple mechanisms', *Br J Dermatol*.10.1093/bjd/ljad305

Petrasca, A., Hambly, R., Molloy, O., Kearns, S., Moran, B., Smith, C. M., Hughes, R., O'Donnell, M., Zaborowski, A., Winter, D., Fletcher, J. M., Kirby, B. and Malara, A. (2023b) 'Innate lymphoid cell (ILC) subsets are enriched in the skin of patients with hidradenitis suppurativa', *PLoS One,* 18(2), pp. e0281688.10.1371/journal.pone.0281688

Piaserico, S., Gisondi, P., Cazzaniga, S. and Naldi, L. (2020) 'Lack of Evidence for an Increased Risk of Severe COVID-19 in Psoriasis Patients on Biologics: A Cohort Study from Northeast Italy', *Am J Clin Dermatol,* 21(5), pp. 749-751.10.1007/s40257-020-00552-w

Pink, A. E., Simpson, M. A., Desai, N., Trembath, R. C. and Barker, J. N. W. (2013) 'gamma-Secretase mutations in hidradenitis suppurativa: new insights into disease pathogenesis', *J Invest Dermatol,* 133(3), pp. 601-607.10.1038/jid.2012.372

Plank, M. W., Kaiko, G. E., Maltby, S., Weaver, J., Tay, H. L., Shen, W., Wilson, M. S., Durum, S. K. and Foster, P. S. (2017) 'Th22 Cells Form a Distinct Th Lineage from Th17 Cells In Vitro with Unique Transcriptional Properties and Tbet-Dependent Th1 Plasticity', *J Immunol,* 198(5), pp. 2182-2190.10.4049/jimmunol.1601480

Povoleri, G. A. M., Lalnunhlimi, S., Steel, K. J. A., Agrawal, S., O'Byrne, A. M., Ridley, M., Kordasti, S., Frederiksen, K. S., Roberts, C. A. and Taams, L. S. (2020) 'Anti-TNF treatment negatively regulates human CD4', *Eur J Immunol,* 50(3), pp. 445-458.10.1002/eji.201948190

Rada, B., Park, J. J., Sil, P., Geiszt, M. and Leto, T. L. (2014) 'NLRP3 inflammasome activation and interleukin-1β release in macrophages require calcium but are independent of calcium-activated NADPH oxidases', *Inflamm Res,* 63(10), pp. 821-30.10.1007/s00011-014-0756-y

Ramirez-Carrozzi, V., Sambandam, A., Luis, E., Lin, Z., Jeet, S., Lesch, J., Hackney, J., Kim, J., Zhou, M., Lai, J., Modrusan, Z., Sai, T., Lee, W., Xu, M., Caplazi, P., Diehl, L., de Voss, J., Balazs, M., Gonzalez, L., Jr., Singh, H., Ouyang, W. and Pappu, R. (2011) 'IL-17C regulates the innate immune function of epithelial cells in an autocrine manner', *Nat Immunol,* 12(12), pp. 1159-66.10.1038/ni.2156

Raphael, I., Nalawade, S., Eagar, T. N. and Forsthuber, T. G. (2015) 'T cell subsets and their signature cytokines in autoimmune and inflammatory diseases', *Cytokine,* 74(1), pp. 5-17.10.1016/j.cyto.2014.09.011

Reddy, S., Strunk, A. and Garg, A. (2019) 'Comparative Overall Comorbidity Burden Among Patients With Hidradenitis Suppurativa', *JAMA Dermatol,* 155(7), pp. 797-802.10.1001/jamadermatol.2019.0164

Reich, K., Armstrong, A. W., Langley, R. G., Flavin, S., Randazzo, B., Li, S., Hsu, M. C., Branigan, P. and Blauvelt, A. (2019) 'Guselkumab versus secukinumab for the treatment of moderate-to-severe psoriasis (ECLIPSE): results from a phase 3, randomised controlled trial', *Lancet,* 394(10201), pp. 831-839.10.1016/S0140-6736(19)31773-8

Reich, K., Thaçi, D., Stingl, G., Andersen, J. S., Hiort, L. C., Lexner, M. O., Winkler, D. and Paul, C. (2022) 'Safety of Brodalumab in Plaque Psoriasis: Integrated Pooled Data from Five Clinical Trials', *Acta Derm Venereol,* 102, pp. adv00683.10.2340/actadv.v102.1993

Reich, K., Warren, R. B., Lebwohl, M., Gooderham, M., Strober, B., Langley, R. G., Paul, C., De Cuyper, D., Vanvoorden, V., Madden, C., Cioffi, C., Peterson, L. and Blauvelt, A. (2021) 'Bimekizumab versus Secukinumab in Plaque Psoriasis', *N Engl J Med,* 385(2), pp. 142-152.10.1056/NEJMoa2102383

Revu, S., Wu, J., Henkel, M., Rittenhouse, N., Menk, A., Delgoffe, G. M., Poholek, A. C. and McGeachy, M. J. (2018) 'IL-23 and IL-1β Drive Human Th17 Cell Differentiation and Metabolic Reprogramming in Absence of CD28 Costimulation', *Cell Rep,* 22(10), pp. 2642-2653.10.1016/j.celrep.2018.02.044

Revuz, J. E., Canoui-Poitrine, F., Wolkenstein, P., Viallette, C., Gabison, G., Pouget, F., Poli, F., Faye, O., Roujeau, J. C., Bonnelye, G., Grob, J. J. and Bastuji-Garin, S. (2008) 'Prevalence and factors associated with

hidradenitis suppurativa: results from two case-control studies', *J Am Acad Dermatol,* 59(4), pp. 596-601.10.1016/j.jaad.2008.06.020

Ring, H. C., Bay, L., Nilsson, M., Kallenbach, K., Miller, I. M., Saunte, D. M., Bjarnsholt, T., Tolker-Nielsen, T. and Jemec, G. B. (2017a) 'Bacterial biofilm in chronic lesions of hidradenitis suppurativa', *Br J Dermatol,* 176(4), pp. 993-1000.10.1111/bjd.15007

Ring, H. C., Sigsgaard, V., Thorsen, J., Fuursted, K., Fabricius, S., Saunte, D. M. and Jemec, G. B. (2019) 'The microbiome of tunnels in hidradenitis suppurativa patients', *J Eur Acad Dermatol Venereol,* 33(9), pp. 1775-1780.10.1111/jdv.15597

Ring, H. C., Thorsen, J., Saunte, D. M., Lilje, B., Bay, L., Riis, P. T., Larsen, N., Andersen, L. O., Nielsen, H. V., Miller, I. M., Bjarnsholt, T., Fuursted, K. and Jemec, G. B. (2017b) 'The Follicular Skin Microbiome in Patients With Hidradenitis Suppurativa and Healthy Controls', *JAMA Dermatol,* 153(9), pp. 897-905.10.1001/jamadermatol.2017.0904

Riverain-Gillet, É., Guet-Revillet, H., Jais, J. P., Ungeheuer, M. N., Duchatelet, S., Delage, M., Lam, T., Hovnanian, A., Nassif, A. and Join-Lambert, O. (2020) 'The Surface Microbiome of Clinically Unaffected Skinfolds in Hidradenitis Suppurativa: A Cross-Sectional Culture-Based and 16S rRNA Gene Amplicon Sequencing Study in 60 Patients', *J Invest Dermatol,* 140(9), pp. 1847-1855.e6.10.1016/j.jid.2020.02.046

Robertson, S. E., Young, J. D., Kitson, S., Pitt, A., Evans, J., Roes, J., Karaoglu, D., Santora, L., Ghayur, T., Liew, F. Y., Gracie, J. A. and McInnes, I. B. (2006) 'Expression and alternative processing of IL-18 in human neutrophils', *Eur J Immunol,* 36(3), pp. 722-31.10.1002/eji.200535402

Romanic, A. M., Adachi, E., Hojima, Y., Engel, J. and Prockop, D. J. (1992) 'Polymerization of pNcollagen I and copolymerization of pNcollagen I with collagen I. A kinetic, thermodynamic, and morphologic study', *J Biol Chem,* 267(31), pp. 22265-71. Available at: https://www.ncbi.nlm.nih.gov/pubmed/1331049

Rosmarin, D., Pandya, A. G., Lebwohl, M., Grimes, P., Hamzavi, I., Gottlieb, A. B., Butler, K., Kuo, F., Sun, K., Ji, T., Howell, M. D. and Harris, J. E. (2020) 'Ruxolitinib cream for treatment of vitiligo: a randomised, controlled, phase 2 trial', *Lancet,* 396(10244), pp. 110-120.10.1016/S0140-6736(20)30609-7

Russo, V. and Alikhan, A. (2016) 'Failure of Anakinra in a Case of Severe Hidradenitis Suppurativa', *J Drugs Dermatol,* 15(6), pp. 772-4. Available at: https://www.ncbi.nlm.nih.gov/pubmed/27272089

Rybski, K. J., Zengin, H. B. and Smoller, B. R. (2023) 'TRPS1: A Marker of Follicular Differentiation', *Dermatopathology (Basel),* 10(2), pp. 173-183.10.3390/dermatopathology10020025

Sabat, R., Jemec, G. B. E., Matusiak, Ł., Kimball, A. B., Prens, E. and Wolk, K. (2020) 'Hidradenitis suppurativa', *Nat Rev Dis Primers,* 6(1), pp. 18.10.1038/s41572-020-0149-1

Sabat, R., Šimaitė, D., Gudjonsson, J. E., Brembach, T. C., Witte, K., Krause, T., Kokolakis, G., Bartnik, E., Nikolaou, C., Rill, N., Coulibaly, B., Levin, C., Herrmann, M., Salinas, G., Leeuw, T., Volk, H. D., Ghoreschi, K. and Wolk, K. (2023) 'Neutrophilic granulocyte-derived B-cell activating factor supports B cells in skin lesions in hidradenitis suppurativa', *J Allergy Clin Immunol,* 151(4), pp. 1015-1026.10.1016/j.jaci.2022.10.034

Sadeghzadeh Bazargan, A., Pashaei, A. and Goodarzi, A. (2023) 'Successful treatment of Hidradenitis Suppurativa with tofacitinib: two cases and a review of the literature', *Oxf Med Case Reports,* 2023(3), pp. omad003.10.1093/omcr/omad003

Sallusto, F., Lenig, D., Förster, R., Lipp, M. and Lanzavecchia, A. (1999) 'Two subsets of memory T lymphocytes with distinct homing potentials and effector functions', *Nature,* 401(6754), pp. 708-12.10.1038/44385

Sanchez, J., Le Jan, S., Muller, C., Francois, C., Renard, Y., Durlach, A., Bernard, P., Reguiai, Z. and Antonicelli, F. (2019) 'Matrix remodelling and MMP expression/activation are associated with hidradenitis suppurativa skin inflammation', *Exp Dermatol,* 28(5), pp. 593-600.10.1111/exd.13919

Sartorius, K., Emtestam, L., Jemec, G. B. and Lapins, J. (2009) 'Objective scoring of hidradenitis suppurativa reflecting the role of tobacco smoking and obesity', *Br J Dermatol,* 161(4), pp. 831-9.10.1111/j.1365-2133.2009.09198.x

Saunte, D. M., Boer, J., Stratigos, A., Szepietowski, J. C., Hamzavi, I., Kim, K. H., Zarchi, K., Antoniou, C., Matusiak, L., Lim, H. W., Williams, M., Kwon, H. H., Gürer, M. A., Mammadova, F., Kaminsky, A., Prens, E., van der Zee, H. H., Bettoli, V., Zauli, S., Hafner, J., Lauchli, S., French, L. E., Riad, H., El-Domyati, M., Abdel-Wahab, H., Kirby, B., Kelly, G., Calderon, P., del Marmol, V., Benhadou, F., Revuz, J., Zouboulis, C. C., Karagiannidis, I., Sartorius, K., Hagströmer, L., McMeniman, E., Ong, N., Dolenc-Voljc, M., Mokos, Z. B., Borradori, L., Hunger, R. E., Sladden, C., Scheinfeld, N., Moftah, N., Emtestam, L., Lapins, J., Doss, N., Kurokawa, I. and Jemec, G. B. (2015) 'Diagnostic delay in hidradenitis suppurativa is a global problem', *Br J Dermatol,* 173(6), pp. 1546-9.10.1111/bjd.14038

Savage, K. T., Santillan, M. R., Flood, K. S., Charrow, A., Porter, M. L. and Kimball, A. B. (2020) 'Tofacitinib shows benefit in conjunction with other therapies in recalcitrant hidradenitis suppurativa patients', *JAAD Case Rep,* 6(2), pp. 99-102.10.1016/j.jdcr.2019.10.010

Schell, S. L., Cong, Z., Sennett, M. L., Gettle, S. L., Longenecker, A. L., Goldberg, S. R., Kirby, J. S., Helm, M. F. and Nelson, A. M. (2023) 'Keratinocytes and immune cells in the epidermis are key drivers of inflammation in hidradenitis suppurativa providing a rationale for novel topical therapies', *Br J Dermatol,* 188(3), pp. 407-419.10.1093/bjd/ljac096

Schlapbach, C., Hanni, T., Yawalkar, N. and Hunger, R. E. (2011) 'Expression of the IL-23/Th17 pathway in lesions of hidradenitis suppurativa', *J Am Acad Dermatol,* 65(4), pp. 790-798.10.1016/j.jaad.2010.07.010

Schmid-Wendtner, M. H. and Korting, H. C. (2006) 'The pH of the skin surface and its impact on the barrier function', *Skin Pharmacol Physiol,* 19(6), pp. 296-302.10.1159/000094670

Schneider-Burrus, S., Tsaousi, A., Barbus, S., Huss-Marp, J., Witte, K., Wolk, K., Fritz, B. and Sabat, R. (2021) 'Features Associated With Quality of Life Impairment in Hidradenitis Suppurativa Patients', *Front Med (Lausanne),* 8, pp. 676241.10.3389/fmed.2021.676241

Schreiber, S., Colombel, J. F., Feagan, B. G., Reich, K., Deodhar, A. A., McInnes, I. B., Porter, B., Das Gupta, A., Pricop, L. and Fox, T. (2019) 'Incidence rates of inflammatory bowel disease in patients with psoriasis, psoriatic arthritis and ankylosing spondylitis treated with secukinumab: a retrospective analysis of pooled data from 21 clinical trials', *Ann Rheum Dis,* 78(4), pp. 473-479.10.1136/annrheumdis-2018-214273

Schutyser, E., Struyf, S. and Van Damme, J. (2003) 'The CC chemokine CCL20 and its receptor CCR6', *Cytokine Growth Factor Rev,* 14(5), pp. 409-26.10.1016/s1359-6101(03)00049-2

Schwaid, A. G. and Spencer, K. B. (2021) 'Strategies for Targeting the NLRP3 Inflammasome in the Clinical and Preclinical Space', *J Med Chem,* 64(1), pp. 101-122.10.1021/acs.jmedchem.0c01307

Seneschal, J., Clark, R. A., Gehad, A., Baecher-Allan, C. M. and Kupper, T. S. (2012) 'Human epidermal Langerhans cells maintain immune homeostasis in skin by activating skin resident regulatory T cells', *Immunity,* 36(5), pp. 873-84.10.1016/j.immuni.2012.03.018

Shaharir, S. S., Jamil, A., Chua, S. H., Arumugam, M. and Rosli, N. (2020) 'A case paradoxical hidradenitis suppurativa with janus kinase inhibitor, literature review and pooled analysis of biological agent-induced HS', *Dermatol Ther,* 33(6), pp. e14021.10.1111/dth.14021

Shahbazi, M. N., Peña-Jimenez, D., Antonucci, F., Drosten, M. and Perez-Moreno, M. (2017) 'Clasp2 ensures mitotic fidelity and prevents differentiation of epidermal keratinocytes', *J Cell Sci,* 130(4), pp. 683-688.10.1242/jcs.194787

Sherman, S., Kridin, K., Bitan, D. T., Leshem, Y. A., Hodak, E. and Cohen, A. D. (2021) 'Hidradenitis suppurativa and atopic dermatitis: A 2-way association', *J Am Acad Dermatol,* 85(6), pp. 1473-1479.10.1016/j.jaad.2020.12.051

Shirshin, E. A., Gurfinkel, Y. I., Priezzhev, A. V., Fadeev, V. V., Lademann, J. and Darvin, M. E. (2017) 'Two-photon autofluorescence lifetime imaging of human skin papillary dermis in vivo: assessment of blood capillaries and structural proteins localization', *Sci Rep,* 7(1), pp. 1171.10.1038/s41598-017-01238-w

Shive, C. L., Jiang, W., Anthony, D. D. and Lederman, M. M. (2015) 'Soluble CD14 is a nonspecific marker of monocyte activation', *AIDS,* 29(10), pp. 1263-5.10.1097/QAD.0000000000000735

Shortman, K. and Heath, W. R. (2010) 'The CD8+ dendritic cell subset', *Immunol Rev,* 234(1), pp. 18-31.10.1111/j.0105-2896.2009.00870.x

Simard, J. C., Cesaro, A., Chapeton-Montes, J., Tardif, M., Antoine, F., Girard, D. and Tessier, P. A. (2013) 'S100A8 and S100A9 induce cytokine expression and regulate the NLRP3 inflammasome via ROS-dependent activation of NF-kappaB(1.)', *PLoS One,* 8(8), pp. e72138.10.1371/journal.pone.0072138

Singh, T. P., Zhang, H. H., Borek, I., Wolf, P., Hedrick, M. N., Singh, S. P., Kelsall, B. L., Clausen, B. E. and Farber, J. M. (2016) 'Monocyte-derived inflammatory Langerhans cells and dermal dendritic cells mediate psoriasis-like inflammation', *Nat Commun,* 7, pp. 13581.10.1038/ncomms13581

Sivaprasad, U., Kinker, K. G., Ericksen, M. B., Lindsey, M., Gibson, A. M., Bass, S. A., Hershey, N. S., Deng, J., Medvedovic, M. and Khurana Hershey, G. K. (2015) 'SERPINB3/B4 contributes to early inflammation and barrier dysfunction in an experimental murine model of atopic dermatitis', *J Invest Dermatol,* 135(1), pp. 160-169.10.1038/jid.2014.353

Smith, C. M., Hambly, R., Gatault, S., Iglesias-Martinez, L. F., Kearns, S., Rea, H., Marasigan, V., Lynam-Loane, K., Kirthi, S., Hughes, R., Fletcher, J. M., Kolch, W. and Kirby, B. (2023) 'B-cell-derived transforming growth factor-β may drive the activation of inflammatory macrophages and contribute to scarring in hidradenitis suppurativa', *Br J Dermatol,* 188(2), pp. 290-310.10.1093/bjd/ljac048

Sojka, D. K., Huang, Y. H. and Fowell, D. J. (2008) 'Mechanisms of regulatory T-cell suppression - a diverse arsenal for a moving target', *Immunology,* 124(1), pp. 13-22.10.1111/j.1365-2567.2008.02813.x

Solé-Boldo, L., Raddatz, G., Schütz, S., Mallm, J. P., Rippe, K., Lonsdorf, A. S., Rodríguez-Paredes, M. and Lyko, F. (2020) 'Single-cell transcriptomes of the human skin reveal age-related loss of fibroblast priming', *Commun Biol,* 3(1), pp. 188.10.1038/s42003-020-0922-4

Stevens, L. J. and Page-McCaw, A. (2012) 'A secreted MMP is required for reepithelialization during wound healing', *Mol Biol Cell,* 23(6), pp. 1068-79.10.1091/mbc.E11-09-0745

Stone, O. J. (1976) 'Hidradenitis suppurativa following acanthosis nigricans. Report of two cases', *Arch Dermatol,* 112(8), pp. 1142. Available at: https://www.ncbi.nlm.nih.gov/pubmed/952534

Stuart, T., Butler, A., Hoffman, P., Hafemeister, C., Papalexi, E., Mauck, W. M., 3rd, Hao, Y., Stoeckius, M., Smibert, P. and Satija, R. (2019) 'Comprehensive Integration of Single-Cell Data', *Cell,* 177(7), pp. 1888-1902 e21.10.1016/j.cell.2019.05.031

Suchanski, J., Tejchman, A., Zacharski, M., Piotrowska, A., Grzegrzolka, J., Chodaczek, G., Nowinska, K., Rys, J., Dziegiel, P., Kieda, C. and Ugorski, M. (2017) 'Podoplanin increases the migration of human fibroblasts and affects the endothelial cell network formation: A possible role for cancer-associated fibroblasts in breast cancer progression', *PLoS One,* 12(9), pp. e0184970.10.1371/journal.pone.0184970

Sugita, S., Kawazoe, Y., Imai, A., Yamada, Y., Horie, S. and Mochizuki, M. (2012) 'Inhibition of Th17 differentiation by anti-TNF-alpha therapy in uveitis patients with Behçet's disease', *Arthritis Res Ther,* 14(3), pp. R99.10.1186/ar3824

Sugiyama, H., Gyulai, R., Toichi, E., Garaczi, E., Shimada, S., Stevens, S. R., McCormick, T. S. and Cooper, K. D. (2005) 'Dysfunctional blood and target tissue CD4+CD25high regulatory T cells in psoriasis: mechanism underlying unrestrained pathogenic effector T cell proliferation', *J Immunol,* 174(1), pp. 164-73.10.4049/jimmunol.174.1.164

Sun, N. Z., Ro, T., Jolly, P. and Sayed, C. J. (2017) 'Non-response to Interleukin-1 Antagonist Canakinumab in Two Patients with Refractory Pyoderma Gangrenosum and Hidradenitis Suppurativa', *J Clin Aesthet Dermatol,* 10(9), pp. 36-38. Available at: https://www.ncbi.nlm.nih.gov/pubmed/29344326

Tabib, T., Morse, C., Wang, T., Chen, W. and Lafyatis, R. (2018) 'SFRP2/DPP4 and FMO1/LSP1 Define Major Fibroblast Populations in Human Skin', *J Invest Dermatol,* 138(4), pp. 802-810.10.1016/j.jid.2017.09.045

Takahashi, K., Yanagi, T., Kitamura, S., Hata, H., Imafuku, K., Iwami, D., Hotta, K., Morita, K., Shinohara, N. and Shimizu, H. (2018) 'Successful treatment of hidradenitis suppurativa with rituximab for a patient with idiopathic carpotarsal osteolysis and chronic active antibody-mediated rejection', *J Dermatol,* 45(5), pp. e116-e117.10.1111/1346-8138.14144

Tamarozzi, F., Wright, H. L., Thomas, H. B., Edwards, S. W. and Taylor, M. J. (2014) 'A lack of confirmation with alternative assays questions the validity of IL-17A expression in human neutrophils using immunohistochemistry', *Immunol Lett,* 162(2 Pt B), pp. 194-8.10.1016/j.imlet.2014.10.025

Tamassia, N., Arruda-Silva, F., Calzetti, F., Lonardi, S., Gasperini, S., Gardiman, E., Bianchetto-Aguilera, F., Gatta, L. B., Girolomoni, G., Mantovani, A., Vermi, W. and Cassatella, M. A. (2018) 'A Reappraisal on the Potential Ability of Human Neutrophils to Express and Produce IL-17 Family Members', *Front Immunol,* 9, pp. 795.10.3389/fimmu.2018.00795

Teunissen, M. B. M., Munneke, J. M., Bernink, J. H., Spuls, P. I., Res, P. C. M., Te Velde, A., Cheuk, S., Brouwer, M. W. D., Menting, S. P., Eidsmo, L., Spits, H., Hazenberg, M. D. and Mjösberg, J. (2014) 'Composition of innate lymphoid cell subsets in the human skin: enrichment of NCR(+) ILC3 in lesional skin and blood of psoriasis patients', *J Invest Dermatol,* 134(9), pp. 2351-2360.10.1038/jid.2014.146

Thomi, R., Kakeda, M., Yawalkar, N., Schlapbach, C. and Hunger, R. E. (2017) 'Increased expression of the interleukin-36 cytokines in lesions of hidradenitis suppurativa', *J Eur Acad Dermatol Venereol,* 31(12), pp. 2091-2096.10.1111/jdv.14389

Tian, Y., Ling, X. Y., Chen, D. L., Zhang, X. Q. and Qiu, C. M. (2020) 'Interleukin-36 receptor antagonist attenuates atherosclerosis development by inhibiting NLRP3 inflammasome', *J Cell Physiol,* 235(12), pp. 9992-9996.10.1002/jcp.29813

Ting, J. P., Kastner, D. L. and Hoffman, H. M. (2006) 'CATERPILLERs, pyrin and hereditary immunological disorders', *Nat Rev Immunol,* 6(3), pp. 183-95.10.1038/nri1788

Tracy, L. E., Minasian, R. A. and Caterson, E. J. (2016) 'Extracellular Matrix and Dermal Fibroblast Function in the Healing Wound', *Adv Wound Care (New Rochelle),* 5(3), pp. 119-136.10.1089/wound.2014.0561

Trifari, S., Kaplan, C. D., Tran, E. H., Crellin, N. K. and Spits, H. (2009) 'Identification of a human helper T cell population that has abundant production of interleukin 22 and is distinct from T(H)-17, T(H)1 and T(H)2 cells', *Nat Immunol,* 10(8), pp. 864-71.10.1038/ni.1770

Tzanetakou, V., Kanni, T., Giatrakou, S., Katoulis, A., Papadavid, E., Netea, M. G., Dinarello, C. A., van der Meer, J. W. M., Rigopoulos, D. and Giamarellos-Bourboulis, E. J. (2016) 'Safety and Efficacy of Anakinra in Severe Hidradenitis Suppurativa: A Randomized Clinical Trial', *JAMA Dermatol,* 152(1), pp. 52-59.10.1001/jamadermatol.2015.3903

Tzellos, T., Yang, H., Mu, F., Calimlim, B. and Signorovitch, J. (2019) 'Impact of hidradenitis suppurativa on work loss, indirect costs and income', *Br J Dermatol,* 181(1), pp. 147-154.10.1111/bjd.17101

UCB 2023. Bimekizumab Phase 3 Data in Hidradenitis Suppurativa Show Clinically Meaningful, Deep and Maintained Response over 48 Weeks.

Uchi, H., Terao, H., Koga, T. and Furue, M. (2000) 'Cytokines and chemokines in the epidermis', *J Dermatol Sci,* 24 Suppl 1, pp. S29-38.10.1016/s0923-1811(00)00138-9

Ulgen, E., Ozisik, O. and Sezerman, O. U. (2019) 'pathfindR: An R Package for Comprehensive Identification of Enriched Pathways in Omics Data Through Active Subnetworks', *Front Genet,* 10, pp. 858.10.3389/fgene.2019.00858

Utsunomiya, A., Chino, T., Utsunomiya, N., Luong, V. H., Tokuriki, A., Naganuma, T., Arita, M., Higashi, K., Saito, K., Suzuki, N., Ohara, A., Sugai, M., Sugawara, K., Tsuruta, D., Oyama, N. and Hasegawa, M. (2020) 'Homeostatic Function of Dermokine in the Skin Barrier and Inflammation', *J Invest Dermatol,* 140(4), pp. 838-849.e9.10.1016/j.jid.2019.09.011

Vaher, H., Kivihall, A., Runnel, T., Raam, L., Prans, E., Maslovskaja, J., Abram, K., Kaldvee, B., Mrowietz, U., Weidinger, S., Kingo, K. and Rebane, A. (2020) 'SERPINB2 and miR-146a/b are coordinately regulated and act in the suppression of psoriasis-associated inflammatory responses in keratinocytes', *Exp Dermatol,* 29(1), pp. 51-60.10.1111/exd.14049

van der Aar, A. M., de Groot, R., Sanchez-Hernandez, M., Taanman, E. W., van Lier, R. A., Teunissen, M. B., de Jong, E. C. and Kapsenberg, M. L. (2011) 'Cutting edge: virus selectively primes human langerhans cells for CD70 expression promoting CD8+ T cell responses', *J Immunol,* 187(7), pp. 3488-92.10.4049/jimmunol.1101105

van der Zee, H. H., de Ruiter, L., Boer, J., van den Broecke, D. G., den Hollander, J. C., Laman, J. D. and Prens, E. P. (2012a) 'Alterations in leucocyte subsets and histomorphology in normal-appearing perilesional skin and early and chronic hidradenitis suppurativa lesions', *Br J Dermatol,* 166(1), pp. 98-106.10.1111/j.1365-2133.2011.10643.x

van der Zee, H. H., de Ruiter, L., van den Broecke, D. G., Dik, W. A., Laman, J. D. and Prens, E. P. (2011) 'Elevated levels of tumour necrosis factor (TNF)-alpha, interleukin (IL)-1beta and IL-10 in hidradenitis suppurativa skin: a rationale for targeting TNF-alpha and IL-1beta', *Br J Dermatol,* 164(6), pp. 1292-8.10.1111/j.1365-2133.2011.10254.x

van der Zee, H. H., Laman, J. D., Boer, J. and Prens, E. P. (2012b) 'Hidradenitis suppurativa: viewpoint on clinical phenotyping, pathogenesis and novel treatments', *Exp Dermatol,* 21(10), pp. 735-9.10.1111/j.1600-0625.2012.01552.x

Vanlaerhoven, A. M. J. D., Ardon, C. B., van Straalen, K. R., Vossen, A. R. J. V., Prens, E. P. and van der Zee, H. H. (2018) 'Hurley III Hidradenitis Suppurativa Has an Aggressive Disease Course', *Dermatology,* 234(5-6), pp. 232-233.10.1159/000491547

Vazquez, B. G., Alikhan, A., Weaver, A. L., Wetter, D. A. and Davis, M. D. (2013) 'Incidence of hidradenitis suppurativa and associated factors: a population-based study of Olmsted County, Minnesota', *J Invest Dermatol,* 133(1), pp. 97-103.10.1038/jid.2012.255

Verdolini, R., Clayton, N., Smith, A., Alwash, N. and Mannello, B. (2013) 'Metformin for the treatment of hidradenitis suppurativa: a little help along the way', *J Eur Acad Dermatol Venereol,* 27(9), pp. 1101-8.10.1111/j.1468-3083.2012.04668.x

von Laffert, M., Helmbold, P., Wohlrab, J., Fiedler, E., Stadie, V. and Marsch, W. C. (2010) 'Hidradenitis suppurativa (acne inversa): early inflammatory events at terminal follicles and at interfollicular epidermis', *Exp Dermatol,* 19(6), pp. 533-7.10.1111/j.1600-0625.2009.00915.x

Vossen, A., Ardon, C. B., van der Zee, H. H., Lubberts, E. and Prens, E. P. (2019a) 'The anti-inflammatory potency of biologics targeting tumour necrosis factor-alpha, interleukin (IL)-17A, IL-12/23 and CD20 in hidradenitis suppurativa: an ex vivo study', *Br J Dermatol,* 181(2), pp. 314-323.10.1111/bjd.17641

Vossen, A., van der Zee, H. H. and Prens, E. P. (2018) 'Hidradenitis Suppurativa: A Systematic Review Integrating Inflammatory Pathways Into a Cohesive Pathogenic Model', *Front Immunol,* 9, pp. 2965.10.3389/fimmu.2018.02965

Vossen, A., van der Zee, H. H., Tsoi, L. C., Xing, X., Devalaraja, M., Gudjonsson, J. E. and Prens, E. P. (2019b) 'Novel cytokine and chemokine markers of hidradenitis suppurativa reflect chronic inflammation and itch', *Allergy,* 74(3), pp. 631-634.10.1111/all.13665

Vossen, A. R. J. V., van Straalen, K. R., Florencia, E. F. and Prens, E. P. (2020) 'Lesional Inflammatory Profile in Hidradenitis Suppurativa Is Not Solely Driven by IL-1', *J Invest Dermatol,* 140(7), pp. 1463-1466.e2.10.1016/j.jid.2020.01.023

Vremec, D. and Shortman, K. (1997) 'Dendritic cell subtypes in mouse lymphoid organs: cross-correlation of surface markers, changes with incubation, and differences among thymus, spleen, and lymph nodes', *J Immunol,* 159(2), pp. 565-73. Available at: https://www.ncbi.nlm.nih.gov/pubmed/9218570

Wang, B., Yang, W., Wen, W., Sun, J., Su, B., Liu, B., Ma, D., Lv, D., Wen, Y., Qu, T., Chen, M., Sun, M., Shen, Y. and Zhang, X. (2010) 'Gamma-secretase gene mutations in familial acne inversa', *Science,* 330(6007), pp. 1065.10.1126/science.1196284

Wang, Q., Zhang, X., Song, X. and Zhang, L. (2018) 'Overexpression of T-cadherin inhibits the proliferation of oral squamous cell carcinoma through the PI3K/AKT/mTOR intracellular signalling pathway', *Arch Oral Biol,* 96, pp. 74-79.10.1016/j.archoralbio.2018.08.018

Wang, R., Ghahary, A., Shen, Q., Scott, P. G., Roy, K. and Tredget, E. E. (2000) 'Hypertrophic scar tissues and fibroblasts produce more transforming growth factor-beta1 mRNA and protein than normal skin and cells', *Wound Repair Regen,* 8(2), pp. 128-37.10.1046/j.1524-475x.2000.00128.x

Wang, Z., Yan, Y. and Wang, B. (2021) 'γ-Secretase Genetics of Hidradenitis Suppurativa: A Systematic Literature Review', *Dermatology,* 237(5), pp. 698-704.10.1159/000512455

Watanabe, R., Gehad, A., Yang, C., Scott, L. L., Teague, J. E., Schlapbach, C., Elco, C. P., Huang, V., Matos, T. R., Kupper, T. S. and Clark, R. A. (2015) 'Human skin is protected by four functionally and phenotypically discrete populations of resident and recirculating memory T cells', *Sci Transl Med,* 7(279), pp. 279ra39.10.1126/scitranslmed.3010302

Weaver, D. J., Reis, E. S., Pandey, M. K., Köhl, G., Harris, N., Gerard, C. and Köhl, J. (2010) 'C5a receptor-deficient dendritic cells promote induction of Treg and Th17 cells', *Eur J Immunol,* 40(3), pp. 710-21.10.1002/eji.200939333

Wieland, C. W., Vogl, T., Ordelman, A., Vloedgraven, H. G., Verwoolde, L. H., Rensen, J. M., Roth, J., Boer, J. and Hessels, J. (2013) 'Myeloid marker S100A8/A9 and lymphocyte marker, soluble interleukin 2 receptor: biomarkers of hidradenitis suppurativa disease activity?', *Br J Dermatol,* 168(6), pp. 1252-8.10.1111/bjd.12234

Wilson, N. J., Boniface, K., Chan, J. R., McKenzie, B. S., Blumenschein, W. M., Mattson, J. D., Basham, B., Smith, K., Chen, T., Morel, F., Lecron, J. C., Kastelein, R. A., Cua, D. J., McClanahan, T. K., Bowman, E. P. and de Waal Malefyt, R. (2007) 'Development, cytokine profile and function of human interleukin 17-producing helper T cells', *Nat Immunol,* 8(9), pp. 950-7.10.1038/ni1497

Wilson, R. P., McGettigan, S. E., Dang, V. D., Kumar, A., Cancro, M. P., Nikbakht, N., Stohl, W. and Debes, G. F. (2019) 'IgM Plasma Cells Reside in Healthy Skin and Accumulate with Chronic Inflammation', *J Invest Dermatol,* 139(12), pp. 2477-2487.10.1016/j.jid.2019.05.009

Witte-Handel, E., Wolk, K., Tsaousi, A., Irmer, M. L., Mossner, R., Shomroni, O., Lingner, T., Witte, K., Kunkel, D., Salinas, G., Jodl, S., Schmidt, N., Sterry, W., Volk, H. D., Giamarellos-Bourboulis, E. J., Pokrywka, A., Docke, W. D., Schneider-Burrus, S. and Sabat, R. (2019) 'The IL-1 Pathway Is Hyperactive in Hidradenitis Suppurativa and Contributes to Skin Infiltration and Destruction', *J Invest Dermatol,* 139(6), pp. 1294-1305.10.1016/j.jid.2018.11.018

Wolk, K., Brembach, T. C., Šimaitė, D., Bartnik, E., Cucinotta, S., Pokrywka, A., Irmer, M. L., Triebus, J., Witte-Händel, E., Salinas, G., Leeuw, T., Volk, H. D., Ghoreschi, K. and Sabat, R. (2021) 'Activity and components of

the granulocyte colony-stimulating factor pathway in hidradenitis suppurativa', *Br J Dermatol,* 185(1), pp. 164-176.10.1111/bjd.19795

Wolk, K., Warszawska, K., Hoeflich, C., Witte, E., Schneider-Burrus, S., Witte, K., Kunz, S., Buss, A., Roewert, H. J., Krause, M., Lukowsky, A., Volk, H. D., Sterry, W. and Sabat, R. (2011) 'Deficiency of IL-22 contributes to a chronic inflammatory disease: pathogenetic mechanisms in acne inversa', *J Immunol,* 186(2), pp. 1228-39.10.4049/jimmunol.0903907

Woodley, D. T. (2017) 'Distinct Fibroblasts in the Papillary and Reticular Dermis: Implications for Wound Healing', *Dermatol Clin,* 35(1), pp. 95-100.10.1016/j.det.2016.07.004

Xia, Y., Vetvicka, V., Yan, J., Hanikýrová, M., Mayadas, T. and Ross, G. D. (1999) 'The beta-glucan-binding lectin site of mouse CR3 (CD11b/CD18) and its function in generating a primed state of the receptor that mediates cytotoxic activation in response to iC3b-opsonized target cells', *J Immunol,* 162(4), pp. 2281-90. Available at: https://www.ncbi.nlm.nih.gov/pubmed/9973505

Xu, Y., Xue, S., Zhou, J., Voorhees, J. J. and Fisher, G. J. (2015) 'Notch and TGF-β pathways cooperatively regulate receptor protein tyrosine phosphatase-κ (PTPRK) gene expression in human primary keratinocytes', *Mol Biol Cell,* 26(6), pp. 1199-206.10.1091/mbc.E14-12-1591

Xue, M. and Jackson, C. J. (2015) 'Extracellular Matrix Reorganization During Wound Healing and Its Impact on Abnormal Scarring', *Adv Wound Care (New Rochelle),* 4(3), pp. 119-136.10.1089/wound.2013.0485

Yan, Y., Chen, R., Wang, X., Hu, K., Huang, L., Lu, M. and Hu, Q. (2019) 'CCL19 and CCR7 Expression, Signaling Pathways, and Adjuvant Functions in Viral Infection and Prevention', *Front Cell Dev Biol,* 7, pp. 212.10.3389/fcell.2019.00212

Yanez, D. A., Lacher, R. K., Vidyarthi, A. and Colegio, O. R. (2017) 'The role of macrophages in skin homeostasis', *Pflugers Arch,* 469(3-4), pp. 455-463.10.1007/s00424-017-1953-7

Yang, L., Anderson, D. E., Baecher-Allan, C., Hastings, W. D., Bettelli, E., Oukka, M., Kuchroo, V. K. and Hafler, D. A. (2008) 'IL-21 and TGF-beta are required for differentiation of human T(H)17 cells', *Nature,* 454(7202), pp. 350-2.10.1038/nature07021

Yang, X. O., Panopoulos, A. D., Nurieva, R., Chang, S. H., Wang, D., Watowich, S. S. and Dong, C. (2007) 'STAT3 regulates cytokine-mediated generation of inflammatory helper T cells', *J Biol Chem,* 282(13), pp. 9358-9363.10.1074/jbc.C600321200

Yao, C., Oh, J. H., Lee, D. H., Bae, J. S., Jin, C. L., Park, C. H. and Chung, J. H. (2015) 'Toll-like receptor family members in skin fibroblasts are functional and have a higher expression compared to skin keratinocytes', *Int J Mol Med,* 35(5), pp. 1443-50.10.3892/ijmm.2015.2146

Yao, L., Zhang, W., Zheng, J., Lu, X. and Zhang, F. (2021) 'miR-199a Targeting PNRC1 to Promote Keratinocyte Proliferation and Invasion in Cholesteatoma', *Biomed Res Int,* 2021, pp. 1442093.10.1155/2021/1442093

Yazdanyar, S. and Jemec, G. B. (2011) 'Hidradenitis suppurativa: a review of cause and treatment', *Curr Opin Infect Dis,* 24(2), pp. 118-23.10.1097/QCO.0b013e3283428d07

Yu, C. C. and Cook, M. G. (1990) 'Hidradenitis suppurativa: a disease of follicular epithelium, rather than apocrine glands', *Br J Dermatol,* 122(6), pp. 763-9.10.1111/j.1365-2133.1990.tb06264.x

Yu, Z., Yu, Q., Xu, H., Dai, X., Yu, Y., Cui, L., Chen, Y., Gu, J., Zhang, X., Guo, C. and Shi, Y. (2022) 'IL-17A Promotes Psoriasis-Associated Keratinocyte Proliferation through ACT1-Dependent Activation of YAP-AREG Axis', *J Invest Dermatol,* 142(9), pp. 2343-2352.10.1016/j.jid.2022.02.016

Zahid, A., Li, B., Kombe, A. J. K., Jin, T. and Tao, J. (2019) 'Pharmacological Inhibitors of the NLRP3 Inflammasome', *Front Immunol,* 10, pp. 2538.10.3389/fimmu.2019.02538

Zhang, L., Yang, X. Q., Cheng, J., Hui, R. S. and Gao, T. W. (2010) 'Increased Th17 cells are accompanied by FoxP3(+) Treg cell accumulation and correlated with psoriasis disease severity', *Clin Immunol,* 135(1), pp. 108-17.10.1016/j.clim.2009.11.008

Zhang, X., Yin, M. and Zhang, L. J. (2019) 'Keratin 6, 16 and 17-Critical Barrier Alarmin Molecules in Skin Wounds and Psoriasis', *Cells,* 8(8).10.3390/cells8080807

Zhang, Y., Reynolds, J. M., Chang, S. H., Martin-Orozco, N., Chung, Y., Nurieva, R. I. and Dong, C. (2009) 'MKP-1 is necessary for T cell activation and function', *J Biol Chem,* 284(45), pp. 30815-24.10.1074/jbc.M109.052472

Zhang, Y., Siegel, A. M., Sun, G., Dimaggio, T., Freeman, A. F. and Milner, J. D. (2019) 'Human T', *J Allergy Clin Immunol,* 143(3), pp. 1108-1118.e4.10.1016/j.jaci.2018.06.036

Zhang, Y., Wang, L., Sun, X. and Li, F. (2023) 'SERPINB4 Promotes Keratinocyte Inflammation via p38MAPK Signaling Pathway', *J Immunol Res,* 2023, pp. 3397940.10.1155/2023/3397940

Zhang, Z., Li, X. J., Liu, Y., Zhang, X., Li, Y. Y. and Xu, W. S. (2007) 'Recombinant human decorin inhibits cell proliferation and downregulates TGF-beta1 production in hypertrophic scar fibroblasts', *Burns,* 33(5), pp. 634-41.10.1016/j.burns.2006.08.018

Zheng, G. X., Terry, J. M., Belgrader, P., Ryvkin, P., Bent, Z. W., Wilson, R., Ziraldo, S. B., Wheeler, T. D., McDermott, G. P., Zhu, J., Gregory, M. T., Shuga, J., Montesclaros, L., Underwood, J. G., Masquelier, D. A., Nishimura, S. Y., Schnall-Levin, M., Wyatt, P. W., Hindson, C. M., Bharadwaj, R., Wong, A., Ness, K. D., Beppu, L. W., Deeg, H. J., McFarland, C., Loeb, K. R., Valente, W. J., Ericson, N. G., Stevens, E. A., Radich, J. P., Mikkelsen, T. S., Hindson, B. J. and Bielas, J. H. (2017) 'Massively parallel digital transcriptional profiling of single cells', *Nat Commun,* 8, pp. 14049.10.1038/ncomms14049

Zheng, M., Karki, R., Williams, E. P., Yang, D., Fitzpatrick, E., Vogel, P., Jonsson, C. B. and Kanneganti, T. D. (2021) 'TLR2 senses the SARS-CoV-2 envelope protein to produce inflammatory cytokines', *Nat Immunol,* 22(7), pp. 829-838.10.1038/s41590-021-00937-x

Zhu, Z., Ding, J., Shankowsky, H. A. and Tredget, E. E. (2013) 'The molecular mechanism of hypertrophic scar', *J Cell Commun Signal,* 7(4), pp. 239-52.10.1007/s12079-013-0195-5

Zouboulis, C. C., Tzellos, T., Kyrgidis, A., Jemec, G. B. E., Bechara, F. G., Giamarellos-Bourboulis, E. J., Ingram, J. R., Kanni, T., Karagiannidis, I., Martorell, A., Matusiak, Ł., Pinter, A., Prens, E. P., Presser, D., Schneider-Burrus, S., von Stebut, E., Szepietowski, J. C., van der Zee, H. H., Wilden, S. M., Sabat, R. and Group, E. H. S. F. I. (2017) 'Development and validation of the International Hidradenitis Suppurativa Severity Score System (IHS4), a novel dynamic scoring system to assess HS severity', *Br J Dermatol,* 177(5), pp. 1401-1409.10.1111/bjd.15748

Zrioual, S., Ecochard, R., Tournadre, A., Lenief, V., Cazalis, M. A. and Miossec, P. (2009) 'Genome-wide comparison between IL-17A- and IL-17F-induced effects in human rheumatoid arthritis synoviocytes', *J Immunol,* 182(5), pp. 3112-20.10.4049/jimmunol.0801967